

1-1-1990

Nature and properties of fragipans in Massachusetts.

David Lloyd Lindbo
University of Massachusetts Amherst

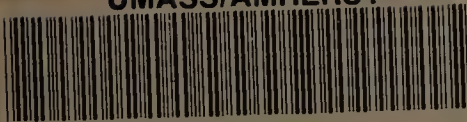
Follow this and additional works at: https://scholarworks.umass.edu/dissertations_1

Recommended Citation

Lindbo, David Lloyd, "Nature and properties of fragipans in Massachusetts." (1990). *Doctoral Dissertations 1896 - February 2014*. 6095.
https://scholarworks.umass.edu/dissertations_1/6095

This Open Access Dissertation is brought to you for free and open access by ScholarWorks@UMass Amherst. It has been accepted for inclusion in Doctoral Dissertations 1896 - February 2014 by an authorized administrator of ScholarWorks@UMass Amherst. For more information, please contact scholarworks@library.umass.edu.

UMASS/AMHERST



312066007712889

NATURE AND PROPERTIES OF FRAGIPANS IN MASSACHUSETTS

A Dissertation Presented

by

DAVID LLOYD LINDBO

Submitted to the Graduate School of the
University of Massachusetts in partial fulfillment
of the requirements for the degree of

DOCTOR OF PHILOSOPHY

May 1990

Department of Plant and Soil Science

© Copyright by David Lloyd Lindbo 1990

All Rights Reserved


NATURE AND PROPERTIES OF FRAGIPANS IN MASSACHUSETTS

A Dissertation Presented

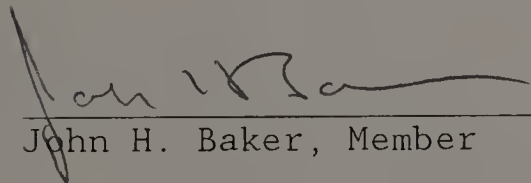
by

DAVID LLOYD LINDBO

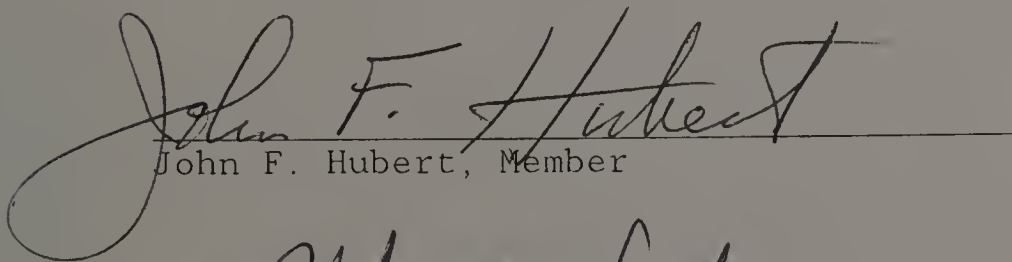
Approved as to style and content by:



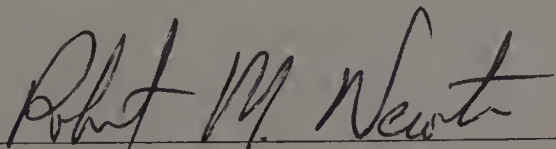
Peter L. M. Veneman, Chair of Committee



John H. Baker, Member



John F. Hubert, Member



Robert M. Newton, Member



Lyle E. Craker, Head
Dept. of Plant and Soil Sciences

For Deb Kozlowski, my wife, her support has made this work easier.

She deserves as much credit as do I, as well as my love.

For my parents, Lloyd and Patricia, and my grandfather Ralph Mead Thompson and in memory of my grandmother Gertrude Thompson, words can not repay the debt I owe you.

In memory of Dr. Nobel K. Peterson who taught me to dig a hole thus making me dirty for the rest of my life.

ACKNOWLEDGEMENTS

Thanks are due to many people who were involved directly and indirectly with this research. First I wish to thank my advisor, Dr. Peter Veneman for allowing me to develop and refine this project in such a way as to develop my self-confidence in the laboratory and in the field. Peter also deserves my gratitude for allowing me to work towards a M.S. in Geology while I was working in this program. In addition, the members of my committee--Dr. John H. Baker, Dr. John F. Hubert, and Dr. Robert M. Newton--deserve my gratitude for reading through my draft in a short period of time and adding their expert advice. Dr. Joseph H. Hartshorn assisted during the first three years of my study. Joe's knowledge of the surficial geology of New England and his willingness to listen and advise were invaluable.

Thanks are also due to Richard F. Yuretich for allowing me to use his XRD equipment, also to Dr. Richard Briggs (Smith College) for teaching me how to use and allowing me to use his SEM. James Doolittle of the SCS in Chester, PA also deserve my thanks for letting me work with him and the GPR unit at three of my sites.

Special thanks must go to Steve Bodine. Steve took his valuable time to teach me the nuances of field and lab work and to never take anything for granted. Many hours were spent bending Steve's ear and bouncing ideas off him while I formulated theories on my research.

I am also indebted to field and laboratory assistants, Judy Barton, Bill Donnelly, John Flemming, and Doug Bozeck who provided me

with much needed support and diversion. Judy deserves additional gratitude for suffering through thousands of dilutions and extractions. Additional support and contribution for which I am thankful came from my friends and colleagues in the lab, Mike Reed and Nadim Khorri. Many hours were spent discussing research with both Mike and Nadim.

The land owners--University of Massachusetts Horticultural Research Center, John Spencer of Elm Hill Farms, and Camp Marshall, The Town of Leicester, ET&L Construction, Resource Control Inc.--where my sites were located were equally as important to the completion of this project. Although I do not know who all the land owners were I wish to thank them all.

My parents, Lloyd and Patricia, gave me much of the fortitude needed to complete this task. They exhibited extreme patience over the last decade as I completed my schooling. I am truly grateful for their support.

My wife, Deb Kozlowski, assisted far more than she can imagine; without her help in the field, in editing and re-editing, and in keeping my spirits up throughout this ordeal I surely would not have been able to complete it. Deb deserves my undying love and gratitude for her unselfish actions while I struggled to complete this project. Equal credit for the completion of this research is due to her.

To all those mentioned thank you again.

ABSTRACT

NATURE AND PROPERTIES OF FRAGIPANS IN MASSACHUSETTS

MAY 1990

DAVID LLOYD LINDBO, B.S., UNIVERSITY OF NEW HAMPSHIRE

M.S., UNIVERSITY OF NEW HAMPSHIRE

M.S., UNIVERSITY OF MASSACHUSETTS

Ph.D., UNIVERSITY OF MASSACHUSETTS

Directed by: Professor Peter L. M. Veneman

A comparison of features between pans developed in the glaciated terrain of Massachusetts and those considered diagnostic to fragipans reveals numerous similarities. The overall morphology of both pan types includes high and low chroma mottles, bleached prism faces (polygons), numerous clay skins, vesicles, evidence of an eluviated horizon, and a massive to platy structure. Most pans observed have a sufficient clay accumulation to qualify as argillic horizons. indicating that illuviation is occurring. The pans also have high bulk densities and low permeabilities. The Massachusetts pans exhibit micromorphology including the presence of: argillans, ferrans, skeletans, grain argillans (clay bridges), and a sepic fabric; all are common pedogenic features and typical to fragipans.

Examination of the chemistry and mineral assemblages (both clay and heavy minerals) of the soils studied also suggests that pedogenic processes have altered the glacial till parent material. The pan is slightly more weathered, typically having lower pH and base saturation, more developed clay minerals, and stained and etched heavy

minerals than the underlying till. Two of the soils investigated have aeolian components that are easily identified based on the heavy mineral assemblages.

New England fragipans exhibit the typical brittle character and slaking in water commonly associated with all fragipans. Shear strength analysis indicates that removal of clay is primarily responsible for a decrease in strength, yet silica is also indicated as contributing to the strength of the pan.

Pebble fabric analysis indicates that the fabric of the pan is consistent with that of the late Wisconsinan Upper Till whereas fabric of the till beneath the pan suggests that it is Illinoian (early Wisconsinan) Lower Till with the exception of the sandy Ridgebury soil. This determination sets the age for the material comprising the pan to approximately 18 ka.

Evidence of pedogenic development is observed in the micromorphology, chemistry, mineralogy, and strength of the fragipans investigated. The similarities between the pans investigated and the taxonomic diagnostic indicators suggest that the pans have formed via similar processes as those developed elsewhere.

TABLE OF CONTENTS

ACKNOWLEDGEMENTS	v
ABSTRACT	vii
LIST OF TABLES	xiv
LIST OF FIGURES	xvi
Chapter	
I. INTRODUCTION	1
II. DISTRIBUTION OF FRAGIPANS	11
III. GEOLOGIC SETTING	17
Physiography	17
Generalized Bedrock and Geologic History	19
Till Deposits	22
Post-glacial	32
IV. PHYSICAL PROPERTIES	37
Previous Work	37
Macromorphology	37
Particle Size Distribution	41
Bulk Density and Moisture Relations	43
Materials and Methods	47
Site Locations and Characteristics	47
General	47
Soils	47
Tills	52
Field Description and Sampling	52
Laboratory	54
General	54
Particle Size Analysis	54
Bulk Density	55
Moisture Retention	55

Results	56
Profile Descriptions of Primary Pedons	56
Pedon 1	53
Pedon 2	63
Pedon 3	69
Pedon 4	77
Pedon 5	77
Description of Selected Till Sites	88
The Ayer Group	91
The Charlemont Group	95
Particle Size Analysis	95
Bulk Density	102
Moisture Retention	105
Discussion	105
Conclusions	115
V. MICROMORPHOLOGY	116
Previous Work	116
Materials and Methods	119
Results	121
Discussion	155
Conclusions	159
VI. CHEMICAL PROPERTIES	160
Previous Work	160
Extracting Agents	161
Materials and Methods	164
Exchange Chemistry	164
pH	164
Organic Carbon	164
Extractable Acidity	165
Cation Exchange Capacity	166
Extractable Elements	166

Results	169
Exchange Chemistry	169
pH	169
Organic Carbon	169
Extractable Acidity	174
Cation Exchange Capacity	174
Extractable Elements	174
Fe	174
Al	181
Mn	181
Si	181
Discussion	188
Exchange Chemistry	188
Extractable Elements	189
Conclusions	189
VII. CLAY MINERAL ANALYSIS	191
Previous Work	191
Clay Minerals in Fragipan Soils	191
Clay Minerals in Glacial Till and Till Derived Soils	192
Clay Mineralogical Studies in New England	193
Materials and Methods	195
Results	197
Pedon 1	197
Pedon 2	197
Pedon 3 and 4	200
Pedon 5	207
Discussion	210
Conclusions	215
VIII. HEAVY MINERALS	217
Previous Work	217
Heavy Mineral Analysis in Soils	217
Heavy Mineral Assemblages in Till	217

Materials and Methods	219
Results	220
Discussion	229
Conclusions	233
XI. STRENGTH ANALYSIS	235
Previous Work	235
Materials and Methods	239
Results	244
Extraction of Potential Bonding Agents	244
Strength Analysis	257
Discussion	260
Conclusions	266
X. FABRIC	268
Previous Work	268
Fabric of New England Tills	270
Materials and Methods	271
Results	272
Tills	272
Soil	272
Discussion	288
Conclusions	290
XI. FORMATION AND CLASSIFICATION	292
Previous Work	292
Mode of Formation	292
General	292
Inherited Properties	293
Relict or Buried Soil	295
Periglacial or Premafrost	295
Pedogenic Formation	296
Self Weight Collapse and Dessication	298
Mode of Formation in Glacial Till	300
Mode of Formation of the Fragipans Investigated	302
Classification	310
Classification of Soils in this Study	311
Conclusions	313
XII. CONCLUSIONS	315

APPENDICES	321
A. SITE LOCATIONS	321
B. PROFILE DESCRIPTIONS	331
C. PHYSICAL DATA	378
D. COMPUTER PROGRAMS	422
E. MICROMORPHOLOGY	426
F. RIDGEBURY VARIATION	437
Introduction	438
Materials and Methods	439
Results and Discussion	440
Macromorphology	440
Micromorphology	446
Conclusions	452
G. GRINDING ANALYSIS	457
H. CHEMICAL DATA	498
I. EXTRACTION GRAPHS	507
Extractable Fe Graphs	508
Extractable Al Graphs	514
Extractable Mn Graphs	520
Extractable Si Graphs	526
J. CLAY MINERAL ANALYSIS	545
Pedon 1	546
Pedon 2	554
Pedon 3	562
Pedon 4	570
Pedon 5	578
K. HEAVY MINERAL ANALYSIS	586
L. COLUMN DATA	590
M. GROUND PENETRATING RADAR	599
Introduction	600
Objectives	600
Materials and Methods	601
Results	605
North Slope	605
West Slope	609
Conclusions	614
BIBLIOGRAPHY	615

LIST OF TABLES

1.	Characteristics common to fragipans (adapted from Soil Survey Staff, 1975).	3
2.	Types of fragipans (adapted from Calhoun, 1980).	6
3.	Worldwide extent of fragipans (adapted from Witty and Knox, 1989).	12
4.	Extent of fragipans in the United States (adapted from Witty and Knox, 1989).	13
5.	Distribution of fragipan and dense till soils in the Northeast region of the United States (after Lindbo and Veneman, 1989).	14
6.	Characteristics of Upper and Lower Till (adapted from Lindbo, 1990).	28
7.	Summary of the characteristics of Upper and Lower Till (after Reed, 1989).	30
8.	Site designations.	49
9.	Parent materials and local bedrock of the primary pedons.	50
10.	Selected morphological features of Pedon 1.	57
11.	Selected morphological features of Pedon 2.	64
12.	Selected morphological features of Pedon 3.	72
13.	Selected morphological features of Pedon 4.	78
14.	Selected morphological features of Pedon 5.	84
15.	Selected morphological features of the Ayer till site. ..	92
16.	Selected morphological features of the Charlemont till site.	95
17.	Field clues used to identify fragipans (adapted from Soil Survey Staff, 1975).	108
18.	Comparison of observed fragipans and tills to field clues.	109

19.	Modal distribution (%) of selected micromorphological features.	122
20.	Micromorphological observations for each Pedon.	147
21.	Summary of extraction procedures used to determine Fe, Al, Mn, and Si.	167
22.	Percent Fe extracted by various procedures.	179
23.	Percent Al extracted by various procedures.	182
24.	Percent Mn extracted by various procedures.	184
25.	Percent Si extracted by various procedures.	186
26.	Procedure to characterize clay mineralogy in selected fragipans and tills in Massachusetts.	196
27.	Statistical analysis of selected heavy minerals.	229
28.	Strength correlation analysis of strength to individual extractable material for all samples.	257
29.	Results of pebble fabric analysis of various horizons in each Pedon.	277
30.	Classification of each Pedon.	312
31.	Selected morphological features of the Ridgebury Pedons. .	444
32.	Micromorphological features of the Ridgebury Pedons.	447

LIST OF FIGURES

1.	Glacial maximum in the Northeast during the late Wisconsinan (after Cunningham and Ciolkosz, 1984).	5
2.	Physiography of Massachusetts (after Denny, 1982).	18
3.	Lithotectonic zones in Massachusetts (after Zen, 1983).	20
4.	Correlation diagram of till nomenclature in New England.	29
5.	Generalized factors affecting soil development in Massachusetts.	36
6.	Textures of fragipan horizons based on soil survey data from throughout the USA. The following three generalized zones can be recognized: 1 = coarse loamy, 2 = loamy, 3 = fine silty (after Lindbo and Veneman, 1989; Soil Survey Staff, 1968; 1974; and 1979).	42
7.	Plot of the soil separates for each horizon by depth for the (A) Grenada series (Soil Survey Staff, 1979); (B) Mardin series (Soil Survey Staff, 1974; and (C) Paxton series (Soil Survey Staff, 1968) (after Lindbo and Veneman, 1989).	44
8.	Site locations.	48
9.	Cross-sectional diagram of Pedon 1.	59
10.	Photograph of Pedon 1.	60
11.	Bleached prism face (BPF) in 2Btx1 of Pedon 1. (A) photograph, (B) schematic. The bar is 5 cm.	61
12.	Contact between 2Btx2 and 3BCm horizons in Pedon 1. (A) photograph, (B) schematic. The knife handle is 8 cm long.	62
13.	Cross-sectional diagram of Pedon 2.	66
14.	Photograph of Pedon 2.	67
15.	Bleached prism face (BPF) containing roots (R) in the 2Btx1 of Pedon 2. Note that in the bottom right of the photograph the roots is sticking out of the profile face. (A) photograph, (B) schematic. The white bar is 10 cm long.	68

16.	Stone line (SL) in the 3Cd1 horizon of Pedon 2. Note the bleached prism face (BPF) terminates above the SL in the 2BCd horizon. Some coarse fragment positions are denoted based on casts (indentations) that they made when the pit was first opened and the face cleaned. (A) photograph, (B) schematic. The bar is 30 cm.	70
17.	Sand lens (SL) in the 3Cd2 horizon (S) of Pedon 2. Note the laminations in the sand and the coarse fragment resting above the SL. (A) photograph, (B) schematic. The top of the knife handle is 2 cm across.	71
18.	Cross-sectional diagram of Pedon 3.	74
19.	Photograph of Pedon 3.	75
20.	Areas of vesicular pores (V) in the BE of Pedon 3. Note how the areas are irregular and noncontinuous. Also coarse fragments (R) occur in both zones. (A) photograph, (B) schematic. The knife handle is 6 cm long.	76
21.	Cross-sectional diagram of Pedon 4.	80
22.	Photograph of Pedon 4.	81
23.	Termination of bleached prism face (BPF) at the top of the 2BCd horizon in Pedon 4. R denotes coarse fragments. (A) photograph, (B) schematic. The bar is 5 cm.	82
24.	Gray or bleached area around coarse fragment in 2Btx2 horizon of Pedon 4. The zone is approximately 1 cm thick and appears lighter in the photograph. (A) photograph, (B) schematic. The knife handle is 2 cm thick.	83
25.	Cross-sectional diagram of Pedon 5.	86
26.	Photograph of Pedon 5.	87
27.	Firm lenses (F) surrounded by loose, sandier material in the 2EB horizon of Pedon 5. (A) photograph, (B) schematic. The bar is 5 cm.	89

28.	Bleached prism face (BPF) in the 2Btx2 horizon of Pedon 5. Note the fine dark streak of roots and organic material running down the center of the BPF. (A) photograph, (B) schematic. The bar is 5 cm.	90
29.	Unoxidized Lower Till, Ayer. LT - Unoxidized Lower Till, T - Talus, Sand - Sand layer. Note that the sand layer appears darker due to water flowing from it. (A) photograph, (B) schematic.	93
30.	Silt/clay beds (B) and faults (F) in the Lower Till, Ayer. (A) photograph, (B) schematic.	94
31.	Soil separates (%) for each horizon by depth for Pedon 1.	97
32.	Soil separates (%) for each horizon by depth for Pedon 2.	98
33.	Soil separates (%) for each horizon by depth for Pedon 3.	99
34.	Soil separates (%) for each horizon by depth for Pedon 4.	100
35.	Soil separates (%) for each horizon by depth for Pedon 5.	101
36.	Clay fraction (%) for each horizon by depth for Pedons 1-5.	103
37.	Bulk density (Mg M^{-3}) for each horizon by depth for Pedons 1-5.	104
38.	Moisture characteristic curves for each horizon of Pedon 3.	106
39.	Moisture characteristic curves for each horizon of Pedon 5.	107
40.	Plan view of the polygonal arrangement of bleached prism faces in the Bx1 of the Ridgebury profile in Spencer, MA. (A) photograph, (B) schematic. The bar is 5 cm.	111

41.	Bleached prism face from the fragipan in a Tillsit soil (Typic Fragiudult) in WV. Note the roots and organic material running down the center of the BPF as seen in Figure 28. (A) photograph, (B) schematic. The knife handle is 6 cm long.	112
42.	Schematic of the apparatus used to impregnate thin sections under vacuum.	120
43.	Photomicrograph from the Ap horizon of Pedon 4. The matrix is dark due to organic material coating the particles. V = void, S = skeleton grain, R = root, M = matrix. (A) photograph, (B) schematic. The bar is 1 mm long.	124
44.	Photomicrograph from the Bw1 horizon of Pedon 4. Less organic material coats the particles in this figure as compared to Figure 43. V = void, S = skeleton grain, R = root. (A) photograph, (B) schematic. The bar is 1 mm long.	126
45.	Photomicrograph from the Bw horizon of Pedon 5. V = void, S = skeleton grain, N = mottle or nodule. (A) photograph, (B) schematic. The bar is 1 mm long.	127
46.	Photomicrograph from the BE horizon of Pedon 4. Argillan in channels and ped faces are discontinuous and broken, some voids do not contain any argillans. V = void, S = skeleton grain, A = argillan. (A) photograph, (B) schematic. The bar is 1 mm long.	128
47.	Photomicrograph from the 2Btx1 horizon of Pedon 3. Vughs and vesicles lined with oriented clay. V = void, S = skeleton grain, A = argillan. (A) photograph, (B) schematic. The bar is 1 mm long.	129
48.	Photomicrograph from the 2Btx1 horizon of Pedon 4. Argillans are continuous and present on ped faces and in channels. V = void, S = skeleton grain, A = argillan. (A) photograph, (B) schematic. The bar is 1 mm long.	130

49. Photomicrograph from the 2Btx1 horizon of Pedon
 2. Channel argillans forming vesicles and
 nearly clogging the entire channel. V = void,
 S = skeleton grain, A = argillan, F = ferran.
 (A) photograph, (B) schematic. The bar is 1 mm
 long. 131
50. Photomicrograph from the 2Btx1 horizon of Pedon
 5. Channel or ped-argillans forming bridges
 between skeleton grains and the S-matrix. V =
 void, S = skeleton grain, A = argillan, B =
 bridge, AL = alban. (A) photograph, (B)
 schematic. The bar is 1 mm long. 132
51. Photomicrograph from the 2Btx2 horizon of Pedon
 5. Channel-argillan forming a bridge between
 skeleton grains. V = void, S = skeleton grain,
 A = argillan, B = bridge. (A) photograph, (B)
 schematic. The bar is 0.25 mm long. 133
52. Photomicrograph from the 2Btx2 horizon of Pedon
 2. Argillan forming a bridge between skeleton
 grains and matrix. V = void, S = skeleton
 grain, A = argillan, B = bridge. (A)
 photograph, (B) schematic. The bar is 0.25 mm
 long. 134
53. Photomicrograph from the bleached prism face
 (BPF) edge in the 2Btx1 horizon of Pedon 3.
 Note the abrupt change from the Fe rich outer
 edge to the Fe poor BPF interior. V = void, S
 = skeleton grain, A = argillan, F = ferran.
 (A) photograph, (B) schematic. The bar is 1 mm
 long. 135
54. Photomicrograph from the bleached prism face
 (BPF) edge in the 2Btx2 horizon of Pedon 1.
 The boundary is demarcated by thick ferrans and
 argillans as well as a small zone of albic
 material. V = void, S = skeleton grain, A =
 argillan, F = ferran, AL = alban. (A)
 photograph, (B) schematic. The bar is 1 mm
 long. 136

55. Photomicrograph from the bleached prism face interior of the 2Btx2 horizon of Pedon 5. There is a small amount of Fe-staining around Fe-rich hornblende (H) and garnet (G) grains, but the remainder of the matrix is devoid of Fe-stains. V = void, skeleton grains are demarcated but not labeled, F = ferran. (A) photograph, (B) schematic. The bar is 1 mm long. 137
56. Photomicrograph from the 2BCd horizon of Pedon 2. The Fe-rich outer edge and Fe-poor interior of a type 2 mottle are illustrated here. S = skeleton grain, F = ferran, AL = alban. (A) photograph, (B) schematic. The bar is 1 mm long. 138
57. Photomicrograph from the 3Cd2 horizon of Pedon 3. Mangans demarcate plate edges. V = void, S = skeleton grain, MN = mangan. (A) photograph, (B) schematic. The bar is 1 mm long. 140
58. Photomicrograph (cross polarized light) of Upper Till. Note that despite the large percentage of skeleton grain they still appear to be matrix supported. The bar is 1 mm long. 141
59. Photomicrograph (cross polarized light) of unoxidized Lower Till. Note that the skeleton grains are matrix supported. The bar is 1 mm long. 142
60. Photomicrograph (cross polarized light) of oriented silt beds in unoxidized Lower Till. F = fine grained silt, C = coarse grained silt. (A) photograph, (B) schematic. The bar is 1 mm long. 143
61. Photomicrograph (cross polarized light) of oriented clay beds in unoxidized Lower Till. S = skeleton grain, T = till, C = clay bed. (A) photograph, (B) schematic. The bar is 1 mm long. 144
62. Photomicrograph of (A) the 2Btx1 horizon of Pedon 1, and (B) the 3Cd2 horizon of Pedon 2. The light areas are skeleton grains, total void space is low. The bar is 1 mm long. 145

63.	Photomicrograph of (A) the 2Btx2 horizon, and (B) the bleached prism face in the 2Btx2 horizon of Pedon 2. Note the dark matrix around the grains in the 2Btx2 horizon and the light matrix in the BPF caused by differences in the amount and nature of the grain cutans and amorphous coatings in each area. The bar is 1 mm long.	150
64.	Scanning electron micrograph of a clay bridge in the 2Btx1 horizon of Pedon 2. The bar is 100 um long.	151
65.	Scanning electron micrograph of a clay bridge in the 2Btx1 horizon of Pedon 2 (enlargement of Figure 64). Note the curved nature of the bridge and the oriented individual particles. The bar is 10 um long.	152
66.	Scanning electron micrograph of a clay bridge in the 2Btx2 horizon of Pedon 5. The bar is 100 um long.	153
67.	Scanning electron micrograph of the 3Cd2 horizon of Pedon 3. Note the massive nature of the material. The bar is 100 um long.	154
68.	Scanning electron micrograph of bleached prism material in the 2Btx2 horizon of Pedon 5. The grains appear to be uncoated. The bar is 100 um long.	156
69.	Photomicrograph (cross polarized light) from the 2Btx2 horizon of Pedon 5. Note that the argillans form geopetal structures in voids. V = void, S = skeleton grain, A = argillan. (A) photograph, (B) schematic. The bar is 1 mm long.	157
70.	pH _w for each horizon by depth in Pedons 1-5.	170
71.	pH _K for each horizon by depth in Pedons 1-5.	171
72.	pH _C for each horizon by depth in Pedons 1-5.	172
73.	Organic carbon (%) for each horizon by depth in Pedons 1-5.	173
74.	Extractable acidity (cmol 100 g ⁻¹) for each horizon by depth in Pedons 1-5.	175

75.	Sum of exchangeable bases (cmol 100 g ⁻¹) for each horizon by depth in Pedons 1-5.	176
76.	Cation exchange capacity (cmol 100 g ⁻¹) for each horizon by depth in Pedons 1-5.	177
77.	Percent base saturation for each horizon by depth in Pedons 1-5.	178
78.	X-ray diffractograms by horizon of the Na-saturated <2µm fraction of Pedon 1. 2.4 nm = mixed-layer supper lattice, 1.4 nm = chlorite and/or vermiculite, 1.21 nm = mixed-layer illite- vermiculite or illite-chloritized vermiculite, 1.0 nm = illite, .846 nm = mixed-layer d003, .715 nm = kaolinite and/or chlorite d002, .501 nm = illite d002, .485 nm = gibbsite, .426 nm = quartz, .358 nm = kaolinite d002 and/or chlorite d004, and .334 nm = illite d003 and quartz.	198
79.	X-ray diffractograms by horizon of the Na-saturated <2µm fraction of Pedon 2. 2.4 nm = mixed-layer supper lattice, 1.4 nm = chlorite and/or vermiculite, 1.21 nm = mixed-layer illite- vermiculite or illite-chloritized vermiculite, 1.0 nm = illite, .846 nm = mixed-layer d003, .715 nm = kaolinite and/or chlorite d002, .501 nm = illite d002, .485 nm = gibbsite, .426 nm = quartz, .358 nm = kaolinite d002 and/or chlorite d004, and .334 nm = illite d003 and quartz.	201
80.	X-ray diffractograms by horizon of the Na-saturated <2µm fraction of Pedon 3. 2.4 nm = mixed-layer supper lattice, 1.4 nm = chlorite and/or vermiculite, 1.21 nm = mixed-layer illite- vermiculite or illite-chloritized vermiculite, 1.0 nm = illite, .846 nm = mixed-layer d003, .715 nm = kaolinite and/or chlorite d002, .501 nm = illite d002, .485 nm = gibbsite, .426 nm = quartz, .358 nm = kaolinite d002 and/or chlorite d004, and .334 nm = illite d003 and quartz.	203

81.	X-ray diffractograms by horizon of the Na-saturated <2um fraction of Pedon 4. 2.4 nm = mixed-layer supper lattice, 1.4 nm = chlorite and/or vermiculite, 1.21 nm = mixed-layer illite-vermiculite or illite-chloritized vermiculite, 1.0 nm = illite, .846 nm = mixed-layer d003, .715 nm = kaolinite and/or chlorite d002, .501 nm = illite d002, .485 nm = gibbsite, .426 nm = quartz, .358 nm = kaolinite d002 and/or chlorite d004, and .334 nm = illite d003 and quartz.	205
82.	X-ray diffractograms by horizon of the Na-saturated <2um fraction of Pedon 5. 2.4 nm = mixed-layer supper lattice, 1.4 nm = chlorite and/or vermiculite, 1.21 nm = mixed-layer illite-vermiculite or illite-chloritized vermiculite, 1.0 nm = illite, .846 nm = mixed-layer d003, .715 nm = kaolinite and/or chlorite d002, .501 nm = illite d002, .485 nm = gibbsite, .426 nm = quartz, .358 nm = kaolinite d002 and/or chlorite d004, and .334 nm = illite d003 and quartz.	208
83.	X-ray diffractograms of the Na-saturated <2u fraction of typical Upper Till, Oxidized Lower Till, and Unoxidized Lower Till. 2.4 nm = mixed-layer supper lattice, 1.4 nm = chlorite and/or vermiculite, 1.21 nm = mixed-layer illite-vermiculite or illite-chloritized vermiculite, 1.0 nm = illite, .846 nm = mixed-layer d003, .715 nm = kaolinite and/or chlorite d002, .501 nm = illite d002, .485 nm = gibbsite, .426 nm = quartz, .358 nm = kaolinite d002 and/or chlorite d004, and .334 nm = illite d003 and quartz.	212
84.	Percent of selected heavy minerals by depth in Pedon 1.	221
85.	Percent of selected heavy minerals by depth in Pedon 2.	222
86.	Percent of selected heavy minerals by depth in Pedon 3.	223
87.	Percent of selected heavy minerals by depth in Pedon 4.	224
88.	Percent of selected heavy minerals by depth in Pedon 5.	225

89.	Garnet grain from the Ap horizon of Pedon 1. Note pitted, jagged and stained surfaces. The bar is 0.05 mm long.	226
90.	Garnet grain from the 2Btxl horizon of Pedon 1. Note pitted, jagged surfaces. The bar is 0.05 mm long.	227
91.	Hornblende grain from the (A) 2Btxl horizon, and (B) 2Cd2 horizon of Pedon 5. Note jagged and stained surfaces on the grain from the fragipan horizon. The bar is 0.05 mm long.	228
92.	Garnet grain from the 3Cd3 horizon of Pedon 2. Note one surface is pitted and jagged, whereas the others are not. The bar is 0.05 mm long.	230
93.	Schematic of the soil coring apparatus used to extract cores for leaching and strength analysis. The inner diameter of the tube is 5 cm.	240
94.	Schematic of the apparatus used for the removal of bonding agents from soil columns. These are arranged in sets of 4 for one treatment.	242
95.	Average amount (mg kg^{-1}) of Fe extracted by each treatment for each site. BTR = Belchertown Ridgebury 2Btxl horizon, BTR/S = Belchertown Ridgebury/Scituate 2Btxl horizon, EHP = Elm Hill Paxton (Pedon 1) 2Btxl horizon, OHW = Orchard Hill Woodbridge (Pedon 4) 2Btxl horizon, OHD = Orchard Hill (Pedon 4) 3Cd horizon, BHW = Buck Hill Woodbridge 2Btxl horizon, BHR = Buck Hill Ridgebury 2Btxl horizon, and BHD = Buck Hill Paxton (Pedon 2) 3Cd3 horizon.	245
96.	Average amount (mg kg^{-1}) of Al extracted by each treatment for each site. BTR = Belchertown Ridgebury 2Btxl horizon, BTR/S = Belchertown Ridgebury/Scituate 2Btxl horizon, EHP = Elm Hill Paxton (Pedon 1) 2Btxl horizon, OHW = Orchard Hill Woodbridge (Pedon 4) 2Btxl horizon, OHD = Orchard Hill (Pedon 4) 3Cd horizon, BHW = Buck Hill Woodbridge 2Btxl horizon, BHR = Buck Hill Ridgebury 2Btxl horizon, and BHD = Buck Hill Paxton (Pedon 2) 3Cd3 horizon.	247

97. Average amount (mg kg^{-1}) of Si extracted by each treatment for each site. BTR = Belchertown Ridgebury 2Btxl horizon, BTR/S = Belchertown Ridgebury/Scituate 2Btxl horizon, EHP = Elm Hill Paxton (Pedon 1) 2Btxl horizon, OHW = Orchard Hill Woodbridge (Pedon 4) 2Btxl horizon, OHD = Orchard Hill (Pedon 4) 3Cd horizon, BHW = Buck Hill Woodbridge 2Btxl horizon, BHR = Buck Hill Ridgebury 2Btxl horizon, and BHD = Buck Hill Paxton (Pedon 2) 3Cd3 horizon. 249
98. Average amount (mg kg^{-1}) of Mn extracted by each treatment for each site. BTR = Belchertown Ridgebury 2Btxl horizon, BTR/S = Belchertown Ridgebury/Scituate 2Btxl horizon, EHP = Elm Hill Paxton (Pedon 1) 2Btxl horizon, OHW = Orchard Hill Woodbridge (Pedon 4) 2Btxl horizon, OHD = Orchard Hill (Pedon 4) 3Cd horizon, BHW = Buck Hill Woodbridge 2Btxl horizon, BHR = Buck Hill Ridgebury 2Btxl horizon, and BHD = Buck Hill Paxton (Pedon 2) 3Cd3 horizon. 251
99. Average amount (g kg^{-1}) of Clay extracted by Na-pyrophosphate for each site. BTR = Belchertown Ridgebury 2Btxl horizon, BTR/S = Belchertown Ridgebury/Scituate 2Btxl horizon, EHP = Elm Hill Paxton (Pedon 1) 2Btxl horizon, OHW = Orchard Hill Woodbridge (Pedon 4) 2Btxl horizon, OHD = Orchard Hill (Pedon 4) 3Cd horizon, BHW = Buck Hill Woodbridge 2Btxl horizon, BHR = Buck Hill Ridgebury 2Btxl horizon, and BHD = Buck Hill Paxton (Pedon 2) 3Cd3 horizon. 253
100. X-ray diffractograms by horizon of the Na-saturated $<2\mu\text{m}$ fraction of clay removed by Na-pyrophosphate from the EHP samples (other diffractograms are in Appendix L). 2.4 nm = mixed-layer supper lattice, 1.4 nm = chlorite and/or vermiculite, 1.21 nm = mixed-layer illite-vermiculite or illite-chloritized vermiculite, 1.0 nm = illite, .846 nm = mixed-layer d003, .715 nm = kaolinite and/or chlorite d002, .501 nm = illite d002, .485 nm = gibbsite, .426 nm = quartz, .358 nm = kaolinite d002 and/or chlorite d004, and .334 nm = illite d003 and quartz. 255

101.	Average unconfined-unconsolidated shear strength of each treatment for each site. BTR = Belchertown Ridgebury 2Btxl horizon, BTR/S = Belchertown Ridgebury/Scituate 2Btxl horizon, EHP = Elm Hill Paxton (Pedon 1) 2Btxl horizon, OHW = Orchard Hill Woodbridge (Pedon 4) 2Btxl horizon, OHD = Orchard Hill (Pedon 4) 3Cd horizon, BHW = Buck Hill Woodbridge 2Btxl horizon, BHR = Buck Hill Ridgebury 2Btxl horizon, and BHD = Buck Hill Paxton (Pedon 2) 3Cd3 horizon.	258
102.	Scanning electron micrograph of the matrix from the CaCl_2 (control) treated column. Note the amount of fine-grained material and bridge. The bar is 100 μm long.	261
103.	Scanning electron micrograph of the matrix from the ammonium-oxalate treated column. Note clay bridge and fine-grained material. The bar is 100 μm long.	262
104.	Scanning electron micrograph of the matrix from the Na-pyrophosphate treated column. Note the small bridges and decreased amount of fine-grained material. The bar is 100 μm long.	263
105.	Scanning electron micrograph of the matrix from the NaOH treated column. Note lack of fine-grained material. The bar is 100 μm long.	264
106.	Overall fabric for the Lower Till plotted in 10^0 increments on an equal area rose diagram. Average trend of 600 pebbles is 335^0	273
107.	Overall fabric for the Upper Till plotted in 10^0 increments on an equal area rose diagram. Average trend of 225 pebbles is 17.6^0 . Note the spread of the data indicating a bimodal distribution.	274
108.	Fabric plotted in 10^0 increments on an equal area rose diagram for A) Unoxidized facies of the Lower Till (300 pebbles), and B) Oxidized facies of the Lower Till (300 pebbles).	275
109.	Fabric plotted on a contoured stereonet for Pedon 1. S1 is the primary (strength) eigenvalue (if greater than .8, a strong fabric exists), V1 is the primary trend, and n = number of observations. .	278

110.	Fabric plotted on contoured stereonet for Pedon 2. S1 is the primary (strength) eigenvalue (if greater than .8, a strong fabric exists), V1 is the primary trend, and n = number of observations.	280
111.	Fabric plotted on contoured stereonet for Pedon 3. S1 is the primary (strength) eigenvalue (if greater than .8, a strong fabric exists), V1 is the primary trend, and n = number of observations.	282
112.	Fabric plotted on contoured stereonet for Pedon 4. S1 is the primary (strength) eigenvalue (if greater than .8, a strong fabric exists), V1 is the primary trend, and n = number of observations.	284
113.	Fabric plotted on a contoured stereonet for Pedon 5. S1 is the primary (strength) eigenvalue (if greater than .8, a strong fabric exists), V1 is the primary trend, and n = number of observations.	286
114.	Schematic illustrating the possible mode of formation of the fragipans investigated in the present study.	308
115.	Photograph of the BTR Pedon, Spencer, MA.	441
116.	Photograph of the OHL Pedon profile, Amherst, MA.	442
117.	Cross-sectional digram of the OHL Pedon.	443
118.	Photomicrograph of A horizon, OHL Pedon. N = nodule, S = skeleton grain, V = void. (A) photograph, (B) schematic. The bar is 1 mm long.	450
119.	Photomicrograph of Bx2 horizon, BTR Pedon. A = argilan, S = skeleton grain, V = void. (A) photograph, (B) schematic. The bar is 1 mm long.	451
120.	Photomicrograph of Bg1 horizon, OHL Pedon. A = argillan, AL = alban, Q = quassiferran, V = void. (A) photograph, (B) schematic. The bar is 1 mm long.	453
121.	Photomicrograph of 2BCm horizon, OHL Pedon. F = ferran, M = mangan, V = void. (A) photograph, (B) schematic. The bar is 1 mm long.	454
122.	Photomicrograph of 3Cd3 horizon, OHL Pedon. F = ferran, M = mangan, V = void. (A) photograph, (B) schematic. The bar is 1 mm long.	455

123.	Cross section of transects (A) 1N and (B) 2N illustrating relationship of pan to the surface. ...	602
124.	Subsurface topography of the north slope area.	604
125.	Cross section of transects (A) 1W, (B) 2W, and (C) 3W illustrating the relationship of the pan to the surface.	606
126.	Three dimensional plot of (A) surface and (B) subsurface of the west slope area.	610
127.	Surface (A) and subsurface (B) topography of the west slope area.	613

CHAPTER I

INTRODUCTION

The history of fragipan research in the northeastern United States extends over the last 40 years (Lindbo and Veneman, 1989). The term 'fragipan' was developed by Winters in the 1940's to refer to dense layers in loess and colluvial deposits in Kentucky and Tennessee (Winters, 1942; Winters and Simonson, 1951). The volume of research papers has grown substantially since that time. When Winters and Simonson's 1951 review paper was published it covered covered fragipans in a scant three pages, whereas the Soil Science Society of America's recent volume devoted to fragipans included 153 pages (Smeck and Ciolkosz, 1989).

The word fragipan is derived from the Latin fragilis meaning brittle. The scientific basis of several of the criteria defining the fragipan horizon in Soil Taxonomy (Soil Survey Staff, 1975, Witty and Knox, 1989) was developed in the Northeastern region, principally by Cline and his students at Cornell University in New York (Carlisle et al., 1957; Grossman et al., 1957; Knox, 1957; Jha and Cline, 1963). Soil Taxonomy (Soil Survey Staff, 1975) states that a fragipan is:

"A loamy or uncommonly a sandy subsurface horizon that may but does not necessarily underlie a cambic, spodic, argillic, or albic horizon. It has a very low content of organic matter, has a high bulk density relative to the horizons above it, and is seemingly cemented when dry, having then hard or very hard

consistence. When moist a fragipan has moderate to weak brittleness, which is the tendency for a ped or clod to rupture suddenly when pressure is applied rather than to undergo slow deformation. A dry fragment slakes or fractures when placed in water."

This definition, while encompassing many properties of a fragipan, is ambiguous as to the key identifying properties leading to contention in classification (Witty and Knox, 1989). One of the most common errors made is categorizing all soils developed on till as having fragipans (Krohelski, 1976). Another common misclassification occurs if the horizon in question is at or near saturation at the time of sampling, when the pan may not exhibit the characteristic brittle behavior and thus not be classified as a fragipan. Since fragipans restrict water movement, significantly affect pedogenesis, and have a major impact on land use it is important to identify them as we recognize other restricting layers such as duripans, caliche, and plinthite.

About one half of the soils in Massachusetts are underlain by a dense hard pan. This pan varies in thickness and occurs at a depth of up to about 1.5 m (Veneman and Bodine, 1982; and Pickering, 1983). In the past, this layer has been defined as a fragipan, but recently a controversy has arisen as to the true nature of this horizon (Calhoun, 1980). This controversy revolves around the degree of pedogenesis that has occurred in these pans. They are commonly developed in dense till deposited during the Wisconsinian and possibly Illinoian

glaciation, thus initially having a high density as well as a massive structure. Other properties of the pan do not appear to be inherited. These include strength, brittle behavior, pore distribution, and the expression of polygons. These properties are all characteristic of fragipans (Table 1).

Table 1. Characteristics common to fragipans (adapted from Soil Survey Staff, 1975).

-
1. Loamy to sandy (uncommon) texture (<35% clay).
 2. May underlie a cambic, spodic, argillic, or albic horizon.
 3. Low to very low organic matter content.
 4. High bulk density relative to overlying horizons.
 5. Seemingly cemented when dry-having then a hard or very hard consistence.
 6. Moderate to weak brittleness when moist.
 7. Slake when placed in water.
 8. Usually mottled and slowly permeable.
 9. Contain faces of bleached material that form a polygonal pattern in plan view.
 10. Clear upper boundary 30 to 100 cm from soil surface and 15 to 200 cm thick.
 11. Roots occur almost exclusively along bleached prism faces (BPF).
 12. Clay skins occur in BPF and in matrix.
 13. Some may have a secondary lenticular or platy structure.
-

The glaciated northern part of the Northeast region has soils developed in glacial deposits such as till, while soils in the unglaciated southern section generally have developed in residual, colluvial, and alluvial parent materials (Figure 1). Consequently, most of the pans in the north have formed in glacial till, whereas those observed south of the glacial limit are found in alluvial or colluvial parent materials (Lindbo and Veneman, 1989). Not all dense horizons observed in glacial till are considered fragipans. The U.S.D.A.-Soil Conservation Service presently does not recognize fragipans in the till soils of New England or northern New York (Calhoun, 1980). In these soils, properties which are normally associated with fragipans, such as high bulk density and brittle behavior in particular, are presumed to have been inherited from the parent material. Calhoun (1980) described three types of dense layers found in the northeast concluding that true genetic fragipans are rare in the glaciated areas (Table 2). Undoubtedly, some characteristics of pans formed in till are geogenic, however it has been shown that, once deposited, tills are altered by post-depositional soil-forming processes (Boulton and Dent, 1974; Boulton and Paul, 1976; DeKimpe et al., 1976; St. Arnaud, 1976; Newton, 1978; Lindbo, 1990).

The presence of fragipans (either geogenic or pedogenic) has a significant impact on land use because of its associated physical properties, such as compactness, low porosity and low hydraulic conductivity. Pans may cause periodic high water tables, higher excavation costs for building construction and the installation of

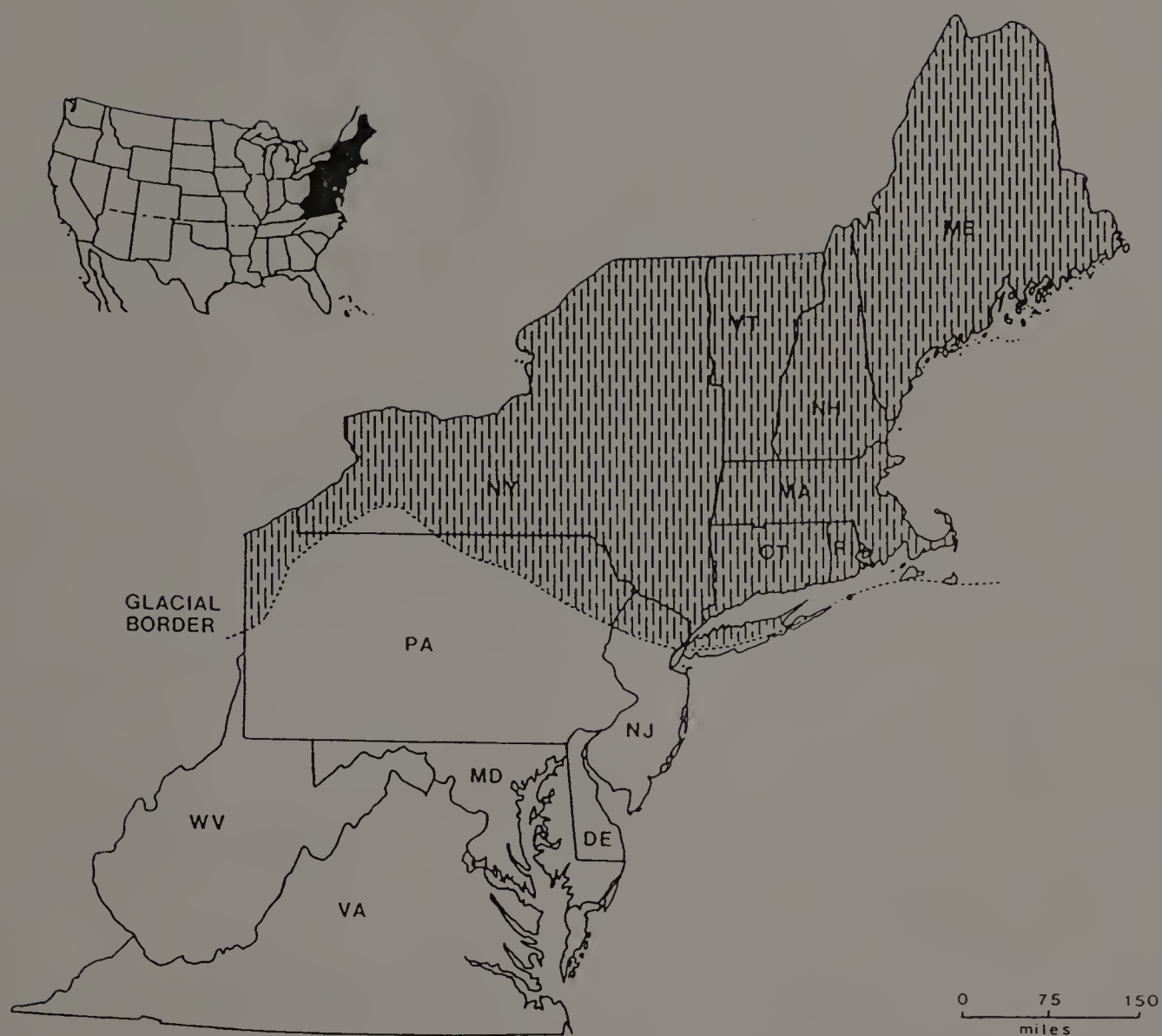


Figure 1. Glacial maximum in the Northeast during the late Wisconsinan (after Cunningham and Ciolkosz, 1984).

subsoil utilities, and a lower suitability for on-site sewage disposal than similar soils without a pan. Recognition of the presence of these dense soil layers, therefore, is important in the land use planning process.

Table 2. Types of fragipans (adapted from Calhoun, 1980).

-
1. Soils with true genetic fragipans.
 2. Soils forming in essentially unaltered, dense basal till.
 3. Soils forming in dense basal tills that have been altered pedogenically.
-

The genesis of fragipans is a critical aspect to understanding its nature. Three ideas have developed over the years to explain how a fragipan forms. Some feel the properties are inherited, while others do not, and a third group feel some properties are inherited but the brittle nature is pedogenic (Smalley and Davin, 1982).

If any material is acting as a bonding agent of the fragipan then it appears obvious that some illuviation and/or reorganization of material has occurred. Despite evidence for this, some feel that the bulk if not all of the properties of the fragipan are inherited from the parent material. If this is the case then by definition these would not be classified as fragipans. Van Vliet and Langohr (1981), Langohr (1987), Fitzpatrick (1980; and personal communication, 1988) feel that the morphology and properties of the pan are best

explained by permafrost and ice segregation, which can cause a platy, lenticular dense structure to a much greater degree than pedogenesis will. Essentially they agree with Fitzpatrick (1956), Nikiforoff (1955), and Nikiforoff et al. (1948), and in part with Lyford et al. (1963). Lyford et al. (1963) stated that there was a relation between ground water and the observed platiness. Since permafrost is also related to the ground water level it stands to reason that the fragipan can be related at least in part to the permafrost level and water table (Lozet and Herbillon, 1971; van Vliet and Langohr, 1981; Langohr, 1987). Another argument for the inheritance of properties is that fragipans are found on older surfaces, particularly in the south (Daniels et al., 1966; Hundall and Williams, 1989). This suggests that pans are relict features and their properties inherited. The feeling that some of the properties of a fragipan are inherited is not without merit yet all features cannot be explained in this way.

Wetting and drying has been proposed as the principal agent in fragipan development. This process is used to account for the translocation of material and the subsequent increase in density and brittleness observed (Yassoglou and Whiteside, 1960; Jha and Cline, 1963; Daniels et al., 1966; Nettleton et al., 1968b; Bryant, 1989). The rearrangement of particles under these conditions could indeed alter the character of the pan, yet wetting and drying may not occur to a great extent in all soils with fragipans. It should be mentioned that the simple illuviation of material as evidenced by numerous accounts of clay skins and vesicles will also account for the observed

brittle character of pans (DeKimpe et al., 1972; 1976; Wang et al., 1974; Lindbo and Veneman, 1989). Further evidence that the fragic properties are not entirely inherited is the crossing of stratigraphic units by fragipans (Franzmeier et al., 1978) and a tendency to follow the topography despite different stratigraphies of its parent material (loess) (Norton and Franzmeier, 1978).

It has been suggested that some aspects of the fragipan are inherited while others have developed in place (Smalley and Davin, 1982; Smeck and Ciolkosz, 1989). In dealing with dense basal till it would appear that the density of the material was indeed inherited, yet the brittle character is not (Jha and Cline, 1963; Miller et al., 1971a; 1971b). Hutchenson and Bailey (1964) have further shown by using $\text{Ca}/(\text{Mg} + \text{Na})$ ratios that there has been severe weathering in the pan, a further indication that at least some properties are not inherited from the parent material. Finally, Bilzi and Ciolkosz (1977) indicated that expression of fragipan morphology increases with time.

The decision to stop recognizing fragipans in New England seems to be based on the premise that pedogenesis has not had a significant effect on the morphology of the soil developed on basal till, thereby discounting the distinct effect the hardpan has on the overlying horizons. The decreased permeability results in soils on a slope being less well-drained than if the same location was not underlain by a pan. Thus, there are implications for classification as well as land use. The blanket approach taken by the SCS in this matter may result in misinterpretation of the soil in question. A clearer understanding

and a complete evaluation of the degree of genesis occurring in these basal till soils is necessary.

The present project evaluates the degree of pedogenesis in the dense New England tills. If several of the soil properties present are due to soil formation, one can conclude that the pan qualifies as a fragipan. One aspect of this research examines various bonding agents and how their removal from the fragipan affects its strength. The major agents believed to be important to the strength of the Massachusetts fragipans are; amorphous iron (Fe), amorphous aluminum (Al), and amorphous silica (Si). Weakly crystalline clay as well as weakly crystalline Fe, Al, and Si may also aid in the character of the pan. If a bonding agent can be correlated to pan strength and a change in the microstructure of the pan, then it is safe to assume some illuviation has occurred and has contributed to the character of the pan. If this is the case then these hard pans would qualify as fragipans as their properties are not totally inherited.

The general objectives of the research are: (i) to characterize physically and chemically a number of Massachusetts pans developed on dense basal till; (ii) investigate the macro- and micromorphology of the pans in relation to pedogenesis; (iii) relate the strength of the pans to particular bonding agents; (iv) evaluate the observed character of the pans in regards to their classification according to Soil Taxonomy and to recent suggestions to redefine fragipans (Calhoun, 1980; Witty and Knox, 1989); and (v) outline a potential mode of formation for Massachusetts pans.

The next chapter (Chapter 2) discusses the occurrence of fragipans from a worldwide to local perspective. This is followed by an overview of the geologic setting of Massachusetts with an emphasis on the glacial and post-glacial record (Chapter 3). The following chapters (Chapters 4-10) are arranged to discuss individual properties or groups of properties observed in the fragipan soils investigated. While each of these chapters may stand alone, they are synthesized in the final chapters into a hypothesis describing the mode of formation and classification of fragipans for this region.

CHAPTER II

DISTRIBUTION OF FRAGIPANS

Fragipans have been identified in many areas throughout the world, most commonly occurring in the mid-latitudes within udic and aquic moisture regimes (Witty and Knox, 1989). The majority of documented fragipans are found in the United States and New Zealand (Table 3). Small scale maps of other countries do not fully differentiate non-fragipan bearing phases from fragipan bearing phases in most soil associations (Witty and Knox, 1989), therefore a complete understanding of where fragipans are located is unclear. The Soil Map of the European Communities (Commission of the European Communities, 1985) indicates map units that are either locally characterized by fragipans (particularly in France) or can be correlated to other fragipan bearing soils. More detailed maps are needed to gain better insight into how fragipan bearing soils relate to topography and parent materials. Other countries that have reported fragipans are Belgium, the Netherlands, Sweden, the United Kingdom, Spain, Brazil, Italy and Australia (Smalley and Davin, 1982; Marsan and Torrent, 1989).

Fragipans have been found in all states east of and adjacent to the Mississippi River along with some western states (Table 4; Wittig et al., 1957; Grossman and Carlisle, 1969; Witty and Knox, 1989). Most commonly associated with Alfisols, Spodosols, Inceptisols, and

Ultisols, they do not occur in areas with a high CaCO_3 content, but primarily in humid regions with excess rainfall and climate ranging from warm to cold. There have also some fragipans mapped as Fragixeralfs in Idaho and Oregon. Over half of the soils containing fragipans are located in seven states: Arkansas, Indiana, Kentucky, Mississippi, New York, Ohio, and Pennsylvania. The majority of fragipan soils are classified as Fragiudalfs or Fragiudults followed by Fragiochrepts, Fragiaqualfs, and Fragiaquepts (Witty and Knox, 1989). Generally Inceptisols with fragipans occur within the glaciated regions of the Northeast, whereas Alfisols and Ultisols with fragipans occur south of the late Wisconsinan glacial limit. Spodosols with fragipans account for less than 5% of observed fragipan soils.

Table 3. Worldwide extent of fragipans (adapted from Witty and Knox, 1989).

Country	Area (km^2)
Canada	5,500*
Czechoslovakia	5,320
France	37,300**
Hungary	170
New Zealand	23,170
Poland	360
Romania	3,740
United States	470,400***

- * Primarily occurring in the Maritime Provinces
- ** Locally characterized by fragipans
- *** Includes soils that are not dominated by the presence of a fragipan

Table 4. Extent of fragipans in the United States (adapted from Witty and Knox, 1989).

STATE	Extent (km ²)	STATE	Extent (km ²)	STATE	Extent (km ²)
AL	4,364	MA	80	OK	831
AR	17,135	MD	1,660	OR	864
DE	36	ME	46	PA	26,768
FL	21	MI	1,132	SC	88
GA	209	MN	127	TN	5,599
ID	872	MO	7,934	TX	299
IL	1,720	MS	15,621	VA	994
IN	8,623	NC	177	VT	502
KS	40	NH	10	WA	67
KY	9,581	NJ	1,937	WI	280
LA	3,366	NY	15,427	WV	1,481
		OH	9,757		

Lindbo and Veneman (1989) reported that 13% of the soils in the Northeast are recognized as having true genetic fragipans, whereas dense till soils (soils that may have previously been classified as containing fragipans as well as soils without fragic properties developed in till) constitute an additional 11% of the soils in this region. These figures were obtained by searching the Map User Unit File (MUUF) data base for mapping units with "Fragi" in the taxonomic name; dense basal tills were estimated by searching the data base for other soils having a horizon in the subsoil with a 1.7 Mg m⁻³ or greater bulk density (Table 5).

Table 5. Distribution of fragipan and dense till soils in the Northeast region of the United States (after Lindbo and Veneman, 1989).

STATE	TOTAL HECTARES	FRAGIPAN HECTARES	%	DENSE TILL HECTARES	%
CONNECTICUT	1,267,585	---	---	303,120	24.0
DELAWARE	512,318	4,047	0.8	-0-	--
DISTRICT OF COLUMBIA	17,872	324	0.5	-0-	--
MAINE	8,384,440	---	---	4,099,410	51.0
MARYLAND	2,550,905	188,185	7.3	-0-	--
MASSACHUSETTS	2,036,855	8,555*	---	529,752	26.0
NEW HAMPSHIRE	2,333,329	7,285*	---	653,185	28.0
NEW JERSEY	1,875,277	135,574	7.2	-0-	--
NEW YORK	12,315,088	3,866,504	31.4	196,279	1.6
PENNSYLVANIA	11,688,154	3,458,161	29.4	-0-	--
RHODE ISLAND	269,983	---	---	70,822	26.2
VERMONT	2,401,773	53,016*	---	384,060	16.0
VIRGINIA	10,310,054	269,125*	2.2	-0-	--
WEST VIRGINIA	6,246,402	416,841*	6.7	-0-	--
TOTAL	62,210,035	8,407,617*	13.7	6,236,628*	10.1

* Tentative figures based on extrapolation of available data.

Fragipans are most commonly mapped in the west-central part of this region, whereas in the most recently glaciated areas mostly dense basal till is mapped (Table 5). Incomplete mapping of some states (Virginia and West Virginia), requires the estimation of fragipan extent based on preliminary information from unsurveyed areas. Soil mapping in Connecticut, Delaware, Maryland, Pennsylvania, and Rhode Island has been completed, although information from those states could change as a result of recorrelation during soil survey up-dates.

Many of the fragipans currently mapped in the New England area and some in New York and Pennsylvania probably will be reclassified as dense basal tills during recorrelation activities.

The influence of Calhoun's suggestions, namely that fragipans are not developed in dense basal till, are evident in the data reported in Table 5. The incorporation of this suggestion into current classification schemes has resulted in fragipans being mapped south of the late Wisconsinan glacial maximum whereas dense basal till is mapped to the north of this maximum. As mapping is completed in individual states the figures may change but the general pattern will not.

Fragipans in New England are found primarily in soils developed on dense basal till. Until recently, these soils were classified with the prefix "Fragi" denoting the presence of a fragipan, but correlation efforts have eliminated this classification from much of the region based, in part, on the idea that the properties of the pan were inherited from the till rather than having pedogenic in origin (Pickering, 1983). Fragipan research in the New England area has been ongoing over the past 27 years (Lyford et al., 1963; Krohelski, 1976, Lord, 1979, Pickering, 1983, Pickering and Veneman, 1984; Reed 1989). These investigations suggest that the observed "pans" in New England are morphologically similar to those observed in unglaciated areas. Most recently a field trip was held in southern New England to address the issue of the presence or absence of fragipans. The overall conclusion was that some soils expressed typical fragipan morphology and should be considered fragipans. It was also noted that not all

soils developed in glacial till having a dense subsoil horizon exhibit fragipan morphology. Possibly, such soils need to be identified at a higher level than series or family as they are presently.

CHAPTER III

GEOLOGIC SETTING

Physiography

The landscape of Massachusetts can be subdivided into five broad physiographic zones. From east to west these include: the Coastal Plain, the Coastal Lowlands, the Central Highlands, the Connecticut Valley, and the Berkshire-Hudson Highlands (Figure 2). Although Massachusetts has been repeatedly glaciated over the last few million years, the overall relief of the landscape is controlled by the complex structures of the underlying bedrock (Schafer and Hartshorn, 1965; Denny, 1982; Zen, 1983). In general, the bedrock structures trend north-south (Zen, 1983), essentially parallel to the major ice movements. Most of the material comprising the till is derived from this bedrock (Mullholland, 1976) and thus the texture, mineralogy, and chemistry is controlled by the local bedrock (Clark, 1986). The bedrock ridges also influenced the course of deglaciation by channeling the disintegrating ice as well as directing the flow of subglacial melt water (Boulton, 1972; Gustavson and Boothroyd, 1987).



Figure 2. Physiography of Massachusetts (after Denny, 1982).

Generalized Bedrock and Geologic History

Zen (1983) identified eight lithotectonic zones in Massachusetts (Figure 3). The Taconic-Berkshire zone and the Milford-Dedham zone contain the oldest rocks (Proterozoic Y and Proterozoic Z, respectively) found in Massachusetts. During the Cambrian, the proto-Atlantic began to form creating an inland sea within the Berkshire-Taconic zone as evidenced by dolostone and marble in the Stockbridge Formation. There was also volcanic activity within this zone which lapsed and later rejuvenated in the Ordovician. Toward the end of the Ordovician, the proto- Atlantic began to close, marking the beginning of the Taconic Orogeny. During this event, allochthonous blocks slid into the Hudson Trough creating the Taconic Mountains. The Cheshire Quartzite (Lower Cambrian) crops out in this region and fragments of it can be found in till sheets blanketing the Berkshire Mountains and in the adjacent Connecticut Valley. The phyllites and schists of the Walloomasac Formation (Middle Ordovician) and Hoosac Formation (Lower Cambrian and Proterozoic Z) influence till composition as well.

Shallow water sedimentation occurred through the Rowe-Hawley to the Nashoba Zone (Figure 3) as the ocean continued to close. Finally during the late Devonian the closure was complete, resulting in massive nap folds, extensive metamorphism of the previously deposited sediments and the emplacement of numerous intrusive bodies. This event is known as the Acadian Orogeny. The present day expression of

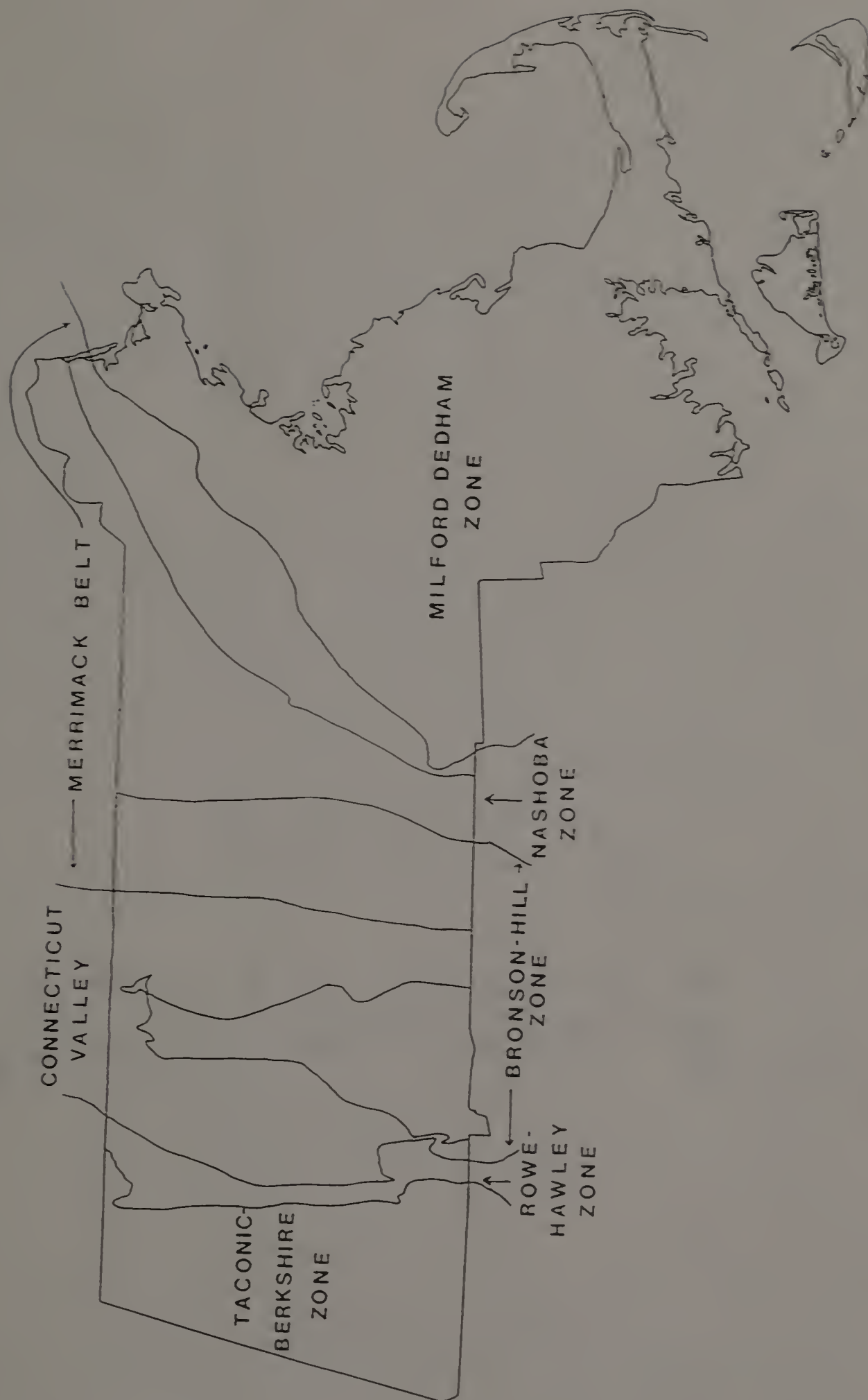


Figure 3. Lithotectonic zones in Massachusetts (after Zen, 1983).

the individual formations is in linear north-south trending bodies. The Partridge Formation (Middle Ordovician) composed of schists, gneisses, and granofels, Paxton Formation (Silurian) composed of schists, calc-silicates, and granofels, and Littleton Formation (Lower Devonian) composed of schists, phyllites, and gneisses significantly contributed to clast and matrix composition of the tills investigated in this area.

A period of quiescence followed the Acadian Orogeny allowing for erosion of the highlands and deposition in low lying swampy areas. The Alleghanian Orogeny further metamorphosed the existing rocks and emplaced more intrusive bodies.

At the end of the Middle Triassic, a rift developed in what is now the Connecticut Valley, associated with the later opening of the Atlantic Ocean. The rift and deformation in the area adjacent to it was active during the Late Triassic and Early Jurassic. During this time, extensive alluvial fans, rivers, and playas deposited mudstones to conglomerates; there were also massive extrusions of basalt in the Early Jurassic. Glacial till now overlying these deposits has a distinct red color and may be difficult to distinguish from weathered bedrock in some areas (J. H. Hartshorn, 1986 personal communication).

The interval between the Middle Jurassic and the Quaternary was a time of extensive erosion during which much of the present landscape evolved (Schafer and Hartshorn, 1965; Denny, 1982). Many of the current drainage systems, including the Connecticut River, were established during this period.

During the Pleistocene, Massachusetts was overridden by at least 2 glacial advances. These advances did little to modify the landscape except for the creation of drumlins, generally composed of a finer textured till, and small scale erosional features (e.g., roche moutonees which are whale back forms). Deglaciation resulted in glaciofluvial deposits which tend to be concentrated in valleys. The Connecticut Valley, like many valleys in New England, was occupied by a large proglacial lake, in this case caused by a drift dam in Rocky Hill, CT. Once this drained, the Connecticut River eroded through the soft clayey lake bottom deposits and continued to act as the major drainage way for much of the region.

Till Deposits

Two texturally distinct tills were recognized in the region over 100 years ago (Upham, 1878). Initially, these two tills were thought to be the englacial and subglacial phase of one glacial event (Upham, 1879). This idea was challenged by Shaler (1889) and later by Fuller (1901), both of whom suggested that the region had been affected by at least two advances. Four glacial events were later identified on Long Island (Fuller, 1914), and on Cape Cod (Woodward and Wigglesworth, 1934). These events were tentatively correlated to those in the Midwest and Europe. Correlations during this early period of stratigraphic research were based on qualitative analysis of color, gross texture, compactness, and selected morphologic features. White (1947), working in Connecticut, designated two tills of

different age as simply the Upper and Lower Till. He described an oxidized zone on the Lower Till as a weathering profile, possibly a soil. Silt caps were commonly observed in the Upper Till while the Lower Till was described as being fissile and commonly fractured (Currier, 1941; Denny, 1941; Moss, 1943). The description, while concise, lacked the support of quantitative data.

Detailed quantitative studies were first reported by Goldthwait (1948). His investigation of numerous large exposures in New Hampshire included texture, bulk density, and moisture content data, from which he concluded that there was no evidence of two advances. He explained the differences, between the tills as observed by others as being caused by water table fluctuations and totally variable modes of transport. Goldthwait did not recognize the occurrence of a paleosol in the till sequence, further suggesting that there could have only been one advance. A year after Goldthwait published his findings, Judson (1949) disputed it partly. Using a quantitative approach, Judson was able to establish characteristics for three tills of differing age. The tills, from youngest to oldest, were the Lexington, Boston, and pre-Boston tills. All were found in eastern Massachusetts with the pre-Boston Till seen only as inclusions in the Boston Till. Although no precise ages could be established it was thought by convention that the Lexington Till was late Wisconsinan, the Boston Till was early Wisconsinan, and the pre-Boston Till was Illinoian or older.

Kaye (1961; 1964) furthered Judson's interpretation, finding additional evidence of multiple tills. Based, first on a core taken during the construction of a parking garage in Boston, Kaye (1961) identified four tills separated by either marine sediments and/or outwash. These were correlated to late Wisconsinan, early Wisconsinan, Illinoian, and Nebraskan. Additional work on Martha's Vineyard identified six tills which had similar ages to those previously reported by Kaye (1964). The source material for the tills was identified as marine sediments making correlation to inland tills with radically different source materials impossible.

Inland investigations by Flint (1961) in Connecticut lead to the addition of two more names to the growing roster of New England tills. He identified the Hamden Till as a loose, sandy till, and the Lake Chamberlain Till as a compact, clayey till each representing a different glaciation. Unlike other workers, Flint resisted the correlation of these units with those described elsewhere, despite similarities. Elsewhere in Connecticut, Pessl (1966; 1971), Pessl and Schafer (1968), and Pease (1970) resurrected the Upper and Lower Till nomenclature. They discussed the "two till problem" in New England concluding that each till represented a distinct glacial event and not different facies of the same event. Pessl's work described in detail the presence of truncated contacts, erosional features at the contact, fabric differences, and weathering (oxidation) of the upper portion of the Lower Till. While Pessl's work was over a wide area of northern Connecticut, Pease was able to concentrate on a continuous seventeen

mile long trench. This continuous exposure allowed him to describe the till to till contacts thus supporting Pessl's conclusions.

Studies in northern New England also addressed the two till problem during this time. Drake (1971) reported on two tills in Central New Hampshire which eventually were interpreted as representing two facies of the Upper Till in an area where the Lower Till was not present. Investigations of surface tills in northern Vermont by Stewart and MacClintock (1971) led to the conclusion that the Shelburne Till (surface till) was an ablation till with a northeast fabric similar to the Upper Till previously described in Connecticut. The Bennington Till (subsurface till) had a northwest fabric, and although it was not discussed in detail, it could be correlated to the Lower Till. A younger till (Burlington Till) overlies parts of the region. As more data was amassed, regional correlations seemed more likely as did support for the presence of two tills of different ages.

The need for a concise regional investigation was filled by Newton (1978). He described, in detail, sites from northern Connecticut to northern New Hampshire. His findings resulted in new nomenclature for the various tills; Bakersville (Upper Till), Thomaston (Lower Till), and PreThomaston Till. Newton's field sites and extensive data base are still used today as a basis of comparison for other studies even though his nomenclature has not been widely adopted.

Throughout this period, the chronostratigraphy of the tills had been determined by assuming that glacial events in the Northeast

corresponded directly to events in the Midwest and Europe. Without some way of accurately dating the tills this process was the best available method. Borns and Calkin (1977) were among the first to establish bracketing dates of the tills. At a two till locality in New Sharon, Maine they found tills separated by glaciolacustrine sediments containing spruce fragments which were ^{14}C dated at >52 ka. Recently this sequence has been seriously questioned by Weddle (1986, 1988). He feels that the sequence represents a complex transport history and that the whole site represents late Wisconsinan events. The spruce fragments are the result of the incorporation of older sediments into the till.

Paleomagnetic studies of selected tills suggested that some of the Lower tills in Massachusetts could be correlated to the 32 ka Lake Mungo excursion (Soloyanis, 1978; Soloyanis and Brown, 1979). This study also found that the paleomagnetism was disturbed by glaciotectonics. A later study indicated that meltout till gives a usable paleomagnetic signal, while lodgement till does not (Thomas, 1984).

The lack of dateable material in the inland areas and the questionable utility of paleomagnetism work has forced workers to look to the terminal moraines along Southern New England in hopes of finding some dateable material. Oldale et al. (1982) and Oldale and Eskenasy (1983) correlated two tills at Sankaty Head, Nantucket Island to the Upper and Lower tills found inland. Shell material taken from the sediments (Sankaty Sand) that separate the tills were dated

between 120 ka and 140 ka using amino acid geochronology. Coral fragments from the sand were similarly dated by U-series at 133 ± 7 ka. These dates (the best available at the present time) indicate that the Lower Till is of Illinoian age, not of Early Wisconsinan age as previously thought.

One of the sites that Newton used in his work has recently been reexamined by Koteff and Pessl (1985). The Nash Stream site in northern New Hampshire contains two tills separated by outwash and a clear erosional surface. The Nash Stream Till (Lower Till) shows evidence of subaerial weathering (oxidation to a depth of up to 7 meters), and is separated from the Stratford Mountain Till (Upper Till) by either a shear zone or thick (up to 23 meters) outwash sand and gravel. Tentatively, the tills are placed as early Wisconsinan and Late Wisconsinan, respectively. This positioning is not based on any numerical dates.

The most recent research on tills suggested that subglacial conditions during the deposition of the Lower Till included lodgement, shear, and attenuation as well as fluvial activity (Lindbo, 1990). Thus the Lower Till is seen as being more heterogeneous than previously observed. Lindbo (1990) compared Upper and Lower Tills concluding that they can be differentiated between based on exchange chemistry, texture, morphology, and fabric (Table 6).

Despite the lack of good exposures in New England numerous studies of the tills have been made resulting in a plethora of names for each type of till (Figure 4) and a substantial data base for each till (Table 7). Most researchers now agree that the tills represent

Table 6. Characteristics of Upper and Lower Till (adapted from Lindbo, 1990).

	Upper Till	Oxidized Lower Till	Unoxidized Lower Till
Color	Light brownish gray to pale olive.	Olive to olive brown, some reddish brown staining on plates.	Olive gray to greenish gray.
Morphology	Loose to dense, common fluvial beds and silt caps, matrix-supported sub-rounded to sub-angular clasts.	Fissile to massive, common joints and plates, silt/clay beds may occur, sand and silt veins common, matrix-supported sub-rounded to angular clasts.	Massive, common joints and silt\clay beds, matrix-supported sub-rounded to angular clasts.
Texture			
% Sand:	68.0	51.6	47.8
% Silt:	26.1	32.3	34.2
% Clay:	5.9	16.1	18.0
Bulk Density (Mg m ⁻³)	1.88	1.77	1.92
pH	5.5	6.4	7.5
CEC (cmol kg ⁻¹)	2.8	6.6	5.2
Pebble Fabric	18 ^o	338 ^o	333 ^o

Upham, 1878	Scaler, 1889; Fuller, 1901; 1914; Woodward, and Wigglesworth, 1934	Whice, 1947	Judson, 1949	Kaye, 1961; 1964	Filinc, 1961	Pessl, 1966; Pessl and Schafer, 1968; Ponse, 1970; Pessl, 1971	Drake, 1971	Stewart and MacClintock, 1971	Newcom, 1978	Dremer, 1984	Kocoff and Pessl, 1985
Englacial	"Younger"	Upper	Lexington	Late Wisconsinan	Hamden	Upper	Soft	Burlington	Bakersville	Roslyn	Stratford Men.
Subglacial							Hard	Shelburne			
	"Older"	Lower	Boston	Early Wisconsinan	Lake Chamberlain	Lower		Bennington	Brown Thomaston Gray Thomaston	Montauk	Nash Stream
			Pre-Boston	Illinoian					Pre-Thomaston		
				Kansan							
				Nebraskan							

Figure 4. Correlation diagram of till nomenclature in New England.

Table 7. Summary of the characteristics of Upper and Lower Till
(after Reed, 1989)

<u>Distribution and Thickness</u>	<u>Upper Till</u>	<u>Lower Till</u>
<p>Ubiquitous throughout the uplands and localized within the Connecticut Valley. Occurs as a discontinuous mantle over the lower till and bedrock and as a collar around some drumlins. It has been reported in depths up to 3 meters.</p>	<p>Ubiquitous throughout the uplands and within the Connecticut Valley. Occurs as thick deposits over 10 meters and comprises the cores of most drumlins.</p>	<p>Ubiquitous throughout the uplands and within the Connecticut Valley. Occurs as thick deposits over 10 meters and comprises the cores of most drumlins.</p>
<u>Color</u>	<p>Unweathered moist colors range from light olive gray to olive (5Y4-6/2-4) with the Triassic provenance tills being redder (10YR4-6/3-5).</p>	<p>There is a great deal of variation from area to area. Common oxidized colors: 2.5Y4-5/2-4 to 5Y3-5/2-3; unoxidized colors: 5Y4-5/1; Connecticut Valley till 7.5YR4-6/5.</p>
<u>Texture and Consistency</u>	<p>Gravel: 11-31 Sand: 55-85 Silt: 11-35 Clay: 2-12 n=128</p> <p>The texture generally is controlled by the local bedrock and shows greater variation than in the lower till. The Upper Till ranges from loose to slightly compact, it may contain dense lenses of siltier material, and it is more porous than the Lower Till. The upper section of this till may be stonier and appears washed. Stones are common throughout the till although they are still matrix supported. Clasts range from angular to rounded. Silt caps are also common.</p>	<p>Gravel: 8-17 Sand: 44-69 Silt: 21-37 Clay: 2-29 n=64</p> <p>No obvious relation has been reported between texture and local bedrock. Basically homogeneous with some depletion of clay at the top. Moderately to extremely compact with low porosity. No silt caps are observed although thin clay films can be found on some small clasts. Stones are less common than in the Upper Till and they are matrix supported. Clasts are generally angular.</p>

Continued, next page

Table 7 cont.

<u>Jointing</u>	<p>Poorly developed joints (both subvertical and subhorizontal), these are better expressed in the siltier phases of the till. Sand and silt, from lenses to deformed layers are common. Some beds are extensive.</p> <p>Common subhorizontal fine jointing in the upper weathering zone produce fissility. Widely spaced vertical joints also occur. Other horizontal layers common. Vertically oriented sand dikes ending in horizontal veins.</p>
<u>Weathering</u>	<p>Commonly weathered to a depth of 1 meter although some weathering to a slightly greater depth has been observed. There is more oxidation of the coarser grained zones and around clasts. Grussified rocks commonly occur adjacent to sound rocks. Contact to the unweathered zone is gradual yet clear.</p> <p>Weathered to depths of 10 meters. Joint surfaces may be coated with Fe and Mn stains. Some fragments also exhibit staining. Staining may follow larger joints into the unoxidized till. Contact with the unoxidized till is commonly sharp although it may occur over the span of 1 meter.</p>
<u>Landforms</u>	<p>Not associated with any particular landform.</p> <p>Cores of drumlins, underlying smooth hillslopes.</p>
<u>Origin</u>	<p>The source material is local unweathered bedrock.</p> <p>Coarse fragments are from unweathered local bedrock, while the matrix is derived from the preexisting weathered bedrock mantle.</p>
<u>Age</u>	<p>Late Wisconsinan</p> <p>Early Wisconsinan or Illinoian.</p>

two glacial events. The presence of the oxidized zone in the Lower Till suggests an extended period of subaerial weathering. This, coupled with erosional contacts, glaciotectionic features in the Lower Till, and the intervening sediments between the tills, provide the evidence to support the two glacial advance theory. The numerical ages of these events is still up for debate. Most would consider the Upper Till to be late Wisconsinan, however, it is the age of the Lower Till which can not be agreed upon. Debates over the existence of early Wisconsinan tills continue throughout parts of North America, as well as New England.

Post-glacial

Deglaciation of southern New England began approximately 17 ka bp. The mode of retreat varied between ice lobes and was commonly non-synchronous (Stone and Peper, 1982). In the major north-south trending valleys the ice remained active but did not remain in one location long enough to build moraines. Instead, ice contact deposits are used to establish ice position during its retreat (Larsen and Hartshorn, 1982). Short lived readvances were common as evidenced by deposits of till over varved clay in the Connecticut Valley (McIlvride, 1982). Topography significantly influenced the mode of retreat in the uplands and the coastal lowlands. Basins were typically occupied by stagnant ice or pro-glacial lakes (Black, 1982). Stagnation zone retreat was most common in eastern portions of Massachusetts (Koteff, 1982). In the more mountainous areas large

section of the glacier were cut off from continued ice supply as the ice thinned over topographic highs (Gerath et al., 1985). As the ice retreated north, climate changed from tundra to forest. This change occurred over the course of a few thousand years (Bonnichsen et al., 1985).

Once the glacier receded, till and other sediments were exposed and subjected to further modification. The main processes involved include aeolian deflation and addition, removal of fine grained material by water action, water table fluctuation, and freeze-thaw or periglacial activity (Boulton and Dent, 1974; Boulton and Paul, 1976).

The removal of fine grained material has been noted to occur subglacially although removal appears most common immediately prior to and post exposure from the overlying ice (Boulton and Dent, 1974). Some of the fine material may migrate vertically and laterally in the till. Such movement has been postulated as a process by which the underlying material becomes denser (possibly forming a fragipan). Removal of fines results in a coarsening upwards in the surface of till and has been noted by Caggiano (1978) and Newton (1978) in Massachusetts tills. Further removal of fines has been attributed to deflation of the surface by wind action. This may account for a decrease in silt sized particles soon after the till is exposed (Boulton and Dent, 1974). However, as the till surface is exposed for a longer period of time aeolian material may be deposited over it resulting in a fine grained aeolian mantle overlying the till (Boulton and Dent, 1974; Fletcher, 1979).

Freshly exposed till commonly is saturated (J. H. Hartshorn, 1987 personal communication). As the water drains the sediment may undergo self-weight collapse resulting in an overconsolidated zone in the till (Boulton and Paul, 1976; Bryant, 1989). Changes in the water table also influence till chemistry. If the water table remains high reducing conditions dominate resulting in gleyed horizons. Subsequent fluctuations in the water table changes some of the characteristics of the till.

Climate is another factor responsible for post-depositional changes in till. Adjacent to glacial ice a periglacial environment (intense frost action and a snow free surface for part of the year) frequently exists either with or without the occurrence of permafrost (Ritter, 1988). Periglacial or permafrost processes may result in structural changes and reorganization of the surficial layers of the exposed till and other glacial sediments. The intensity of late Pleistocene periglacial activity may have been greater than that observed in the Arctic today. This increase in activity results in deeper freezing and thawing and possible dessication of the ground during the summer months (Bryan, 1949; Budel, 1959; Bonnicksen et al., 1985).

The periglacial post-glacial New England climate of 13 to 14 ka (Davis and Jacobson, 1985) may have to be extended to 10 ka if the reports of pingos in Lake Hitchcock sediments are accurate (G. Ashley, 1990, personal communication). Also, the confirmation of these features suggests that permafrost was much more extensive than previously thought (c.f. Gustavson and Boothroyd, 1987). Features,

such as stone stripes and solifluction lobes, observed elsewhere in Massachusetts (c.f. Stout, 1952; Lyford et al., 1963) suggest that a periglacial environment existed and was relatively intense. However, not all researchers agree with this conclusion, citing evidence for rapid revegetation and the rare occurrence of periglacial features (Schafer and Hartshorn, 1965; Flint, 1971).

The periglacial climate (if it existed in the first place) graded into a climate similar to that of the present. Forest vegetation has dominated the landscape for at least the last 10,000 years (Pritchett, 1979). Under these climatic conditions bioturbation, illuviation, and eluviation (soil development) have dominated post-depositional alteration of the glacial deposits.

Soils in this region have thus been influenced by glacial activity and deposition, followed by post-glacial alteration, and soil development (Figure 5).

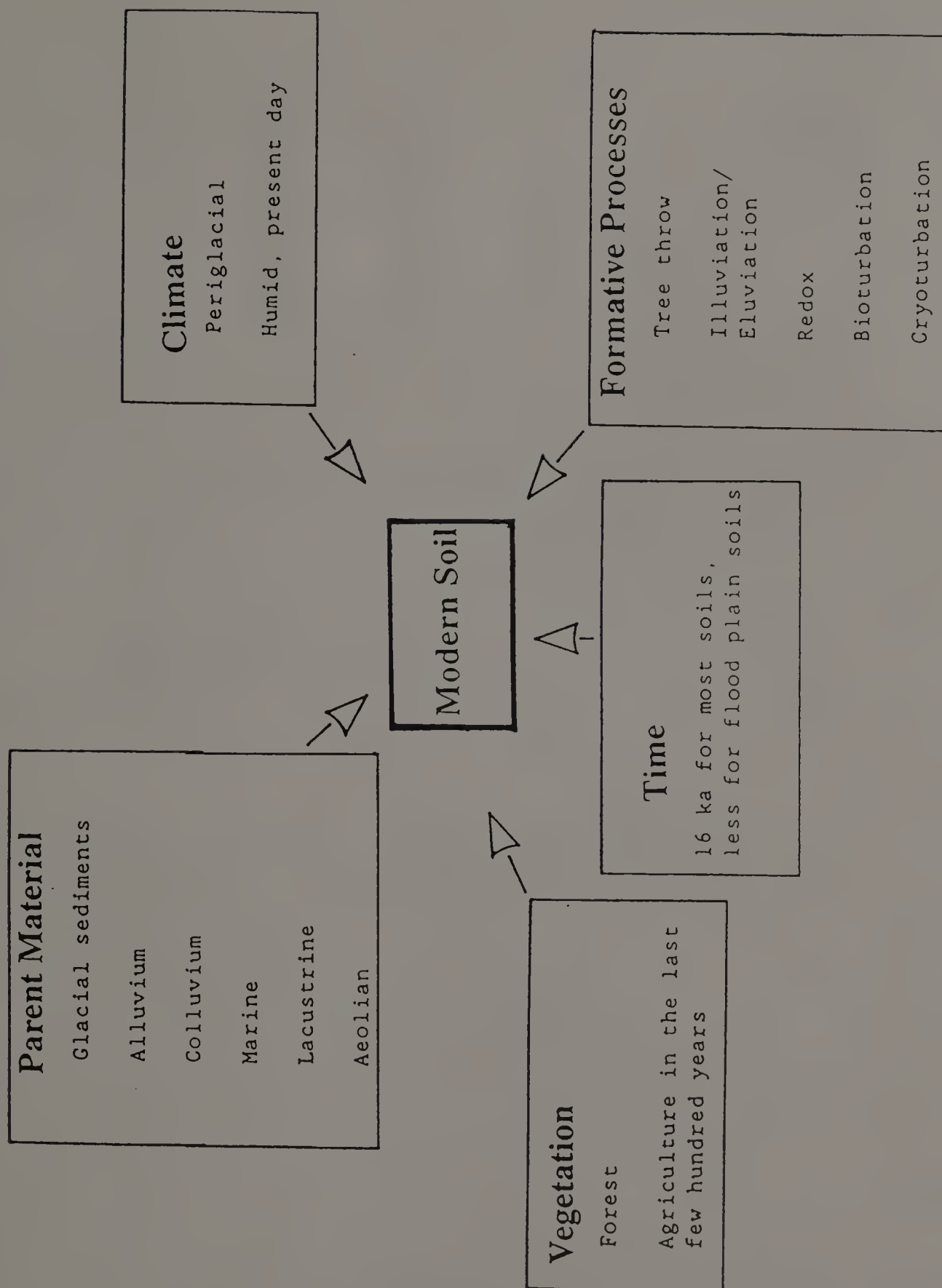


Figure 5. Generalized factors affecting soil development in Massachusetts.

CHAPTER IV

PHYSICAL PROPERTIES

Previous Work

Macromorphology

The morphology common to fragipan soils is discussed in detail by Grossman and Carlisle (1969). In Soil Taxonomy (Soil Survey Staff, 1975) many of their observations were incorporated in the fragipan description (Smalley and Davin, 1982). Macromorphological features common to most fragipans include: mottles, polygons with bleached faces, varied structures within the polygons, a strong relation of polygons to texture and drainage conditions, and clay-lined pores and vesicles (c.f. Table 1, Chapter 1).

High and low chroma mottles are observed in fragipans depending on drainage conditions. The area adjacent to the bleached faces may show strong evidence of localized Fe staining (Williams and Farvolden, 1967). The high amounts of Fe within the pan as reported by Nettleton et al. (1968b) add to the expression of high chroma mottles (DeKimpe and McKeague, 1974). Manganese (Mn) concretions or mottles also appear on the surfaces of platy peds (Matthews, 1976; and Miller et al., 1971b).

Often one of the fragipan's most striking features in plan view are large prisms or polygons bounded by vertical or near vertical

planes (Nikiforoff et al., 1948; Nikiforoff, 1955). The polygons range from 20-60 cm in diameter with the bleached face commonly 2 cm across. Between the bleached face and the interior a thin zone (1 mm - 10 mm) of Fe staining is common (Ranney et al., 1975; Williams and Farvolden, 1967). Ranney et al. (1975) further describe the faces as zones of water movement and accumulation of material. Water movement removes some material but it also tends to illuviate clay leading to the formation of bridges and clay skins along the edge of the feature. Williams and Farvolden (1967) indicate that the oxidation zone common to the bleached prism faces occurs because the water moving down the face is higher in dissolved oxygen than the surroundings. The oxygen diffuses and results in localized oxidation of Fe. The morphology of the prism faces has been explained as due to preferential flow of water which may be oxygen poor due to the microbiological activity around roots (Ranney et al., 1975; Williams and Farvolden, 1967; Payton, 1980; Jha and Cline, 1963). Lyford et al. (1963) found that roots were almost exclusively found along the prism faces and not in the interior.

Polygons are not always present in a fragipan (Daniels et al., 1966), particularly in coarse-textured pans (Wang et al., 1974; Nettleton et al., 1968a). In general, there is agreement that polygons form more readily in medium to fine-textured soils (Carlisle et al., 1957; Petersen et al., 1970; Hanna et al., 1975; Harlan and Franzmeyer, 1977; Steinhardt and Franzmeier, 1979). Some drainage classes exhibit better polygon development than others, with moderately well drained and somewhat poorly drained soils showing the

most distinct polygons overall (Carlisle et al., 1967; Petersen et al., 1970; Grossman and Carlisle, 1969; Wang et al., 1974; Hanna et al., 1975; Harlan and Franzmeier, 1977).

In most cases the presence of polygons constitutes the major structure within the pan. In other cases a secondary structure may occur and may overwhelm the polygon expression, or there may be no secondary structure at all (Nettleton et al., 1968a). Platy or lenticular structure is the most common secondary structure associated with the fragipan (Lyford et al., 1963; Miller et al., 1971b; Yassoglou and Whiteside, 1960; Crampton, 1966; van Vliet and Langohr, 1981; Grossman and Carlisle, 1969). Conversely, Jha and Cline (1963) observed a fragipan with a massive structure whereas Horn and Rutledge (1965) investigated one with an angular to subangular structure. In part these structures (platy, massive, or angular) may be inherited from the parent material or mode of deposition (Grossman and Carlisle, 1969; Nikiforoff et al., 1948; and van Vliet and Langohr, 1981).

Typically fragipans restrict vertical water movement. Large and continuous vertical pores exist primarily in the joints or polygon faces (Williams and Farvolden, 1967). In general, the pores that are observed are vesicular and filled with clay (Yassoglou and Whiteside, 1960; DeKimpe et al., 1972). Wang et al. (1974) found that more clay skins occurred in the lower half of the fragipan, suggesting that, as Grossman and Carlisle (1969) had stated previously, illuviation of clay and silt is common. Lyford et al. (1963) described in detail the distribution and nature of the pores

they observed. In short, the pores are tortuous, seldom continuous, often bulbous and lined with clay. They may be branching but do not connect to allow drainage. The nature of the pores suggests that some reorientation and redistribution of clay and fine silt are occurring in fragipans.

In general, fragipans are subparallel to the surface and possibly controlled by groundwater (Lyford et al., 1963) or by permafrost (van Vliet and Langohr, 1981). This position indicates that the pan is related to formative processes (pedologic, hydrologic, or geologic) rather than stratigraphic relationships. Because the pan may cut across stratigraphic boundaries it is not a relict feature. Steinhardt and Franzmeier (1979) observed this in fragipans developed in loess.

The presence of fragipans in the soils of the Northeastern region has a distinct influence on soil moisture conditions. Most profiles in drumlins and drumloidal ridges show low chroma colors within the soil solum in the backslope position (Hanna et al., 1975; Veneman and Bodine, 1982), indicating moderately well drained conditions, while soils in similar landscapes in the Midwest are mostly well-drained (Milfred and Hole, 1970). In the upper footslope position, somewhat poorly drained soils are frequently encountered. The low chroma morphology is caused by reducing conditions due to lower permeabilities in the pan that lead to perched water tables allowing for the mobilization of iron. Judging from the soil morphology, field observations, and actual measurements, it seems that the pan is only saturated during the late winter and early spring and remains

unsaturated for the remainder of the year (Reed, 1989; Scotter et al., 1979). Therefore the presence of the pan appears to have a pronounced influence on the moisture regime in these soils and as such has a pronounced effect on soil development as well. Non-fragipan, dense basal tills often show the same type of phenomena but to a lesser extent.

Particle Size Distribution

The Soil Survey Staff (1975) describes fragipans as having commonly loamy textures, with less than 35% clay. Few fragipans have greater than 35% clay (Hutcherson et al., 1959) and none have been found with over 60% clay (Grossman and Carlisle, 1969). The minimum clay content reported is 2% (DeKimpe et al., 1972), with the most common range being between 13% and 25% clay (Jha and Cline, 1963; Grossman and Carlisle, 1969; Petersen et al., 1970; Hutcherson and Bailey, 1964). The fine to medium textured soils within this textural range show the greatest fragipan development and expression (Carlisle et al., 1957; Wang et al., 1974; Harlan and Franzmeier, 1977; Payton, 1980).

Some general trends in the textural data for fragipans can be seen by plotting reported data from various Soil Survey Investigations Reports (Figure 6). The fragipans in loess clearly fall within the silty textural classes, while the fragipans developed in tills in southern New England predominantly have sandy-loam textures. The fragipans in New York and Pennsylvania are intermediate depending on

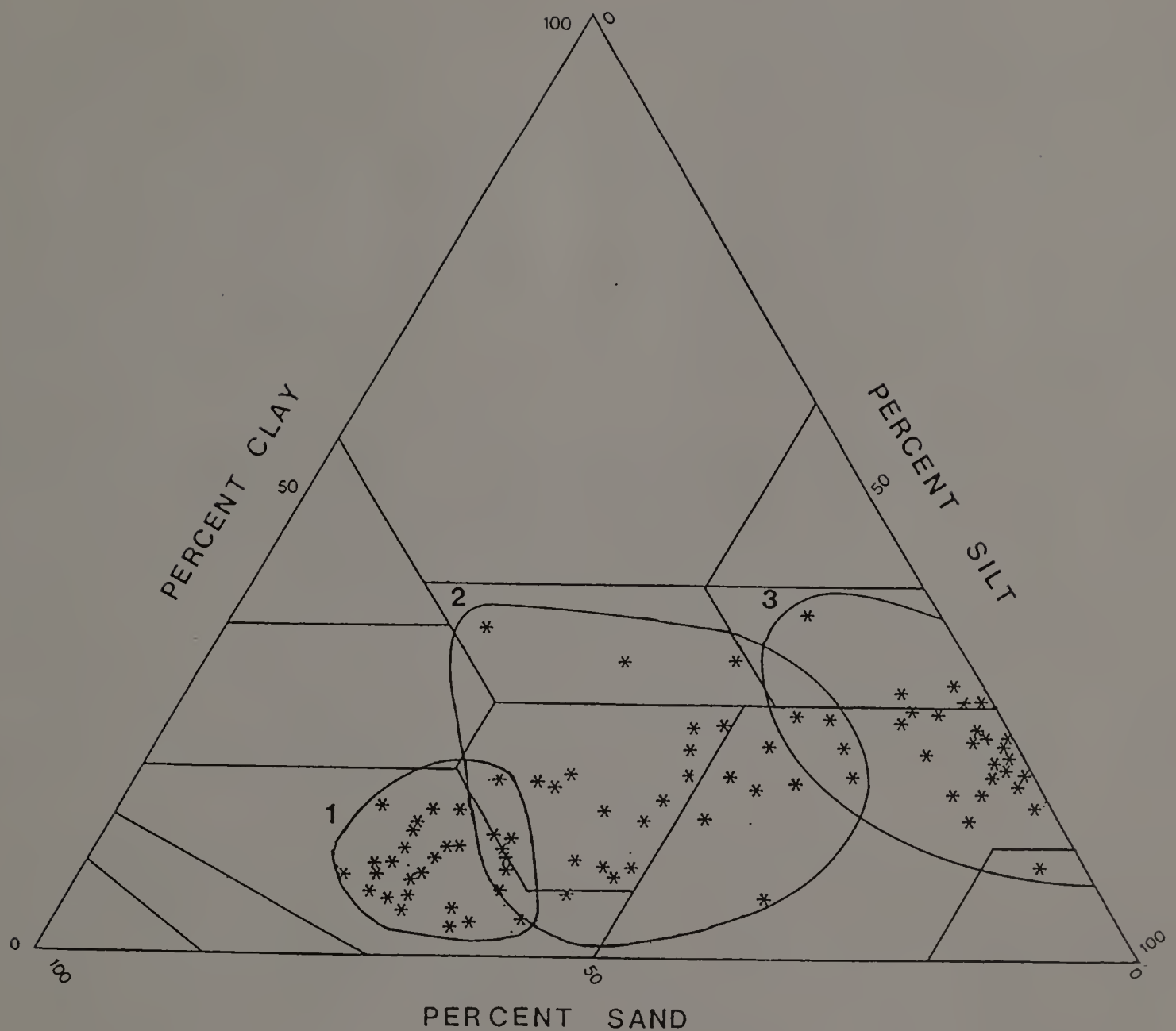


Figure 6. Textures of fragipan horizons based on soil survey data from throughout the USA. The following three generalized zones can be recognized: 1 = coarse loamy, 2 = loamy, 3 = fine silty (after Lindbo and Veneman, 1989; Soil Survey Staff, 1968; 1974; and 1979).

the parent material. Fragipans are not found in parent materials having a combined clay and silt content less than 35%.

In some cases the pans are found to contain the maximum amount of clay for the given profile (Hutcherson and Bailey, 1964; Grossman et al., 1959a). For example, coatings of oriented clay are quite common in the upper part of fragipans developed in glacial till, indicating illuviation of clay (Grossman and Carlisle, 1969; Wang, 1971). The loess derived fragipan of the Grenada series (Soil Survey Staff, 1979), as well as those of the Mardin series formed on loamy till (Soil Survey Staff, 1974), show this increase in clay distinctly (Figure 7). In the sandy-loam fragipans of New England (Soil Survey Staff, 1968), this clay accumulation often is significant enough (Figure 7) to qualify some of these pans as argillic horizons. Further proof that illuviation occurs can be found in the bleached prism faces of polygons occurring in pans. These areas may differ slightly in texture suggesting some particle migration (Ranney et al., 1975). In contrast, Nettleton et al. (1968a) found that in North Carolina the clay content was lowest in pan interiors. This was explained by the bisequal nature of the soil, as the parent material of the upper solum may have had a greater clay content.

Bulk Density and Moisture Relations

Fragipans have a bulk density that ranges from 1.65 to 2.15 Mg m⁻³ (Miller et al., 1971a; Daniels et al., 1966; Grossman and Carlisle, 1969; Veneman and Bodine, 1982). The reported values always show that the bulk density of the fragic horizon is higher than that

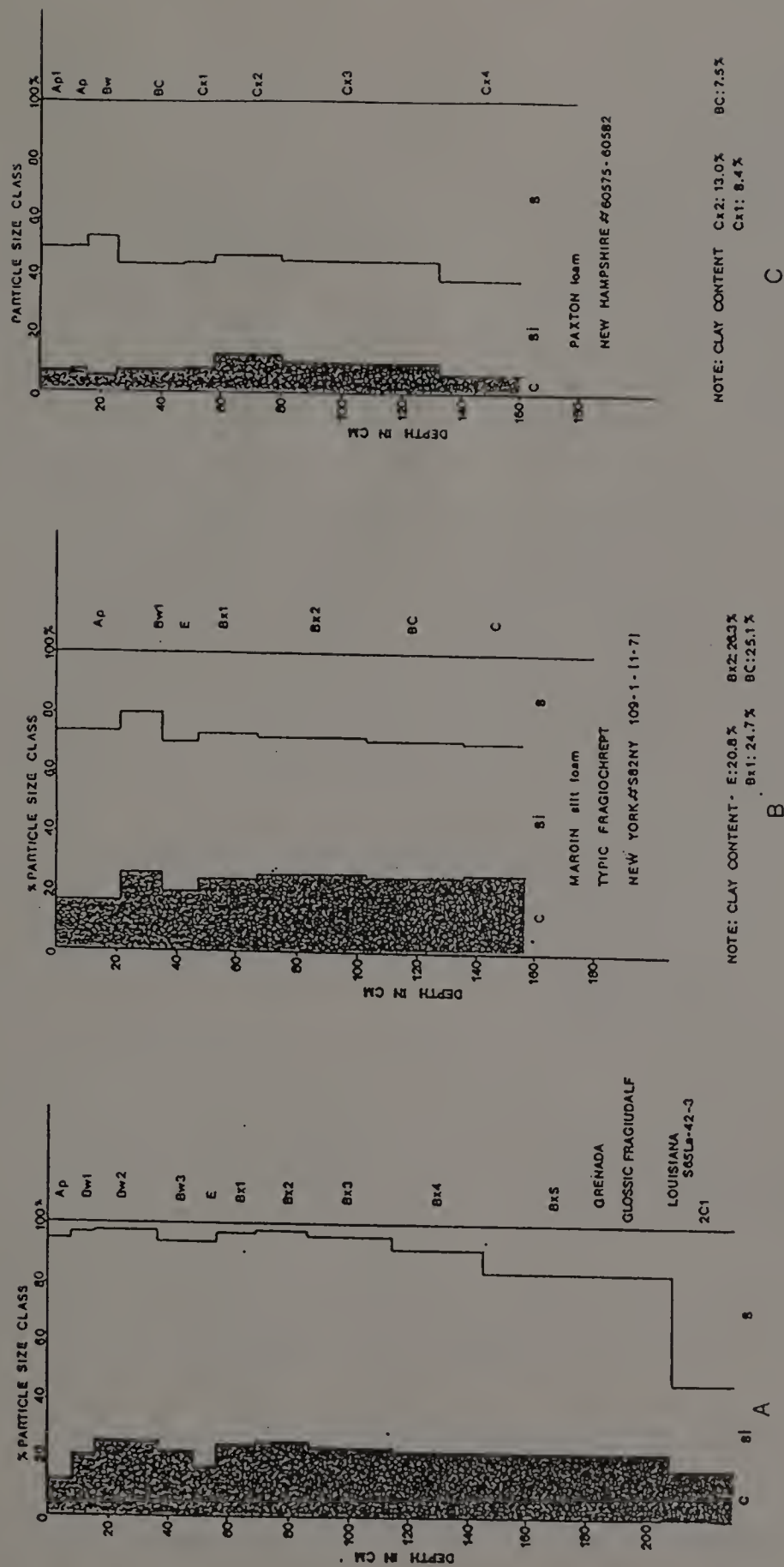


Figure 7. Plot of the soil separates for each horizon by depth for the (A) Grenada series (Soil Survey Staff, 1979); (B) Mardin series (Soil Survey Staff, 1974); and (C) Paxton series (Soil Survey Staff, 1968) (after Lindbo and Veneman, 1989).

of the overlying horizons (DeKimpe et al., 1972; Grossman and Carlisle, 1969; van Vliet and Langohr, 1981; Jha and Cline, 1963). Bulk density is found to decrease below the fragipan in most cases (Smalley and Davin, 1982). In some instances the extremely high bulk densities may be inherited from the parent material (Smith and Callahan, 1987), yet reorganization and subsequent increases in bulk density are common (Jha and Cline, 1963; Boulton and Dent, 1974; Scotter et al., 1979; Wang et al., 1974; Miller et al., 1971a; Petersen et al., 1970). Fritton (Fritton and Olson, 1972; Fritton et al., 1983) showed that the high density of a fragipan developed in glacial till reestablished itself in a period of less than 10 years after disturbance. In a laboratory setting, Krohelski (1976) found that the brittleness and high density can be recreated within 24 hours using fragipan material free of organic matter. Bryant (1989) found similar results in fragipan materials from New York state.

Soils within the same catena express differing fragipan bulk densities depending on their position in the landscape. The moderately well drained to the more poorly drained members show not only the greatest fragipan expression but also the highest bulk densities (Wang et al., 1974; Grossman et al., 1959a; Carlisle et al., 1957; Daniels et al., 1966; Nettleton et al., 1968a; Hanna et al., 1975; Petersen et al., 1970; Veneman and Bodine, 1982). The higher bulk density of the pan results in a lower pore volume (Lozet and Herbillon, 1971), restricting water movement and water may actually pond on the pan surface (Franzmeier et al., 1978). The polygon cracks common to fragipans may act as conduits for water movement (Williams

and Farvolden, 1967; Jha and Cline, 1963). Water may also move across the top of the pan or between the plates which are subparallel to the surface (Franzmeier et al., 1978; Lyford, 1963; Reed, 1989). Such movement may create the appearance of an eluvial horizon.

Water retention data indicate that pores in the fragic horizon are small since there is still a significant percent of the pore space occupied by water at low water potentials (Rutledge and Horn, 1965; Yassoglou and Whiteside, 1960; DeKimpe, 1970; Reed, 1989).

Fragipan identification is based on a series of field clues rather than any specific laboratory analysis. In order to ascertain whether the pans observed in this study qualify as fragipans detailed morphological descriptions are compared to the ideals set forth in Soil Taxonomy (Soil Survey Staff, 1985). In addition, textural analysis and bulk density are used to further define the presence or absence of argillic and fragipan horizons. It can be assumed that the presence of a argillic horizon in association with a pan suggests that illuviation has occurred which indicates pedogenesis within the pan.

Materials and Methods

Site Locations and Characteristics

General. Five primary pedons were selected based on the following criteria: i) developed in dense basal till; ii) accessible to a backhoe; and iii) presence of fragipan morphology. Vegetation on most sites was either pasture (open) or apple orchard. Supportive pedons were used to establish site conditions and topographic influence on the primary pedons. In addition, freshly exposed till sites were characterized and used to compare properties of the soil to those of the till. The sites were located in east-central and west-central Massachusetts (Figure 8 and Table 8). Maps of individual site locations are in Appendix A. All sites were located on drumlins or drumloidal ridges with bedrock over 5 meters below the surface (Table 9). Only the Amherst pedons were located in the Connecticut Valley, others were located in the central highlands. These soils had a relatively thin (0.3-0.7 m) aeolian component overlying and mixed into the underlying till.

Soils. The Brookfield site was located on Blanchard Hill (a drumlin), on the grounds of Elm Hill Farm. The present vegetation was a mixture of young and old apple trees as well as grasses. The primary pedon (Pedon 1) was located approximately 2 meters vertically below and 40 meters south of the summit of the drumlin. Supportive pedons were located on the west slope of the drumlin with EHR and EHDP3 being in the upper toeslope position and EHW and EHDP2 being in

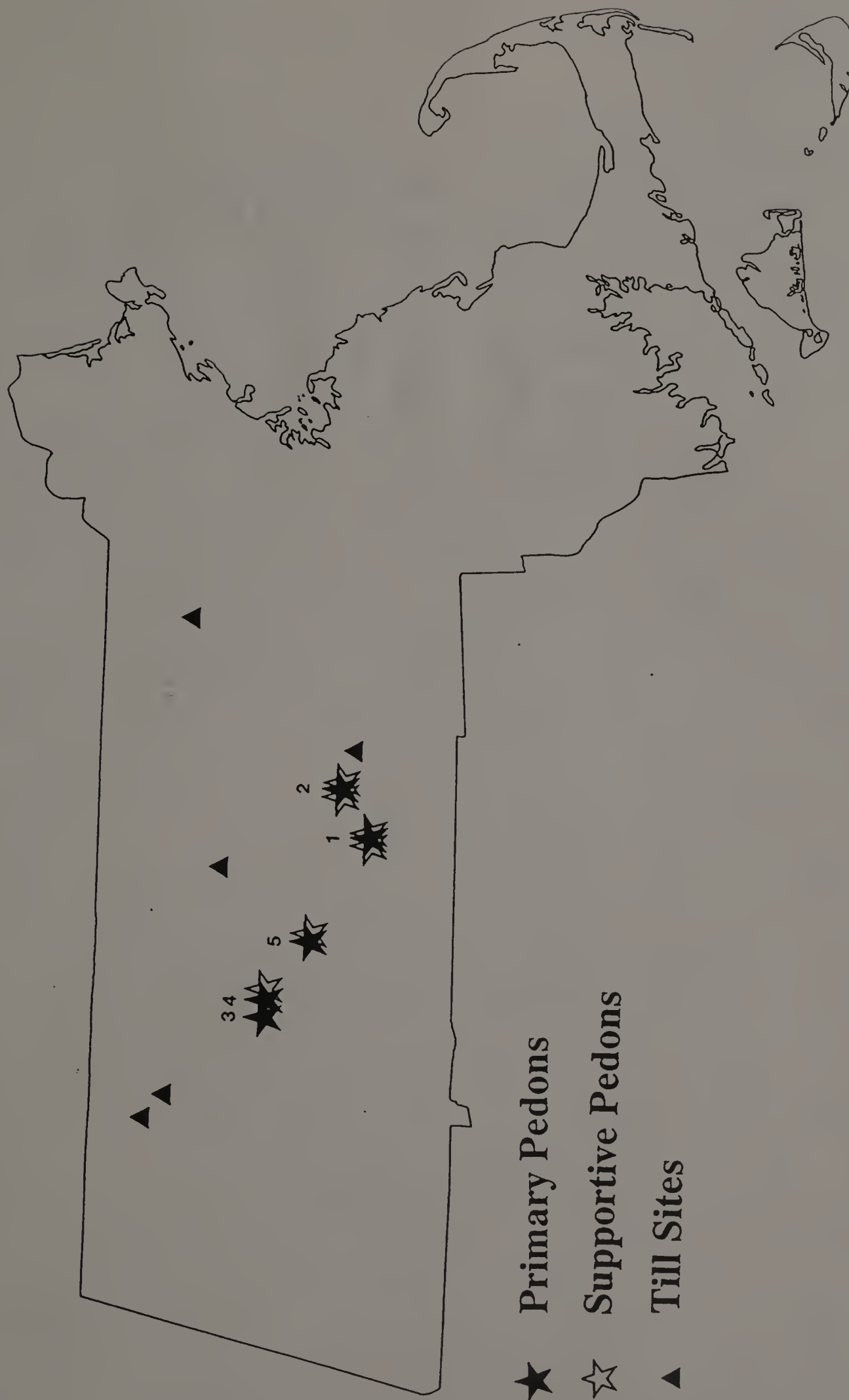


Figure 8. Site Locations.

Table 8. Site designations.

Location	Designation	Soil Series or Till Type
<u>Primary Pedons</u>		
Brookfield (Blanchard Hill)	Pedon 1	Paxton
Spencer (Buck Hill)	Pedon 2	Paxton
Amherst (Orchard Hill)	Pedon 3	Paxton
Amherst (Orchard Hill)	Pedon 4	Woodbridge
Belchertown (Horticultural Research Center)	Pedon 5	Ridgebury
<u>Supportitive</u>		
Brookfield	EHP	Paxton
	EHW	Woodbridge
	EHR	Ridgebury/Woodbridge
	EHDP2	Paxton
	EHDP3	unclassified
Spencer	BHP	Paxton
	BHW	Woodbridge
	BHR	Ridgebury
Amherst	OHW	Woodbridge
	OHL	Ridgebury
Belchertown	BTR	Ridgebury
	BTR/S	Ridgebury/Scituate
<u>Till</u>		
Leicester	LTD	Upper, Lower (Oxidized and Unoxidized) Till
Ayer	AY	Upper, Lower (Oxidized and Unoxidized) Till
Barre	BA	Upper, Lower (Oxidized and Unoxidized) Till
Buckland	BU	Lower, Unoxidized Till
Charlemont	CH	Upper, Lower (Unoxidized) Till

Table 9. Parent materials and local bedrock of the primary pedons.

Pedon	Classification	Parent Material	Local Bedrock
Pedon 1 (Paxton)	Typic Dystrochrept (coarse-loamy, mixed, mesic)*	Lower Till	Sulfidic Mica Schist
Pedon 2 (Paxton)	Typic Dystrochrept (coarse-loamy, mixed, mesic)*	Lower Till	Biotite Granofels and Calc-Silicate Granofels
Pedon 3 (Paxton)	Typic Dystrochrept (coarse-loamy, mixed, mesic)*	Lower Till	Red Sandstone, Arkose, Tonalite, and Sulfidic Schist
Pedon 4 (Woodbridge)	Typic Dystrochrept (coarse-loamy, mixed, mesic)*	Lower Till	Red Sandstone, Arkose, Tonalite, and Sulfidic Schist
Pedon 5 (Ridgebury)	Aeric Haplaquept (coarse-loamy, mixed, mesic)**	Upper Till	Biotite Tonalite and Hornblende Gabbro
* Previous USDA-SCS classification:		Typic Fragiochrept (coarse-loamy, mixed, mesic)	
** Previous USDA-SCS classification:		Aeric Fragiaquept (coarse-loamy, mixed, mesic)	

the footslope position (Appendix A). The site has no artificial drainage. There has been some localized disturbance of the upper 0.5 meter where large apple trees were removed 10 years prior to this study.

The Spencer site, located on the northwest slope of a drumloidal ridge, was on the grounds of the Buck Hill Conservation Center, Camp Marshall. Vegetation varies from young spruce trees (Christmas trees) and pasture (Pedon 2 and BHP), abandoned pasture (BHW), to hardwood forest (BHR). Pedon 2 and BHP were located mid-slope on a slight plateau at the edge of the spruce trees and hardwood forest. The other supportive pedons were located on the foreslope (BHW) or on the toeslope (BHR). Apart from the planting of the spruce trees the site has been undisturbed.

Located on the University of Massachusetts campus, the Amherst site has been used for numerous studies the latest being Pickering (1983) and Reed and Veneman (1986). The site was located on the east side of a drumlin (Orchard Hill) in an abandoned orchard/pasture. Pedon 3 was situated on the upper backslope approximately 4 meters vertically below the summit, Pedon 4 and OHW were on the lower backslope, and OHL was located on the lower toeslope or step tread. The lower portions of the slope had tile drains and terraces installed, although these have not been functional during the last 15 years.

The University of Massachusetts, Horticultural Research Center are the location of the Belchertown site. The soils were located at

the edge of an apple orchard on the west-facing slope of a drumloidal, bedrock controlled ridge. All the soils were in the toeslope position approximately 15 meters apart parallel to the slope (Pedon 5 was at the lowest and BTR/S was highest relative topographic position of the three soils studied at this site). Tile drainage has been installed throughout the toe- and footslope area. This site was also used by Reed (1989) for his investigation of moisture regimes.

Tills. Till sites were chosen based primarily on the size of the exposure. Leicester, Ayer, and Barre sites were situated either at or near landfills that were utilizing the till as daily cover. This resulted in large, unweathered exposures. At the three sites oxidized and unoxidized facies of the Lower Till were studied in detail (c.f. Lindbo, 1990). The Charlemont and Buckland sites were adjacent to streams which eroded the banks and exposed till during floods in the spring of 1987. These sites, while not as extensive as the first three discussed, are excellent examples of Upper and unoxidized Lower Till.

Field Description and Sampling

After pits (clean faces at till sites) were established 1.5 to 3 meters in depth, soil descriptions using established methodology were made (SCS, 1984). Fragipans, designated by the suffix "x" on the horizon identification, were identified by the presence of vertical streaking, polygons, and a noticable change in the consistency. Dense horizons, indicated by the "d" suffix, were those horizons that lacked vertical streaking or polygons but remained hard under the range of

moisture conditions seen in the field. Argillic horizons, indicated by the suffix "t" were difficult to determine in the field due to the overall low clay content, however, they were tentatively identified by the occurrence of clay skins. The BC transition zone was characterized by an increase in low chroma, type 2 mottles (Fanning and Fanning, 1989) and the termination of the vertical streaks in all soils but those from the Belchertown site where the fragipan was contained within part of it. Photographs of the overall profile as well as details were taken prior to sampling. The photographs and the detailed diagrams of the pit face were used to construct cross-section diagrams of the primary pedons to complement the profile descriptions. Selected elements of profile descriptions are located within the text. The complete profile descriptions are located in Appendix B.

The soils were sampled after the profile description was completed. Bulk samples (1-5 kg) were taken for each horizon. Where possible, extra samples of the bleached prism face were taken as well as subsamples of the fragipan based on depth. At least eight clods from the center of each horizon were collected and coated with a liquid polymer (6 to 1 ratio acetone to powdered saran) in the field. The clods were used for bulk density and moisture retention characterization (SCS, 1984). Also at this time, oriented blocks for thin section analysis (Chapter 5) and cores for strength analysis (Chapter 9) were sampled.

Laboratory

General. Bulk samples were air-dried for about 24 hours and passed through a 2-mm sieve, and air-dried for an additional 2 to 3 days. Once dry, the fine (<2mm) and coarse (>2mm) fractions were weighed and the percent coarse fragments was calculated.

Three subsamples were removed from the fine fraction, one for particle size and two for chemical analysis. One of the subsamples for chemical analysis was pulverized in a Spex Shatter Box. Chemical analysis will be discussed in Chapter 6.

Particle Size Analysis. Particle size analysis was performed using the hydrometer method (Day, 1965). Prior to dispersal of a 50 g sample in 125 ml of 5% Na-hexametaphosphate (Calgon), organic matter was removed from the A and upper B horizons by boiling the sample in approximately 30 ml of H_2O_2 . Sands were removed by wet sieving through a 50-um sieve, dried and then fractionated into very coarse sand 2000-1000 um, coarse sand 1000-500 um, medium sand 500-250 um, fine sand 250-100 um, and very fine sand 100-50 um by dry sieving. The remaining silt plus clay suspension was placed in a sedimentation cylinder and 8 fractions were determined by hydrometer assuming that the particles settle according to Stokes Law. After the last reading the mixture was resuspended and a 25 ml aliquot was taken at a depth of 15 cm. Another sample was taken and centrifuged at 10000 rpm for 20 minutes. A 25 ml aliquot was taken after centrifugation, and both aliquots were dried at $105^{\circ}C$ overnight. The former sample (representing silt + clay + dissolved solids) and the latter sample (representing dissolved solids) were used to calculate the total silt

plus clay. Summing the total weight of the sands and the calculated weight of the silt plus clay equaled the total weight of the sample. Selected data from this analysis is presented in the following sections, and additional data is located in Appendix C.

Bulk Density. Three or four 60+ cm³ clods were used to determine bulk density (SCS, 1984). After the volume was determined the clods were dried at 105° C for 24 to 48 hours at which time they were weighed. The saran coat was removed by heating the clod to 500° C for 4 hours. The clod material was sieved through a 2-mm sieve and the weight of the coarse fragments was determined. Bulk density of the fine fraction (<2 mm) was then calculated (Appendix D).

Moisture Retention. Moisture characteristic curves were determined for all horizons investigated using clods not used in the bulk density determination. The clods were cut with a diamond saw to create a flat surface and saturated from the bottom with water. A thin layer of saturated kaolinite and tissue paper was used to cover the pressure plates to improve hydraulic contact between the clods and the plate. Moisture contents by volume of the fine fraction (<2 mm) were determined at pressures of 10, 30, 50, 70, 90, 100, 200, 400, and 1500 kPa (computer program in Appendix D). Measurements were made when equilibrium was reached (no outflow of water from the plates for 12 hours), usually after one week. Data from the primary pedons is discussed in the text, other data is located in Appendix C.

Results

Profile Descriptions of Primary Pedons

Pedon 1. Pedon 1 has developed in loamy till overlain by a thin (40 to 50 cm thick) mantle of aeolian material (Table 10, Figures 9 and 10). The upper horizons have a low coarse fragment content reflecting an aeolian influence. The influence of aeolian material decreases in the Bw2 and is absent in the Bt. A strong plow layer is still evident even though the area has been out of cultivation for over 50 years (John Spencer, personal communication, 1985). Argillans up to 1 mm thick occur through the Bt and into the 2Btx horizons but do not extend into the BCm. A weak platy structure becomes noticeable in the lower Bw2 and strengthens throughout the Bt and into the 2Btx horizons. At the boundary between the Bt and 2Btx1 some albans occur and some uncoated sand grains (skeletons) adhering to ped faces and some albans are present. Fragipan horizons are typified by bleached prism faces (BPF) (Figure 11) that form a polygonal network. Some BPF appear as non-continuous isolated vertical streaks. Weak development of BPF is visible in the Bt whereas the 2Btx1 has better expressed BPF. Brittle behavior was noted in the 2Btx horizons but not in other horizons. The lower boundary of the 2Btx2 is abrupt at the 3BCm in what appears to be a lithologic discontinuity (Figure 12). The 3BCm is a moderately cemented sand and gravel layer where individual fragments are typically stained with iron and manganese. Some of the stains common to the BCm extend into the upper portions of

Table 10. Selected morphological features of Pedon 1.

Hor.	Color	Mottles	Texture; Structure; Consistence	Special features
Ap	10YR 3/3	none	Fine sandy loam; Granular; Loose	Abundant roots
Bw1	10YR 4/6	none	Fine sandy loam; Weak sub-angular blocky; Very friable	Common roots; common krotovinas some with neoalbans in center
Bw2	10YR 5/8	none	Fine sandy loam; Weak sub-angular blocky; Friable	as Bw1 and some krotovinas are sand filled; weak argillans; weak plates at boundary
Bt	10YR 5/4	10YR 6/1 7.5YR 4/6	Fine sandy loam; Weak platy; Friable to firm	Common argillans; few faint vertical bands grade into BPF; roots follow ped faces; few skeletans and albans more common with depth
2Btx1	10YR 4/6 7.5YR 4/6	10YR 6/1 7.5YR 5/6	Loam; Weak platy, coarse prismatic; Firm and brittle	BPF common 10-20 cm apart; roots confined to BPF; common argillans; few mangans; and skeletans
2Btx2	10YR 4/6 7.5YR 4/6	10YR 6/1 10YR 7/1 10YR 7/2 7.5YR 5/6	Loam; Platy, coarse prismatic; Very firm and brittle	as 2Btx1 with some Fe cemented areas at lower boundary; BPF are 40 cm apart; mangans are more common with depth

Continued, next page

Table 10 cont.

3BCm	7.5YR 4/4 10YR 4/6 5YR 3/4	none	Coarse sand; Structureless; Hard	Cemented by Fe and Mn
4Cd	7.5YR 5/6 7.5YR 5/0 N 6/0	none	Fine sandy loam; Platy; Firm to friable	Banded and stained by Fe from overlying horizon

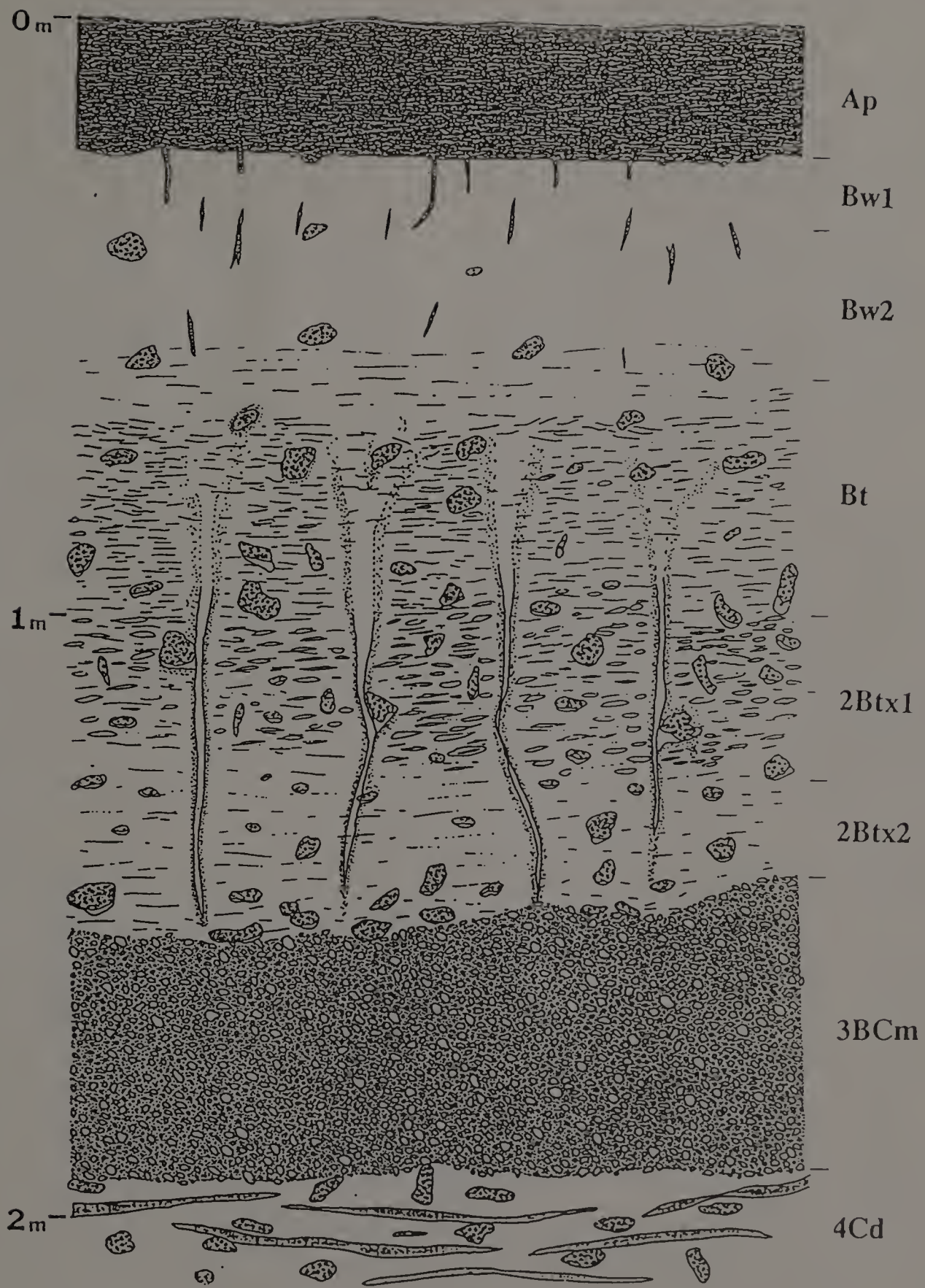


Figure 9. Cross-sectional diagram of Pedon 1.

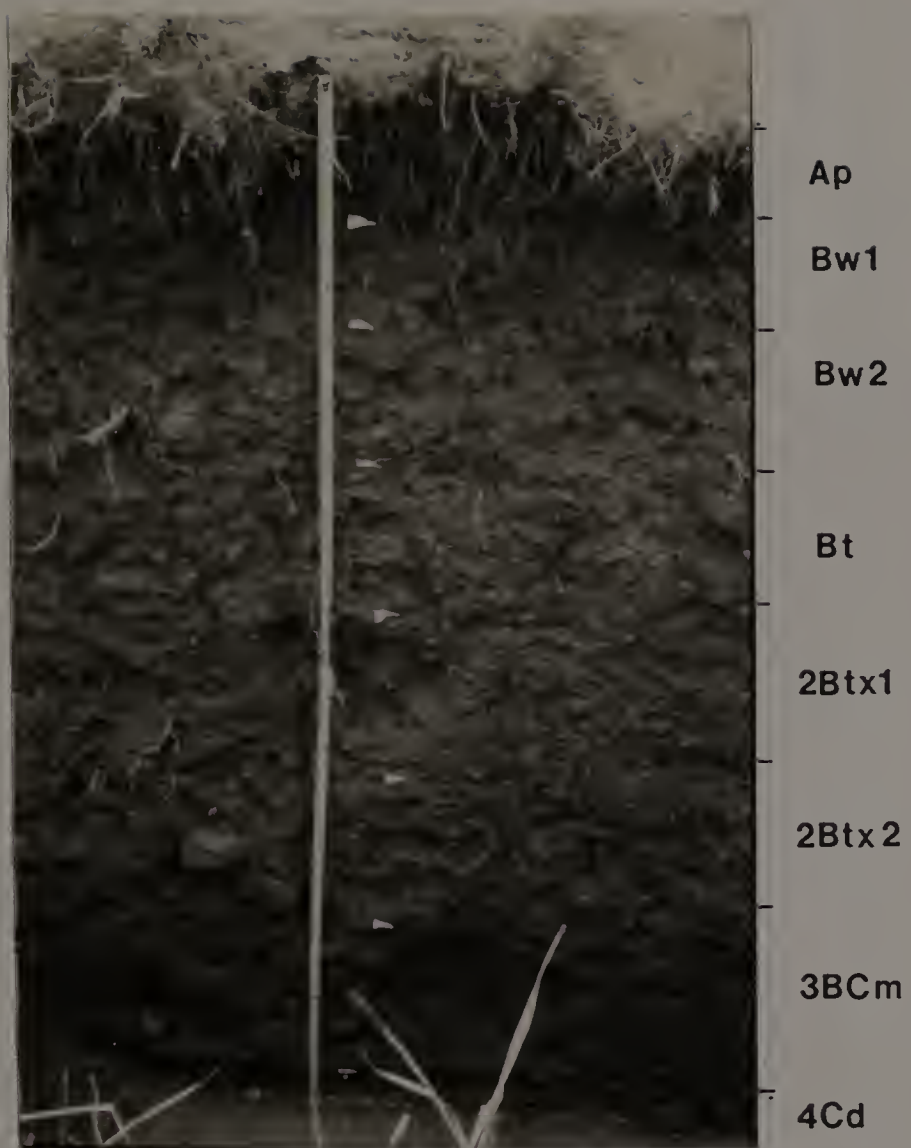
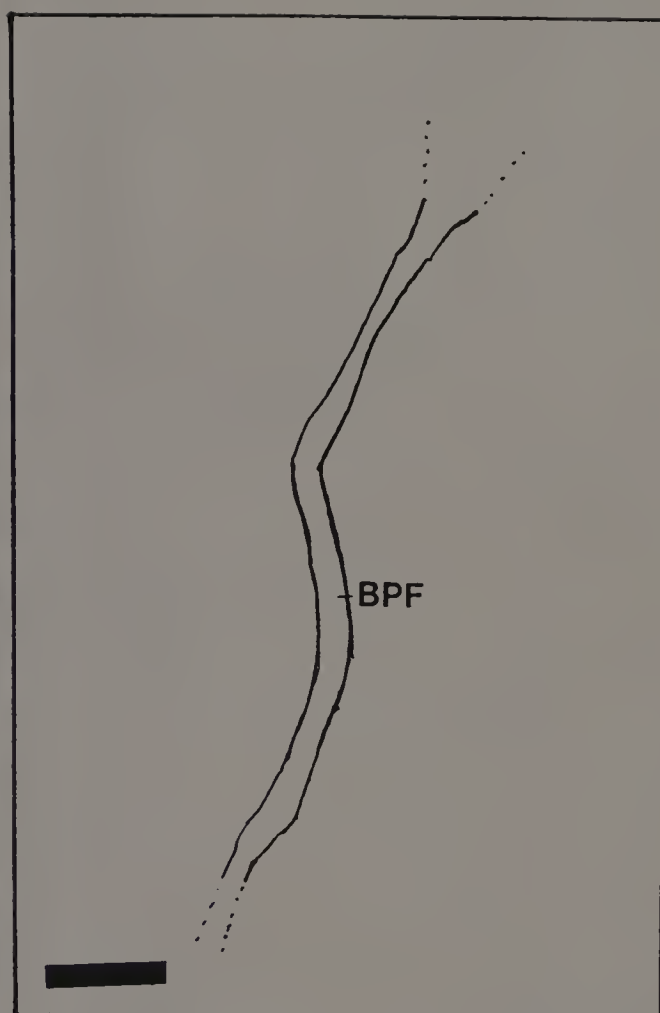


Figure 10. Photograph of Pedon 1.



A

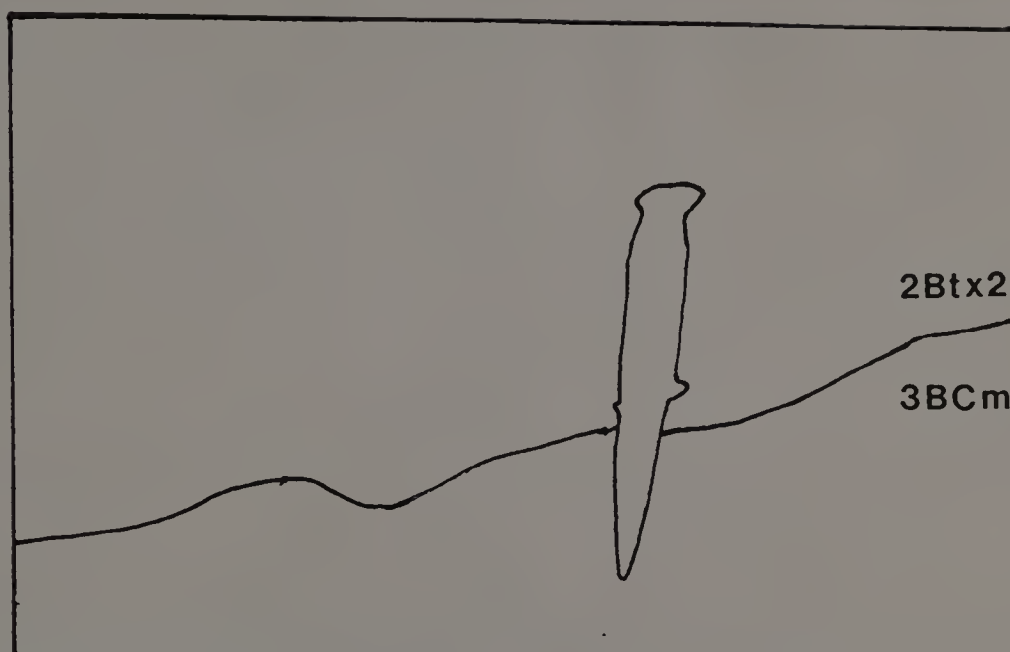


B

Figure 11. Bleached prism face (BPF) in 2Btx1 of Pedon 1.
 (A) photograph, (B) schematic. The bar is 5 cm.



A



B

Figure 12. Contact between 2Btx2 and 3BCm horizons in Pedon 1. (A) photograph, (B) schematic. The knife handle is 8 cm long.

the 4Cd. The 4Cd was not examined in great detail as it was below the water table during sampling.

Pedon 2. Pedon 2 has developed on loamy till with a slightly thinner aeolian mantle (30 to 40 cm) than the one observed in Pedon 1 (Table 11, Figures 13 and 14). The Ap boundary is still distinct despite limited agricultural activity at the site in the recent past. Mixing between the till and aeolian component occurs in the BE as evidenced by the complicated color patterns and increase in coarse fragment content. Krotovinas occur throughout the Bw's and BE although the frequency decreases with depth. In some instances krotovinas appear to terminate a few centimeters above the initiation of BPF in the 2Btx1. BPF in the upper portion of the 2Btx1 are wider than at their terminus in the 2Btx2. Argillans are rare in the lower BE occurring in conducting pores often adjacent to skeletans. The frequency and thickness of argillans increases in the the 2Btx horizons where they are observed occurring on peds and coarse fragments and coating some interiors of voids. The BPF and brittleness allow for the identification of the fragipan. The pan effectively excludes roots except within the BPF (Figure 15). The interior of the BPF is generally gray with a 1 to 4-cm reddish-brown Fe-stained rind between the BPF interior and the matrix of the fragipan. Type 2 mottles (gray or reduced interiors with reddish-brown exteriors or rinds) increase in frequency and size through the lower 2Btx1 and into the 3Cd1. These mottles are most pervasive in the 2BCd where the BPF terminate. The soil on the undersides of some rock fragments is of the same color as that within the BPF, and in the

Table 11. Selected morphological features of Pedon 2.

Hor.	Color	Mottles	Texture; Structure; Consistence	Special features
Ap	10YR 4/2	none	Fine sandy loam; Granular; Friable	Abundant roots
Bw1	10YR 5/4	none	Fine sandy loam; Granular; Friable	Common roots; common krotovinas
Bw2	10YR 6/6	10YR 4/6	Fine sandy loam; Weak sub-angular blocky; Friable	as Bw1 and some krotovinas contain skeletans
BE	10YR 6/6 10YR 5/3 2.5Y 5/4	10YR 7/1 7.5YR 4/4	Fine sandy loam; Weak sub-angular blocky; Friable to firm	Common roots in krotovinas; common skeletans in vughs; rare argillans
2Btx1	2.5Y 4/2 2.5Y 4/4	10YR 7/1	Fine sandy loam; Weak platy, coarse prismatic; Firm and brittle	BPF common 50-70 cm apart; roots confined to BPF; common argillans; few mangans
2Btx2	2.5Y 4/4 2.5Y 5/4	5Y 7/1 7.5YR 4/4	Fine sandy loam; Weak platy, coarse prismatic; Very firm and brittle	as 2Btx1 platy character increases with depth; mottling increases with depth.

Continued, next page

Table 11 cont.

2BCd	2.5Y	4/4	2.5Y 5/2 7.5YR 4/4	Fine sandy loam; Platy; Firm	BPF end; rocks have a bleached area around them; common argillans and mangans on plates
3Cd1	2.5Y	4/4	2.5Y 5/2 7.5YR 4/4	Fine sandy loam; Platy; Firm to friable	Stone line; rare argillans; rocks surrounded by bleached area
3Cd2	2.5Y 2.5Y	4/4 5/4	2.5Y 5/2 7.5YR 4/4	Fine sandy loam; Platy; Firm to friable	Rare argillans; common ferrans; many mangans on plates
3Cd3	2.5Y	4/2	7.5YR 4/4 2.5Y 5/2	Fine sandy loam; Platy: Friable to firm	as 3Cd2

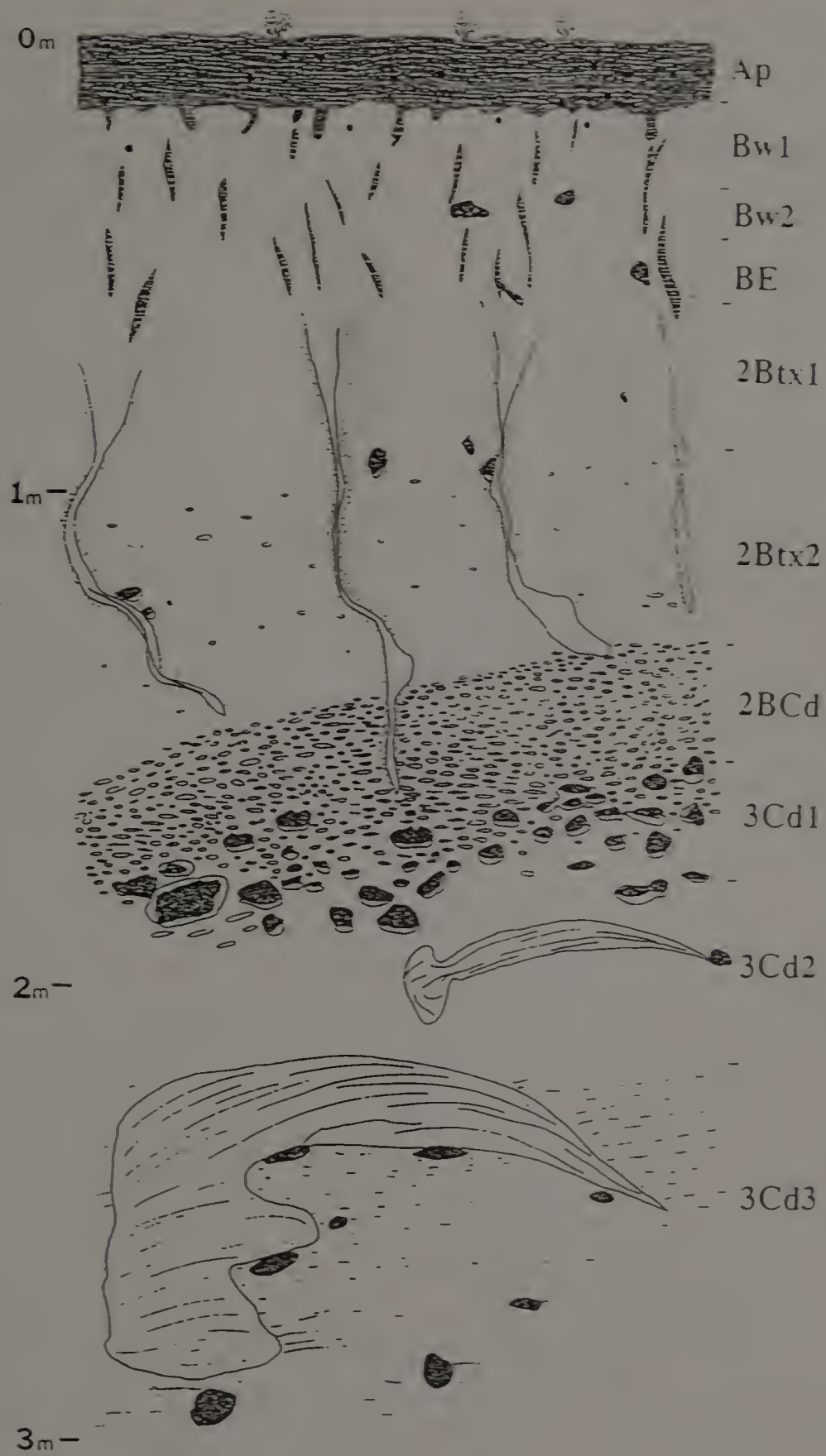


Figure 13. Cross-sectional diagram of Pedon 2.

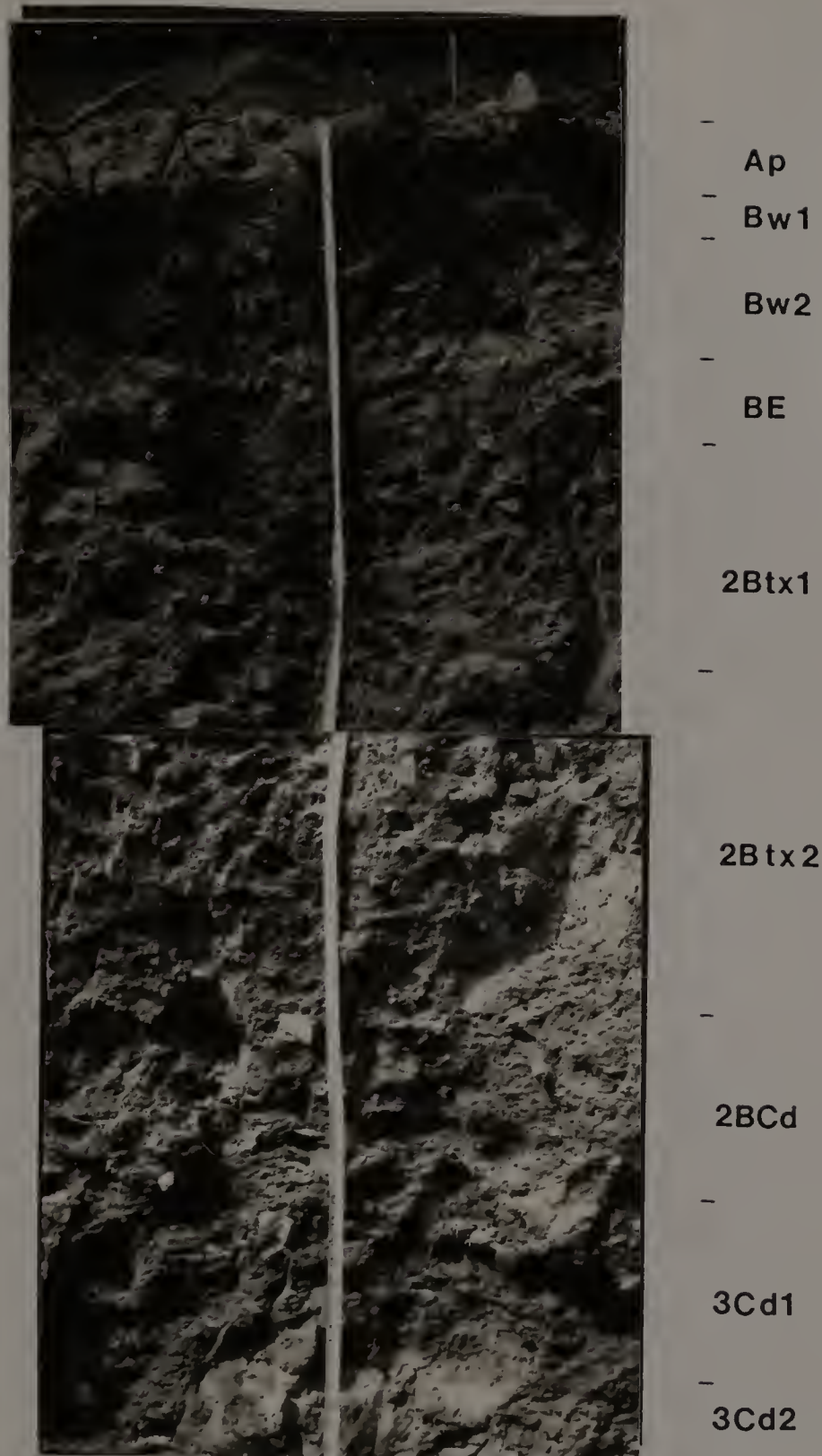
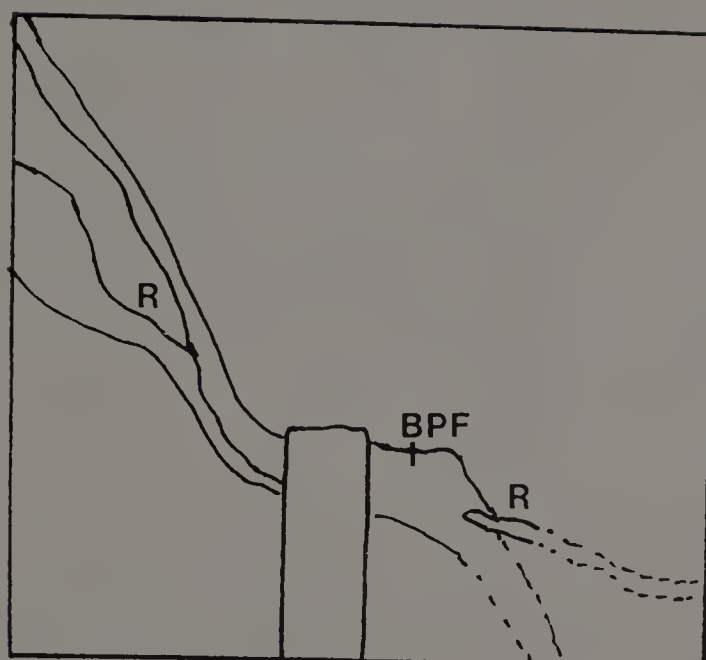


Figure 14. Photograph of Pedon 2.



A



B

Figure 15. Bleached prism face (BPF) containing roots (R) in the 2Btx1 of Pedon 2. Note that in the bottom right of the photograph the roots is sticking out of the profile face. (A) photograph, (B) schematic. The white bar is 10 cm long.

3Cd1 this zone completely surrounds most stones. A weak platy structure exists throughout the fragipan, intensifying in the 3Cd horizons. Commonly the plates are demarcated by mangans and ferrans.

A stone line is observed beneath the 2BCd within the 3Cd1. This feature appears to separate the weathered till (B horizons) from the unweathered till (Figure 16). Mottling ceases below the 3Cd1 and argillans become scarcer with depth, whereas plates are still coated with Fe and Mn. A sorted, laminated, non-continuous sand lens 20 to 80 cm thick occurs within the 3Cd2 and 3Cd3, and is probably an inherited feature from the deposition of the till (Figure 17). The bottom of the pit was at 270 cm below the surface and did not intersect the water table.

Pedon 3. Pedon 3 has developed on loamy till with an aeolian mantle similar in thickness to Pedon 2 (Table 12, Figures 18 and 19). The Ap boundary is smooth and abrupt except where krotovina extend into the Bw. Coarse fragment content increases quickly from the Ap to the Bw. Vesicles, some containing skeletans, are rare at the base of the Bw becoming more common within the BE (Figure 20). Krotovinas are spaced further apart in the BE and do not extend into the 2Btx1. Type 2 mottles occur in the lower BE overlying the fragipan. The BE contains both individual skeletans and channel argillans whereas the fragipan horizons predominantly contain argillans. Roots become scarcer with depth and as with Pedon 2 occur only within BPF in the fragipan. The BPF, similar in appearance to those observed in Pedons 1 and 2, terminate at the top of the 2BCd which is morphologically similar to the 2BCd in Pedon 2. Structure varies from a weak

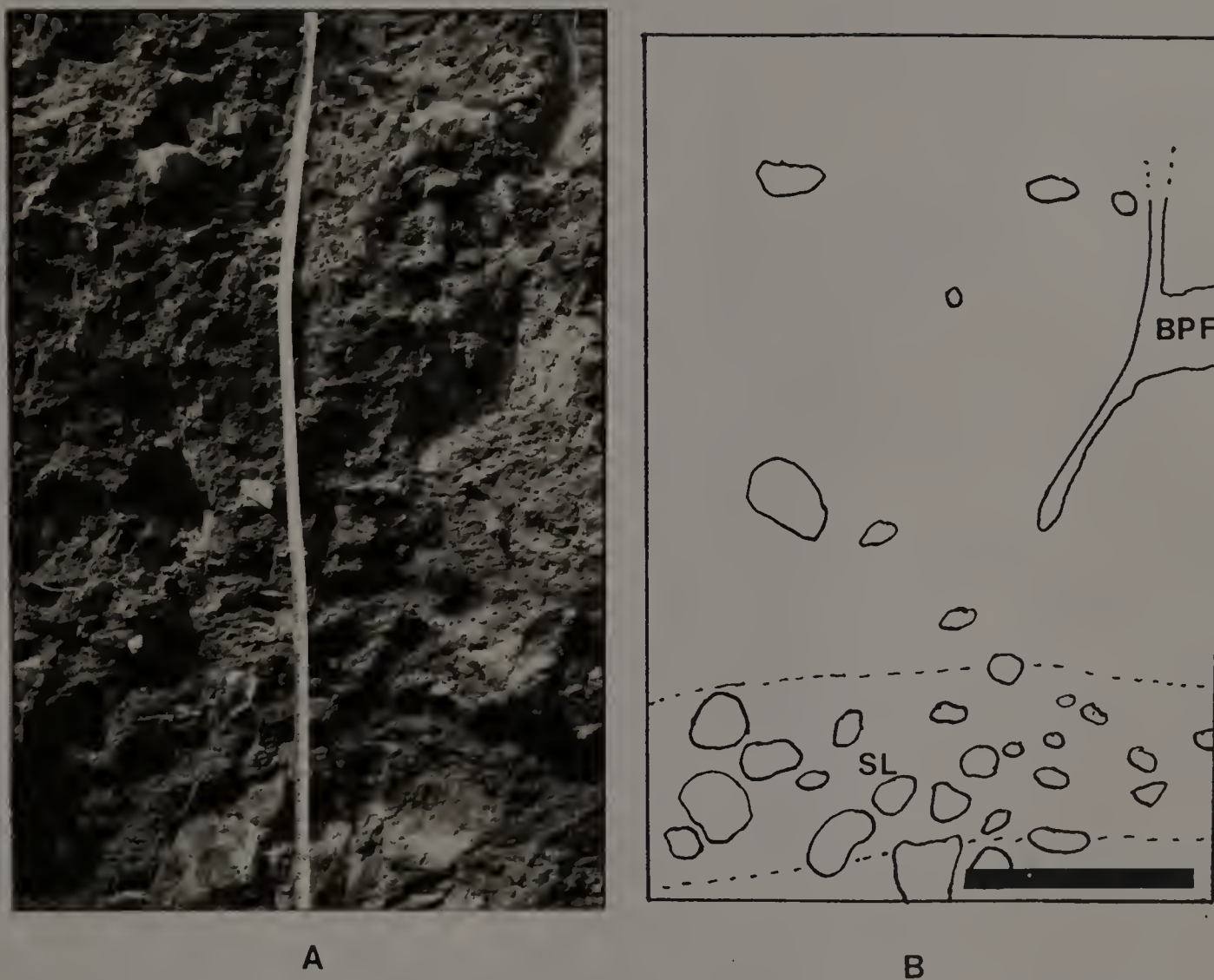
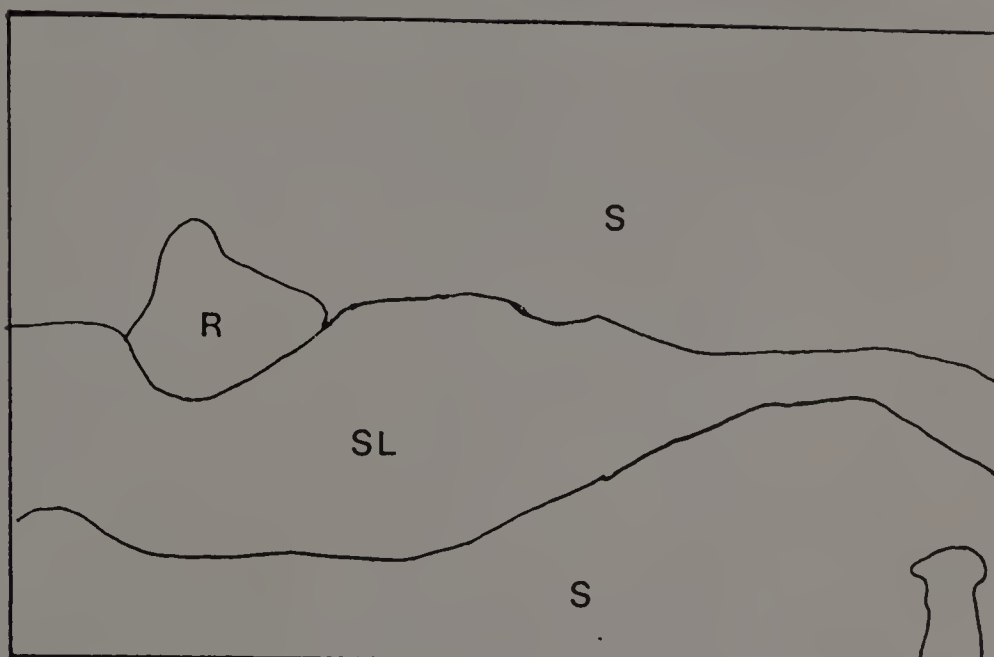


Figure 16. Stone line (SL) in the 3Cd1 horizon of Pedon 2. Note the bleached prism face (BPF) terminates above the SL in the 2BCd horizon. Some coarse fragment positions are denoted based on casts (indentations) that they made when the pit was first opened and the face cleaned. (A) photograph, (B) schematic. The bar is 30 cm.



A



B

Figure 17. Sand lens (SL) in the 3Cd2 horizon (S) of Pedon 2. Note the laminations in the sand and the coarse fragment resting above the SL. (A) photograph, (B) schematic. The top of the knife handle is 2 cm across.

Table 12. Selected morphological features of Pedon 3.

Hor.	Color	Mottles	Texture; Structure; Consistence	Special features
Ap	10YR 3/3	none	Fine sandy loam; Granular; Friable	Abundant roots
Bw	10YR 5/6	none	Fine sandy loam; Weak sub- angular blocky; Friable	Common roots; common krotovinas some with neoalbans and skeletans in center; few vesicles with skeletans occur at base of horizon
BE	10YR 5/3	10YR 6/1 7.5YR 5/8	Fine sandy loam; Weak sub- angular blocky; Friable to firm	as Bw; common skeletans; few argillans; weak plates at boundary
2Btx1	10YR 4/3 10YR 5/3	10YR 6/1 7.5YR 5/8 7.5YR 4/6	Fine sandy loam; Weak platy, coarse prismatic; Firm and brittle	BPF begin and contain few roots; common argillans; few skeletans associated with BPF; few mangans and ferrans on peds and rocks
2Btx2	10YR 3/3 7.5YR 3/4	10YR 6/1 7.5YR 5/8 7.5YR 4/6	Fine sandy loam; Weak platy, coarse prismatic; Firm and brittle	BPF terminate; other features as in 2Btx1

Continued, next page

Table 12 cont.

2BCd	7.5YR 3/4 10YR 5/3	10YR 6/1 7.5YR 5/8 7.5YR 4/6	Fine sandy loam; Weak platy; Firm	Few argillans on plates; common mangans and ferrans on plates and rocks; no vesicles
3Cd1	7.5YR 3/4	10YR 6/4	Fine sandy loam; weak platy; Firm to friable	as 2BCd
3Cd2	7.5YR 3/4	none	Fine sandy loam; Weak platy; Friable to firm	Common mangans on plates

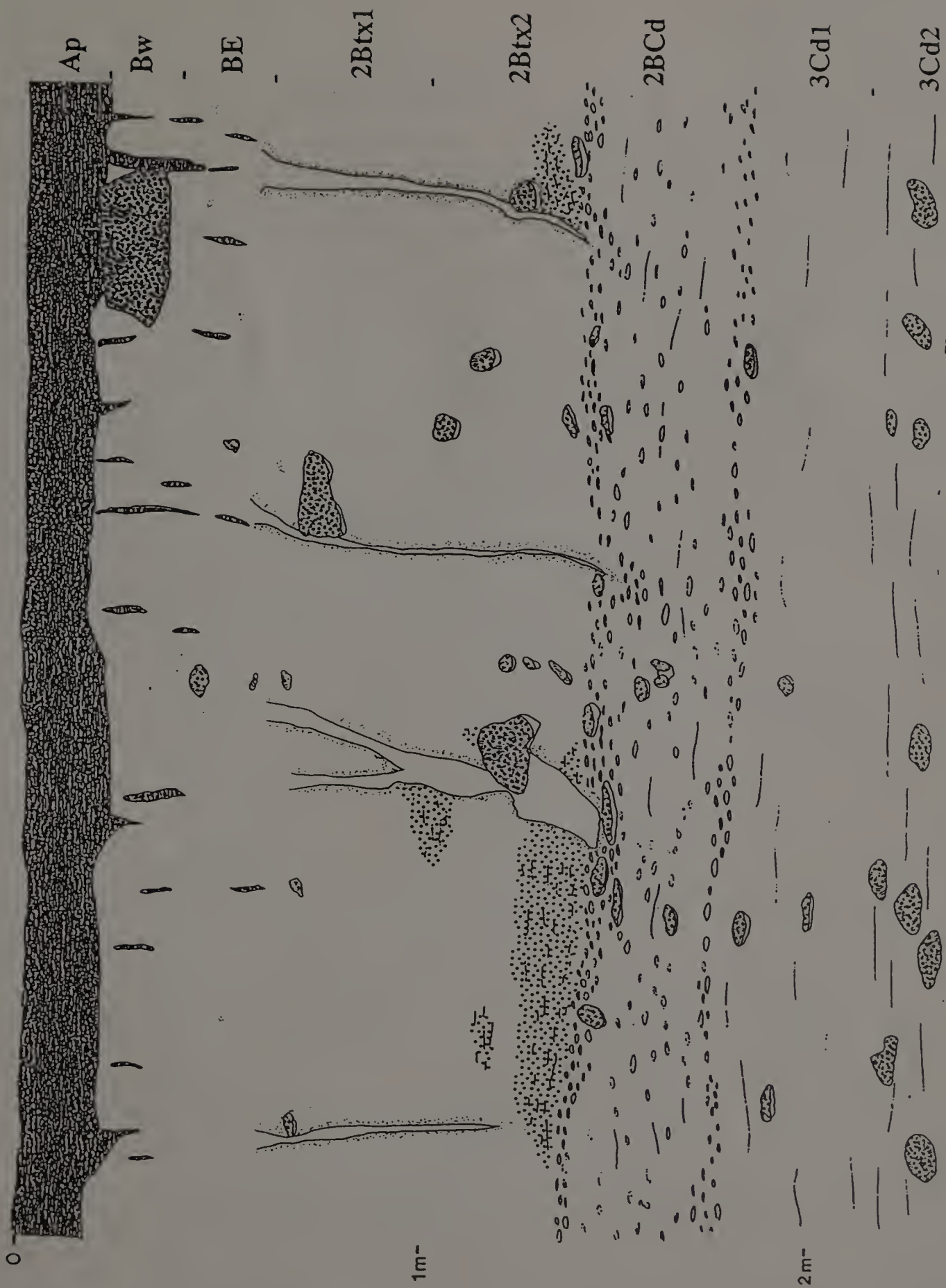


Figure 18. Cross-sectional diagram of Pedon 3.

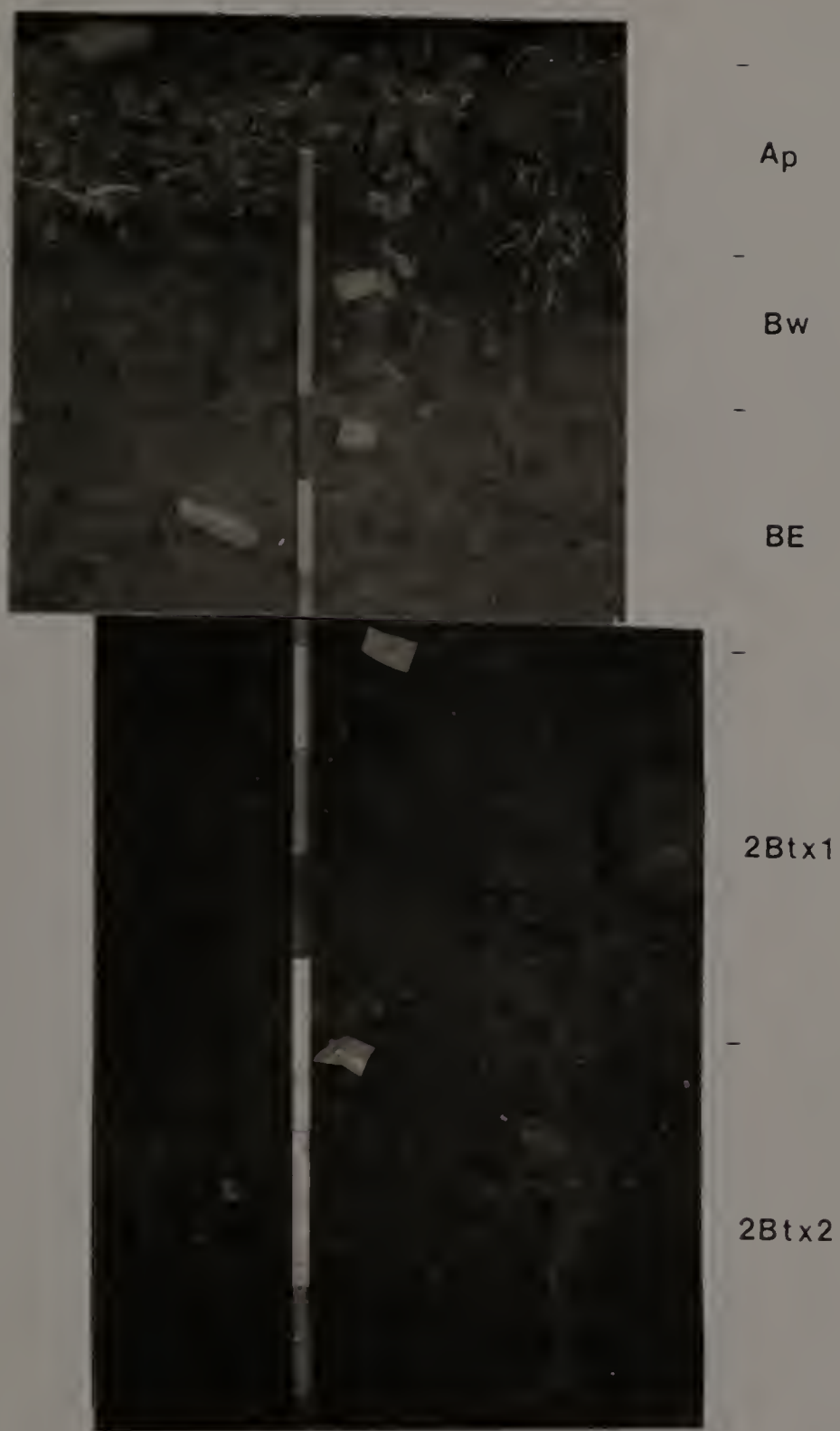
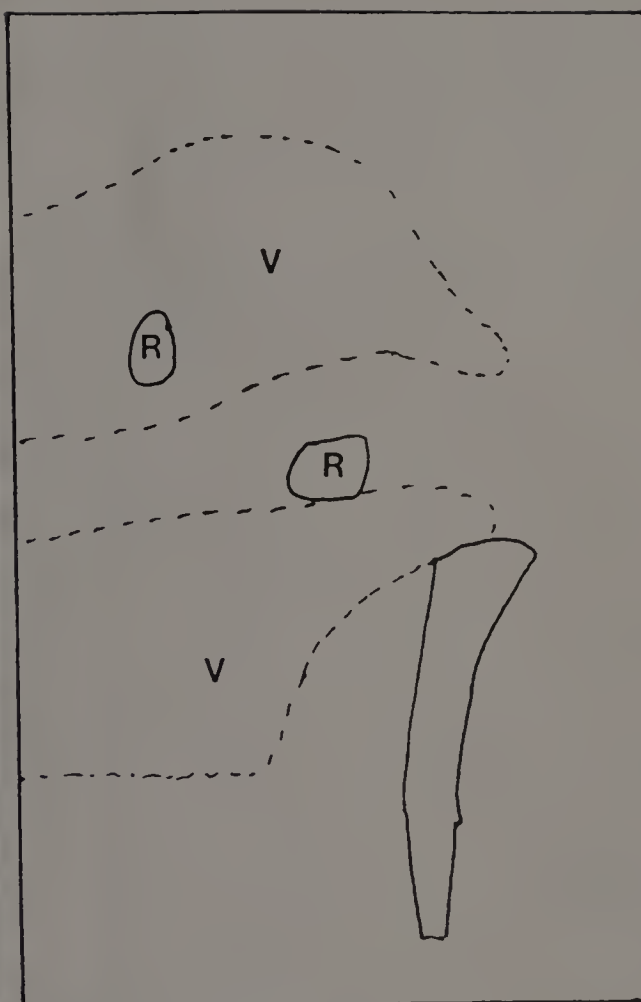


Figure 19. Photograph of Pedon 3.



A



B

Figure 20. Areas of vesicular pores (V) in the BE of Pedon 3. Note how the areas are irregular and noncontinuous. Also coarse fragments (R) occur in both zones. (A) photograph, (B) schematic. The knife handle is 6 cm long.

granular/sub-angular blocky in the upper horizons to a moderate platy structure in the Cd horizons. The plates are coated by Mn and Fe and may contain small, faint mottles. The fragipan has the strongest consistency although the Cd's can be firm and approximately 30% of the BE is firm and brittle. Some coarse fragments are arkosic and probably derived from the nearby Triassic formations. At the time of sampling the water table was at 200 cm and had been observed as high as 120 cm (Pickering, 1983).

Pedon 4. Pedon 4 is located approximately 75 meters east of Pedon 3. It is developed on loamy till with a 50 to 60-cm thick aeolian cap (Table 13, Figures 21 and 22). Most of the features observed in this Pedon are similar to those seen in Pedon 3, however due to a change in drainage class (Pedon 3 is well-drained and Pedon 4 is moderately well-drained) the colors in Pedon 4 are brighter. The BPF are prominent and their termini are distinct (Figure 23). Also of note in this profile are the gray areas surrounding most large coarse fragments (Figure 24) similar to those observed in the 3Cdl horizon of Pedon 2. At the time of sampling the water table was observed at 40 cm below the surface.

Pedon 5. Pedon 5 is the only primary pedon that has developed in sandy till and is somewhat poorly to poorly drained (Table 14, Figures 25 and 26). As with the other pedons, Pedon 5 has a aeolian cap 40 to 50 cm thick. The drainage conditions make the contact between the Ap and the Bw distinct. High chroma mottles are common within the Ap, Bw, and BE, whereas low chroma mottles begin to appear in the Bw and are common throughout the B and 2BC horizons. The BE and 2BC horizons

Table 13. Selected morphological features of Pedon 4.

Hor.	Color	Mottles	Texture; Structure; Consistence	Special features
Ap	10YR 3/2	none	Fine sandy loam; Granular; Loose	Abundant roots
Bw1	10YR 4/6	7.5YR 5/8	Fine sandy loam; Weak sub-angular blocky; Friable	Common roots; common krotovinas some with neoalbans in center; common vesicles; few sekeletans
Bw2	10YR 5/6	10YR 5/3 10YR 6/3	Fine sandy loam; Weak sub-angular blocky; Friable	as Bw1; rare argillans
BE	10YR 5/4 7.5YR 4/4	10YR 5/3 7.5YR 5/2	Fine sandy loam; Weak sub-angular blocky; Friable to firm	as Bw2; common skeletans; few argillans; weak plates at boundary
2Btx1	7.5YR 4/4	5Y 6/1 7.5YR 5/8	Fine sandy loam; Weak platy, coarse prismatic; Firm and brittle	BPF begin and contain few roots; common argillans; common skeletans associated with BPF; few mangans and ferrans on peds and rocks

Continued, next page

Table 13 cont.

2Btx2	7.5YR 4/4	5Y 6/1	Fine sandy	BPF terminate; albans occur on the undersides of rocks; other features in 2Btx1
	7.5YR 3/4	10YR 7/1	loam;	
	7.5YR 5/8	Weak platy, coarse prismatic; Firm and brittle		
2BCd	7.5YR 4/4	5Y 6/1	Fine sandy	Few argillans on plates; common mangans and ferrans on plates and rocks; no vesicles
	7.5YR 3/4	7.5YR 5/8	loam;	
	10YR 7/1	Weak platy; Firm		
3Cd	7.5YR 4/4	7.5YR 5/8	Fine sandy loam; Weak platy; Firm to friable	Common mangans on plates

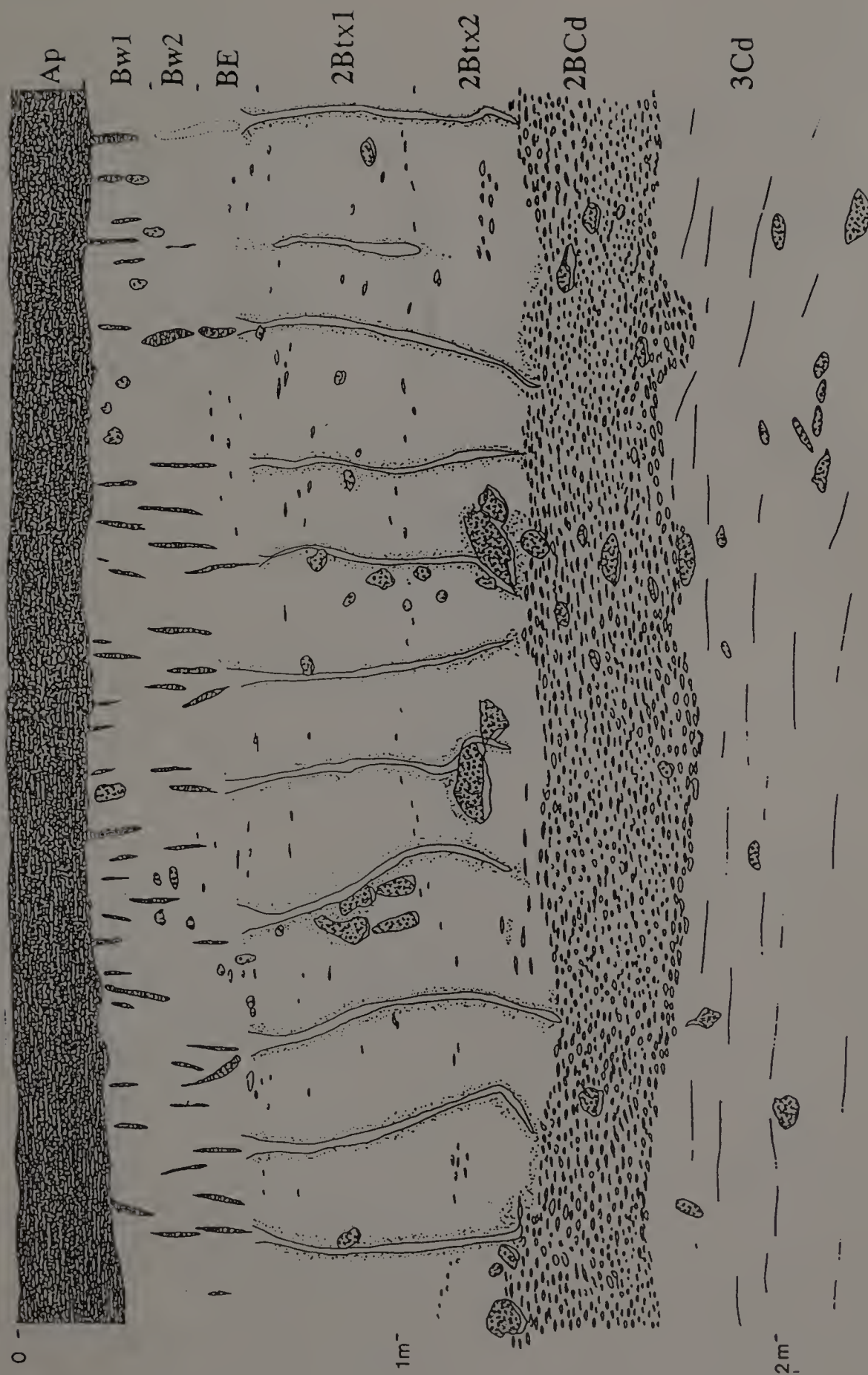


Figure 21. Cross-sectional diagram of Pedon 4.

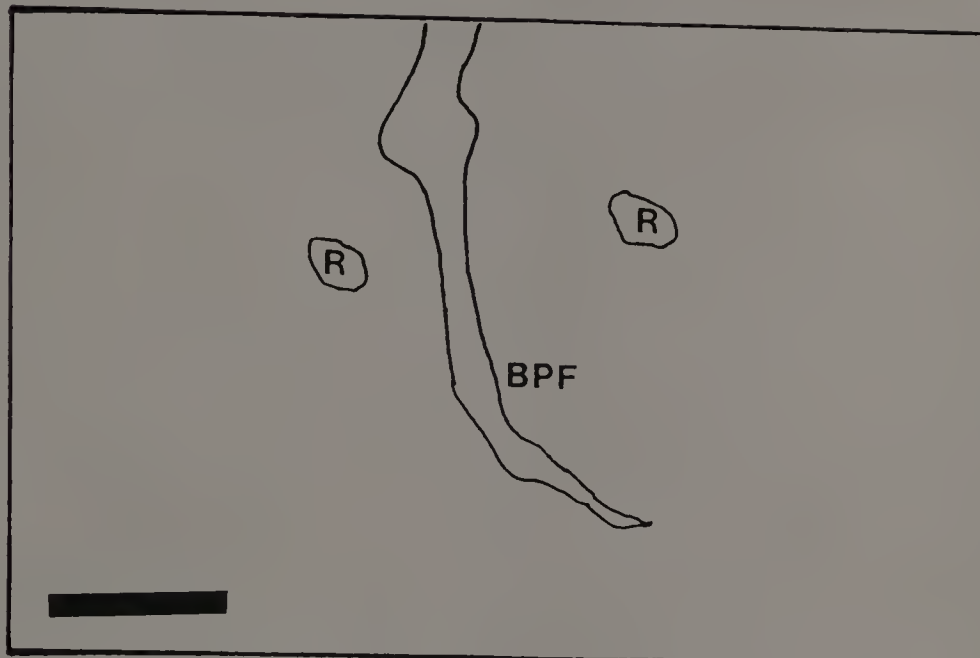


-
Ap
-
Bw1
-
Bw2
-
BE
-
2Btx1
-
2Btx2
-
2BCd
-
3Cd

Figure 22. Photograph of Pedon 4.



A

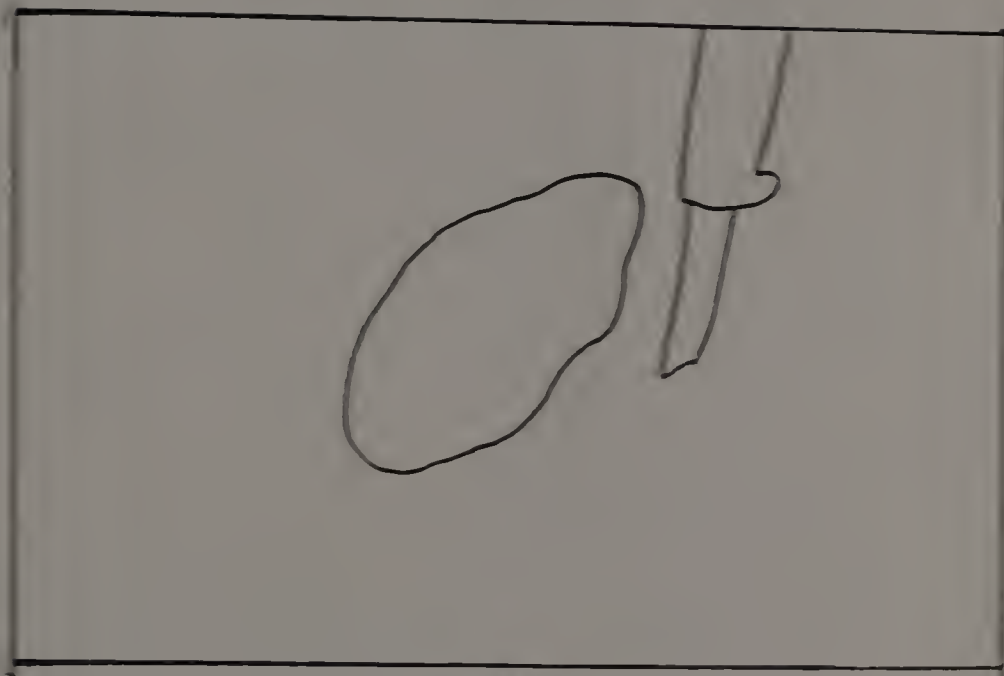


B

Figure 23. Termination of bleached prism face (BPF) at the top of the 2BCd horizon in Pedon 4. R denotes coarse fragments. (A) photograph, (B) schematic. The bar is 5 cm.



A



B

Figure 14 Gray or bleached area around coarse fragment in 2Btx2 horizon of Pedon 4. The zone is approximately 1 cm thick and appears lighter in the photograph. (A) photograph, (B) schematic. The knife handle is 1 cm thick.

Table 14. Selected morphological features of Pedon 5.

Hor.	Color	Mottles	Texture; Structure; Consistence	Special features
Ap	10YR 3/1 10YR 3/2	7.5YR 5/6	Fine sandy loam; weak platy to blocky; Friable	Abundant roots
Bw	10YR 5/4 10YR 6/4	10YR 7/1 7.5YR 5/6	Fine sandy loam; Weak sub- angular blocky; Friable	Common roots; common krotovinas
BE	10YR 6/3	10YR 7/1 7.5YR 5/6	Loamy sand single grain to granular; Friable to slightly firm	as Bw and some krotovinas are sand filled; common albans and skeletans
2EB	10YR 7/2 10YR 5/3 10YR 5/4 7.5YR 4/6	10YR 7/1	Loamy fine sand; Weak platy; Friable to firm	Common lenses of firm material surrounded by sand; few roots; rare argillans; few mangans rocks; few vesicles; BPF are faint at base of the horizon
2Btx1	10YR 5/3 10YR 6/4	7.5YR 4/6	Loamy fine sand; weak platy, coarse prismatic; Firm and brittle	BPF common; neoalbans and quassiferrans associated with some voids; common mangans on surfaces; common argillans; common skeletans in BPF

Continued, next page

Table 14 cont.

2Btx2	5Y 4/6 10YR 5/1	7.5YR 4/6	Fine sandy loam; weak platy, coarse prismatic; Firm and brittle	as 2Btx1; BPF narrow and terminate at base of horizon; few vesicles
2Cd1	5GY 6/1	none	Fine sandy loam; Platy; Firm to friable	Very few argillans; few mangans; common silt caps
2Cd2	5GY 6/1	none	Loamy fine sand; Platy; Firm	as 2Cd1

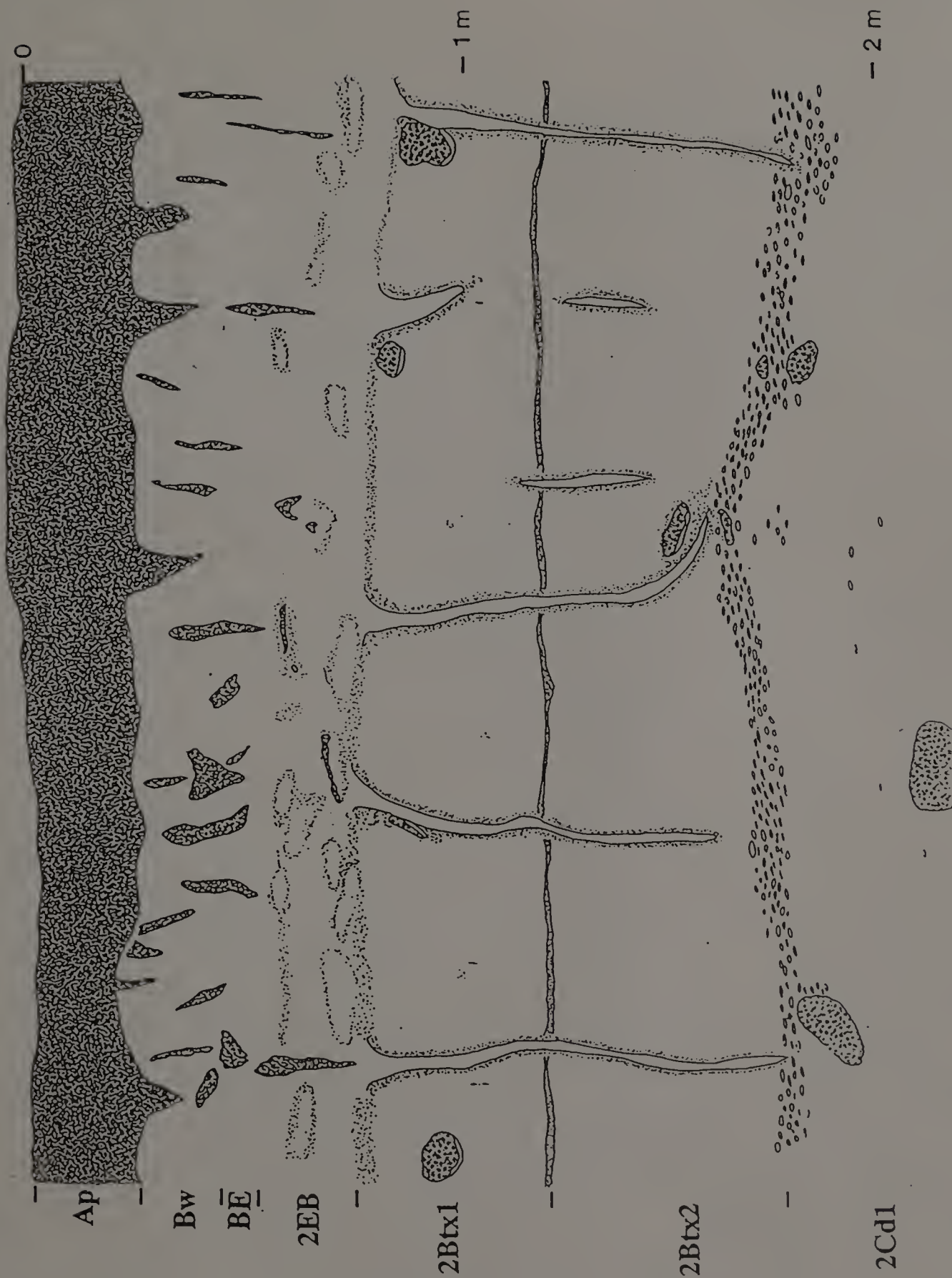


Figure 25. Cross-sectional diagram of Pedon 5.

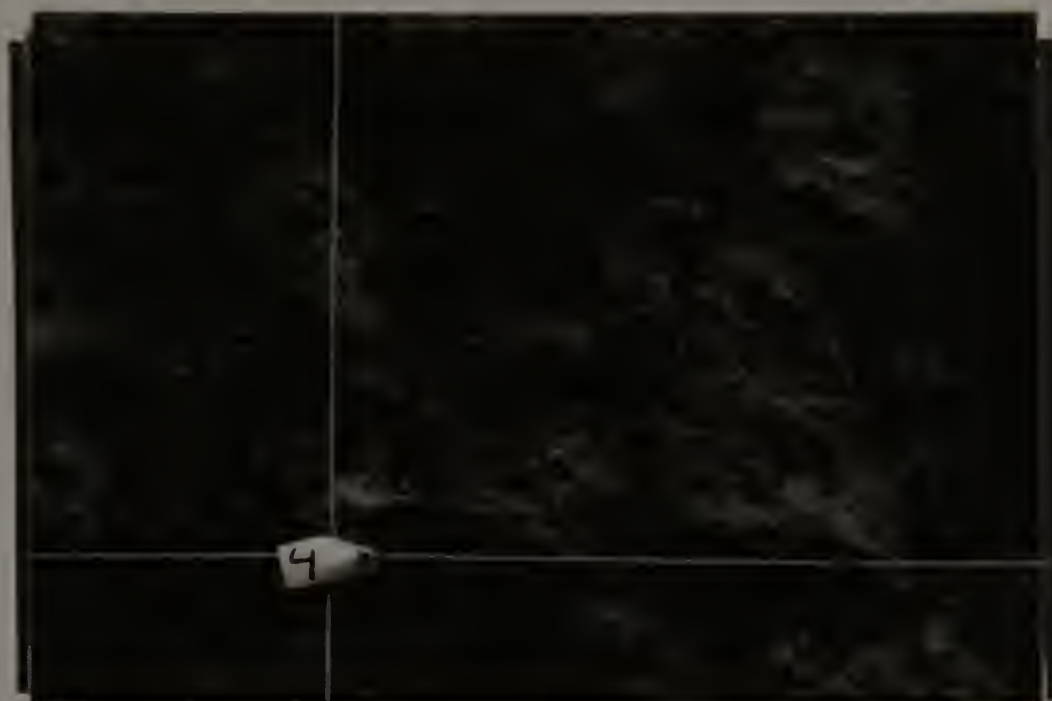


Figure 26. Photograph of Pedon 5.

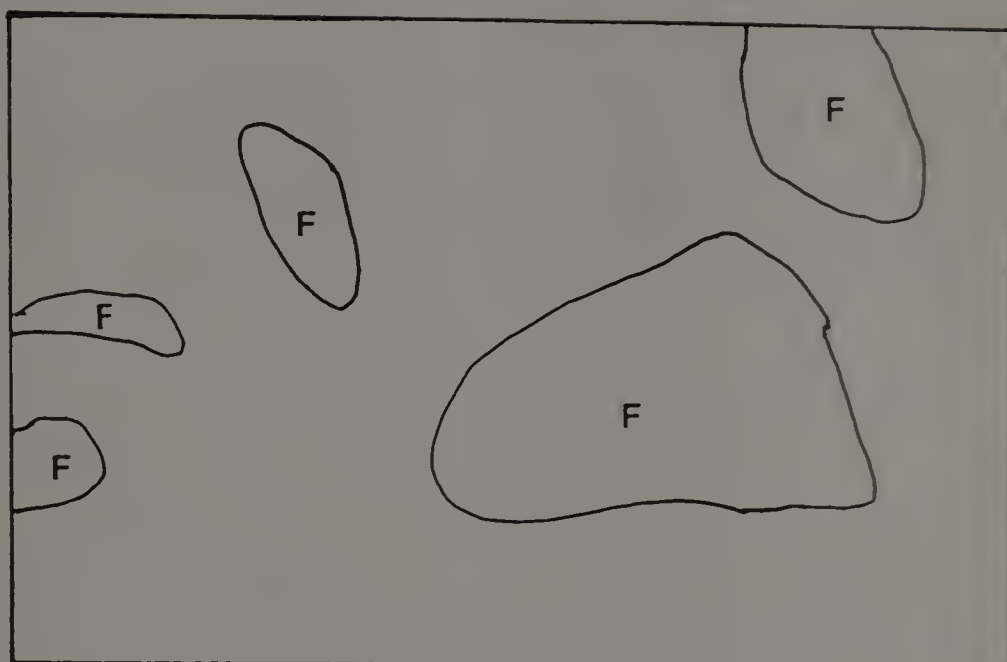
contain lenses of firm material, similar to fragipan material, with sandier margins; the sandy margins appear more extensive in the BE (Figure 27). The sandy zones commonly contain clean sand grains at the outer margins and very thin argillans in the interiors. The frequency and size of the sandy lenses decrease with depth grading into a weak platy structure in the fragipan. The fragipan (2BCtx1 and 2BCtx2) is identified by BPF and firm, brittle behavior. The BPF begin in the lower 2BC and commonly occur under large krotovinas. The interiors of the BPF are grayer than the matrix and are bounded by a thin, Fe-stained rind (Figure 28). Argillans are common on peds, coarse fragments and voids. Neoalban, quasiferrans occur in association with some of the larger voids, and some of the plates are thinly coated with Fe and Mn. Also common within the fragipan are silt caps on top of most coarse fragments. The majority of the coarse fragments are tonalite. About half of these fragments are grussified (rotten), the others show little evidence of weathering. The water table at the time of sampling was observed at 30 cm although it has been observed at or near the ground surface (Reed, 1989).

Description of Selected Till Sites

The till sites investigated can be broken down into two groups based on the type of exposure: the Ayer group (Leicester, Barre, and Ayer) are large exposures with Upper and both facies of the Lower Till, and the Charlemont group (Charlemont and Buckland) are small exposure of the unoxidized Lower and Upper Till. Descriptions for



A



B

Figure 27. Firm lenses (F) surrounded by loose, sandier material in the 2EB horizon of Pedon 5. (A) photograph, (B) schematic. The bar is 5 cm.

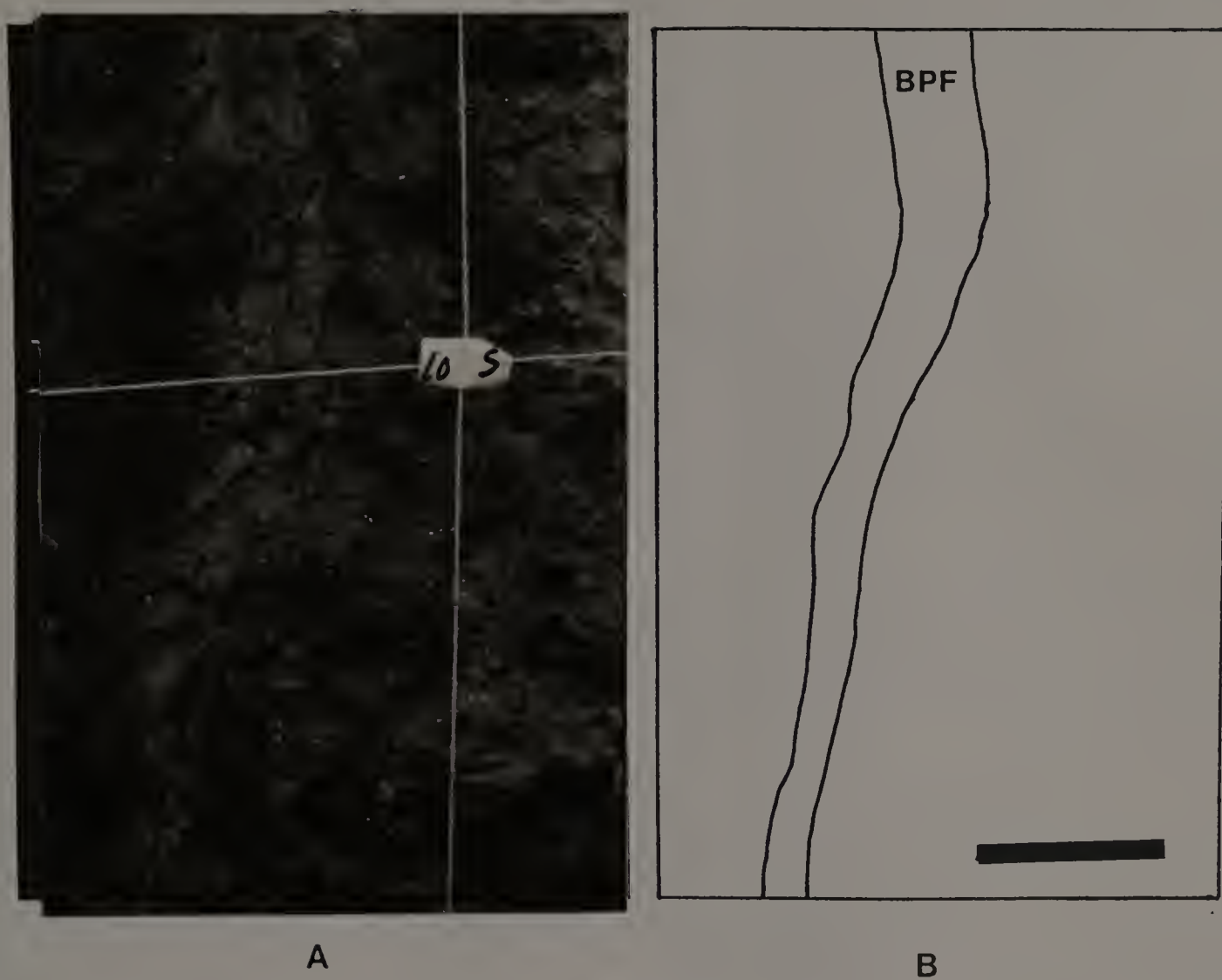


Figure 28. Bleached prism face (BPF) in the 2Btx2 horizon of Pedon 5. Note the fine dark streak of roots and organic material running down the center of the BPF. (A) photograph, (B) schematic. The bar is 5 cm.

all members of each group are presented in Appendix B whereas only one description for each is presented in the text.

The Ayer Group. The site in Ayer is located in a till strip mine which was cut into a drumlin in the Pingryville section of Ayer. The Lower Till is being mined for landfill cover for use throughout the state and this exposure changes daily. Upper Till was observed as a surficial drape over the Lower Till in an 8 by 3-meter thick section where the intervening contact was not exposed. The remaining area of this site consisted of a 25-meter thick exposure of oxidized and unoxidized Lower Till (Table 15). The contact between oxidized and unoxidized facies was inferred because the head wall containing the presumed contact was unscalable at the time of sampling.

The Lower Till is massive and hard with colors ranging from gray to olive (Figures 29). Joints are common in both facies although they are more closely spaced at the top of the oxidized facies. Throughout much of the section well sorted layers of very fine sand, silt, or clay occur. These laminae are commonly contorted over an amplitude of 10 to 20 cm by subglacial shearing (Figure 30). The beds increase in frequency with depth and are interrupted by a 50-cm thick horizontal coarse sand bed which is crosscut by fine grained dikes of silt and clay. Beneath this layer the number of discrete bands of silt and clay decrease and eventually disappear.

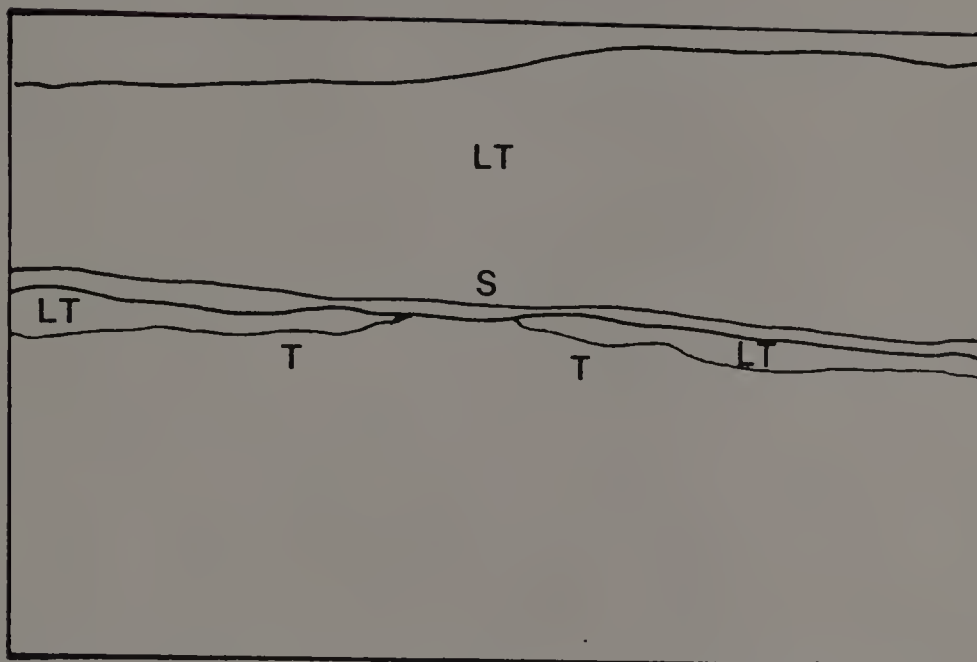
The limited exposure of the Upper Till is characterized by a loose, sandy 1.5-meter zone overlying a slightly denser sandy zone. Lenses of denser till along with discontinuous beds of water worked sediment also occur throughout the deposit. This till is much stonier

Table 15. Selected morphological features of the Ayer till site.

Depth in meters	Color	Features
<u>Upper Till</u>		
1.0-2.5	2.5Y 6/2	Loose to hard, sandy till with bands of water worked material
2.5-4.5	5Y 6/4	Firm to friable, sandy till with thin silty bands
<u>Lower Till</u>		
0-2.0	5Y 4/3	Fissile, firm to friable, oxidized till with 5YR 3/4 staining (ferrans and mangans) on plates
2.0-3.0	5Y 4/3	Fissile, hard oxidized till with staining on plates and thin clustered sand veins
3.0-10.0	5Y 4/3	Massive, hard oxidized till other features as above
10.0-12.0	5Y 4/4	Massive, hard oxidized till with less joints or plates but common sand veins
12.0-17.0	5Y 4/2	Massive, hard unoxidized till with deformed silt/clay beds prevalent
17.0-21.0	5Y 4/2	As above with more silt/clay beds showing more deformation
21.0-21.7	2.5Y 5/4	Slighly compact but very friable coarse saturated sand
21.7-25+	5Y 4/1 5GY 4/1	Massive, hard unoxidized till with numerous deformed silt/clay beds

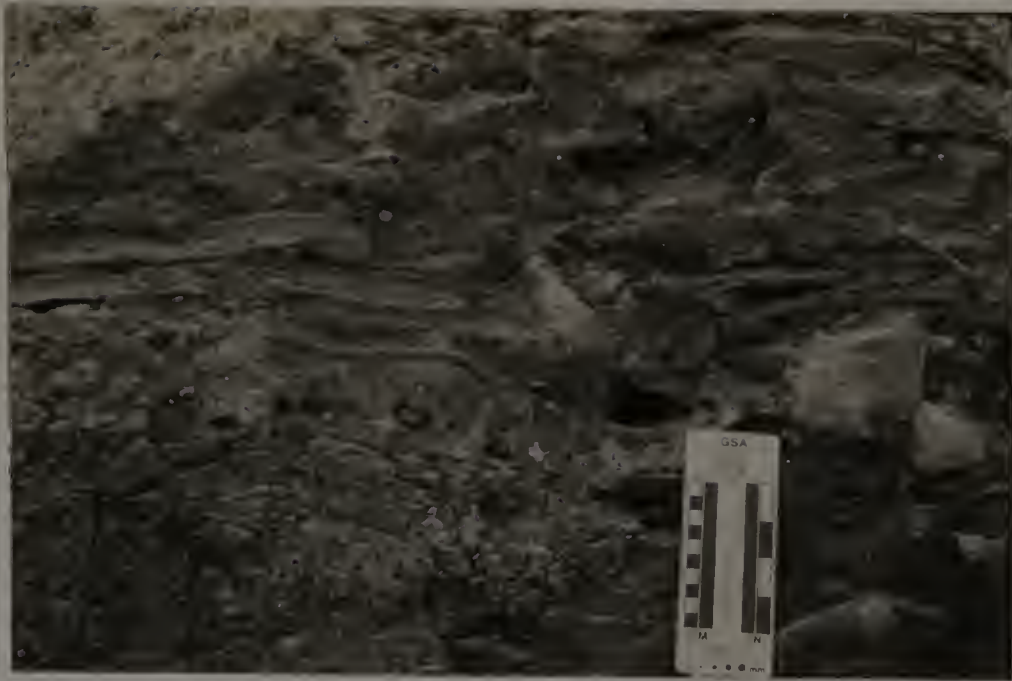


A

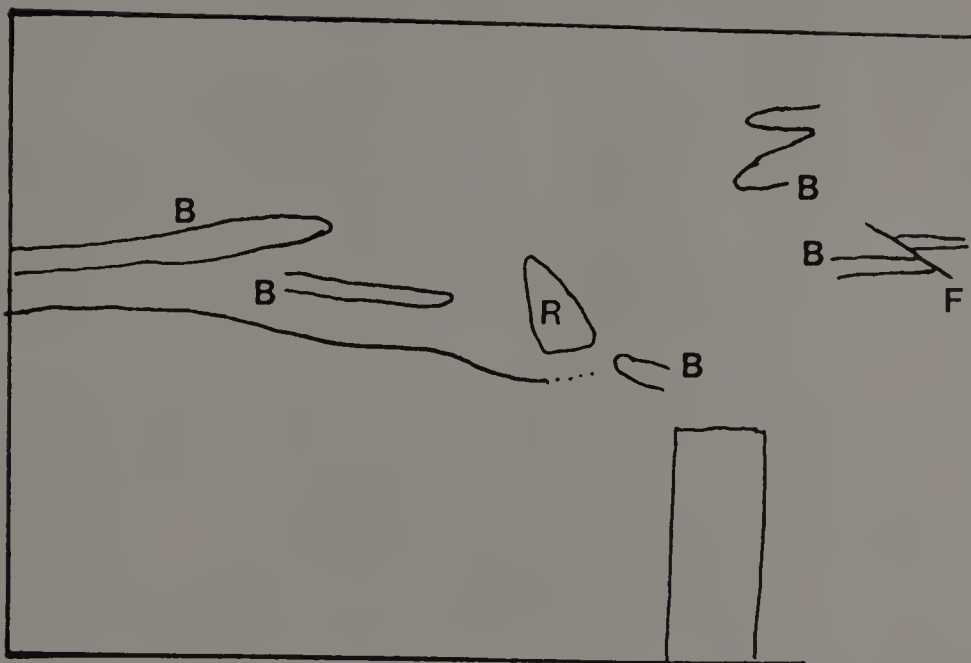


B

Figure 29. Unoxidized Lower Till, Ayer. LT - Unoxidized Lower Till, T - Talus, Sand - Sand layer. Note that the sand layer appears darker due to water flowing from it. (A) photograph, (B) schematic.



A



B

Figure 30. Silt/clay beds (B) and faults (F) in the Lower Till, Ayer. (A) photograph, (B) schematic.

than the Lower Till, but clasts are still matrix supported. Clasts in the Upper Till range from rounded to subangular shapes while the clasts in the Lower Till are predominantly subangular and angular.

The Charlemont Group Sections exposing both Upper and Lower Till occur along Albee Brook in Charlemont. The two tills are not seen in superposition, appearing to be separated by a bedrock high. The massive, dark gray (5Y4/1) unoxidized Lower Till occurs 600-800 meters upstream of the Upper Till outcrop. The till is massive and dark gray (5Y4/1) with numerous joints. The joint planes are enhanced by water flowing over the surface of the outcrop. Coarse fragments are angular and matrix supported (Table 16). The sandy, olive (5Y4/3-4) Upper Till exposure was masked by talus in its lower portions, however, a 3-meter thick section was available for inspection. Silt caps were common on the subangular matrix supported coarse fragments. Some of the coarse fragments were grussified while others of the same lithology were not. Olive yellow (5Y6/6) sand lenses and thin subvertical sand bands were common. Near the contact between the outwash and the till an iron stained yellowish brown (10YR5/8) band of till was observed.

Particle Size Analysis

Pedons 1 and 2 exhibit a slight fining with depth whereas the other 3 pedons coarsen with depth (Figures 31-35). Increases in the sand content are noticable in the BE horizons of Pedons 2 and 5 and in the BCm horizon of Pedon 1. In general the sand contents of Pedons 3 and 4 increase with depth, although not as sharply as in Pedon 5.

Table 16. Selected morphological features of the Charlemont till site.

Depth in meters	Color	Features
<u>Upper Till</u>		
1.2-2.2	5Y 4/3	Firm to friable sandy till with common silt caps
2.2-3.0	5Y 4/3	Firm sandy till, some plates present bounded by a thin sandier zone
3.0-4.0+	5Y 4/3	Firm platy sandy till with silt caps and sand lenses common
<u>Lower Till</u>		
0-1.0+	5GY 4/1	Massive, firm unoxidized till with numerous shear planes demarcated by thin slickensides

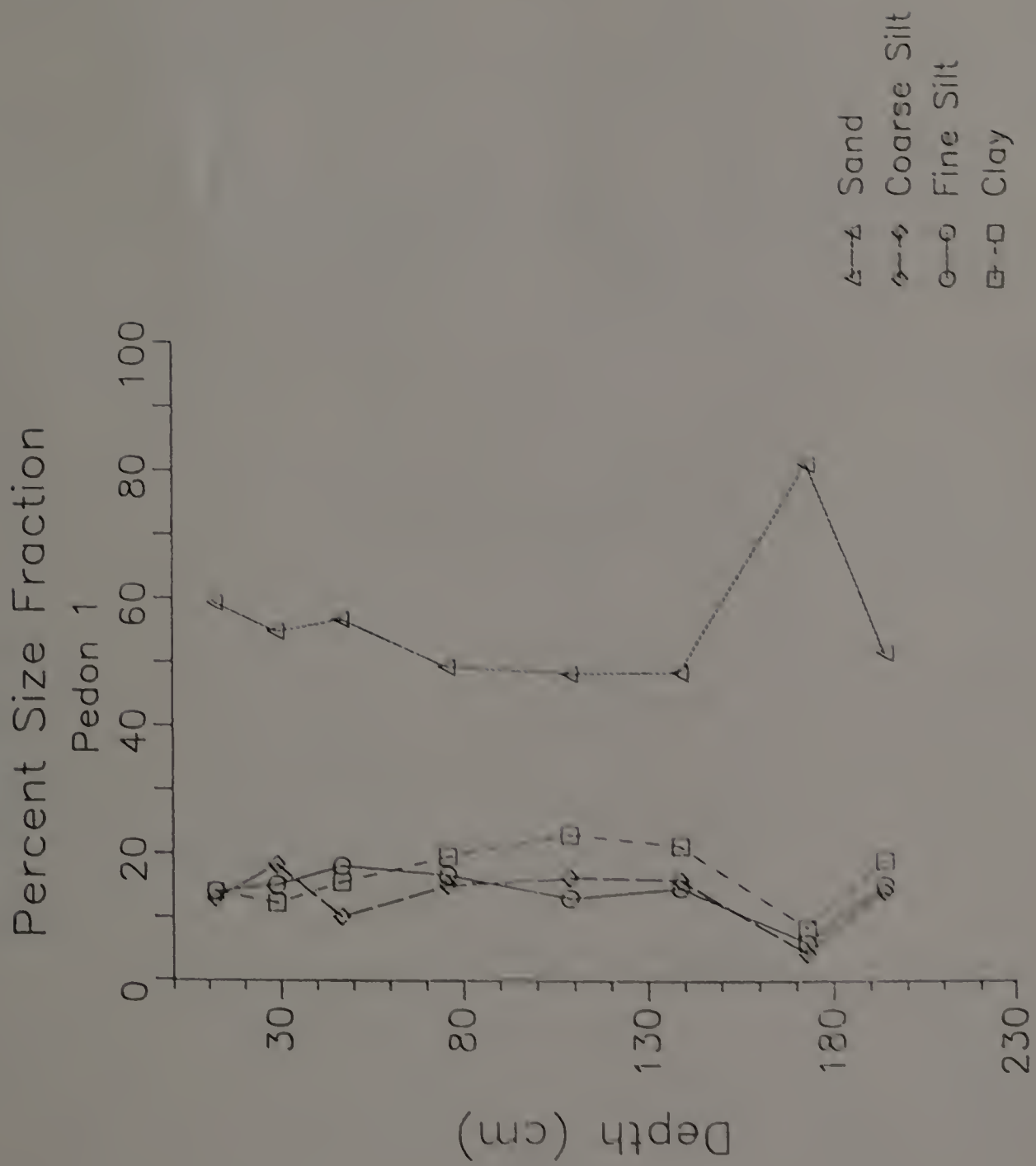


Figure 31. Soil separates (%) for each horizon by depth for Pedon 1.

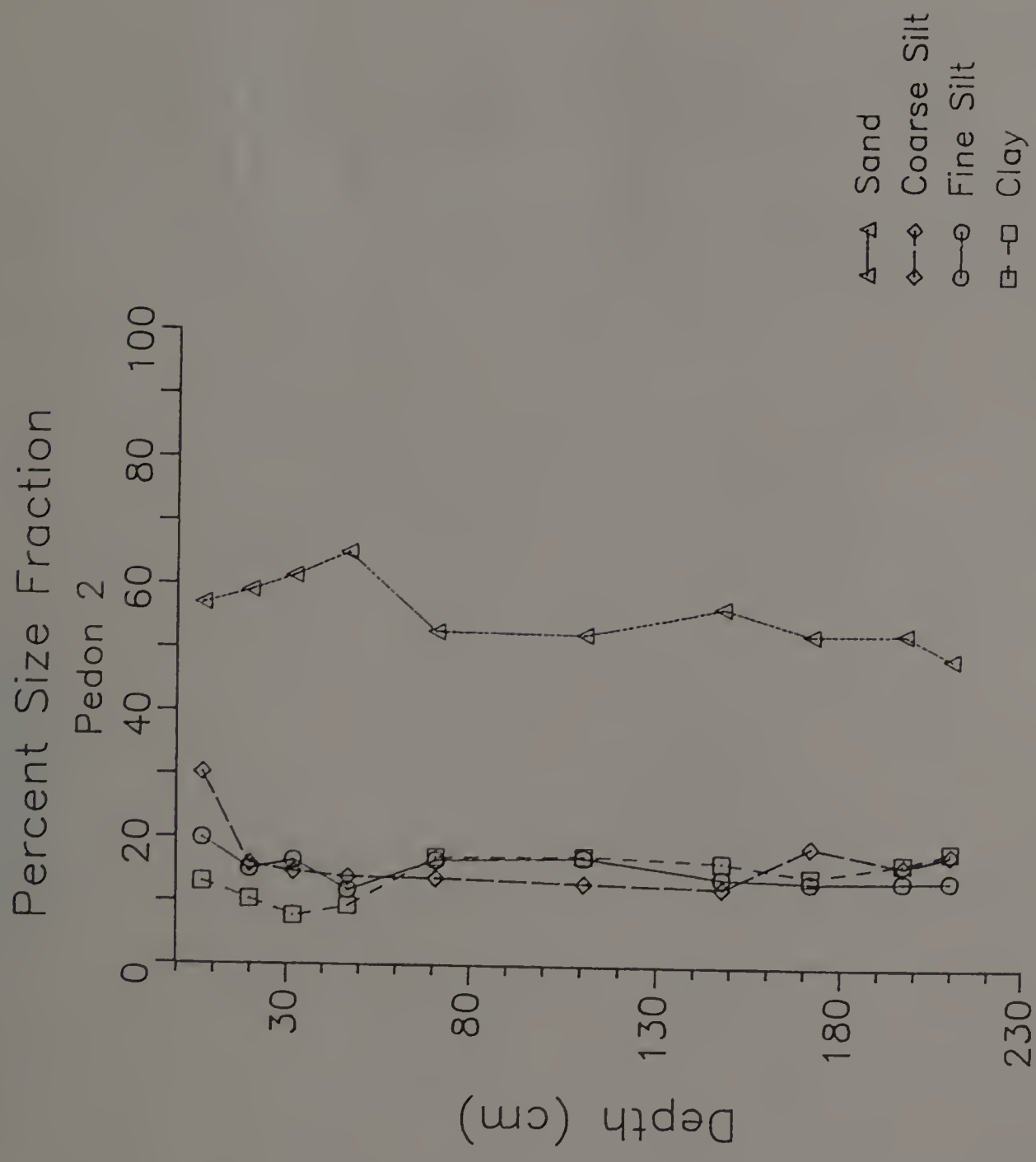


Figure 32. Soil separates (%) for each horizon by depth for Pedon 2.

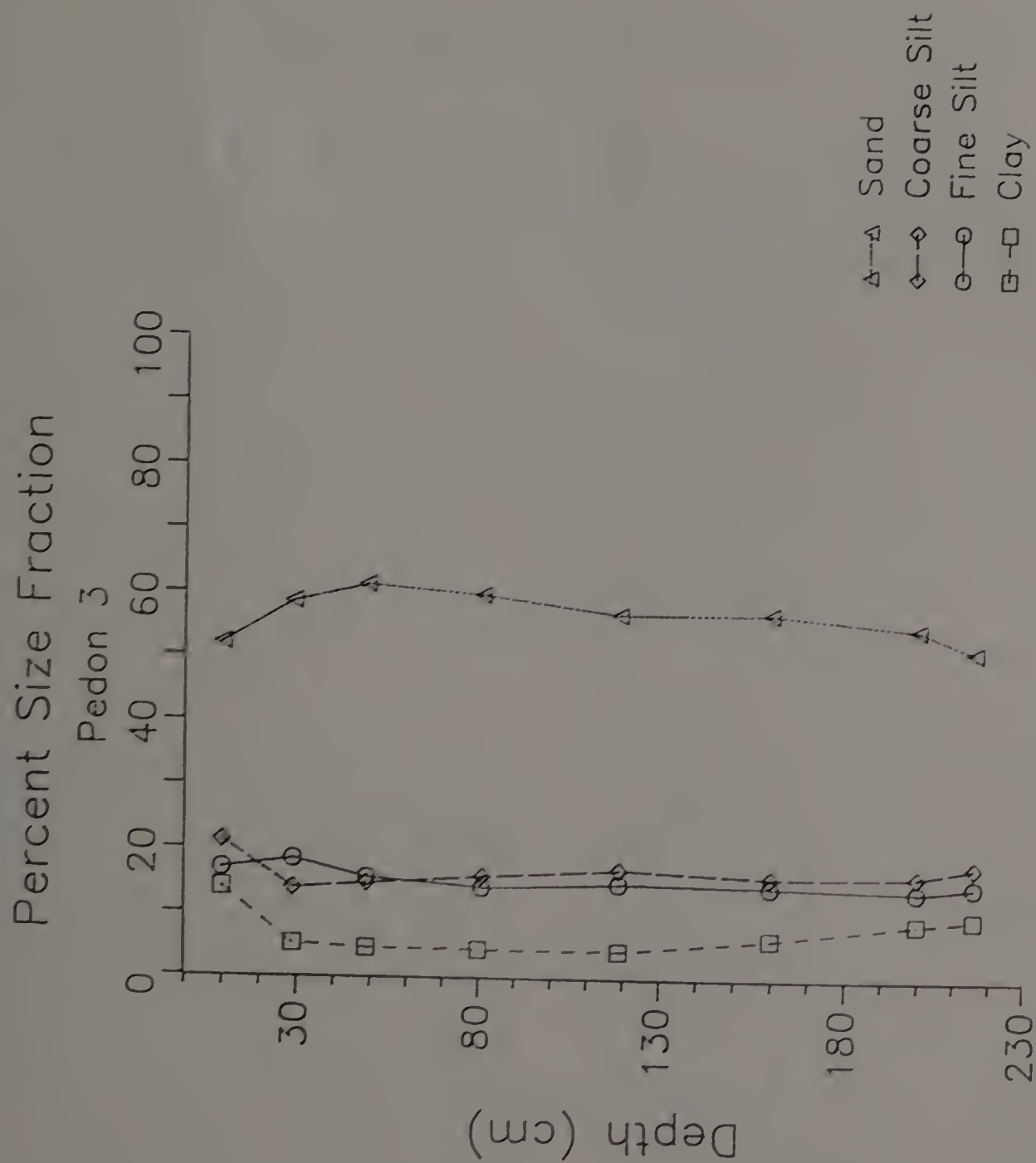


Figure 33. Soil separates (%) for each horizon by depth for Pedon 3.

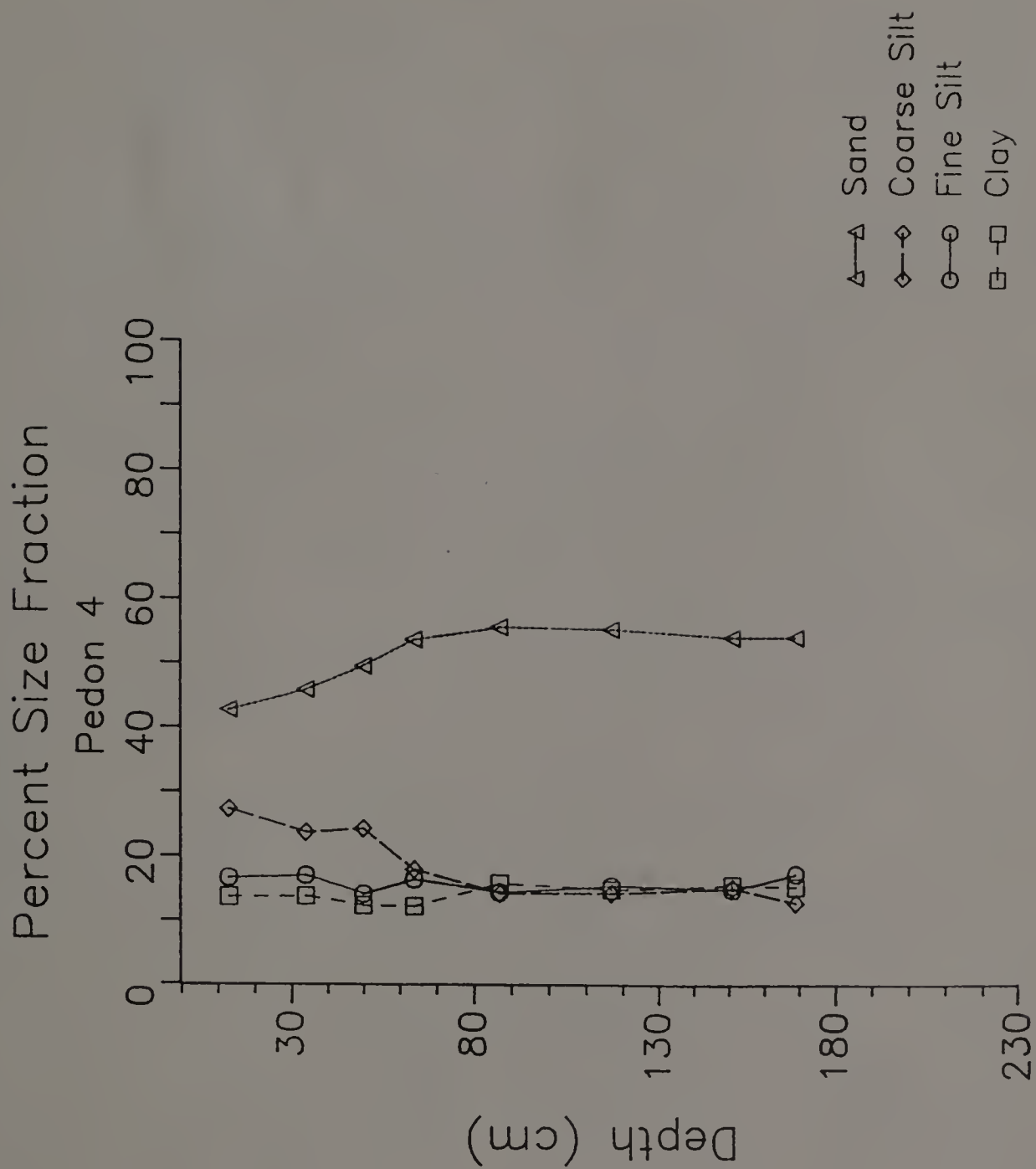


Figure 34. Soil separates (%) for each horizon by depth for Pedon 4.

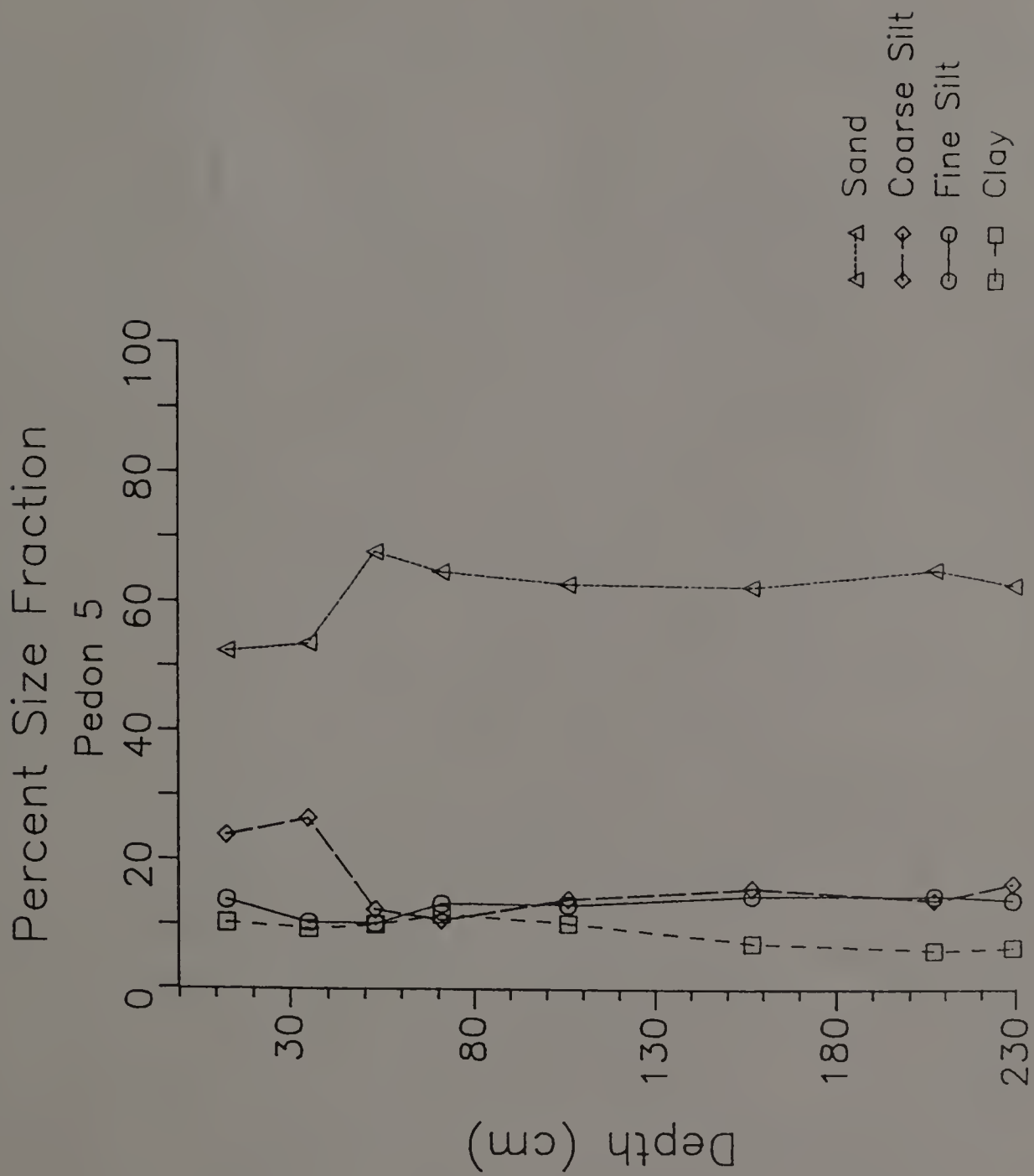


Figure 35. Soil separates (%) for each horizon by depth for Pedon 5.

Within Pedons 1 and 2 as the sand content decreases, the clay content increases. Silt content is not as variable as sand or clay content in any of the pedons. Combined silt and clay contents are 35% or greater in all pedons.

A more detailed look at the clay content confirms the field description of argillic horizons in all pedons but Pedon 3 (Figure 36). Pedons 1 and 2 have the largest increase in clay (approximately 10%) and Pedons 4 and 5 have a smaller increase (5 and 3% respectively). Based solely on the clay content from particle size analysis no argillic horizon can be identified in Pedon 3, however the clay content remains about the same through the B horizons and increases in the Cd horizons due to a change in lithology. Argillans were observed in the field and in thin section at $> 1\%$ (c.f. Chapter 5) thus indicating the presence of an argillic horizon. A change in lithology also accounts for the abrupt drop in the clay content in the BCm horizon in Pedon 1.

Bulk Density

Bulk density (BD) increases with depth in all pedons (Figure 37). There is a gradual increase in BD in the horizons above the fragipan and in most instances the horizon that immediately overlies the fragipan has a BD close to that of the fragipan. Beneath the fragipan the bulk density decreases slightly. Relatively unweathered till has a bulk density of about 1.8 Mg m^{-3} .

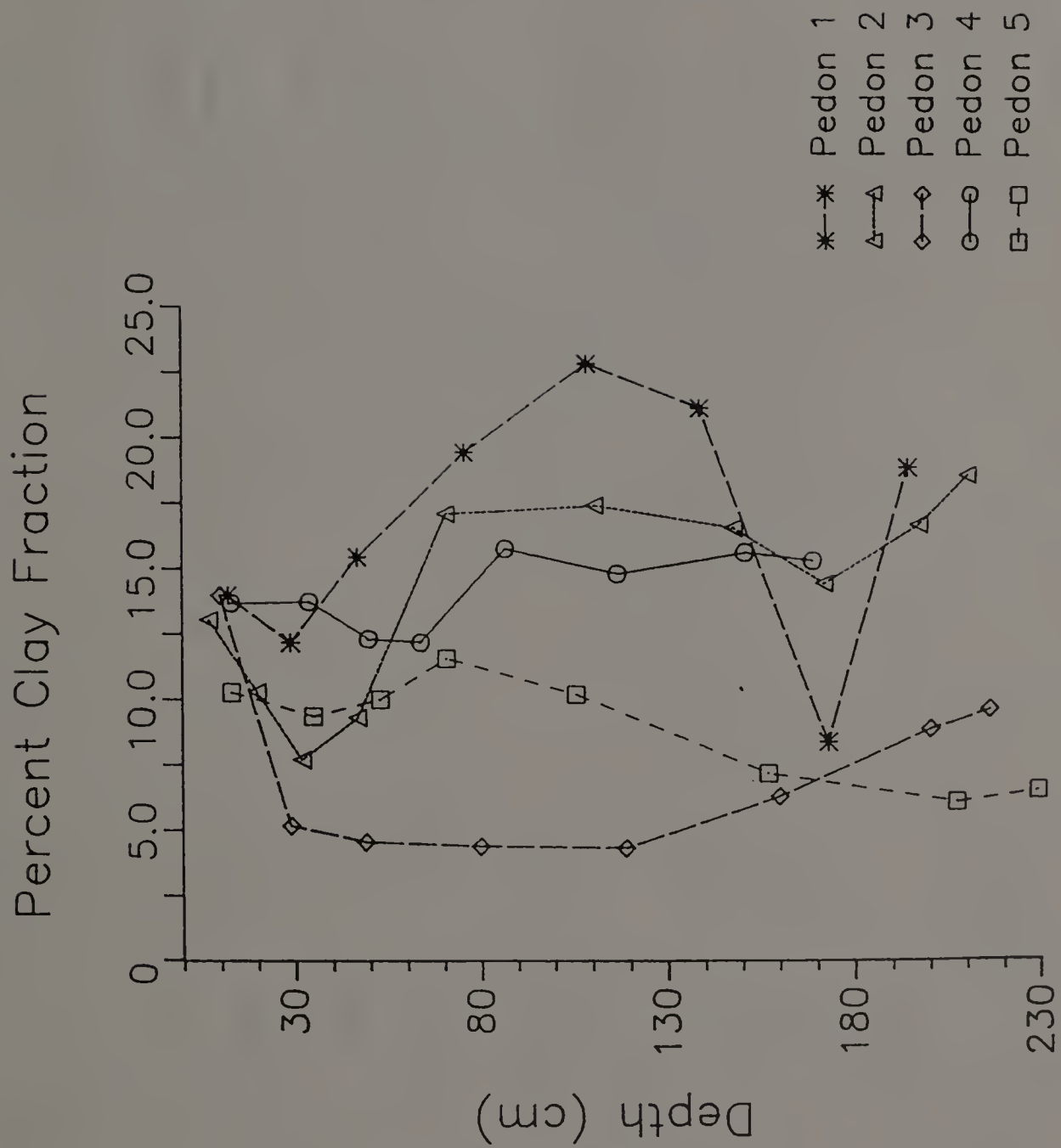


Figure 36. Clay fraction (%) for each horizon by depth for Pedons 1-5.

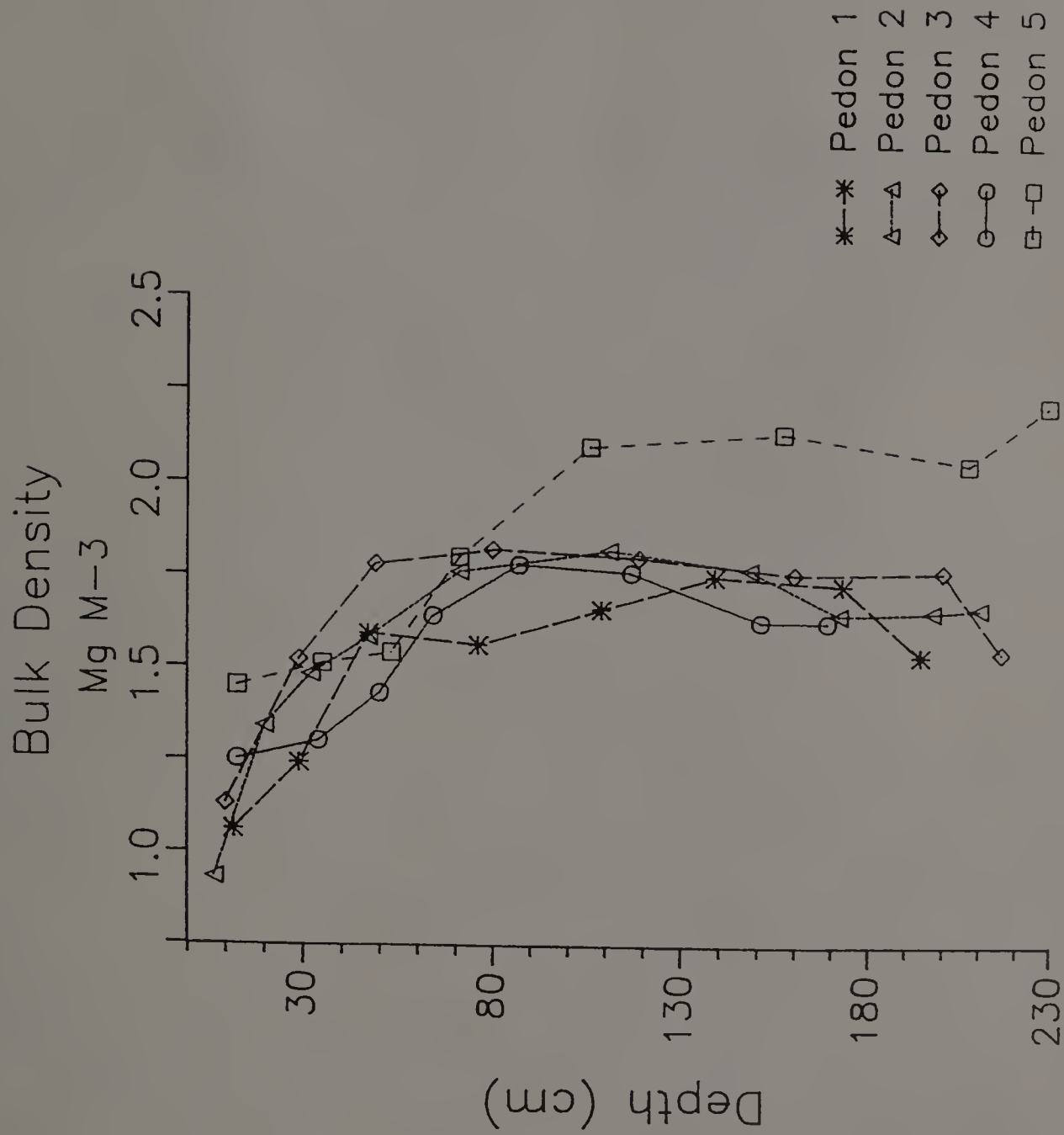


Figure 37. Bulk density (Mg M⁻³) for each horizon by depth for Pedons 1-5.

Moisture Retention

At low pressures, water is lost from large packing voids and from marco-pores. This phenomenon is reflected by a rapid decrease in moisture content of the upper, less compact horizons as evidenced by Pedon 3 and 5 (Figure 38 and 39). In general the lower, compact, dense horizons retained water at higher pressures. Bleached prism face (BPF) material behaves similarly to the fragipan horizons (Figure 39). The abrupt changes noted at 100 and 400 kPa are most likely due to a change in the apparatus being used rather than to changes in the soil.

Discussion

Fragipans are the only diagnostic horizons that have no laboratory procedure to confirm identification (Soil Survey Staff, 1975). According to Soil Taxonomy (Soil Survey Staff, 1975) the identification rests with 7 field clues recognizing that a combination of these must be used because there is no single unique property of fragipans (Table 17). Smalley and Davin (1982) incorporated these clues into a useful flow diagram that further assists in recognizing a fragipan. A comparison between the soils observed in this study and the clues in Soil Taxonomy indicate that these soils do contain fragipans (Table 18).

Most of the observed pans underlie an eluvial horizon or a horizon that has eluvial features (clues 1 and 2). These features include: gray mottles above the pan; clean, uncoated sand grains; and a depletion of clay in some overlying horizon. The gray, low chroma

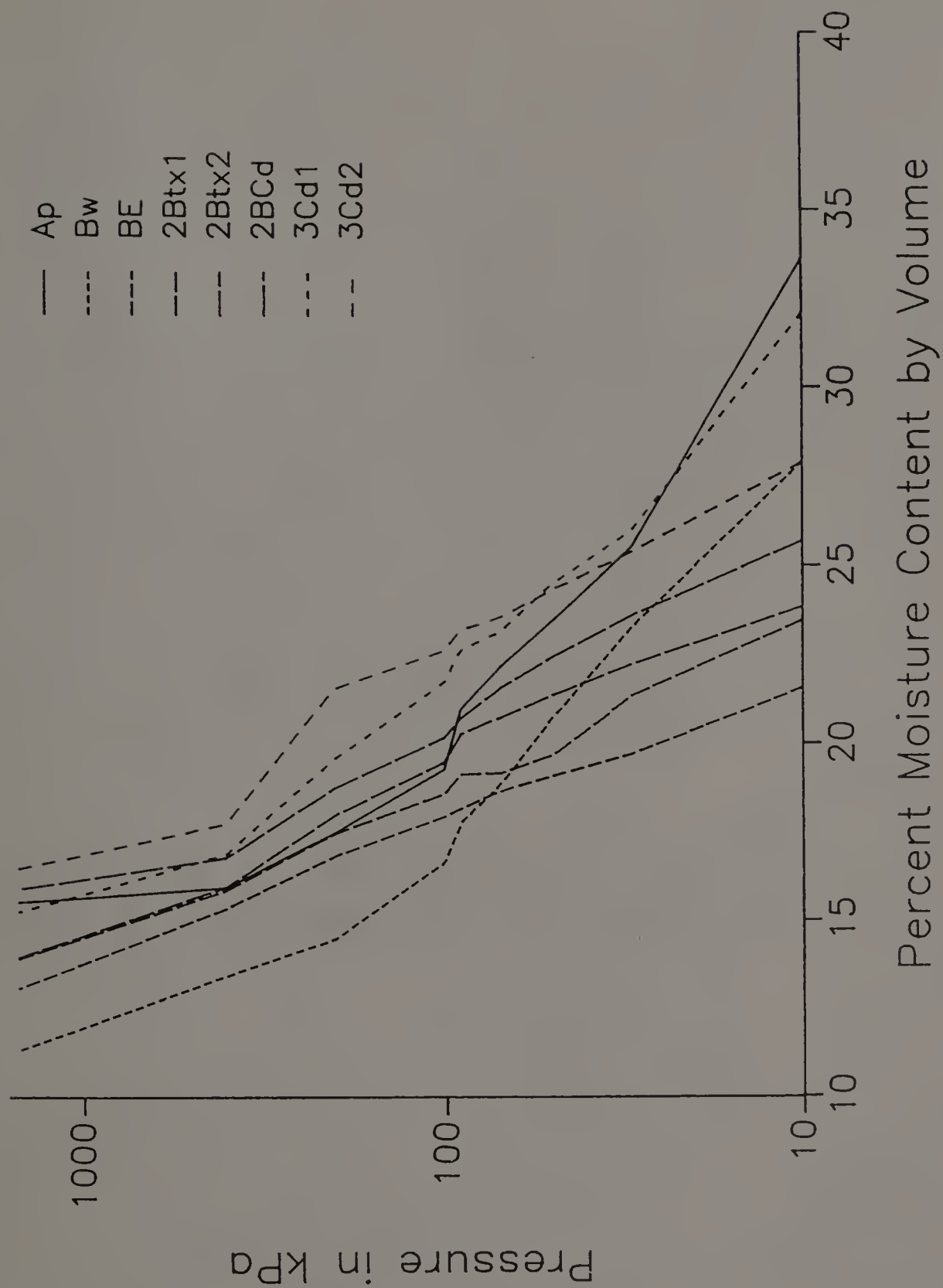


Figure 38. Moisture characteristic curves for each horizon of Pedon 3.

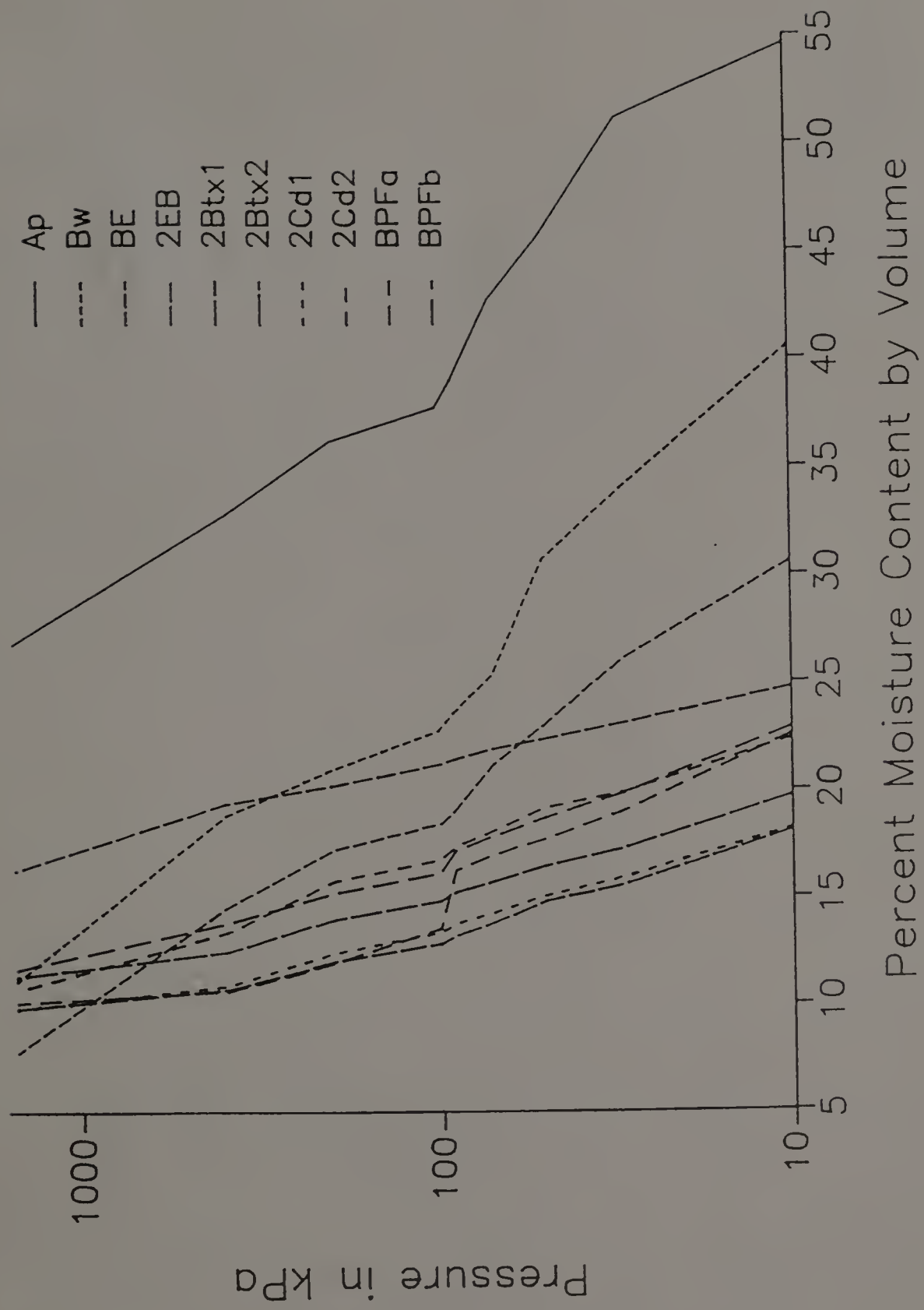


Figure 39. Moisture characteristic curves for each horizon of Pedon 5.

Table 17. Field clues used to identify fragipans (adapted from Soil Survey Staff, 1975).

-
1. Fragipans occur below, but not necessarily immediately below, an eluvial horizon unless truncated.
 2. An E horizon occurs between the pan and overlying cambic or argillic horizons. The E is characterized by uncoated sand and silt grains. Water moves laterally along the pan surface.
 3. Bleached prism faces are common in pans that are not saturated year-round and may or may not occur in saturated pans.
 4. Over 60% of the matrix is firm to brittle.
 5. Fine roots are virtually absent from the matrix but may occur in the bleached prism faces.
 6. The texture is finer than loamy fine sand.
 7. Air-dried fragments slake in water.
-

Table 18. Comparison of observed fragipans and tills to field clues.

Clue	Pedon					Till	
	1	2	3	4	5	Ayer	Charlemont
Below eluvial horizon	No ¹	Yes	Yes	Yes	Yes	No	No
Cambic or argillic overlies the pan, uncoated sand grains, lateral water movement	Yes ¹	Yes	Yes	Yes	Yes	No ²	No ²
BPF common	Yes	Yes	Yes	Yes	Yes	No	No
Over 60% firm matrix	Yes	Yes	Yes	Yes	Yes	Yes ³	Yes ³
Fine roots absent except in BPF	Yes	Yes	Yes	Yes	Yes	Yes	Yes
Finer than loamy fine sand	Yes	Yes	Yes	Yes	Yes	Yes	No (UT) Yes (LT)
Slake in water	Yes	Yes	Yes	Yes	Yes	No ⁴	No ⁴

- 1 Pedon 1 does not contain an eluvial horizon, however there are skeletans and albans at the base of the Bt indicating some eluviation.
- 2 The soils above the tills may contain eluvial horizons and evidence of lateral water movement but this is unrelated to the features observed in the till.
- 3 The Upper Till may have firm as well as friable zones varying from 25 to 90% of the deposit. The Lower Till, except for the more platy zones, is firm to hard.
- 4 The Upper Till slakes rapidly in water whereas the Lower Till slakes at a slower rate or may not slake at all.

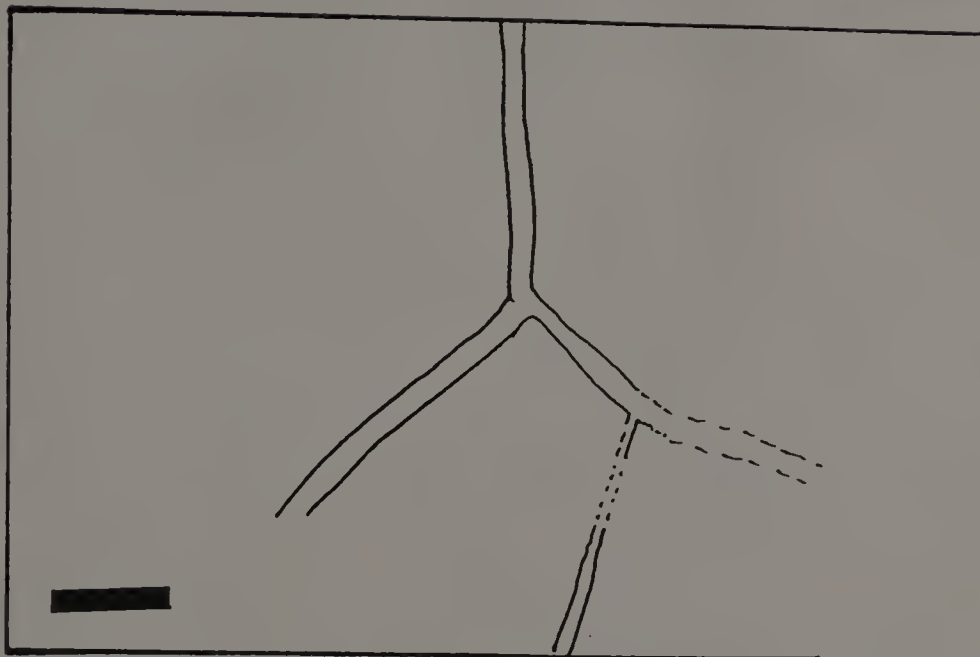
mottles are most likely caused by water perching above the pan for some period in the year, causing localized reducing conditions. Because these mottles may be adjacent to high chroma rinds or mottles, part of the matrix must be an oxidizing environment.

Bleached prism faces (BPF) are observed in most moderately well, and well-drained soils and in some poorly drained and somewhat poorly drained soils (clue 3). BPF occurred in all the soils investigated in the present study, and when the BPF are exposed in plan view they form a roughly polygonal pattern (Figure 40). The BPF from a Tillsit soil (Typic Fragiudult) observed in West Virginia (Figure 41) was nearly identical to the pans observed in Massachusetts apart from the yellower matrix color, and its size, shape, and expression. It also appears that the morphology of the BPF seen in Massachusetts are similar to those in the Mardin soil (Typic Fragiochrept) and the Empeyville soil (Aquic Fragiorthod) in New York. These two soils have developed in glacial till in similar conditions to the soils investigated in this study and are currently viewed as having fragipans by the SCS (Calhoun, 1980; W. Waltman, 1987, personal communication). In view of this similarity, the soils in Massachusetts should be considered fragipans as well.

By definition, in a fragipan the majority of the matrix (>60%) must be brittle to very firm depending on moisture content (clue 4). The high density of the observed pans attest to its firmness. The brittle nature is observed in most pans although Pedon 1 was not as brittle as the others. Pedon 1 may have been less brittle due to its high clay and water content at time of sampling. Other pedons with



A

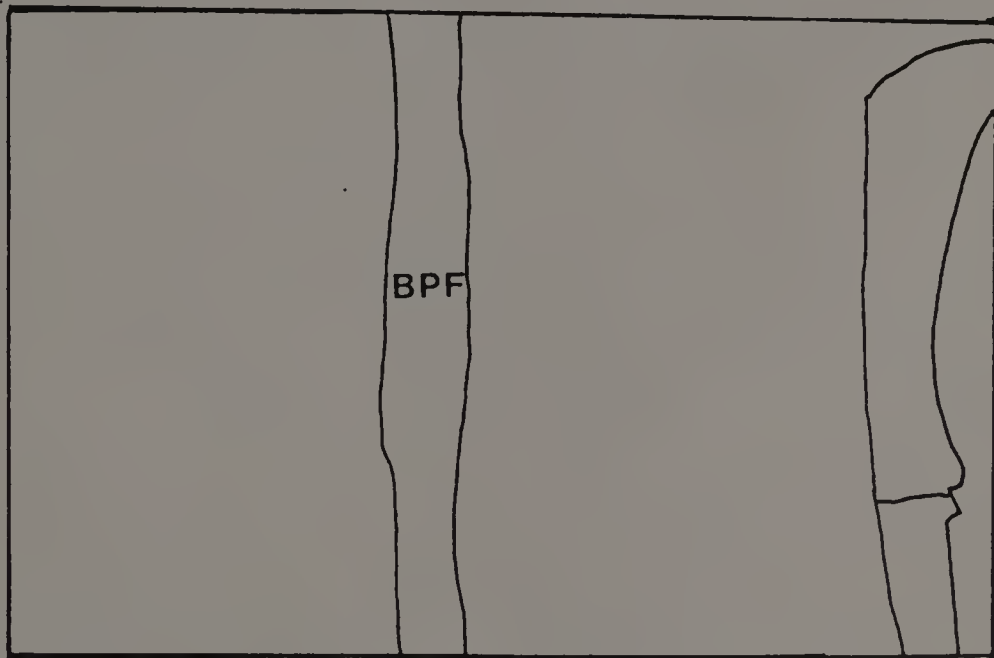


B

Figure 40. Plan view of the polygonal arrangement of bleached prism faces in the Bx1 of the Ridgebury profile in Spencer, MA. (A) photograph, (B) schematic. The bar is 5 cm.



A



B

Figure 41. Bleached prism face from the fragipan of a Tilsit soil (Typic Fragiudult) in WV. Note the roots and organic material running down the center of the BPF as seen in Figure 28. A) photograph, B) schematic. The knife handle is 6 cm long.

high water contents at sampling time were observed to be less brittle until the samples dried slightly. Pickering and Veneman (1984) observed the strength was inversely related to moisture content, thus a drier sample would appear stronger and more brittle. No direct measurements of the brittle behavior of the soil were taken in the field, although laboratory analysis was performed (Chapter 9). Also the total percentage of the brittle matrix was not quantitatively measured but the entire matrix excluding the BPF was observed to be brittle. A feature related to the consistency of the pan is its ability to slake in water (clue 7), a phenomenon observed in all the pedons investigated.

The dense nature of the fragipan effectively excludes roots except within the BPF (clue 5). Root penetration within the BPF and exclusion from the matrix is common to the observed soils. Roots were most common in the BPF of Pedon 2 and their presence may be helpful in explaining the BPF morphology. The area around the roots may be oxygen depleted (reducing) due to an increase in respiration of microorganisms associated with the roots. The localized reduction may account for the gray coloration and may result in the mobilization of some Fe. As the reduced Fe moves away from the reduced zone it encounters a more oxidized matrix and is consequently oxidized, resulting in the red-brown rind surrounding the gray interior of the BPF.

Textural analysis of the pans indicated that most can be classified as argillic horizons. In all instances the pans contained < 35% clay but were finer than fine sand, typically fine sandy loam

(clue 6). Identifying the pans in this study as argillic horizons has a bearing on the final classification of the soils as discussed in Chapter 11.

Witty and Knox (1989) proposed a revised fragipan definition to include some positive evidence of pedogenesis. Clay films, low chroma mottles, and BPF are all formed by pedogenesis and are present in the primary and supportive pedons. Clay films occur in voids and on ped surfaces throughout the pan although they may become less prevalent in the extreme interior of the brittle matrix. Low chroma mottles are particularly noticable within the less well-drained pedons and at the top and bottom of the pans in the more well-drained pedons. While the exact mode of formation of the BPF remains to be determined their presence typifies fragipans. All of the afore mentioned physical features are common to Massachusetts fragipans.

A comparison of the till descriptions and properties to those of the soils illustrates a few similarities and some major differences. Bulk density (BD) is similar between the till and the pans although in most of the soils the pans had a slightly higher BD than the 3Cd horizon (till). Moisture retention in the 3Cd horizons was also similar to those in the fragipans. Morphologically the till was very different from the fragipans. BPF, clay skins, and mottles were all absent from the till but common to the fragipans. The fluvial features of the Upper Till and shear and attenuation features of the Lower Till were absent from the fragipans. This may indicate that some mixing has occurred between the pan and overlying horizons. A few

beds that may have had a fluvial origin were observed in Pedon 5 above the pan. These could be due to slope position rather than to the till deposit. The morphologic changes in the pan indicate that it has been pedogenically altered from the glacial till.

Conclusions

The morphology and physical properties of the soils investigated indicated that some horizons currently classified by the Soil Conservation Service as a Cd or Cr horizon should be classified as a Bx or Btx horizon. The pans observed have the typical fragipan morphology with BPF, mottles, and clay skins. They typically underlie eluvial zones, contain few roots (only in the BPF), and air-dried clods slake when emersed in water. The pans show a higher BD than overlying horizons. The high BD probably is inherited from the till parent material but the morphologic features are not. Textural analysis indicates the pans have less than 35 percent clay and are finer in textural classification than fine sand. The analysis also indicates that most of the pans can be classified as argillic horizons as well as fragipans.

The argument that the pans studied are mostly geogenic is not valid. The pedogenic features (mottles, clay skins, increase in clay content, and BPF) have been superimposed over many of the features observed in the original till. Of all the physical properties investigated only the BD appears to be inherited from the till and even that may have increased slightly as a result of fragipan formation.

CHAPTER V

MICROMORPHOLOGY

Previous Work

Soil micromorphological studies throughout North America have indicated several features common to fragipan horizons. These include grain and channel argillans, ferrans, ferriargillans, and sepic fabrics (Smith and Callahan, 1987; Miller et al., 1971; Wang, 1971; Grossman and Cline, 1969). Several researchers have reported argillans occurring as linings of voids and as bridges between skeletal grains (Nettleton, et al, 1968; Jha and Cline, 1963; Knox, 1957), while others have reported amorphous silica as forming bridges between grains (Norton, et al, 1984). The presence of illuviated argillans and ferriargillans in Bx horizons and the absence of such features in C horizons suggests pedogenic development. Grossman and Carlisle (1969) did not distinguish between fragipans developed in different parent materials. Today the nature of the parent materials and the development of fragipan soils in them have become a key element in the controversy over geogenic versus pedogenic development. Essentially three types of environments or parent materials are involved with pan formation and classification: non-glacial, periglacial and loess, and glacial.

Hardpans of the Delmarva area have been studied by Nikiforoff et al. (1948) and Nikiforoff (1955). Observations based on optical

techniques, illustrated an abundance of oriented clay bodies, close packing, and clay bridges. These findings were echoed by Rutledge and Horn (1965) in Arkansas. They described fabrics as being sepic with a large number of illuviation cutans associated with voids. They concluded that the arrangement of clay within the fragipan is critical to the pan's development and properties. Sepic fabric, close packing, and argillans as well as translocated clay in a pan developed on residual material were also reported by Nettleton et al. (1968b), and most recently by Smith and Callahan (1987). They too felt the arrangement of clay particles was important to pan formation. McKeague and Sprout (1975) looked at non-glacially derived hardpans. Their investigations of a duripan concluded that cementing was not obvious using standard optical techniques yet grain argillans were visible. Essentially fragipans developed in a non-glacially derived parent material showed the common features of sepic fabric, grain argillans, argillans and close packing.

Fragipans in periglacial terrain in Europe have shown both a sepic and plasmic fabric (van Vliet and Langohr, 1981). The pans commonly have planar voids which are anastomosed, resulting in the platy character of the pan. Further studies indicate that these voids are commonly stained with Fe and coated with clay (Ranney et al., 1975). Oriented clay associated both with voids and as bridges between grains is a standard feature of fragipans (Chartres, 1985; Grossman et al., 1959b; Miller et al., 1971b; Norton and Franzmeier, 1978). By etching thin sections, as Price and Jenkins (1980) suggested, Norton et al. (1983) were able to expose bridges for

detailed SEM study. Chartres (1985) and Norton et al. (1984) used the EMP and EDXRA to further study the bridges, concluding that Si was an important component of the bridging. Norton et al. (1984) concluded also that Al played a role in the bridges. The presence of these two elements suggest that clay or possibly amorphous Si and Al are part of grain argillans. These observations did not depart from the overall view expressed by Grossman and Carlisle (1969).

The existence of fragipans developed on glacial material is, as mentioned, somewhat controversial. Comparison of the micromorphology of "true" fragipans (non-glacial) to those of till derived fragipans is one step in comparing their development. As in the previously mentioned studies, bridges (grain argillans), argillans, and close packing have been observed in till derived pans (Jha and Cline, 1963; Knox, 1957; Lynn and Grossman, 1970; McCracken and Weed, 1963; Wang et al., 1974; Yassaglou and Whiteside, 1960). Knox (1957) stated that the oriented clay accounts for at least part of the pan's rigidity, a point that Rutledge and Horn (1965) also agree with although they were investigating non-till pans. Further evidence of illuviation is suggested by Crampton's (1965) observation that intergranular areas are clogged with clay. SEM observations show bridges that appear similar to those shown by others in "true" fragipans (Lynn and Grossman, 1970; Wang et al., 1974). During his examination of tills in New England, Newton (1978) observed oriented clay which he attributed to post-depositional changes in the till. The evidence indicates that illuviation has resulted in argillans within the till

derived pans. These pans exhibited the same general features observed by others in fragipans developed on different parent material. The conclusion drawn by Yassoglou and Whiteside (1960) was that the till derived pan was indeed pedogenic and therefore a true fragipan.

Assessment of the microphology of soil investigated is critical in understanding how they formed and how they compare to pans observed elsewhere. If it can be demonstrated that the pans in question have similar features to "true" fragipans than the argument that till derived pans are fragipans is strengthened. Significant illuviation of clay can also be identified and used to confirm that some of the pans studied can be classified as argillic horizons. Finally, investigation of unweathered till in thin section enhances the understanding of the degree of pedogenesis and the amount of inherited features that have occurred.

Materials and Methods

Thin sections were prepared using methods described by Osmond (1958), Innes and Pluth (1970), McCarrick and Protz (1978), and Waldron (1983). This involved inserting a 5 x 5 x 2.5 cm sheet metal frame into the soil and removing the surrounding soil until the frame could easily be removed without disturbing the soil it contained. Orientation of the blocks were noted and the blocks were air-dried for at least one month and then impregnated under vacuum with low viscosity Spurr embedding medium (Figure 42 represents a schematic of the apparatus used). Samples were cut, polished, mounted to a frosted glass slide and ground to approximately 30 μm . A cover slip was then

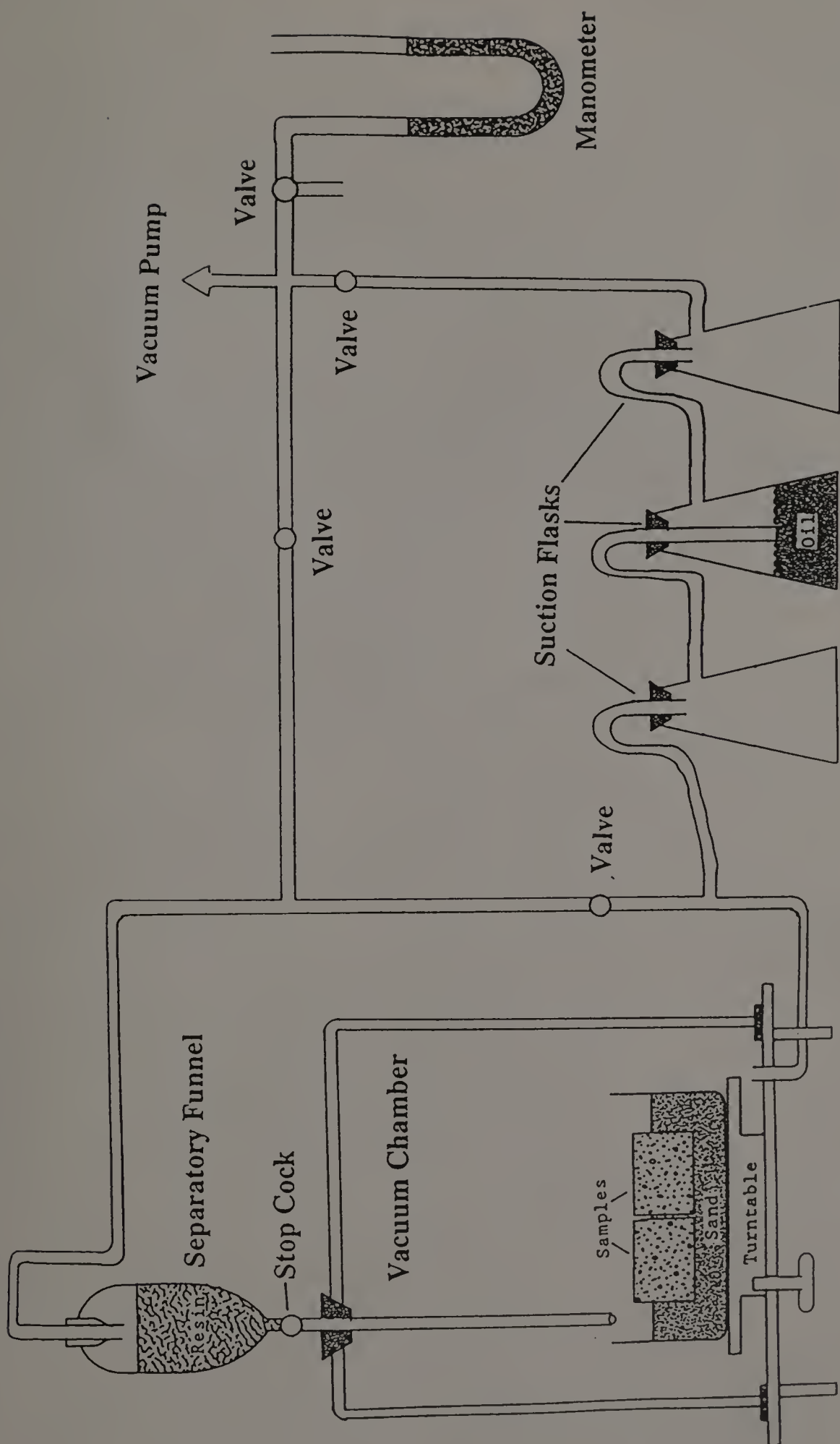


Figure 42. Schematic of the apparatus used to impregnate thin sections under vacuum.

fixed onto the thin section with Canada Balsam. If subsequent electron microscopy analysis was required the Canada Balsam could be heated and the cover slip easily removed.

Thin sections were analysed under both plain and polarized light and described using the terminology of Brewer (1976). Modal distributions of selected features were ascertained by point counts with a petrographic microscope equipped with a click stage. In addition to optical examination, SEM and EDXRA investigations were performed on small peds with natural surfaces, which were mounted on 1/4" diameter aluminum stubs with graphite paint. The small ped samples were coated with a Au-Pd alloy for 3 to 4 minutes in a Sputter Coater (Bisdom et al., 1983). Prior to coating the samples, drawings of the visible surface features were made with the aid of a dissecting microscope. These drawings aided in determining which features were being observed with the SEM. Observations and analyses were carried out on a JEOL JSM25S with a Kevex attachment for EDXRA.

Results

Modal distribution data based on point counts indicate a maximum argillan expression in the fragipan horizons (Table 19 and Appendix E). A notable exception was observed when the 2Btx horizons were overlain by a Bt horizon. Cutans are less common in the Ap, Bw and BE horizons although some noteworthy features are present. The Ap horizons are dominated by a dark, organic rich matrix with some root fragments and a few papules (Figure 43). There is little discernable structure within the horizon. Bw horizons contain less organic materials in the

Table 19. Modal distribution (%) of selected micromorphological features.

PEDON 1

	Bt	2Btx1	BPF	2Btx2	BPF	3BCm	4Cd
Matrix and							
Voids <40 um	39.2	35.9	40.0	50.9	45.1	14.1	47.4
Weathered Gr.	22.8	13.6	20.0	11.7	15.3	16.7	10.8
Unweathered Gr.	7.1	13.3	15.2	17.2	18.4	33.7	22.5
Argillans	13.6	13.6	12.2	7.0	8.6	1.5	1.1
Grain Cutans	5.3	4.9	3.8	3.3	2.4	4.1	1.0
Mangans	0.0	1.6	0.0	0.4	0.0	1.2	2.3
Ferrans	5.7	12.3	1.8	3.0	0.6	10.9	8.6
Voids >40 um	5.7	5.8	10.4	4.6	10.4	17.4	5.1
Opaque	0.1	0.4	2.0	0.6	0.0	0.1	1.2
n=	1433	1133	413	1047	316	917	912

PEDON 2

	Bw2	BE	2Btx1	2Btx2	BPF	2BCd	3Cd1	3Cd2
Matrix and								
Voids <40 um	42.0	42.6	40.6	42.2	23.4	43.8	66.3	52.9
Weathered Gr.	29.1	16.7	19.3	20.0	31.6	22.4	11.5	13.1
Unweathered Gr.	16.3	14.8	11.8	13.7	24.2	22.6	9.2	21.2
Argillans	0.0	4.7	10.6	6.6	0.6	2.8	0.0	0.0
Grain Cutans	1.5	3.2	3.7	3.8	0.0	1.2	0.0	0.2
Mangans	0.0	0.0	0.0	0.0	0.0	0.2	1.6	0.3
Ferrans	0.9	1.3	2.2	7.0	0.6	3.0	3.6	2.8
Voids >40 um	7.1	16.4	11.5	6.0	19.1	3.3	7.5	9.3
Opaque	0.3	0.3	0.6	1.0	0.6	0.7	0.3	0.3
n=	326	317	321	936	351	602	305	650

PEDON 3

	BE	2Btx1	2Btx2	2BCd	3Cd1
Matrix and					
Voids <40 um	46.5	44.8	45.9	45.6	53.5
Weathered Gr.	23.3	23.3	16.4	15.4	14.4
Unweathered Gr.	9.8	14.3	14.2	27.0	22.1
Argillans	0.7	4.2	5.3	2.0	0.0
Grain Cutans	0.8	1.7	1.3	1.3	0.8
Mangans	0.0	0.2	0.3	0.2	0.9
Ferrans	1.8	4.0	1.8	3.0	4.6
Voids >40 um	17.1	7.5	14.7	4.7	3.4
Opagues	0.0	0.0	0.0	0.7	0.0
n=	598	574	538	987	637

Continued, next page

Table 19 cont.

PEDON 4

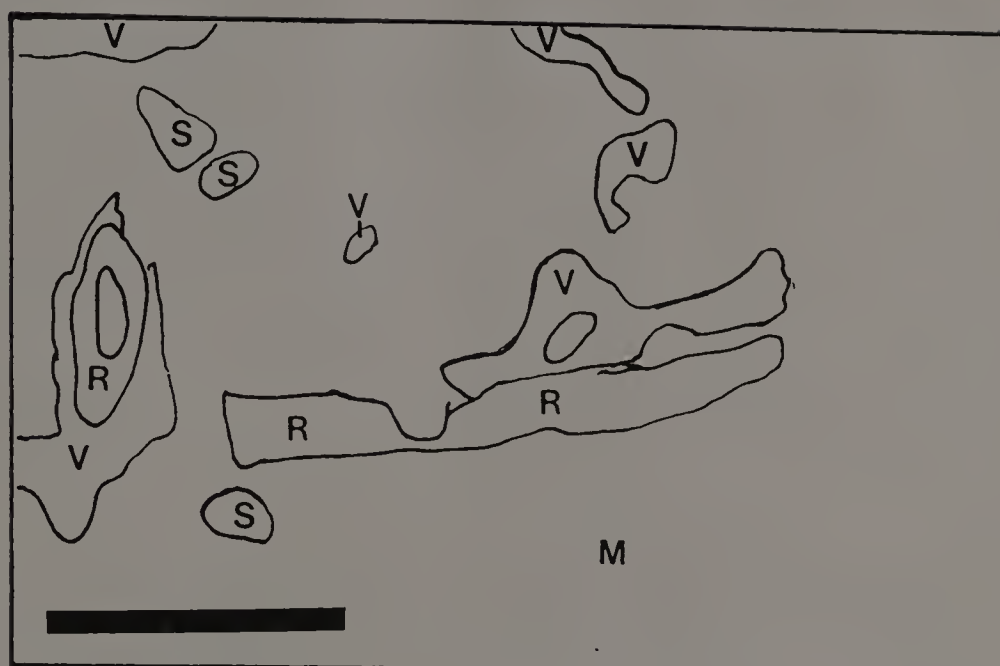
	Ap	Bw1	Bw2	BE	2Btx1	2Btx2	2BCd	3Cd
Matrix and								
Voids <40 um	67.7	60.2	56.2	48.0	44.5	41.7	41.9	44.6
Weathered Gr.	11.2	13.6	15.6	17.8	21.7	16.3	16.6	20.6
Unweathered Gr.	10.5	12.1	15.1	19.1	13.7	12.5	22.1	19.5
Argillans	0.0	0.0	0.6	2.6	8.7	7.7	3.3	1.0
Grain Cutans	0.8	0.7	0.8	2.1	3.6	4.5	2.0	0.7
Mangans (Roots)	(0.5)	(1.0)	0.0	0.0	0.4	0.0	0.0	0.0
Ferrans	2.1	1.7	5.3	3.3	3.1	3.5	5.9	2.6
Voids >40 um	5.4	9.8	2.9	6.0	3.1	3.5	7.5	11.8
Opaques	1.9	0.9	1.6	1.2	1.4	1.3	0.8	0.6
n=	596	755	627	520	1231	312	470	331

PEDON 5

	BE	2EB	2Btx1	2Btx2	BPF	2Cd1	2Cd2
Matrix and							
Voids < 40 um	50.9	35.7	44.8	41.8	27.8	46.0	49.2
Weathered Gr.	34.4	41.9	21.0	20.8	35.0	22.9	24.6
Unweathered Gr.	9.5	10.3	12.9	23.1	26.6	23.9	22.9
Argillans	0.0	0.9	5.5	3.6	1.8	1.0	0.4
Grain Cutans	0.1	0.6	3.0	2.8	0.0	0.9	0.2
Mangans	0.0	0.0	0.4	0.5	0.0	0.2	0.2
Ferrans	1.2	1.1	5.2	1.6	0.9	0.9	0.6
Voids >40 um	3.4	10.0	6.1	5.9	6.5	4.2	1.7
Opaque	0.6	0.0	1.1	0.0	1.2	0.0	0.0
n=	617	651	1025	880	338	920	951



A



B

Figure 43. Photomicrograph from the Ap horizon of Pedon 4. The matrix is dark due to organic material coating the particles. V = void, S = skeleton grain, R = root, M = matrix. (A) photograph, (B) schematic. The bar is 1 mm long.

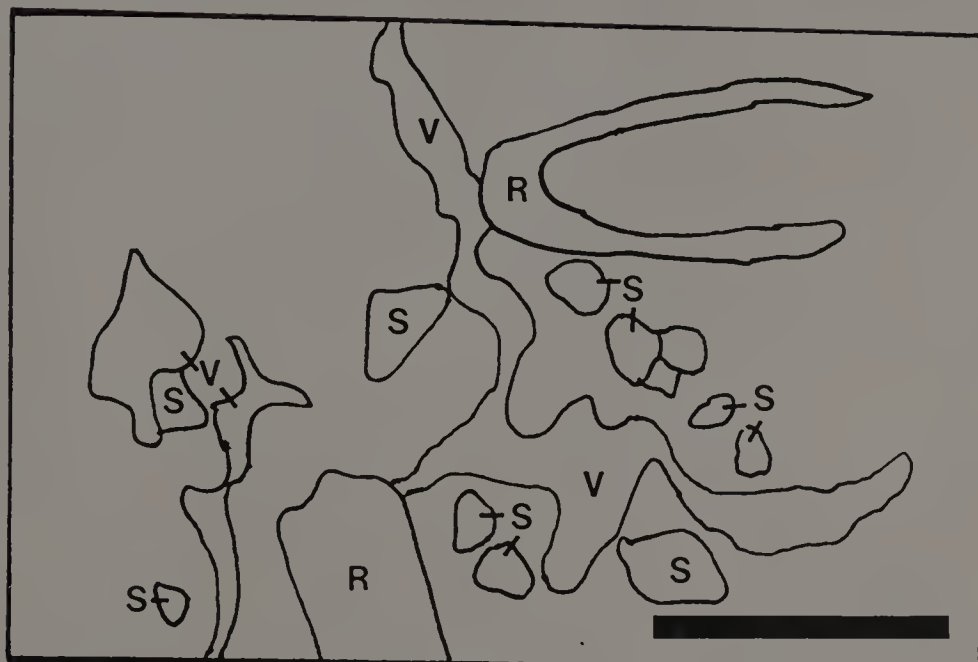
matrix, with the exception of krotovinas, than observed in the Ap horizons. Bw horizons typically contain a few papules and a rare argillan (Figure 44). Pedon 5 however contains numerous ferrans and Fe-rich nodules (Figure 45) characteristic of poorly drained conditions (Appendix F). The horizons (BE and 2BC) that directly overlie the 2Btx horizon with the exception of the Bt horizon in Pedon 1, contain a few argillans, occurring more frequently towards the bottom of the horizon, yet these are not well defined and appear to be degrading (Figure 46).

In all cases there are sufficient amounts of yellow illuviation argillans to classify each fragipan horizon as an argillic horizon according to Soil Taxonomy (page 26-27). Much of the clay forming the argillans occurs as linings of vughs, vesicles, (Figure 47-49), and as bridges between skeletal grains (Figures 50-52). The bleached prism faces (BPF) contain a lower amount of argillans, while directly adjacent to the prism face ferrans, ferriargillans and argillans are common (Figures 53 and 54). Interiors of BPF are almost devoid of cutanic features (Figure 55). The features associated with the bleached prism faces commonly are visible on the macroscopic scale as well.

Below the fragipan in the 2BCd horizons, argillans are still present but they are less common and not as well developed as in overlying horizons. Ferrans and Fe-nodules commonly occur on the surfaces of plates or in association with the pervasive type 2 mottles typical of the 2BCd horizons (Figure 56). The Cd horizons are dominated by the s-matrix and unweathered grains. Few argillans occur



A

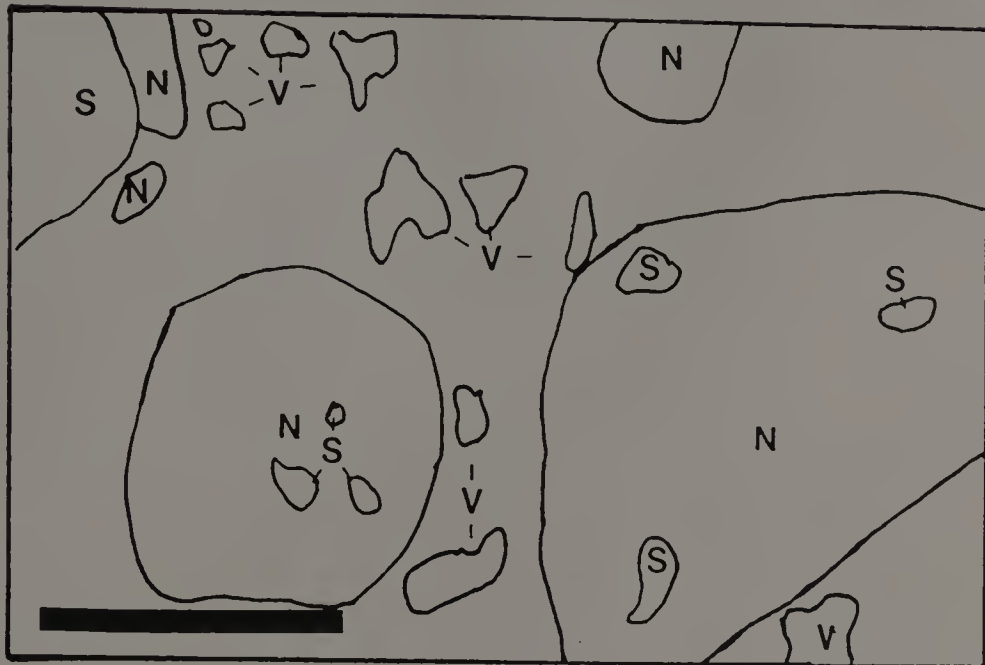


B

Figure 44. Photomicrograph from the Bw1 horizon of Pedon 4. Less organic material coats the particles in this figure as compared to Figure 43. V = void, S = skeleton grain, R = root. (A) photograph, (B) schematic. The bar is 1 mm long.

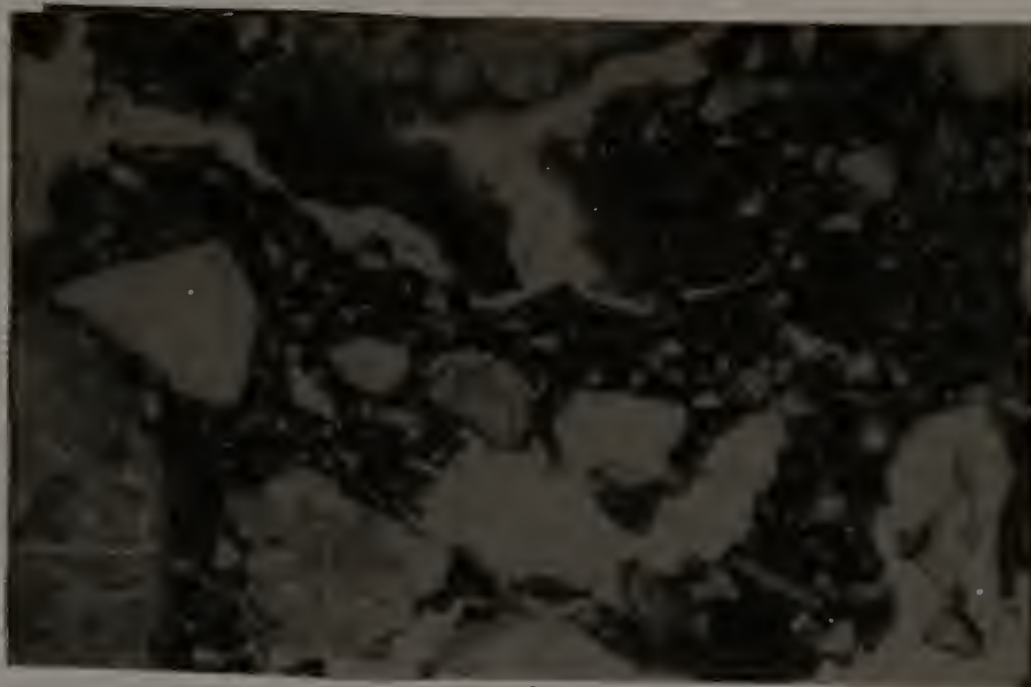


A

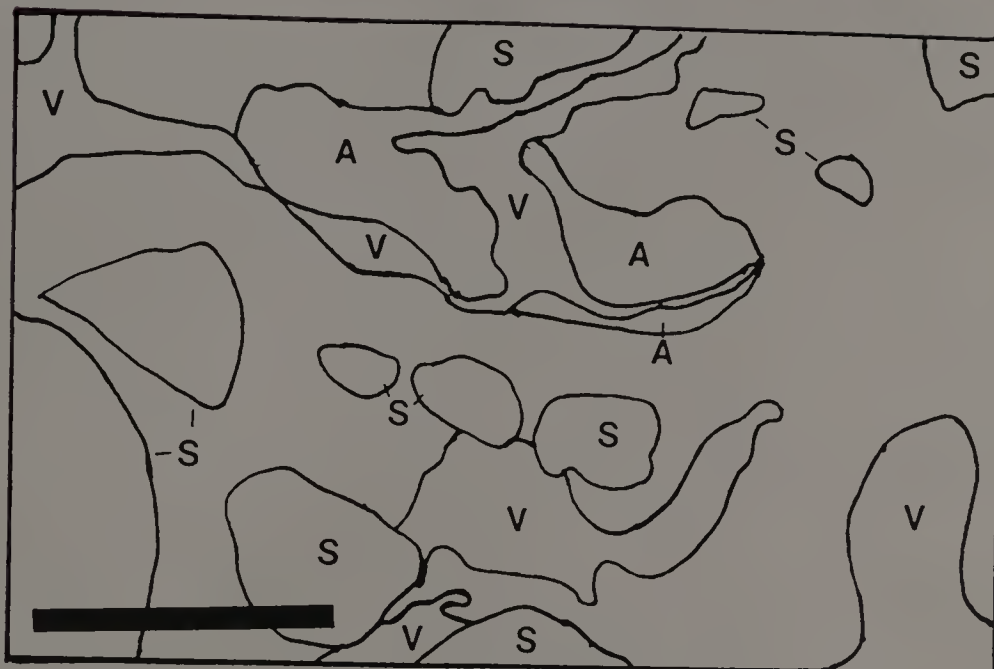


B

Figure 45. Photomicrograph from the Bw horizon of Pedon 5.
 V = void, S = skeleton grain, N = mottle or
 nodule. (A) photograph, (B) schematic. The bar
 is 1 mm long.



A

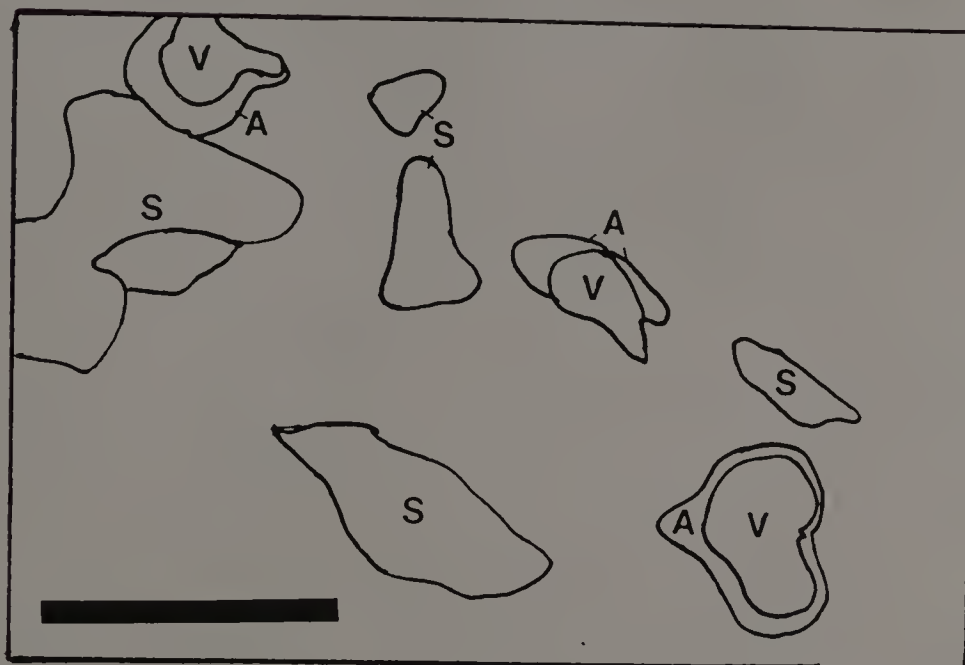


B

Figure 46. Photomicrograph from the BE horizon of Pedon 4. Argillan in channels and ped faces are discontinuous and broken, some voids do not contain any argillans. V = void, S = skeleton grain, A = argillan. (A) photograph, (B) schematic. The bar is 1 mm long.



A

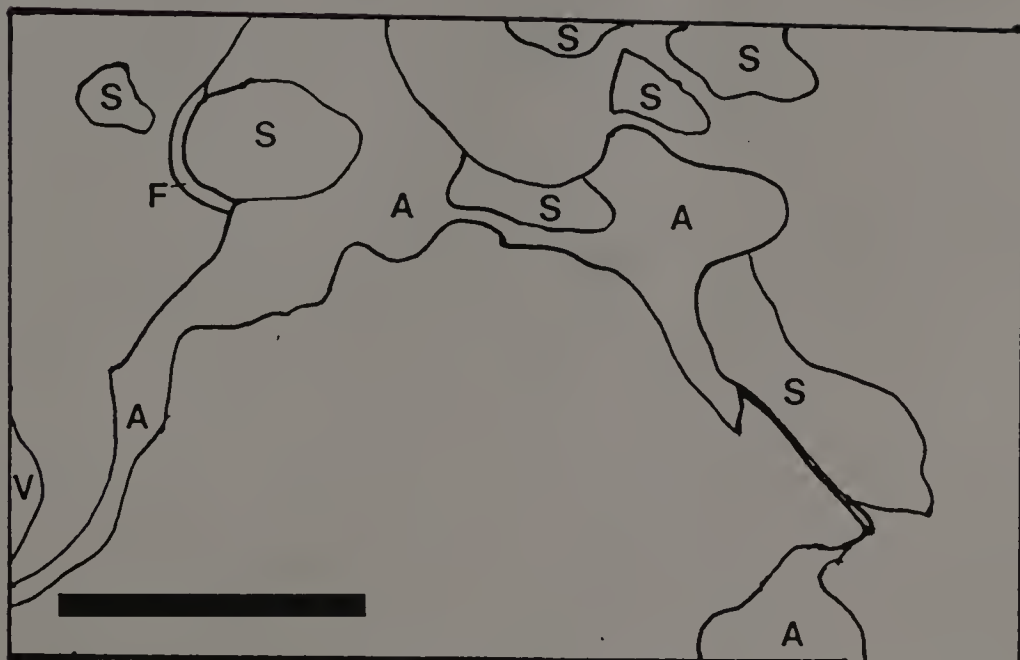


B

Figure 47. Photomicrograph from the 2Btx1 horizon of Pedon 3. Vughs and vesicles lined with oriented clay. V = void, S = skeleton grain, A = argillan. (A) photograph, (B) schematic. The bar is 1 mm long.

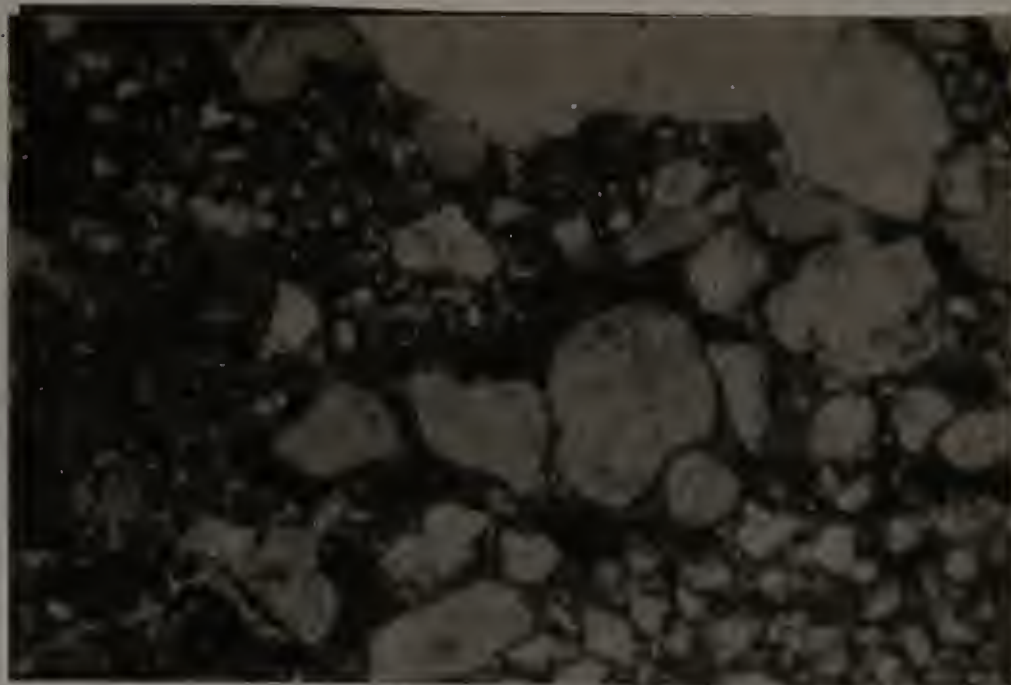


A

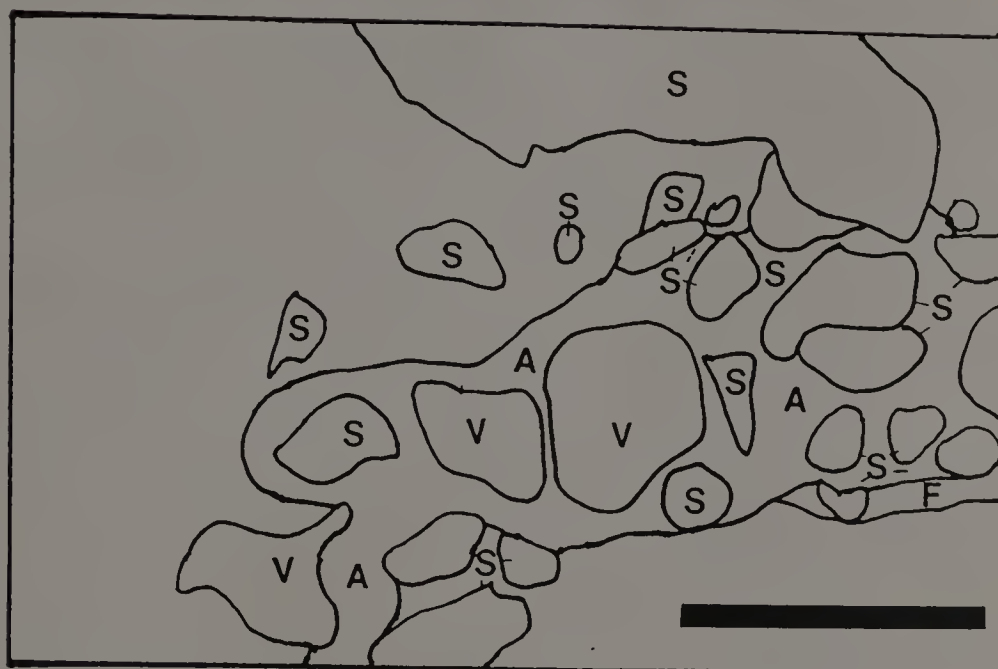


B

Figure 48. Photomicrograph from the 2Btx1 horizon of Pedon 4. Argillans are continuous and present on ped faces and in channels. V = void, S = skeleton grain, A = argillan. (A) photograph, (B) schematic. The bar is 1 mm long.



A

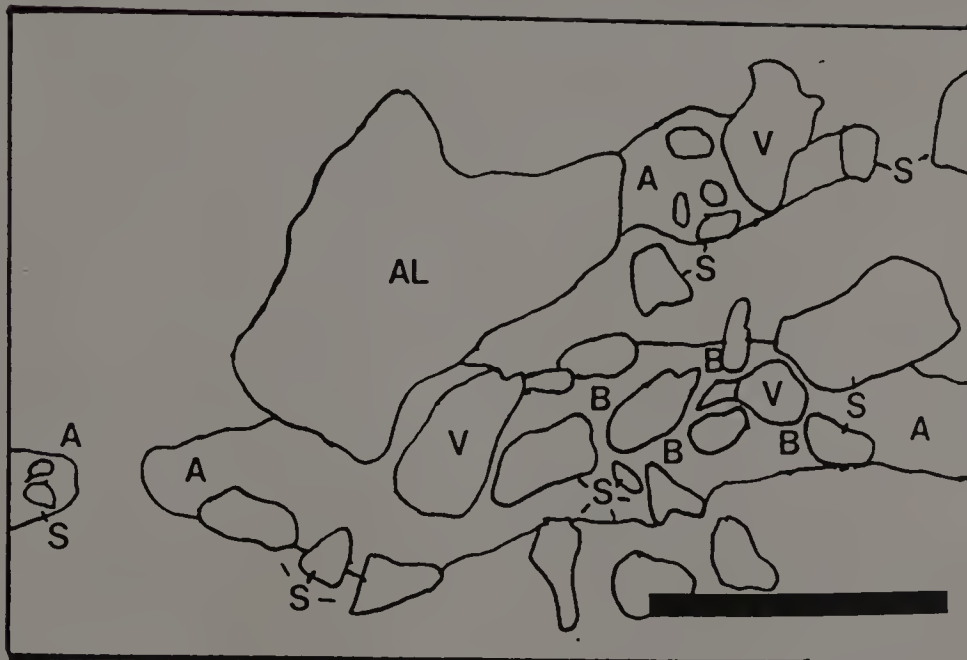


B

Figure 49. Photomicrograph from the 2Btx1 horizon of Pedon 2. Channel argillans forming vesicles and nearly clogging the entire channel. V = void, S = skeleton grain, A = argillan, F = ferran. (A) photograph, (B) schematic. The bar is 1 mm long.

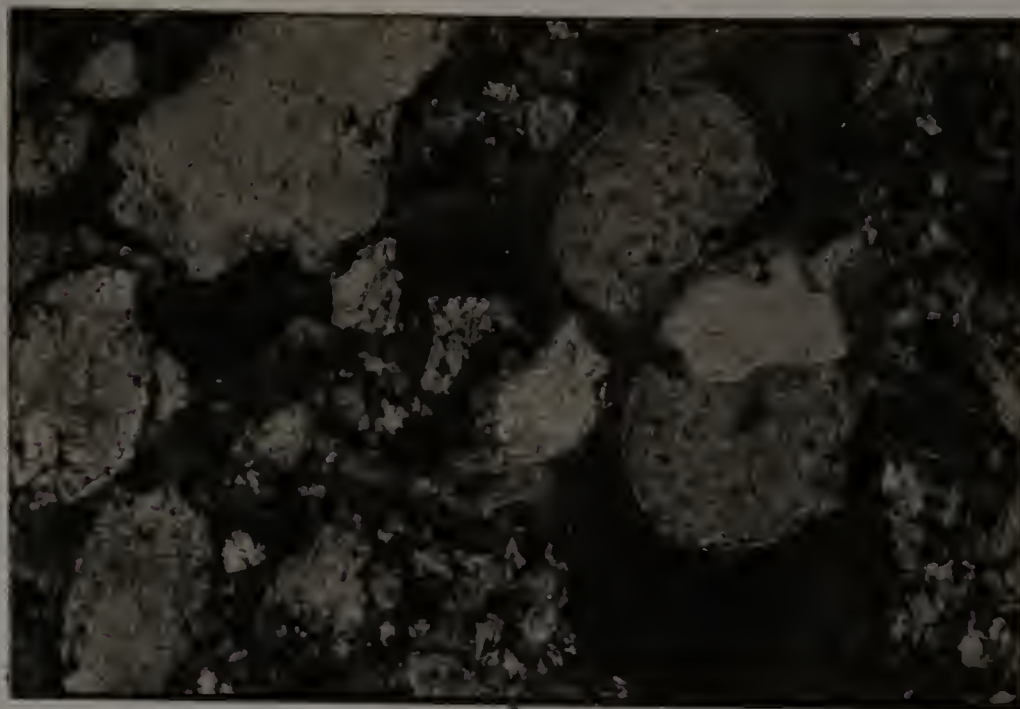


A

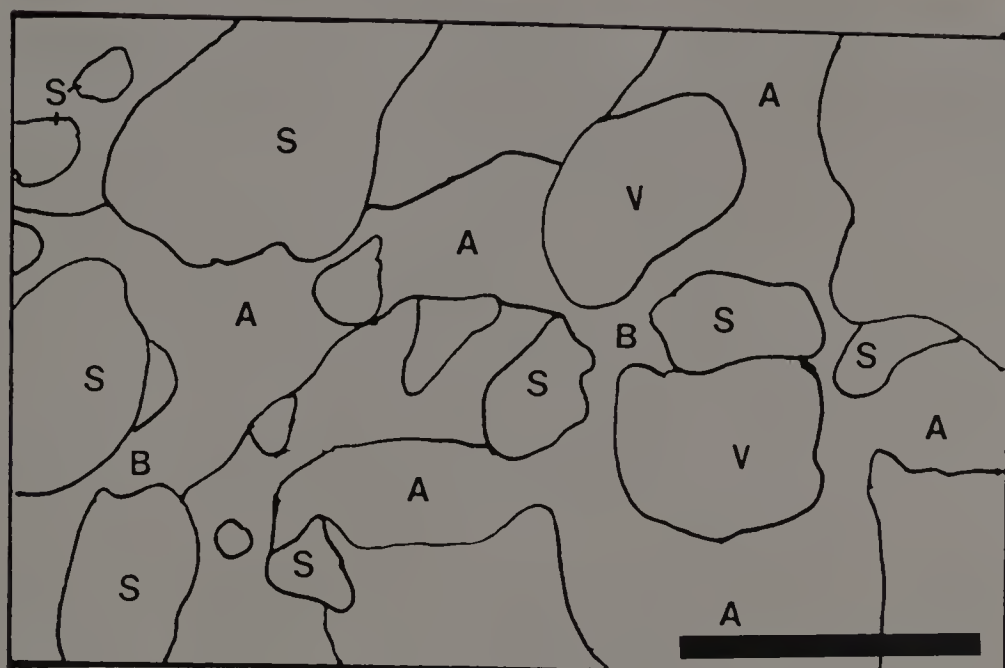


B

Figure 50. Photomicrograph from the 2Btxl horizon of Pedon 5. Channel or ped-argillans forming bridges between skeleton grains and the S-matrix. V = void, S = skeleton grain, A = argillan, B = bridge, AL = alban. (A) photograph, (B) schematic. The bar is 1 mm long.



A

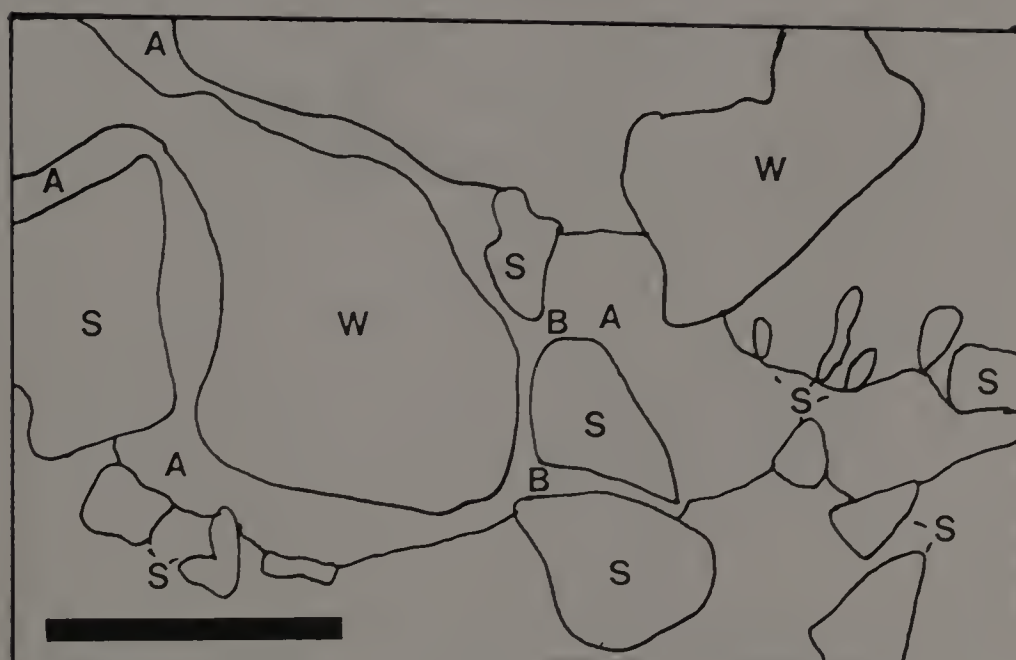


B

Figure 51. Photomicrograph from the 2Btx2 horizon of Pedon 5. Channel-argillan forming a bridge between skeleton grains. V = void, S = skeleton grain, A = argillan, B = bridge. (A) photograph, (B) schematic. The bar is 0.25 mm long.



A

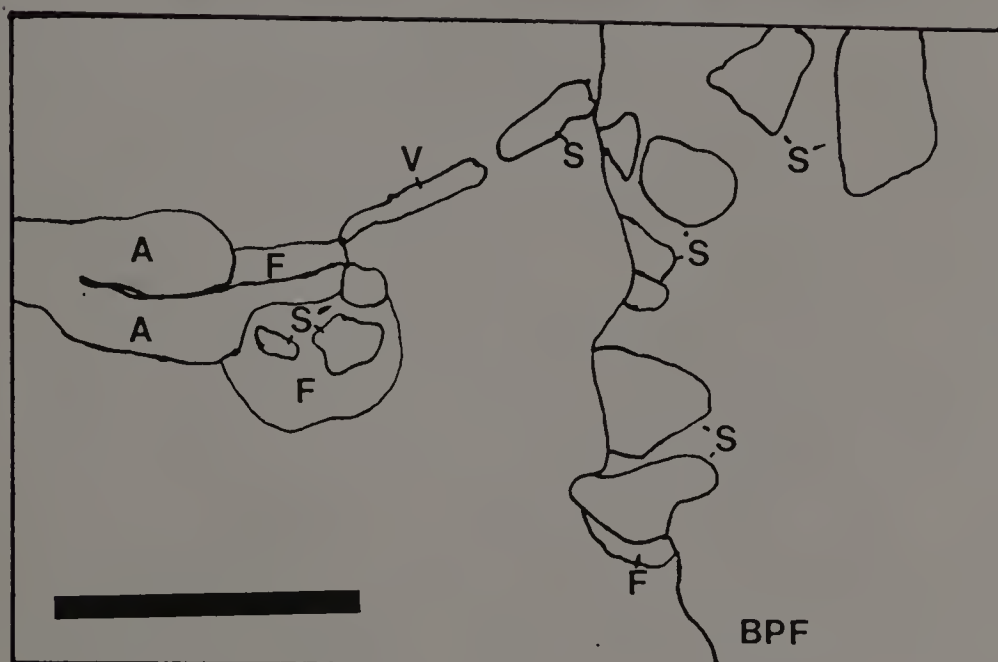


B

Figure 52. Photomicrograph from the 2Btx2 horizon of Pedon 2. Argillan forming a bridge between skeleton grains and matrix. V = void, S = skeleton grain, A = argillan, B = bridge. (A) photograph, (B) schematic. The bar is 0.25 mm long.



A

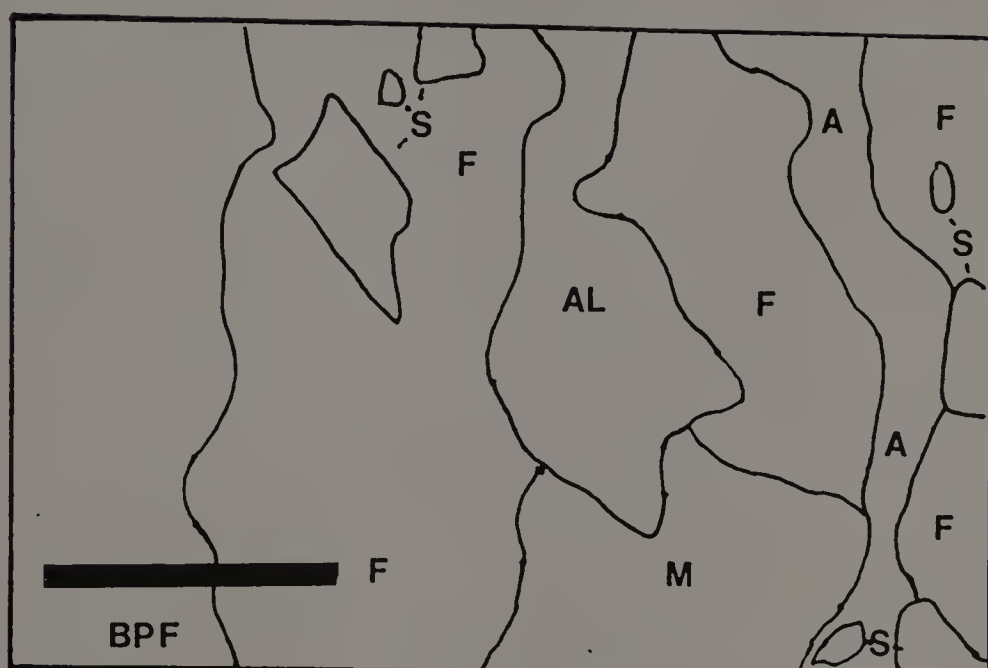


B

Figure 53. Photomicrograph from the bleached prism face (BPF) edge in the 2Btxl horizon of Pedon 3. Note the abrupt change from the Fe rich outer edge to the Fe poor BPF interior. V = void, S = skeleton grain, A = argillan, F = ferran. (A) photograph, (B) schematic. The bar is 1 mm long.

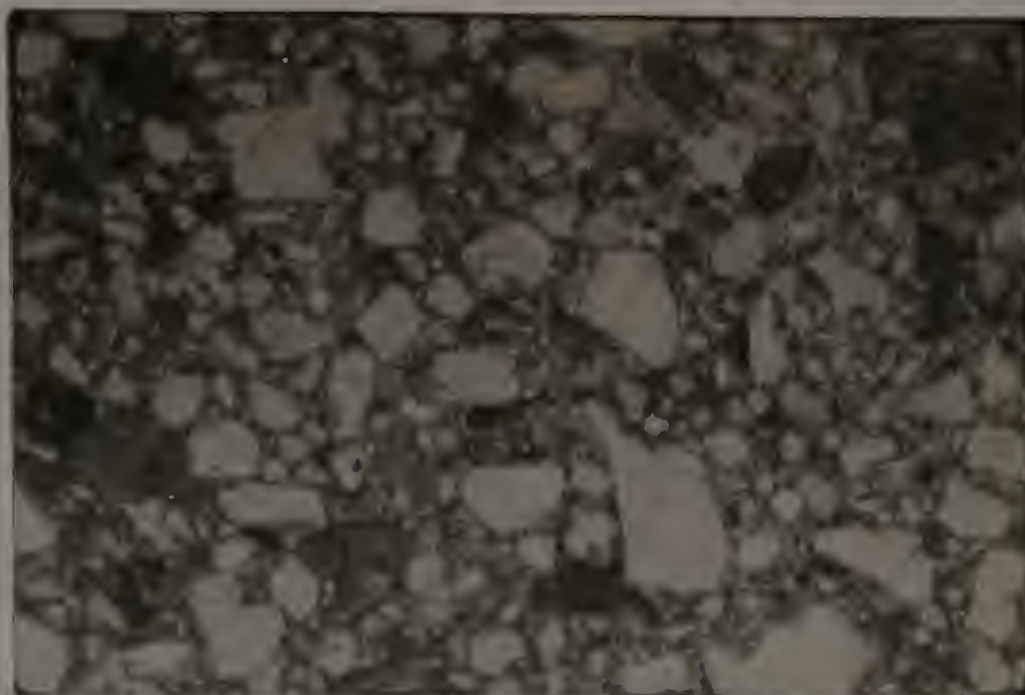


A

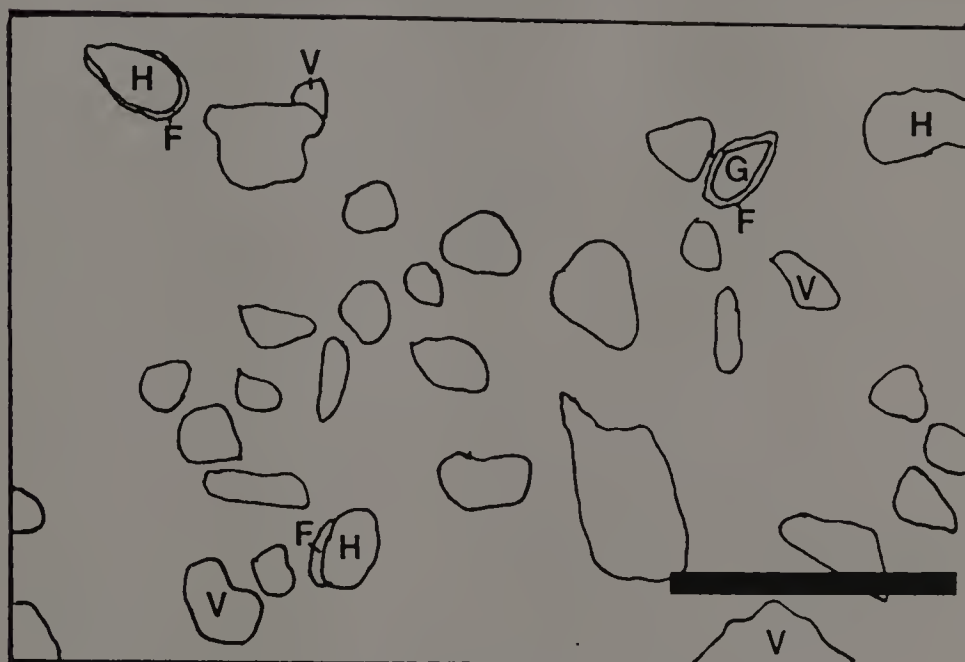


B

Figure 54. Photomicrograph from the bleached prism face (BPF) edge in the 2Btx2 horizon of Pedon 1. The boundary is demarcated by thick ferrans and argillans as well as a small zone of albic material. V = void, S = skeleton grain, A = argillan, F = ferran, AL = alban. (A) photograph, (B) schematic. The bar is 1 mm long.

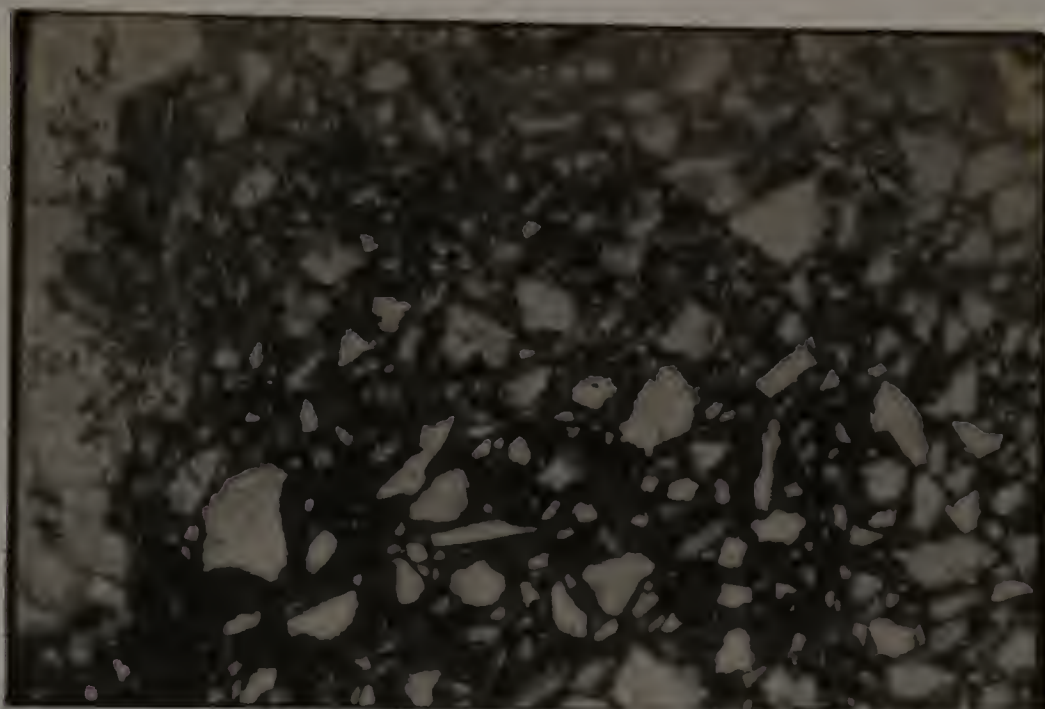


A

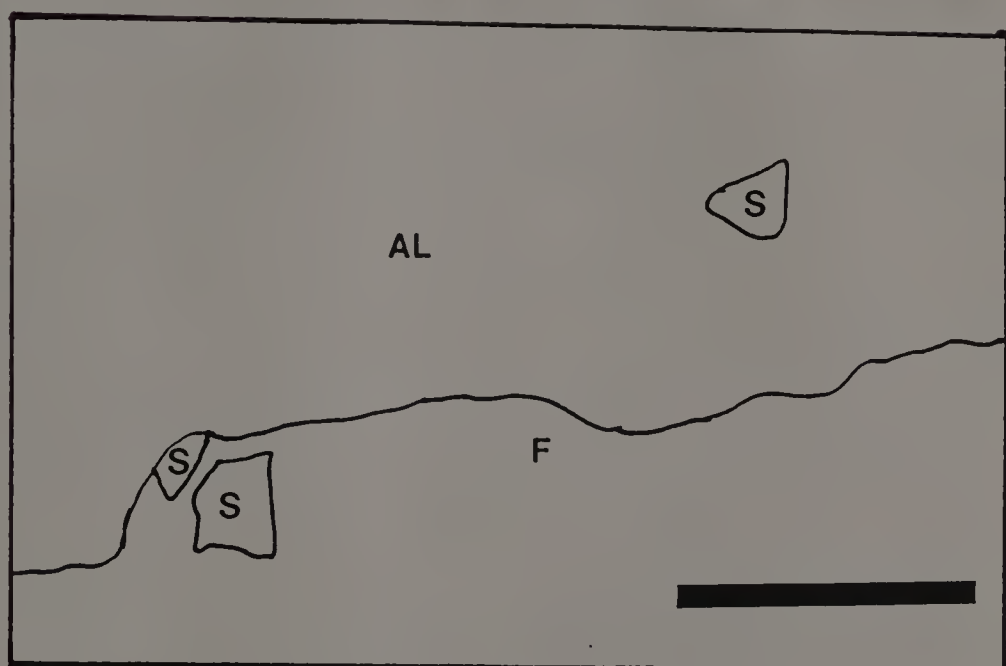


B

Figure 55. Photomicrograph from the bleached prism face interior of the 2Btx2 horizon of Pedon 5. There is a small amount of Fe-staining around Fe-rich hornblende (H) and garnet (G) grains, but the remainder of the matrix is devoid of Fe-stains. V = void, skeleton grains are demarcated but not labeled, F = ferran. (A) photograph, (B) schematic. The bar is 1 mm long.



A



B

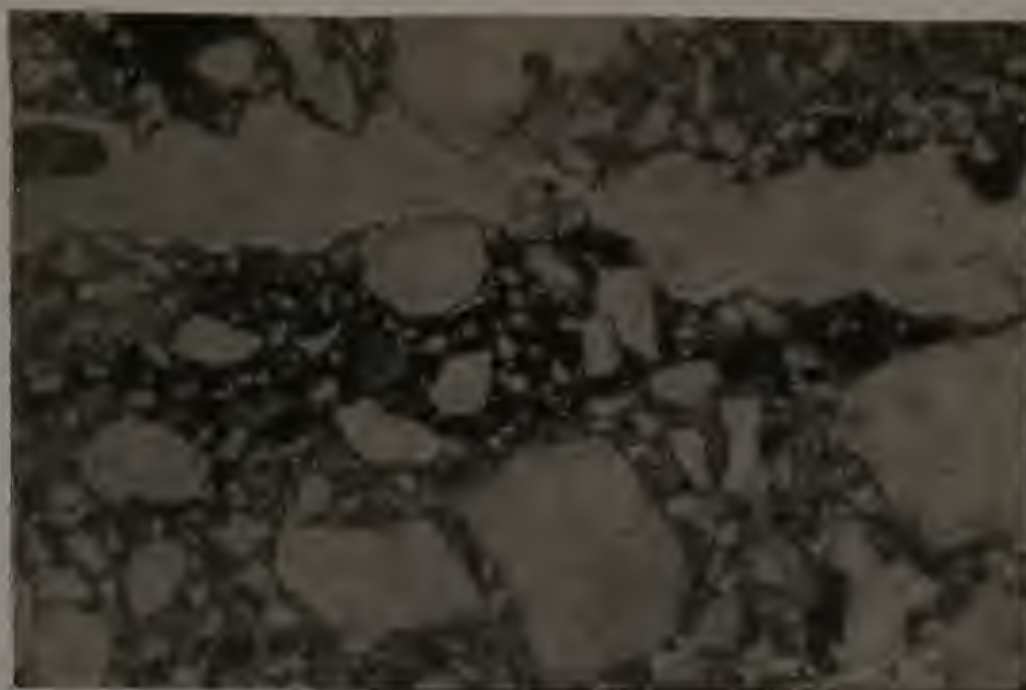
Figure 56. Photomicrograph from the 2BCd horizon of Pedon 2. The Fe-rich outer edge and Fe-poor interior of a type 2 mottle are illustrated here. S = skeleton grain, F = ferran, AL = alban. (A) photograph, (B) schematic. The bar is 1 mm long.

in the Cd horizons although ferrans and mangans are common (Figure 57). The Cd horizons are similar to unweathered till (Figures 58 and 59). Oriented clay is observed in the Lower Till but it is associated with shear and attenuation planes rather than as pedological features (Figures 60 and 61).

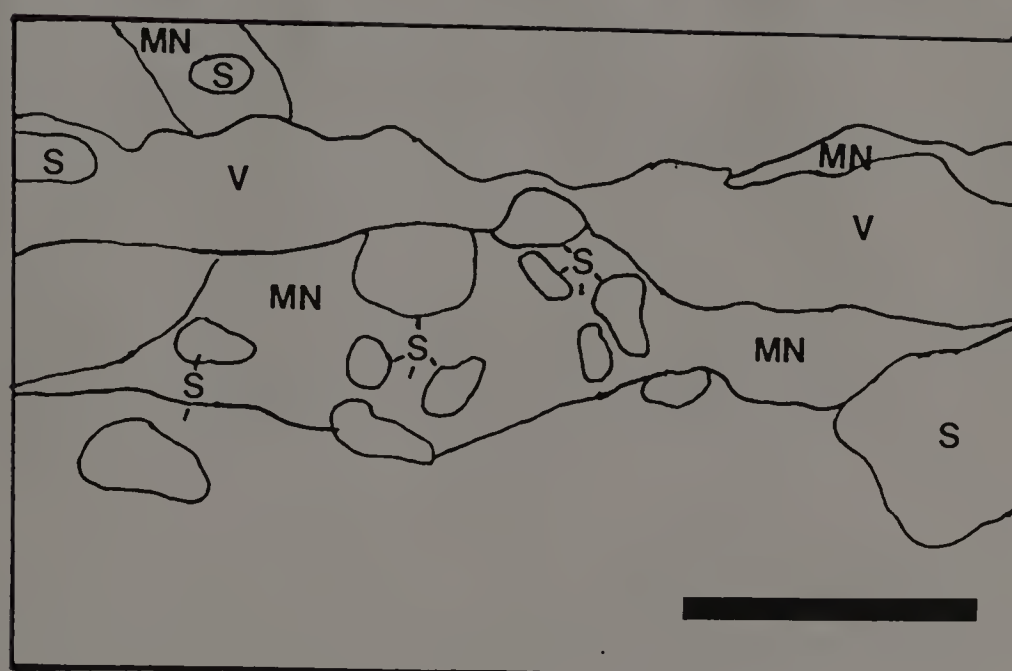
In general, void space decreased with depth (Table 18 and Figure 62) with packing voids rare in the Bt, 2Btx, 2BCd, and 3Cd horizons. The voids that did occur commonly are filled with plasma or illuviation features. The overall fabric of the matrix becomes denser with depth. Voids occur more often in the overlying Bw and BE horizons as well as within the bleached prism faces, appearing to be continuous with a few contained degrading argillans. Skeletal grains in the prism faces have fewer coatings than grains in the adjacent fragic material (Figure 63). The zone appears as a wide continuous alban cutting through the fragipan.

Plasmic fabrics in the BE and Bw horizons range from argillasepic to insepic. The fragipan horizon appears denser with a greater degree of plasmic organization present and fabrics ranging from skel-insepic to skel-vosepic (Table 20). These fabrics contrast with the argillasepic and insepic fabrics of the 3Cd horizons. 2BCd horizons, while generally similar in fabric to that of the 2Btx horizons, are less distinct.

Scanning electron microscopy (SEM) indicates that bridges and grain cutans are common within the Bx horizons (Figure 64-66) and the massive, dense nature of the Cd horizons is confirmed. (Figure 67). A few small bridges and incomplete grain coatings occur randomly within



A



B

Figure 57. Photomicrograph from the 3Cd2 horizon of Pedon 3. Mangans demarcate plate edges. V = void, S = skeleton grain, MN = mangan. (A) photograph, (B) schematic. The bar is 1 mm long.

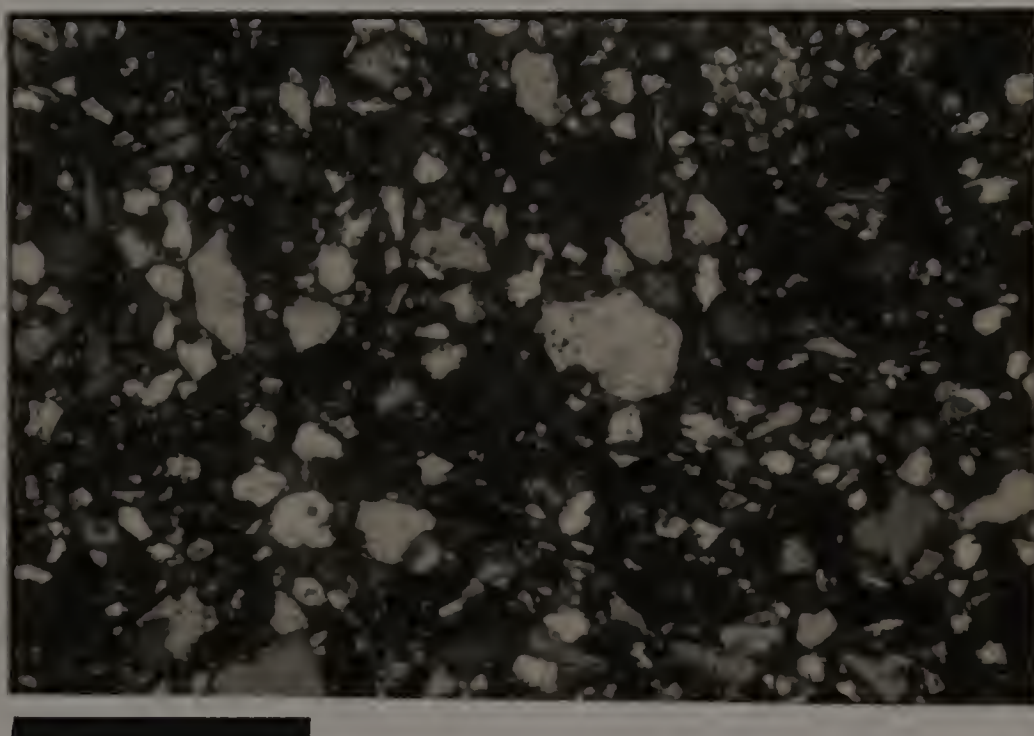


Figure 58. Photomicrograph (cross polarized light) of Upper Till. Note that despite the large percentage of skeleton grain they still appear to be matrix supported. The bar is 1 mm long.

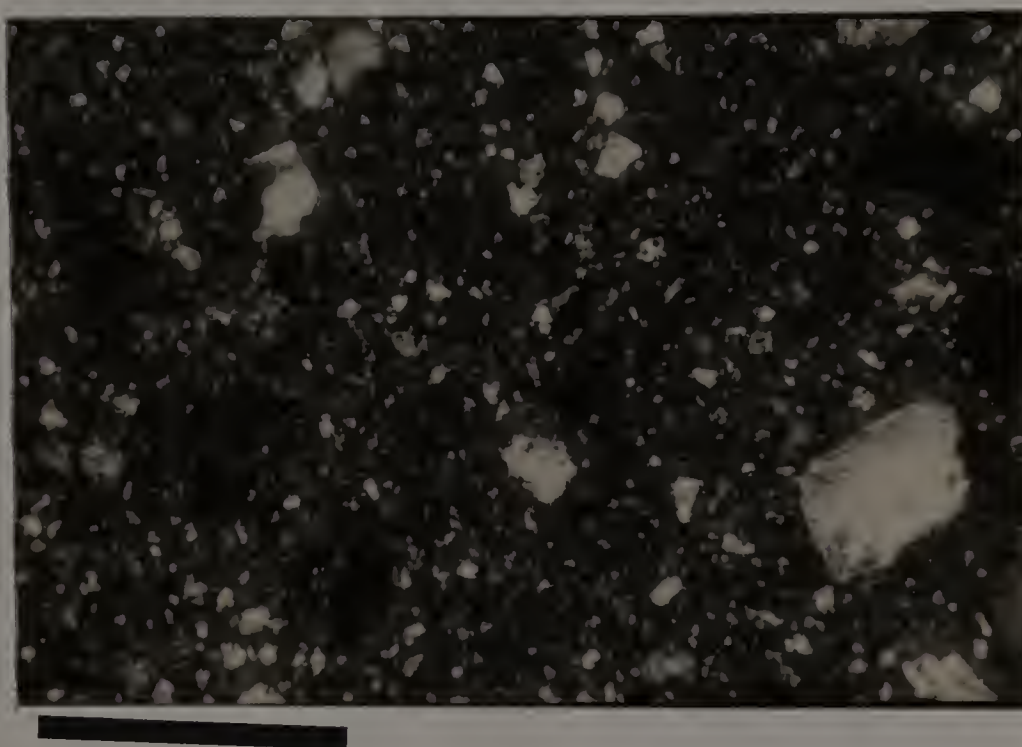
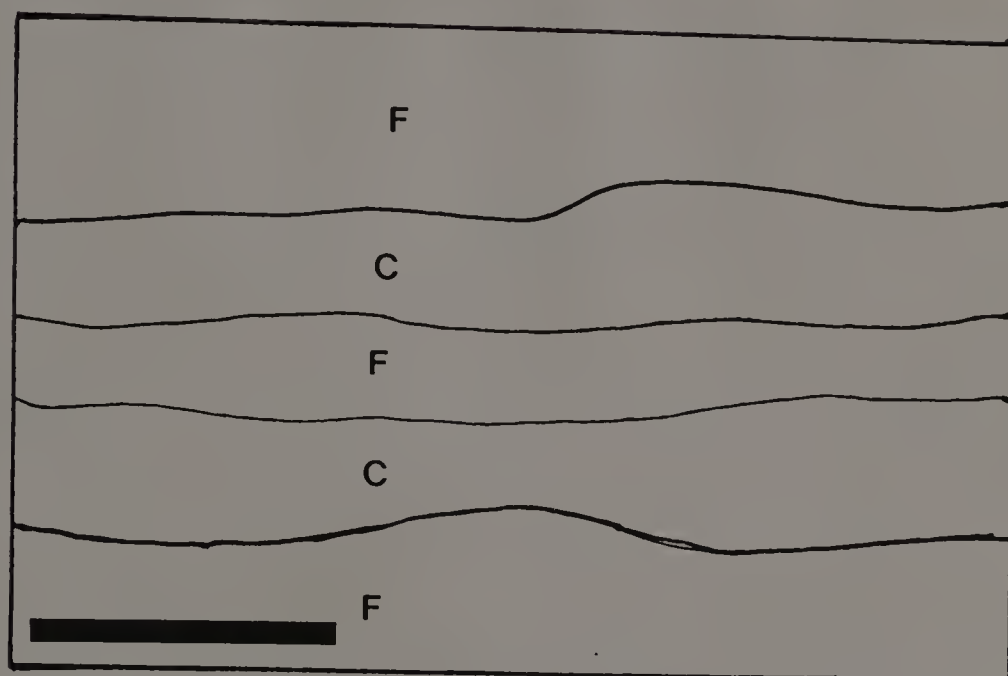


Figure 59. Photomicrograph (cross polarized light) of unoxidized Lower Till. Note that the skeleton grains are matrix supported. The bar is 1 mm long.

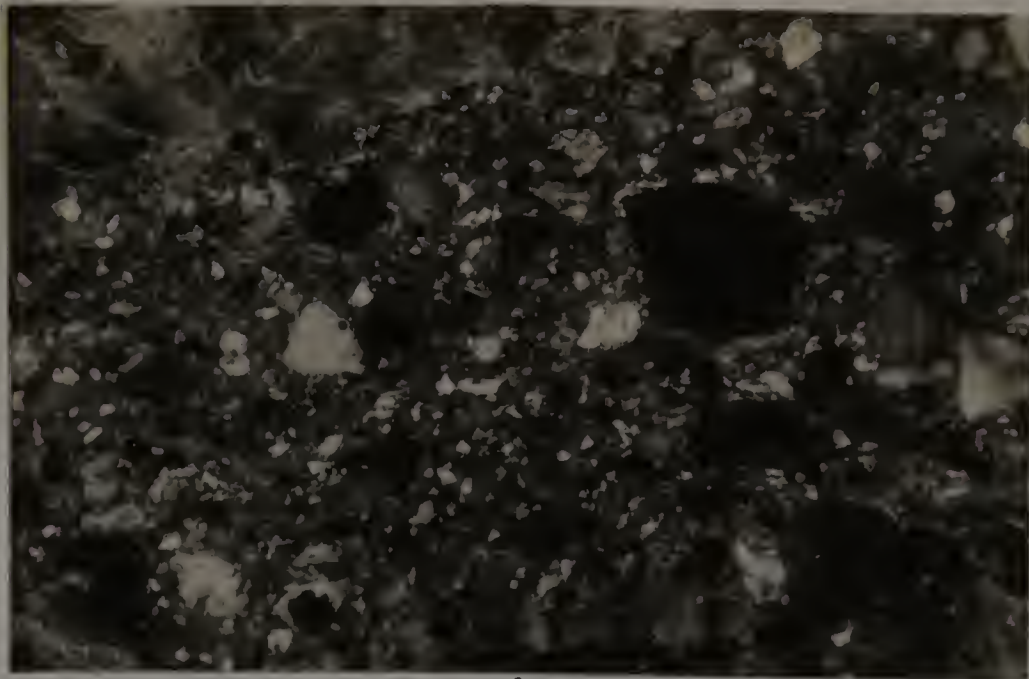


A



B

Figure 60. Photomicrograph (cross polarized light) of oriented silt beds in unoxidized Lower Till. F = fine grained silt, C = coarse grained silt. (A) photograph, (B) schematic. The bar is 1 mm long.



A

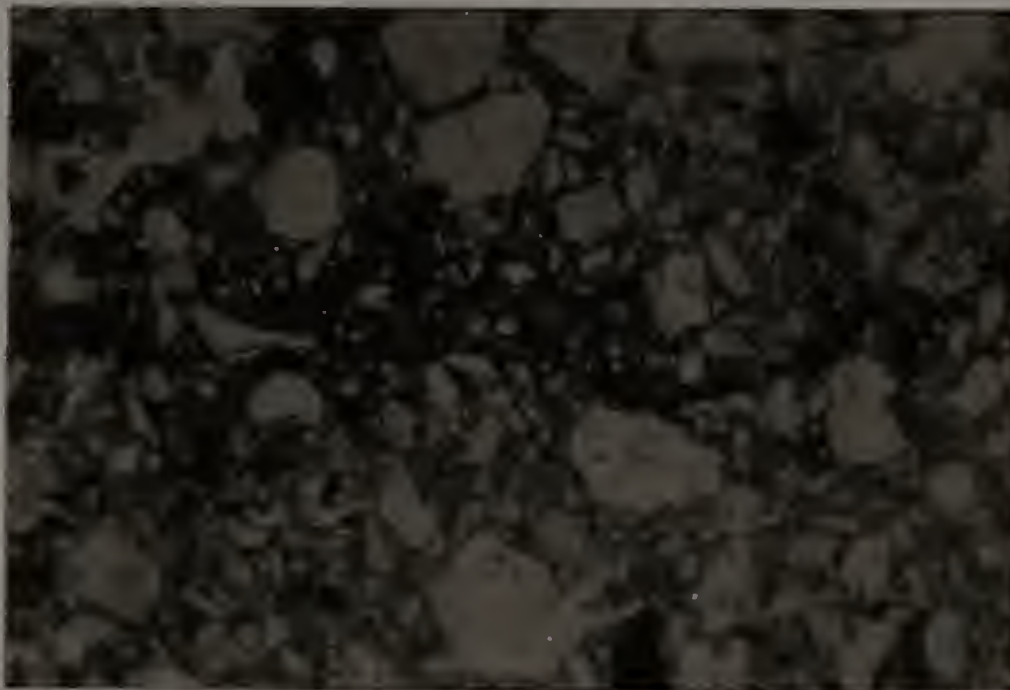


B

Figure 61. Photomicrograph (cross polarized light) of oriented clay beds in unoxidized Lower Till. S = skeleton grain, T = till, C = clay bed. (A) photograph, (B) schematic. The bar is 1 mm long.



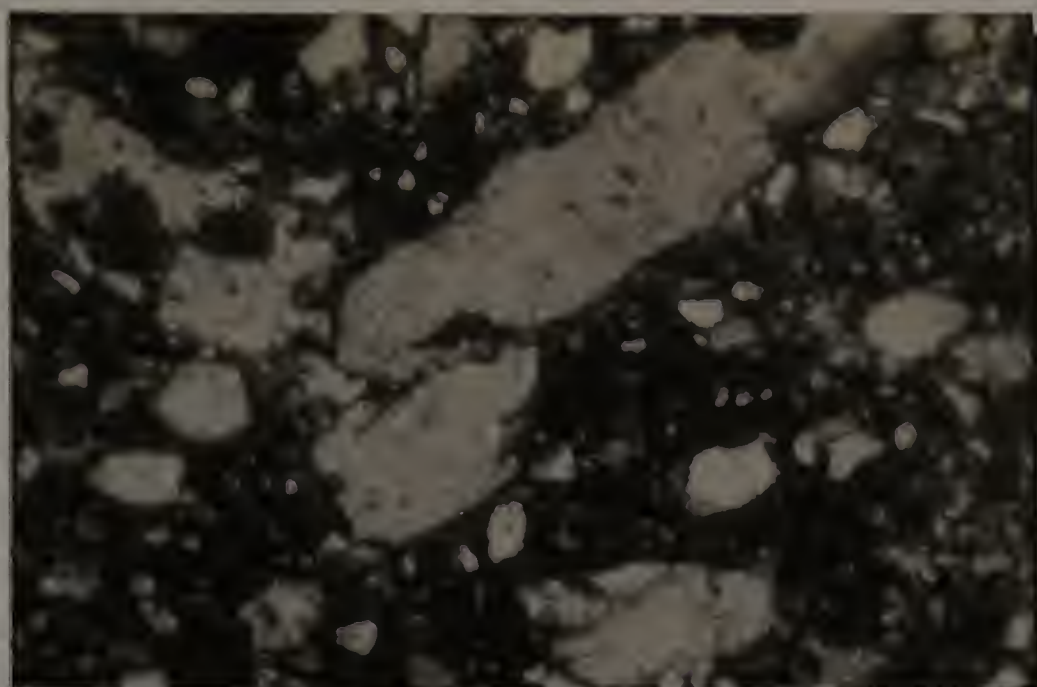
A



B



Figure 62. Photomicrograph of (A) the 2Btxl horizon of Pedon 1, and (B) the 3Cd2 horizon of Pedon 2. The light areas are skeleton grains, total void space is low. The bar is 1 mm long.



A



B

Figure 63. Photomicrograph of (A) the 2Btx2 horizon, and (B) the bleached prism face in the 2Btx2 horizon of Pedon 2. Note the dark matrix around the grains in the 2Btx2 horizon and the light matrix in the BPF caused by differences in the amount and nature of the grain cutans and amorphous coatings in each area. The bar is 1 mm long.

Table 20. Micromorphological observations for each Pedon.

Horizon	Plasmic Fabric	Pedological Features
<u>Pedon 1</u>		
Bt	Mosepic	Common papules, diffuse Fe-nodules, argillans, and ferriargillans; few albens and skeletans; very few roots
2Btx1	Mosepic with vo-skelsepic	Common papules, Fe-nodules, argillans, ferriargillans, ferrans, mangans, and albens; common grain to grain argillans and ferriargillans
2Btx2	Mosepic with vo-skelsepic	Common papules, Fe-nodules, argillans, ferriargillans, and ferrans; common grain to grain argillans and ferriargillans; few to common albens; few mangans
3BCm	Silasepic	Common ferrans, Fe-nodules, and mangans; very few argillans and ferriargillans
4Cd	Silasepic to	Common ferrans, Fe-nodules, and albens; few argillans
<u>Pedon 2</u>		
Bw1	Insepic with minor vosepic	Common papules, roots, and organic debris; very few ferrans, thin argillans, and fecal pellets
Bw2	Insepic with minor vosepic	Common papules and organic debris; few roots, ferrans, and thin argillans
BE	Insepic	Common papules and ferrans, few to common argillans; few skeletans
2Btx1	In- to mosepic to minor vo-skelsepic more developed with depth	Common papules, Fe-nodules, argillans, ferriargillans, ferrans, and albens; common grain to grain argillans and ferriargillans; very few mangans on large coarse fragments

Continued, next page

Table 20 cont.

2Btx2	Mosepic with some areas of skel-vosepik and omnisepik	Common papules, Fe-nodules, argillans, ferriargillans, and ferrans; common grain to grain argillans and ferriargillans; few to common albans; very few mangans
2BCd	In- to mosepic	Common papules, Fe-nodules, argillans, ferriargillans, and ferrans; few to common albans; few mangans
3Cd1	Insepik	Common ferrans; few to common mangans; few papules; very few argillans
3Cd2	Silasepic minor argillasepic	Common ferrans; few mangans and papules; very few argillans

Pedon 3

BE	Insepik	Common papules and ferrans, few argillans and skeletans
2Btx1	In- to mosepic to minor vo-skelsepik more developed with depth	Common papules, argillans, ferriargillans, ferrans, and albans; common grain to grain argillans and ferriargillans; few Fe-nodules; very few mangans
2Btx2	Mosepic with some skel-vosepik	Common papules, Fe-nodules, argillans, ferriargillans, and ferrans; common grain to grain argillans and ferriargillans; few to common albans; very few mangans
2BCd	In- to mosepic	Common papules, diffuse Fe-nodules, argillans, ferriargillans, and ferrans; few to common albans; few mangans
3Cd1	Insepik to silasepic	Common ferrans; few mangans and papules; very few argillans

Continued, next page

Table 20 cont.

Pedon 4

Ap	Silasepic	Common papules, Fe-nodules, fecal pellets, roots, and organic debris
Bw1	Argillasepic to silasepic	Common papules, roots, and organic debris; few diffuse Fe-nodules and ferrans; very few thin argillans and fecal pellets
Bw2	Silasepic	Common papules and diffuse Fe-nodules; few ferrans; very few thin argillans, fecal pellets, and organic debris
BE	Insepic	Common papules and ferrans, few to common argillans; few diffuse Fe-nodules, and skeletans
2Btx1	In- to mosepic to minor vo-skelsepic more developed with depth	Common papules, argillans, Fe-nodules, ferriargillans, ferrans, and albans; common grain to grain argillans and ferriargillans; few Fe-nodules, and mangans
2Btx2	Mosepic to skel-vosepic	Common papules, Fe-nodules, argillans, ferriargillans, and ferrans; common grain to grain argillans and ferriargillans; few to common albans; very few mangans
2BCd	In- to mosepic	Common papules, diffuse Fe-nodules, argillans, ferriargillans, and ferrans; few to common albans; few mangans
3Cd	Insepic to silasepic	Common ferrans; few mangans and papules; very few argillans

Continued, next page

Table 20 cont.

Pedon 5

Bw	Silasepic	Common Fe-nodules and papules
BE	Silasepic	Common papules and diffuse Fe-nodules; very few skeletans
2EB	Silasepic	Common papules, diffuse Fe-nodules, and thin ferriargillans and argillans; few ferrans and skeletans
2Btx1	Silasepic to mosepic and skel-vosepik	Common papules, Fe-nodules, argillans, ferriargillans, ferrans, albans, and silt caps, common grain to grain argillans and ferriargillans; very few mangans
2Btx2	Insepik to mosepic and skel-vosepik	Common papules, Fe-nodules, argillans, ferriargillans, ferans, and silt caps, common grain to grain argillans and ferriargillans; few to common albans; very few mangans; argillans, ferriargillans, and ferrans decrease with depth
2Cd1	Silasepic to mosepic	Few papules, argillans, and diffuse Fe- nodules; very few ferrans
2Cd2	Silasepic to mosepic	Few papules and diffuse Fe-nodules; very few argillans and ferrans



Figure 64. Scanning electron micrograph of a clay bridge in the 2Btx1 horizon of Pedon 2. The bar is 100 μ m long.



Figure 65. Scanning electron micrograph of a clay bridge in the 2Btx1 horizon of Pedon 2 (enlargement of Figure 64). Note the curved nature of the bridge and the oriented individual particles. The bar is 10 μm long.



Figure 66. Scanning electron micrograph of a clay bridge in the 2Btx2 horizon of Pedon 5. The bar is 100 μ m long.



Figure 67. Scanning electron micrograph of the 3Cd2 horizon of Pedon 3. Note the massive nature of the material. The bar is 100 μm long.

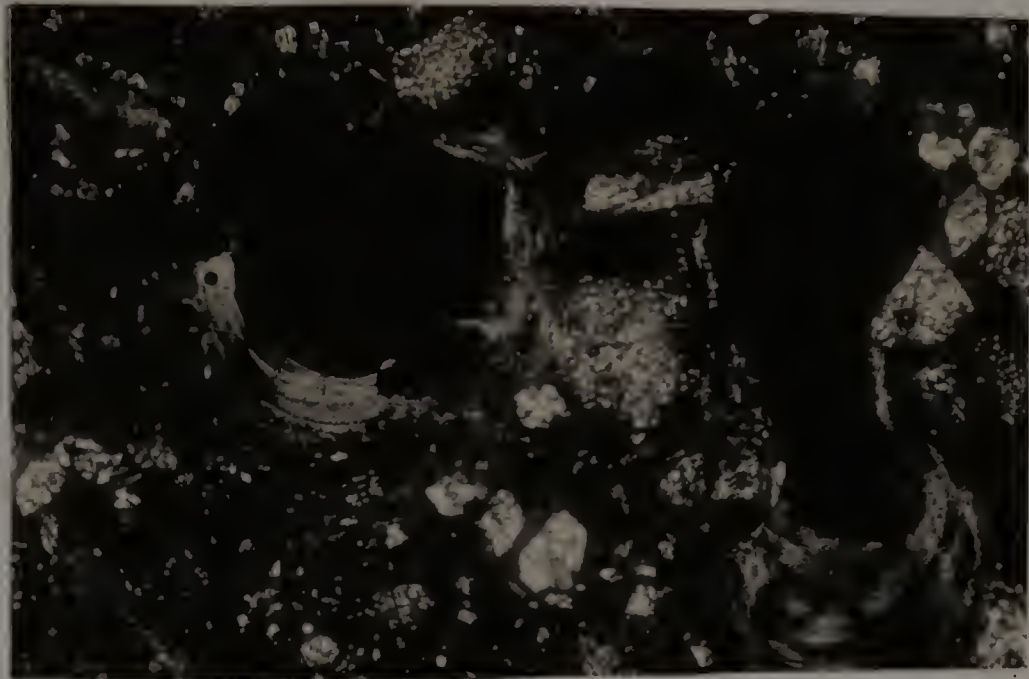
the bleached prism face although clean skeletal grains dominated the zone (Figure 68). A single EDXRA analysis of a bridge in the 2Btx1 horizon of Pedon 5 is composed of Si, Al, and K. This suggests that the bridge is composed of clay, possibly illite.

Discussion

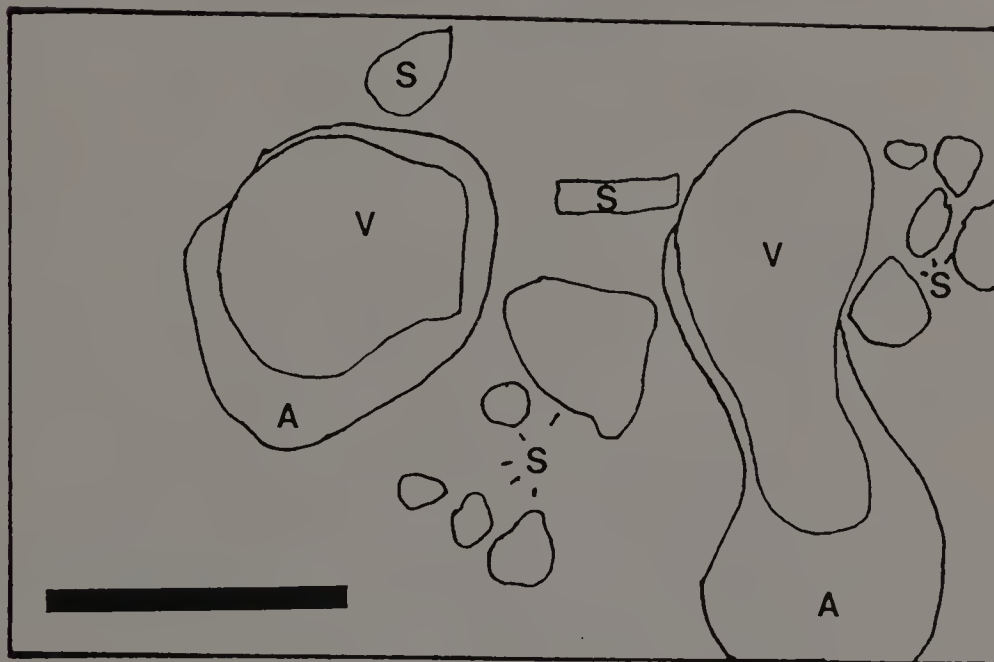
Results of observations of thin section observations of Massachusetts fragipans are similar to results of other micromorphic studies of fragipans. Illuviated clay in voids and as bridges between sand grains are ubiquitous. Investigations of fragipans developed in a wide range of parent materials have described the same features (Knox, 1957; Grossman et al., 1959; Jha and Cline, 1963; Horn and Rutledge, 1965; Wang, 1971; Wang et al., 1974; Smith and Callahan, 1987). The occurrence of partially degrading argillans above the fragipan implies that newly mobilized clay is moving vertically into the fragipan or laterally across the fragipan. Wang (1971) observed similar degradation in a fragipan soil in New York. The presence of geopetal structures (Figure 69) suggest that clay moves into the fragipans from above rather than solely moving across it. Below the fragipans most argillans are not well developed and less abundant indicating that less lessivage has occurred. Nodules and ferrans are typically related to redox conditions rather than to illuviation. Changes in redox potential best explain the presence of ferrans adjacent to the BPF (c.f. Chapter 4) although the Fe is probably complexed in overlying horizons and moved into the fragipan through the BPF. Much of the flow of water through the fragipan occurs in the



Figure 68. Scanning electron micrograph of bleached prism material in the 2Btx2 horizon of Pedon 5. The grains appear to be uncoated. The bar is 100 μ m long.



A



B

Figure 69. Photomicrograph (cross polarized light) from the 2Btx2 horizon of Pedon 5. Note that the argillans form geopetal structures in voids. V = void, S = skeleton grain, A = argillan. (A) photograph, (B) schematic. The bar is 1 mm long.

BPF and illuvial cutanic features commonly are observed adjacent to them, however, argillans and grain cutans are observed throughout the fragipan matrix. Argillans in horizons above and below the Bx horizons have been described as remnants or as being degraded while the argillans in the pans are forming currently (Jha and Cline, 1963; Miller et al., 1971). Well developed argillans and ferriargillans support the conclusion that illuviation is an ongoing process in these fragipans.

Determination of plasmic fabric is a subjective exercise due to the wide spectrum of features to be described (Brewer, 1976). Skel-insepic to vosepic fabrics are observed most often in the fragipans, whereas asepic and skelsepic fabrics are observed in horizons above and below the pan respectively (Table 20). The fabric seen in the till samples are skelsepic to asepic except in areas affected by shear and attenuation (Lindbo, 1990). It is unlikely that the fabrics observed in the fragipans are inherited as the plasmic fabric in the till is less developed than that in the fragipans. Other investigators have described similar plasmic fabrics in fragipans developed from a wide range of parent materials. The plasmic fabrics described in fragipans include skel-insepic (Miller et al., 1971; Norton et al., 1984; Smith and Callahan, 1987), skel-mosepic (Smith and Callahan, 1987), and invosepic (Horn and Rutledge, 1965); whereas those observed in C horizons are asepic to skelsepic fabrics (Smith and Callahan, 1987). The present study fits in well with previous observations further indicating that the fragipans observed in

Massachusetts have undergone pedogenesis and are not fully inherited features.

Based on previous work (Horn and Rutledge, 1965; Smith and Callahan, 1987), the presence of strong illuviated features as observed in the pedons investigated, indicates a period of intense and/or prolonged pedogenic activity. The features observed in the soils from this study are the same regardless as to the type of bedrock suggesting that the micromorphology of the fragipans is not dependent on local bedrock lithology, although the parent material (i.e. till type, colluvium, or aeolian material) does have an influence on micromorphology (c.f. Appendix F) as does drainage.

Conclusions

Based on the available information from other micromorphic investigations of fragipans it appeared that the soils investigated in this study show enough similarities to be formally recognized as fragipans. These features include well developed illuvial argillans, ferriargillans, bleached prism faces, and vosepic and skel-insepic fabrics. Enough illuviated clay is present to classify the Bx horizons as argillic as well as fragipan horizons. The dense nature of the material is similar to that observed in the Cd horizons, although the fragipans showed greater development of fabric and other micromorphic features. The use of thin section analysis showed significant pedogenic development in these Massachusetts fragipans.

CHAPTER VI

CHEMICAL PROPERTIES

Previous Work

The only truly unique chemical properties found in fragipans are a low organic matter and very low to zero CaCO_3 content (Grossman and Carlisle, 1969; Soil Survey Staff, 1975; Smalley and Davin, 1982). In addition, fragipans have been observed to contain moderate to high levels of extractable Fe (Steinhardt and Franzmeier, 1979; Nettleton et al., 1968b; Crampton, 1965). High Fe content has been positively related to clay content (Grossman and Carlisle, 1969; McCabe et al., 1978; Harlan et al., 1977), as has high Al content (Harlan et al., 1977). Both extractable Fe and Al have been used as tests to determine the location of the fragipan and to explain its brittleness (Yassoglou and Whiteside, 1960; Horn and Rutledge, 1965; Nettleton et al., 1968b). Recently, the presence of extractable Si has been linked to fragipan expression (Steinhardt and Franzmeier, 1979; Franzmeier et al., 1978; Harlan et al., 1977; Norton and Franzmeier, 1978; Karathanasis, 1987a, 1987b, 1989; Franzmier et al., 1989), however extractable Fe, Al, and Si do not always appear concentrated in the fragipan (DeKimpe, 1970; DeKimpe et al., 1972) thus they are not necessarily diagnostic of fragipans. Therefore, it can be assumed that fragipan chemistry varies due to location and parent material. Attempts have also been made to correlate brittle behavior in the

fragipan to the extraction of bonding agents which will be discussed in Chapter 9.

Extracting Agents

Many investigations have been carried out to determine the most suitable reagent for removing various soil constituents and to correlate these constituents to various soil forming processes. McKeague and Day (1966) used ammonium-oxalate and dithionite-citrate-bicarbonate (CBD) to determine the fraction of inorganic Fe and Al removed. At pH 2 and pH 3 oxalate extracted virtually the same amount of Fe and Al but less was extracted at pH 4.2. Oxalate at pH 3 was determined to be the most satisfactory extractant for inorganic and organic amorphous Fe and Al. The dithionite extracted more Fe than any of the oxalate treatments since it extracts not only the amorphous component but also some of the more crystalline Fe as well. McKeague (1967) compared ammonium-oxalate at pH 3, 0.1 M sodium-pyrophosphate at pH 10, and 0.1M sodium-pyrophosphate combined with dithionite as used by Franzmeier et al. (1965). The oxalate extracted inorganic and organic non-crystalline complexes, while the pyrophosphate-dithionite solution extracted crystalline complexes as well. The pyrophosphate extracted sesquioxides causing the solution to become turbid. Na-pyrophosphate was concluded to be the most specific extractant for organically bound amorphous Fe and Al. McKeague and Day (1969) and McKeague et al. (1971) suggested that ammonium-oxalate and pyrophosphate were good extractants for differentiating soils by the amount of organically and inorganically complexed extractable Fe and Al they contain. They reported that while various sodium-dithionite

extractions may remove more Fe and Al (Deshpande et al., 1968), the oxalate extraction is more selective in its removal of amorphous Fe. Borggaard (1976) reported that Na-EDTA worked as well as oxalate with slightly greater selectivity although the solution may become turbid and require centrifuging. Recently, Ross et al. (1985) reported hydroxylamine to be more efficient and simpler in procedure with a solution to soil ratio of 250:1 than either oxalate or Na-EDTA.

Potassium-pyrophosphate has also been used as an extractant for Al and Fe (Bascomb, 1968). Using a large solution to soil ratio Bascomb compared 0.1M K-pyrophosphate at pH 10 and pH 7, concluding that the pH 10 solution extracted organic complexes and the active or mobile $\text{Fe}(\text{OH})_3$ phase best, while the pH 7 solution extracted the older, more crystalline phase. Neither solution extracted Al or Si well.

The particle size and mineralogy of the soil being extracted have as much bearing on the results as the extractant (Arshard et al., 1972). Both dithionite and oxalate extracted more Fe, Al, and Mg as the particle size of the soil decreased, and as the amount of trioctahedral layered silicates increased. Potassium-pyrophosphate did not follow the same trends. The pyrophosphate at pH 10 and pH 7 removes organically bound Fe along with the organic complex. Giovannini and Sequi (1976) used acetylacetone in benzene to remove the organically bound Fe but not the organic matter as the solution is non-polar. This results in the extremely specific removal of Fe in about 200 hours. Giovannini and Sequi indicated that the use of acetylacetone in benzene was a better method than the use of

pyrophosphate, however Bascomb and Thanigasalam (1978) disagreed. They observed that as surface area decreased the amount of Fe removed by acetylacetone decreased, whereas the amount of pyrophosphate extracted Fe was independent of surface area. They concluded that pyrophosphate is most suitable for soils with amorphous and poorly crystalline Fe oxides. The effect of a slight change in the acetylacetone matrix was investigated by Hallmark and Smeck (1979a). They compared pyrophosphate, oxalate, and acetylacetone-0.1M HCl solution and used their results to establish a positive link between amorphous material removed and the presence of a fragipan developed in loess. The acetylacetone extractable-Al was the only extractant to give a positive correlation to the fragipan horizon. Steinhardt (1982), using 0.5N NaOH, found that extracted silica was highest in the fragipan horizons. The values attained for the NaOH were up to 10 times higher than those found for CBD. Prior to Steinhardt's comparison of NaOH to CBD, Knox (1957) used NaOH to extract colloidal Si. NaOH was also used by Franzmeier et al. (1978) and by Steinhardt and Franzmeier (1979) to extract Si and hydrous Al. DeKimpe and Laverdiere's (1982) findings did not agree entirely with the aforementioned as they concluded NaOH was a poor extractor of oxides compared to the other solutions they used. Their results showed CBD 1:1>tiron/citrate>CBD/citrate>citrate>NaOH/citrate in terms of oxides extracted. They concluded that NaOH actually dissolved some crystalline minerals, but did not remove much Fe_2O_3 as the Fe is less soluble at the higher pH's.

Although the exchange chemistry of fragipans has not been correlated to its expression and properties it is useful to investigate changes in the soil due to pedogenic factors. If the exchange chemistry indicates that weathering has occurred it stands to reason that the pan has been altered and is not entirely inherited. Numerous studies have attempted to correlate various extractable elements to a fragipan with limited success. The present study evaluates eight extractions methods in hopes to find some correlation between the pan and extractable elements.

Materials and Methods

Exchange Chemistry

pH. Hydrogen ion concentration (pH) was measured in separate 1:1 (20 g of sample to 20 ml of solution) mixtures of sample to distilled/deionized H₂O, 1N KCl, and 0.01M CaCl₂ (McClean, 1982). This procedure used unground sample passed through a 2-mm sieve only.

Organic Carbon. Organic carbon was determined by wet digestion following the Modified Mebius Procedure (Nelson and Sommers, 1982). Two grams of ground sample (passed through a 2-mm sieve and pulverized in a Spex Shatter Box) were added to 10 ml of 0.5N potassium-dichromate (K₂Cr₄O₇), 15 ml H₂SO₄, and 8 ml of distilled/deionized H₂O. The solution was boiled for 30 minutes, removed from heat, approximately 50 ml distilled/deionized H₂O was added, and the mixture cooled to room temperature in a water bath. Five drops of indicator (0.100g N-phenylanthranilic acid and 0.107 g sodium-carbonate

dissolved in 100 ml H₂O) was added and the solution titrated with 0.2N FeSO₄ to a light green end point. Percent organic carbon was calculated using formula 1, where ml blank and ml sample refer to the ml of titrant used, N refers to the exact normality of the titrant, and g refers to the grams of sample used. As the amount of organic carbon increases less sample is required.

$$\%O. C. = \frac{\text{ml Blank} - \text{ml Sample}}{\text{g Sample}} \times N \text{ of FeSO}_4 \times 0.3 \quad (1)$$

Extractable Acidity. Extractable acidity was determined using the modified barium chloride-triethanolamine (BaCl₂-TEA) method (Peech et al., 1962). Ten grams of unground sample was added to 100 ml of BaCl₂-TEA at pH 8 and allowed to react overnight. The solution was filtered and brought to 250 ml with BaCl₂-TEA. The solution was then titrated with 0.2N HCl using 5 drops of indicator (0.22g bromocresol green, 0.075g methyl red, 3.5 ml 0.1N NaOH, in 96 ml 95% EtOH). Centimoles per kilogram extractable acidity was calculated using formula 2, where ml blank and ml sample are the ml of tritrant used, N refers to the normality of the HCl, and g sample is the sample weight.

$$\text{Ex. Acidity} = (\text{ml blank} - \text{ml sample}) \times (\text{M acid}) \times (100\text{g/g sample}) \quad (2)$$

Cation Exchange Capacity. The major basic cations (Ca^{2+} , Mg^{2+} , Na^{+} , and K^{+}) were extracted with 1N ammonium-acetate (NH_4AOC) at pH 7. Twenty-five grams of unground sample was added to 50 ml of extractant and allowed to react overnight (Rhoades, 1982). The sample was filtered, washed, and brought to 250 ml with the extractant. Concentrations of each cation were determined by means of atomic absorption or emission. Centimoles per kilogram of exchangeable cations were determined using formula 3, where ppm is the concentration from the AA/AE, D is the dilution factor, F is a conversion factor, and g is the weight of sample. Factors used in the determination are as follows: $\text{Ca} = 1.2475$, $\text{Mg} = 2.0566$, $\text{Na} = 1.08744$, $\text{K} = 0.63939$.

$$\text{Ex. Cation} = (\text{ppm}) \times (\text{D}) \times (\text{F}) / (\text{g}) \tag{3}$$

Cation exchange capacity was calculated by summing the exchangeable bases with the extractable acidity and percent base saturation was calculated by dividing the sum of cations by the total CEC and multiplying by 100.

Extractable Elements.

Extractable Fe, Mn, Al, and Si were determined from ten separate extraction procedures (Table 21). In addition, the effects of differing grinding techniques were evaluated for eight extractions on two soils (Appendix G).

Table 21. Summary of extraction procedures used to determine Fe, Al, Mn, and Si.

Citrate-Dithionite (CD) after Holmgren (1967)

2 g sample
2 g Na-dithionite; 20 g Na-citrate
125 ml Distilled-deionized water
Shake overnight (16 hours), bring to 250 ml
Centrifuge, dilute, and analyse.

Pyrophosphate @ pH 10 (PYRO) after Bascomb (1968)

0.5 g sample
50 ml 0.1 M Na-pyrophosphate
Shake overnight (16 hours), bring to 100 ml
Centrifuge, dilute, and analyse.

Ammonium-Oxalate @ pH 3 (OX) after McKeague and Day (1966)

1 g sample
40 ml 0.2 M NH_4 -Oxalate
Shake in darkness overnight (16 hours), bring to 100 ml
Centrifuge, dilute, and analyse.

Acetylacetone (AA) after Hallmark and Smeck (1979a)

5 g soil
30 ml 2% Acetylacetone in 0.1 M HCl
Shake for 1 hour, filter, bring to 100 ml.

Hydroxylamine-Hydrochloride (HH1) after Chao and Theobald (1976) and
Chao and Zhou (1983)

0.1 g soil
25 ml 0.25 M hydroxylamine-hydrochloride in 0.25 M HCl
Shake at 150 rpm in a 50°C water bath for 30 minutes
Bring to 50 ml and centrifuge.

Hydroxylamine-Hydrochloride (HH2) after Chao and Theobald (1976)
Chao and Zhou (1983) and Ross
et al. (1985)

0.1 g soil
25 ml 0.25 M hydroxylamine-hydrochloride in 0.25 M HCl
Shake overnight (16 hours)
Bring to 50 ml and centrifuge.

Continued, next page

Table 21 cont.

NaOH (NaOH) after Franzmeier et al. (1978)

0.1 g soil

100 ml 0.5 M NaOH

Bring to 100°C for 2.5 minutes

Cool, bring to 250 ml, and centrifuge.

Citrate-Bicarbonate-Dithionite (CBD) after McKeague and Day (1966)

2 g soil

2.5 ml 1 M Na-Bicarbonate, 20 ml 0.3 M Na-Citrate

Bring to 80°C in a water bath

Add 0.5 g Na-Dithionite, stir for 1 minute

Add 10 ml NaCl, bring to 250 ml, and centrifuge.

Na-EDTA (EDTA) after Borggaard (1976)

1 g soil

50 ml 0.1 M Na-EDTA

Shake for 48 hours, bring to 100 ml

Centrifuge.

Calcium-Chloride (CaCl)

1 g soil

50 ml 0.025N CaCl₂

Shake overnight (16 hours)

Bring to 100 ml and centrifuge.

Fe, Mn, and Al were all analysed by atomic absorption or emission spectroscopy. Si was analysed colorometrically (Hallmark et al., 1982).

Results

Exchange Chemistry

pH. The pH_w (water extract) increases from the Ap horizons to the Cd horizons (Figure 70). Most of the pedons have a gradual increase with depth with the pH_w maximum occurring in the Cd horizons. In Pedon 2 pH values increase through the BE and then rapidly decrease in the 2Btx1 from which the pH_w then rises to a maximum in the 3Cd2. As expected, pH_K (KCl extract) values are lower by approximately 0.5 pH units but the same general trend as pH_w is observed with the major exception of Pedon 1 (Figure 71). Pedon 1 has a pH_K maximum in the lower fragipan horizon followed by a drop in pH_K . The pH_C (CaCl_2 extract) shows a similar decrease in overall pH values when compared to the pH_w values but again the trends with depth are similar (Figure 72). Interestingly, Pedon 5 has the highest pH_w and pH_C values, probably caused by agricultural practices at the site. Pedons 1-4 have lower pH values in their solums than their corresponding parent material (oxidized Lower Till), whereas Pedon 5 has higher values than observed in the Upper Till (Appendix H).

Organic Carbon. Percent organic carbon (OC) follows the expected trend, a rapid decrease from a maximum in the Ap horizons to low values in the fragipan and lower horizons (Figure 73).

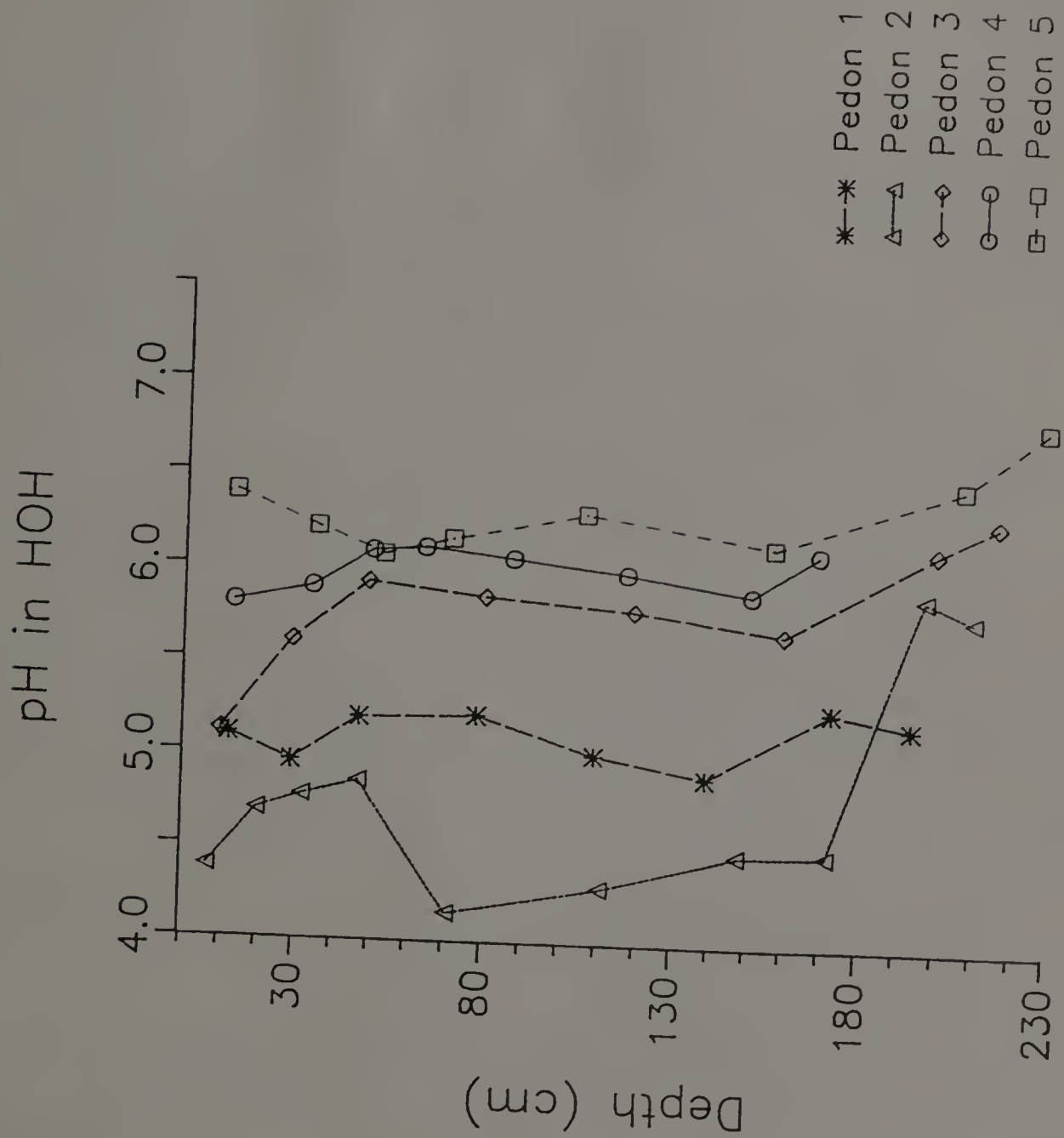


Figure 70. pH_w for each horizon by depth in Pedons 1-5.

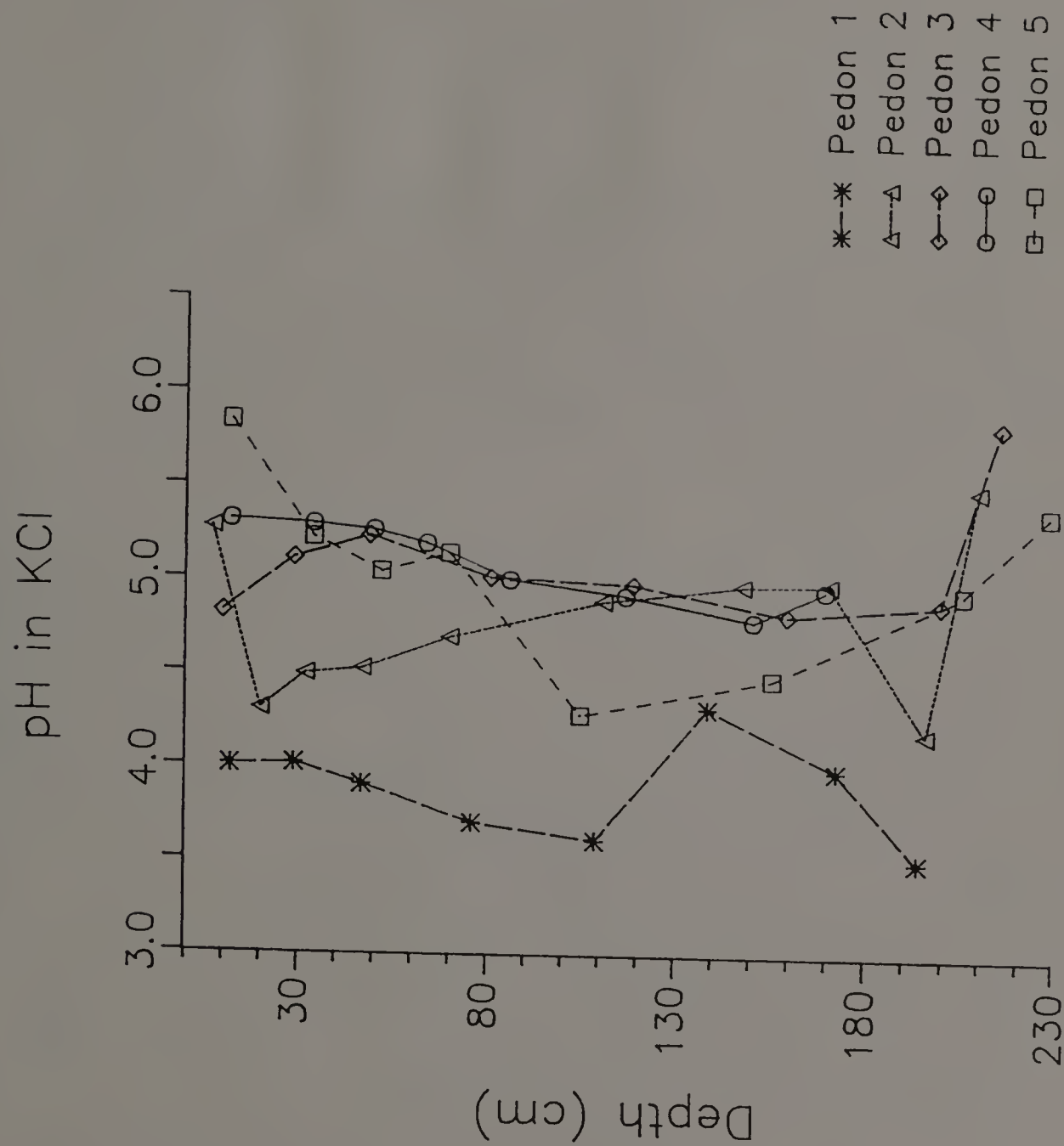


Figure 71. pH_K for each horizon by depth in Pedons 1-5.

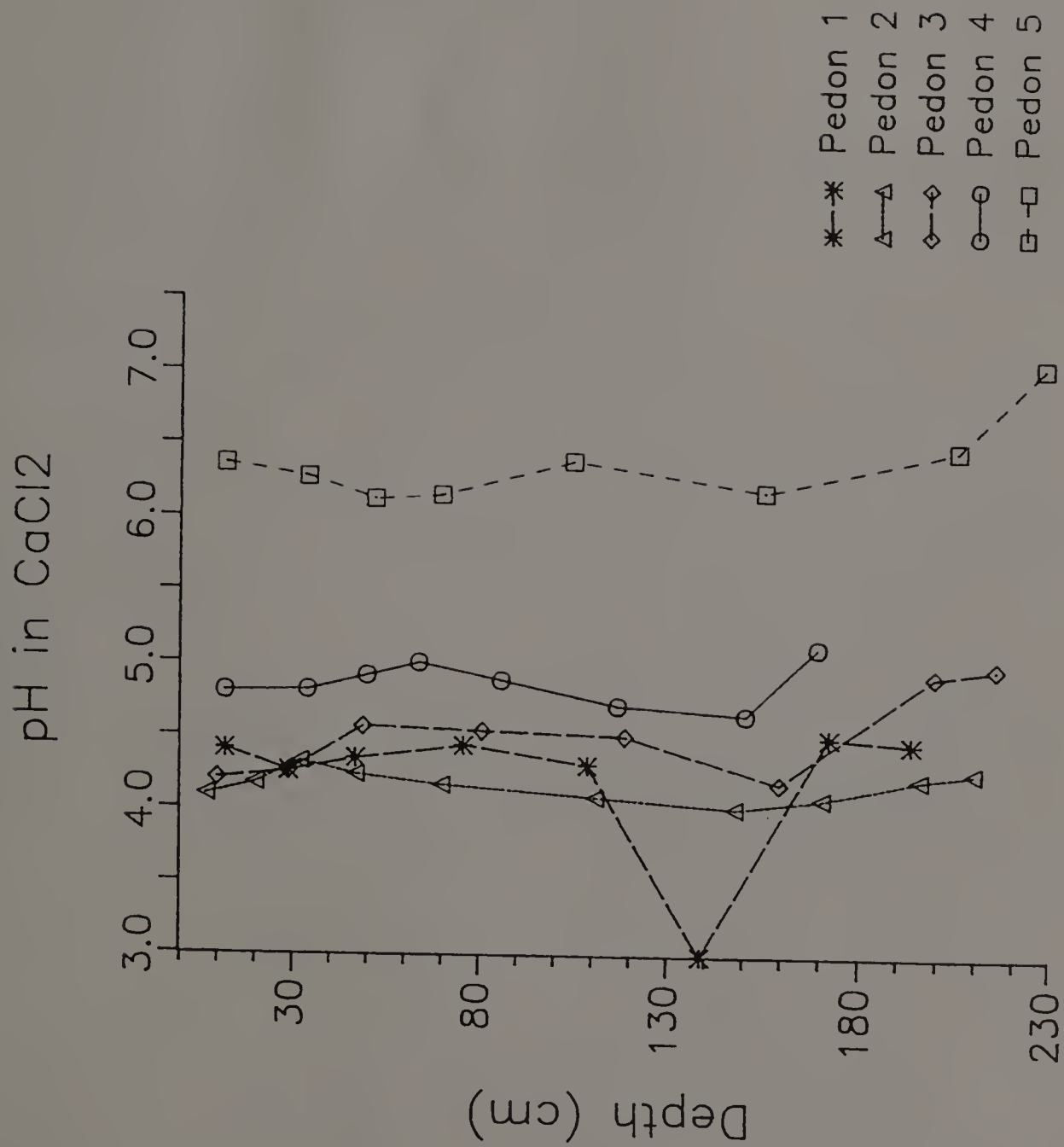


Figure 72. pH_C for each horizon by depth in Pedons 1-5.

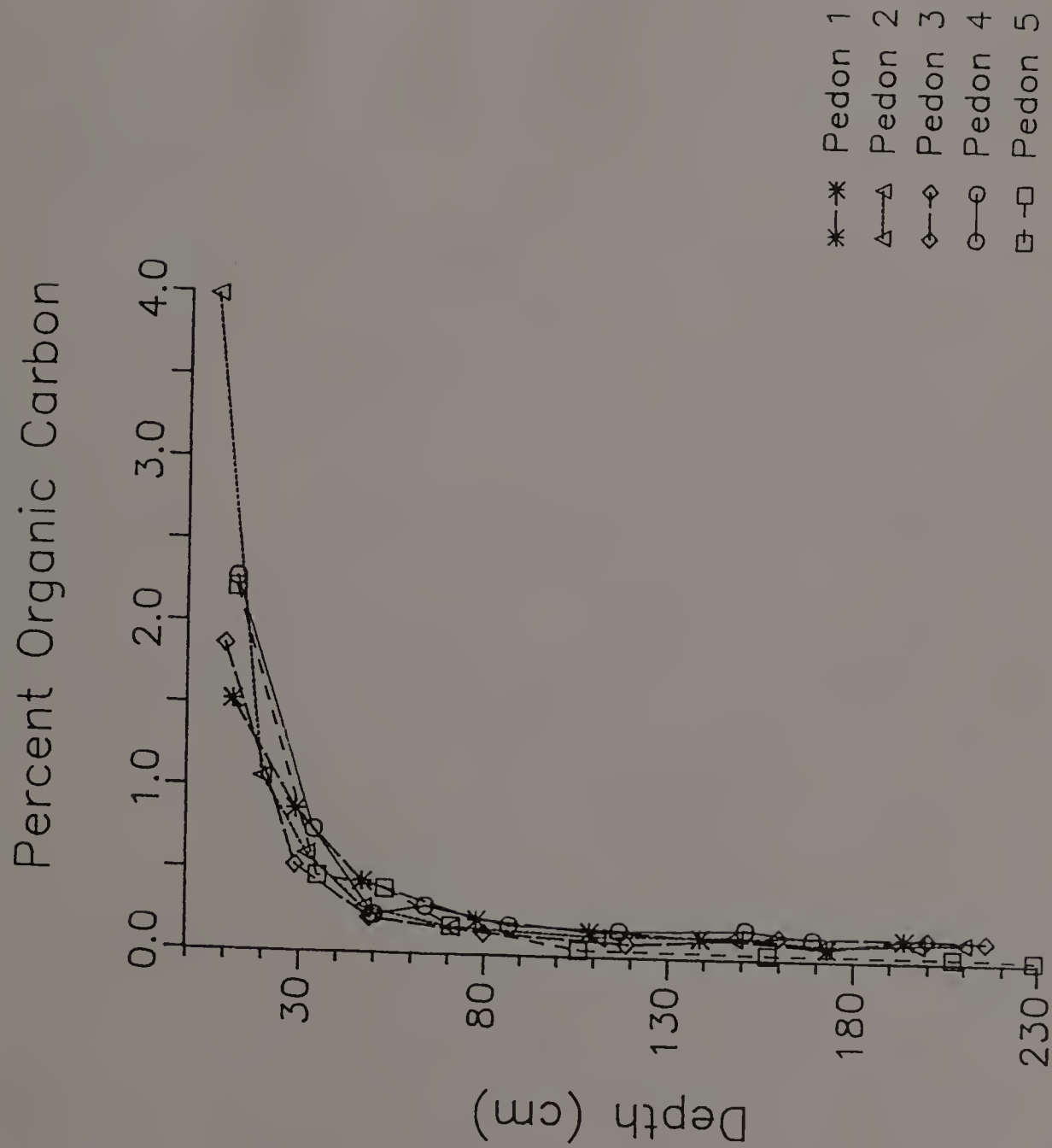


Figure 73. Organic carbon (%) for each horizon by depth in Pedons 1-5.

Extractable Acidity. Extractable acidity (EA) follows the same trend as OC (Figure 74). The lowest EA values (0 cmol kg^{-1}) are observed in the lower horizons of Pedon 5.

Cation Exchange Capacity. The sum of exchangeable bases (SEB) and total cation exchange capacity (CEC) are high in the Ap horizons, decrease in the B horizons and increase in the Cd horizons (Figures 75 and 76). Pedon 5 does not follow this trend, showing a decrease in both SEB and CEC with depth. Despite its sandy texture and lower CEC, the SEB of Pedon 5's Ap is higher than that of the other pedons suggesting an influence from active liming and fertilization practices. Percent base saturation (BS) increases with depth in all the pedons reaching 100% in the 2BCx1 and 2Cd horizons in Pedon 5 (Figure 77). Also of note is that the majority of the horizons in Pedons 3, 4, and 5 have a BS of 35% or greater as do the 2BCd and 3Cd horizons of Pedon 2. The lower BS of Pedon 1 corresponds to its lower pH_K and higher EA.

Extractable Elements

Fe. The percent Fe extracted by CD, OX, and CBD appears to follow the clay curve with peaks corresponding to clay bulges in and above the pan (Table 22, Appendix I, and c.f. Figure 36). The PYRO extractable Fe decreases with depth as does the AA, NaOH, and EDTA although the decrease is slight in the latter three. There is an initial decrease in the HH extractable Fe followed by an increase in the lower horizons. None of the extractants appear to correlate extractable Fe with the presence of fragipan horizons.

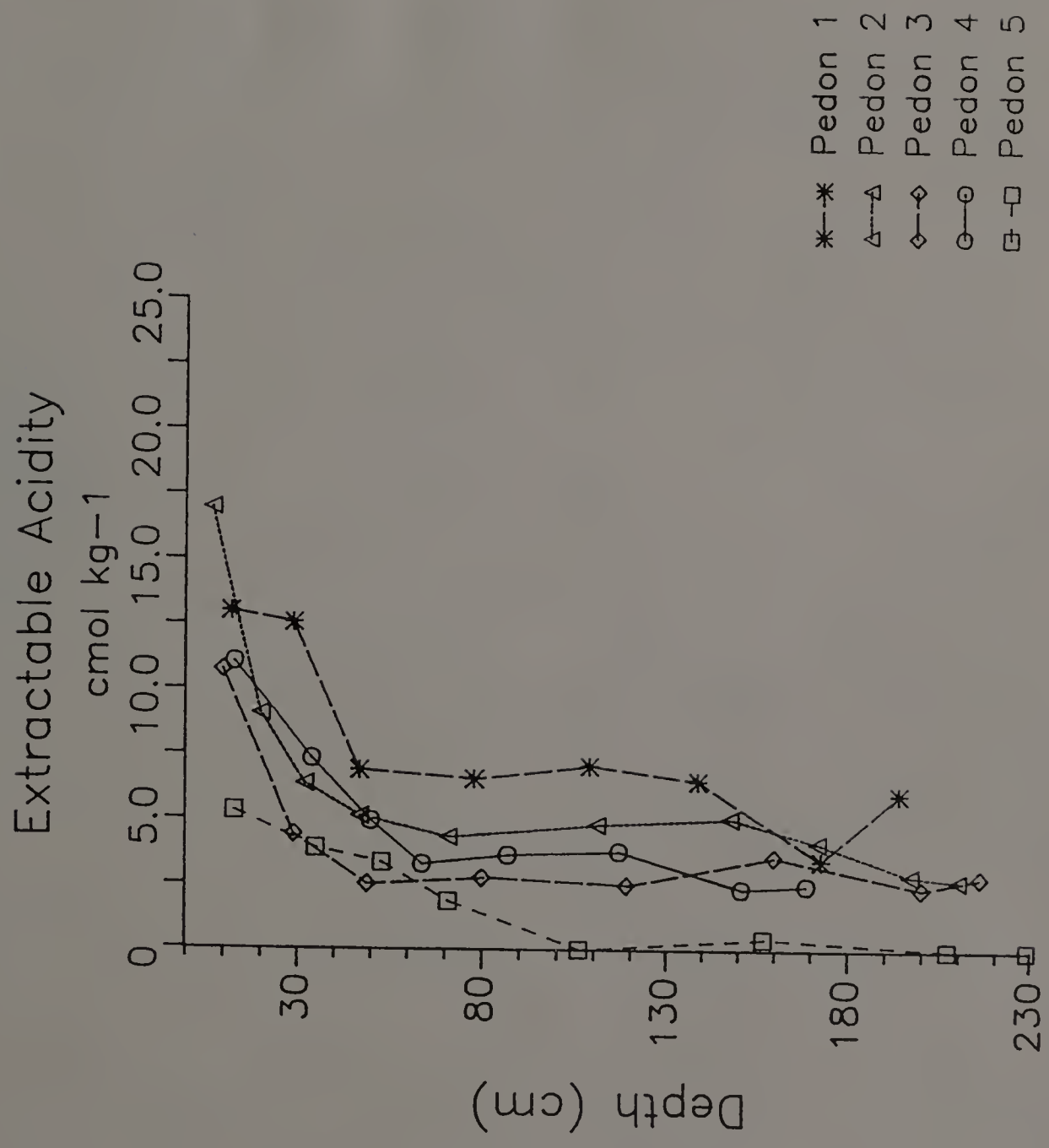


Figure 74. Extractable acidity (cmol 100 g⁻¹) for each horizon by depth in Pedons 1-5.

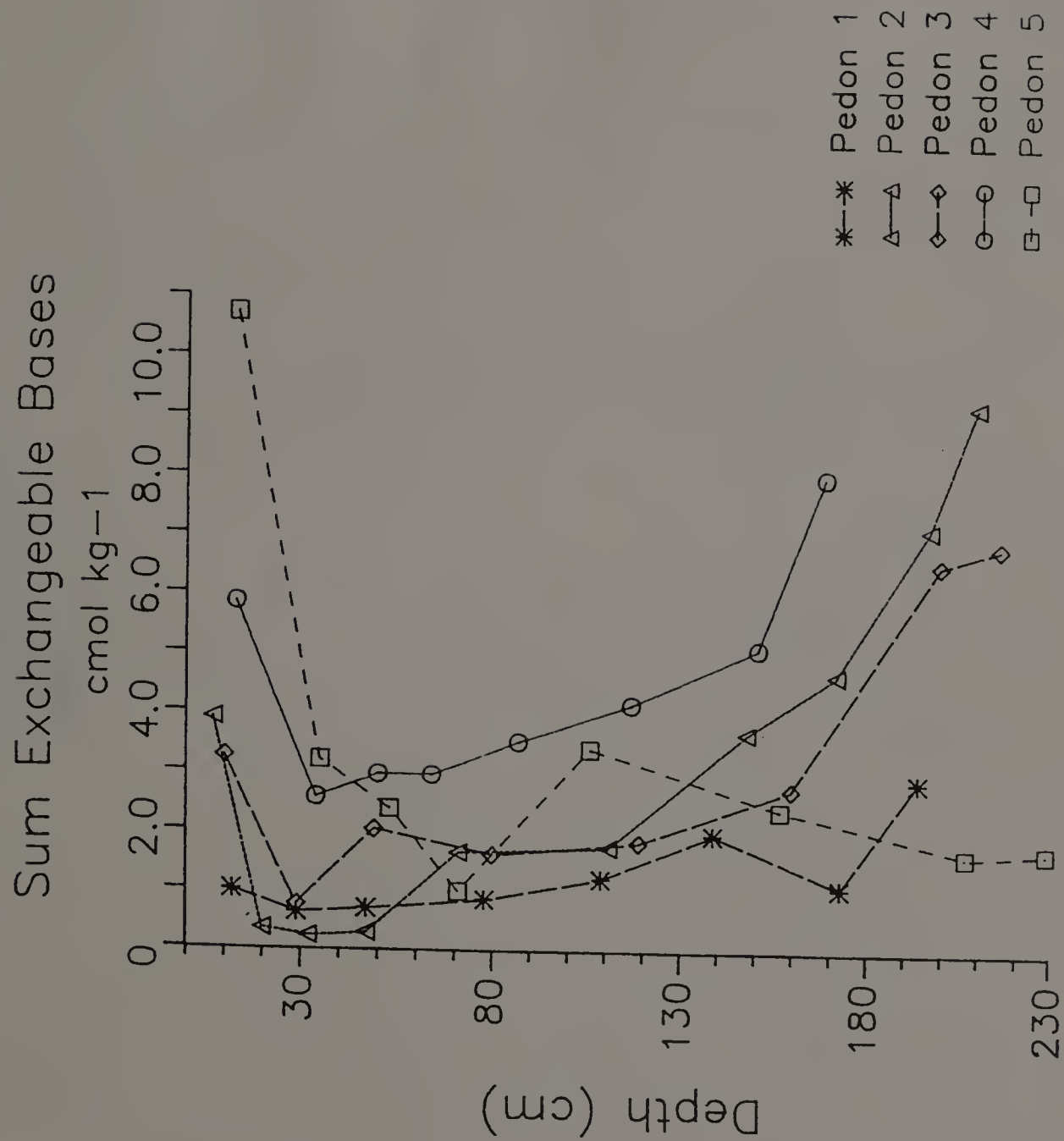


Figure 75. Sum of exchangeable bases (cmol 100 g⁻¹) for each horizon by depth in Pedons 1-5.

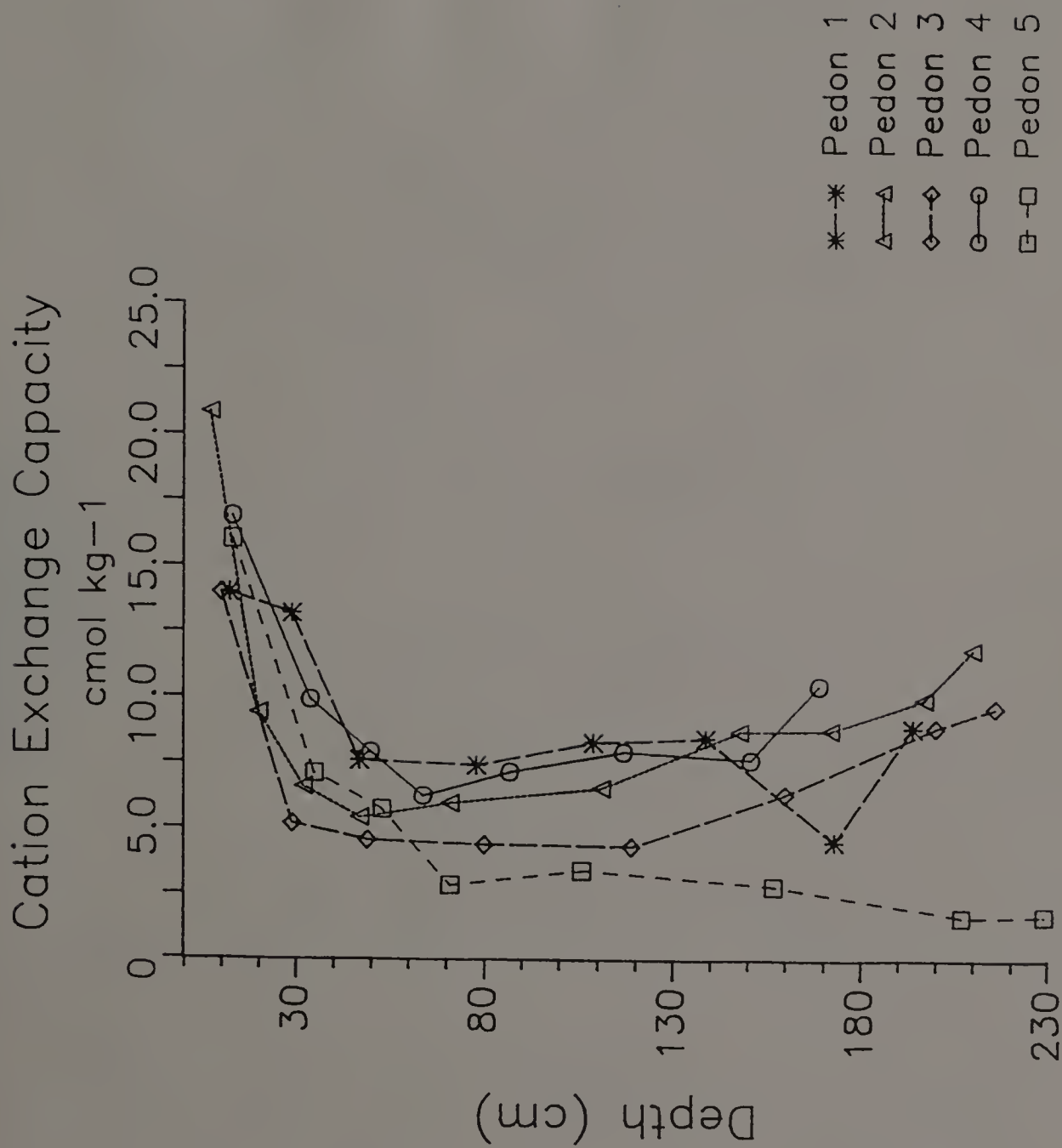


Figure 76. Cation exchange capacity (cmol 100 g⁻¹) for each horizon by depth in Pedons 1-5.

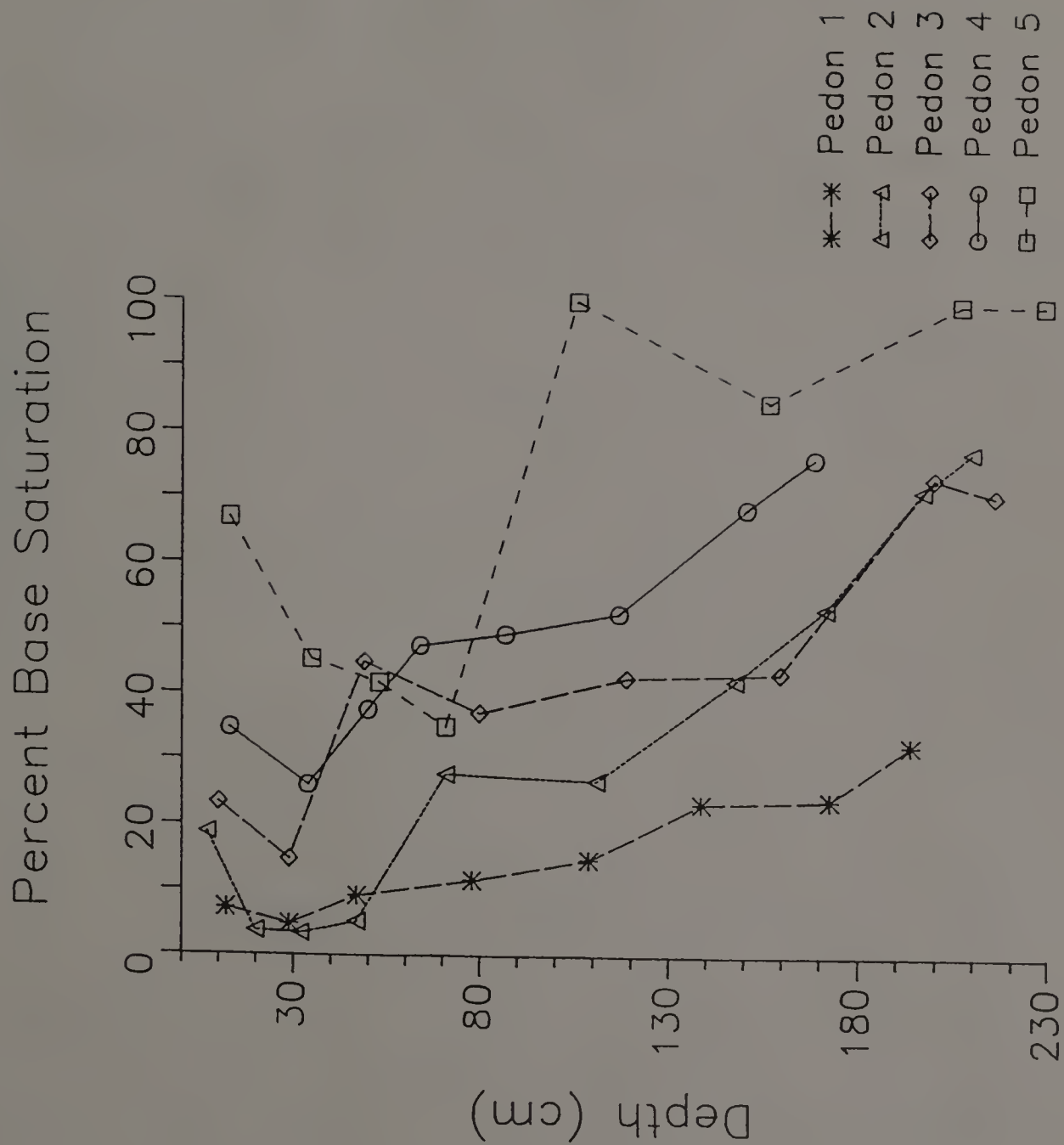


Figure 77. Percent base saturation for each horizon by depth in Pedons 1-5.

Table 22. Percent Fe extracted by variuos procedures.

Pedon 1

Hori.	CD	PYRO	OX	CBD	AA	HH1	HH2	NaOH	EDTA
Ap	1.54	0.36	0.930	1.096	0.093	0.247	0.230	1.52	0.130
Bw1	1.71	0.32	0.995	1.113	0.068	0.236	0.326	0.133	0.095
Bw2	1.98	0.21	0.900	0.918	0.055	0.145	0.262	0.158	0.058
Bt	2.82	0.13	1.765	1.789	0.075	0.203	0.354	0.134	0.079
2Btx1	3.13	0.08	2.335	1.915	0.093	0.220	0.398	0.165	0.082
2Btx2	2.10	0.08	1.525	1.457	0.093	0.277	0.463	0.170	0.089
3BCm	1.92	0.07	1.680	1.416	0.092	0.241	0.256	0.124	0.106
4Cd	3.02	0.09	2.490	1.680	0.108	0.289	0.525	0.144	0.117
BPF	1.71	0.08	1.520	1.227	0.098	0.364	0.428	0.136	0.093

Pedon 2

Hori.	CD	PYRO	OX	CBD	AA	HH1	HH2	NaOH	EDTA
Ap	1.21	0.57	1.105	0.549	0.079	0.219	0.447	0.205	0.138
Bw1	1.09	0.42	1.025	0.890	0.074	0.246	0.375	0.160	0.112
Bw2	0.97	0.32	0.855	0.550	0.072	0.197	0.312	0.142	0.094
BE	0.86	0.23	0.715	0.423	0.063	0.113	0.191	0.100	0.053
2Btx1	0.21	0.19	1.165	0.938	0.096	0.186	0.291	0.106	0.085
2Btx2	0.91	0.21	1.525	0.943	0.115	0.24	0.422	0.126	0.109
2BCd	1.45	0.11	1.410	1.064	0.109	0.234	0.412	0.183	0.103
3Cd1	1.38	0.23	1.235	0.835	0.121	0.242	0.343	0.163	0.105
3Cd2	1.41	0.10	1.150	0.325	0.137	0.246	0.334	0.121	0.113
3Cd3	1.62	0.11	1.365	0.435	0.155	0.306	0.486	0.146	0.116
Sand	0.57	0.08	0.455	0.342	0.098	0.132	0.131	0.064	0.081
BPF	1.13	0.13	1.285	0.792	0.118	0.239	0.389	0.086	0.121

Pedon 3

Hori.	CD	PYRO	OX	CBD	AA	HH1	HH2	NaOH	EDTA
Ap	1.08	0.40	0.845	0.270	0.121	0.426	0.284	0.160	0.139
Bw	1.06	0.31	0.825	0.737	0.102	0.247	0.274	0.124	0.105
BE	1.08	0.15	0.705	0.623	0.088	0.214	0.232	0.091	0.081
2Btx1	1.18	0.13	0.995	0.719	0.108	0.244	0.267	0.083	0.102
2Btx2	1.25	0.15	1.155	0.287	0.130	0.331	0.357	0.088	0.122
2BCd	1.34	0.23	1.360	0.302	0.156	0.323	0.413	0.097	0.155
3Cd1	1.47	0.16	1.455	0.540	0.174	0.364	0.426	0.079	0.127
3Cd3	1.525	0.18	1.510	0.998	0.155	0.366	0.453	0.079	0.151

Continued, next page

Table 22 cont.

Pedon 4

Hori.	CD	PYRO	OX	CBD	AA	HH1	HH2	NaOH	EDTA
Ap	1.30	0.58	1.340	0.468	0.095	0.327	0.390	0.052	0.226
Bw1	1.40	0.50	1.535	1.179	0.093	0.354	0.413	0.140	0.165
Bw2	1.38	0.38	1.445	0.379	0.107	0.321	0.411	0.124	0.167
BE	1.13	0.31	0.990	0.563	0.091	0.205	0.328	0.098	0.087
2Btx1	1.34	0.15	1.325	0.367	0.108	0.208	0.337	0.073	0.100
2Btx2	1.49	0.17	1.690	1.223	0.137	0.271	0.419	0.069	0.142
2BCd	1.61	0.18	1.730	0.371	0.134	0.246	0.399	0.112	0.123
3Cd	1.65	0.19	1.600	0.471	0.124	0.253	0.409	0.064	0.123

Pedon 5

Hori.	CD	PYRO	OX	CBD	AA	HH1	HH2	NaOH	EDTA
Ap	0.46	0.29	0.695	0.262	0.089	0.240	0.228	0.102	0.196
Bw	0.50	0.22	0.440	0.224	0.081	0.158	0.136	0.095	0.101
BE	0.46	0.16	0.345	0.160	0.089	0.114	0.143	0.114	0.075
2EB	0.45	0.14	0.385	0.242	0.066	0.107	0.112	0.115	0.049
2Btx1	0.41	0.04	0.270	0.212	0.080	0.143	0.128	0.091	0.048
2Btx2	0.37	0.03	0.150	0.131	0.049	0.092	0.071	0.061	0.028
2Cd1	0.33	0.04	0.155	0.090	0.042	0.078	0.064	0.078	0.032
2Cd2	0.39	0.05	0.245	0.077	0.072	0.122	0.091	0.091	0.056
BPF	0.39	0.08	0.265	0.097	0.081	0.146	0.110	0.114	0.072

Al. As with Fe, PYRO extractable Al, and to a lesser extent AA and HH extractable Al, decrease with depth (Table 23 and Appendix I). CD and CBD extract more Al in the upper Bw and Ap horizons than in the lower horizons whereas OX despite an overall decrease in extractable Al with depth has relative peaks occurring in the 2Bx horizon of Pedons 2, 4, and 5. NaOH appears to be the most efficient at extracting Al. In general, the NaOH extractable Al peaks above the pan in the upper Bw horizons and is then followed by a decrease. No correlation between extractable Al and the fragipan was noticeable.

Mn. The percent of extractable Mn decreases with depth for each of the procedures used with a few exceptions (Table 24 and Appendix I). Relative higher values in the BCm (Pedon 1) and BCd (Pedon 3) horizons occur in each extraction. There is also a slight increase in Mn extracted by AA, HH, and EDTA associated with the Bx horizons, however, it is insignificant in terms of classification.

Si. Extractable Si is more variable than the other extractable elements (Table 25 and Appendix I). CD, CBD, and OX extractable Si increased from the Ap and upper B horizons into the lower B horizons and then remains approximately the same with depth whereas AA and EDTA extractable Si decreases with depth. Overall PYRO extractable Si decreases from the Ap horizons to the Cd horizons with relative peaks occurring in the Bx horizons of Pedons 1, 3, and 5, and both above and below the Bx horizons of Pedons 2 and 4. NaOH proved to be the best extractor of Si with relative peaks occurring above the pan or in it.

Table 23. Percent Al extracted by various procedures.

Pedon 1

Hori.	CD	PYRO	OX	CBD	AA	HH1	HH2	NaOH	EDTA
Ap	0.413	0.460	0.83	0.416	0.249	0.575	0.387	1.218	----
Bw1	0.431	0.400	0.85	0.376	0.190	0.515	0.390	1.333	----
Bw2	0.288	0.190	0.050	0.114	0.117	0.265	0.304	1.293	----
Bt	0.288	0.180	0.61	0.250	0.134	0.310	0.322	1.515	----
2Btx1	0.306	0.180	0.53	0.245	0.144	0.315	0.359	1.103	----
2Btx2	0.238	0.150	0.45	0.145	0.131	0.335	0.338	1.175	----
3BCm	0.219	0.120	0.61	0.148	0.124	0.220	0.200	0.823	----
BPF	0.213	0.190	0.38	0.149	0.158	0.415	0.428	1.348	----

Pedon 2

Hori.	CD	PYRO	OX	CBD	AA	HH1	HH2	NaOH	EDTA
Ap	0.488	0.490	0.89	0.342	0.304	0.545	0.418	1.410	----
Bw1	0.494	0.510	0.094	0.449	0.350	0.680	0.626	1.510	----
Bw2	0.413	0.450	0.90	0.312	0.345	0.580	0.526	1.375	----
BE	0.300	0.400	0.56	0.193	0.329	0.465	0.387	1.298	----
2Btx1	0.250	0.250	0.55	0.180	0.251	0.380	0.390	1.445	----
2Btx2	0.319	0.340	0.68	0.157	0.271	0.405	0.457	1.483	----
2BCd	0.225	0.220	0.63	0.167	0.241	0.345	0.413	1.378	----
3Cd1	0.225	0.100	0.54	0.119	0.252	0.345	0.342	1.258	----
3Cd2	0.206	0.190	0.49	0.061	0.257	0.350	0.520	1.163	----
3Cd3	0.213	0.180	0.38	0.062	0.258	0.365	0.403	0.950	----
Sand	0.100	0.130	0.23	0.052	0.174	0.165	0.139	0.368	----
BPF	0.206	0.210	0.50	0.137	0.220	0.310	0.371	0.975	----

Pedon 3

Hori.	CD	PYRO	OX	CBD	AA	HH1	HH2	NaOH	EDTA
Ap	0.462	0.520	0.58	0.185	0.286	0.445	0.302	0.743	----
Bw	0.387	0.420	0.57	0.279	0.230	0.405	0.296	0.740	----
BE	0.325	0.280	0.46	0.161	0.212	0.330	0.247	0.648	----
2Btx1	0.300	0.220	0.39	0.123	0.190	0.250	0.208	0.650	----
2Btx2	0.287	0.220	0.39	0.048	0.186	0.285	0.213	0.610	----
2BCd	0.312	0.260	0.45	0.047	0.198	0.265	0.252	0.648	----
3Cd1	0.262	0.160	0.31	0.059	0.188	0.255	0.213	0.433	----
3Cd2	0.300	0.180	0.33	0.098	0.198	0.270	0.231	0.395	----

Continued, next page

Table 23 cont.

Pedon 4

Hori.	CD	PYRO	OX	CBD	AA	HH1	HH2	NaOH	EDTA
Ap	0.525	0.54	0.71	0.268	0.262	0.485	0.358	0.975	----
Bw1	0.475	0.48	0.72	0.383	0.266	0.465	0.361	1.288	----
Bw2	0.425	0.36	0.61	0.136	0.212	0.350	0.296	0.965	----
BE	0.287	0.30	0.42	0.149	0.176	0.245	0.240	0.713	----
2Btx1	0.290	0.20	0.39	0.081	0.194	0.245	0.235	0.690	----
2Btx2	0.270	0.20	0.45	0.148	0.192	0.275	0.254	0.680	----
2BCd	0.287	0.180	0.39	0.056	0.198	0.245	0.229	0.688	----
3Cd	0.280	0.14	0.33	0.460	0.184	0.235	0.289	0.435	

Pedon 5

Hori.	CD	PYRO	OX	CBD	AA	HH1	HH2	NaOH	EDTA
Ap	0.263	0.270	0.63	0.183	0.209	0.350	0.246	0.625	----
Bw	0.188	0.280	0.38	0.116	0.185	0.230	0.179	0.833	----
BE	0.213	0.280	0.38	0.101	0.249	0.230	0.244	0.073	----
2EB	0.188	0.180	0.38	0.085	0.187	0.220	0.153	0.655	----
2Btx1	0.075	0.040	0.43	0.013	0.107	0.145	0.114	0.360	----
2Btx2	0.050	0.030	0.16	0.005	0.072	0.085	0.070	0.388	----
BPF	0.138	0.150	0.30	0.029	0.190	0.210	0.124	0.583	----
2Cd1	0.050	0.050	0.13	0.006	0.083	0.085	0.073	0.350	----
2Cd2	0.088	0.070	0.17	0.007	0.123	0.130	0.084	0.350	----

Table 24. Percent Mn etracted by various procedures.

Pedon 1

Hori.	CD	PYRO	OX	CBD	AA	HH1	HH2	NaOH	EDTA
Ap	0.081	0.090	0.028	0.067	0.025	0.066	0.045	----	0.095
Bw1	0.057	0.043	0.003	0.047	0.009	0.047	0.029	----	0.046
Bw2	0.014	0.011	0.004	0.008	0.004	0.011	0.007	----	0.009
Bt	0.015	0.007	0.005	0.011	0.005	0.011	0.007	----	0.006
2Btx1	0.010	0.004	0.003	0.006	0.004	0.006	0.004	----	0.004
2Btx2	0.013	0.009	0.004	0.010	0.008	0.011	0.008	----	0.009
3BCm	0.042	0.016	0.020	0.035	0.014	0.037	0.019	----	0.035
4Cd	0.018	0.012	0.008	0.013	0.010	0.015	0.009	----	0.013
BPF	0.004	0.003	0.002	0.002	0.002	0.003	0.002	----	0.001

Pedon 2

Hori.	CD	PYRO	OX	CBD	AA	HH1	HH2	NaOH	EDTA
Ap	0.011	0.022	0.005	0.007	0.008	0.008	0.007	----	0.010
Bw1	0.006	0.013	0.003	0.004	0.003	0.004	0.004	----	0.003
Bw2	0.004	0.011	0.002	0.003	0.002	0.002	0.003	----	0.002
BE	0.005	0.011	0.004	0.005	0.003	0.003	0.003	----	0.003
2Btx1	0.017	0.014	0.008	0.003	0.008	0.012	0.008	----	0.012
2Btx2	0.011	0.012	0.006	0.014	0.006	0.009	0.008	----	0.008
2BCd	0.008	0.012	0.004	0.010	0.004	0.005	0.005	----	0.004
3Cd1	0.012	0.011	0.005	0.007	0.008	0.008	0.059	----	0.009
3Cd2	0.012	0.013	0.005	0.005	0.009	0.009	0.068	----	0.009
3Cd3	0.012	0.018	0.005	0.005	0.010	0.010	0.008	----	0.010
Sand	0.007	0.014	0.003	0.005	0.005	0.005	0.003	----	0.005
BPF	0.007	0.012	0.003	0.004	0.003	0.004	0.004	----	0.003

Pedon 3

Hori.	CD	PYRO	OX	CBD	AA	HH1	HH2	NaOH	EDTA
Ap	0.038	0.054	0.011	0.019	0.023	0.032	0.016	----	0.030
Bw	0.018	0.026	0.003	0.013	0.009	0.011	0.007	----	0.011
BE	0.019	0.019	0.003	0.014	0.006	0.013	0.007	----	0.009
2Btx1	0.024	0.018	0.010	0.019	0.009	0.017	0.009	----	0.014
2Btx2	0.026	0.019	0.007	0.010	0.009	0.019	0.011	----	0.013
2BCd	0.040	0.032	0.013	0.014	0.018	0.027	0.017	----	0.030
3Cd1	0.027	0.026	0.012	0.014	0.012	0.020	0.012	----	0.019
3Cd2	0.019	0.021	0.003	0.013	0.010	0.012	0.008	----	0.011

Continued, next page

Table 24 cont.

Pedon 4

Hori.	CD	PYRO	OX	CBD	AA	HH1	HH2	NaOH	EDTA
Ap	0.056	0.075	0.027	0.029	0.016	0.039	0.026	----	0.043
Bw1	0.037	0.038	0.009	0.028	0.008	0.023	0.015	----	0.023
Bw2	0.034	0.032	0.014	0.015	0.009	0.022	0.014	----	0.019
BE	0.025	0.029	0.005	0.018	0.007	0.015	0.010	----	0.012
2Btx1	0.020	0.016	0.004	0.008	0.007	0.011	0.008	----	0.008
2Btx2	0.019	0.017	0.006	0.013	0.008	0.011	0.008	----	0.009
2BCd	0.017	0.018	0.002	0.006	0.008	0.010	0.006	----	0.008
3Cd	0.019	0.018	0.002	0.007	0.010	0.010	0.008	----	0.011

Pedon 5

Hori.	CD	PYRO	OX	CBD	AA	HH1	HH2	NaOH	EDTA
Ap	0.028	0.049	0.027	0.019	0.019	0.027	0.017	----	0.029
Bw	0.005	0.018	0.002	0.002	0.002	0.003	0.001	----	0.003
BE	0.005	0.018	0.002	0.002	0.003	0.002	0.002	----	0.002
2EB	0.005	0.016	0.003	0.003	0.002	0.002	0.001	----	0.001
2Btx1	0.006	0.015	0.004	0.004	0.004	0.005	0.003	----	0.003
2Btx2	0.009	0.016	0.005	0.006	0.005	0.007	0.004	----	0.005
BPF	0.004	0.015	0.002	0.001	0.002	0.002	0.001	----	0.001
2Cd1	0.004	0.016	0.002	0.002	0.003	0.003	0.002	----	0.003
2Cd2	0.008	0.018	0.004	0.004	0.006	0.006	0.004	----	0.005

Table 25. Percent Si extracted by various procedures.

Pedon 1

Hori.	CD	PYRO	OX	CBD	AA	HH1	HH2	NaOH	EDTA
Ap	0.194	0.611	0.197	0.043	1.722	----	0.537	5.06	0.064
Bw1	0.220	0.518	0.261	0.049	1.513	----	0.850	6.24	0.026
Bw2	0.185	0.440	0.122	0.047	1.251	----	0.530	8.64	0.032
Bt	0.246	0.317	0.242	0.055	1.520	----	0.596	9.72	0.073
2Btx1	0.238	0.209	0.162	0.072	1.645	----	0.581	8.34	0.104
2Btx2	0.234	0.411	0.144	0.059	1.332	----	0.559	6.94	0.071
3BCm	0.152	0.324	0.147	0.051	1.534	----	0.341	1.40	0.071
4Cd	0.291	0.148	0.210	0.057	1.770	----	0.390	6.64	0.114
BPF	0.339	0.396	0.137	0.047	1.550	----	0.828	7.53	0.077

Pedon 2

Hori.	CD	PYRO	OX	CBD	AA	HH1	HH2	NaOH	EDTA
Ap	0.078	0.569	0.194	0.039	1.659	----	0.537	7.02	0.076
Bw1	0.119	0.559	0.359	0.080	2.501	----	0.596	3.70	0.138
Bw2	0.153	0.648	0.332	0.079	3.169	----	0.282	3.71	0.138
BE	0.094	0.799	0.309	0.053	2.981	----	0.545	3.50	0.173
2Btx1	0.204	0.463	0.305	0.064	2.413	----	0.588	8.70	0.176
2Btx2	0.153	0.586	0.353	0.061	2.683	----	0.515	5.82	0.249
2BCd	0.163	0.781	0.358	0.073	2.335	----	0.778	7.54	0.173
3Cd1	0.189	0.452	0.247	0.074	2.002	----	0.646	7.77	0.218
3Cd2	0.208	0.568	0.202	0.040	3.128	----	0.355	6.29	0.246
3Cd3	0.211	0.436	0.333	0.051	3.169	----	0.683	6.53	0.114
Sand	0.112	0.390	0.112	0.052	2.084	----	0.253	6.32	0.102
BPF	0.180	0.693	0.381	0.048	2.105	----	0.668	9.20	0.068

Pedon 3

Hori.	CD	PYRO	OX	CBD	AA	HH1	HH2	NaOH	EDTA
Ap	0.119	0.237	0.168	0.051	1.868	----	0.268	8.38	0.106
Bw	0.122	0.293	0.160	0.038	1.976	----	0.435	8.22	0.155
BE	0.137	0.359	0.275	0.029	1.973	----	0.472	9.88	0.156
2Btx1	0.172	0.681	0.288	0.062	1.715	----	0.545	7.33	0.162
2Btx2	0.172	0.361	0.246	0.053	1.916	----	0.457	4.57	0.144
2BCd	0.212	0.317	0.372	0.153	2.125	----	0.537	6.87	0.154
3Cd1	0.157	0.507	0.238	0.058	2.689	----	0.588	5.07	0.180
3Cd2	0.151	0.360	0.256	0.054	1.729	----	----	6.49	0.205

Continued, next page

Table 25 cont.

Pedon 4

Hori.	CD	PYRO	OX	CBD	AA	HH1	HH2	NaOH	EDTA
Ap	0.046	0.302	0.144	0.031	1.729	----	0.231	3.58	0.124
Bw1	0.116	0.326	0.366	0.092	2.028	----	0.392	6.03	0.186
Bw2	0.177	0.246	0.306	0.029	1.931	----	0.523	4.54	0.170
BE	0.107	0.264	0.265	0.061	1.652	----	0.443	8.05	0.156
2Btx1	0.174	0.271	0.235	0.044	2.063	----	0.377	3.76	0.171
2Btx2	0.244	0.340	0.180	0.026	2.105	----	0.523	4.49	0.209
2BCd	0.169	0.433	0.356	0.073	1.973	----	0.413	6.99	0.143
3Cd	0.294	0.328	0.226	0.047	2.136	----	0.632	5.04	0.147

Pedon 5

Hori.	CD	PYRO	OX	CBD	AA	HH1	HH2	NaOH	EDTA
Ap	0.081	0.124	0.190	0.050	1.25	----	0.122	7.31	0.087
Bw	0.026	0.097	0.197	0.036	1.38	----	0.122	9.69	0.064
BE	0.050	0.079	0.144	0.046	2.22	----	0.275	5.80	0.113
2EB	0.036	0.063	0.132	0.037	2.14	----	0.281	0.42	0.103
2Btx1	0.068	0.063	0.193	0.042	2.47	----	0.428	6.67	0.119
2Btx2	0.025	0.108	0.199	0.029	2.01	----	0.210	4.60	0.076
BPF	0.096	0.073	0.168	0.028	2.26	----	0.422	5.33	0.152
2Cd1	0.043	0.050	0.169	0.033	1.58	----	0.348	4.34	0.052
2Cd2	0.058	0.068	0.223	0.038	2.45	----	0.261	5.17	0.106

Discussion

Exchange Chemistry

There is an overall increase in pH, and SEB, whereas OC and EA decrease with depth in all samples. The decrease in EA indicates a lower potential acidity with depth, which is correlated to a decrease in OC and extractable Al. Because pH_K is indicative of slowly exchangeable Al complexes it stands to reason that as EA decreases pH_K would increase as well as exchangeable bases and pH_w . The observed inverse relation of EA to SEB and pH values is most likely caused by a combination of leaching, liming, and parent material chemistry. Any expected decrease in both pH and SEB in the Ap horizons may be offset by liming practices. Reed (1989) reported that at the site where Pedon 5 is located lime had been applied within the last 8 years. The only other site (Pedon 1) where active agricultural practices had occurred in the recent past (<10 yrs.) also had a slightly higher pH in the Ap horizon. Pedons 1-4 all developed in the oxidized Lower Till which had a slightly higher pH and SEB than the soil horizons above it (c.f. Lindbo, 1990 and Appendix H). This, in part, explains the observed increase in those parameters with depth. Pedon 5 on the other hand has developed in the more acid Upper Till yet at depth has a relatively high pH. In this instance leaching of bases from the horizons above and lateral down slope movement of water containing bases accounts for the observed pH. Texture accounts for some of the observed variation resulting in lower CEC in sandier textured soils (i.e. Pedons 3, 5, and the BCm horizon in Pedon 1).

Extractable Elements

There is no apparent correlation of Fe, Al, or Mn extracted by any method to fragipan occurrence. The CD, OX, CBD, and possibly HH extractable Fe can be related to clay content. Extractable Mn by any method peaked in horizons that have significant Mn cementation (BCm, Pedon 1) or mangans (BCd, Pedon 3). With the exception of NaOH and PYRO Si was extracted poorly by all methods. Both NaOH and PYRO extractable Si appear higher in the pan or in adjacent horizons, however, the relations are not consistent. The observed variation does not appear correlated with any particular horizon from pedon to pedon. Recently, Karathanasis (1987a; 1987b; and 1989) and Franzmeier et al. (1989) have correlated Si with fragipans, and earlier Steinhardt et al. (1982) illustrated that NaOH extractable Si is strongly correlated to the fragipan horizon. The data presented in this study, while not conclusive, does suggest that NaOH extractable Si is higher in or adjacent to the pan, but the results are from a limited number of samples.

Conclusions

The soil chemistry suggests that illuviation of bases from lime applications resulted in an increase in the pH in Pedon 5. The pedons developed in the oxidized Lower Till also exhibit pedogenic changes in the form of increasing BS and SEB with depth to values that are similar to those of the parent material. As clay contents increase CEC rises. Finally, as expected OC decreases with depth.

The various elements extracted by different procedures did not correlate to fragipan expression although some extractable Fe could be correlated to clay content, and Mn could be correlated to mangan occurrence or Mn cementation. The NaOH extractable Si and to a lesser extent PYRO extractable Si were highest in or adjacent to the pan, however, more pedons need to be evaluated in this region before definite conclusions can be reached regarding the effectiveness two of these extraction procedures.

The overall chemistry of the soils does not conclusively show that one particular element or group of elements are directly related to the formation or identification of the pan. These findings basically agree with Grossman and Carlisle (1969). However, work simliar to that of Karathanasis (1989) could prove useful in understanding the solution chemistry of the fragipans in this area.

CHAPTER VII

CLAY MINERAL ANALYSIS

Previous Work

Clay Minerals in Fragipan Soils

While fragipans do not appear to contain any unique minerals (Smalley and Davin, 1982), they lack carbonate minerals as a general rule (Grossman and Carlisle, 1969). The lack of a relationship between fragipan expression and mineralogy was reported by Daniels et al. (1966). They showed that amount of feldspar in the very fine sand fraction was not related to pan development, yet Nettleton et al. (1968a) found that pans were more common in felspathic rather than quartz rich areas. Nettleton et al. (1968a) also concluded that old, highly weathered formations better supported the development of pans. The wide range of areas that fragipans occur in suggest varied bedrock sources and mineralogy.

Like the overall mineralogy, the clay mineralogy of the pan is not unique. Fragipan soil clay mineralogy is often the same as comparable horizons in soils without fragipans (Grossman and Carlisle, 1969). While the clay may be important to the character of the fragipan, it appears to correlate best to the general bedrock of the area and not to the fragipan itself. DeKimpe et al. (1972) indicated that micas dominated the clay fraction of a fragipan which developed in slaty till. They also found interstratified chlorite-

vermiculite minerals with the pan showing a slightly higher chlorite concentration which may be explained by weathering and illuviation. Knox (1959) argued that illite was common and perhaps critical in the fragic character of the pan he studied, yet DeKimpe (1970) investigated a pan where illite was not a major constituent. Montmorillonite has been found by Grossman et al. (1959b) and by Anderson and White (1958) in soils developed from loess in the Mississippi Valley. This finding leads to the conclusion that the soils had been strongly weathered and illuviated. East and North of the Mississippi Valley the clay mineralogy changes again. Fragipans of the mid-Atlantic coast contain less montmorillonite and more kaolinite (Nikiforoff et al., 1948; Nettleton et al., 1968b). Furthermore, the kaolinite was shown to be imperfectly crystalline with some amorphous material (Nettleton et al., 1968b) suggesting that these soils may have been subjected to more severe or longer periods of weathering.

Clay Minerals in Glacial Till and Till Derived Soils

Stratigraphic, weathering, and age relationships are commonly assessed using clay mineral assemblages. If two tills are stratigraphically the same they should have similar clay mineralogy if all other factors are equal (Kempton et al., 1971). Assumptions regarding the initial clay mineralogy allows for the investigation of weathering of the clays and relative age determination. Commonly, chlorite will alter to vermiculite, whereas illite will alter to

mixed-layer illite/vermiculite, with both eventually altering to smectite and/or kaolinite (Steward and Mickelson, 1976; Newton, 1978). Thus older, more weathered assemblages contain less illite. Identification of weathered zones and paleosols is useful in determining paleoclimates, as well as serving as a stratigraphic marker (Willman et al., 1966; Johnson et al., 1971; Newton, 1978; Glass and Killey, 1986).

Clay Mineralogical Studies in New England

Clay mineralogy has been successfully used in parts of New England (Newton, 1978; Lord, 1979; Retelle, 1979) and adjacent Quebec (DeKimpe et al., 1979) for differentiating between till sheets of different age. Newton (1978) studied the clay mineralogy of the Upper (Bakersville) and Lower (Thomaston) Till in detail. Both tills contained illite and chlorite in the unweathered or less weathered section of many exposures. In the Lower Till four zones were identified based on the clay assemblage. The upper two zones were exclusive to the oxidized zone with Zone I defined by mixed-layer illite/vermiculite that did not collapse on K saturation, and Zone II in which the mixed-layer did collapse on K saturation. Zone III contained no mixed-layer but did contain discrete vermiculite; and Zone IV was composed of unweathered chlorite and illite. Zones III and IV occur in the transition zone between the oxidized and unoxidized facies and in the unoxidized facies, respectively. A trace amount of kaolinite was also found in Zone IV. The Upper Till was observed to be similar to the Lower Till but contained little mixed-

layer clay, indicating that it was not as highly weathered as the Lower Till. The occurrence of Zones I and II suggest that an extended period of weathering on the surface of the Lower Till occurred prior to deposition of the Upper Till. They may also be related to Holocene soil formation (Lindbo, 1990).

Despite the complex bedrock geology of the region, Newton also concluded that the source areas of the tills were similar enough with regards to clay mineralogy that bedrock influence could be disregarded (c.f. Lord, 1979). On the other hand, Bodine (1986) found that clay weathering, in particular depotassification and chloritization, was influenced by the primary sheet silicates present in the local bedrock and till thus a rough correlation between parent rock, till and soil clay minerals can be seen. In general, depotassification was viewed to be rapid in the solum with interlayer removal occurring readily in the upper B and the A horizons. The occurrence of neo-formed gibbsite although unexpected was attributed to the breakdown of chlorite. Bodine also noted that kaolinite was present in some C horizons which were also rich in unexpanded micas. He attributed the kaolinite and interstratified mica-vermiculite in the lower horizons to being inherited from preglacial material and interglacial (or interstadial) weathering respectively. Kaolinite was also observed in unoxidized Lower Till thus furthering the hypothesis that some pre-existing material was incorporated into the till (Lindbo, 1990).

Despite the observations that no clay mineral is unique to the pan an understanding of the changes in the clay mineral assemblages

with depth assists in determining the extent of soil genesis that has occurred in the pedons studied. If the clay mineral assemblage of the pan is more developed (weathered) than that in the underlying Cd horizons and till some pedogenesis must have taken place.

Materials and Methods

The less than 2 micron fraction (<2 μm) was used in determining the clay mineralogy. Approximately 50 g of sieved sample was dispersed and centrifuged to separate the <2 μm fraction from the rest of the sample. Treatments used are outlined in Table 26. Only till samples from Ayer and Leicester received the full spectrum of treatments, while others were only analysed for the three Na treatments. Clay samples were smeared on petrographic slides and diffractograms were obtained using a Siemens diffractometer with nickel-filtered copper K_{α} radiation at 35KV and 20 ma. Samples were run from 2° to 30° at 2° 20 per minute.

Mica was identified by peaks at 1.0, 0.5, and 0.334 nm. Chlorite and chloritized vermiculite were identified by a 1.4, 0.72, and 0.354 nm peak. Chlorite was generally unaffected by heating @ 550°C or other treatments, whereas chloritized vermiculite collapsed to 1.0 nm upon heating. Mixed-layer mica/vermiculite was identified by a 1.2 and 0.349 nm peak which collapsed upon heating. A super-lattice peak was sometimes observed at 2.4 nm. Kaolinite was difficult to identify as chlorite and chloritized vermiculite d(002) and d(004) overlap kaolinite's 0.715 and 0.358 nm peaks. The absence of chlorite and the good crystallinity of kaolinite allowed for the identification of

kaolinite in some horizons. In the situation where the kaolinite was well crystallized its 0.358 nm d(002) peak could be differentiated from the chlorite or chloritized vermiculite d(004) peak at 0.354 nm. Finally, minor amounts of gibbsite were identified by a peak at 0.485 nm. Complete sets of diffractograms showing all treatment effects are in Appendix J.

Table 26. Procedure to characterize clay mineralogy in selected fragipans and tills in Massachusetts.

Sample Preparation and Fractionation

Particle Size Fractionation-Centrifugation
Dispersal of Clay Particles-1N Na-Acetate and
Agitation

X-Ray Diffraction

Mounted on glass slides

Treatments- Na-saturated, Na-saturated and heated @ 550^o for 1 hour,
Na-saturated and glycol solvated
Mg-saturated, Mg-saturated and glycerol solvated
K-saturated, K-saturated and heated @ 550^o for 1 hour

Results

Pedon 1

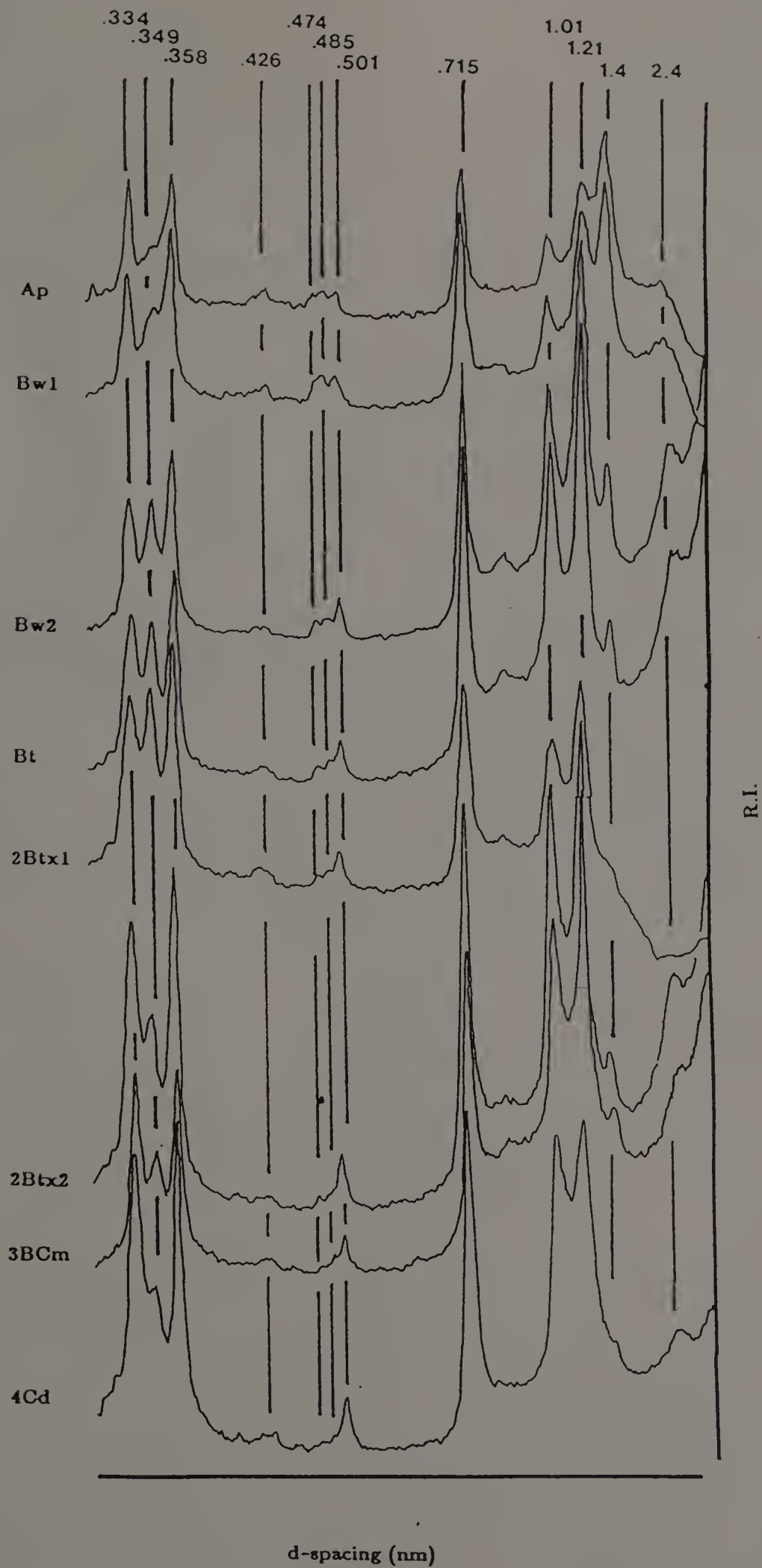
The upper solum of Pedon 1 is dominated by chloritized vermiculite. The intensity of this peak decreases with depth and is rapidly overshadowed by a strongly developed interstratified mica/vermiculite in the Bw2. This mixed-layer phase retains a super lattice peak throughout the profile although its intensity is greatest in the middle to lower B horizons (Figure 78).

The amount of mica appears to increase with depth until it is nearly as common as the mixed-layer phase. Likewise the 0.715 nm peak of kaolinite increases with depth. This peak can be identified solely as kaolinite due to the lack of significant 1.4 nm minerals in the 4Cd horizon. Gibbsite may occur as a minor constituent in the solum.

Pedon 2

The Ap and upper Bw horizons have a strongly developed chlorite and chloritized vermiculite component as well as a significant mica component. Gibbsite is present throughout the upper horizons but is absent in the pan and below. The mixed-layer mica-vermiculite does not account for a great proportion of the clay assemblage in the upper two horizons, but occur more commonly with depth at the expense of the chlorite and chloritized vermiculite reaching a maximum within the fragipan horizons. The super lattice peak of the mixed-layer clay indicates that a small amount is present in the 3Cd3 horizon where the 1.2 nm peak is difficult to distinguish from the large mica peak at

Figure 78. X-ray diffractograms by horizon of the Na-saturated <2um fraction of Pedon 1. 2.4 nm = mixed-layer supper lattice, 1.4 nm = chlorite and/or vermiculite, 1.21 nm = mixed-layer illite-vermiculite or illite-chloritized vermiculite, 1.0 nm = illite, .846 nm = mixed-layer d003, .715 nm = kaolinite and/or chlorite d002, .501 nm = illite d002, .485 nm = gibbsite, .426 nm = quartz, .358 nm = kaolinite d002 and/or chlorite d004, and .334 nm = illite d003 and quartz.



1.0 nm. Below the pan mica content increases, eventually dominating the assemblage (Figure 79).

The presence of chlorite in the lower horizons makes the identification of kaolinite somewhat more difficult, however the good crystallinity of the kaolinite allows for the separation of the 0.354 nm peak of chlorite from the 0.358 nm peak of kaolinite in the 3Cd2 horizon. Although this separation is not possible everywhere in the profile it does suggest that kaolinite is present.

The clay mineral assemblage of the BPF appeared nearly identical to that of the pan. There was however a slightly greater mixed-layer component and a trace amount of gibbsite present similar to that observed in the BE horizon.

Pedons 3 and 4

Both Pedons 3 and 4 are located at the same site and have similar clay mineral assemblages (Figure 80 and 81). A 1.4 nm peak occurs throughout the profile intensifying slightly in the unweathered till. Heat treatments indicate that the 1.4 nm peak represents both chloritized vermiculite, which collapses when heated, and chlorite, which is heat stable. The relative proportions of chlorite appears to be greatest in the mid-horizons. Likewise, a mixed-layer component is at a maximum in the pan although the super lattice peak is not well expressed.

Mica dominates the lower horizons in Pedon 4 and all the horizons in Pedon 3. Kaolinite may be present but can not be conclusively identified because of the large proportion of chlorite present.

Figure 79. X-ray diffractograms by horizon of the Na-saturated <2 μ m fraction of Pedon 2. 2.4 nm = mixed-layer super lattice, 1.4 nm = chlorite and/or vermiculite, 1.21 nm = mixed-layer illite-vermiculite or illite-chloritized vermiculite, 1.0 nm = illite, .846 nm = mixed-layer d003, .715 nm = kaolinite and/or chlorite d002, .501 nm = illite d002, .485 nm = gibbsite, .426 nm = quartz, .358 nm = kaolinite d002 and/or chlorite d004, and .334 nm = illite d003 and quartz.

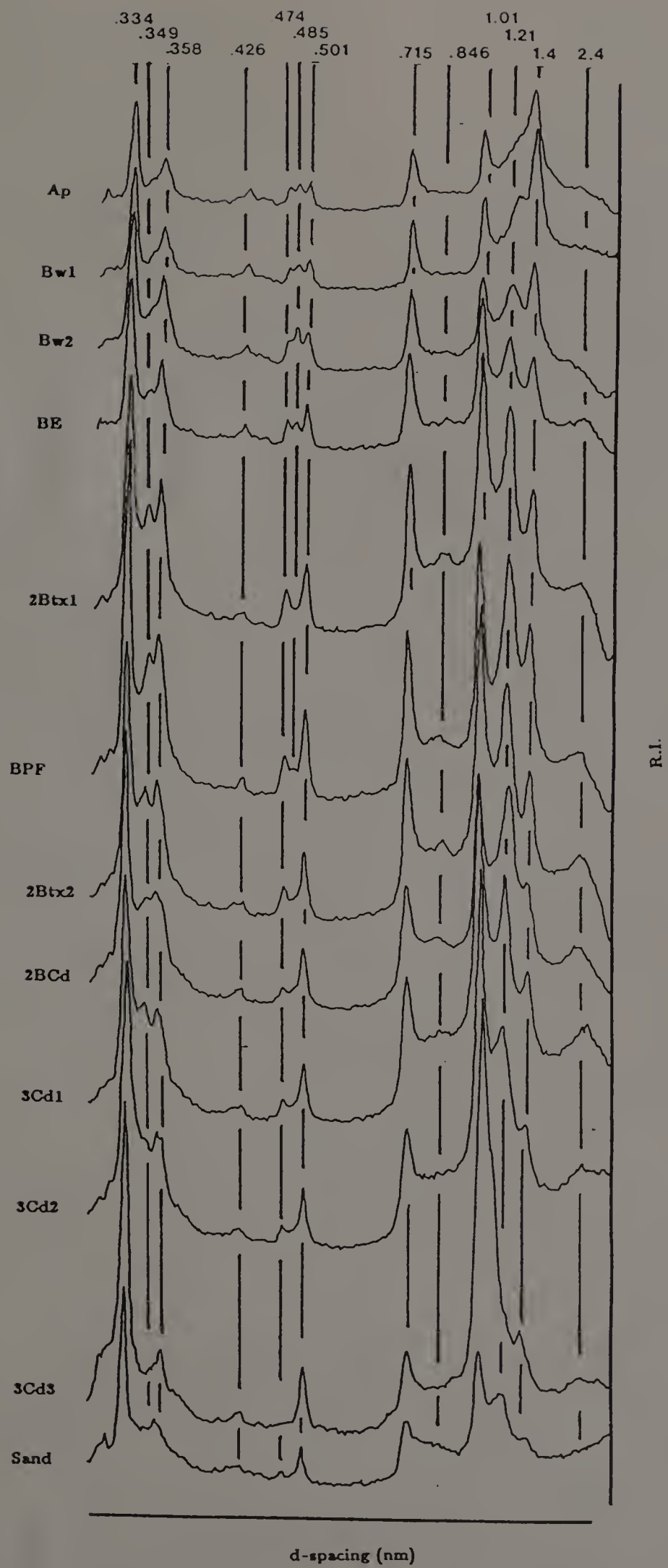


Figure 80. X-ray diffractograms by horizon of the Na-saturated <2um fraction of Pedon 3. 2.4 nm = mixed-layer supper lattice, 1.4 nm = chlorite and/or vermiculite, 1.21 nm = mixed-layer illite-vermiculite or illite-chloritized vermiculite, 1.0 nm = illite, .846 nm = mixed-layer d003, .715 nm = kaolinite and/or chlorite d002, .501 nm = illite d002, .485 nm = gibbsite, .426 nm = quartz, .358 nm = kaolinite d002 and/or chlorite d004, and .334 nm = illite d003 and quartz.

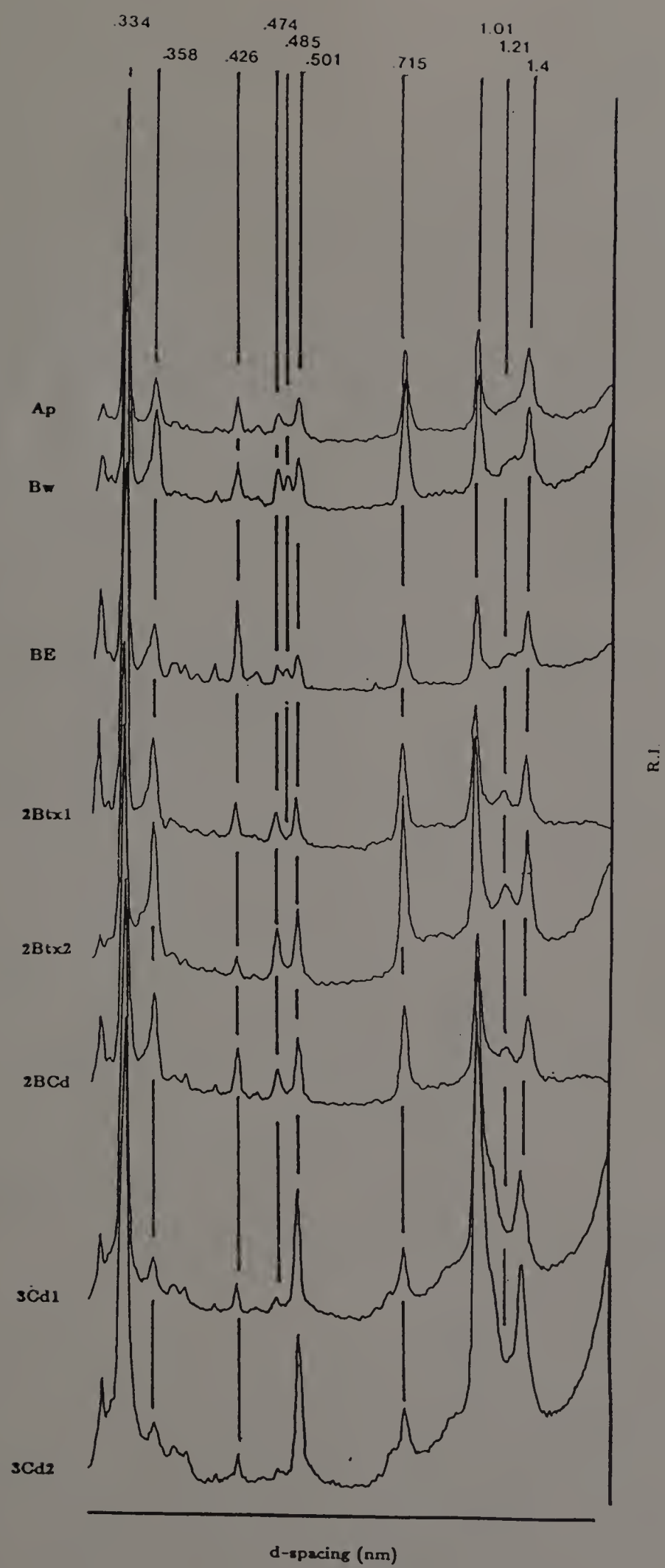
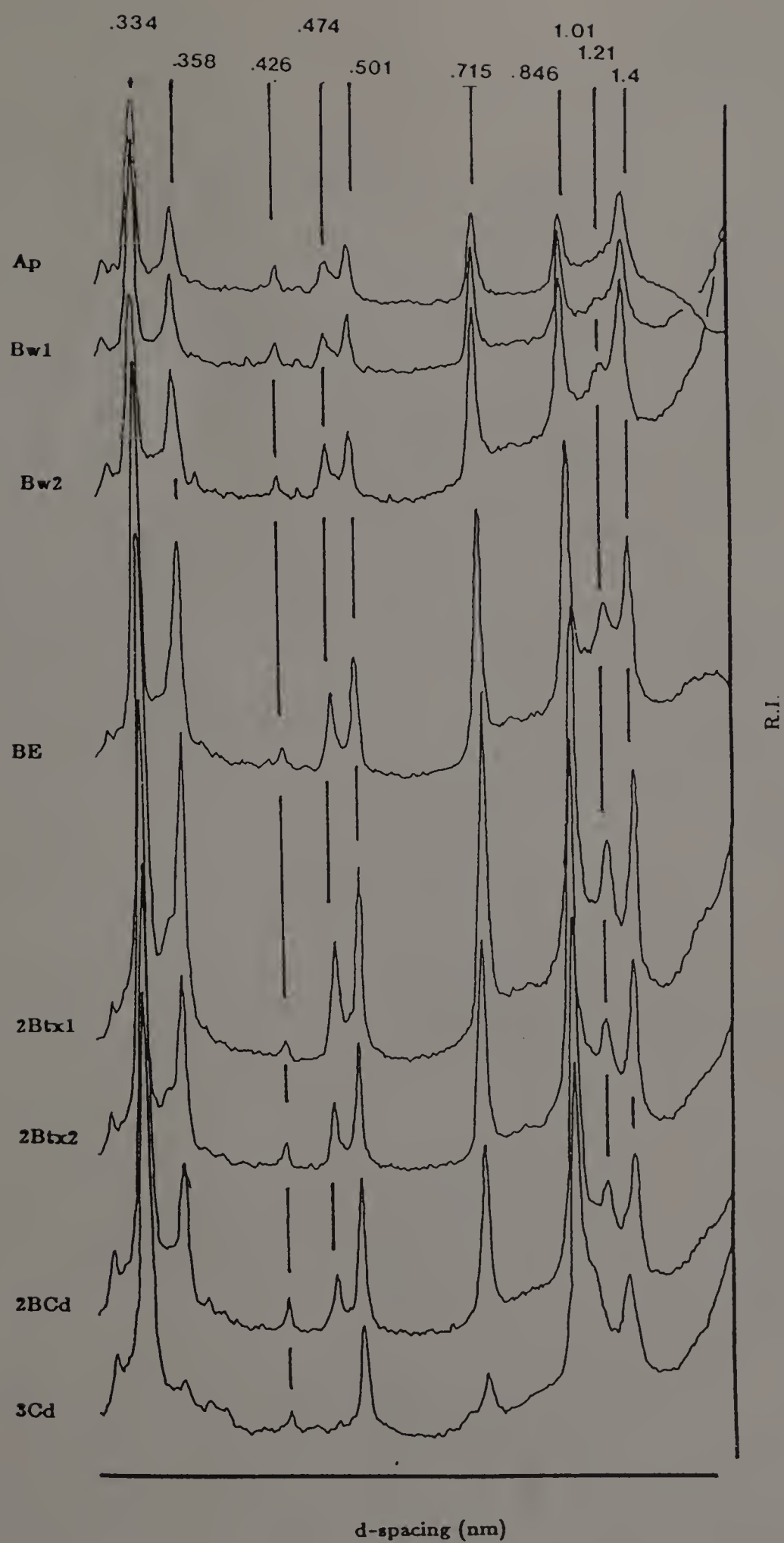


Figure 81. X-ray diffractograms by horizon of the Na-saturated <2 μ m fraction of Pedon 4. 2.4 nm = mixed-layer super lattice, 1.4 nm = chlorite and/or vermiculite, 1.21 nm = mixed-layer illite-vermiculite or illite-chloritized vermiculite, 1.0 nm = illite, .846 nm = mixed-layer d003, .715 nm = kaolinite and/or chlorite d002, .501 nm = illite d002, .485 nm = gibbsite, .426 nm = quartz, .358 nm = kaolinite d002 and/or chlorite d004, and .334 nm = illite d003 and quartz.



Gibbsite on the other hand is easily identified only in the upper B horizons of Pedon 3.

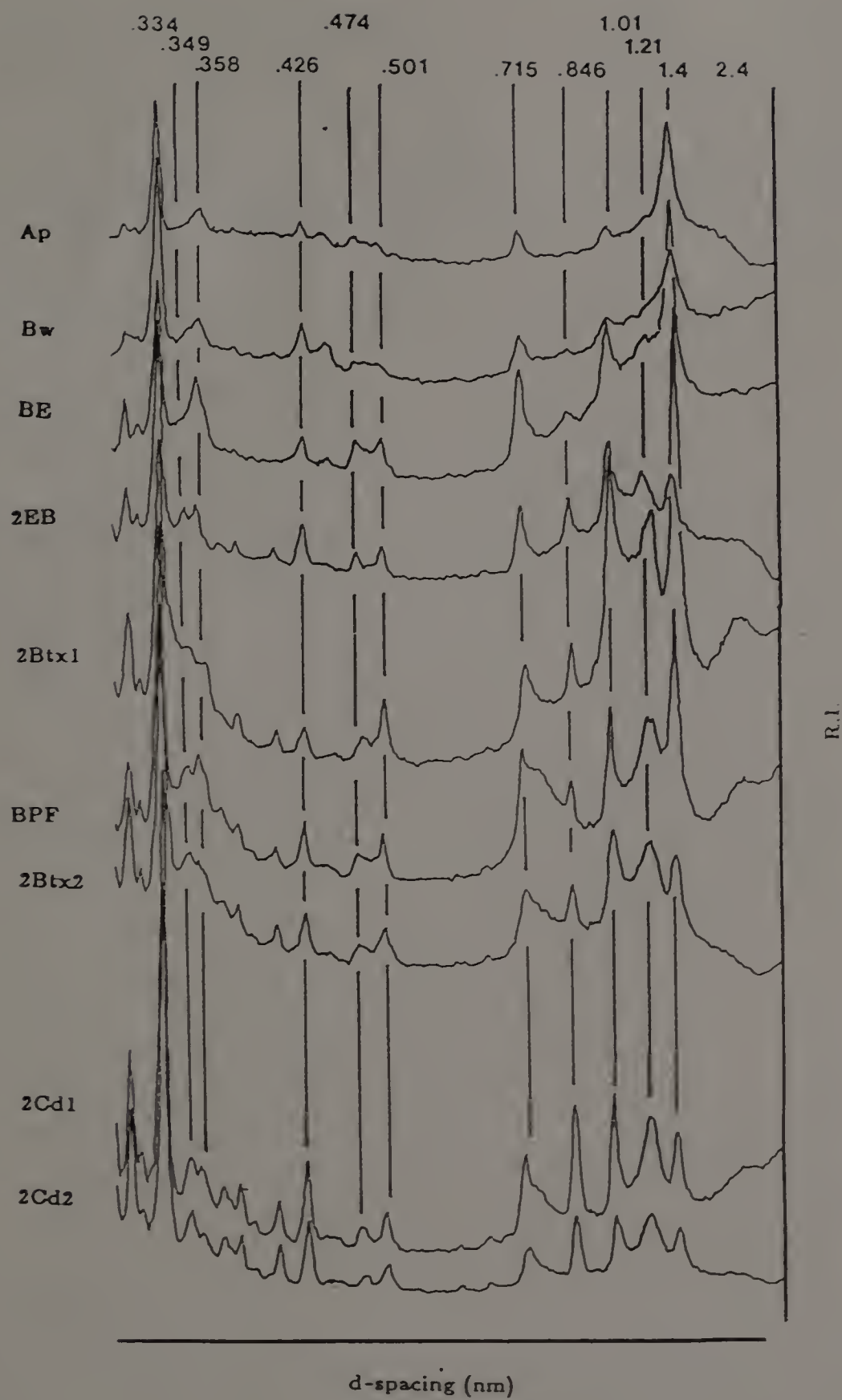
Pedon 5

A general increase in crystallinity (more well defined, sharp peaks) at the high angle, low d-spacing portion of the diffractograms in the lower horizons indicates the presence of relatively fresh feldspars in the clay fraction (Figure 82). In addition, the 0.846 nm peak throughout the profile corresponds to amphibole (hornblende) occurring in the clay fraction. Thus is expected based on the high hornblende content in the heavy mineral assemblage (c.f. Chapter 8).

Apart from the non-sheet silicates, Pedon 5 follows a similar pattern of clay mineral distribution as the other pedons; the chlorite and/or chloritized vermiculite component is strongest in the upper solum and decreases with depth, and chlorite becomes the dominant component of the peak with depth. Mixed-layer mica-vermiculite reaches a maximum in the pan but persists into the till, and the mica component increases with depth. Unlike Pedon 2, the BPF of Pedon 5 is similar to the 2BC horizon but not to the 2BCtx1 horizon, although the amphibole and 0.715 nm peak are not as well defined.

Also noteworthy is the lack of gibbsite throughout the profile. Kaolinite was not detected although the chlorite's interference may mask its presence. Because Pedon 5 has developed in the sandy Upper Till, the observed differences between pedons can be expected.

Figure 82. X-ray diffractograms by horizon of the Na-saturated <2 μ m fraction of Pedon 5. 2.4 nm = mixed-layer super lattice, 1.4 nm = chlorite and/or vermiculite, 1.21 nm = mixed-layer illite-vermiculite or illite-chloritized vermiculite, 1.0 nm = illite, .846 nm = mixed-layer d003, .715 nm = kaolinite and/or chlorite d002, .501 nm = illite d002, .485 nm = gibbsite, .426 nm = quartz, .358 nm = kaolinite d002 and/or chlorite d004, and .334 nm = illite d003 and quartz.



Discussion

Overall there appears to be no unique clay mineral or clay mineral assemblage present in the pan. A comparison of the assemblages observed in this study to those for the non-pan soils of Bodine (1986) indicate similar assemblages. The lack of a unique mineralogy agrees with Grossman and Carlisle's (1969) assesment of pan mineralogy.

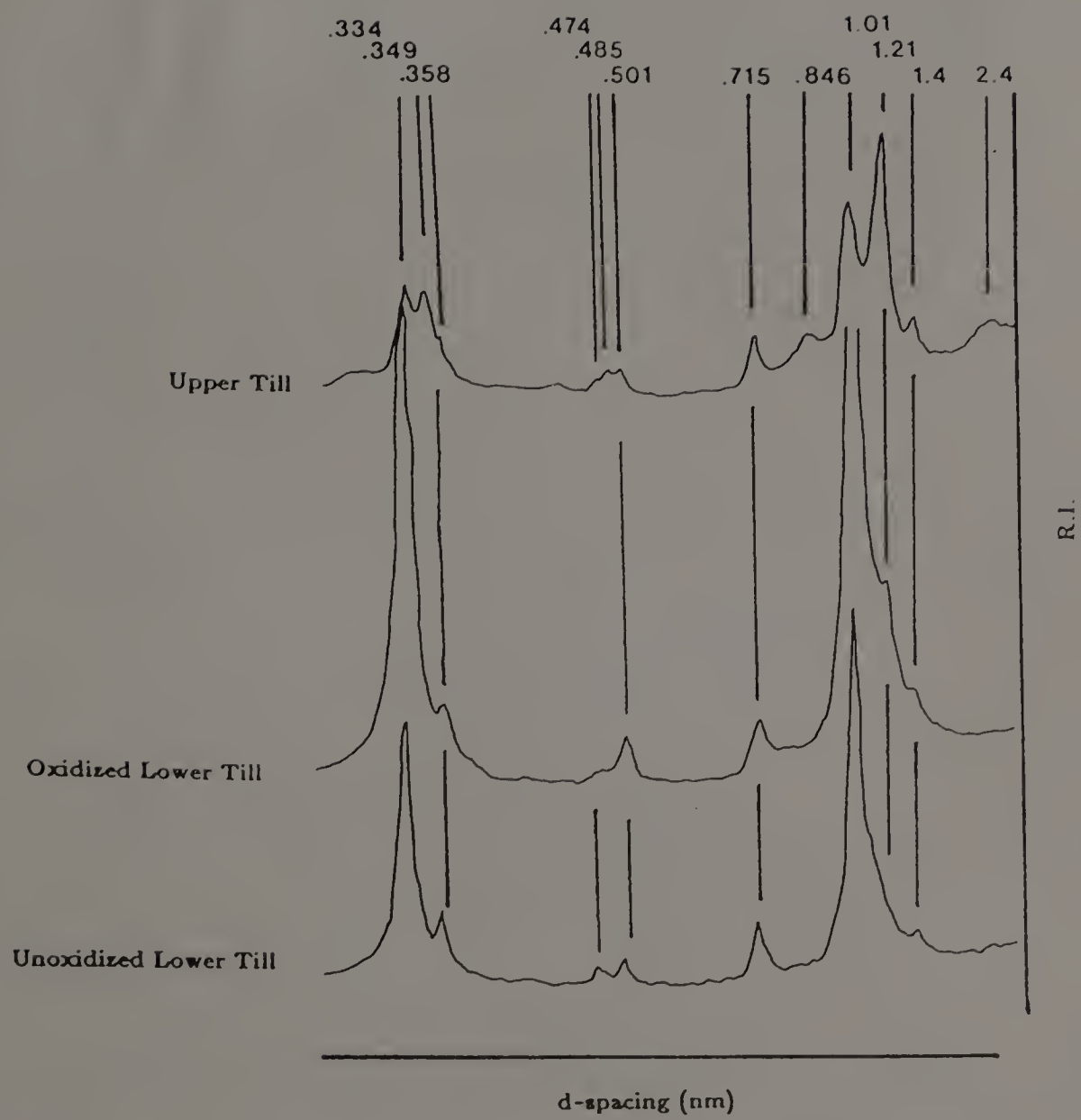
Although the clay mineral analysis provides no simple way to identify the pan it does illustrate a weathering sequence common, in varying degrees, to each pedon. The common sequence has chlorite and/or chloritized vermiculite occurring in the upper solum with the chloritized vermiculite component decreasing and chlorite increasing with depth; interstratified mica/vermiculite increases with depth usually attaining a maximum within the pan and decreasing below it; mica is usually common throughout the profile and in Pedons 1, 2, and 5 increases steadily with depth; gibbsite, when present, is highest in the upper solum especially when there is a low chlorite component; and kaolinite is generally present only in the lower horizons (till). The formation of chloritized vermiculite/vermiculite from mica and chlorite is rapid in the upper solum due to the near complete removal of interlayer potassium (depotassification) and the hydrated interlayer (brucite) followed in some instances by the precipitation of aluminum hydroxy interlayers on the opened interlayers. This process appears incomplete at the present as some chlorite and mica remains in the upper solum. This process appears less rapid deeper within the profile as evidenced by the increase in the mixed-layer

component at the expense of the more completely expanded mineral. This zone represents the first stage of depotassification where alternate interlayer K is removed resulting in an interstratified mica/vermiculite. The second stage would result in the formation of vermiculite (Newton, 1978; Bodine, 1986). Below the pan, mica content generally increases and the mixed-layer clay tends to decrease suggesting that the pan is more weathered than the underlying till (Figure 83).

Although the pan does appear to have a more developed clay mineral assemblage than the till (Cd horizons) some aspects of the assemblage may be inherited directly. Pedons 1-4 have all developed in the oxidized Lower Till which may contain a significant amount of mixed-layer clays (Newton, 1978). It is not unlikely that these clays were inherited by the pan's upper horizons, thus the clay mineral assemblage could have had a head start in developing (Bodine, 1986). Despite this head start the present assemblage in the pan is not the same as that observed in the till, thus some degree of weathering or pedogenic alteration of the clay minerals must have occurred throughout the profiles making the actual degree of inheritance difficult to quantify.

The influence of the till upon the clay assemblage is best seen in Pedon 5. Because Pedon 5 is developed on the younger, coarser textured Upper Till, the clay mineral assemblage is less weathered within the lower horizons as evidenced by the presence of feldspars in the 2BCx horizons and below. The changes in mineralogy with depth are

Figure 83. X-ray diffractograms of the Na-saturated <2 μ fraction of typical Upper Till, Oxidized Lower Till, and Unoxidized Lower Till. 2.4 nm = mixed-layer super lattice, 1.4 nm = chlorite and/or vermiculite, 1.21 nm = mixed-layer illite-vermiculite or illite-chloritized vermiculite, 1.0 nm = illite, .846 nm = mixed-layer d003, .715 nm = kaolinite and/or chlorite d002, .501 nm = illite d002, .485 nm = gibbsite, .426 nm = quartz, .358 nm = kaolinite d002 and/or chlorite d004, and .334 nm = illite d003 and quartz.



not as gradual in this pedon, reflecting a possible weathering discontinuity between the BE and 2BCxl horizons. The lower horizons appear less weathered and more similar to unweathered till than do the upper horizons. Nevertheless the pan is still more weathered than the underlying 2Cd horizons.

Although a similar sequence of assemblages occurs within each pedon the exact minerals and their relative abundances do differ. These differences are best explained by the variation in local bedrock present at each site (c.f. Bodine, 1986). Such effects of lithology are clearly visible when comparing Pedons 1 and 2. The dominant lithology in Pedon 1 is sulfidic biotite schist low in chlorite, whereas in Pedon 2 biotite granofels with chlorite dominate the lithology (Zen, 1983; Bodine, 1986). The clay mineral assemblage reflects these differences as chlorite is all but absent in Pedon 1 but is common in Pedon 2. The presence of amphibole in Pedon 5, and its absence elsewhere is further indication of the influence of local lithology on the initial clay mineral assemblage.

At first glance, the BPF of Pedons 2 and 5 seem to act differently as the BPF of Pedon 2 has a similar assemblage to the 2Btxl, whereas the BPF in Pedon 5 has an assemblage similar to the 2BC horizon, not the 2Btxl. However, both BPF have components similar to overlying horizons with Pedon 5 being most similar to the horizon above it. The illuviation of material into the BPF could account for such an observation. It has been established (Reed, 1989), especially for the Pedon 5 location, that water moves rapidly through the BPF thus material could be washed in from above. However, with the BPF

acting as a conduit it would appear likely that eluviation would dominate, although some translocation could occur. In-situ weathering of minerals present in the BPF could also account for the assemblage. Roots are present in most of the BPF thus organic acids and respiration by-products would be concentrated. This coupled with an increased amount of water moving through the feature results in a greater amount of weathering. It is likely that both processes occur but due to drainage conditions, texture, and parent material differences, the effectiveness of one over the other will vary. Regardless as to which process dominates, the assemblage of the BPF further illustrates that on-going pedogenesis is occurring within the pan.

Conclusions

No unique clay mineral or clay mineral assemblage is present in the fragipan soils studied. The influence of local lithology accounts for much of the observed variation in assemblages. The major influence can be seen by viewing the clay in the Cd horizons in order to establish which mineral assemblage was present prior to Holocene alteration. The clay minerals definitely have been pedogenically altered at least through the fragipan as evidenced by the common occurrence of well developed interstratified mica/vermiculite and its associated super lattice peak. Although some aspects of the assemblage may be inherited, the current weathering sequence clearly superimposes this influence. At the very least the clay mineral

assemblages illustrate that the pan has been pedogenically affected by modern pedogenic processes. At best, the assemblages lend credence to a possible pedogenic origin of the fragipans observed in this study.

CHAPTER VIII

HEAVY MINERALS

Previous Work

Heavy Mineral Analysis in Soils

Analysis of heavy mineral assemblage is not a routine procedure in soil genesis studies, however, they are used to study weathering rates (Ruhe, 1969; Birkeland, 1974). Cremeens et al. (1988) measured etch pits in hornblende grains as well as in some light minerals to compare weathering rates. In situations where a soil is thought to have multiple parent materials, as is the case with some fragipan soils, the heavy mineral assemblage should be different dependent on parent material. Such a difference could be used to differentiate between soil horizons with different parent materials as it is used to differentiate between tills.

Heavy Mineral Assemblages in Till

Heavy mineral analysis has been used since the 1930's to determine till provenance (Derry, 1933). Recent investigations of multiple till sheets in the Great Lakes region of Canada (Gywn and Dreimanis, 1979) identified the source areas as well as differentiated between till units. The identification of the provenance allows for the construction of flow lines, thus establishing the direction of the movement of the ice sheet at the time of till deposition.

Tills in the Mid-continent have been identified based on heavy mineralogy, but the same can not be said for New England. Newton (1978) and Lindbo (1990) indicated that there were no differences in the assemblage between the oxidized and unoxidized facies of the Lower Tills. Lindbo (1990) reported that at locations where both Upper and Lower were present, the heavy mineral assemblage was similar in both tills despite other physical and mineralogical differences. Both researchers noted that garnet and hornblende were more weathered at the surface of the oxidized till. Hematite staining was common around these minerals and typically the color was observed to bleed into the matrix. In the Upper Till at Newton's Warwick site, a slight change in amphibole content with depth was attributed to a minor change in ice flow direction.

Dermer (1984) utilized heavy minerals with more success than Newton. She found slight differences from east to west in hornblende and garnet concentration and was able to correlate assemblages in the Upper (Roslyn) Till on Long Island to particular source areas to the north. Once source areas were identified, flow lines were established using the heavy mineral data and other existing flow indicators. This work resulted in the identification of various ice lobes for the late Wisconsinan in Long Island.

Heavy mineral analysis assists in determining the extent of aeolian input, mixing between the till, pan, and overlying material, and weathering relations through the profile. If the pan is essentially unaltered till the heavy minerals should be similarily

weathered. On the other hand, an increase in weathered minerals may indicate pedogenic processes.

Materials and Methods

Heavy minerals in the very fine sand fraction of selected samples were used to determine the character of the assemblage. Fifty grams of sieved (< 2-mm) soil were gently agitated overnight in 2% sodium-bicarbonate at pH 9.5 (Cremeens et al., 1987). This procedure was found to remove surface staining without damage to the mineral. The sample was later wet sieved to remove fines, dried and sieved, saving the very fine sand fraction. Heavy minerals were separated by placing a 2-gram sample in a test tube containing tetrabromoethane (TBE) and centrifuging at 1000 rpm for 10 minutes. The heavy minerals were concentrated at the bottom of the tube and removed by inserting a fine bulb pipet through the light minerals at the top and suctioning the heavy minerals from the bottom. The minerals were washed in acetone to remove any residual TBE. After drying they were weighed, split, and mounted on a slide in Canada Balsam. Ribbon traverses were made counting 200 to 400 minerals per sample and the counts were converted to percentages (Hubert, 1973). Complete data tables are in Appendix K.

To determine whether individual mineral percentages changed with depth, the horizons above the fragipan, generally considered to contain a significant aeolian component (Fletcher, 1976), were compared to the pan and 3Cd horizons, generally considered to be dense basal till (Calhoun, 1980). An additional comparison was made between

the pan horizons and the 3Cd horizons when a sufficient number of samples were analysed.

Results

Pedons 4 and 5 have highly significant differences between the individual heavy minerals in the upper versus lower portions of the profile (Table 27 and Figures 84-88). The difference observed in hornblende in Pedon 5 was not expected but is relatively small in comparison to that in Pedon 4. Pedon 3 has a small but significant increase in hornblende in the upper horizons. The heavy minerals in Pedons 1 and 2, while exhibiting some variation, are not significantly different. The BCm horizon of Pedon 1 was not included in the statistical analysis as it clearly represented a different provenance based on its low tremolite and high hornblende content (Figure 84). Comparisons between the pan and the 3Cd horizons show that only the garnet content of Pedon 3 was significantly different. This is most likely due to a small increase in the content in the lower 2Btx horizon.

Individual mineral grains, particularly hornblende, garnet, and pyroxene, show signs of severe weathering in the Ap and Bw horizons (Figure 89). The degree of weathering based on etch pits and saw-like terminations appears to decrease slightly with depth, but the minerals in the pans are still weathered (Figure 90). In Pedon 5 less etching is apparent in the 2Cd horizons than in the 2BCx horizons (Figure 91). The minerals in the 3Cd horizons of the other four pedons varied in

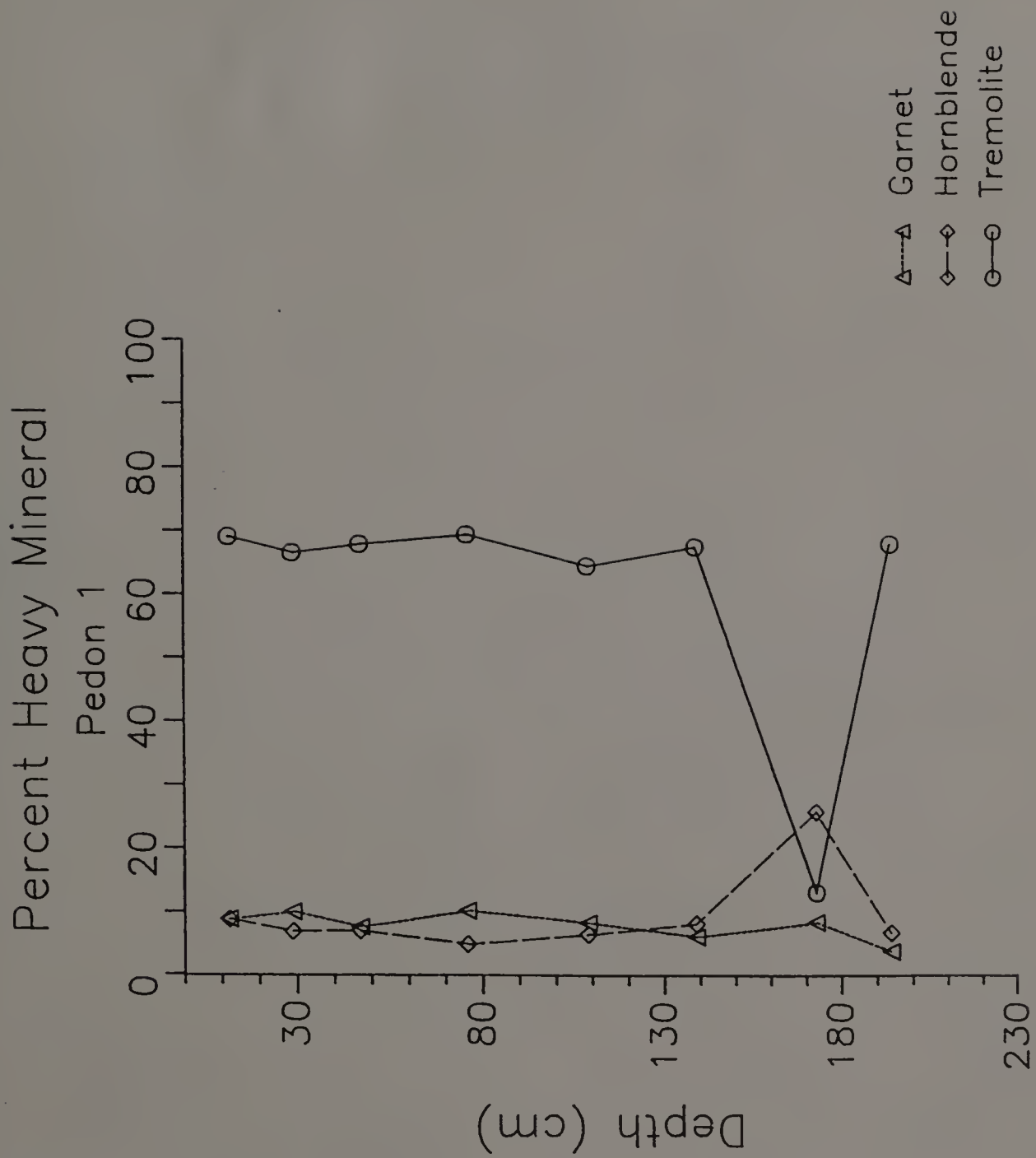


Figure 84. Percent of selected heavy minerals by depth in Pedon 1.

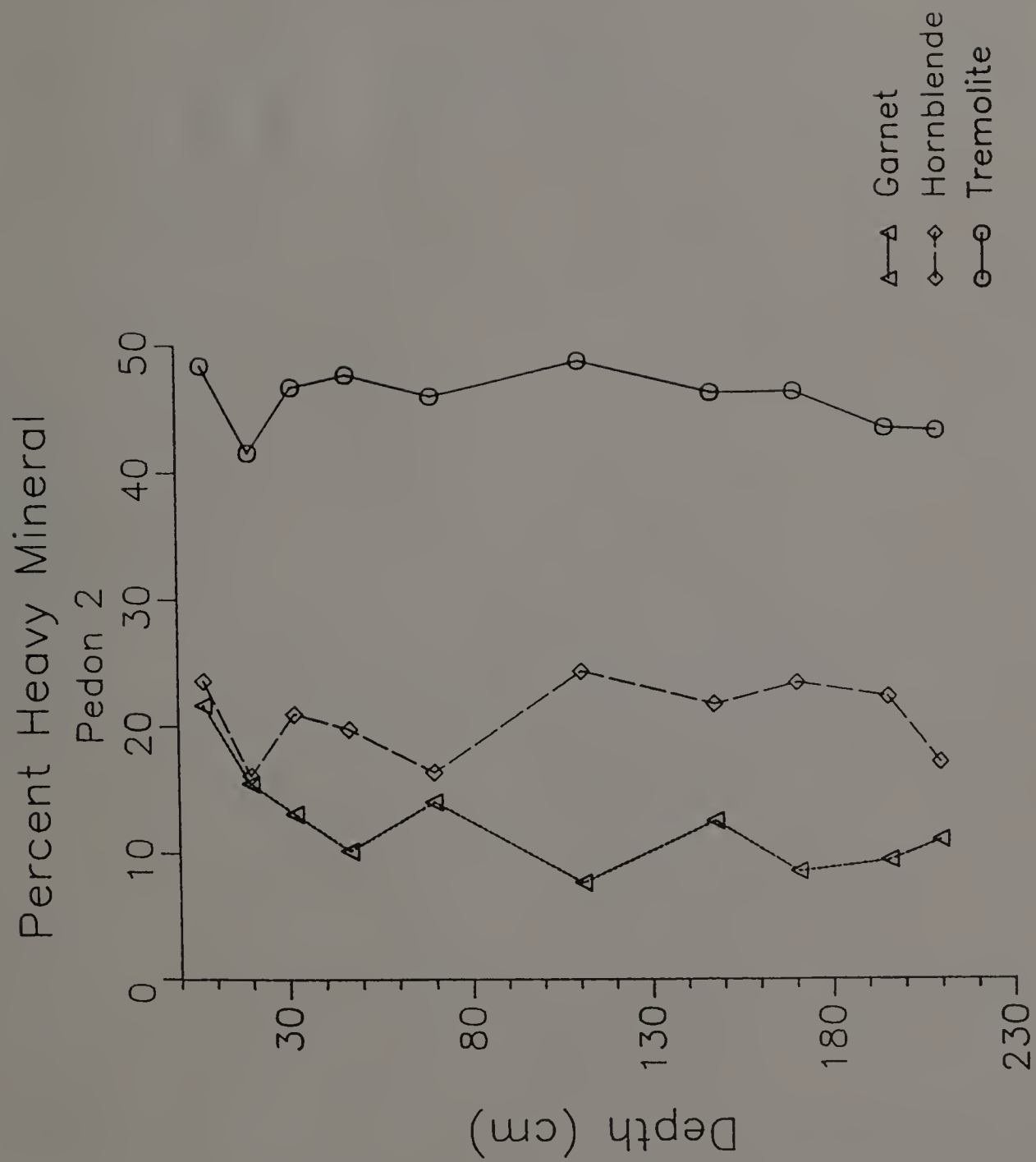


Figure 85. Percent of selected heavy minerals by depth in Pedon 2.

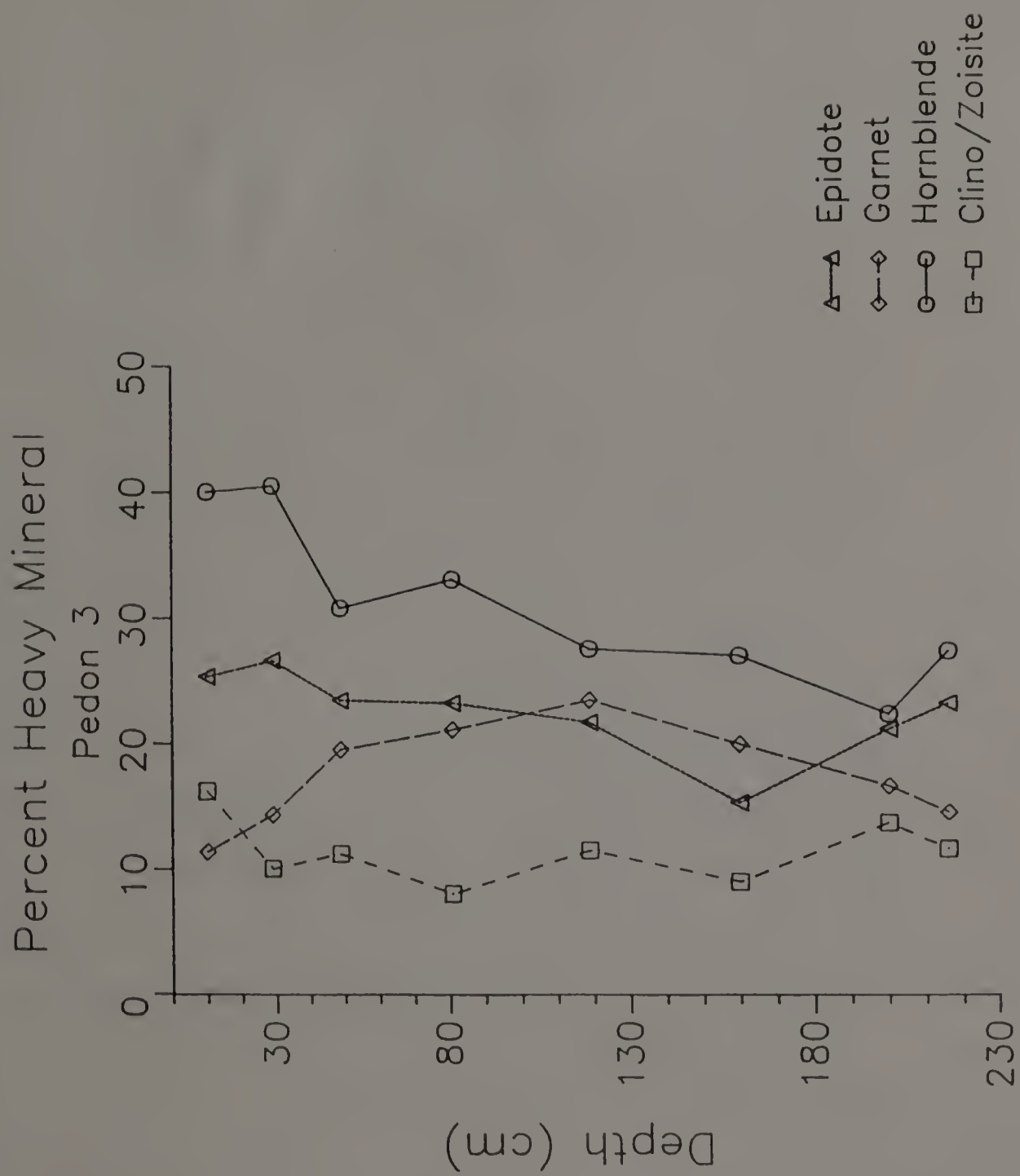


Figure 86. Percent of selected heavy minerals by depth in Pedon 3.

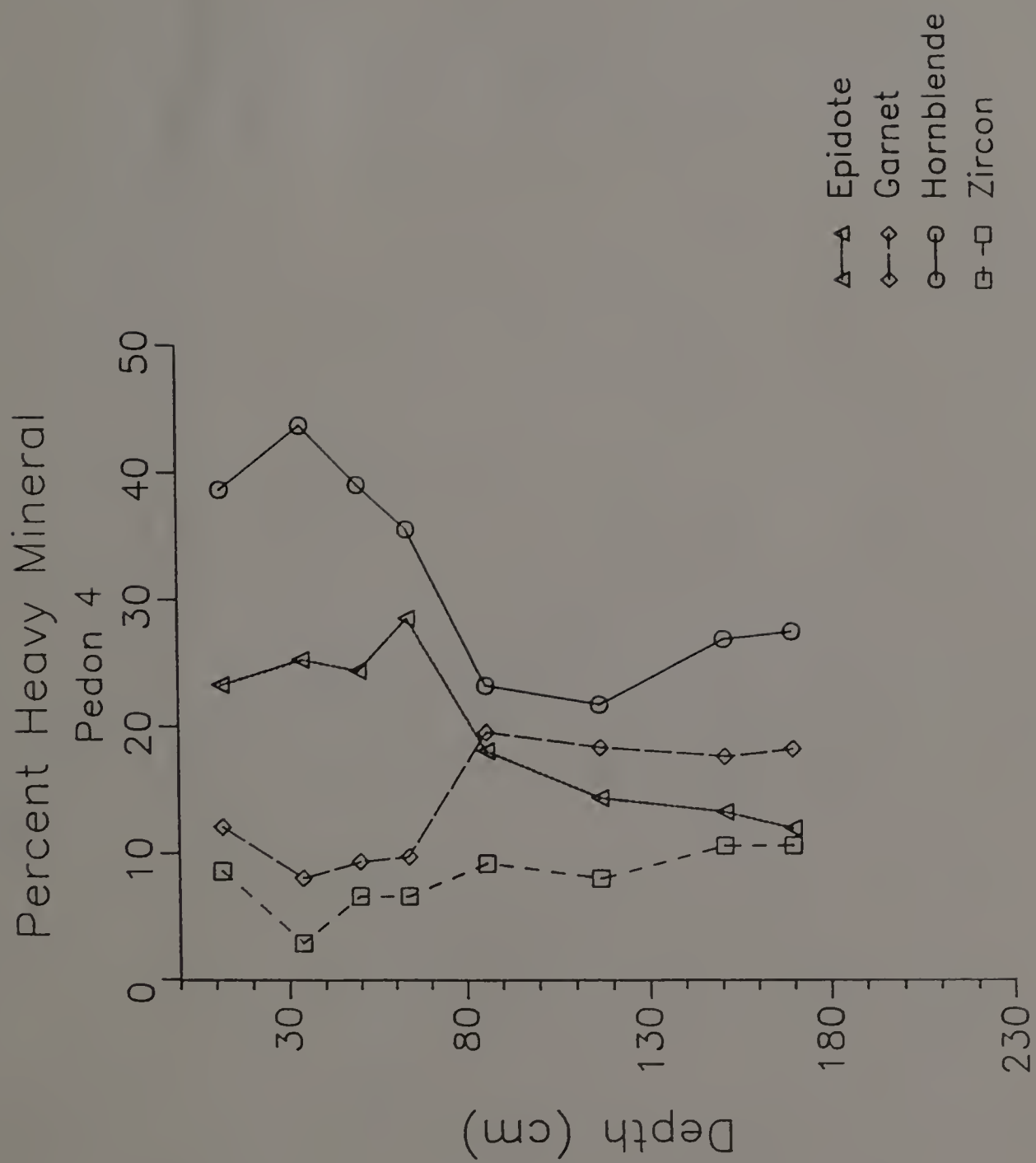


Figure 87. Percent of selected heavy minerals by depth in Pedon 4.

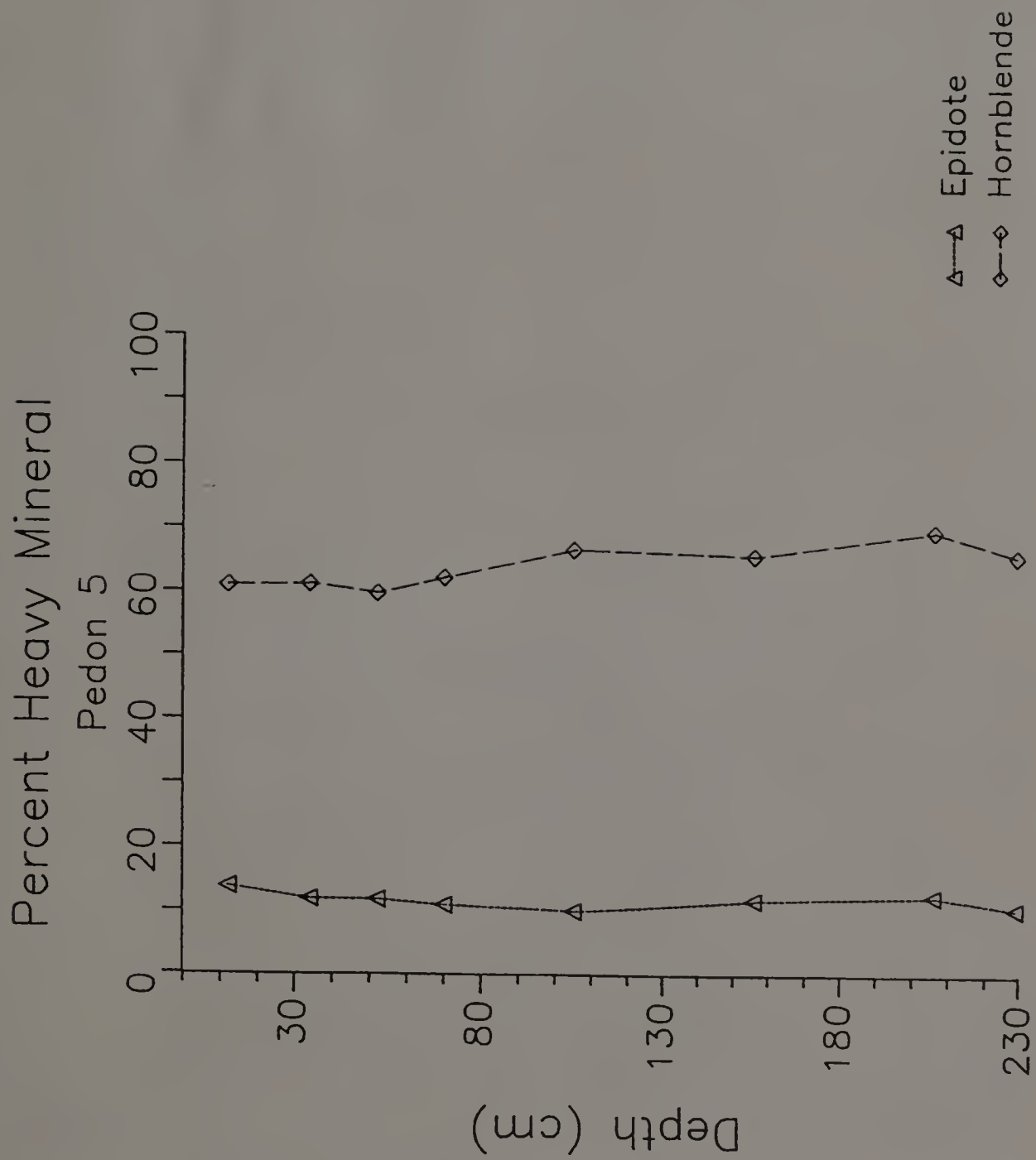


Figure 88. Percent of selected heavy minerals by depth in Pedon 5.



Figure 89. Garnet grain from the Ap horizon of Pedon 1.
Note pitted, jagged and stained surfaces. The bar
is 0.05 mm long.



Figure 90. Garnet grain from the 2Btx1 horizon of Pedon 1.
Noted pitted, jagged surfaces. The bar is 0.05 mm
long.



A



B



Figure 91. Hornblende grain from the (A) 2Btx1 horizon, and (B) 2Cd2 horizon of Pedon 5. Note jagged and stained surfaces on the grain from the fragipan horizon. The bar is 0.05 mm long.

the degree of etching (Figure 92). Staining by iron oxides and organic matter is most common in the upper horizons and is almost non-existent in the 2Cd horizons of Pedon 5.

Table 27. Statistical analysis of selected heavy minerals.

Comparison	Mineral	Pedon				
		1	2	3	4	5
Upper vs Lower Horizons ¹	Epidote	--	--	NS	HS	NS
	Garnet	NS	NS	NS	HS	--
	Hornblende	NS	NS	S	HS	HS
	Tremolite	NS	NS	--	--	--
	Zircon	--	--	--	S	--
	Clino/Zoisite	--	--	NS	S	--
Fragipan vs 3Cd Horizons	Epidote	--	--	NS	--	--
	Garnet	--	NS	S	--	--
	Hornblende	--	NS	NS	--	--
	Tremolite	--	NS	--	--	--
	Clino/Zoisite	--	--	NS	--	--

NS-Not Significant, S-Significant (95%), HS-Highly Significant (99%)

1 Upper horizons refer to Ap through the horizon just above the pan; lower horizons refer to the horizons developed in till.

Discussion

There is no individual or group of heavy minerals that is exclusive to the pan. This does not mean however, that the heavy mineral assemblages are not useful in understanding the genesis of the pedons studied. On the contrary, changes in relative mineralogy are



Figure 92. Garnet grain from the 3Cd3 horizon of Pedon 2.
Note one surface is pitted and jagged, whereas the
others are not. The bar is 0.05 mm long.

useful in determining the influence of different parent materials, weathering relationships, and degree of pedoturbation.

The macromorphology of all pedons suggests that the upper horizons contain some aeolian material which is most noticable in Pedons 3, 4, and 5. The heavy mineral assemblage confirms the aeolian input in these profiles especially in Pedon 4. Although Pedons 4 and 3 are separated by only a few hundred meters, Pedon 3 does not exhibit the same changes in heavy minerals with depth. This could be caused by down-slope movement of the upper aeolian cap in the form of soil creep. This seems unlikely however, as Pedon 4 which is down slope from Pedon 3, does not exhibit a greater concentration of any of the heavy minerals associated with either pedon. Because of their topographic position it is possible that Pedon 4 received a greater, that is thicker, aeolian input. Although this can not be conclusively demonstrated it appears likely as the lower pedon, Pedon 4, would lie in the lee of Orchard Hill where the air would be calmer, albeit slightly, and increased deposition could occur. These hypotheses explain the observed assemblages based on geomorphic processes, but soil forming processes also may have played a role in developing the assemblage. Pedoturbation by frost action, tree throw, and bioturbation is likely to homogenize the assemblages. Such homogenization of the heavy mineral assemblages is evident in Pedons 1 and 2 where there are no statistical differences in the assemblage between the upper and lower portions of the profiles. This same phenomenon is seen to a lesser extent in Pedon 5 (note the epidote content) and in Pedon 3. Pedon 5 does have a difference in hornblende

content but this difference is numerically small and there does appear to be a gradual transition between the BE, BC, and BCxl horizons indicating mixing between these horizons. In the field, this mixing zone is characterized by sand lenses surrounding lenses of pan-like material and may represent some slope movement as well as pedoturbation. Despite differences in hornblende content in Pedon 3 the other minerals appear uniformly distributed in all the horizons except the upper two horizons. These horizons represent the thickness of the remaining unmixed aeolian mantle with the lower horizons illustrating a zone of mixing.

The observation of etched grains is qualitative but such observations are important in understanding the degree of weathering that has occurred in the soils. If weathering has been significant, easily weathered grains such as hornblende and pyroxenes will be etched. In the relatively acid conditions common to the soils in southern New England garnet probably also will show signs of etching and pitting (Fuchtbauer, 1972). The 2Cd horizons of Pedon 5 are the least weathered of all the observed horizons. This is consistent with observation of heavy minerals in the Upper Till showing only slight weathering of the afore mentioned minerals (Newton, 1978; Lindbo, 1990). The horizons above the 2Cd horizons in Pedon 5 have a increasing degree of etching and pitting towards the surface. This trend is also observed in the other pedons which have developed in the loamy, oxidized Lower Till. In these pedons, the degree of etching in the pan appears greater than that in the 3Cd horizons but an argument

could be made that the observed weathering is inherited because the oxidized Lower Till has been shown to contain weathered mineral grains. However, there is no discernable abrupt change in the degree of etching throughout the profiles, suggesting that there is no weathering discontinuity or that such a discontinuity has been overprinted by the current weathering cycle. Whereas some etching could be inherited, it mostly occurred post-depositionally. This interpretation is supported by the observation that the clay mineral assemblage indicates weathering throughout the profiles (Chapter 7).

Overall the heavy mineral assemblages of the 3Cd and 2Bx horizons are statistically the same with only a slight difference in garnet content of Pedon 3. This suggests that both the pan and till (3Cd's) are derived from the same material (source) and/or that significant mixing has occurred between them. A substantial amount of mixing seems unlikely as a well developed stone line separates the pan from the till in Pedon 2. Pebble fabric (Chapter 10) suggests that the pan material has been reoriented during the late Wisconsinan thus the most likely source for the pan is the till. An event that could reorient pebbles may have also abraded some heavy minerals resulting in fewer etched grains being inherited in the pan. Therefore, the observed etching is not entirely inherited and is the result of Holocene weathering indicating that the pan has been affected by pedogenesis.

Conclusions

The heavy mineral assemblages did not identify a common mineral within the pan. Instead, the assemblages illustrated differences in

provenance between some horizons. In particular the BCm of Pedon 1 was identified as being derived from a dissimilar source than the rest of the pedon. The influence of aeolian material was clearly expressed in Pedon 4 and partially in Pedons 3 and 5. The assemblages also were useful in showing that the underlying till assemblage is basically the same as the pan assemblage. This indicates that the pan is developed in the locally derived till. Although parent material differences were evident, a large degree of homogeneity was observed in most pedons indicating that pedoturbation had resulted in the mixing of till and aeolian materials. Such mixing implies that pedogenesis is an ongoing process modifying the properties of the soils. Further indication that pedogenesis has affected the soils are the presence of etched and pitted grains throughout the profiles with the degree of weathering decreasing with depth. The heavy mineral weathering agrees with observation of the clay mineral assemblages (Chapter 7).

CHAPTER IX

STRENGTH ANALYSIS

Previous Work

Brittle consistency is one of the properties used most often to distinguish fragipans from other horizons (Grossman and Carlisle, 1969). While brittleness commonly is used to describe the consistency of the fragipan in the field, the term is highly subjective. A dry fragipan ped is very brittle, yielding abruptly when compressed. A moist ped is not as brittle and may yield slowly to applied pressure. This first suggests that there is some cementation of the pan, yet as Anderson and White (1958) showed fragipan peds slake when placed in water, indicating the lack of cementation.

Attempts have been made to quantify the strength or brittle behavior of the fragipan. Grossman et al. (1959a) used the "drop-shatter" method on soil clods to show that strength increased with depth in the soil. In a more quantitative approach using a triaxial soil compression apparatus, Grossman and Cline (1957) determined that rupture of the pan material occurred between 390 and 2450 kPa. Later work by Lenhardt (1983) confirmed these values for several fragipan soils in New York state. Pickering (1983) and Pickering and Veneman (1984) reported the unconfined compressive strength of a glacial till pan in southern New England to be about 100 kPa, falling within the range of reported strength values

for of glacial till (Dejong and Harris, 1971; Quigley, 1975). They also investigated the use of a pocket penetrometer to evaluate strengths. This device was found to give variable results depending on the moisture content of the sample. Unfortunately, none of these tests addresses the question of the sources of the brittleness.

The brittleness, presumably, is the result of the cementation of soil particles. This phenomenon is evident from the sudden rupture of a soil ped upon the application of pressure, resulting in the instantaneous destruction of the soil aggregate. Grossman and Cline (1957) suggested that clay acting as a bridge between silt and sand grains is the main cause of the brittle nature of the pan. This feeling has been supported by many since it was proposed (Knox, 1959; Wang et al., 1974; Yassoglou and Whiteside, 1960; Veneman and Bodine, 1982; DeKimpe et al., 1972; Hutcheson and Bailey, 1964; Buurman and Jongmans, 1975; Payton, 1980). Buurman and Jongmans (1975) suggested a model for the contribution of clay to the strength of the pan. Firstly, clay would be removed from overlying horizons by water. Subsequently, soil water was removed by evapotranspiration when the soil dried out and a meniscus of water would form around and between particles. The clay would be oriented with the water film and as the film disappeared the clay would be deposited in a position between larger grains and act as a bridge. In cases where the process of soil drying due to evaporation seems unlikely water removal due to drainage is possible.

Another aspect of the Buurman and Jongmans model is the idea that close packing of material (or high bulk density) can occur and

cause brittle behavior. Nettleton et al. (1968b) felt that as clay was removed, slumping of the remaining material may occur, thus causing close packing and subsequent increase in density and brittleness (c.f. Bryant, 1989). This mechanism of gross particle reorganization was further supported by Yassoglou and Whiteside (1960); Fritton and Olson (1972); Jha and Cline (1963); DeKimpe and McKeague (1974); and Habecker et al. (1990).

Several researchers have attempted to associate a particular agent with brittle behavior. Silicon has been found in sodium-hydroxide (NaOH) extracts of fragipan material and in natural pore fluids and therefore is postulated as contributing to the bonding, possibly in the form of weakly crystalline silicate clay or as an amorphous compound (Norton et al., 1984; Steinhardt et al., 1982; Steinhardt and Franzmeier, 1979; Franzmeier et al., 1978; Harlan et al., 1977; Norton and Franzmeier, 1978; Karathanasis, 1987a; 1987b; 1989; Franzmeier et al., 1989; Smeck et al., 1989). Thus a silica rich precipitate may contribute significantly to the brittleness in fragipans, especially those developed in loess (Franzmeier et al., 1978, Harlan et al., 1977, Norton and Franzmeier, 1978; Steinhardt and Franzmeier, 1979; Hallmark and Smeck, 1979a and 1979b; Karathanasis, 1987a; 1987b; 1989). The process by which this occurs (c. f. Franzmeier et al., 1989) is similar to that described by Buurman and Jongmans (1975) for clay bonding. Plant roots remove water preferentially over silicic acid thus concentrating the acid in small pores. This causes the precipitation of a stable silica-rich compound

that will not dissolve with an influx of water containing appreciable amounts of silicic acid. This model adequately explains a possible bonding mechanism, however, it also suggests that the pan may be the initial stage in the formation of a duripan.

In addition to clay and amorphous silica, amorphous oxides of Fe, Al, and Mn also may contribute to the fragic character of some horizons (Anderson and White, 1958; Nettleton et al., 1968b; Steele et al., 1969; Grossman et al., 1959c; McCabe et al., 1978; Matthews, 1976; Horn and Rutledge, 1965). Iron (Fe) and aluminum (Al) have also been used as indicators of the presence of the fragipan and to explain its brittleness (Yassoglou and Whiteside, 1960; Horn and Rutledge, 1965; Nettleton et al., 1968b). However, crystalline silicates or well crystallized Fe and Al oxides or hydrous oxides are not very likely cementing agents, as the fragipan material slakes in water, losing its brittleness when moistened (Anderson and White, 1959; Soil Survey Staff, 1975). Also Fe is mobile when reduced, therefore it is unlikely that it could act as a cement in poorly drained soils under reducing conditions (Franzmeier et al., 1989). Others have stated that the presence of amorphous Fe, Al, and Mn oxides and hydroxides may be related more to the high clay content in the pan rather than to actual bonding (Harlan et al., 1977). Identification of the premier bonding agents in fragipans remains elusive.

Using a different approach, Bryant (1989) associated at least part of the brittleness in New York fragipans, with a relatively high angle of internal friction caused by self weight collapse or collapse

of a saturated sediment, with a cohesive force resulting from the presence of some chemical bonding agent as a secondary factor.

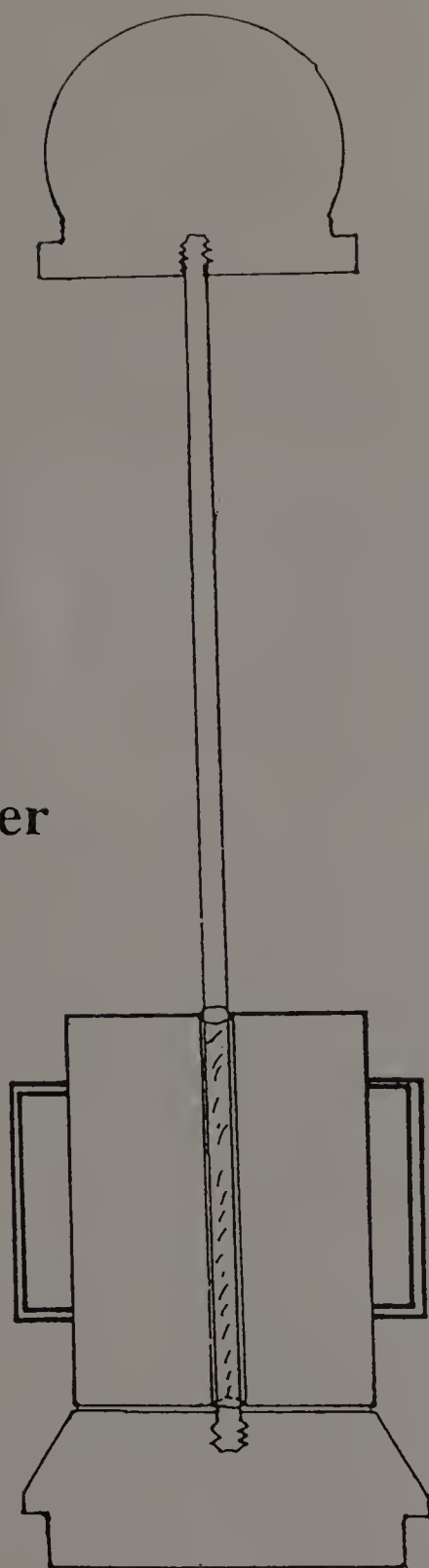
Finally, Lozet and Herbillon (1971) state that they found no clear cement. They feel that a combination of the afore mentioned factors influences the consistency of the pan.

The nature of the pans observed in New England often is attributed to properties inherited from the glacial till in which they formed (Calhoun, 1980). The identification of bonding agents in the pan is one more way to illustrate that pedogenic development also has occurred. In order to assess this, the potential bonding agent must be removed to determine the agents effect on the strength character of the pan.

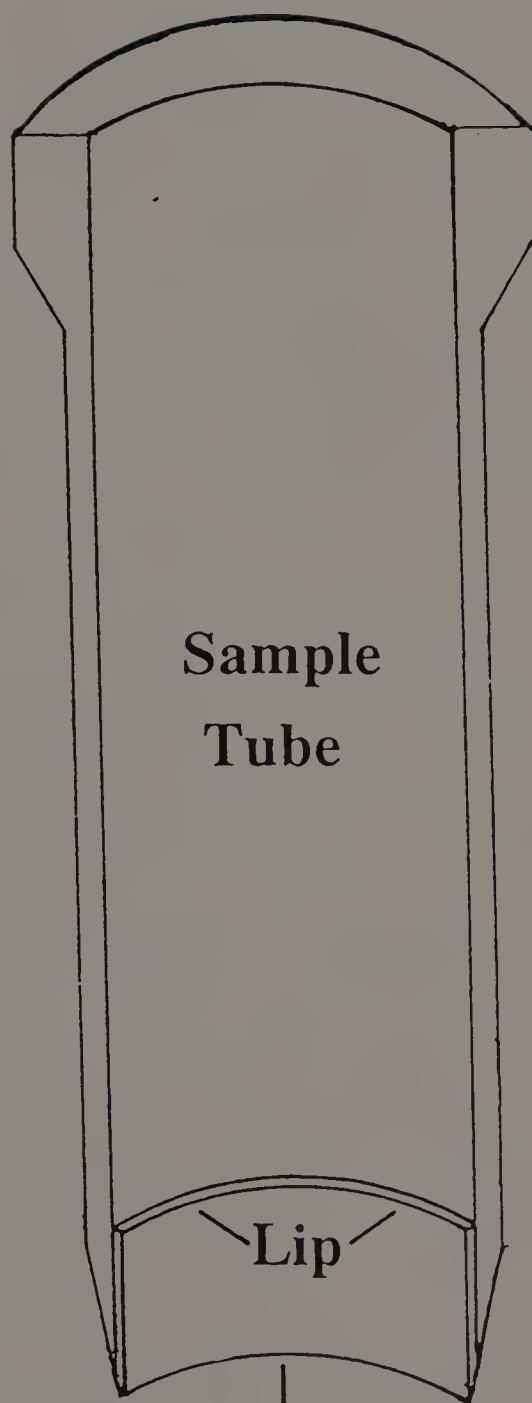
Materials and Methods

Undisturbed soil columns approximately 5 cm in diameter and over 15 cm in length were extracted from the pan using a soil coring device similar to that described by Ruark (1985) (Figure 93). Pickering and Veneman (1984) reported that cores taken with this device had a maximum 1.5 mm zone of disturbance, with values of 0.5 mm to 1.0 mm being more common. In rockier soils this zone may extend further into the core. The cores were brought back to the lab inside thin plastic tubes and cut to 15 cm in length with a diamond saw. The cutting was done slowly to prevent disturbance. The cores were examined to ensure that there were no visible signs of disturbance and then placed on

Slide Hammer



Sample
Tube



Cutting Edge

Figure 93. Schematic of the soil coring apparatus used to extract cores for leaching and strength analysis. The inner diameter of the tube is 5 cm.

sponges and wetted for at least one week. During this procedure the cores remained in field orientation.

Various methods have been used to encase cores for leaching experiments (Gephart, 1979; Hallmark and Smeck, 1979b; Norton et al., 1984) yet these all proved unsatisfactory due to economic and time constraints. For this research the plastic liner used in the initial sampling procedure was removed with a scalpel from the saturated, oriented cores. A clear plexiglass tube approximately 20 cm long and 7 cm inside diameter, was placed around the core without touching it. The gap between the plexiglass and the core was filled with liquid parafin and allowed to cool overnight. The bottom of the column (core, parafin, and plexiglass) was covered with a pad of glass wool and a 1-mm mesh nylon screen. The screen was secured with a rubber band and tape (Figure 94). A minimum of sixteen cores from each sampling site were required in order to ensure four replications of each leaching treatment. During the set up procedure the cores remained wetted by direct basal contact with saturated sponges. Before leaching, a layer of fine sand was placed on top of the core to prevent puddling. A constant head of the extracting solution was maintained with a mariotte device.

The following solutions were used in the leaching experiments: 0.2M NH_4 oxalate at pH 3, 0.1M Na-pyrophosphate at pH 10, 0.5M NaOH , while 0.025M CaCl_2 was used as a control. The oxalate was chosen to selectively extract old amorphous Fe and Al materials, while the pyrophosphate was assumed to extract the younger more mobile and

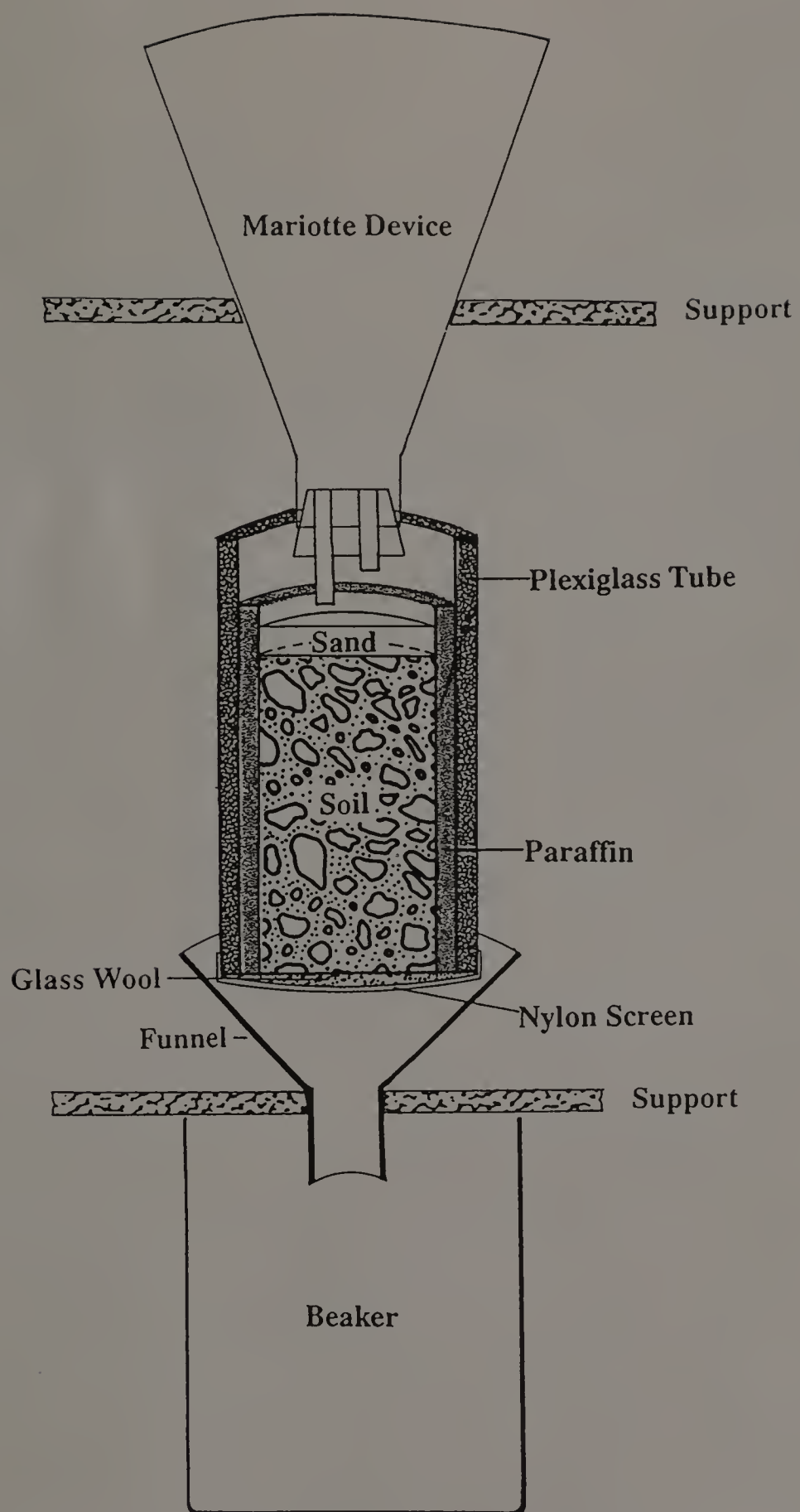


Figure 94. Schematic of the apparatus used for the removal of bonding agents from soil columns. These are arranged in sets of 4 for one treatment.

organically bound Fe and Al amorphous minerals. Sodium-hydroxide was selected to extract amorphous Si.

Approximately 65 pore volumes of extracting solution were leached through each column. Leachate samples for analysis of Fe, Al, Si and Mn were removed after the fifteenth, twenty-fifth, thirty-fifth, forty-fifth, fifty-fifth, and sixty-fifth pore volume, respectively. An additional sample to determine the amount of clay was taken from the four samples leached with pyrophosphate. Fresh extracting solution was used each time after the supernatant samples were taken.

Upon completion of the leaching process the columns were air-dried for at least one month and then oven-dried at 45°C for at least one week. After drying the columns were placed in a freezer for about one hour, facilitating the extraction of the cores from the tubes. The cores remained encased in parafin for at least one more hour to equilibrate to room temperature. Both the top and bottom of the core were made flat prior to placing it in the unconfined compression apparatus for an unconsolidated-undrained shear (UU) test. Once in the device, the parafin was scored and removed. After failure, sub-samples with known orientation were saved for micromorphological examination, and the remainder of the sample was saved for physical and chemical investigations.

Results

Extraction of Potential Bonding Agents

Iron is extracted best by oxalate (Figure 95). The oxalate extracted approximately 1 order of magnitude more Fe than pyrophosphate or NaOH did, because oxalate complexes Fe more strongly. Similarly, oxalate extracted Al more efficiently than pyrophosphate although NaOH extracted Al nearly as much and sometimes more than the oxalate (Figure 96). The extraction procedures confirm that NaOH extracts Al in similar amounts as oxalate (c. f. Chapter 6). Silicon was removed in the greatest amounts by NaOH followed by oxalate, the latter removing about 2 times more Si than the pyrophosphate (Figure 97). Manganese was removed in the smallest amount, insignificant in comparison to the other three elements analyzed (Figure 98). Oxalate extracted the most and NaOH the least amount of Mn. During the first run of column extractions it was noticed that clay was being leached by the Na-pyrophosphate. In subsequent runs the amount of clay removed was determined and the clay mineralogy was characterized for selected samples. Clay removal ranged from a low 15 g/kg to 47 g/kg with an average of about 26 g/kg (Figure 99). The clay minerals present in the pyrophosphate leachate were somewhat dissimilar to those found in the overall horizon (c. f. Chapter 7). Mica generally dominated followed by the mixed-layer component (Figure 100). The analyses were commonly performed at a lower impulse setting in order to attain peak heights great enough to determine the mineralogy. This

Figure 95. Average amount (mg kg^{-1}) of Fe extracted by each treatment for each site. BTR = Belchertown Ridgebury 2Btxl horizon, BTR/S = Belchertown Ridgebury/Scituate 2Btxl horizon, EHP = Elm Hill Paxton (Pedon 1) 2Btxl horizon, OHW = Orchard Hill Woodbridge (Pedon 4) 2Btxl horizon, OHD = Orchard Hill (Pedon 4) 3Cd horizon, BHW = Buck Hill Woodbridge 2Btxl horizon, BHR = Buck Hill Ridgebury 2Btxl horizon, and BHD = Buck Hill Paxton (Pedon 2) 3Cd3 horizon.

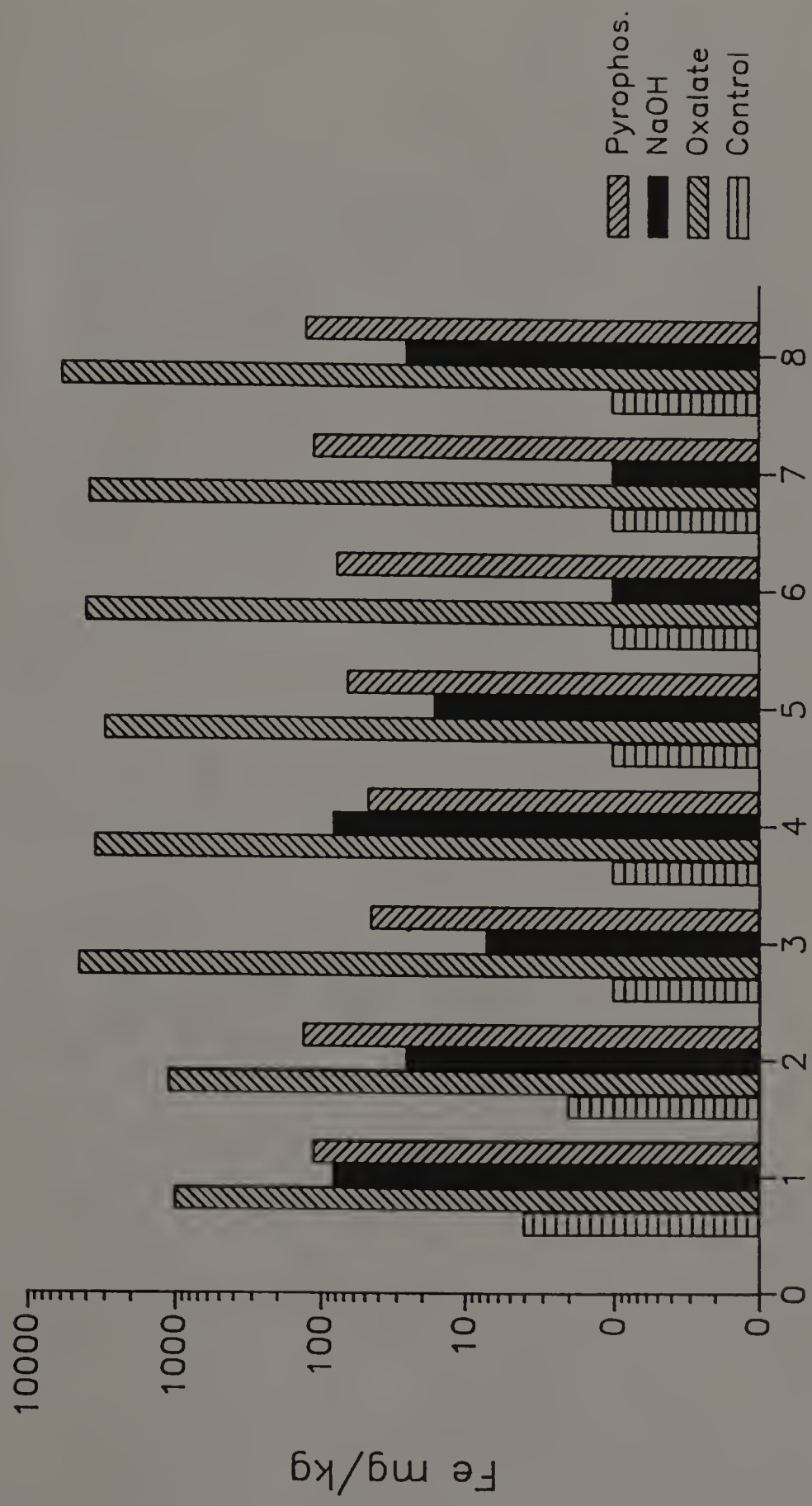


Figure 96. Average amount (mg kg^{-1}) of Al extracted by each treatment for each site. BTR = Belchertown Ridgebury 2Btxl horizon, BTR/S = Belchertown Ridgebury/Scituate 2Btxl horizon, EHP = Elm Hill Paxton (Pedon 1) 2Btxl horizon, OHW = Orchard Hill Woodbridge (Pedon 4) 2Btxl horizon, OHD = Orchard Hill (Pedon 4) 3Cd horizon, BHW = Buck Hill Woodbridge 2Btxl horizon, BHR = Buck Hill Ridgebury 2Btxl horizon, and BHD = Buck Hill Paxton (Pedon 2) 3Cd3 horizon.

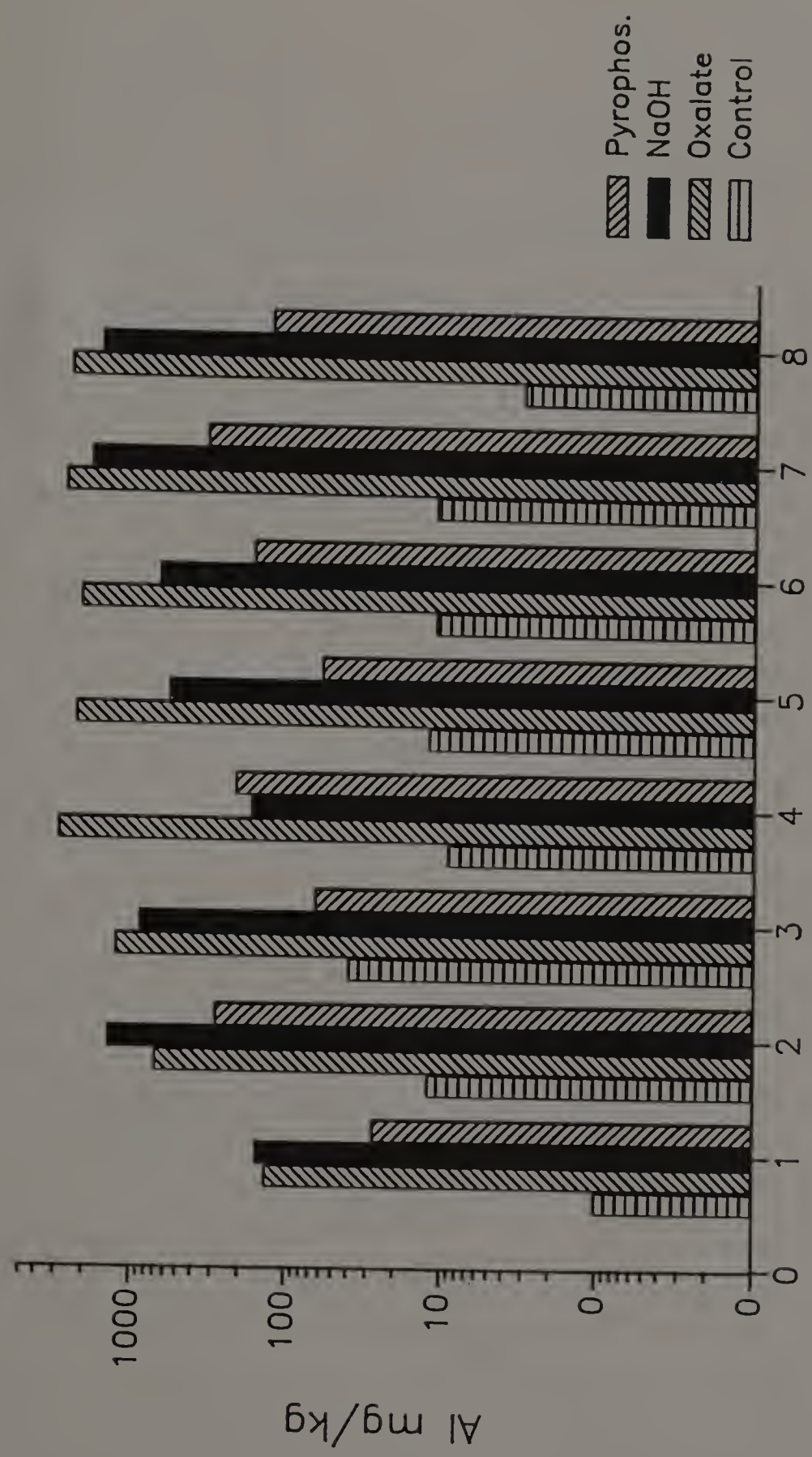


Figure 97. Average amount (mg kg^{-1}) of Si extracted by each treatment for each site. BTR = Belchertown Ridgebury 2Btxl horizon, BTR/S = Belchertown Ridgebury/Scituate 2Btxl horizon, EHP = Elm Hill Paxton (Pedon 1) 2Btxl horizon, OHW = Orchard Hill Woodbridge (Pedon 4) 2Btxl horizon, OHD = Orchard Hill (Pedon 4) 3Cd horizon, BHW = Buck Hill Woodbridge 2Btxl horizon, BHR = Buck Hill Ridgebury 2Btxl horizon, and BHD = Buck Hill Paxton (Pedon 2) 3Cd3 horizon.

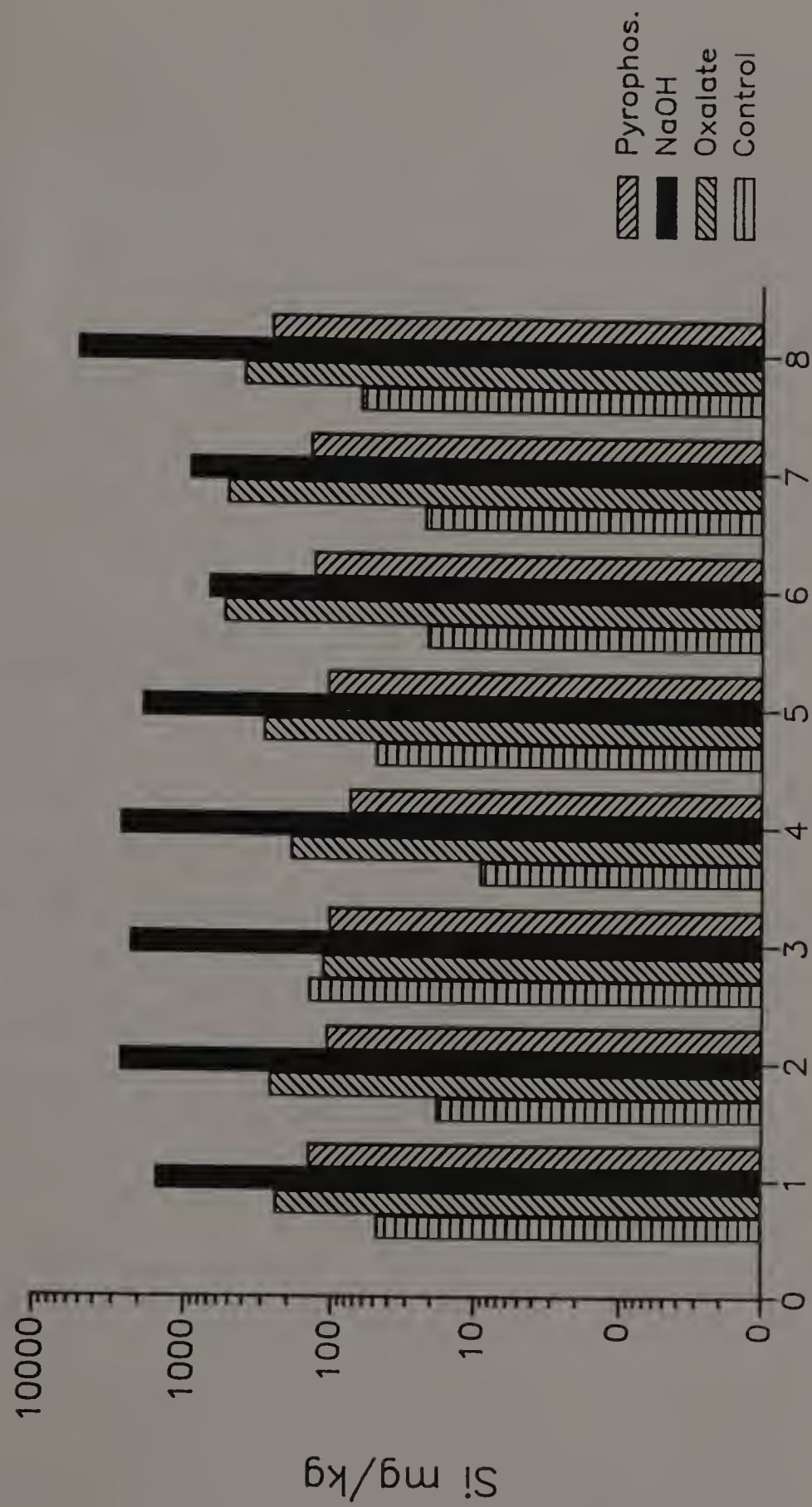


Figure 98. Average amount (mg kg^{-1}) of Mn extracted by each treatment for each site. BTR = Belchertown Ridgebury 2Btxl horizon, BTR/S = Belchertown Ridgebury/Scituate 2Btxl horizon, EHP = Elm Hill Paxton (Pedon 1) 2Btxl horizon, OHW = Orchard Hill Woodbridge (Pedon 4) 2Btxl horizon, OHD = Orchard Hill (Pedon 4) 3Cd horizon, BHW = Buck Hill Woodbridge 2Btxl horizon, BHR = Buck Hill Ridgebury 2Btxl horizon, and BHD = Buck Hill Paxton (Pedon 2) 3Cd3 horizon.

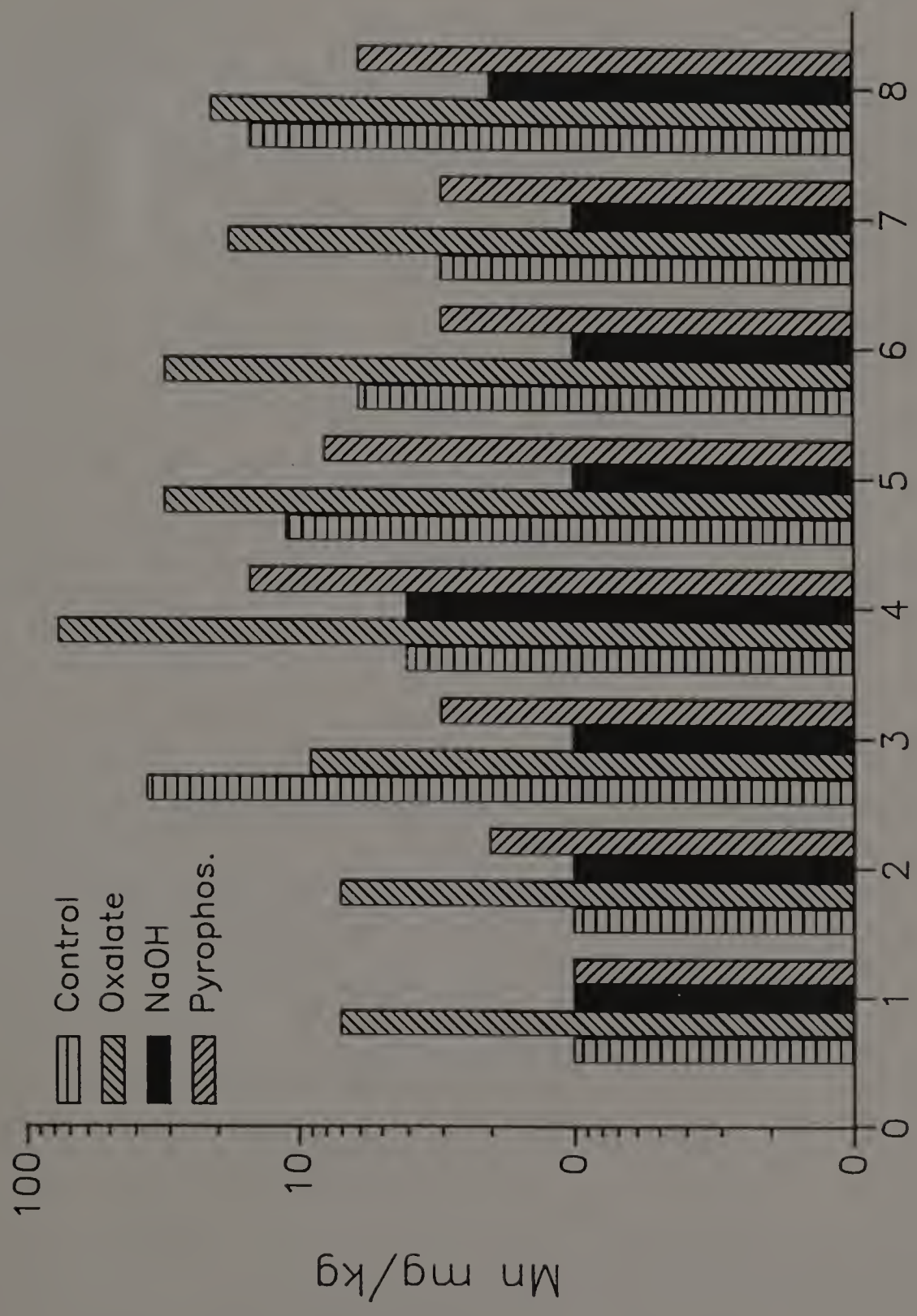


Figure 99. Average amount (g kg^{-1}) of Clay extracted by Na-pyrophosphate for each site. BTR = Belchertown Ridgebury 2Btxl horizon, BTR/S = Belchertown Ridgebury/Scituate 2Btxl horizon, EHP = Elm Hill Paxton (Pedon 1) 2Btxl horizon, OHW = Orchard Hill Woodbridge (Pedon 4) 2Btxl horizon, OHD = Orchard Hill (Pedon 4) 3Cd horizon, BHW = Buck Hill Woodbridge 2Btxl horizon, BHR = Buck Hill Ridgebury 2Btxl horizon, and BHD = Buck Hill Paxton (Pedon 2) 3Cd3 horizon.

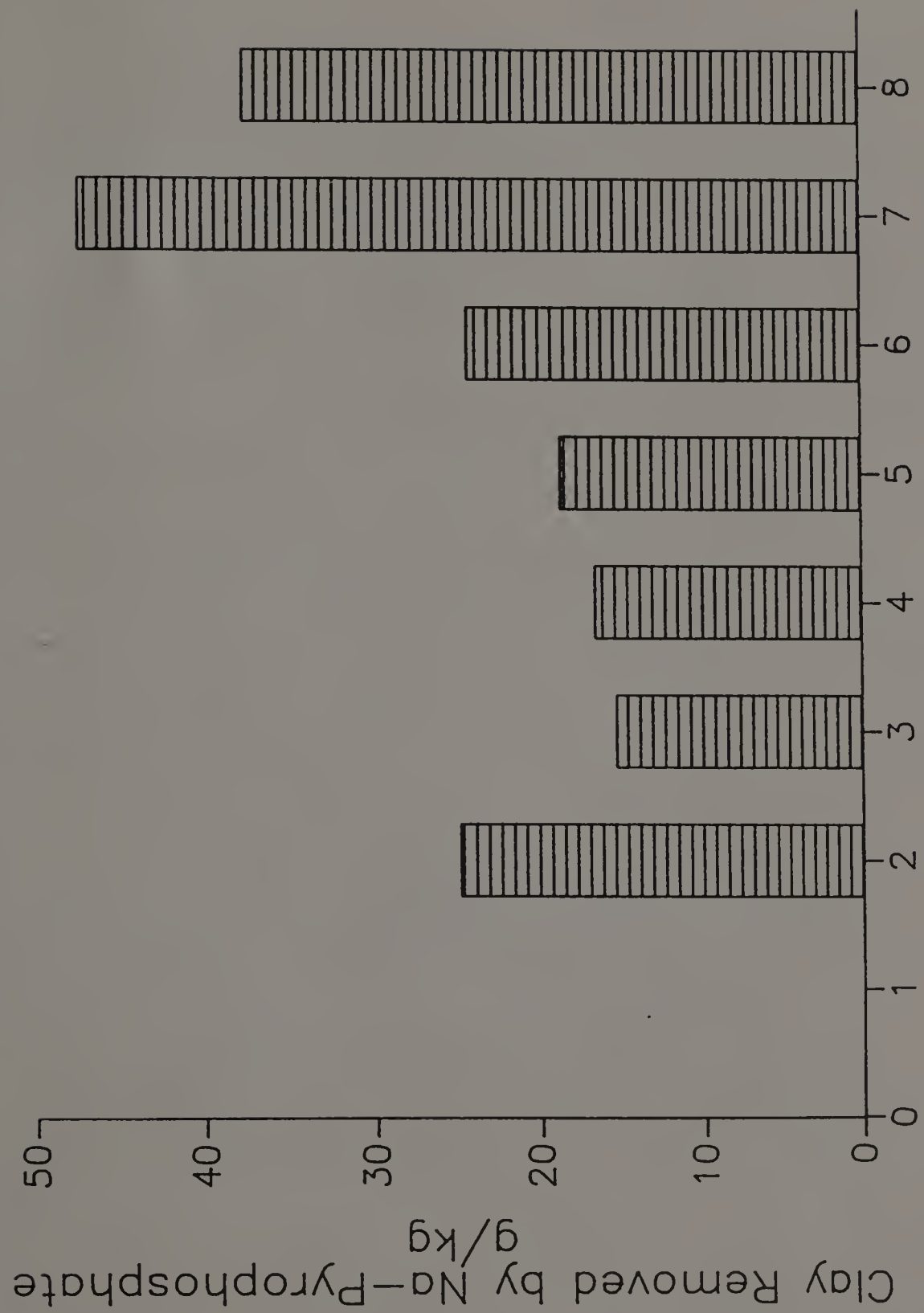
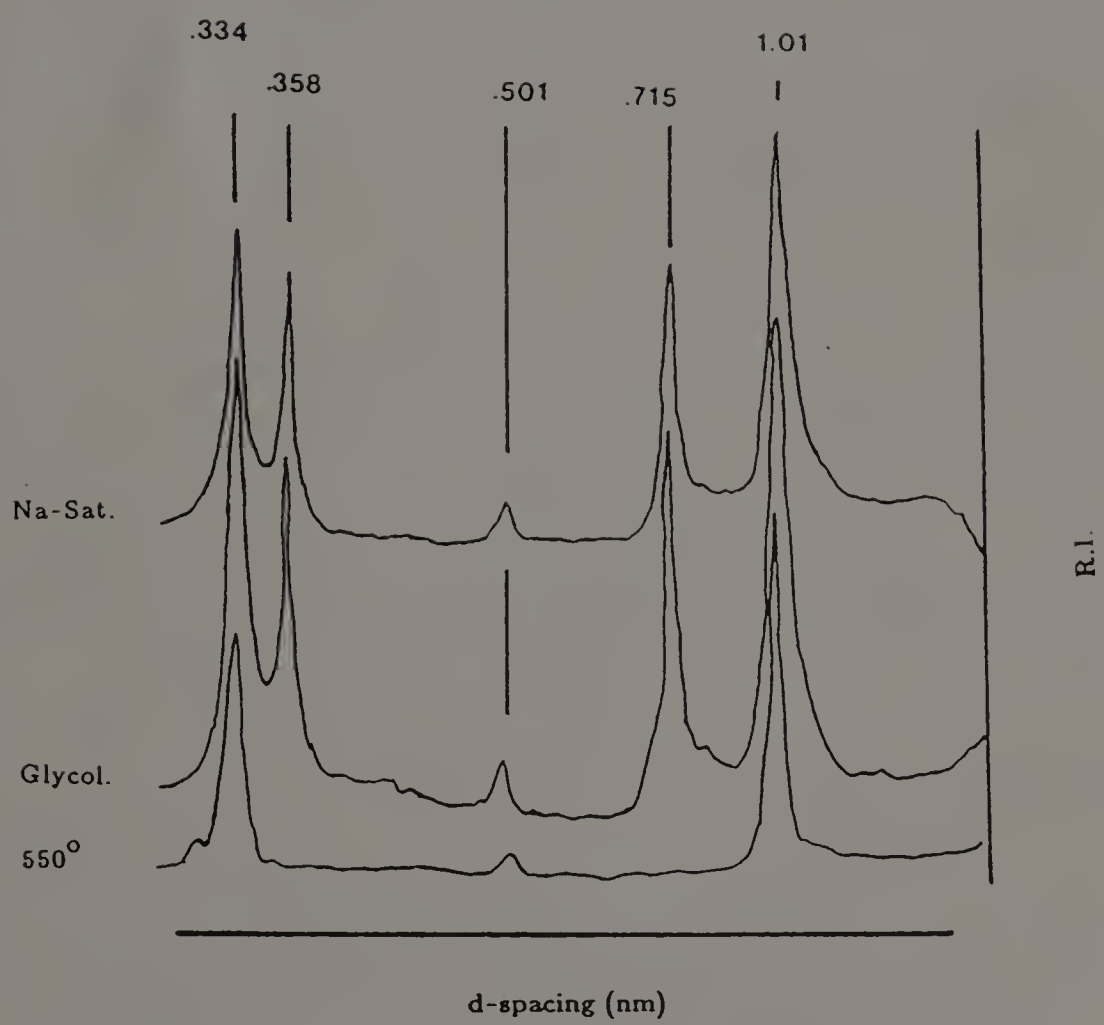


Figure 100. X-ray diffractograms by horizon of the Na-saturated <2um fraction of clay removed by Na-pyrophosphate from the EHP samples (other diffractograms are in Appendix L). 2.4 nm = mixed-layer supper lattice, 1.4 nm = chlorite and/or vermiculite, 1.21 nm = mixed-layer illite-vermiculite or illite-chloritized vermiculite, 1.0 nm = illite, .846 nm = mixed-layer d003, .715 nm = kaolinite and/or chlorite d002, .501 nm = illite d002, .485 nm = gibbsite, .426 nm = quartz, .358 nm = kaolinite d002 and/or chlorite d004, and .334 nm = illite d003 and quartz.



suggests that the clays were not as crystalline in the leachate as in situ (Appendix L).

Strength Analysis

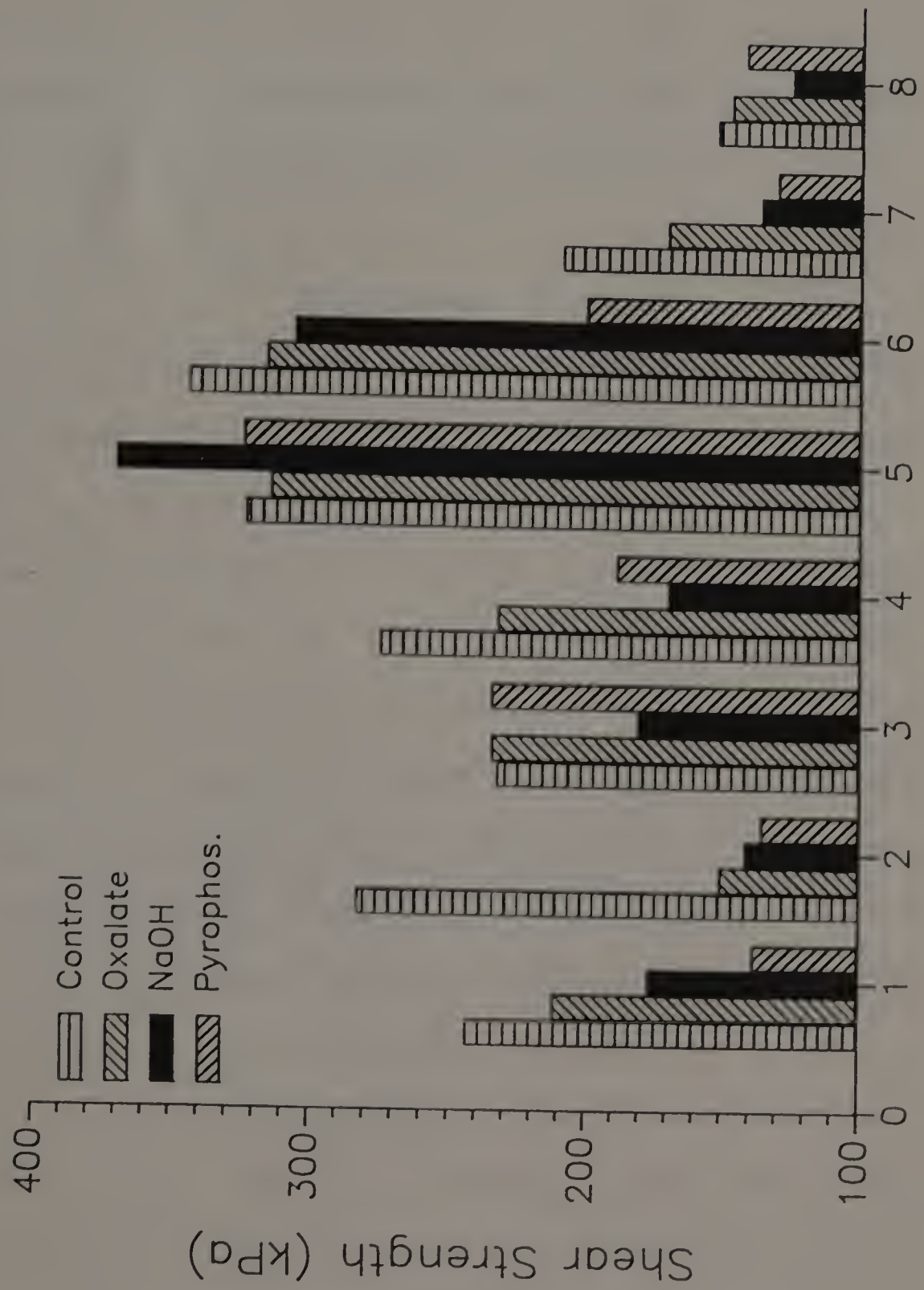
The overall means of the shear strength (Figure 101) suggest that the various extraction procedures have an effect on strength, however the means of 5 out of the 8 sets were not statistically different. Despite the lack of significant differences, the pyropohsphate and NaOH strength values were generally lowest and the control strength the highest. Correlation analysis of strength versus extracted materials indicates that Na-pyrophosphate extracted clay is best correlated with an ($r^2 = 0.601$) followed by NaOH extractable Si ($r^2 = 0.282$) (Table 28).

Table 28. Strength correlation analysis of strength to individual extractable material for all samples.

Strength versus					
	Ox-Fe	Ox-Al	NaOH-Al	NaOH-Si	Pyro-Clay
r^2	0.270	0.071	0.139	0.282	0.601

Thin sections of failed column samples were examined with a microscope and with SEM. SEM analysis indicated that both

Figure 101. Average unconfined-unconsolidated shear strength of each treatment for each site. BTR = Belchertown Ridgebury 2Btxl horizon, BTR/S = Belchertown Ridgebury/Scituate 2Btxl horizon, EHP = Elm Hill Paxton (Pedon 1) 2Btxl horizon, OHW = Orchard Hill Woodbridge (Pedon 4) 2Btxl horizon, OHD = Orchard Hill (Pedon 4) 3Cd horizon, BHW = Buck Hill Woodbridge 2Btxl horizon, BHR = Buck Hill Ridgebury 2Btxl horizon, and BHD = Buck Hill Paxton (Pedon 2) 3Cd3 horizon.



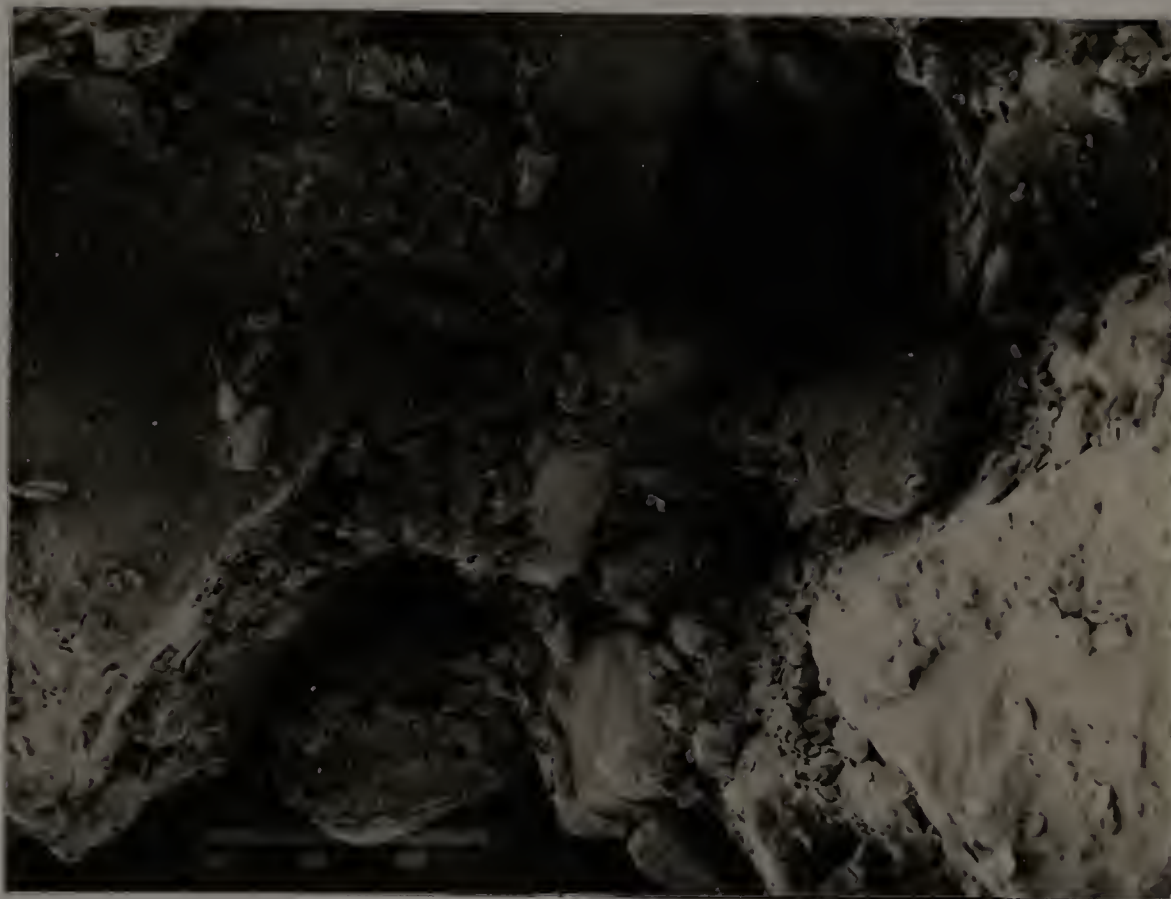


Figure 102. Scanning electron micrograph of the matrix from the CaCl_2 (control) treated column. Note the amount of fine-grained material and bridge. The bar is 100 μm long.



Figure 103. Scanning electron micrograph of the matrix from the ammonium-oxalate treated column. Note clay bridge and fine-grained material. The bar is 100 μm long.



Figure 104. Scanning electron micrograph of the matrix from the Na-pyrophosphate treated column. Note the small bridges and decreased amount of fine-grained material. The bar is 100 μm long.



Figure 105. Scanning electron micrograph of the matrix from the NaOH treated column. Note lack of fine-grained material. The bar is 100 μm long.

Unfortunately, the data suggest that dispersal was not consistent in each sample resulting in variability within and between samples.

Bonding in the soil may result from precipitation of silica (Franzmeier et al., 1989) and/or the partial dissolution and deposition of clay (Buurman and Jongmans, 1975). Such bonds were not immediately apparent when samples were observed microscopically, although the overall matrix did appear to be more open than that of the undisturbed samples. Strength reduction associated with NaOH extraction is most likely due to partial or complete destruction of Si bonds. The NaOH probably did not cause the clay to disperse as did the Na-pyrophosphate, because the ionic strength of the NaOH solution was greater. The exact nature of the bonds affected by the NaOH can only be speculated upon because no direct observations were made.

The samples of till (from Orchard Hill--OHD-- and Buck Hill--BHD) were not statistically different from the pans (Orchard Hill Woodbridge--OHW--, Buck Hill Woodbridge--BHW--, and Buck Hill Ridgebury--BHR) which developed from them. However, the tills did not exhibit a strength reduction due to the Na-pyrophosphate extraction nor much reduction due to NaOH extraction even though clay was removed by Na-pyrophosphate and Si by the NaOH extraction. This lends credence to the theory that clay and Si may stabilize the strength of the pan although the density is primarily inherited from the till (Calhoun, 1980).

Changes in strength due to removal of bonding agents are not conclusive based on statistical analysis of the data. The large amount of variability observed within a given treatment accounted for

the lack of statistical significance. This variability is caused by the nature of the material (Habecker et al., 1990) and the mode of sampling. The till samples used in the study have a high stone content making sampling difficult. It was not uncommon to remove a core only to find gravel lodged in the tube in such a way to make the core unusable. Typically, coarse fragments would be shattered if they were cut by the sampling tube also making the core unusable. It was not only this obvious disturbance that presented a problem, in some instances the core entirely surrounded a coarse fragment resulting in the cross section to be dominated not by soil but by stone. Another problem was the presence of BPF material with different strength values. Attempts were made to avoid the BPF but this was not always possible. The diameter of the core was probably too small to overcome the afore mentioned inhomogeneties within the pan. Finally, four replicates were not a statistically large enough number of samples to adequately overcome the variability of the soil, even within the same horizon.

Conclusions

Despite problems with sample size and the lack of statistical significance, the reduction in strength due to leaching with selected extractants indicates that the pan is affected by some kind of bonding agent. Removal of clay by pyrophosphate and to a lesser degree of Si by NaOH caused a reduction in strength in some samples. Both clay and Si removal appeared to cause some changes in the microstructure of the

fragipan samples suggesting that both are related to observed strength properties because similar reductions were not seen in the till samples. Presence of bonding agents in the pan supports the theory that the brittle behavior results from post-depositional processes and that the pan at least in part is pedogenic in origin. The exact process by which the bonding agents occur in the pan is unclear from the data collected in this set of experiments.

Any additional investigations along this line should use larger diameter cores and more samples should be tested to ensure that the large variability is accounted for.

UMASS/AMHERST



312066007712914

NATURE AND PROPERTIES OF FRAGIPANS IN MASSACHUSETTS

A Dissertation Presented

by

DAVID LLOYD LINDBO

Submitted to the Graduate School of the
University of Massachusetts in partial fulfillment
of the requirements for the degree of

DOCTOR OF PHILOSOPHY

May 1990

Department of Plant and Soil Science

CHAPTER X

FABRIC

Previous Work

Pebble fabric rarely has been reported in soil genesis studies but it does have a application in determining the origin of some parent materials. Snyder and Bryant (1985) used the orientation of 25 pebbles to identify colluvium as the parent material in a study of fragipans in the Salamanca re-entrant in New York. Such analysis also could be useful in the present investigation.

It has long been noted that stones in till may have a preferred orientation (Andrews, 1971b). Till fabric analysis is an outgrowth of this observation, focused on the significance of a preferred orientation and dip of clasts within the till. Ritcher (1932; 1936) was among the first to quantify and explain his findings, noting that oblong clasts are oriented parallel to ice flow. However, he also noted that some clasts appeared transverse to ice flow. Holmes (1941) expanded on these findings by taking extensive measurements of clast morphology, orientation, and dip of long and intermediate axes and postulating on how the fabrics were produced. This work remains one of the benchmark papers in till fabric analysis.

The use of till fabric analysis continued into the following decades. Emphasis shifted from using results as a descriptive tool to more process oriented studies (Hoppe, 1952; Wright, 1957; Glen et al.,

1957). As the amount of data increased, researchers developed models using till fabrics to assist in explaining depositional processes in different till types (Westgate and Dreimanis, 1967; Boulton, 1968; Cowan, 1968). Studies also concentrated on statistical interpretation of the data to determine variability between and within sites (Hill, 1968). Andrews (1971b) identified four broad fields of fabric studies; determination of regional flow direction, determination of variability, investigation of till genesis, and examination of sedimentological history of specific features. Ehlers and Stephen (1983) indicated that clast direction is the best method to understand ice movement direction.

Studies reported through the late 1960's basically agreed that the preferred orientation indicated ice movement but there were still debates regarding processes (Andrews, 1971b; Boulton, 1971). Other problems with till fabric studies included a lack of agreement on standard methods, experimental design, analysis of data, and on the effect of stone morphology (Andrews, 1971a). Methods and design criteria were outlined by Andrews (1971a; 1971b) and Derbyshire et al. (1976). These criteria seem to have been widely adopted although Lawson (1980) has indicated that in studies attempting to describe regional flow patterns it is advantageous to study small numbers of samples at many sites.

Mark (1974) discussed various statistical approaches to analysing fabric data suggesting that contoured stereo plots and eigenvalue analysis relate fabric to fabric forming processes. The plane of dip

generally was found to be up ice, and if dip was extremely shallow Mark concluded that fabric alone was insufficient to indicate direction of movement.

Stone geometry and post-depositional factors have been shown to influence fabric. Holmes (1941) and Drake (1974) concluded rod and blade shaped clasts are the best indicators of past ice movement. Drake also noted that some rods were oriented transverse to flow. Ramsden and Westgate (1971) concluded that a shift in fabric within the same till unit at different locales in Alberta, Canada was due to post-depositional, en mass reorientation of a large block of till. Recently, Lawson (1980) concluded that multimodal fabrics are indicative of post-depositional changes in orientation.

Fabric of New England Till

Fabric is yet another way in which the Upper and Lower Till have been identified (Flint, 1961; Pessl, 1966; Pessl and Schafer, 1968). Pessl and Schafer (1968) summarized the previous work on fabric indicating that the Lower Till fabric trended north-northwest (N 5-15° W) with a range from north to northwest, and the Upper Till fabric trended northeast (N 25-35° E) with a range north-northeast to east-northeast. They also reported that the fabric orientation of the Upper Till was to the northwest above the contact with the Lower Till and shifted to the northeast towards the top of the column. They explained this as a shift in ice flow during the later stages of glaciation.

Recently, Lindbo (1990) confirmed the previous studies and reported that in Massachusetts the fabric of the Lower Till trended northwest (N 25-35° W) and the Upper Till Northeast (N 25-35° E). While slight variation between sites is observed, such variation is not uncommon in till fabric studies and is easily be explained by localized topographic effects.

The origin (age) of the till in which the pans have developed has been based on their textural similarity to either the Upper (sandy) or Lower (silty) Till (Krohelski, 1976). The observation of a stone line (3Cdl in Pedon 2) and the sand and gravel horizon (3BCm in Pedon 1) forced the questioning of this previous hypothesis. In order to determine if the pan could be developed in reworked Lower Till pebble fabrics were measured and compared to fabrics establish for each till type in the region. If the pan was shown to have an Upper Till fabric it must have been reoriented during deposition. Thus soil development would comence with the retreat of the late Wisconsinan ice rather that earlier events.

Materials and Methods

Fabric measurements were taken from the 2Bx horizons at each of the pedons and from the 3Cd horizons at Pedons 2, 3, and 4. Fabric was also determined for the till sites. All analysis followed the procedures outlined by Andrews (1971b), Derbyshire et al. (1976), and Lawson (1980). Between 25 and 176 oblong clasts were measured for trend and dip at each horizon or site. Prior to making measurements a

vertical face was cleaned thus removing any disturbed samples.

Individual clasts, either rod or blade shaped, were removed from the face in a fashion that left a cast where the clast had been. A brass rod was then inserted into the cast parallel to the direction of the long axis. The trend and dip of the rod was then recorded.

Once field measurements were complete the data for each site was statistically analyzed to determine eigenvalues and plotted on contoured stereonet. Till fabrics were combined to establish a regional trend.

Results

Till

A visual inspection of the combined rose diagram for the Lower Till (Figure 106) indicates that the pebbles trend to the northwest, while that of the Upper Till suggests a northeast orientation (Figure 107). There is a slight difference between the fabric of the oxidized and unoxidized Lower Till with the oxidized facies trending slightly more northerly (Figure 108). The pebbles generally plunged to the north at all sites. The majority of the fabrics in both tills were unimodal although more polymodal fabrics were observed in the Upper Till (Figure 107).

Soil

Strength values (S1) for the majority of the fabrics are above 0.8 indicating a strong fabric (Table 29). The 3Cd1 horizon of Pedon



Figure 106. Overall fabric for the Lower Till plotted in 10° increments on an equal area rose diagram. Average trend of 600 pebbles is 335° .

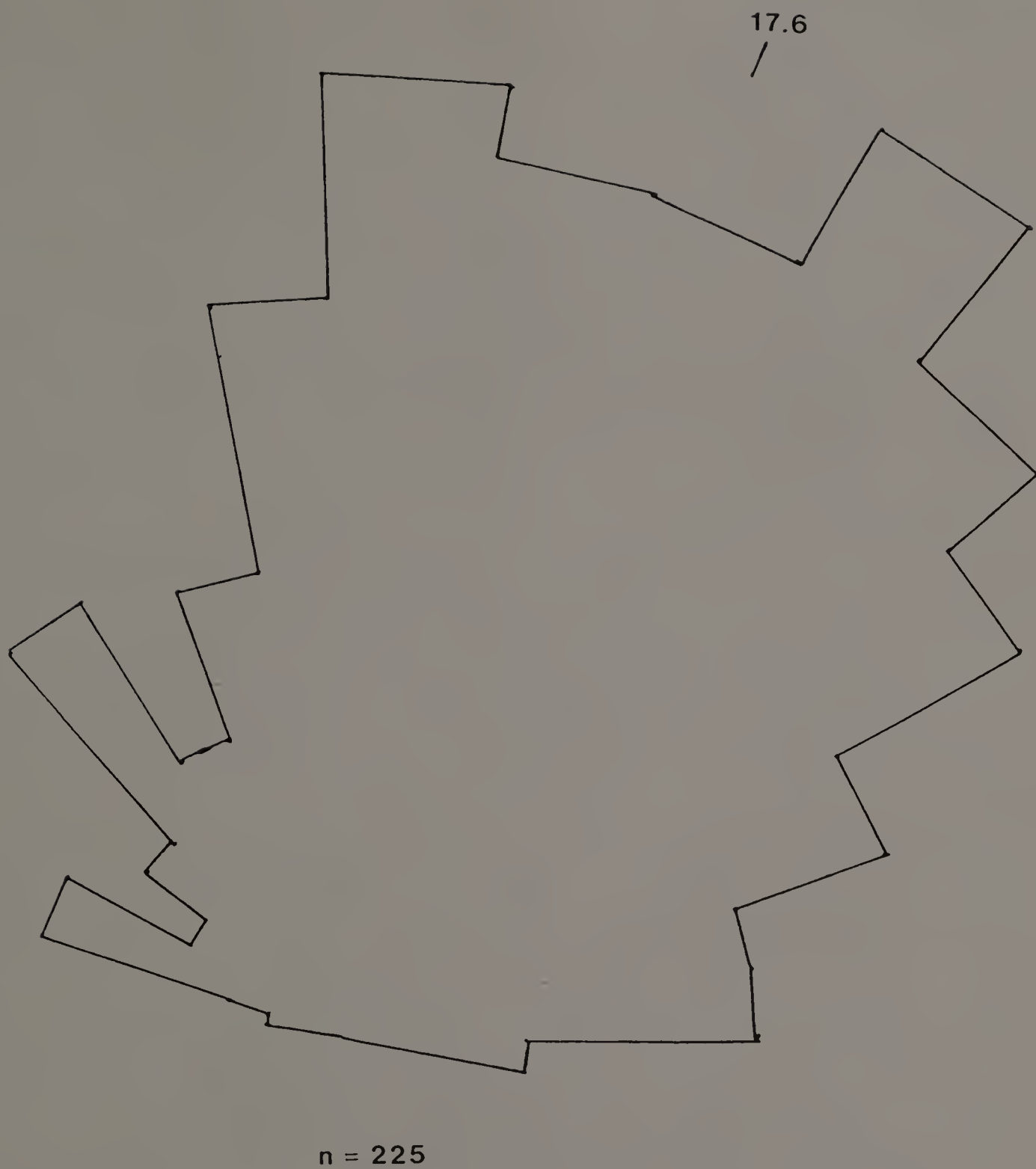
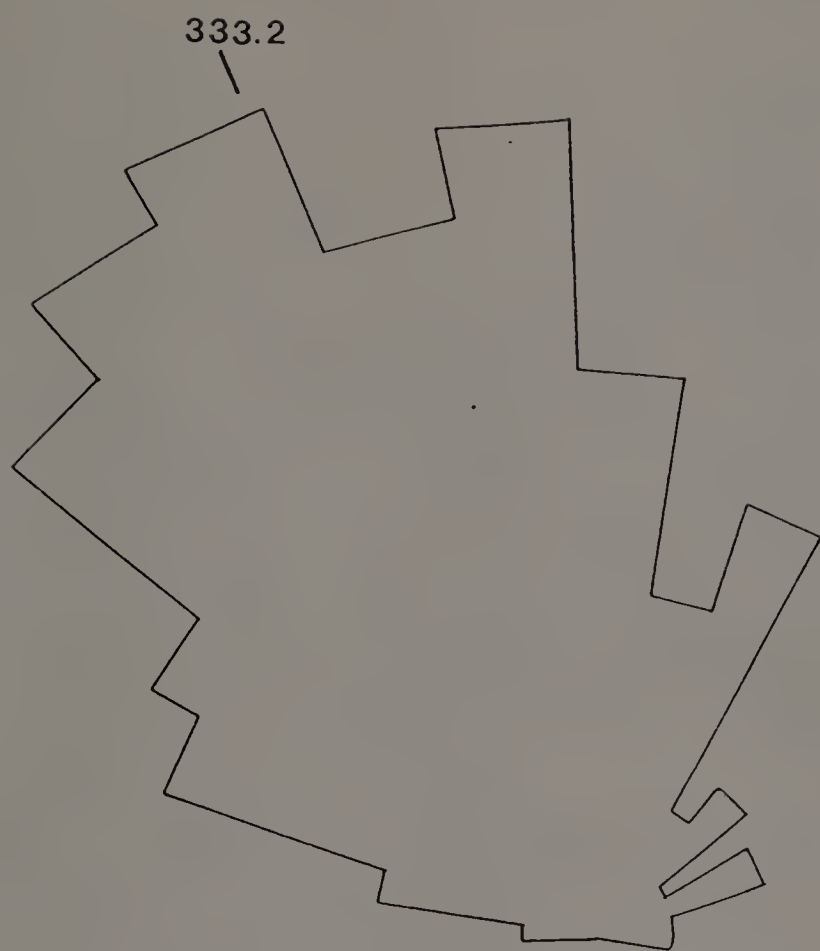
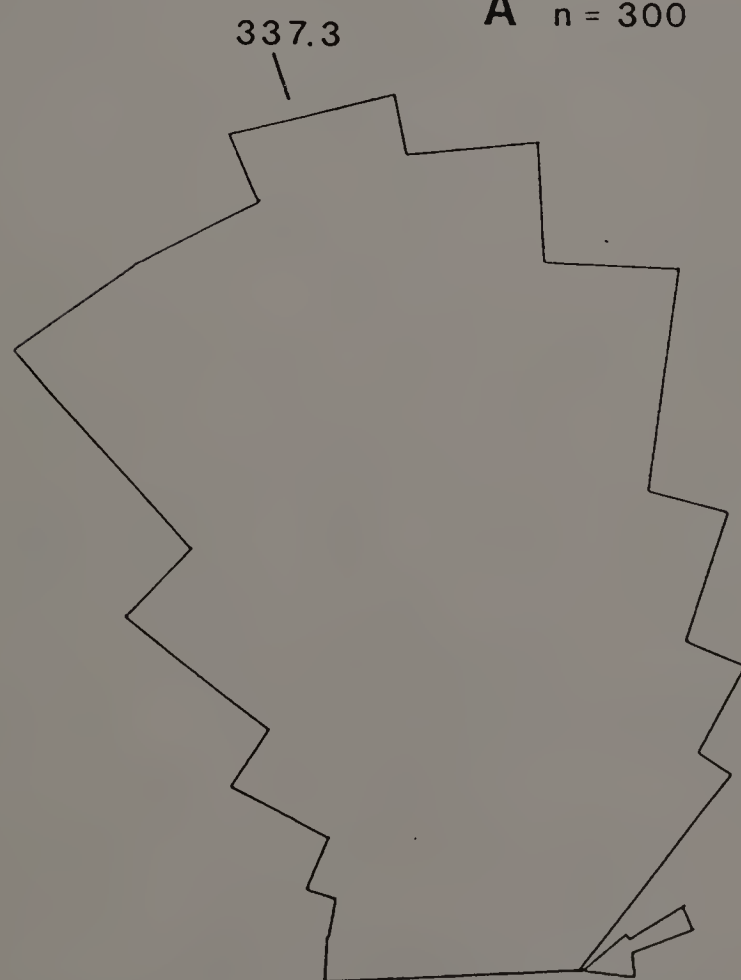


Figure 107. Overall fabric for the Upper Till plotted in 10° increments on an equal area rose diagram. Average trend of 225 pebbles is 17.6° . Note the spread of the data indicating a bimodal distribution.

Figure 108. Fabric plotted in 10^0 increments on an equal area rose diagram for A) Unoxidized facies of the Lower Till (300 pebbles), and B) Oxidized facies of the Lower Till (300 pebbles).



A n = 300



B n = 300

Table 29. Results of pebble fabric analysis of various horizons in each Pedon.

Horizon	Char.	PEDON				
		1	2	3	4	5
2Bx	V1	47.9	28.7	2.9	35.9	47.9
	S1	0.9031	0.9318	0.9305	0.8473	0.9094
	n	176	100	25	25	25
3Cd1	V1		11.1			
	S1	--	0.7283	--	--	--
	n		51			
3Cd	V1		356.9	336.0	325.7	
	S1	--	0.8174	0.8796	0.9032	--
	n		100	25	25	

V1 = Primary vector (0 = north, 180 = south)

S1 = Strength of primary vector (> 0.8 is strong)

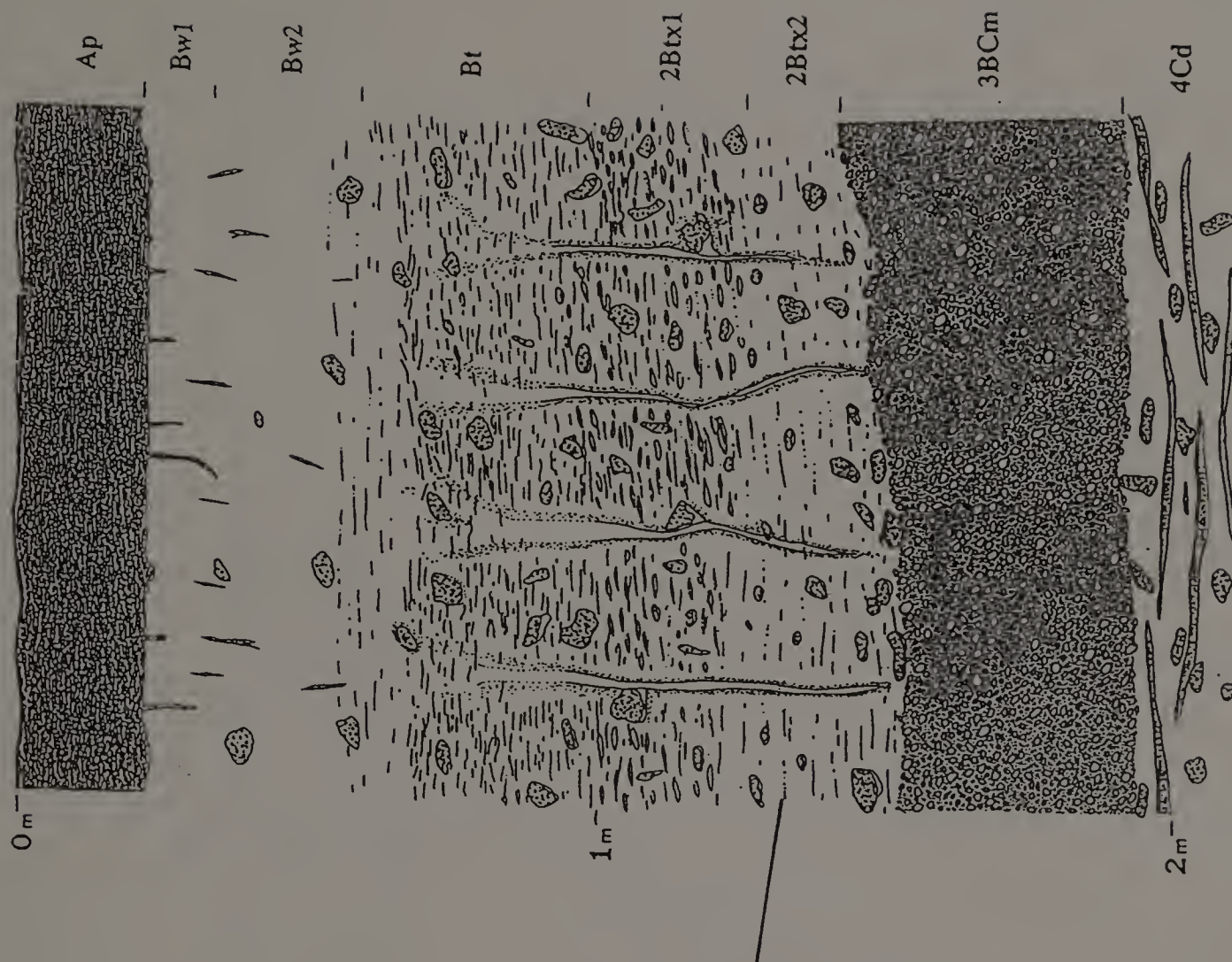
n = number of samples

2 is the only exception having a slightly weaker fabric (0.7283).

Pebble fabrics from the 2Bx horizons all trend to the east with Pedon 3 trending almost due north (Table 29 and Figures 109-113). Pedon 5 is developed in Upper Till and therefore it is expected to have a northeast trend but the other pedons are developed in Lower Till and should have a northwest trend. This is obviously not the case for the 2Bx horizons but the lower Cd horizons do have the expected northwest trend of the Lower Till (Table 29). There does not appear to be any structural or lithological discontinuity between the 2Bx horizon or

Figure 109. Fabric plotted on a contoured stereonet for Pedon

1. S_1 is the primary (strength) eigenvalue (if greater than .8, a strong fabric exists), V_1 is the primary trend, and n = number of observations.



2Btx2

$V1 = 47.9$
 $S1 = 0.9031$
 $n = 176$



Figure 110. Fabric plotted on contoured stereonet for Pedon 2. S1 is the primary (strength) eigenvalue (if greater than .8, a strong fabric exists), V1 is the primary trend, and n = number of observations.

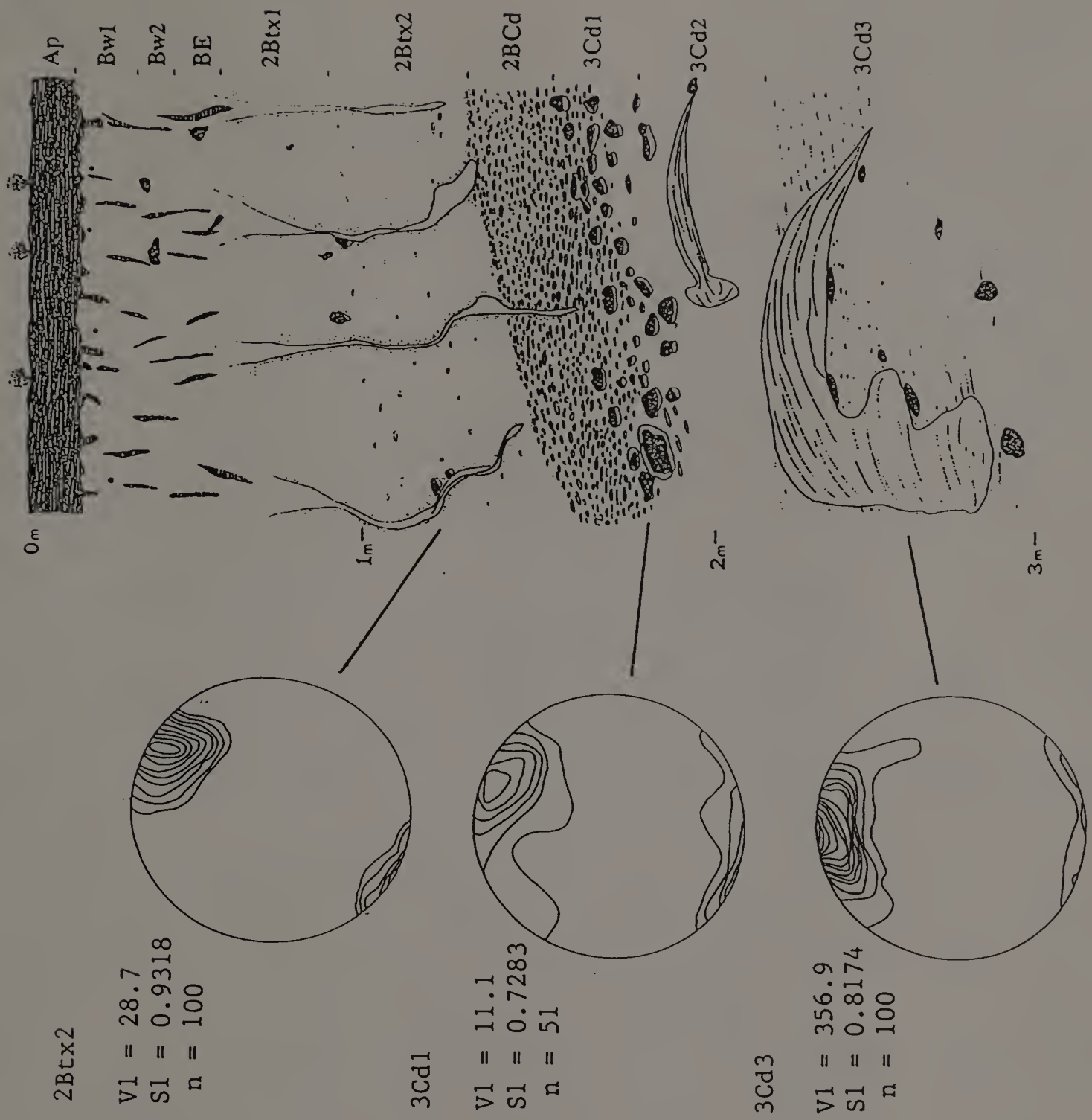
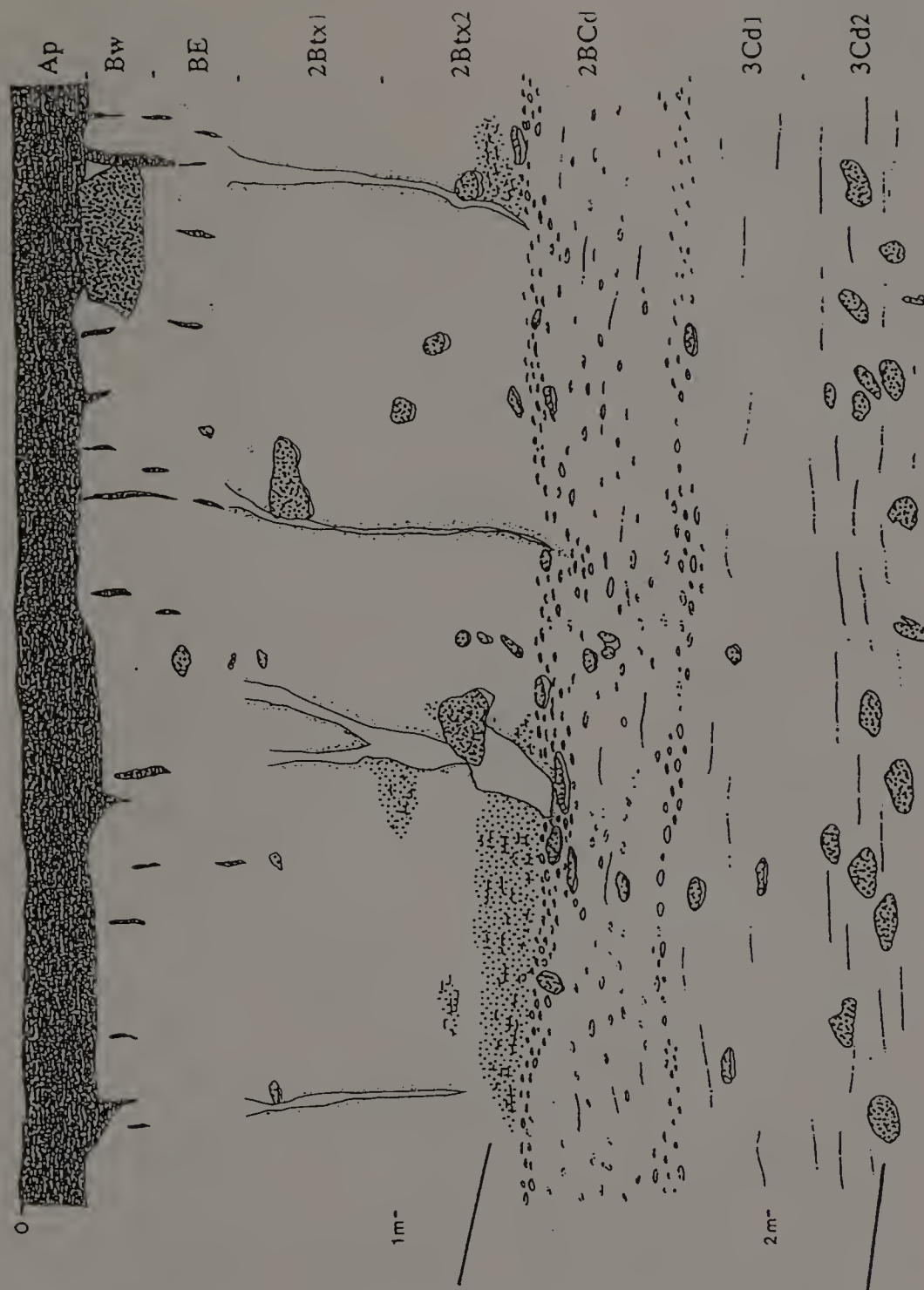
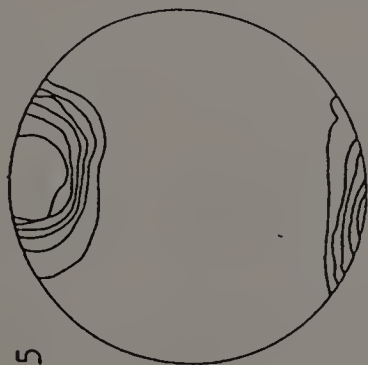


Figure 111. Fabric plotted on contoured stereonet for Pedon
3. S1 is the primary (strength) eigenvalue (if
greater than .8, a strong fabric exists), V1 is
the primary trend, and n = number of observations.



2Btx2

V1 = 2.9
S1 = 0.9305
n = 25



3Cd2

V1 = 336.0
S1 = 0.8796
n = 25

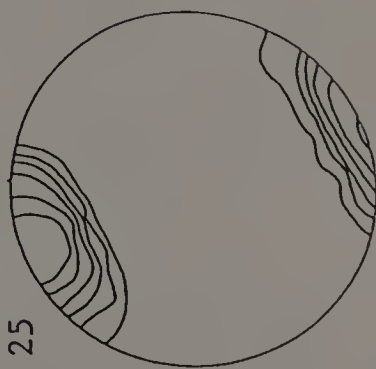
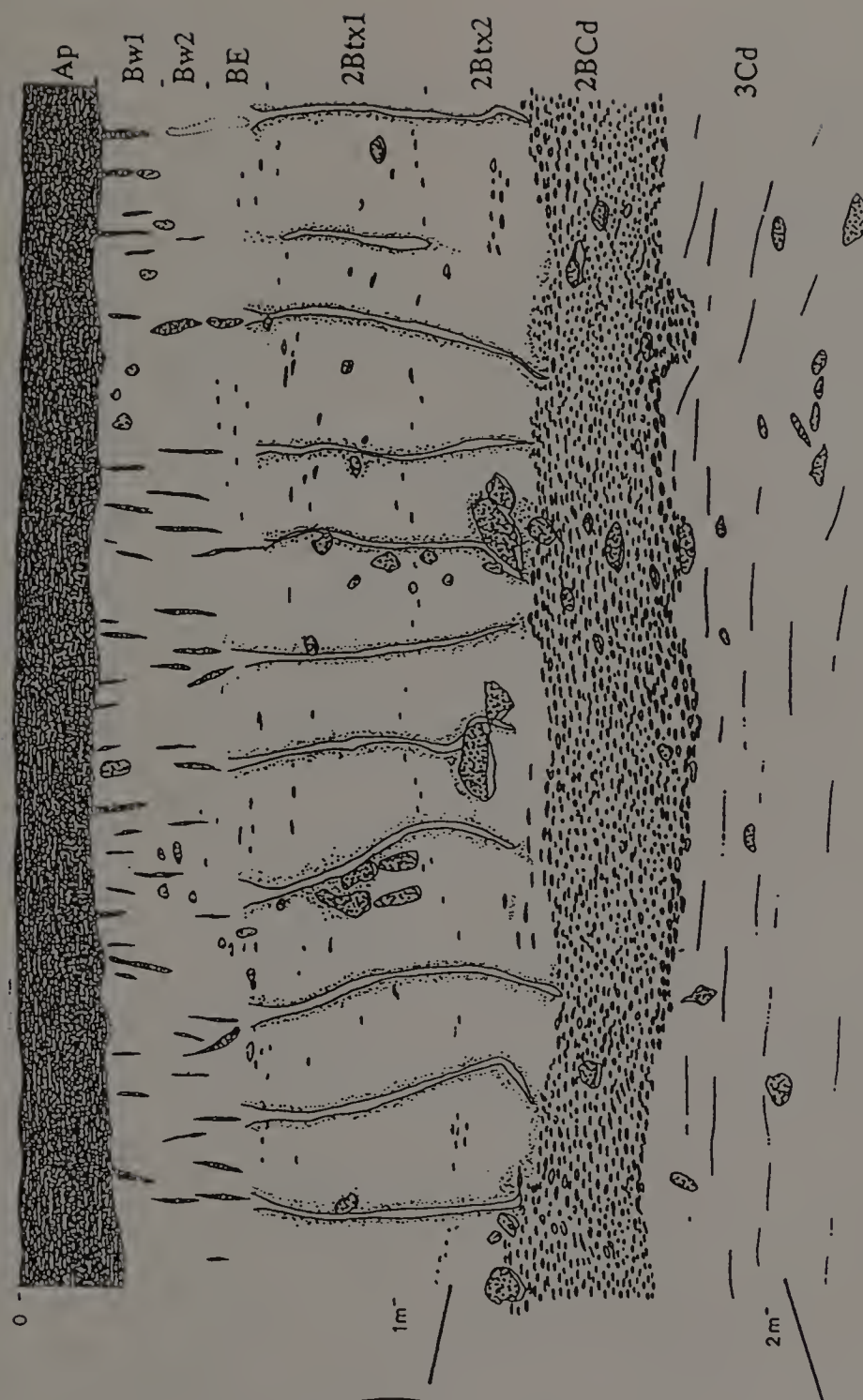
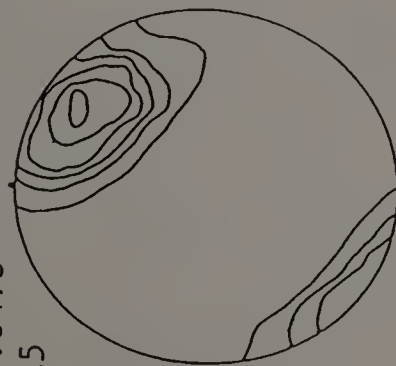


Figure 112. Fabric plotted on contoured stereonet for Pedon
4. S1 is the primary (strength) eigenvalue (if
greater than .8, a strong fabric exists), V1 is
the primary trend, and n = number of observations.



2Btx2

V1 = 35.9
S1 = 0.8473
n = 25



3Cd

V1 = 325.7
S1 = 0.9032
n = 25

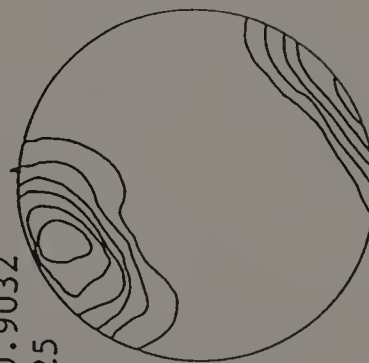
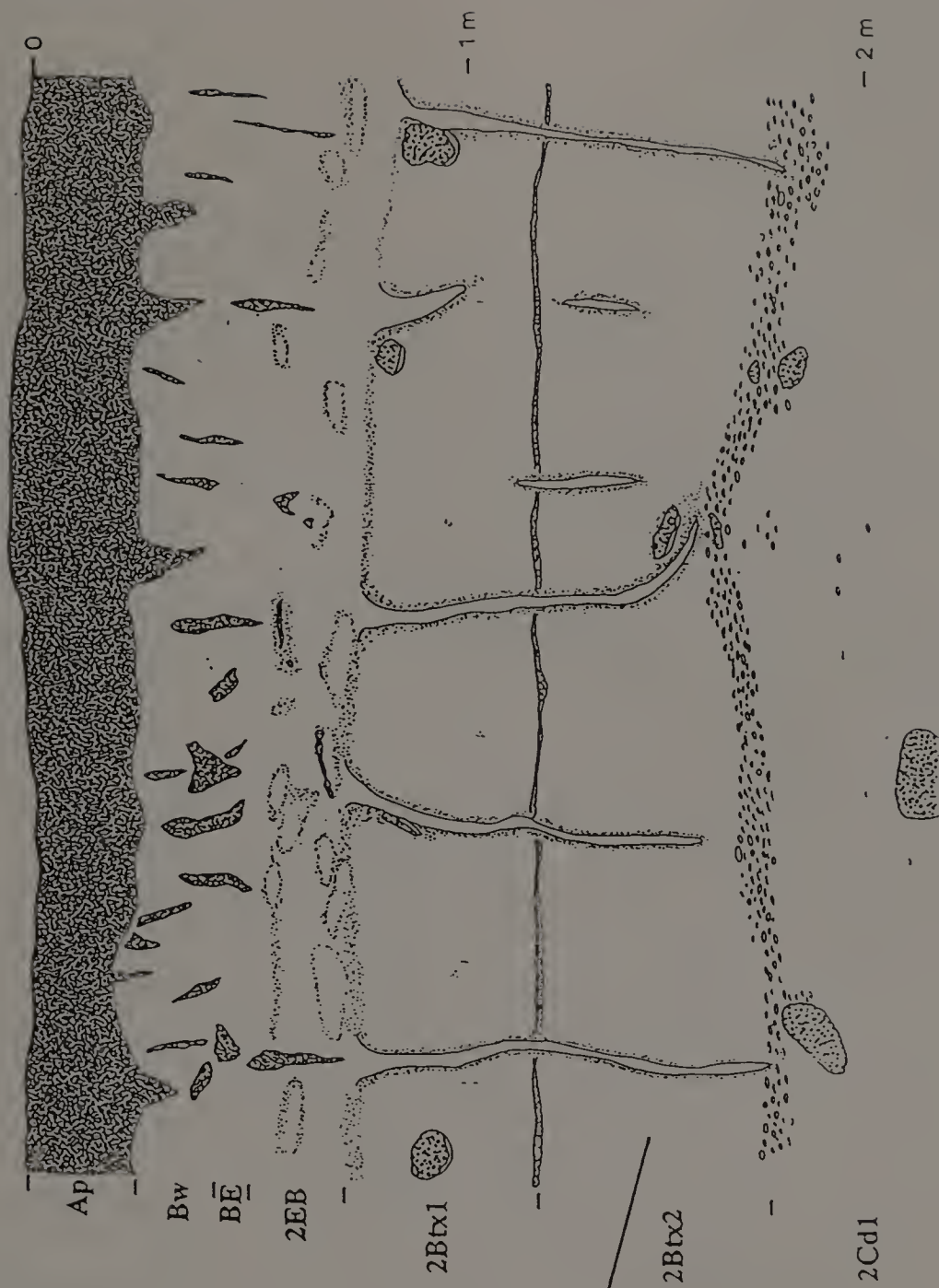
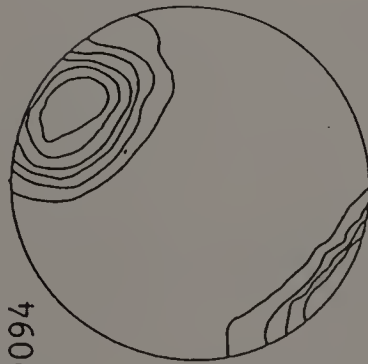


Figure 113. Fabric plotted on a contoured stereonet for Pedon 5. S1 is the primary (strength) eigenvalue (if greater than .8, a strong fabric exists), V1 is the primary trend, and n = number of observations.



2Btx2

V1 = 35.6
 S1 = 0.9094
 n = 25



the 3Cd horizons where both sets of fabric were measured in either Pedons 3 or 4. Although physical and chemical properties of Pedon 2 do suggest a gradual change from the 2Bx to 3Cd horizons a stone line (3Cdl) does occur between the pan and parent material indicating a lag deposit of some type. An abrupt change in lithology was most noticable between the pan and parent material of Pedon 1 which were separated by a cemented sand and gravel layer.

Discussion

Fabrics of Upper and Lower Till have been established by Pessl and Schafer (1968) and Lindbo (1990). The fabric of the 2Bx of Pedon 5 agrees with the fabric of the Upper Till in which it developed. This is not surprising as Pedon 5 has texture and morphology similar to that of the Upper Till. The fabrics of the 3Cd horizon of Pedons 2, 3, and 4, all presumed to be Lower Till, fit into their prescribed niche as being similar to the fabric of the Lower Till, however the 2Bx horizons do not have the same fabric. These horizons have Upper Till fabrics suggesting that they were either deposited during a shift in Illinoian (or early Wisconsinan) ice sheet direction and are therefore part of the Lower Till or deposited by the late Wisconsinan Ice Sheet and are therefore part of the Upper Till.

A shift in ice flow is the easiest explanation of the observed small shift in trend, however the change in trend recorded (30° to 70°) is too great to be attributed solely to a shift in ice. Also observed discontinuities between horizons do not support the idea of continuous deposition under shifting ice flow conditions. By default

it appears that the material composing the pans was deposited by late Wisconsinan ice making it equivalent to Upper Till, even though its physical properties are very different from the typical, sandy Upper Till of the literature. It seems likely that the pan material was incorporated locally by the late Wisconsin ice and slightly reworked thus changing the pebble orientation but not the overall mineralogy (c.f. Chapter 8), chemistry (Chapter 6), or some of the physical properties (Chapter 5). Such material has been termed deformation till (Boulton, 1987) and is envisioned to occur in a thin, mobile, highly deformable layer at the glacier sole. Under the proper interface conditions of ice to thin mobile sediments (as is the case of the pan material) it appears likely that short transport distance and/or complete erosion is possible (Menzies, 1987). Such a process accounts for the reworking of local till and its deposition it with slight modifications.

The observation of a stone line (Pedin 2) and a sand and gravel layer (Pedin 1) indicate that a surface may have been exposed prior to the deposition of the overlying pan material or at the least the material above and below the discontinuity are different in terms of deposition history (Ruhe, 1959; Birkeland, 1984). In Pedons 3 and 4 a discontinuity between the pan and the 3Cd horizons is not readily visible although the BPF end in a zone containing many mottles and a more pronounced platy structure.

The implication of the pan developing in Lower Till that has been reworked by late Wisconsinan ice is far reaching. First, the length

of time for pedogenic development is set at 15 to 17 ka. Second, if the till has been reworked enough to change the fabric no structures could have been inherited and some mineral abrasion must have occurred. Third, the micromorphic features would not be preserved during the reorientation process. Thus the observed features; BPF, mottles, and argillans must have developed since 17 ka. This suggests that the pedons studied have undergone significant pedogenic development and that all of the observed features could not be inherited from the till.

Conclusions

Fabric analysis forced a reinterpretation of the parent material and glacial history of some of the pedons. The fabric of Pedon 5 indicates that the pan is developed in Upper Till as its morphology and physical properties suggest. The fabrics of the other primary pedons were more difficult to explain. Prior to the analysis of fabric it was assumed that the loamy pans were developed in Lower Till but the fabric analysis suggests a different possibility. In all instances the fabrics in the pan indicated that the material was deposited or at least modified by late Wisconsinan ice, whereas the 3Cd horizons suggested deposition by Illinoian ice. The most likely explanation for the observed fabrics is that the pan material was deposited as a thin deformation till derived from the local loamy Lower Till. The source for the pan material must have been local as the heavy mineral assemblage in the pan is not different from that in the 3Cd horizons.

This interpretation of the age and mode of deposition of the pan implies that the features observed must have developed in the last 17 ka and could not be entirely inherited from the Lower (Illinoian) Till or interstadial weathering. Significant pedogenesis appears to have occurred within the pans, further indicating that these pans should be considered to be pedogenically derived.

CHAPTER XI

FORMATION AND CLASSIFICATION

Previous Work

Mode of Formation

General. Even after four decades of fragipan research the exact mode of formation in tills is still unclear. It may be possible that several different processes produce a similar end product, the fragipan. Understanding the genesis of fragipans is critical to an understanding of its inherent properties and to the development of appropriate diagnostic taxonomic criteria. Theories for fragipan formation can be broken down into 5 broad groups: 1) Inherited properties; 2) Relict or buried features; 3) Periglacial or permafrost features; 4) Pedogenically derived features; and 5) Self weight collapse and dessication. Undoubtably there is overlap between these theories but each has been envoked to explain the characteristics associated with a fragipan.

Any theory must be able to explain some if not all of the features associated with a pan. Smalley and Davin (1982) selected four features as the most critical ones to be explained by any theory. First is the consistancy of the pan, that is both its brittle and hard nature. Second is its close packed structure or, as Franzmeier et al. (1989) pointed out, more correctly, its high bulk density. Third, the

horizon is relatively impervious and drains slowly. Finally, the fourth feature is the polygonal structure commonly associated with the overall pan morphology.

Inherited Properties. The degree to which properties of a fragipan are inherited is the crux for the on-going debate over the geogenic versus pedogenic origin of fragipans (Calhoun, 1980). In instances where the pans have developed in glacial tills the high bulk densities and platy structure has been attributed to compaction of the overriding ice mass. Investigations of recently exposed, previously overridden till in Iceland have shown that the till has some of the physical properties associated with fragipans (Boulton and Dent, 1974). Till is not the only parent material that has been shown to impart a high bulk density to the pan. Norton and Franzmeier (1978) found that lower loess in which pans commonly are developed, had a slightly higher bulk density than the upper loess. While this could be interpreted that the bulk density was inherited from the lower loess, the firmness in the loess represented only weak development when compared to the pan. Thus a material having a high bulk density may not have other properties associated with fragipans.

Problems do exist with the theory that pans are inherited features. If the compaction by ice was the sole process causing high bulk density than the pan horizons should be no denser than underlying horizons. Grossman (1954) observed that some pans in glacial till in New York had a slightly higher bulk density than the underlying till suggesting that the density in the pan was not due solely to the

compaction of overlying ice. Also, within the glaciated terrain of the Northeast, Hanna et al. (1975) observed that many fragipans were developed in congeliturbate (colluvium) derived from glacial till. Pans developed in this material were similar to those developed in till, however, it is unlikely that the high densities present in the congeliturbate could be inherited from the weight of the ice since it was never overridden. They concluded therefore, that the pans had a pedogenic origin.

A recent paper by Gustavson and Boothroyd (1987) indicated that till may be totally saturated when deposited. If the till is in this condition then the density must be imparted after the water drains--exposure to the air--and pedogenesis begins. Other descriptions of till indicate that not all till is deposited under direct glacial pressure and the high bulk density associated with till may be due to processes other than ice pressure.

While it is likely that density and associated low permeability could be inherited from the parent material other features could not. In particular the BPF can not easily be explained as being inherited from the parent material. A case can be made, however, that such features are formed by permafrost or under periglacial conditions rather than by pedogenic processes. This theory will be discussed in a following section.

At best some of the density and permeability could be inherited, while other features are not. A wholly geogenic origin for fragipans is not entirely feasible.

Relict or Buried Soil. This theory suggests that the pan formed in an earlier weathering cycle and is unrelated to the present one. Nikiforoff (1955) may have been the first to suggest this mode of formation, suggesting that the burial of the pan by loess or some other rapid burial mechanism would preserve its features. Present weathering (pedogenesis) could be expected to translocate clay and other materials but would not significantly alter the pan.

This theory does not explain how the pan formed in the first place, thus it adds little to our understanding of fragipan genesis. Also the theory fails because not all pans are covered by loess or some other material. If pans were formed via this process the depth to the pan should be variable due to the type of material and the process involved in the burial of the original pan. The depth to the pan is consistent (80 to 120 cm), and the pan is usually parallel to the surface. Also Norton and Franzmeier (1978) have observed that the pan may cut across stratigraphic boundaries. These observations do not support the concept of a pan being a buried horizon.

Periglacial or Permafrost. In parts of Europe and the UK fragipans are directly correlated to the occurrence of permafrost during the late Pleistocene (Fitzpatrick, 1956; 1987; van Vliet and Langhor, 1981; van Vliet-Lanoe, 1985). The BPF show a strong resemblance to ice wedges and other features associated with a periglacial environment and the products of ice lens formation are similar to those observed in a fragipan. Van Vliet and Langhor (1981) attribute the coarse prismatic structure (BPF) of fragipans to the

defrosting and dessication processes. The increased density in the pan is formed in a similar way as the growth of ice wedges compacts the remaining soil. Ice lenses account for the platy sub-structures (Fitzpatrick, 1987). Thus both macro- and some meso-features in a fragipan can be explained by periglacial processes (Habecker et al., 1990).

This theory explains most of the features associated with fragipans, the major objection being that pans are found in areas well outside the limits of periglacial activity, particularly in the southern United States. The permafrost theory can not be ruled out entirely as it does explain fragipan morphology within areas that could have been in a periglacial environment.

Pedogenic Formation. This theory assumes that fragipans are pedogenic in origin and are continuing to form. In general, researchers ascribing to this theory look for the evidence of translocated material accumulating in the pan and attempt to correlate the strength of the pan to some bonding agent. Clay bridging, amorphous to weakly crystalline Fe, Mn, Al, and Si and H-bonding have all been used to explain the brittle behavior of the pan (c.f. Chapter 9).

Fragipans show a relatively small but significant increase in clay content with associated argillans indicating illuviation of clay. Grossman and Cline (1957) suggested that clay acting as a bridge between silt and sand grains was the main cause of the brittle nature of the pan. This theory has been supported by many since it was proposed (Knox, 1959; Wang et al., 1974; Yassoglou and Whiteside, 1960; Veneman and Bodine, 1982; DeKimpe et al., 1972; Hutcheson and

Bailey, 1964; Buurman and Jongmans, 1975; Payton, 1980). Buurman and Jongmans (1975) suggested that clay movement by water followed by evaporation (or removal by transpiration) at lower depths in the horizons (in the pan), concentrated the clay between and around larger grains forming a bridge.

Amorphous oxides of Fe, Al, and Mn may also contribute to the fragile character of some horizons (Anderson and White, 1958; Nettleton et al., 1968b; Steele et al., 1969; Grossman et al., 1959c; McCabe et al., 1978; Matthews, 1976; Horn and Rutledge, 1965), although the presence of amorphous Fe, Al, and Mn oxides and hydroxides may be related more to the high clay content in the pan rather than to actual bonding (Harlan et al., 1977). Well crystallized Fe and Al oxides or hydrous oxides are not very likely cementing agents, as the fragipan material slakes in water, losing its brittleness when moistened (Anderson and White, 1959; Soil Survey Staff, 1975). Also Fe is mobile when reduced, therefore it is unlikely that it could act as a cement in poorly drained soils under reducing conditions (Franzmeier et al., 1989).

Silicon has been found in sodium-hydroxide (NaOH) extracts of fragipan material and in natural pore fluids and therefore can be considered as contributing to the bonding, possibly in the form of weakly crystalline silicate clay or as an amorphous compound (Norton et al., 1984; Steinhardt et al., 1982; Steinhardt and Franzmeier, 1979; Franzmeier et al., 1978; Harlan et al., 1977; Norton and Franzmeier, 1978; Karathanasis, 1987a; 1987b; 1989; Franzmeier et al.,

1989; Smeck et al., 1989). Thus a silica rich precipitate contributes significantly to the brittleness in fragipans, especially those developed in loess (Franzmeier et al., 1978, Harlan et al., 1977, Norton and Franzmeier, 1978; Steinhardt and Franzmeier, 1979; Hallmark and Smeck, 1979a and 1979b; Karathanasis, 1987a; 1987b; 1989). The process by which this occurs (c. f. Franzmeier et al., 1989) is similar to that described by Buurman and Jongmans (1975) for clay bonding.

All the mechanisms for bonding rely on the translocation and concentration of material in the pan to explain strength and density but do not explain morphology completely. The theories assume that BPF formation occurs along weak cracks in the pan caused by some undefined process. These fractures are subsequently altered as water flows through and roots penetrate. Thus the initial processes by which the BPF form are not as important as their present morphology explained by pedogenic formation.

Self Weight Collapse and Dessication. Dessication or physical ripening has been suggested as the principal cause of fragipan development, accounting for the translocation of clay and possibly of silt, and for the subsequent increase in density and brittleness observed to accompany polygon formation (Daniels et al., 1966; Yassoglou and Whiteside, 1960; Nettleton et al., 1968b; Jha and Cline, 1963; Boulton and Paul, 1976; Bryant, 1989). The rearrangement of particles by desiccation could indeed alter the character of the pan, yet extreme wetting and drying may not have occurred to a sufficient extent in all soils with fragipans. Ranney et al. (1975)

reported that crack fillings in Pennsylvanian fragipans seemed more related to the overlying materials than to the pan. This led them to the conclusion that the pan had undergone extreme dessication resulting in the infilling of cracks with material from above.

Numerous investigators have attempted to ascertain the effectiveness of synthetic ripening on bulk density. Fritton (Fritton and Olson, 1972; Fritton et al., 1983) showed that the high density of a fragipan developed in glacial till was reestablished in a period of < 10 years after total disturbance. Krohelski (1976) and Bryant (1989) indicated that synthetically laboratory ripened pan material attained essentially the same bulk density as observed in the field. Krohelski (1976) also indicated that lab ripened material had the same brittleness associated with the original pan.

Another aspect of this theory is that the upper portion of a dessicated sediment would most likely be exposed to numerous wet-dry cycles causing it to show a maximum densification with a decrease in lower horizons. Fragipans commonly are denser than the material that underlies them, thus fitting in with this theory.

Handy (1973) describes a possible mechanism for the rapid consolidation of water saturated loess, resulting in instant densification of the soil. Wet sediment collapses as water is rapidly removed causing an immediate increase in density and a volume reduction. The same principles may apply to the consolidation of saturated till deposits, resulting in relatively small cracks upon drying of the sediment. Based on morphological observations, the

polygons in pedogenically affected tills probably are not only the result of ice wedging but were formed when cracks developed initially due to desiccation. This allowed roots to enter the dense subsoil widening the cracks and creating a preferential flow path for percolating soil water (Dabney and Selim, 1987).

How does the bonding occur? The dessication theory does not fully address this question. One can assume however that bonding occurs by other pedogenic processes which dominate formation after the initial collapse or densification of the sediment. Therefore densification occurs in the early stages of soil formation and bonding occurs later (or at a steady rate throughout formation).

Each theory has its merits but not one stands alone in explaining all the properties of all pans. Modes of formation most applicable to the pans in the glaciated Northeast are the permafrost, pedogenic, and dessication theories. A combination of the processes involved in each of these theories can account for fragipan genesis. It is also likely that not all processes occur equally within a given pan depending on its parent material, topographic position, and its location.

Mode of Formation in Glacial Till

In much of the Northeast, Midwest, and maritime provinces of Canada fragipans or fragipan like horizons have developed in Wisconsinan till. Much of the till is acid (low CaCO_3) and has a high initial density. The high density of the parent material makes the fragipans appear to be inherited features rather than formed post-

depositionally. However, examination of the pans formed in till suggests a significant pedogenic origin.

Fragipans have been found to coincide with or occur directly underneath argillic horizons (Antoine, 1970; Miller et al., 1971a; 1971b; Wang, 1971) or form in bisequal soils with an Ex horizon separating the pan from an overlying spodic or argillic horizon (Olson and Hole, 1968; Miller et al., 1971a; 1971b). Fragipans have also been reported to simply underlie an E horizon or material similar to one (Grossman and Cline, 1957; Lyford et al., 1963). The sequence of horizons observed in till derived pans (till-pans) is similar to pans derived in non-glacially derived material (c.f. Smith and Daniels, 1989), although not all till derived pans have been described as having E or Ex horizons.

Researchers do not agree which material within the till-pans is responsible for the observed strength and brittle behavior. Clay forming bridges between grains, as well as an increase in the coarse clay content has been observed in till-pans from Minnesota to New England and parts of Canada (Knox, 1957; Lyford et al., 1963; Antoine, 1971; Wang, 1971; Wang et al., 1974). Closer to the glacial margins in the Midwest the brittle behavior of the till-pans appears to be caused by the precipitation of amorphous Al and Si at contact points between grains (Hallmark and Smeck, 1979a). Interestingly, pans do not form in high-lime or calcareous till. Wang (1971) postulated that in order for a pan to form in calcareous till the lime must first be totally leached away. Once this has occurred, the soil develops along

the same pathway as its low-lime counter part. Such an observation further strengthens the pedogenic origin of till-pans.

Mode of Formation of the Fragipans Investigated

Establishing the mode of formation for a fragipan soil is complicated due to the numerous pathways that can be followed all of which may result in the formation of a fragipan or fragipan-like horizon. The starting point for the development of the pedons investigated appears to be the same. The fabric data in the 2Bx horizons of the loamy pans (Pedons 1-4) suggests that the till parent material possibly is oxidized Lower Till reworked and redeposited by the late Wisconsinan ice sheet. This gives all five pedons an approximate age of 15 to 17 ka.

Once the age of the soil has been established the amount or degree of inherited features must be discussed. There is little doubt that some of the observed high density is directly inherited from the till parent material. The tills have a density ranging from 1.77 to 2.20 Mg M⁻³ (Lindbo, 1990), and the density of the pans falls within this range. It is, however, noteworthy that the pan commonly has a density above that of the till that directly underlies it. The consistency of deep till samples a few to tens of meters below the surface is extremely hard, but the samples do not appear to have the same brittle behavior as the pan. These deep till samples do not slake in water as readily as pan samples. The till directly below the pan, especially the oxidized Lower Till, is slightly more friable.

This friability may be due to its platy nature which could be inherited from an earlier weathering cycle. The sandy Upper Till does not exhibit the platy character as strongly.

Whereas the density and the platy character may be inherited other features are not. Argillans are delicate and it is unlikely that they would survive the forces needed to reorient the pebbles in the oxidized Lower Till. Some argillans are found in the till, both Upper and oxidized Lower, but these are thin and poorly developed in comparison to those seen in the pans and above. While most argillans are not likely to survive transport and deposition of the till, grain argillans could be formed during transport as fine grained material is plastered onto coarse fragments.

Although a convincing argument is made for why most argillans are not inherited features their presence must be placed into a genetic context. The dense and nearly impermeable nature of the pan makes the presence of argillans within the matrix difficult to explain by illuvation or lessivage. In these instances the argillans have two likely origins. Immediately after deposition, the till was probably saturated or at least had a high water content. Rapid draining and dessication would cause not only a consolidation of the material but would also result in some reorganization of the fine grained material including clay. Given a high water content, the clay could move during dewatering eventually clogging pores and vesicles, coating surfaces, and bridging some larger grains. This process could be renewed during repetitive wet-dry cycles resulting in argillans deep within the matrix of the pan. The model of clay bridging proposed by

Buurman and Jongmans (1975) may occur as well within the matrix of the pan. It is probably more active in Pedons 4 and 5 which are wetter than the other pedons. As the afore mentioned processes are proceeding, clay could also be moved into the pan from the overlying horizons. The major pathways for water movement occur along ped faces as well as through the BPF. Commonly the ped faces adjacent to the BPF have strongly developed argillans and secondary ped faces have slightly less well developed ones. The continual movement of water through the BPF apparently keeps them fairly clear of illuviated clay, although the clay mineralogy does indicate that some illuviation does occur.

Illuviation of clay into the BPF and the pan is only one indication of pedogenic alteration of clay. All the pedons show a more weathered clay mineral assemblage in the pan than in the till beneath the pan. A comparison of the initial clay mineral assemblage represented by till samples taken far below the soil surface (c.f. Newton, 1978; Lindbo, 1990) to the assemblage within the pan clearly indicates alteration of the clays in the till. Undoubtably, some clay minerals are inherited, but these would act as a starting point for continued alteration during the Holocene weathering as suggested by Bodine (1986).

The most distinctive morphological feature of fragipans are the BPF. These are common to all the pedons discussed in the present study. As with the fragipan as a whole the genesis of the BPF takes on multiple pathways and processes. The Lower Till, and to a lesser

extent the Upper Till, typically is jointed both horizontally and vertically. The vertical joints are exploited by water to by-pass the denser, less permeable till, resulting in some preferential leaching along the joints. As soil development continued and vegetation is established, tree roots follow the established joints. The influx of organic material results in a reducing environment leading to the grey color of the BPF. The ferrans typical to the outer edges of the BPF form as the reduced water in the BPF interacts with the more oxidized matrix causing the precipitation of iron oxides and hydroxides. This later stage of development of the BPF morphology occurs regardless of how the initial joints or cracks form.

Another explanation for the formation of the BPF is that they formed during initial dessication of the wet till. A qualitative experiment was conducted in the lab where a slury of pan material from Pedon 5 was allowed to drain rapidly and dessicate at room temperature and at a temperature below freezing. The sample at room temperature developed a 1-cm wide crack at the top which rapidly tapered out, while the frozen sample developed a much thinner crack. Subsequent to dessication the samples were thin sectioned (c.f. Chapter 5 for procedure). Cursory examination indicated numerous vesicles and a dense matrix. The rapid formation of the cracks suggests that physical ripening, self weight collapse, and dessication are all important processes in forming the BPF and some of the typical fragipan morphology. However the initial development of the cracks must be followed by the illuviation/eluviation processes mentioned above.

The frozen sample was not as well fractured as the unfrozen one but that does not rule out periglacial processes as acting on the pan material. Indeed there are features within the pan and non-pan till such as a lenticular structures and siltcaps (Fitzpatrick, 1987; E. A. Fitzpatrick, personal communication, 1988) that indicate a periglacial environment existed after the ice sheet receded. Despite a passing similarity between ice wedges and the BPF it is felt that the BPF are too narrow and do not contain material typical of an ice wedge pseudomorph (J. Brigham-Grette, personal communication, 1987). Some of the features in the pans are influenced by freeze-thaw or periglacial conditions, however, such influences are of less importance than physical ripening and subsequent illuviation/eluviation processes.

Other morphologic features common to the pan and adjacent horizons are numerous mottles of varying types and degrees. Most of these are indicative of redox conditions--low chroma indicating more reduced conditions--while others relate to the formation of the pan and soil as a whole. The type 2 mottles common in the 2BCd horizons below the pan suggest localized water saturation and reducing conditions for part of the year. This may be due to ground water or water which flows through the BPF only to be slowed or perched in the 2BCd horizons. If the water is poorly oxygenated localized reduction in the vicinity of joints and other voids occurs, causing Fe to be mobilized. The Fe when exposed to a slightly more aerobic environment precipitates forming a quassiferran around the low chroma mottle. Only pedogenic processes could account for these features.

The BE or E like material (albans and skeletans) found above the pan are likely caused by the perching of water above the pan and the subsequent lateral movement of water across the pan. Although some water and dissolved or suspended material does move into the pan via the BPF and other channels lateral movement is more common, as indicated by higher horizontal than vertical conductivity (Reed, 1989). Also the degree of expression of the eluvial zone depends on the location of the soil on the slope with mid and downslope positions (Pedons 2, 4, and 5) having a better expressed BE than the upslope or summit positions (Pedons 1 and 3).

The brittleness of the pan is best explained by a combination of processes. The data regarding the strength of the pan suggests the effect of clay and Si. As previously mentioned, clay bridging is formed during initial dessication of the material. The Si bonding most likely occurred in later stages of soil development, possibly following the processes described by Franzmeier et al. (1989). This process could also account for bonds formed by other elements as well.

It is apparent that many processes have contributed to the genesis of the fragipan soils investigated (Figure 114). If the till was deposited with a low initial water content, it most likely had a high bulk density and a platy or fissile character. Under these conditions joints due to shearing may also have occurred. However, it is more plausible that the till was deposited wet, and upon exposure drained, collapsed, compacted, and/or dessicated depending on local conditions. During this early stage of soil development cracks due to

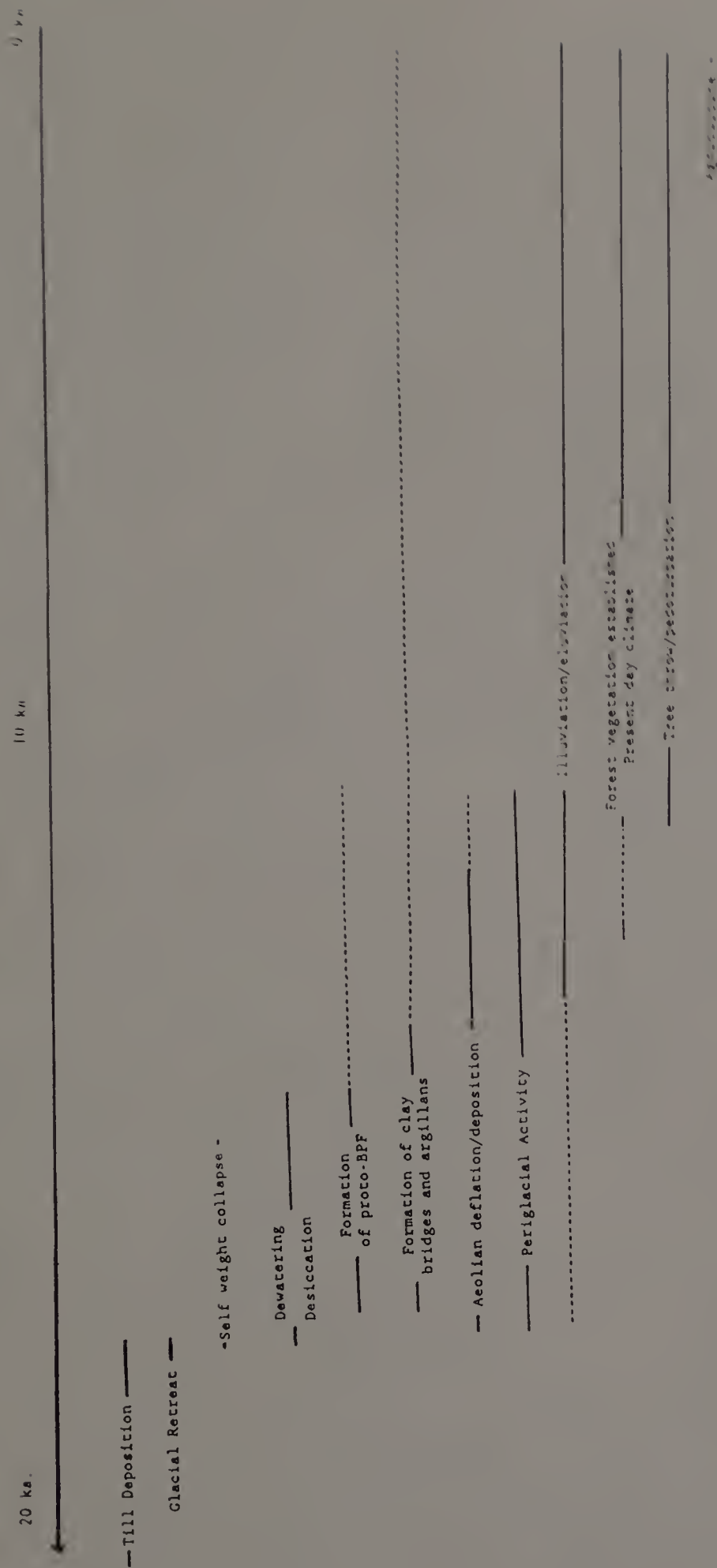


Figure 114. Schematic illustrating the possible mode of formation of the fragipans investigated in the present study

desiccation form. These cracks were the proto-BPF and became conduits for renewed water movement. Also during initial dewatering some matrix reorientation is likely, resulting in the formation of clay bridges and other argillans. The afore mentioned processes occur rapidly upon exposure. As the exposed surfaces dry they become susceptible to wind action which initially deflates the surface. Eventually the aeolian material begins to accumulate and as the surfaces become stabilized the amount of aeolian deposition subsides. A periglacial climate may have existed during this period resulting in some cryoturbation of the till, incorporation of aeolian components, silt cap formation, and lenticular structures appearing in the upper till surfaces. Illuviation and eluviation were proceeding during this time, becoming the dominant soil forming processes as the climate ameliorated. Clay translocation into the pan was due primarily to lessivage and continues into the present. The development of the typical BPF morphology, while begun during the initial dessication of the till was enhanced as roots and water movement. Mottle formation also occurred during this period and continues today, as does E horizon development, although it appears its formation is more dependent upon lateral than vertical water movement. In some profiles, the E or BE horizon is not well developed due to additional input of material from above and a limited amount of lateral water movement across the pan. In some areas tree throw or other pedoturbation may reduce the expression of the E and BE horizons. The most recent stage of development has occurred within the last 200 to 300 years with the implementation of agricultural practices. The

major effects are the formation of a distinct plow layer and the addition of lime to the upper soil horizons.

Classification

Fragipans are identified at the great group level. The presence of horizons which do not meet all the fragipan criteria, yet exhibit significant fragic character, is indicated by Fragic subgroups in the Ultisol and Alfisol orders. The diagnostic criteria for the fragipan listed in Soil Taxonomy (Soil Survey Staff, 1975) (c.f. Table 1 and 17) constitute a listing of general properties, rather than providing a clear basis for separating fragipans from fragipan-like materials. Due to the lack of exclusive, clearly defined criteria, a combination of several criteria is generally considered diagnostic. This may reflect, in part, the apparent confusion as to what constitutes a true fragipan.

There is a clear need to improve the definition of the fragipan horizon to provide exclusive diagnostic criteria. The proposals presented by Smith and Callahan (1987) and Witty and Knox (1989) may fulfill this need. Lindbo and Veneman (1989) have suggested an appropriate Fragic subgroups in the Inceptisol order, to accommodate soil materials which have some fragic properties yet do not meet all the criteria of the fragipan horizon. Use of the subscript "x" would indicate a fragipan or a fragic horizon, as recommended by Calhoun (1980). The subscript "d" should be used to indicate horizons which have a bulk density exceeding 1.70 Mg m^{-3} yet do not meet any of the

standards of genetic soil horizons (h, s, t, or x subscripts) or lithic (R-horizon) or paralithic (r subscript) contacts.

Classification of Soils in this Study

As with any classification endeavor the first step is to determine what diagnostic horizons are present. Both Soil Taxonomy and Keys to Soil Taxonomy (Soil Survey Staff, 1975; 1988 respectively) were consulted in identifying the diagnostic horizons and the subsequent classification. All of the pedons contain an ochric epipedon, although in both Pedons 1 and 5 it approaches an umbric epipedon (Table 30). Based on the discussion in Chapters 4 and 5 all the pedons appear to have a fragipan and an argillic horizon. Pedon 1 has an argillic overlying the fragipan horizon; however, most pedons have the pan coinciding with the argillic horizon with a BE overlying it. Moisture regimes, determined in previous studies and based on morphology (Pickering and Veneman, 1984; Reed, 1989), indicate that Pedon 5 has an aquic regime and the others have a udic moisture regime. Based on the presence of an argillic diagnostic horizon and a high base saturation the soils are classified as Alfisols rather than Inceptisols. If the argillic horizon was not present then the soils would be classified as Inceptisols. Suborder classification is based on moisture regime thus Pedon 5 is an aqualf and the other pedons are udalfs. The presence of a fragipan makes the great group classification for all the pedons fragi-. Finally subgroup classification results in Pedon 5 classified Aeric due to a matrix chroma greater than 2; Pedons 2, 3, and 4 are all Ochreptic due to an

Table 30. Classification of each Pedon.

	1	2	Pedon 3	4	5
Epipedon	Ochric	Ochric	Ochric	Ochric	Ochric
Diagnostic Horizons	Argillic	Argillic	Argillic	Argillic	Argillic
	Fragipan	Fragipan	Fragipan	Fragipan	Fragipan
Moisture Regime	Udic	Udic	Udic	Udic	Aquic
ALFISOLS					
Suborder	Udalfs	Udalfs	Udalfs	Udalfs	Aqualfs
Great Group	Fragi- udalf	Fragi- udalf	Fragi- udalf	Fragi- udalf	Fragi- aqualf
Subgroup	Typic Fragi- udalf	Ochreptic Fragi- udalf	Ochreptic Fragi- udalf	Ochreptic Fragi- udalf	Aeric Fragi- aqualf
INCEPTISOLS					
Suborder	Ochrept	Ochrept	Ochrept	Ochrept	Aquept
Great Group	Fragi- ochrept	Fragi- ochrept	Fragi- ochrept	Fragi- ochrept	Fragi- aquept
Subgroup	Typic Fragi- ochrept	Typic Fragi- ochrept	Typic Fragi- ochrept	Typic Fragi- ochrept	Typic Fragi- aquept

ochric epipedon and the argillic horizon coinciding with the fragipan; and, Pedon 1 is Typic due to the argillic horizon occurring above the pan (Table 30).

The above classification scheme assumes that the soils are Alfisols. The central concept of Alfisols may not be met in this region due to slightly higher precipitation and a more acidic parent material than observed in regions traditionally considered to have Alfisols. Most likely the soils investigated fall in the transition zone between Alfisols and Inceptisols, and based on the presence of illuviated clay they are more Alfisol-like than Inceptisol-like (Table 30).

Conclusions

The current controversy over the presence of fragipans in the Northeast revolves around the mode of formation. Calhoun (1980) suggested that most pans developed on till were not true pedogenically derived pans. Instead he felt that the observed properties were inherited, although some till he acknowledged was pedogenically altered. The mode of formation presented here disputes this claim by illustrating that the observed properties were formed post-depositionally by pedogenic processes (Figure 110). The mode of formation consists of multiple pathways affecting each soil in a slightly different fashion thus accounting for observed variability. The mode discussed may only apply to pans developed in this region, although it may have implications to other till derived pans.

Classification, based on observed properties, suggests that the soils are all Alfisols. Such a classification may not meet the ideal concept of an Alfisol but appears accurate based on the occurrence of illuviated clay.

CHAPTER XII

CONCLUSIONS

Unlike many other diagnostic horizons fragipans do not have a specific set of absolute criteria for identification. Instead the identification relies on a series of field clues listed in Soil Taxonomy (Soil Survey Staff, 1975). Based solely on these clues the soils investigated all contain fragipans. This conclusion is contrary to Calhoun (1980), that Massachusetts, as well as most of the glaciated Northeast but excluding parts of New York, does not contain fragipans. Calhoun based his statements on the premise that the till derived pans inherited a high bulk density from the compaction of the overriding ice; and that pedogenesis has not occurred in the pan or that it has had limited effect on the present morphology and properties of the pan. These ideas were undoubtedly influenced by a limited number of deep observations of till derived pans in New England and the practice of identifying pans by a Cx in Massachusetts rather than as a Bx or Btx as in New York (P. Veneman, 1987, personal communication). Also because much of the pioneering work in fragipans was done by Cline and his students at Cornell, those soils could not be reclassified as not containing fragipans. The result of Calhoun's paper was a reclassification of fragipan soils in much of the glaciated Northeast to non-fragipans.

The most recent suggestion to modify the existing definition results from the 1989 Soil Science Society of America publication

devoted to fragipans (Smeck and Ciolkosz, 1989). Witty and Knox's (1989) characteristics aptly describe fragipan properties and suggests that not all pans are alike. The characteristics also recognized that E horizons are not always present and are likely caused by low vertical saturated hydraulic conductivity.

The soils investigated not only meet the criteria established by Soil Taxonomy and Witty and Knox (1989), but also have been formed either in part or in whole by pedogenic processes thus satisfying the criteria set forth by Calhoun (1980). Such processes are evident in the overall morphology of the pans. The BPF are common to all the pedons, showing distinct signs of Fe reduction and subsequent oxidation adjacent to them, with clay films present at their boundaries. In addition, some pores and channels within the matrix of the pan are coated with clay. Mottling, another indication of pedogenesis, is common throughout the pan and appears concentrated in the horizon beneath the fragipan in the more well-drained sites. Apart from the evidence of illuviation some of the pedons exhibit a BE horizon or areas that appear eluviated above the pan. Although these features may be due primarily to the movement of water across the top of the pan, they are nonetheless pedogenic in origin. Micromorphic examination confirms the macromorphologic interpretation illustrating that argillans are common to the pan in amounts indicative of argillic horizons. In addition, argillans in the form of interparticle connections (clay bridges) are common and may account for the strength and brittleness of the pan. It is unlikely that the argillans are

inherited from a previous weathering cycle as the till in which the pans have developed was deposited or reworked during the last period of glaciation (late Wisconsinan). This observation is based on similarities between pebble fabrics in the pans and Upper Till deposits. Other physical characteristics such as moisture retention, bulk density, and slaking in water are similar to those discussed by Grossman and Carlisle (1969).

Both the heavy and clay mineral assemblages suggest some development of the pedons. The clay minerals, while not unique to the pan, illustrated a gradual change from the most weathered minerals occurring in the Ap horizons to less weathered ones in the Cd horizons. The clay mineral assemblages in the pan were transitional illustrating some degree of alteration. The heavy mineral assemblages were similar throughout most of the horizons of a given soil, but minerals in the pans appeared more etched than those in lower horizons suggesting the pan has been more weathered than the lower horizons. The heavy mineral assemblage also identifies aeolian components in Pedons 3, 4, and 5.

Unfortunately, chemical analysis of the soils could not conclusively identify any unique pan component. An increase in pH, CEC and bases was noted through the pan and into the Cd horizons. This increase suggests that some alteration in the soil chemistry has occurred but such changes do not appear to be directly related to the formation of the pan. The chemistry does suggest pedogenesis has occurred.

The mechanism responsible for the strength or brittle behavior in the pan was not conclusively proven. Results suggest a combination of clay and to a lesser extent Si being responsible for the observed brittle behavior. However, a small sample size and heterogeneities in the pan were not conducive to adequate statistical separation of the results.

Synthesis of the data generated by the characterization analyses into a mode of formation for the pedons investigated suggests that a combination of processes are responsible for the present structure and morphology of the pan. Formation of the pan begins rapidly upon deposition and exposure of the till. Dessication, self weight collapse, and physical ripening occur in the early stages of pedogenic development. If there was a strong periglacial climate post-glacially (Gail Ashely, 1990, personal communication) then some of the features may have resulted from periglacial processes. Shortly after exposure came the addition and pedoturbation of aeolian material. The amount of aeolian component was not the same in all soils resulting in some soils having a distinct aeolian mantle while others did not. As vegetation became established the surface stabilized, and eluviation and illuviation became the dominant soil processes. Localized oxidation and reduction resulted in redoximorphic features in the soil. Finally, agricultural practices raised the pH of the upper horizons by liming and created a plow layer.

The results of the characterization not only suggest that the soils contain pedogenic fragipans but that they should be classified as Alfisols. This classification is based on the evidence of

significant clay movement into the fragipan and some of the overlying horizons. The high base saturation is indicative of Alfisols rather than Inceptisols. This interpretation is a departure from traditional view points and more characterization of similar soils is needed to ascertain if these conclusions are typical of a wide variety of soils in the area or just isolated occurrences.

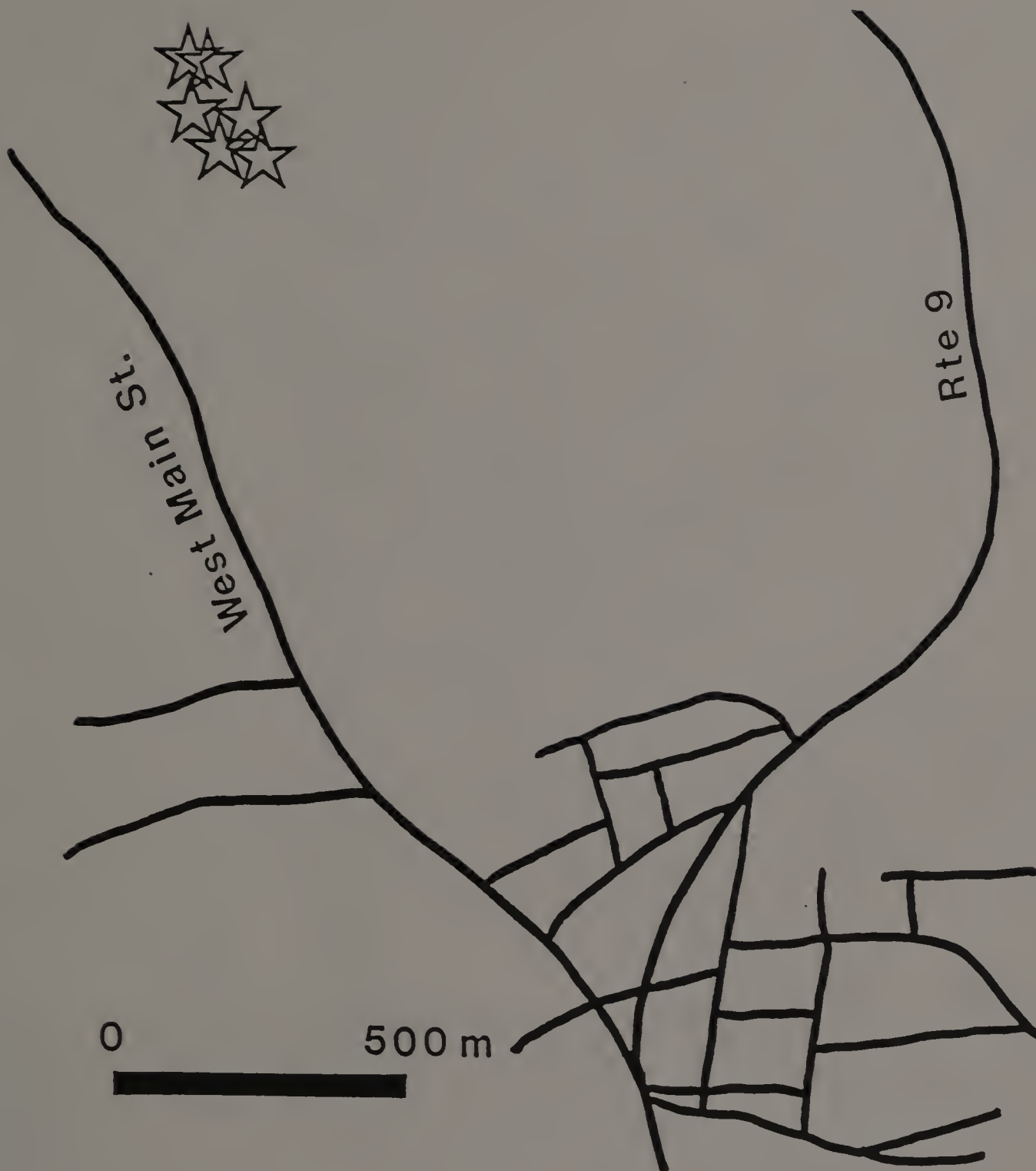
The general conclusions drawn about the fragipan soils investigated in this study are:

1. Fragipans as described by Soil Taxonomy and Witty and Knox (1989) do occur in soils in Massachusetts.
2. The fragipans are pedogenically derived.
3. The presence of fragipans have a distinct impact on the genesis, morphology, and land use of the soils.
4. Fragipans are formed in transported material (glacial till) and are subject to consolidation even after being disturbed.
5. While the brittleness in fragipans formed in non-glaciated deposits is due to cementation primarily by amorphous silica, the fragic character in till derived pans is, in part, the result of clay bridging with associated bonding by Si.
6. Fragipan and dense basal till soils must be described, sampled, and studied to a depth of at least 1.8 m to permit a satisfactory assessment of the character of these soils.
7. There is a need to develop better criteria to separate fragipans from materials which exhibit fragic character.

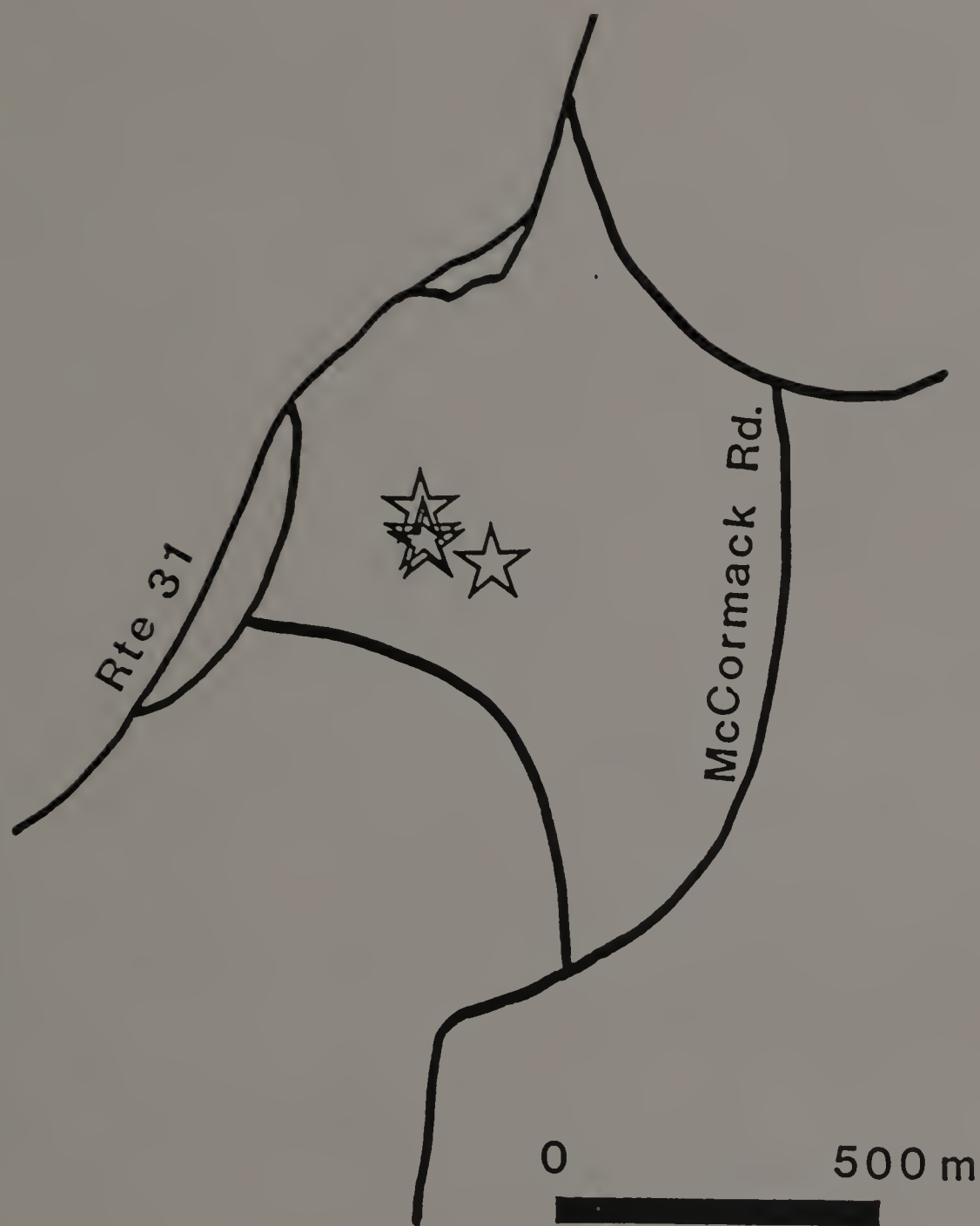
8. The soils investigated have undergone significant pedogenesis and meet criteria to be classified as Alfisols.

Future areas where research could be done in Massachusetts include: solution chemistry of soil water to look for Si or other potential binding agents; and synthetically ripening fragipan material under controlled conditions to ascertain some of its physical properties.

APPENDIX A
SITE LOCATIONS



Blanchard Hill, Brookfield



Buck Hill, Spencer



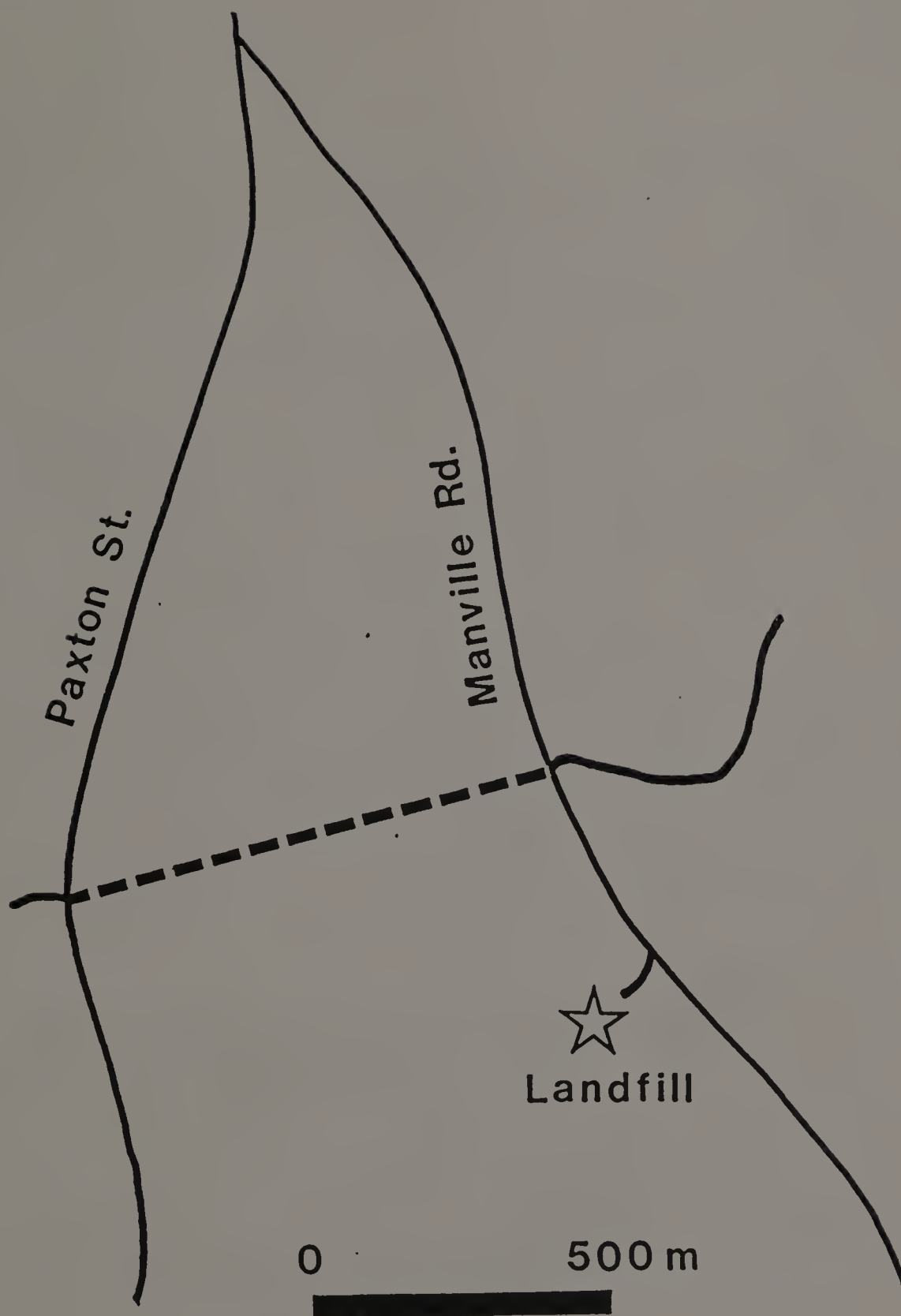
0 500 m

A horizontal black scale bar representing 500 meters.

Orchard Hill, Amherst



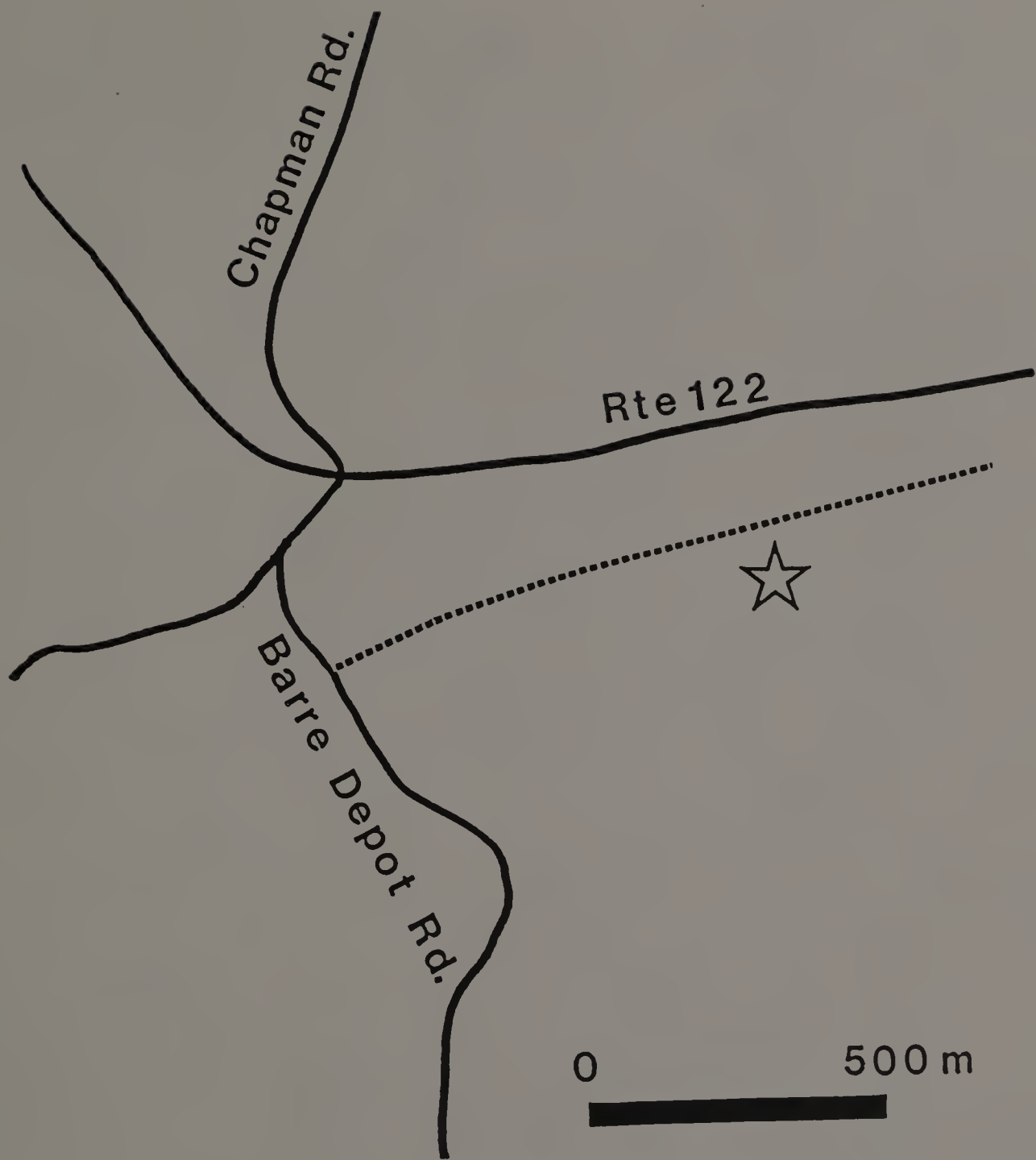
Horticultural Research Center, Belchertown



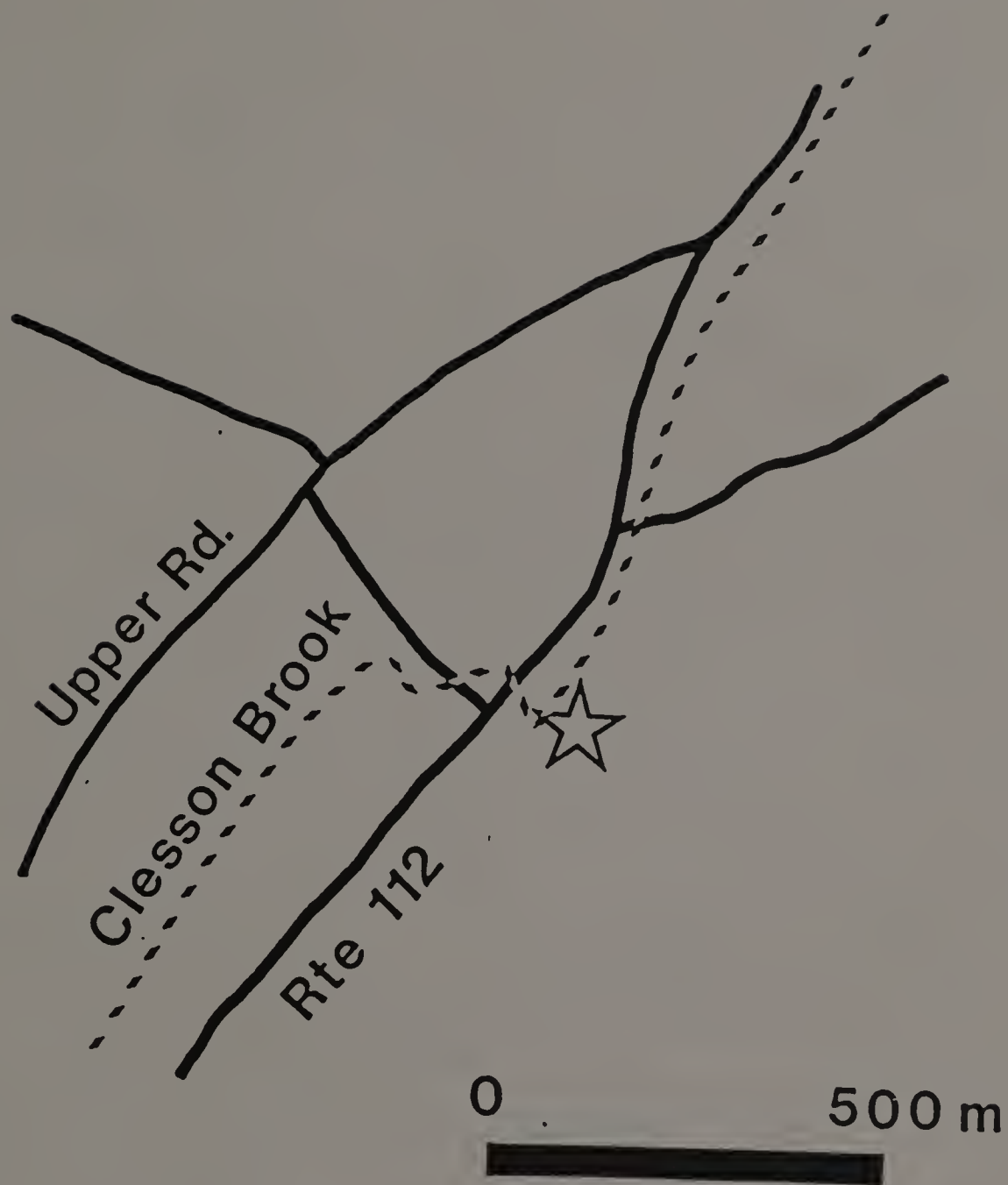
Leicester Town Landfill, Leicester



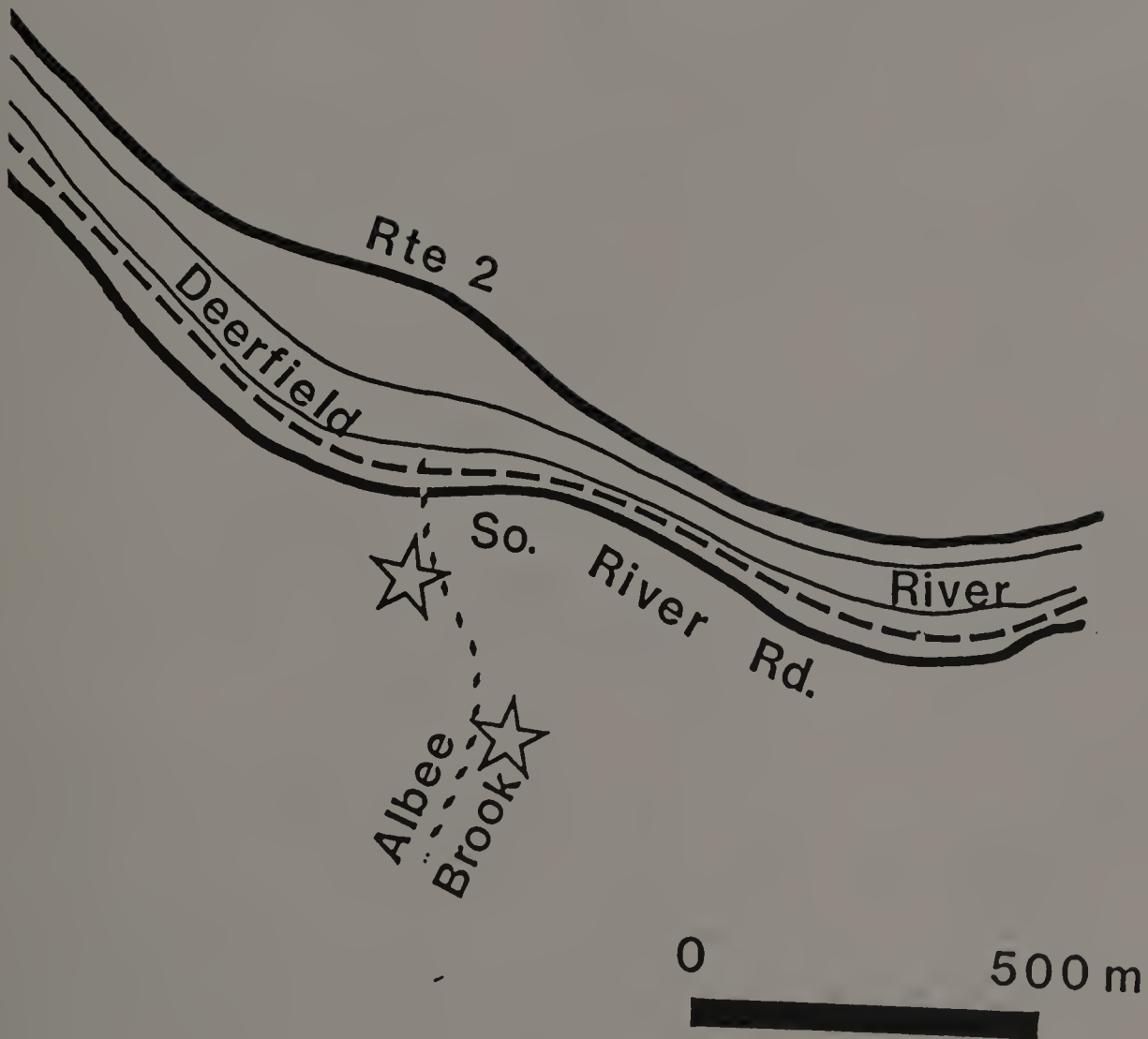
Ayer



Barre Landfill, Barre



Clesson Brook, Buckland



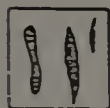
Albee Brook, Charlemont

APPENDIX B

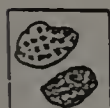
PROFILE DESCRIPTIONS



A Horizon



Krotonia



Rock Fragments



Low Chroma Mottles



Bleached Prism Face With Fe Staining At Edges



High Chroma Mottles And Bands



Platy Structure (Mn coated in Cd, Low chroma along plates in Dt and Dtx)



Fe And Mn Cemented Sand And Gravel



Laminated Sand Lenses



High Chroma Bands



Rock Fragments With Adjacent Low Chroma Areas



Root Within Bleached Prism Face



Band Weakly Cemented by Fe



Sand Lenses



Roots

Key to Cross Section Diagrams

Soil: Paxton (Pedon 1)

Location: Blanchard Hill, Elm Hill Farm, Worchester County,
Brookfield, Massachusetts

Drainage: Well-drained

Position: 13 meters below the summit of the drumlin

Slope and Aspect: 3%, West

Landuse: Orchard with 2-5 year old dwarf apple trees and grass

Date: July 1987

Horizon	Depth (cm)	Description
Ap	0-23	Dark brown (10YR 3/3) fine sandy loam; granular; abundant roots; worm holes (krotovina) 0.2-1cm in dia. (abundant); boundary abrupt and smooth except where krotovina penetrate into the Bw1; fine medium and coarse roots very common.
Bw1	23-34	Dark yellowish brown (10YR 4/6) fine sandy loam matrix; dark brown (10YR 3/3) krotovina; granular to weak subangular blocky; roots common; many follow krotovina; krotovina commonly filled with sand; krotovina commonly have neo alban in center; boundary gradual and smooth.
Bw2	34-59	Yellowish brown (10YR 5/8) fine sandy loam matrix; brown to dark brown (10YR 4/3) krotovina; weak subangular blocky; roots common, predominate between peds and krotovina; krotovina are commonly sand-filled or contain neo albans; weak argillans occurring on fragments; boundary gradual to diffuse; some weak platiness occurs at boundary.

Bt	59-92	Yellowish brown matrix (10YR 5/4) fine sandy loam; common light gray to gray and strong brown (10YR 6/1 and 7.5YR 5/6) mottles adjacent to ped faces; some sand grains are uncoated; weak fine platy structure; friable to firm in spots; few to common yellowish brown (10YR 5/6) argillans (1mm maximum); 10% coarse fragments some be grussified; very faint pale brown (10YR 6/3) vertical bands, 3 cm in diameter and 10-20 cm apart; roots common follow ped faces and around stones; vertical bands grading into BPF in 2Btx1; boundary is clear and smooth.
2Btx1	92-125	Light yellowish brown and strong brown (10YR 4/6 and 7.5YR 4/6) loam matrix; common medium light gray to gray and strong brown (10YR 6/1 and 7.5YR 5/6) mottles adjacent to ped faces and stones; weak to moderate platy structure; roots confined to vertical cracks and ped faces; 10-15% coarse fragments; few black (10YR 2/1) mangans around stones and plates; vertical faces (cracks) are grayish brown to brown (10YR 5/2-5/3), 3-5 cm wide and 10-20 cm apart, connected to the vertical bands above; may also occur unconnected and +/-30 cm apart; mottling is actually color differences around plates; brown (7.5YR 5/4) border around vertical faces; boundary is clear and smooth.
2Btx2	125-162	Light yellowish brown and strong brown (10YR 4/6 and 7.5YR 4/6) loam matrix; light gray to gray, light gray, and strong brown (10YR 6/1, 7/1, 7/2, and 7.5YR 5/6) common medium mottles; PCF light gray and light gray to gray (10YR 6/1 and 7/1) interior, 2-3 cm with strong brown (7.5YR 5/8) border about 40 cm apart; black (10YR 2/1) mangans become more common with depth; some areas are 2-3 cm thick, 10-15 cm long and cemented with Fe and Mn, dusky red and dark reddish brown (2.5YR 3/2 and 2.5/4), more common and large with depth; common yellowish brown (10YR 5/6) argillans, 1-2 mm thick; boundary is abrupt and smooth; firm to very firm.

3BCm	162-194	Brown to dark brown, dark yellowish brown, and dark reddish brown (7.5YR 4/4, 10YR 4/6, and 5YR 3/4) coarse sand matrix; sandy texture; coarse platy banded yet irregular; very hard; up to 20% coarse fragments.
------	---------	---

4Cd	194+	Strong brown (7.5YR 5/6) fine sandy loam, with horizontal band of gray (7.5YR 5/0) and gray (N 6/0); platy; fine textured.
-----	------	--

Water table at 160 cm (7/87)

Soil: Paxton (Pedon 2)

Location: Buck Hill 4-H Camp, Camp Marshall, Worchester Conservation District, Worchester County, Spencer, Massachusetts

Drainage: Well-drained

Position: Mid-slope on the north side of a southwest trending knoll

Slope and Aspect: 5%, Northwest

Landuse: Spruce Christmas trees, grasses

Date: August 1987

Horizon	Depth (cm)	Description
Ap	0-14	Dark grayish brown (10YR 4/2) fine sandy loam; weak coarse granular to weak coarse subangular blocky; friable; common fine, medium, coarse roots; 5% coarse fragments; irregular boundary due to krotovina tonguing into Bw1; abrupt, smooth boundary.
Bw1	14-25	Yellowish brown (10YR 5/4) fine sandy loam; weak coarse granular; friable; common fine, medium, coarse roots; 7% coarse fragments; common 2-5 cm diameter dark grayish brown (10YR 4/2) krotovina 20-30 cm apart; roots occur more often in krotovinas; gradual wavy boundary.
Bw2	25-39	Brownish yellow (10YR 6/6) fine sandy loam; weak coarse subangular blocky; friable; common fine and coarse roots, few medium roots commonly occurring in dark brown (10YR 4/3) krotovina; krotovina 3-6 cm diameter, 30-50 cm apart; few skeletons associated with vughs in krotovina; few small faint light yellowish brown (10YR 4/6) mottles; 7% coarse fragments; gradual wavy boundary.

BE	39-55	<p>Brownish yellow, 45%, (10YR 6/6) brown, 30%, (10YR 5/3), and light olive brown, 25%, (2.5Y 5/4) fine sandy loam matrix; horizon appears mixed (congeliturbated); friable, 75%, to firm, 25%; common fine and coarse roots within krotovina and friable matrix; few krotovina dark yellowish brown (10YR 4/4) 50 cm apart, 4 cm diameter; common skeletons in vughs with yellowish brown (10YR 5/4) thin rare argillans adjacent to them; massive to weak coarse angular blocky; common medium distinct dark brown (7.5YR 4/4) and light gray (10YR 7/1) mottles; boundary irregular gradual; 10% coarse fragments; horizon lower boundary demarked by the initiation of bleached prism faces (BPF).</p>
2Btx1	55-88	<p>Dark grayish brown (2.5Y 4/2) and olive brown (2.5Y 4/4) fine loamy sand matrix; weak coarse platy with moderate very coarse prismatic overprint; firm and brittle; few fine and coarse roots confined to BPF; BPF are 12 cm wide generally occur under a krotovina and are 50-60 cm apart; interior of BPF gray (5Y 6/1) with dark brown (7.5YR 4/4) iron rich rind; common thin to medium yellowish brown (10YR 5/4) argillans on common medium vesicles, peds, and coarse fragments; few dark brown (7.5YR 3/2) mangans on tops of rocks; common small distinct light gray (10YR 7/1) mottles; 12% coarse fragments; gradual wavy boundary.</p>
2Btx2	88-126	<p>Olive brown, 60%, (2.5Y 4/4) and light olive brown, 40%, (2.5Y 5/4) fine sandy loam matrix; moderate very coarse prismatic overprinting weak coarse platy; very firm and brittle; few coarse roots confined to BPF BPF interior light gray (5Y 7/1) with dark brown (7.5YR 4/4) rind; BPF 3-10 cm wide, rind 1-3 cm wide; few skeletons within BPF and common argillans within rind; dark yellowish brown (10YR 4/4) medium argillans common in matrix as coatings; common gray bleached area adjacent to stones usually on</p>

2Btx2 continued		underside up to 5 cm thick; mangan, dark brown (7.5YR 3/2) common of peds and upper surface of rocks; medium vesicle common, concentrated near plate boundaries; lower horizon boundary demarked by an end to BPF and the start of reticulated mottles; platy character increase with depth; 15% coarse fragments; light gray (5Y 7/1) common fine distinct mottles increase with depth, becoming more lens shaped and developing a dark brown (7.5YR 4/4) outer rind; abrupt wavy boundary.
2BCd	126-160	Olive brown (2.5Y 4/4) fine sandy loam matrix; moderate coarse platy; firm to friable along plates; no roots; many large distinct reticulated mottles; interior grayish brown (2.2Y 5/2), exterior dark brown (7.5YR 4/4), 1 cm thick and up to 10 cm long bounded by plates; rarely BPF from BCx2 enters into the horizon; mottles and plates are lenticular; common mangans on rocks surfaces and plate boundaries; few thick olive brown (2.5Y 4/6) argillans on plates; undersides of rocks show bleached areas grayish brown (2.5Y 5/2); 15% coarse fragments; gradual wavy boundary.
3Cd1	160-183	Olive brown (2.5Y 4/4) fine sandy loam matrix; moderate coarse platy; firm to friable; many large distinct reticulated mottles; interior grayish brown (2.5Y 5/2), exterior dark brown (7.5YR 4/4); few thin weak red (2.5YR 5/2) and light reddish brown (2.5YR 6/4) argillans; common dark brown (7.5YR 4/4) mangans on lenticular plates and stones; rocks have a bleached grayish brown (2.5Y 5/2) 1 cm wide zone around them, more prominent on the underside; 50% coarse fragments (stone line); gradual wavy boundary.
3Cd2	183-210	Olive brown, 75%, (2.5Y 4/4) and light olive brown, 25%, (2.5Y 5/4) fine sandy loam matrix; moderate coarse platy; slightly firm to friable; few medium grayish brown (2.5Y 5/2) and dark

3Cd2 continued brown (7.5YR 4/4) mottles; no argillans; many dark brown (7.5YR 3/4) mangans; no argillans; many dark brown (7.5YR 3/4) mangans; common strong brown (7.5YR 4/6) ferrans; 10% coarse fragments; gradual smooth boundary.

3Cd3 210-305+ Dark grayish brown (2.5Y 4/2) fine sand loam; slightly firm to friable; moderate coarse platy; few medium dark brown (7.5YR 4/4) and few fine grayish brown (2.5Y 5/2); mottles; many mangans on plates.

Special feature in 3Cd2 and 3Cd3, large yellow (10YR 7/8) and reddish yellow (7.5YR 6/8) sand lens 20-80 cm. thick; laminated; very abrupt boundaries; few strong brown (7.5YR 5/8) mottles.

Water table below pit floor. (8/87)

Soil: Paxton (Pedon 3)

Location: Orchard Hill, University of Massachusetts, Hampshire
County, Amherst, Massachusetts

Drainage: Well-drained

Position: 25 meters east of the summit of a drumlin

Slope and Aspect: 5%, East

Landuse: Abandoned orchard/pasture, first stage regrowth including
poison ivy, blackberry, gray birch, and grass

Date: September 1987

Horizon	Depth (cm)	Description
Ap	0-20	Dark brown (10YR 3/3) fine sandy loam; weak fine granular; friable; many fine, medium and coarse roots; krotovinas at base of horizon cause mixing between Ap and Bw; 1% coarse fragments; abrupt irregular boundary.
Bw	20-37	Yellowish brown (10YR 5/6) fine sandy loam; weak fine subangular blocky; friable; many fine and medium roots; few coarse roots occur primarily in dark brown (10YR 3/3) krotovina (many); few skeletons with large voids in vesicles occur toward bottom of horizon; 5% coarse fragments; abrupt smooth boundary.
BE	37-61	Brown (10YR 5/3) fine sandy loam; weak fine subangular blocky to massive; friable to firm (30%) common coarse roots in dark brown and yellowish brown (10YR 3/3 and 10YR 5/6) krotovinas; krotovinas occur 20-50 cm apart; common uncoated grains (skeletons); few fine channel argillans yellowish brown (10YR 5/4); common coarse distinct gray (10YR 6/1) mottles surrounded by strong brown (7.5YR 5/8) quasiferran; 5% coarse fragments; diffuse irregular boundary.

2Btx1	61-100	Brown (10YR 4/3 to 10YR 5/3) fine sandy loam; weak fine platy overprinted by coarse prismatic; very firm and brittle; few medium roots confined to bleached prism faces (BPF); BPF light yellowish brown (10YR 6/4) interior with strong brown (7.5YR 5/6) ferrans along edges; BPF 3-8 cm wide and 50-70 cm apart; argillan lined vesicles common; argillans dark yellowish brown (10YR 4/6) common on peds rocks and grains up to 0.5 mm thick; few skeletans occur in conjunction with BPF mainly; few ferran strong brown (7.5YR 5/8) and mangans black (7.5YR 2/1) occur on rocks and peds; common large distinct gray (10YR 6/1), strong brown (7.5YR 5/8), and strong brown (7.5YR 4/6) mottles; 10% coarse fragments; gradual smooth boundary.
2Btx2	100-137	Dark brown (10YR 3/3 to 7.5YR 3/4) fine sandy loam; as 2Btx1 but BPF better developed; mangans more common than ferrans; BPF pinch out at bottom of horizon; grade into horizontal mottles lenticular 2-5 cm long, 1 cm wide with pale brown (10YR 6/3) interiors and strong brown (7.5YR 5/6) exteriors; 15% coarse fragments; abrupt wavy boundary.
2BCd	137-183	Dark brown (7.5YR 3/4) fine sandy loam; moderate medium platy; firm to friable; common large distinct gray (10YR 6/1) interior, strong brown (7.5YR 5/8 and 7.5YR 4/6) exterior mottles; mottles are 5 cm long by 1 cm wide; few argillans dark yellowish brown (10YR 4/6) on plates; common to many mangans very dark brown to black (7.5YR 2/1) on plates and rocks; no vesicles evident; 15% coarse fragments; abrupt smooth boundary.
3Cd1	183-216	Dark brown (7.5YR 3/4) fine sandy loam; as 2BCd but friable to firm; few fine faint light yellowish brown (10YR 6/4) mottles; many mangans very dark brown to black (7.5YR 2/1); gradual smooth boundary.
3Cd2	216+	Dark brown (7.5YR 3/4) fine sandy loam; fine platy moderate; friable.

Soil: Woodbridge (Pedon 4)

Location: Orchard Hill, University of Massachusetts, Hampshire County,
Amherst, Massachusetts

Drainage: Moderately well-drained

Position: Mid-slope approximately 100 meters from the summit of a
drumlin

Slope and Aspect: 3%, East

Landuse: Abandoned orchard/pasture with first stage regrowth
including poison ivy, gray birch, and grasses

Date: October 1987

Horizon	Depth (cm)	Description
Ap	0-25	Very dark grayish brown (10YR 3/2) fine sandy loam; weak medium granular; loose to friable; many fine medium and coarse roots; common fine krotovina dark yellowish brown (10YR 4/6) at base of horizon; few clear small brown to dark brown (10YR 4/3) mottles; 1% coarse fragments; abrupt irregular boundary.
Bw1	25-43	Dark yellowish brown (10YR 4/6) fine sandy loam; weak medium subangular blocky; friable; many fine medium coarse roots; roots follow krotovina; krotovina are very dark grayish brown and brown to dark brown (10YR 3/2 and 10YR 4/3), 5 to 10 cm apart, and 2-3 cm in diameter; few uncoated sand grains (skeletons); common 0.1 mm vesicles; few fine distinct strong brown (7.5YR 5/8) mottles; 2% coarse fragments; gradual smooth boundary.
Bw2	43-57	Yellowish brown (10YR 5/6) fine sandy loam; weak medium subangular blocky; friable; common fine and coarse roots; few medium roots; roots follow krotovina; and along ped faces; common krotovina,

Bw2 continued		brown to dark brown (10YR 4/3) 10 cm apart and 2 cm in diameter; few faint medium, brown and pale brown (10YR 5/3 and 10YR 6/3) mottles; very thin 0.1 mm yellowish brown (10YR 5/4) argillans on few vesicles which are up to 1 mm in dia.; 4% coarse fragments; abrupt wavy boundary.
BE	57-70	Mixture of brown to dark brown and yellowish brown (7.5YR 4/4 and 10YR 5/4) fine sandy loam; moderate medium subangular blocky; friable to firm (40%); few coarse roots following few brown to dark brown (10YR 4/3) krotovinas, which are 30 cm apart and 4 cm in dia.; common medium vesicles and peds; argillans thin 0.3 mm and yellowish brown (10YR 5/4); few uncoated sand grains; few medium faint brown (10YR 5/3) and brown (7.5YR 5/2) mottles; 10% coarse fragments; gradual smooth boundary.
2Btx1	70-102	Brown to dark brown (7.5YR 4/4) dominates with some areas of yellowish brown (10YR 5/4) fine sandy loam; weak medium subangular blocky; weak thin platy overprinted by very coarse prismatic structure; few coarse roots confined to bleached prism faces (BPF); BPF 30-50 cm apart 4-8 cm wide (wider at top), light gray to gray (5Y 6/1) face with 1-2 cm thick ferrans red (2.5YR 5/8) vertical streaks at edges; common uncoated grains within BPF; vesicles of 2 mm dia. lined and filled with clay common above start of BPF a krotovina from the BE is common; common grayish brown 10YR 5/2) argillans up to 0.7 mm thick coating peds voids and grains; common distinct large light gray to gray and strong brown (5Y 6/1 and 7.5YR 5/8) generally elongated; very firm and brittle; 10% coarse fragments; gradual smooth boundary.
2Btx2	102-132	Brown to dark brown (7.5YR 4/4) fine sandy loam; weak medium subangular blocky, moderate thin platy overprinted by very coarse prismatic structure; very firm and brittle; very few coarse roots confined to BPF; BPF are light gray to gray (5Y 6/1) interior with a 2 mm strong brown (7.5YR

2Btx2 continued		5/8) ferran at edges; BPF 30-50 cm apart and 3 cm wide, terminating at base of horizon; common distinct large light gray to gray, light gray, and strong brown (5Y 6/1, 10YR 7/1, and 7.5YR 5/8) commonly elongate mottles; surrounding rocks and thicker on the undersides are neo albans, light gray to gray (10YR 6/1); grayish brown (10YR 5/2) argillans common on peds, grains, and rocks; few vesicles 0.5 to 1 mm; common mangans very dark brown to black (7.5YR 2/1) on plates; 12% coarse fragments; abrupt wavy boundary.
2BCd	132-167	Brown to dark brown and dark brown (7.5YR 4/4 and 7.5YR 3/4) fine sandy loam; moderate thick platy; firm to friable; no roots; no krotovina; few thin grayish brown (10YR 5/2) argillans on peds and in few fine vesicles; common mangans, dark brown (7.5YR 3/2) on plates and rocks; many distinct large light gray to gray, light gray, and strong brown (5Y 6/1, 10YR 7/1, and 7.5YR 5/8) mottles arranged in elongated fashion with 7/1 and 6/1 interiors and 5/8 exteriors; 20% coarse fragments; gradual smooth boundary.
3Cd	167+	Brown to dark brown (7.5YR 4/4) fine sandy loam; moderate to strong platy; friable to firm (40%); common mangans, dark brown (7.5YR 3/2) on plates and rocks; few distinct small, strong brown (7.5YR 5/8) mottles; no low chroma mottles; 20% rock fragments.

Water table at 40 cm. (10/87)

Soil: Ridgebury (Pedon 5)

Location: Horticultural Research Center, University of Massachusetts,
Hampshire County, Belchertown, Massachusetts

Drainage: Somewhat poorly drained

Position: Toe-slope of north-south trending bedrock controlled
drumloidal ridge

Slope and Aspect: 3%, West

Landuse: Orchard with 30 year old apple trees and grass

Date: July 1987

Horizon	Depth (cm)	Description
Ap	0-25	Very dark gray (10YR 3/1) with some (20%) very dark grayish brown (10YR 3/2) fine sandy loam; moderate coarse subangular, blocky when dry, weak medium platy when moist; friable; many fine medium to coarse krotovina, dark brown (10YR 3/3) and yellowish brown (10YR 5/4); many fine to coarse roots common large and medium distinct strong brown (7.5YR 5/6) mottles; boundary abrupt, irregular, due to krotovina; no living worms were observed.
Bw	25-44	Yellowish brown (10YR 5/4) fine sandy loam with 25% light yellowish brown (10YR 6/4) loamy sand lenses moderate coarse granular, and weak coarse subangular blocky; friable; many roots, all sizes, fine and coarse occur in very dark brown (10YR 3/2) and in very dark gray (10YR 3/1); 2.5 cm diameter krotovina; krotovinas 20-40 cm apart, many medium distinct strong brown (7.5YR 5/6) and light gray (10YR 7/1) mottles; mottles become more dominant with depth in the profile; gradual wavy boundary.

BE	44-57	<p>Pale brown (10YR 6/3) loamy sand; weak medium granular to single grain; friable; many roots of all sizes occurring in association with very dark gray (10YR 3/1) and very dark grayish brown (10YR 3/2) krotovinas; krotovina 40-60 cm apart, 2-5 cm diameter; many medium distinct strong brown (7.5YR 5/6) and light gray (10YR 7/1) mottles; some grains are uncoated; boundary is irregular yet clear; the horizon appears to pinch out in places.</p>
2EB	57-81	<p>Loamy fine sand matrix colors include light gray 35% (10YR 7/2), brown 25% (10YR 5/3), yellowish brown, 15%, (10YR 5/4), and strong brown, 25%, (7.5YR 4/6); weak coarse platy; friable to slightly firm lenses (25%); few roots of all sizes confined to few, 2-5 cm diameter very dark grayish brown (10YR 3/2) to strong brown (7.5YR 4/6) krotovinas; sandy zones mantling brown (10YR 5/3) firm lenses; krotovinas 50-70 cm apart; common large distinct light gray (10YR 7/1) mottles; sandy areas mantle; firm lenses similar material to fragipan horizons; within sandy area few very dark gray (7.5YR 3/1) mangans; few thin yellowish brown (10YR 5/4) and very pale brown (10YR 7/3) argillans on peds, coarse fragments, and in few fine vesicles; tops of bleached prism faces (BPF) commonly begin under krotovina; BPF interior light gray (10YR 7/2) with strong brown (7.5YR 4/6) rind; BPF are not very distinct and not always continuous; BPF 12-14 cm wide, rind 1-2 cm wide and 50-70 cm apart; gradual wavy boundary.</p>
2Btx1	81-129	<p>Brown (10YR 5/3) and light yellowish brown (10YR 6/4) loamy fine sand matrix; weak coarse platy with moderate very coarse prismatic overprint; very firm; few roots, fine and coarse, commonly confined to BPF; BPF interior light gray (10YR 7/1), rind strong brown (10YR 4/5) and some interior of BPF light gray (5Y 7/1); BPF interior contains uncoated sand grains with thin argillans</p>

2Btx1 continued	<p>at boundaries of rind; common fine distinct strong brown (7.5YR 4/6) mottles; common thin to medium yellowish brown (10YR 5/4) argillans on peds, fine to medium common vesicles and coating coarse fragments; common very dark gray (7.5YR 3/1) mangans on fragments and some ped-faces; manganese and iron cement sand band, 1-3 cm. thick; occurs at boundary dark brown (7.5YR 4/4) to dark reddish brown (5YR 3/3); abrupt wavy boundary.</p>
2Btx2 129-184	<p>Gray (5Y 5/1) and (10YR 5/1) fine sandy loam matrix; moderate coarse platy with moderate very coarse prismatic overprint; very firm; few fine roots confined to BPF; BPF interior gray (5Y 6/1) with strong brown (7.5YR 4/6) rind; BPF 3 cm. wide, narrowing and ending abruptly at base of horizon; BPF contains striped sand grains in center with thin argillans at and within the rind; grayish brown (10YR 5/2) thin argillans common on common medium vesicles, peds and fragments; many fragments of tonalite are grussified; very dark gray (7.5YR 3/1) mangans common on peds and fragments; gradual wavy boundary.</p>
2Cd1 184-229	<p>Greenish gray (5GY 6/1) fine sandy loam matrix; moderate fine to medium platy; friable to firm; few argillans; few mangan; common silt caps; very few grussified tonalites fragments.</p>
2Cd2 229+	<p>Greenish gray (5GY 6/1) loamy fine sand matrix; moderate medium platy; firm; common silt caps; few mangan; very few grussified tonalites fragments.</p>

Soil: Paxton

Location: Blanchard Hill, Elm Hill Farm, Worchester County,
Brookfield, Massachusetts

Drainage: Well drained

Slope, aspect: 3%, Southwest

Position: 10 meters below summit of drumlin

Landuse: Apple orchard, 3-5 year old dwarf apple trees, grass

Horizon	Depth (cm)	Description
Ap	0-18	Very dark grayish brown (10YR 3/2) fine sand; moderate medium granular; loose to very friable; common fine roots; 5% coarse fragments; abrupt irregular boundary.
Bw1	18-30	Dark yellowish brown (10YR 4/4) fine sandy loam; weak fine granular to weak fine subangular blocky; friable; common fine roots occurring primarily in dark brown (10YR 3/3) krotovinas; few faint fine yellowish red (5YR 5/8) mottles; 10% coarse fragments; gradual smooth boundary.
Bw2	30-51	Brown (10YR 5/3) fine sandy loam; weak fine subangular blocky; friable; few fine roots associated with dark brown (10YR 3/3) krotovinas; few fine distinct strong brown (7.5YR 5/8) mottles; few thin argillans, yellowish brown (10YR 5/6) around sand grains; 10% coarse fragments; smooth clear boundary.
Bt	51-76	Olive brown (2.5Y 4/4) fine sandy loam; weak fine subangular blocky to moderate medium platy; friable to firm (50%); few fine roots occurring along plates; some roots show neo albans of light gray to gray (10YR 6/1) adjacent to them; common fine distinct strong brown (7.5YR 5/8) mottles; thin to medium (0.5-0.7mm) argillans of light olive brown (2.5Y 5/4) on peds, rocks, and sand grains; 15% coarse fragments; clear smooth boundary.

2Btx1 76+ Olive brown (2.5Y 4/4) loam; moderate medium platy to weak fine subangular block with very weak coarse prismatic overprint; firm and brittle; common fine distinct yellowish red (5YR 4/6 and 5YR 5/8) mottles; few dark reddish brown (5YR 2.5/2) mangans on upper surfaces of rocks; few red (2.5YR 4/8) ferrans adjacent to rocks and on some plates; few fine distinct (5YR 5/0 and 5YR 6/0) mottles common around rocks; common argillan of light olive brown (2.5Y 5/4) up to 1mm thick on peds and rocks; 25% coarse fragments

Soil: Woodbridge

Location: Blanchard Hill, Elm Hill Farm, Worchester County,
Brookfield, Massachusetts

Drainage: Moderately well drained

Slope, aspect: 10%. Southwest

Position: Upper foot-slope 200 meters from summit of drumlin

Landuse: Apple orchard, 30+ year old trees, grasses

Horizon	Depth (cm)	Description
---------	------------	-------------

Ap	0-23	Very dark grayish brown (10YR 3/2) fine sandy loam; loose to friable; many fine medium and coarse roots; dark yellowish brown (10YR 4/4) inclusions within krotovina in lower portions of horizon; 5% coarse fragments; abrupt irregular boundary.
----	------	--

Bw1	23-41	Brown to dark brown (10YR 4/3) fine sandy loam; weak fine subangular blocky; friable; many fine and few medium roots commonly associated with very dark gray (10YR 3/1) krotovina; few fine distinct yellowish red (5YR 5/8), and few fine distinct strong brown (7.5YR 5/8) mottles; 5% coarse fragments; gradual smooth boundary.
-----	-------	---

Bw2	41-56	Brown to dark brown (10YR 4/3) fine sandy loam; weak fine subangular blocky; friable to firm (20%); few fine roots commonly associated with few very dark grayish brown (10YR 3/2) krotovina; few fine faint yellowish brown (10YR 5/6) mottles; common thin irregular argillans, dark yellowish brown (10YR 4/4) on ped surfaces; 5% coarse fragments; clear smooth boundary.
-----	-------	--

2Btx1	56-76	<p>Light olive brown (2.5Y 5/4) fine sandy loam; weak fine subangular blocky to weak thin platy; firm; very few fine roots confined to area between plates; common fine faint strong brown (7.5YR 5/8) and brown to dark brown (7.5YR 4/4) mottles; common fine distinct strong brown and dark brown (7.5YR 4/8 and 7.5YR 3/2) mottles; common dark brown (7.5YR 3/2) mangans on ped surfaces and rocks; common yellowish brown (10YR 5/4) thin 0.5 to 1mm argillans on peds and vesicles; 15% coarse fragments; gradual smooth boundary.</p>
2Btx2	76+	<p>Brown to dark brown (10YR 4/3) fine sandy loam; weak fine subangular blocky to weak fine platy, weakly overprinted by coarse prismatic; BPF gray with ferrans at edges, strong brown (7.5YR 5/6); BPF 2-5cm thick and 30-70cm apart; common dark brown (7.5YR 3/2) mangans on plates and rocks; common vesicles some lined with argillans, light olive brown (2.5Y 5/4); argillans occur up to 1mm thick on ped surfaces; 20% coarse fragments.</p>

Soil: Ridgebury

Location: Blanchard Hill, Elm Hill Farm, Worchester County,
Brookfield, Massachusetts

Drainage: Somewhat poorly drained

Slope, aspect: 3%, Southwest

Position: Foot-slope 225 meters from summit of drumlin

Landuse: Apple orchard, 30+ year old trees, grass

Horizon	Depth (cm)	Description
Ap	0-25	Very dark brown (10YR 2/2) fine sandy loam; weak fine granular; loose to friable; many fine, few medium roots; krotovina common, dark yellowish brown (10YR 4/6); the lower 2-8cm of the horizon contains an irregular non-continuous layer of charcoal, black (2.5Y 2/0); 5% coarse fragments; wavy abrupt boundary.
Bw1	25-41	Dark yellowish brown (10YR 4/6) fine sandy loam; weak fine subangular blocky; friable; common fine, few medium roots; few very dark grayish brown (10YR 3/2) krotovina with roots concentrated in them; few fine 0.1 mm argillan on grains; few fine (0.5cm diameter) charcoal pieces, black (2.5y 2/0); 10% coarse fragments; gradual smooth boundary.
BE	41-56	Grayish brown to light olive brown (2.5Y 5/3) fine sandy loam; weak fine subangular blocky; friable; few fine roots; few medium faint light yellowish brown and grayish brown (2.5Y 6/4 and 2.5Y 5/2) mottles; few fine faint dark yellowish brown (10YR 4/4); argillan, light olive brown (2.5Y 5/4) thin (0.3 mm) on peds, grains, and vesicles; 10% coarse fragments; smooth clear boundary.

- 2Bx1 56-66 Grayish brown to light olive brown (2.5Y 5/3) fine sandy loam; weak medium subangular blocky to weak fine platy; friable to firm (50%); many fine faint olive gray (5Y 5/2) mottles; common fine faint dark yellowish brown (10YR 3/4) mottles; few fine roots along plates; many vesicles filled with light olive brown (2.5Y 5/4) argillans; argillans up to 0.7 mm thick coat peds and stones; 10% coarse fragments; gradual smooth boundary.
- 2Bx2 66+ Olive (5Y 5/3) fine sandy loam; moderate medium subangular blocky to weak fine platy with weak overprint of coarse prismatic; firm to very firm and brittle; few fine roots in upper portion of horizon; weakly developed polygon network; BPF, gray (5Y 6/1) with brown to dark brown ferrans (7.5YR 4/4); few fine prominent brown to dark brown (7.5YR 4/4), common fine prominent dark yellowish brown (10YR 4/6), and common large distinct light gray to gray (5Y 6/1) mottles; common argillans grayish brown to light olive brown (2.5Y 5/3) on peds and in common vesicles up to 1 mm thick; 20% coarse fragments.

Water table at 71 cm (8/85)

Soil: Woodbridge

Location: Blanchard Hill, Elm Hill Farm, Worcester County,
Brookfield, Massachusetts

Drainage: Moderately well drained

Slope, aspect: 5%, Southwest

Position: Foot-slope below the break in slope at the base of a small
terrace, 225 meters from summit of drumlin

Landuse: Pasture area adjacent to an apple orchard with 30+ year old trees

Horizon	Depth (cm)	Description
Ap	0-25	Dark brown matrix (10YR 3/3) loamy sand; granular; abundant roots; krotovina 0.2-2 cm. in dia. (worms), abundant slightly finer granular structure and they contain more roots; boundary clear abrupt except for krotovina.
Bw1	25-38	Dark yellowish brown (10YR 4/6) fine sandy loam matrix; dark brown and dark grayish brown krotovina (10YR 3/3 and 10YR 4/2); granular to weak subangular blocky; roots common, follow krotovina; common sand filling and neoalban associated with krotovina; boundary gradual.
Bw2	38-50	Strong brown (7.5YR 4/6) loamy sand matrix; brown to dark brown krotovinas (10YR 4/3); weak to moderate subangular blocky; roots common as in Bw1; few fine argillans; boundary gradual to diffuse.
BE	50-78	Strong brown (7.5YR 5/6) friable loamy sand matrix; dark yellowish brown (10YR 4/4) firm matrix; occurs as lenses intermixed with no common sizes; weak platy structure to subangular blocky; few dark brown (10YR 3/3) krotovinas filled with sand; roots common in friable but not in firm material; grayish brown to light gray (10YR 5/2 to 6/1) coating on some peds; 0.1 to 0.5 cm. thick; abrupt to gradual boundary.
2BCx	78-108	Dark yellowish brown (10YR 4/4) loamy sand; firm; few thin 0.1 to 0.3 cm. argillans of yellowish brown (10YR 5/6); few roots; weak platy structure.

3BCm	108+	Fe/Mn cemented; coarser textured; brown to dark brown, dark reddish brown, and dark yellowish brown (7.5YR 4/4, 5YR 3/4, and 10YR 4/6) loamy sand matrix colors; coarse platy; banded irregularly; very hard; 25% coarse fragments.
------	------	---

Soil: Unclassified

Location: Blanchard Hill, Elm Hill Farm, Worchester County,
Brookfield, Massachusetts

Drainage: Undetermined

Slope, aspect: 5%, Southwest

Position: Foot-slope 10 meters below the break in slope at the base of
a small terrace, 235 meters from summit of drumlin

Landuse: Pasture area adjacent to an apple orchard with 30+ year old
trees

Horizon	Depth (cm)	Description
Ap	0-24	Very dark brown (10YR 2/2) loamy sand; roots abundant; common krotovina, dark yellowish brown (10YR 3/6) to dark brown (10YR 3/6); diameter .3 to 1 cm; discontinuous bands of black (10YR 2/1); granular structure; undulating abrupt boundary.
Bw1	24-37	Dark brown (7.5YR 4/4) fine sandy loam; granular structure; continuis fine vescile and very fine argillans; friable; 5% coarse fragments; roots common; krotovina common .3 to 1 cm. very dark gray (10YR 3/1); krotovina contain sand and neoalbans; few medium vesicles 2 mm diameter; gradual boundary.
Bw2	37-63	Dark yellowish brown (10YR 4/6) loamy sand; krotovina dark brown (10YR 4/3)and very dark grayish brown(10YR 3/2); friable; granular structure; few argillans 1-2 mm thick, vesicles common; gradual lower boundary.
2BCd	63-96	Yellowish brown (10YR 5/8) intermixed with yellowish brown (10YR 5/6) loamy sand; firm; 10% coarse fragments; numerous argillans; silt caps brownish yellow (10YR 6/6); krotovina less dominant to nonexistant; roots on ped faces; indurated pockets strong brown (7.5YR 5/6), sandier texture; grussified fragments; small mangans, black (10YR 2/1); horizon coarsens with depth; structure weak and platy; fine and weak fine subangular, lower boundary undulating.

3BCm	56-138	<p>Matrix is varigated: brown to dark brown, yellowish brown, and very dark brown (7.5YR 4/4, 10YR 5/6, and 10YR 2/2) loamy sand; bands--irregular and discontinuous, of dark reddish brown (5YR 3/2 and 3/3), 3-5mm thick, following moderate fine platy structure; 20% coarse fragments; plates Mn and Fe stained with dark reddish brown (5YR 2.5/2); argillans common on faces and coarse fragments; gravelly sand texture; vesicles common; cementation increases with depth; hard to extremely hard; boundary abrupt.</p>
4Cr	138+	<p>Red, reddish yellow and yellowish red (2.5YR 5/8, 5YR 6/8 and 5/8); colors are in irregular bands, reddish yellow (5YR 6/8) dominates; firm to hard; weathered Brimfield schist.</p>

Soil: Paxton

Location: Buck Hill, Camp Marshall, Worchester County Conservation District, Worchester County Spencer, Massachusetts

Drainage: Well drained

Slope, aspect: 5%, Northwest

Position: Mid-slope on knoll

Landuse: Abandoned pasture with Christmas trees (spruce) and grass

Horizon	Depth (cm)	Description
Ap	0-20	Dark yellowish brown (10YR 3/4) fine sandy loam; weak granular structure; loose to very friable; many fine medium and coarse roots; 3-5% coarse fragments; abrupt wavy boundary.
Bw1	20-36	Dark yellowish brown (10YR 4/4) fine sandy loam; weak fine subangular blocky; loose to friable; few coarse roots, common medium to fine roots; fine roots occur primarily in common, dark yellowish brown (10YR 3/4) krotovinas; 5% coarse fragments; gradual smooth boundary.
Bw2	36-48	Olive brown (2.5Y 4/4) fine sandy loam; moderate medium subangular blocky; friable; few medium, common fine roots; fine and medium roots occur primarily in few dark yellowish brown (10YR 3/4) krotovinas; few thin (0.1-0.3mm thick); argillans, light olive brown (2.5Y 5/4) around coarse sand grains and rocks; few mangans, black (7.5YR 2/0) occur as coating around rocks; 5-10% coarse fragments; gradual smooth boundary.
BE	48-58	Light olive brown (2.5Y 5/4) fine sandy loam; weak to moderate medium subangular blocky with weak fine platy; friable to slightly firm (less than 10%); few medium and fine roots occurring primarily with few dark yellowish brown (10YR 3/4) krotovinas; few thin argillans, light olive brown (2.5Y 5/4) around coarse sand grains and rocks; less developed argillan associated with ped faces; faint fine few reddish yellow (7.5YR 6/8) mottles; 5-10% coarse fragments; clear smooth boundary.

- 2Btx1 58-74 Light olive brown (2.5Y 5/4 to 2.5Y 5/5) fine sandy loam matrix; moderate medium platy with overprinted coarse prismatic; firm to very firm and brittle; bleached prism faces (BPF), light brownish gray (2.5Y 6/2) 2-8cm wide with strong brown (7.5YR 5/8) ferrans 1-4mm wide adjacent to them; common light olive brown (2.5Y 5/4) argillans 0.3mm-0.7mm thick on peds, grains and coarse fragments; few fine distinct mottles, brown to dark brown (7.5YR 4/4); few fine roots occurring primarily along the BPF; BPF 40-60cm apart; 10-20% coarse fragments; clear smooth boundary.
- 2Btx2 74+ As 2Btx1 but: argillans up to 1mm; matrix light olive brown to grayish brown (2.5Y 5/4 to 2.5Y 5/3) fine sandy loam; few lenticular mottles, strong brown (7.5YR 5/8) exteriors with light olive brown (2.5Y 5/4) interiors; very firm and brittle; BPF 50-60cm apart; few faint fine strong brown mottles (7.5YR 5/6); coarse fragments up to 20%.

Soil: Woodbridge

Location: Buck Hill, Camp Marshall, Worcester County Conservation District, Worcester County, Spencer, Massachusetts

Drainage: Moderately well drained

Slope, aspect: 8%, West

Position: Mid-slope of a drumloidial ridge

Landuse: Abandoned pasture with regrowth of grass, low and high bush blueberries, young white pine and red maple

Horizon	Depth (cm)	Description
Ap	0-20	Dark brown (10YR 3/3) loam; moderate medium granular; friable to loose; many fine roots; common medium and coarse roots; 1-3cm lenses of very dark brown (10YR 2/2) discontinuous; 1 to 3% coarse fragments; abrupt irregular boundary.
Bw1	20-30	Dark yellowish brown (10YR 4/6) loam; weak fine subangular blocky to weak fine granular; friable to loose; common fine roots; few medium roots both primarily occur in common coarse dark brown (10YR 3/3) krotovinas; very fine yellowish brown (10YR 5/4) argillans irregularly coating grains; few fine faint yellowish brown (10YR 5/4) mottles.
Bw2	30-48	Yellowish brown (10YR 5/5) fine sandy loam; moderate coarse subangular blocky; friable; common fine roots occurring in few coarse dark yellowish brown (10YR 3/4) krotovinas; fine yellowish brown (10YR 5/4) argillans on sand grains and some peds; few fine faint yellowish brown (10YR 5/8) mottles; few medium distinct light brownish gray and grayish brown (2.5Y 6/2 and 2.5Y 5/2) mottles; 10% coarse fragments; gradual smooth boundary.

- 2Bx1 48-61 Olive brown (2.5Y 4/4) loamy fine sand; moderate medium subangular block with secondary weak thin platy , overprinted by coarse prismatic; firm to very firm and brittle; limited to very dark brown (10YR 2/2) krotovina only at top of horizon; few fine roots confined to Bleached Prism Faces (BPF); BPF is grayish brown (2.5Y 5/2) with yellowish brown (10YR 5/6) ferran (1-3mm thick) at boundary; BPF 2-10cm wide, 40-70cm apart; few fine faint argillans on peds, grains and rocks; undersides of rocks is grayish brown (2.5Y 5/2) and may extend 2-5cm below rock; 15% coarse fragments; gradual smooth boundary.
- 2Bx2 61+ Olive brown (2.5Y 4/4) fine sandy loam; Structure, consistency, and BPF are the same as 2Brl; argillans are as in 2Brl but more developed (i.e. thicker); few fine distinct dark yellowish brown (10YR 4/6) mottles; common fine faint grayish brown (2.5Y 5/2) mottles; 20% coarse fragments.

Water table at 97 cm (8/85)

Soil: Ridgebury

Location: Buck Hill, Camp Marshall, Worchester County Conservation District, Worchester County, Spencer, Massachusetts

Drainage: Somewhat poorly drained

Slope, aspect: 3%, Southwest

Position: Toe-slope; seasonal drainage way

Landuse: Woodland including red maple, red oak, beech, ferns, and skunk cabbage

Horizon	Depth (cm)	Description
Oa	2.5-0	Black (10YR 2/1 rubbed); highly decomposed leaf litter; many fine, medium and coarse roots; irregular gradual boundary.
A	0-11	Very dark grayish brown (2.5Y 3/2) fine sandy loam; weak medium granular; loose; many fine, medium, and coarse roots; few 3mm dia. brown to dark brown (10YR 4/3) krotovina; common medium distinct strong brown (7.5YR 5/6) mottles; 3% coarse fragments; clear irregular boundary.
Bw	11-23	Light olive brown (2.5Y 5/4) fine sandy loam; weak fine subangular blocky; friable to firm (25%); common fine roots occurring in very dark grayish brown (2.5Y 3/2) krotovinas; common large faint grayish brown (2.5Y 5/2) mottles; few faint fine dark yellowish brown (10YR 4/6) mottles; few fine grayish brown (2.5Y 5/2) argillans on sand grains; 15% coarse fragments; gradual smooth boundary.
Bx1	23-46	Grayish brown (2.5Y 5/2) fine sandy loam; weak fine subangular blocky to weak thin platy overprinted by coarse prismatic; firm to vry firm and brittle; few fine roots confined to bleached prism faces (BPF); BPF of light olive gray (5Y 6/2) center with dark yellowish brown (10YR 4/6) ferrans at boundary; ferran 2-4mm thick; BPF 3-10cm wide and 40-60cm apart; common argillans 0.3-0.7mm thick on peds, grains, and rocks; silt caps common; few very dark brown (10YR 2/2) krotovinas at top of horizon; 20% coarse fragments; gradual smooth boundary.

Bx2 46+ Grayish brown (2.5Y 5/2) loamy sand; same as Bx1 except: no krotovina; common ferran, fine to medium, dark yellowish brown (10YR 4/6 and 10YR 3/6); common fine distinct, light gray to gray (2.5Y 6/0) mottles; ferrans may surround light gray to gray mottles (2.5Y 6/0); 25% coarse fragments.

Water table at 30cm (8/85)

Soil: Woodbridge

Location: Orchard Hill, University of Massachusetts, Hampshire
County, Amherst, Massachusetts

Drainage: Moderately well drained

Slope, aspect: 5%, East

Position: Mid-slope 100 meters from summit of drumlin

Landuse: Abandoned orchard, first stage regrowth including poison
ivy, gray birch, and grass

Horizon	Depth (cm)	Description
---------	------------	-------------

Ap	0-30.5	Very dark grayish brown (10YR 3/2) very fine sandy loam; weak medium granular structure; loose to friable; few worm cast, very dark gray (10YR 3/1); common medium to fine roots; 2-5% coarse fragments; abrupt wavy boundary.
----	--------	--

Bw1	30.5-53	Dark yellowish brown (10YR 4/4) fine sandy loam; weak medium granular to weak fine subangular blocky structure; friable; common krotovina (worm holes), very dark gray and very dark brown (10YR 3/1 and 10YR 2/2); few fine distinct mottles, strong brown (7.5YR 5/8); common fine and medium roots; fine roots are concentrated within the krotovinas; 5-10% coarse fragments; gradual wavy boundary.
-----	---------	--

Bw2	53-74	Yellowish brown (10YR 5/4) fine sandy loam; weak fine to medium subangular blocky; common krotovina, very dark gray(10YR 3/1); friable; few medium distinct mottles, strong brown and light yellowish brown (7.5YR 5/8, 7.5YR 5/6, and 10YR 6/4); few fine mangans coating peds and coarse fragments predominantly on the top of the feature, black (7.5YR 2/0); few fine to very fine argillans, light yellowish brown (10YR 6/4) occur around coarse fragments; few fine roots occurring mainly in or adjacent to krotovina; some roots show neo albans around them, light gray (10YR 7/2); 10-15% coarse fragments; gradual wavy boundary.
-----	-------	---

BE	74-94	Dark yellowish brown (10YR 4/6) fine sandy loam; weak medium subangular blocky; few krotovina, very dark gray (10YR 3/1); friable with 10-20% firm peds; common medium distinct mottles, strong brown and dark yellowish brown (7.5YR 5/8, 7.5YR 5/6, and 10YR 4/6); few fine mangans occurring mainly on tops of features, black (7.5YR 2/0); few medium reticulated or complex mottled bands 4-12mm in cross section; center of mottled area is grayish brown (2.5Y 5/2), outer edges are strong brown (7.5YR 5/8); few uncoated grains are visible adjacent to voids (skeletans); few fine to very fine argillans, light yellowish brown (10YR 6/4); few fine roots commonly associated with krotovina and with fine light gray (10YR 7/2) neo albans; 10-15% coarse fragments; clear smooth boundary.
2Btx1	94-122	Light olive brown (2.5Y 5/4) fine sandy loam; weak fine subangular blocky to weak medium platy; overprinted by a very coarse prismatic polygonal structure; very firm and brittle; 10% friable material present located between prisms; common medium distinct mottles, strong brown (7.5YR 5/8 and 7.5YR 5/6); bleached prism faces (BPF), grayish brown (2.5Y 5/2) 10-40mm wide with strong brown (7.5YR 5/8) at matrix boundary 2-10mm wide; the BPF do not occur regularly and at times are difficult to trace. They occure between 20 and 60cm apart and are vertically oriented. Common argillans up to 0.5mm thick and light yellowish brown (10YR 6/4); few fine roots confined to BPF; 15% coarse fragments; gradual smooth boundary.
2Btx2	122+	Grayish brown to light olive brown (2.5Y 5/3) fine sandy loam; weak medium platy; overprinted by very coarse polygonal prismatic structure; very firm and brittle; few medium distinct mottles, strong brown (7.5YR 5/6 and 7.5YR 5/8); polygons well expressed; BPF light brownish gray to light gray (2.5Y 6/2 to 2.5Y 7/2), up to 40mm wide; edges 5-15 mm and strong brown (7.5YR 5/8); BPF 40-60cm apart. Beneath coarse fragments neo albans form, light brownish gray (2.5Y 6/2); argillans common up to 1mm thick and light olive brown (2.5Y 5/4); fine roots are rare and occur only in BPF; 15-25% coarse fragments ranging from rounded to angular.

Water table at 150 cm (5/85)

Soil: Ridgebury

Location: Orchard Hill, University of Massachusetts, Hampshire
County, Amherst, Massachusetts

Drainage: Poorly drained

Slope, aspect: 3%, East

Position: Toe-slope at edge of wetland

Landuse: Abandoned orchard and pasture area adjacent to wetland,
vegetation includes gray birch, high bush blueberries, and
grass

Horizon	Depth (cm)	Description
Ap	0-21	Very dark gray (10YR 3/1) very fine sandy loam matrix; massive to weak coarse angular blocky; friable; many coarse, medium fine roots; common medium distinct light yellowish brown (2.5Y 6/4) and common medium distinct strong brown (7.5YR 5/6) mottles; krotovina extend into Bw making boundary irregular yet abrupt.
Bw	21-40	Light yellowish brown (2.5Y 6/4) and light olive brown (2.5Y 5/4) loam matrix; weak coarse subangular blocky; friable; many coarse and fine roots, few medium roots; common 2-5 cm. diameter very dark gray (10YR 3/1) and very dark grayish brown (10YR 3/2) krotovina; common medium gray (5Y 6/1) and gray (5Y 5/1) mottles; some mottles associated with root channels and voids (neoalbans); few small strong brown (7.5YR 5/6) mottles (quassiferrans in some cases); 2% coarse fragments; gradual smooth boundary.
Bgl	40-52	Greenish gray (5GY 6/1) to greenish gray (5G 6/1) silt loam matrix; weak coarse subangular blocky; friable; many fine roots; common very dark gray (10YR 3/1) 2-5 cm. diameter krotovina; common neo- and quassiferrans yellowish brown (10YR 3/1) may occur in bands; common medium olive yellow (2.5Y 6/6) mottles; few gray (5Y 6/1) neoalbans; few thin argillans; less than 1% coarse fragments; silt; irregular gradual boundary.

Bg2	52-76	Gray (5Y 6/1) loamy sand matrix; massive; few fine roots; few large grayish brown and dark yellowish brown (2.5Y 5/2 and 10YR 4/6) mottles, may occur in bands up to 5 cm. thick and 20 to 50 cm. long, wavy and sandier than surrounding areas; 10 to 15% coarse fragments; few pockets of cemented sand dark brown (7.5YR 4/4); coarse fragments are rounded, some are gussified; gradual wavy boundary.
2Bw	76-90	Light olive brown (2.5Y 5/4) loamy sand matrix; massive; slightly firm; very few fine roots; 10% of horizon is cement with iron dark brown (7.5YR 4/4); sandier than Bg2; 15% coarse fragments mostly rounded; common medium to large black (5YR 2.5/1), dark reddish brown (5YR 2.5/2), and red (2.5YR 5/8) mottles; some rock fragments coated with manganese; clear wavy boundary.
2BCm	90-102	Overall matrix dark yellowish brown (10YR 4/6) sand; massive; hard cemented; 30-50% rounded coarse fragments; many fragments manganese coated; few gussified fragments; other colours present with the horizon as discontinuous bands include black (N 2.5/0), reddish black (5YR 2.5/2), yellowish red (5YR 5/6), and reddish yellow (7.5YR 6/8); abrupt wavy boundary.
3Cd1	102-144	Dark brown (10YR 3/3) loamy sand; weak coarse angular blocky; slightly firm; few fine roots with neobands light brownish gray (10YR 6/2) commonly associated with the root channels; common vesicles 0.25-0.75mm. diameter; few fine argillans dark yellowish brown (10YR 3/4); few fine dark reddish brown (5YR 3/3) mottles; 7% angular coarse fragments; gradual; smooth boundary.
3Cd2	144-160	Dark yellowish brown (10YR 4/4) fine sandy loam; massive; slightly firm; few fine roots with yellow (2.5Y 7/6) areas around them; common fine to medium olive brown (2.5Y 4/4), olive yellow (2.5Y 6/6), and dark reddish brown (5YR 3/3) mottles; separated below by a non-continuous, thin (2 cm.), dark reddish brown (5YR 3/3) band; clear wavy boundary.

3Cd3	160-175	Olive brown (2.5Y 4/4) loamy sand; massive; soft due to moisture; few large dark reddish brown (5YR 3/3) and olive yellow (2.5Y 6/6) mottles, 5% coarse fragments, mainly angular; abrupt wavy boundary.
4Cm	175-187	Black (5Y 2.5/0) loamy coarse sand matrix; massive; hard cemented; sandy gravel; 50% coarse fragments mainly rounded; cemented bands 5 by 10 cm. reddish black (5R 2.5/1), yellowish red (5Y 5/6), and reddish yellow (7.5YR 6/8); iron and manganese cement; few grussified rocks; abrupt smooth boundary.
5Cd4	187-220	Yellowish red (5YR 4/6) loamy sand; weak to moderate coarse platy; firm; banded horizontally with noncontinuous 0.2 to 1 cm. thick and up to 1 m long yellowish red (5YR 5/8), reddish yellow (5YR 6/8), red (2.5YR 5/8), yellowish brown (10YR 5/8), and iron stains; sandier layers less abundant dark reddish brown (2.5YR 3/4); 10% angular coarse fragments; abrupt smooth boundary.
5Cd5	220-250+	Light gray (N 7/0) to gray (5Y 6/1) loamy sand matrix; moderate coarse platy; firm; strong brown (7.5YR 5/6) and yellowish brown (10YR 5/8); iron stains on plates.

Soil: Ridgebury (as described by M. Reed, 1985, personal communication)

Location: Horticultural Research Center, University of Massachusetts, Hampshire County, Belchertown, Massachusetts

Drainage: Somewhat poorly drained

Slope, aspect: 3%, West

Position: Foot-slope

Landuse: Apple orchard, 30 year old trees, grass

Horizon	Depth (cm)	Description
Ap	0-22	Very dark grayish loam (10YR 3/2); weak to medium coarse platy, breaking up to weak fine to medium granular structure; friable to firm; common, very fine to medium roots; abrupt wavy boundary.
Bw1	22-37	Yellowish brown loam (10YR 5/6); common fine to medium distinct strong brown (7.5YR 5/8) and few to common fine prominent red (2.5YR 4/8) mottles; weak coarse subangular blocky structure; friable; common (in matrix) to many (in krotovinas) very fine to fine roots; 3-5% coarse fragments; common medium to coarse (5-25mm) tubular very dark grayish brown (10YR 3/2) krotovinas extend downwards from Ap horizon, through the B horizons where they are common, to the top of the BTR, where they are few; common very fine to medium pores (0.5 to 3.0mm); gradual wavy boundary.
Bw2	37-51	Light olive brown loam (2.5Y 5/5); many medium to coarse prominent strong brown (7.5YR 5/8); and common medium faint grayish brown (2.5Y 5/3) mottles (first occurrence of these at 33cm.); mottling increases markedly just above lower horizon; massive in place parting to weak fine to medium subangular blocky structure; friable; roots and pores same as in Bw1; some larger (40mm) krotovinas present, two of which run laterally on top of the lower horizon; 5% coarse fragments; abrupt wavy boundary.

2Br (2BE)	51-88	<p>Ligth olive brown fine sandy loam (2.5Y 5/4); interstratified with many lenses of coarser textured brown (7.5YR 4/5) and finer textured greenish gray (5GY 5/1) materials in nearly equal proportions (25-30% each); massive in place parting to discontinuous medium coarse lenticular structure; firm to very firm when moist, very hard and often brittle when dry; few very fine roots limited to top 8cm.; 8-10% coarse fragments; common very fine to fine vesicles and bands of interconnected vughs at top part of horizon, tapering off in occurrence with depth; few distinct clay skins in vertical channels; gray streaks begin near the top of this horizon forming distinct polygons with depth; abrupt smooth boundary.</p>
2Btr (2Btx1)	88+	<p>Olive (5Y 5/3) fine sandy loam; coarse prominent strong brown (7.5YR 5/8) quasiferrans about coarse (5-15mm) prominent, branched greenish gray (5GY 6/1) polygons spaced approximately 60cm. apart; massive in place parting to moderately coarse platy when dry; very firm when moist, extremely hard and noticeably brittle when dry; common distinct argillans about vesicles and vughs; vesicles are common very fine to fine occurring randomly or in horizontal bands as do less common interconnected vughs (with argillans), less dense occurrences of vesicles and vughs (lacking argillans); 6-7% coarse fragments, appearing more highly weathered than those in overlying horizons; no roots or krotovinas.</p>

Location: Leicester

Depth in meters	Description
--------------------	-------------

Upper Till

- | | |
|---------|--|
| 0-1.0 | Overlying soil. |
| 1.0-3.0 | Loose to slightly hard in pockets, sandy, stoney, light yellowish brown (2.5Y6/4) till with bands and lenses of sandier or siltier material ranging from a few millimeters to tens of centimeters in thickness; some appear to have undergone post-depositional folding and faulting; coarse fragments are matrix supported. |
| 3.0-4.0 | Hard, sandy, stoney, light yellowish brown (2.5Y6/4) till with few light gray (2.5Y7/2) mottles; common bands up to 10 cm thick of siltier material commonly contorted due to post-depositional folding and faulting; coarse fragments are matrix supported and are less numerous than in the till above. |

Lower Till

- | | |
|---------|---|
| 0-1.5 | Fissile olive (5Y4/4) oxidized till with dark reddish brown (5YR3/3) staining on the plate surfaces; common subvertical joints dipping 30 to 45 degrees south; other subvertical joints with no consistent dip are common; some joint surfaces are stained with brown (7.5YR4/4) iron oxide stains; thin clay skins on some plates and coating some pebbles; few discontinuous sand veins ranging from subhorizontal to subvertical; coarse fragments are matrix supported. |
| 1.5-2.0 | Massive olive (5Y4/3) oxidized till with minor fissility; south dipping joints shallow and pinch out; other joints still common along with sand veins and dikes, some stained with brown (7.5YR4/4) iron oxide; coarse fragments are matrix supported; lower boundary is marked by an abrupt color change indicating a transition from the oxidized Lower Till to the unoxidized Lower Till. |
| 2.0-3.0 | Massive gray (5Y5/1) unoxidized till with common joints, few stained with brown (7.5YR4/4) iron oxide; matrix supported coarse fragments. |

3.0-5.0+ Massive gray (5Y5/1) to light olive gray (5Y6/2) unoxidized till with common joints; common silt and sand beds a few millimeters to centimeters thick laterally continuous and contorted due to post-depositional folding and faulting; matrix supported coarse fragments.

Location: Ayer

Depth
in meters

Description

Upper Till

- 0-1.0 Canton and/or Montauk soil series overlies the deposit.
- 1.0-2.5 Loose to slightly hard in pockets, sandy, stoney, light brownish gray (2.5Y6/2) till with bands and lenses of sandier water worked (well sorted and laminated) material up to 40 cm thick; coarse fragments are subrounded to subangular and matrix supported.
- 2.5-4.5 Firmer, sandy, stoney, pale olive (5Y6/4) till with light brownish gray (2.5Y6/2) bands several cm thick of sandier or siltier material commonly laminated and dipping 5-10 degrees to the west; coarse fragments are subrounded to subangular and matrix supported.

Lower Till

- 0-2.0 Fissile olive (5Y4/3) oxidized till with dark reddish brown (5YR3/4) staining on the plate surfaces; common subvertical joints some with fine sand on the joint surface; thin clay skins on some plates and coating some pebbles; coarse fragments are matrix supported.
- 2.0-3.0 Fissile, dense olive (5Y4/3) oxidized till with dark reddish brown (5YR3/4) staining on plates; joints common with sand veins and dikes, some stained with brown (7.5YR4/4) iron oxide; few olive (5Y5/4) sand veins up to 2 cm thick and clustered in groups of alternating veins up to 40 cm thick; most of these beds are slightly to extremely deformed; coarse fragments are matrix supported.
- 3.0-10.0 Massive olive (5Y4/3) oxidized till with joints, few stained with brown (7.5YR4/4) iron oxide; sand veins common as described in the overlying unit although they are more prevalent; matrix supported coarse fragments.
- 10.0-12.0 Massive olive (5Y4/4) oxidized till with few joints; sand veins common as described in the overlying unit although they are more prevalent; matrix supported coarse fragments; lower boundary is marked by a gradual transition from the oxidized till to the unoxidized till.

- 12.0-17.0 Massive olive gray (5Y4/2) with few widely spaced joints some with very fine sand along them; common olive gray (5Y5/2) to pale yellow (5Y7/4) sand and clay veins up to 2 cm thick and clustered in groups of alternating veins up to 60 cm thick spaced up to 1 m apart; most of these beds are slightly to extremely deformed; coarse fragments are matrix supported.
- 17.0-21.0 Massive olive gray (5Y4/2) with very few widely spaced joints some with very fine sand along them; common olive gray (5Y5/2) to pale yellow (5Y7/4) sand and clay veins up to 2 cm thick and clustered in groups of alternating veins up to 60 cm thick spaced up to 50 cm apart; most of these beds are slightly to extremely deformed; few coarse fragments coated with dark reddish brown (5YR3/4) stains; coarse fragments are matrix supported.
- 21.0-21.7 Slightly compacted light olive brown (2.5Y5/4) medium to coarse sand; the sand is saturated; common fine grained olive gray (5Y5/2) dikes cross cut the horizon; few coarse fragments present.
- 21.7-25+ Massive dark gray (5Y4/1) to dark greenish gray (5GY4/1) with few widely spaced joints; few olive gray (5Y5/2) to pale yellow (5Y7/4) sand and clay veins up to 2 cm thick and clustered in groups of alternating veins up to 60 cm thick spaced up to 2 m apart; most of these beds are slightly to extremely deformed; coarse fragments are matrix supported.

Location: Barre

Depth in meters	Description
--------------------	-------------

Upper Till

0-1.0	Loose, sandy, stoney, gray (2.5Y6/0) till; coarse fragments are subrounded to subangular and matrix supported.
-------	--

Lower Till

0-1.0	Fissile light olive brown (2.5Y5/4) oxidized till with dark reddish brown (5YR3/4) staining on the plate surfaces; common subvertical joints with fine sand along joint planes; thin clay skins on some plates and coating some pebbles; coarse fragments are matrix supported.
1.0-4.0	Fissile, dense olive brown (2.5Y4/4) oxidized till with dark reddish brown (5YR3/4) staining on some plates; joints common with pale yellow (5Y 7/4) sand veins and dikes, some stained with brown (7.5YR4/4) iron oxide; few olive (5Y5/6) sand veins up to 2 centimeters thick and clustered in groups of alternating veins up to 40 centimeters thick; some of these beds are slightly to extremely deformed; matrix supported subangular coarse fragments; lower boundary is marked by a gradual transition from the oxidized till to the unoxidized till.
4.0-9.0+	Massive dark gray (5Y4/1) with few widely spaced joints some with very fine sand along them; common olive gray (5Y5/2) to pale yellow (5Y7/4) sand and clay veins up to 15 centimeters thick and clustered in groups of alternating veins up to 60 centimeters thick spaced up to 1 meter apart; most of these beds are slightly to extremely deformed, the deformation may have resulted in the overthickening of sandier layers; some groups of beds are parallel to others; coarse fragments are matrix supported.

Location: Buckland: Lower Till

Depth in meters	Description
0-3.0+	Massive dark greenish gray (5GY4/1) to dark gray unoxidized till with numerous shear planes oriented N 10 W to N 20 W, dipping 10-30 degrees S, a few dip 10 degrees N; shear planes are opened by running water yet matrix is unsaturated; smaller shears are present yet more difficult to see; slight thin slickensides appear on shear planes; coarse fragments seem to accumulate adjacent to shears and are matrix supported.

Location: Charlemont

Depth in Meters	Description
--------------------	-------------

Upper Till

- | | |
|----------|--|
| 0-1.2 | Sandy gravel outwash. |
| 1.2-2.2 | Sandy, massive olive (5Y4/3) sandy till; silt caps occur on the larger coarse fragments; 10% coarse fragments grussified; bands (horizontal) of iron stained till of yellowish brown (10YR 5/8) 2-4 mm thick occur at outwash-till interface; coarse fragments are matrix supported. |
| 2.2-3.0 | Sandy, massive olive (5Y4/3) slightly platy till; abundant silt caps; common sand lenses olive yellow (5Y 6/6); some sandier bands 1-5 mm thick are subvertical while others outline 2 cm plates in till; coarse fragments are matrix supported. |
| 3.0-4.0+ | Sandy, massive olive (5Y4/3-4) platy till; abundant silt caps; common olive yellow (5Y 6/6) sand lenses; many rocks grussified; coarse fragments are matrix supported. |

NOTES: coarse fragments increase with depth; most sand lenses in middle layer; boundaries very diffuse.

Lower Till

- | | |
|--------|--|
| 0-1.0+ | Massive dark greenish gray (5GY4/1) to dark gray unoxidized till with numerous shear planes; thin slickensides appear on shear planes; subangular coarse fragments are matrix supported. |
|--------|--|

APPENDIX C
PHYSICAL DATA

Coarse Fragment Data

Primary Pedons

Pedon 1

Horizon	Depth (cm)	%C.F.	19mm	8mm	4.75mm	2mm	B.D (Mg m ⁻³)
Ap	0-23	27.22	110.0	168.0	95.0	228.0	1.06
Bw1	23-34	32.85	84.7	219.0	141.8	335.6	1.24
Bw2	34-59	36.40	367.0	187.0	149.6	566.4	1.59
Bt	59-92	44.17	503.0	367.7	518.0	472.0	1.56
2Btx1	92-125	26.76	102.0	250.0	188.0	277.0	1.66
2Btx2	125-152	30.46	238.0	347.3	405.0	64.2	1.75
3BCm	152-194	50.78	587.0	539.0	555.0	967.0	1.73
4Cd1	194+	47.90	53.0	201.0	249.2	342.0	1.54
PCF	124	78.38	0.0	0.0	329.0	70.0	1.68

Pedon 2

Horizon	Depth (cm)	%C.F.	19mm	8mm	4.75mm	2mm	B.D (Mg m ⁻³)
Ap	0-14	11.64	69.3	27.6	8.4	13.7	0.93
Bw1	14-25	35.15	234.6	144.8	62.0	85.5	1.34
Bw2	25-39	27.20	173.4	173.8	88.2	147.6	1.48
BE	39-55	32.60	614.6	347.4	191.8	323.3	1.58
2Btx1	55-86	36.82	126.8	201.3	152.7	246.7	1.76
2Btx2	86-136	39.92	166.8	212.5	332.4	345.7	1.82
2BCd	136-160	32.98	69.0	135.4	326.3	299.8	1.77
3Cd1	160-183	39.34	282.4	370.2	181.7	203.4	1.65
3Cd2	183-210	45.41	598.2	325.1	231.2	314.1	1.66
3Cd3	210+	5.75	0.0	11.8	21.2	33.1	1.67
Sand	196.2	39.59	330.1	393.2	335.4	316.8	1.66

Pedon 3

Horizon	Depth (cm)	%C.F.	19mm	8mm	4.75mm	2mm	B.D (Mg m ⁻³)
Ap	0-20	15.60	0.0	57.2	18.1	47.8	1.13
Bw	20-37	19.22	0.0	96.6	30.7	53.4	1.52
BE	37-61	31.09	233.0	125.7	65.8	131.2	1.78
2Btx1	61-100	28.53	128.5	141.8	90.7	151.9	1.82
2Btx2	100-137	18.88	18.8	193.8	110.9	157.4	1.80
2BCd	137-183	32.00	312.0	181.7	121.4	201.1	1.76
3Cd1	183-216	33.18	354.8	328.6	190.3	264.6	1.77
3Cd2	216+	35.98	345.6	401.8	158.4	229.2	1.55

Pedon 4

Horizon	Depth (cm)	%C.F.	19mm	8mm	4.75mm	2mm	B.D (Mg m ⁻³)
Ap	0-25	10.43	39.8	35.9	28.0	40.2	1.25
Bw1	25-43	12.38	63.1	89.5	45.7	73.3	1.30
Bw2	43-57	11.68	19.7	67.9	25.3	52.2	1.43
BE	57-71	26.38	206.4	165.2	87.2	143.0	1.64
2Btx1	71-102	26.64	253.1	174.9	145.2	307.7	1.78
2Btx2	102-132	26.46	215.2	221.1	129.4	208.7	1.76
2BCd	132-169	28.73	250.0	306.0	126.2	204.8	1.63
3Cd	169+	29.52	337.1	215.2	109.2	190.2	1.63

Pedon 5

Horizon	Depth (cm)	%C.F.	19mm	8mm	4.75mm	2mm	B.D (Mg m ⁻³)
Ap	0-25	4.60	12.1	18.3	18.3	27.8	1.45
Bw	25-45	8.43	88.8	40.7	27.6	68.3	1.51
BE	45-60	10.54	22.6	77.5	29.2	71.7	1.54
2EB	60-81	18.78	25.3	88.6	126.3	186.4	1.80
2Btx1	81-130	10.54	26.5	64.0	55.8	152.6	2.10
2Btx2	130-184	16.86	189.6	85.7	53.0	148.2	2.14
2Cd1	184-229	17.63	118.3	272.1	184.2	384.9	2.06
2Cd2	229+	22.94	279.3	184.1	249.4	486.6	2.22
PCF		8.76	0.0	9.3	9.8	23.9	2.02/1.99

Secondary Sites

EHP

Horizon	Depth (cm)	%C.F.	19mm	8mm	4.75mm	2mm	B.D (Mg m ⁻³)
Ap	0-18	33.63	46.7	67.4	83.2	167.1	1.59
Bw1	18-30	25.72	45.2	76.5	60.9	180.5	1.77
Bw2	30-51	24.76	32.0	80.5	64.1	181.5	1.81
Bt	51-76	20.31	11.0	98.1	77.9	197.8	1.88
2Btx1	76+	25.16	77.8	48.7	50.7	140.6	1.97

EHW

Horizon	Depth (cm)	%C.F.	19mm	8mm	4.75mm	2mm	B.D (Mg m ⁻³)
Ap	0-23	18.80	22.9	28.8	22.4	75.1	1.40
Bw1	23-41	21.92	0.0	47.2	68.3	153.9	1.56
Bw2	41-56	21.70	133.7	53.8	74.7	262.6	1.58
2Btx1	56-76	22.16	128.5	73.0	51.6	206.4	1.71
2Btx2	76+	20.49	24.3	57.8	99.0	326.2	1.86

EHR

Horizon	Depth (cm)	%C.F.	19mm	8mm	4.75mm	2mm	B.D (Mg m ⁻³)
Ap	0-25	16.49	0.0	43.1	25.4	53.7	1.24
Bw1	25-41	16.11	36.6	56.7	38.8	101.5	1.30
BE	41-56	13.49	0.0	28.3	56.8	216.3	1.47
2Bx1	56-66	20.70	27.1	79.8	139.1	182.8	1.61
2Bx2	66+	15.13	75.6	37.7	24.8	97.4	1.78

EHDP2

Horizon	Depth (cm)	%C.F.	19mm	8mm	4.75mm	2mm	B.D (Mg m ⁻³)
Ap	0-25	20.45	116.0	78.0	51.0	165.0	1.09
Bw1	25-38	0.00	0.0	0.0	0.0	0.0	1.51
Bw2	38-50	18.57	0.0	71.9	97.8	330.0	1.50
BE	50-78	0.00	0.0	0.0	0.0	0.0	1.62
2BCx	78-108	16.85	0.0	100.0	103.6	403.3	1.60
3BCm	108+	35.36	165.7	262.4	235.0	580.9	1.69

EHDP3

Horizon	Depth (cm)	%C.F.	19mm	8mm (in grams)	4.75mm	2mm	B.D (Mg m ⁻³)
Ap	0-24	10.80	42.0	5.0	33.0	107.0	1.09
Bw1	24-37	36.94	245.1	217.4	181.8	364.9	1.34
Bw2	37-63	76.97	440.0	180.0	170.0	383.0	1.32
2BCd	63-96	51.22	735.0	545.0	500.0	930.2	1.71
3BCm	96-138	61.90	1990.0	581.0	380.1	354.0	1.30
4Cr	138+	68.41	63.0	61.0	49.0	76.0	--

BHP

Horizon	Depth (cm)	%C.F.	19mm	8mm (in grams)	4.75mm	2mm	B.D (Mg m ⁻³)
Ap	0-20	21.02	38.6	65.0	24.4	64.0	0.93
Bw1	20-36	26.54	80.8	83.7	46.6	65.8	1.36
Bw2	36-48	22.64	61.4	89.9	51.8	93.0	1.48
BE	48-58	36.62	221.3	116.3	42.6	109.3	1.56
2Btx1	58-74	37.26	172.0	163.7	91.2	135.7	1.86
2Btx2	74+	26.11	136.8	124.3	109.3	211.1	1.95

BHW

Horizon	Depth (cm)	%C.F.	19mm	8mm (in grams)	4.75mm	2mm	B.D (Mg m ⁻³)
Ap	0-20	30.81	148.6	158.2	53.1	148.7	1.25
Bw1	20-30	33.96	239.0	116.1	91.0	158.7	1.32
Bw2	30-48	27.55	95.8	105.4	94.9	158.5	1.46
2Bx1	48-61	43.45	649.0	207.9	178.5	228.5	1.75
2Bx2	61+	38.66	406.9	298.7	273.7	106.7	1.80
PCF		8.76	0.0	8.7	6.1	12.8	

BHR

Horizon	Depth (cm)	%C.F.	19mm	8mm (in grams)	4.75mm	2mm	B.D (Mg m ⁻³)
A	3-11	20.54	26.1	55.7	19.5	34.9	1.20
Bw	11-28	16.54	50.5	58.0	37.8	102.9	1.41
Bx1	28-46	17.88	38.0	111.7	148.8	288.0	1.85
Bx2	46+	26.94	30.8	116.3	193.5	303.6	2.10
PCF		13.11	0.0	30.9	29.3	62.2	--

OHW

Horizon	Depth (cm)	%C.F.	19mm	8mm (in grams)	4.75mm	2mm	B.D (Mg m ⁻³)
Ap	0-31	12.97	62.5	30.5	14.1	40.0	1.23
Bw1	31-53	38.48	498.1	128.6	113.5	281.2	1.39
Bw2	53-74	20.71	321.2	159.7	100.7	186.5	1.68
BE	74-94	19.91	206.9	78.7	28.0	171.2	1.64
2Btx1a	94-107	26.55	331.3	170.8	93.5	174.1	1.63
2Btx1b	107-122	28.74	223.5	223.1	151.6	275.3	1.84
2Btx2a	122-137	40.35	828.9	173.9	86.8	292.8	1.97
2Btx2b	137+	44.08	1610.0	392.2	211.5	408.2	1.87

OHL

Horizon	Depth (cm)	%C.F.	19mm	8mm (in grams)	4.75mm	2mm	B.D (Mg m ⁻³)
Ap	0-21	3.88	0.0	36.8	11.4	29.7	0.99
Bw	21-40	0.21	0.0	4.8	0.0	2.0	1.28
Bg1	40-52	3.87	33.7	13.1	37.9	54.7	1.70
Bg2	52-76	18.94	66.3	385.8	180.2	251.5	1.88
2Bw	76-90	41.14	828.5	431.8	259.6	396.6	1.76
2Bcm	90-102	43.63	638.9	515.3	219.6	316.3	1.75
3Cd1	102-144	32.76	717.7	525.2	209.3	269.3	1.76
3Cd2	144-160	20.52	360.8	276.4	121.3	207.3	1.74
3Cd3	160-175	21.67	363.8	337.7	146.8	262.7	1.79
4Cm	175-187	26.11	238.6	256.8	158.7	243.4	1.62
5Cd4	187-220	24.08	324.0	244.4	169.0	277.3	1.66
5Cd5	220+	17.51	29.7	93.8	37.0	55.8	--

BTR/S

Horizon	Depth (cm)	%C.F.	19mm	8mm (in grams)	4.75mm	2mm	B.D (Mg m ⁻³)
Ap	0-18	2.45	0.0	5.8	13.0	34.0	1.30
Bw1	18-46	10.32	0.0	101.0	81.3	186.6	1.46
Bw2	46-71	9.23	21.3	56.0	72.7	172.6	1.45
2BE a	71-81	13.97	76.7	134.4	132.0	214.2	1.91
2BE b	81-91	12.71	11.2	97.8	104.8	174.1	2.05
2Btx1a	91-102	11.10	19.7	85.7	83.9	173.8	2.15
2Btx1b	102+	7.40	57.1	65.2	37.6	96.3	2.21
BPF	85	9.19	0.0	14.2	12.3	21.3	--

BTR

Horizon	Depth (cm)	%C.F.	19mm	8mm (in grams)	4.75mm	2mm	B.D (Mg m ⁻³)
2Btx1a	91	5.38	15.4	58.3	40.9	86.7	1.94
2Btx1b	107	13.98	56.8	38.2	37.9	82.1	1.99
2Btx2a	122	9.25	44.5	34.3	23.6	51.4	1.95
2Btx2b	137	7.61	14.5	93.3	55.1	111.3	1.92
BPF	115	3.79	0.0	12.7	20.6	51.0	1.85

Fine Earth Fraction

Primary Pedons

Pedon 1

Hori.	Depth (cm)	VC	C	Sand M	F	VF	Total Sand	Silt C	F	Clay	Tex. USDA
Ap	0-23	6.05	8.98	11.85	18.19	14.10	59.17	12.83	14.06	13.95	FSL
Bw1	23-34	4.20	7.37	11.18	17.84	14.07	54.66	18.20	15.00	12.15	FSL
Bw2	34-59	5.28	8.22	11.37	18.53	13.23	56.63	9.99	17.94	15.44	FSL
Bt	59-92	3.85	6.62	9.11	15.85	13.69	49.12	14.94	16.50	19.45	FSL
2Btx1	92-125	5.77	7.06	9.22	15.02	11.04	48.11	16.14	12.90	22.86	L
2Btx2	125-152	4.79	7.54	10.03	15.91	10.15	48.42	15.83	14.58	21.18	L
3BCm	152-194	12.46	18.34	19.40	21.41	9.70	81.31	4.29	6.01	8.40	CS
4Cd	194+	4.10	5.58	7.70	20.33	14.01	51.72	14.19	15.14	18.95	FSL

Pedon 2

Hori.	Depth (cm)	VC	C	Sand M	F	VF	Total Sand	Silt C	F	Clay	Tex. USDA
Ap	0-14	2.75	7.19	11.29	23.49	12.13	56.85	30.15	19.83	13.00	FSL
Bw1	14-25	5.78	8.34	12.21	21.88	10.76	58.97	15.78	15.01	10.25	FSL
Bw2	25-39	5.40	8.95	13.30	26.28	7.40	61.33	14.60	16.42	7.66	FSL
BE	39-55	5.22	8.43	13.40	31.36	6.69	65.10	13.84	11.79	9.28	FSL
2Btx1	55-86	3.40	7.18	10.89	20.01	11.14	52.62	13.69	16.59	17.10	FSL
2Btx2	86-136	3.62	6.63	11.41	23.78	6.97	52.41	13.04	17.13	17.43	FSL
2BCd	136-160	4.21	7.77	12.13	25.46	7.33	56.90	12.47	14.03	16.60	FSL
3Cd1	160-183	4.64	6.91	10.33	20.42	10.44	52.74	19.20	13.58	14.49	FSL
3Cd2	183-210	4.56	7.25	11.51	21.57	8.24	53.13	16.28	13.83	16.77	FSL
3Cd3	210+	3.94	6.23	10.15	20.97	7.93	49.22	18.19	13.94	18.66	FSL
Sand	196	1.35	8.41	36.74	39.59	8.19	94.28	0.54	3.15	2.03	S
BPF	148	3.32	7.61	13.85	24.43	11.75	60.96	4.29	17.38	17.38	FSL

Pedon 3

Hori.	Depth (cm)	VC	C	Sand M	F	VF	Total Sand	Silt C	F	Clay	Tex. USDA
Ap	0-20	2.26	5.85	10.08	16.28	17.50	51.97	21.23	16.88	9.93	FSL
Bw	20-37	5.46	8.18	11.82	17.35	15.77	58.58	13.90	18.42	9.11	FSL
BE	37-61	5.55	10.84	14.22	19.25	11.39	61.25	14.72	15.53	8.51	FSL
2Btx1	61-100	5.89	10.94	13.98	19.11	9.85	59.77	15.86	14.08	10.29	FSL
2Btx2	100-137	5.28	9.42	13.38	18.92	9.89	56.89	17.03	14.82	11.27	FSL
2BCd	137-183	5.52	10.64	13.70	18.57	8.78	57.21	15.99	14.46	12.34	FSL
3Cd1	183-216	4.50	10.03	14.18	18.59	8.56	55.06	16.33	13.86	13.96	FSL
3Cd2	216+	5.50	9.61	12.73	16.73	7.06	51.63	17.89	14.79	15.69	FSL

Pedon 4

Hori.	Depth (cm)	VC	C	Sand M	F	VF	Total Sand	Silt C	F	Clay	Tex. USDA
Ap	0-25	1.94	4.55	7.71	12.43	15.93	42.56	27.22	16.56	13.67	FSL
Bw1	25-43	2.23	4.62	7.10	10.51	21.29	45.75	23.60	16.92	13.74	FSL
Bw2	43-57	2.68	5.10	8.01	13.98	19.69	49.46	24.21	14.04	12.30	FSL
BE	57-71	4.13	8.36	12.25	17.65	11.25	53.64	17.84	16.36	12.17	FSL
2Btx1	71-102	5.60	9.82	13.55	18.69	8.02	55.68	14.19	14.35	15.79	FSL
2Btx2	102-132	6.34	10.60	13.05	17.57	7.86	55.42	14.29	15.45	14.84	FSL
2BCd	132-169	5.99	10.72	12.87	18.13	6.54	54.25	15.19	14.88	15.69	FSL
3Cd	169+	5.86	10.97	13.30	17.06	7.14	54.35	12.86	17.41	15.39	FSL

Pedon 5

Hori.	Depth (cm)	VC	C	Sand M	F	VF	Total Sand	Silt C	F	Clay	Tex. USDA
Ap	0-25	2.30	5.52	10.65	20.21	13.55	52.23	23.76	13.75	10.27	FSL
Bw	25-45	2.09	5.78	10.95	21.44	19.70	53.43	26.39	10.25	9.35	FSL
BE	45-60	3.79	7.98	13.78	24.05	18.06	67.66	12.24	10.11	10.00	LS
2EB	60-81	3.05	7.45	15.00	23.48	15.63	64.61	10.63	13.19	11.57	LFS
2Btx1	81-130	3.44	8.99	15.76	22.52	12.07	62.78	13.97	13.06	10.20	LFS
2Btx2	130-184	3.29	8.20	15.58	24.16	11.24	62.47	15.74	14.59	7.20	FSL
2Cd1	184-229	3.56	8.35	15.02	23.38	15.07	65.38	13.90	14.61	6.11	LFS
2Cd2	229+	3.22	8.09	15.14	23.48	13.04	62.97	16.56	13.91	6.56	FSL
BPF		4.16	8.69	15.21	24.33	12.73	65.12	14.07	13.44	7.38	LFS

Secondary Sites

EHP

Hori.	Depth (cm)	VC	C	Sand M	F	VF	Total Sand	Silt C	F	Clay	Tex. USDA
Ap	0-18	6.27	8.53	11.39	13.61	19.90	59.70	13.32	16.09	10.89	FS
Bw1	18-30	6.43	7.74	10.96	13.21	18.50	56.84	8.71	17.75	16.70	FSL
Bw2	30-51	5.36	7.28	9.74	12.41	18.31	53.10	8.32	20.33	18.25	FSL
Bt	51-76	5.13	6.86	8.24	12.55	17.87	50.65	12.16	18.09	19.10	FSL
2Btx1	76+	5.37	7.14	9.48	11.13	16.90	50.02	12.76	16.11	21.11	L

EHW

Hori.	Depth (cm)	VC	C	Sand M	F	VF	Total Sand	Silt C	F	Clay	Tex. USDA
Ap	0-23	5.21	7.75	9.67	9.67	15.02	47.32	21.02	16.36	15.30	FSL
Bw1	23-41	6.80	8.73	10.74	12.36	18.09	56.72	19.66	13.86	9.76	FSL
Bw2	41-56	5.98	8.20	11.56	11.09	19.01	55.84	14.45	14.34	15.37	FSL
2Btx1	56-76	5.29	7.64	10.84	10.13	15.56	49.46	16.36	17.09	17.09	FSL
2Btx2	76+	5.03	7.86	10.68	10.76	18.35	52.68	17.16	12.07	18.09	FSL

EHR

Hori.	Depth (cm)	VC	C	Sand M	F	VF	Total Sand	Silt C	F	Clay	Tex. USDA
Ap	0-25	5.67	6.85	9.62	10.60	19.80	52.54	20.80	14.40	12.26	FSL
Bw1	25-41	4.54	6.15	8.81	10.39	21.34	51.23	26.59	16.37	5.81	FSL
BE	41-56	5.93	6.31	8.47	8.36	19.49	48.56	23.40	17.99	10.05	FSL
2Bx1	56-66	4.13	6.06	8.27	9.87	20.07	48.40	25.52	18.06	8.02	FSL
2Bx2	66+	3.83	4.78	8.67	10.54	22.65	50.47	23.90	16.40	9.23	FSL

EHDP2

Hori.	Depth (cm)	VC	C	Sand M	F	VF	Total Sand	Silt C	F	Clay	Tex. USDA
Ap	0-25	6.58	9.74	11.86	18.37	9.37	55.92	13.68	15.69	14.71	LS
Bw1	25-38	5.82	9.56	11.07	18.91	8.42	53.78	14.36	18.16	13.71	FSL
Bw2	38-50	5.70	9.61	12.54	20.74	7.85	65.44	12.85	15.08	13.64	LS
BE	50-78	6.80	10.95	15.44	24.82	6.40	64.41	9.44	13.69	12.46	LS
2BCx	78-108	5.11	10.93	15.29	22.77	7.60	61.70	12.07	11.23	15.01	LS
3BCm	108+	6.26	10.88	14.98	23.08	8.68	63.88	12.03	11.69	12.41	LS

EHDP3

Hori.	Depth (cm)	VC	C	Sand M	F	VF	Total Sand	Silt C	F	Clay	Tex. USDA
Ap	0-24	6.17	9.52	12.36	18.79	9.01	55.85	11.04	13.99	19.13	FSL
Bw1	24-37	6.13	10.47	12.81	18.92	7.86	56.19	14.84	13.70	15.28	FSL
Bw2	37-63	8.65	11.31	12.83	15.81	8.45	57.05	13.98	12.46	16.52	FSL
2BCd	63-96	6.90	10.57	12.60	22.43	14.82	67.32	14.13	9.12	9.44	LS
3BCm	96-138	9.76	14.44	14.40	19.21	9.36	67.17	23.22	13.38	9.62	SL

BHP

Hori.	Depth (cm)	VC	C	Sand M	F	VF	Total Sand	Silt C	F	Clay	Tex. USDA
Ap	0-20	4.38	6.07	10.55	12.78	18.87	52.65	17.34	17.37	12.64	FSL
Bw1	20-36	5.16	7.20	11.42	14.68	22.25	60.71	15.57	16.50	7.22	FSL
Bw2	36-48	5.33	7.96	12.69	14.58	21.01	61.57	14.85	16.40	7.18	FSL
BE	48-58	5.63	8.36	13.32	15.16	21.49	63.96	18.86	12.25	5.11	FSL
2Btx1	58-74	6.17	8.02	11.86	15.26	20.64	61.95	10.87	17.13	10.05	FSL
2Btx2	74+	4.18	6.31	10.21	13.63	17.71	52.04	14.79	18.09	15.08	FSL

BEV

Horiz	Depth (cm)	WC	C	Sand H	F	VF	Total Sand	Silt: C	F	Clay	Tex. USDA
Ap	0-20	5.22	6.94	10.77	13.48	17.80	54.51	9.01	15.65	20.84	L
Bw1	20-30	5.87	5.85	8.18	13.66	17.36	48.92	8.84	18.54	23.78	L
Bw2	30-48	4.29	6.52	10.30	13.20	17.77	51.98	11.24	18.38	18.39	FSL
2Bx1	48-61	4.66	7.18	10.68	20.21	16.15	58.98	11.61	17.96	11.15	LPS
2Bx2	61+	4.06	6.79	10.32	20.73	12.84	54.94	14.58	17.27	13.21	FSL
BPF		3.53	6.20	9.66	18.70	11.49	49.58	15.98	18.74	15.70	FSL

BCR

Horiz	Depth (cm)	WC	C	Sand H	F	VF	Total Sand	Silt: C	F	Clay	Tex. USDA
A	0-11	3.79	6.06	10.83	13.66	16.78	50.94	22.59	14.82	11.65	FSL
Bw	11-28	4.83	6.97	11.27	15.05	21.37	59.49	17.89	16.45	6.17	FSL
Bx1	28-46	5.79	7.91	11.48	19.36	17.06	62.04	17.73	13.65	6.58	FSL
Bx2	46+	6.48	11.38	14.85	22.84	14.43	70.61	13.83	9.58	6.56	LS
BPF		4.72	7.37	10.98	17.08	15.74	56.22	19.55	15.65	8.58	FSL

CEV

Horiz	Depth (cm)	WC	C	Sand H	F	VF	Total Sand	Silt: C	F	Clay	Tex. USDA
Ap	0-31	2.20	4.35	6.96	5.88	23.51	43.10	26.79	14.53	15.58	VFSL
Bw1	31-53	5.54	8.41	12.10	11.19	19.15	56.39	13.05	17.32	13.24	FSL
Bw2	53-74	5.57	8.19	11.17	9.77	18.22	52.83	12.64	18.28	16.25	FSL
Bx	74-94	1.90	4.01	6.68	5.67	23.55	41.81	24.45	18.89	14.85	FSL
2Btx1a	94-107	6.59	9.68	12.83	16.67	13.49	58.37	15.33	14.72	12.69	FSL
2Btx1b	107-122	5.60	9.37	11.38	14.78	12.75	54.98	16.57	15.73	13.69	FSL
2Btx1a	122-137	6.92	10.72	13.23	18.48	11.38	60.73	10.83	15.20	13.17	LS
2Btx2b	137+	6.70	10.91	12.60	16.68	11.33	57.62	11.88	15.21	15.22	FSL

OHL

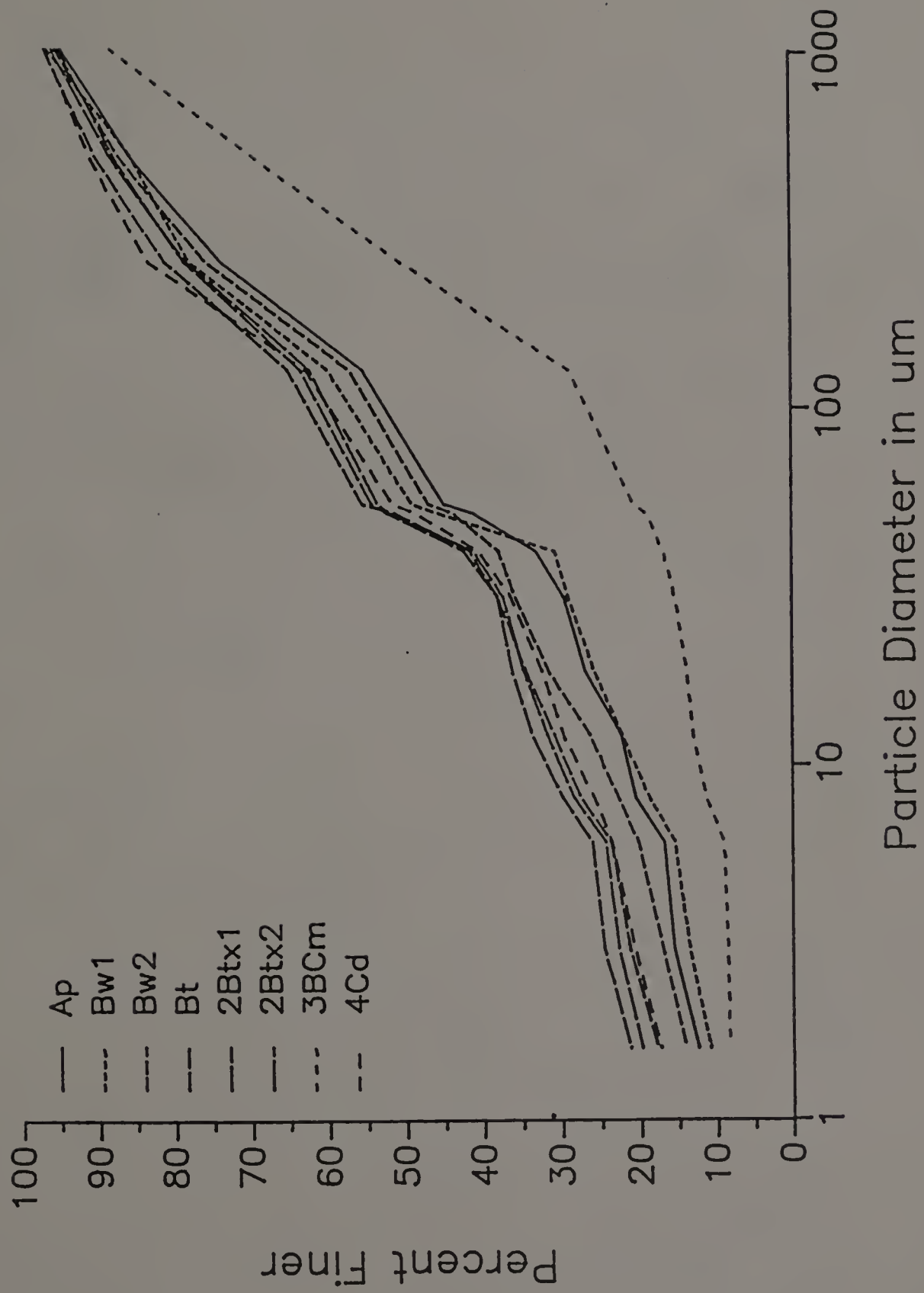
Hori.	Depth (cm)	VC	C	Sand M	F	VF	Total Sand	Silt C	F	Clay	Tex. USDA
Ap	0-21	2.30	4.13	6.78	11.96	18.28	43.45	29.77	17.41	9.38	VFSL
Bw	21-40	0.29	0.52	1.47	12.22	18.61	33.11	46.26	15.88	4.76	L
Bg1	40-52	0.66	2.21	5.37	15.16	15.02	38.42	36.90	16.59	8.10	SiL
Bg2	52-76	4.19	13.85	22.85	20.32	10.80	72.01	12.16	10.03	5.81	LS
2Bw	76-90	7.91	15.03	25.40	24.64	8.89	81.87	5.45	9.00	3.69	LS
2BCm	90-102	14.18	21.49	30.76	22.74	3.93	93.10	1.17	3.79	1.95	S
3Cd1	102-144	5.21	11.27	18.80	22.10	9.65	67.33	12.00	11.61	9.06	LS
3Cd2	144-160	5.65	9.05	14.33	24.64	12.00	65.67	19.12	11.17	4.05	FSL
3Cd3	160-175	6.24	9.88	14.91	24.85	13.13	69.01	16.76	10.07	4.17	LS
4Cm	175-187	9.56	15.28	17.41	22.22	9.44	73.91	15.46	7.35	3.28	LCS
5Cd4	187-220	6.37	11.12	17.86	31.07	10.57	76.99	12.42	9.17	1.43	LS
5Cd5	220+	4.92	9.55	14.94	24.46	15.85	69.72	13.05	12.06	5.17	LS

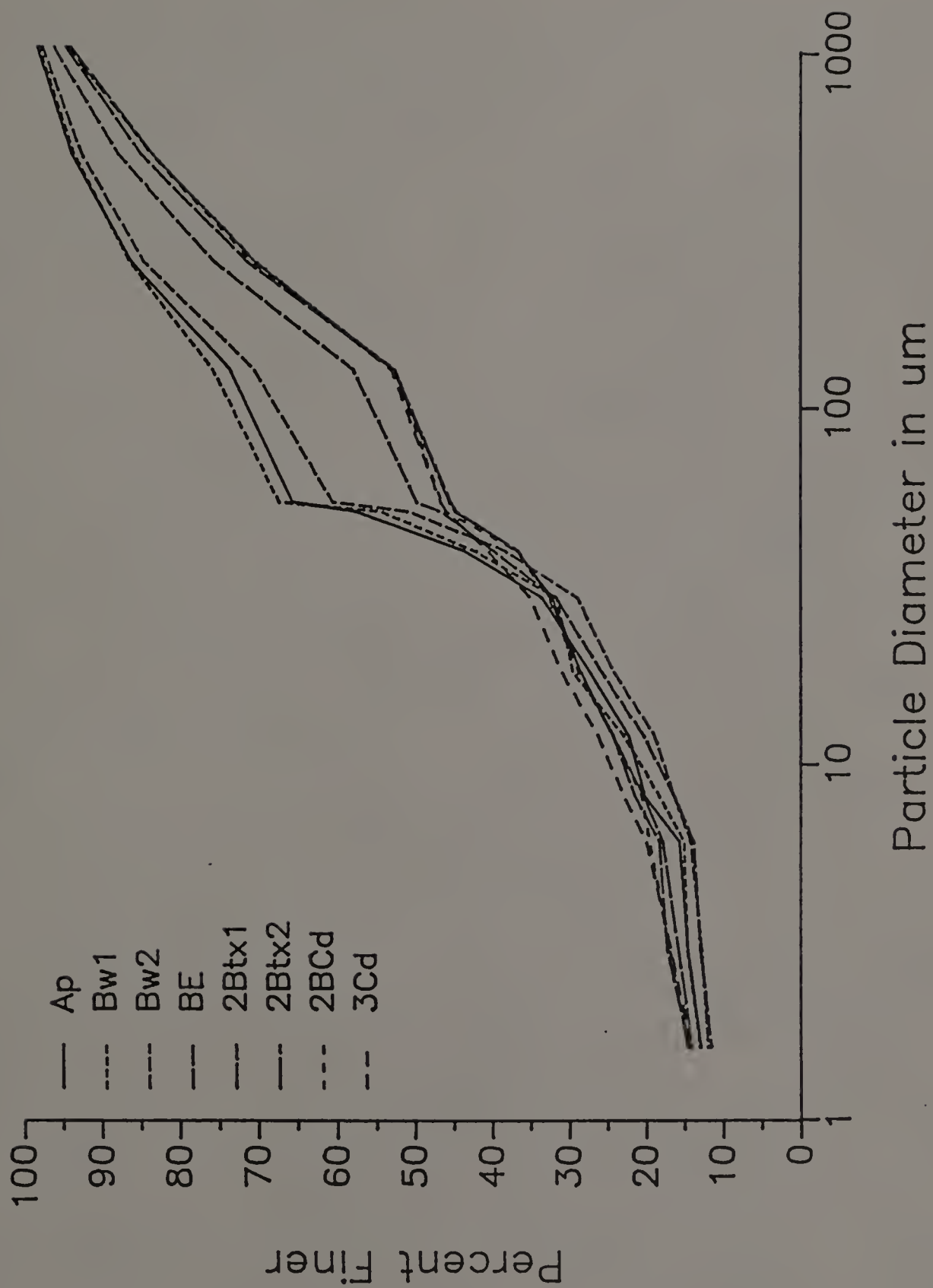
BTR/S

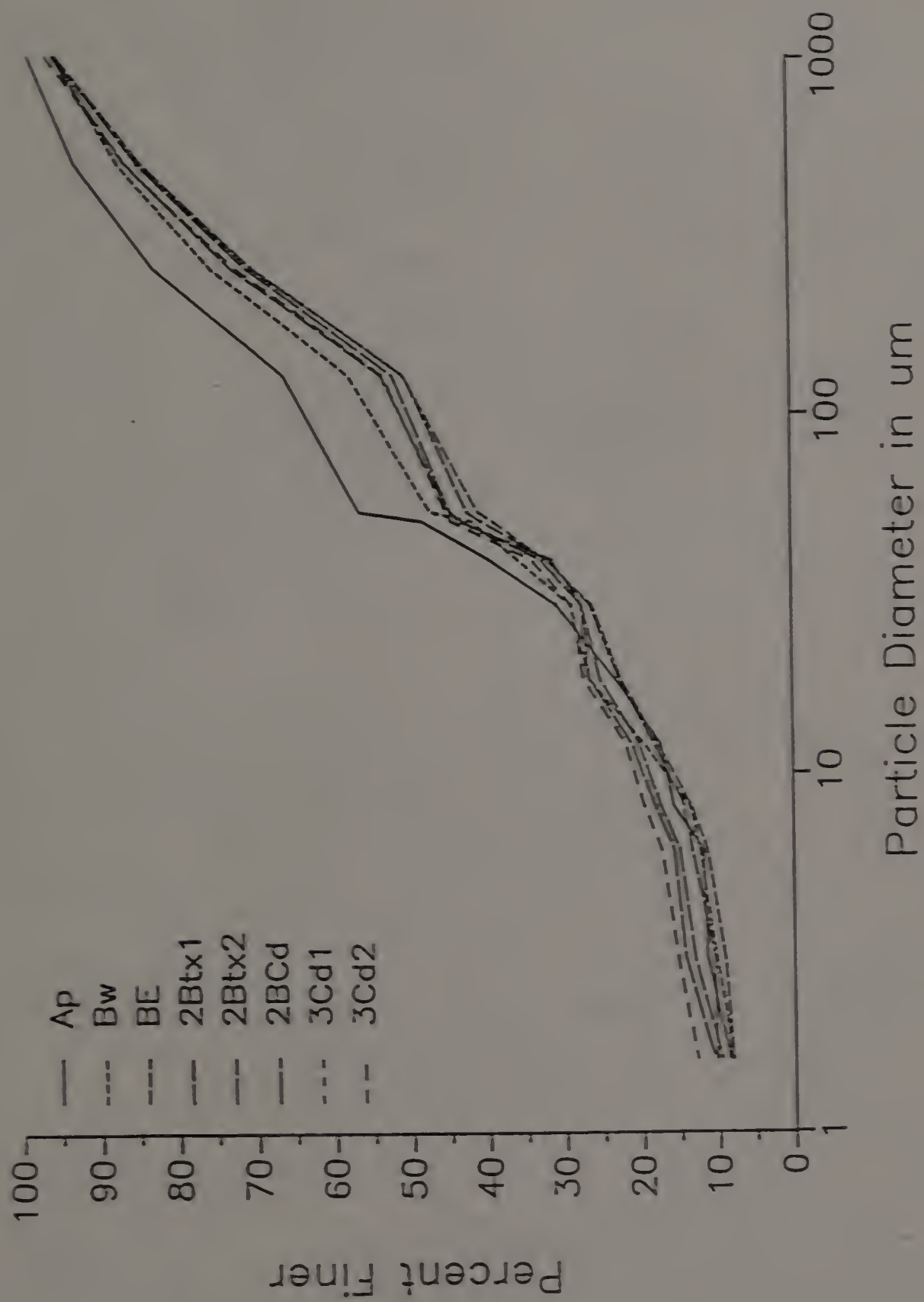
Hori.	Depth (cm)	VC	C	Sand M	F	VF	Total Sand	Silt C	F	Clay	Tex. USDA
Ap	0-18	2.10	5.50	11.28	14.74	23.56	57.18	19.28	12.20	11.34	FSL
Bw1	18-46	3.10	7.51	13.40	16.28	26.07	66.36	12.22	9.79	11.63	LS
Bw2	46-71	3.06	7.50	14.66	19.04	25.56	69.82	15.99	10.14	4.05	LS
2BE a	71-81	3.70	8.19	15.47	18.33	21.63	67.32	12.56	14.08	6.04	LS
2BE b	81-91	3.66	8.83	16.63	19.91	24.19	73.22	8.68	10.46	7.64	LS
2Btx1a	91-102	2.77	6.21	12.38	16.67	18.80	56.83	16.03	17.69	9.45	FSL
2Btx1b	102+	2.71	6.29	12.52	17.58	20.82	59.92	14.95	16.08	9.05	FSL
BPF	85	4.23	9.10	17.30	19.58	19.92	70.13	13.82	10.03	6.02	LS

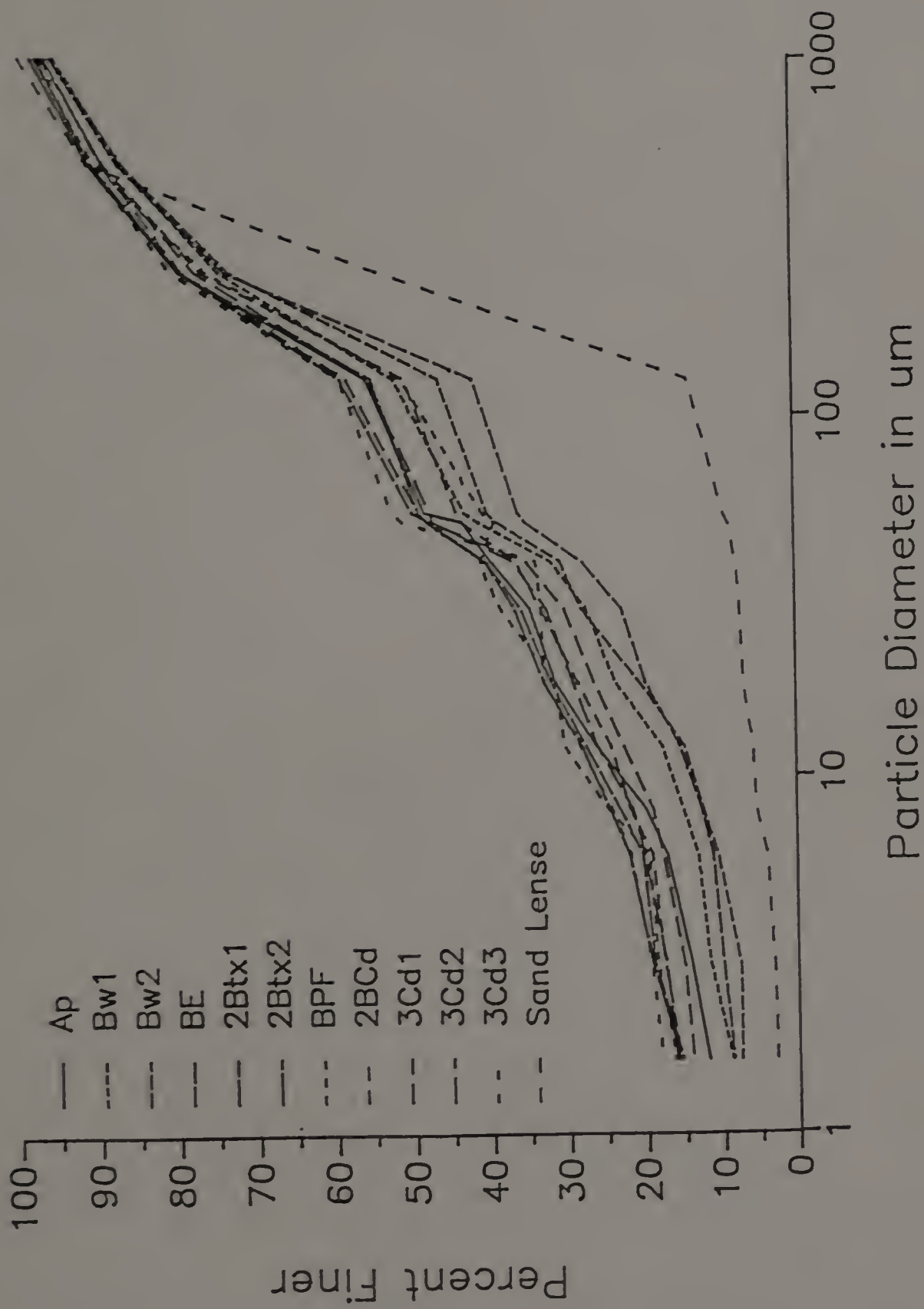
BTR

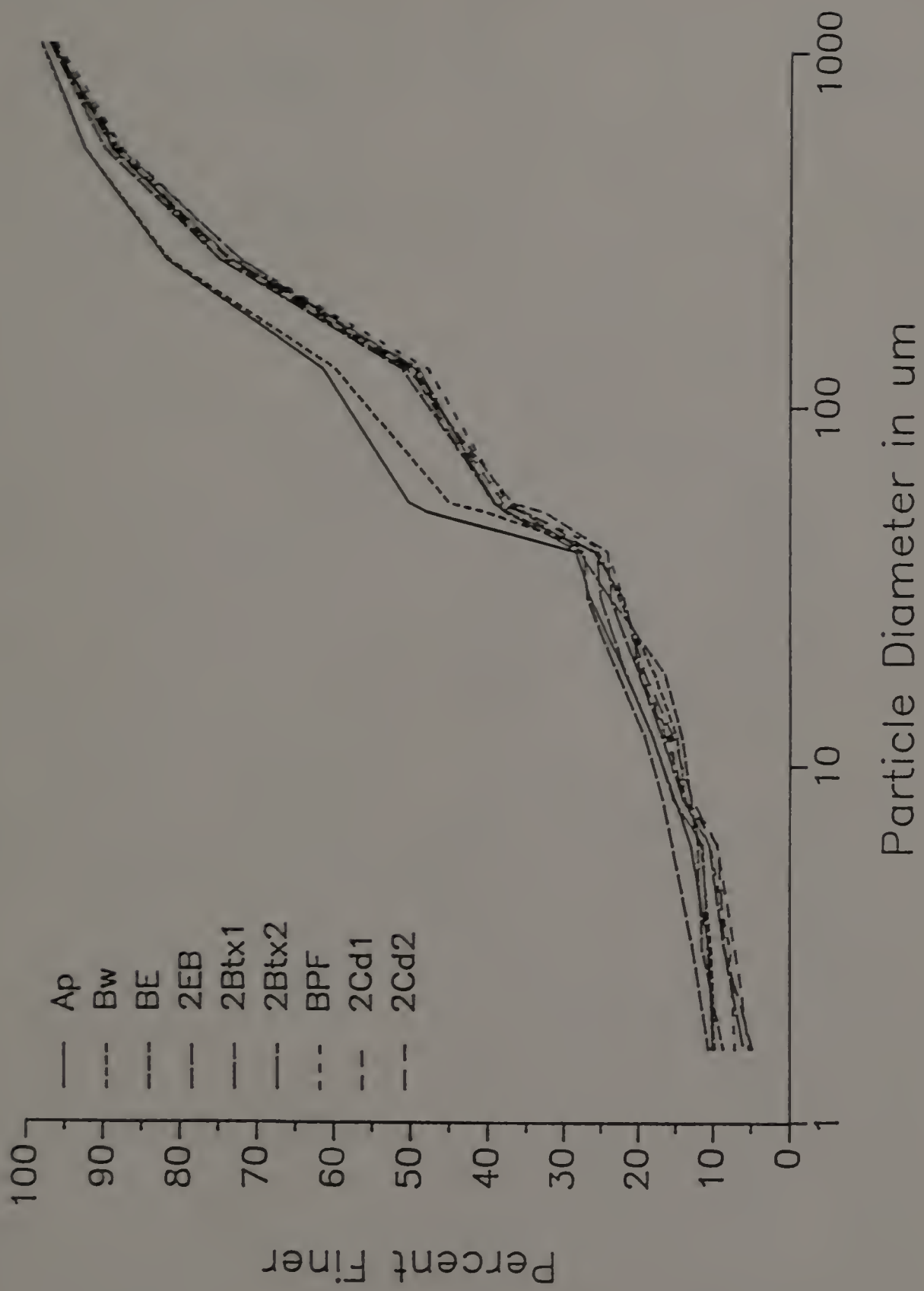
Hori.	Depth (cm)	VC	C	Sand M	F	VF	Total Sand	Silt C	F	Clay	Tex. USDA
2BE	91	3.82	7.90	14.64	23.23	10.28	59.87	10.16	16.84	13.14	LS
2Btx1	107	4.26	8.81	15.32	23.40	12.26	64.05	6.25	14.14	15.56	FSL
2Btx1	122	4.73	8.60	14.94	23.94	12.59	64.77	5.53	14.96	14.74	LS
2Btx1	137	5.00	9.51	14.89	21.93	12.04	63.37	8.18	16.05	12.40	LS
BPF	115	3.63	7.40	12.95	22.66	17.52	64.16	11.32	12.97	11.55	LS











Till Sites

Charlemont

Horizon	Depth (cm)	%C.F.	19mm	8mm (in grams)	4.75mm	2mm	B.D (Mg m ⁻³)
Outwash	0-122	98.31	667.1	626.2	598.3	842.4	--
UT A	122-216	95.44	480.3	462.7	223.9	315.3	1.88
UT B	216-299	96.10	515.7	355.5	146.2	229.7	1.98
UT C	299-401	95.88	609.6	449.2	222.7	321.7	1.93
LT Ox		33.04	175.8	139.2	112.4	684.3	--
LT Unox		30.38	218.8	186.5	159.0	487.6	1.83

Buckland

Horizon	Depth (cm)	%C.F.	19mm	8mm (in grams)	4.75mm	2mm	B.D (Mg m ⁻³)
StCa		62.91	1641.0	802.3	423.0	785.0	--
S&G		78.15	2702.0	870.0	241.5	372.0	--
10cm ox		31.97	0.0	340.0	258.0	1258.0	1.83
Unox		31.01	214.3	487.4	860.5	510.8	1.79

Till Sites

Upper Till

Sample	VC	Sand		F	VF	Total Sand	Silt		Clay
		C	M				C	F	
<u>LTD</u>									
UT1	4.65	6.71	11.38	26.58	21.34	70.67	13.23	16.32	7.45
UT2	4.74	7.00	11.17	30.89	13.64	67.42	13.98	18.58	5.13
UT3	6.13	6.91	9.87	22.62	18.49	64.02	15.21	20.77	5.73
UT4	5.70	5.62	8.35	18.35	16.56	54.46	20.36	25.06	8.39
UT5	3.80	4.91	8.45	18.23	17.83	52.23	14.34	32.45	11.63
<u>AY</u>									
UT1	8.12	10.27	11.32	12.26	10.64	52.62	18.41	28.98	6.59
UT2	5.09	12.15	14.83	23.38	7.36	62.80	18.79	18.40	4.15
UT3	9.36	13.27	14.12	10.73	7.97	55.47	16.40	28.17	6.17
UT4	7.00	11.75	11.72	19.93	18.83	59.25	25.21	19.93	7.69
UT5	6.77	8.71	9.51	16.92	16.43	58.35	20.37	21.30	5.97
<u>BA</u>									
UT1	7.36	9.39	12.59	17.55	12.29	59.19	15.74	25.09	15.25
UT2	9.41	14.39	18.28	21.58	9.72	73.38	10.23	16.39	7.85
<u>CH</u>									
UTA	6.83	9.22	14.36	34.01	11.95	76.37	10.69	9.50	3.44
UTB	5.39	5.95	9.99	32.84	17.37	71.54	16.65	8.62	3.20
UTC	11.38	11.98	16.58	37.56	15.81	93.31	2.28	2.40	2.00

Oxidized Lower Till

Sample	VC	Sand		F	VF	Total Sand	Silt		Clay
		C	M				C	F	
<u>LTD</u>									
OT1	4.08	6.33	9.83	20.00	13.70	53.90	15.37	30.69	18.82
OT2	3.61	5.60	10.11	20.83	14.14	54.30	13.85	31.86	15.72
OT3	3.65	5.33	9.25	19.64	13.65	51.54	14.47	34.02	17.26
OT4	4.30	5.27	9.41	19.93	13.88	52.80	11.33	35.88	18.72
OT5	3.58	5.24	9.94	26.48	8.37	53.60	16.66	29.74	16.90
<u>AY</u>									
OT1	4.69	6.42	8.49	14.19	8.25	42.04	21.68	36.29	13.81
OT2	4.54	6.48	8.70	12.78	10.21	42.71	22.49	34.81	16.07
OT3	4.91	7.35	9.28	13.87	8.71	42.97	19.15	36.78	19.37
OT4	3.97	5.15	7.07	10.84	8.72	35.77	12.15	52.08	19.45
OT5	5.01	7.24	8.94	13.61	9.99	44.81	20.74	34.48	14.03
<u>BA</u>									
OT1	4.67	7.41	11.51	17.05	11.97	52.61	17.93	29.46	19.51
OT2	5.85	8.79	12.74	22.67	9.33	59.38	14.74	25.89	15.47

Unoxidized Lower Till

Sample	VC	Sand		F	VF	Total Sand	Silt		Clay
		C	M				C	F	
<u>LTD</u>									
LT1	3.70	5.45	9.34	19.82	15.52	53.83	13.00	33.18	18.82
LT2	3.84	5.70	9.87	20.28	13.61	53.30	13.88	32.82	16.61
LT3	3.77	5.12	9.22	18.86	14.53	51.51	14.57	33.94	18.98
LT4	4.59	5.27	8.81	18.39	12.80	49.86	15.03	35.11	18.16
LT5	4.60	5.29	8.85	18.38	12.77	49.88	16.96	33.15	17.81
<u>AY</u>									
LT1	2.94	4.34	6.62	10.65	5.55	30.11	18.16	51.74	27.74
LT2	5.11	6.44	9.18	13.37	10.22	44.31	22.08	33.61	17.05
LT3	3.89	6.24	8.36	12.63	7.96	39.09	14.60	46.32	23.26
LT4A	4.33	5.24	7.07	10.45	8.51	35.61	21.17	43.23	20.18
LT4B	5.11	7.69	7.75	9.89	5.80	36.34	19.00	44.77	24.75
LT5	5.54	6.38	8.30	12.64	10.64	43.51	22.71	33.79	17.63
LTSAND	20.06	33.90	24.83	8.25	2.31	89.37	3.70	6.96	4.51
<u>BA</u>									
LT1	5.04	6.31	9.33	14.73	12.34	47.74	17.14	35.11	21.70
LT2	5.75	9.04	12.67	19.32	10.40	57.20	14.75	28.08	15.62
CH LT	1.27	4.45	10.94	22.43	8.07	47.16	23.61	15.05	14.19
BU LT	4.06	4.08	6.37	20.81	8.12	46.91	15.36	19.24	18.50

Till Bulk Density

Upper Till
Sample B.D. g/cm³

LTD UT	1.82
AY UT	1.78
BA UT1	1.84
BA UT2	1.91
CH UTA	1.88
CH UTB	1.98
CH UTC	1.93

Oxidized Lower Till
Sample B.D. g/cm³

LTD OT	1.53
AY OT	1.93
BA OT	1.98

Unoxidized Lower Till
Sample B.D. g/cm³

LTD LT	1.96
AY LT	1.90
BA LT	2.03
BU LT	1.79
CH LT	1.83

Moisture Retention Data

Primary Sites

Pedon 1

Horizon	Pressure (kPa)								
	10	30	50	70	90	100	200	400	1500
Ap	27.30	24.98	23.87	22.89	22.38	21.32	20.44	18.89	8.61
s.d.	1.53	2.28	1.90	1.52	1.46	1.47	1.54	1.45	5.73
Bw1	25.67	22.83	21.31	20.49	19.63	18.56	17.66	16.08	12.18
s.d.	0.66	0.83	0.61	0.62	0.72	0.54	0.62	0.65	0.66
Bw2	27.46	24.97	23.76	22.93	22.05	20.99	19.79	18.44	16.89
s.d.	0.77	1.13	1.18	1.12	1.09	1.09	1.14	1.28	1.52
Bt	27.63	25.16	24.15	23.32	22.89	22.27	21.35	20.31	16.52
s.d.	0.46	0.78	0.83	0.85	0.82	0.79	0.91	1.06	1.15
2Btx1a	33.45	30.62	29.14	28.18	27.60	26.37	24.86	22.81	19.49
s.d.	0.99	0.77	0.70	0.71	0.77	1.03	0.97	1.66	0.68
2Btx1b	33.38	31.06	30.01	29.11	28.58	27.74	26.27	24.18	18.79
s.d.	0.41	1.05	0.29	0.17	0.13	0.16	0.22	0.37	0.76
2Btx2a	35.14	30.70	29.45	28.48	27.96	27.38	24.52	24.11	19.02
s.d.	1.93	0.33	0.27	0.25	0.27	0.25	3.04	0.35	0.92
2Btx2b	33.10	30.50	29.10	28.12	27.49	26.88	24.86	22.15	18.37
s.d.	1.96	1.80	1.67	1.62	1.61	1.62	1.49	1.76	0.75
3BCm	18.73	14.90	12.90	11.91	11.57	10.78	10.47	10.02	8.42
s.d.	2.30	1.25	0.84	0.98	1.10	1.07	1.15	1.13	0.73
4Cd	31.26	29.16	27.93	27.10	26.80	25.19	24.49	23.01	19.51
s.d.	3.83	3.59	3.54	3.46	3.31	3.38	3.17	2.97	2.64
BPF	31.60	29.90	28.27	27.33	26.89	26.21	24.94	23.72	19.86
s.d.	1.69	1.81	1.82	1.85	1.58	1.74	1.72	1.70	1.90

Table 1

Horizon	Pressure (kPa)								
	10	30	50	70	90	100	200	400	1500
Sw	27.27	21.07	20.07	18.48	18.14	17.51	16.83	15.88	9.03
s.d.	8.17	6.01	4.85	4.61	4.67	4.76	4.51	4.51	4.50
SE	18.73	25.50	22.91	21.71	20.79	20.31	19.41	17.98	8.20
s.d.	4.63	3.64	3.84	3.76	3.63	3.67	3.45	3.46	2.40
13tx1	21.48	19.49	18.67	18.04	17.77	17.26	16.48	15.90	10.91
s.d.	1.56	1.85	2.02	2.13	2.24	2.21	2.39	2.64	2.51
13tx2	28.88	26.62	25.82	25.17	24.76	24.47	23.43	22.34	15.78
s.d.	1.29	1.27	1.26	1.25	1.27	1.24	1.25	1.28	0.41
23Cd	28.62	26.05	24.73	23.84	23.45	23.02	21.46	18.88	12.90
s.d.	0.96	0.81	0.82	0.81	0.85	0.76	1.16	1.53	0.83
3Cd1	28.10	25.32	24.38	22.45	21.70	21.40	19.84	17.40	10.17
s.d.	4.02	4.21	4.22	4.16	4.27	4.20	3.69	3.22	0.95
3Cd2	34.61	31.49	30.17	29.12	28.33	27.83	26.47	24.02	14.09
s.d.	2.42	2.22	2.22	2.25	2.24	2.31	2.29	2.44	2.07
3Cd3	43.81	41.50	40.51	39.62	38.87	38.47	37.08	35.16	22.52
s.d.	15.87	15.88	15.90	15.90	15.76	15.79	15.81	15.82	12.62
SAND	29.53	17.30	15.82	15.02	14.35	14.18	13.32	12.43	4.40
s.d.	5.24	4.39	4.30	4.26	4.35	4.16	4.09	4.13	0.43

Pedon 3

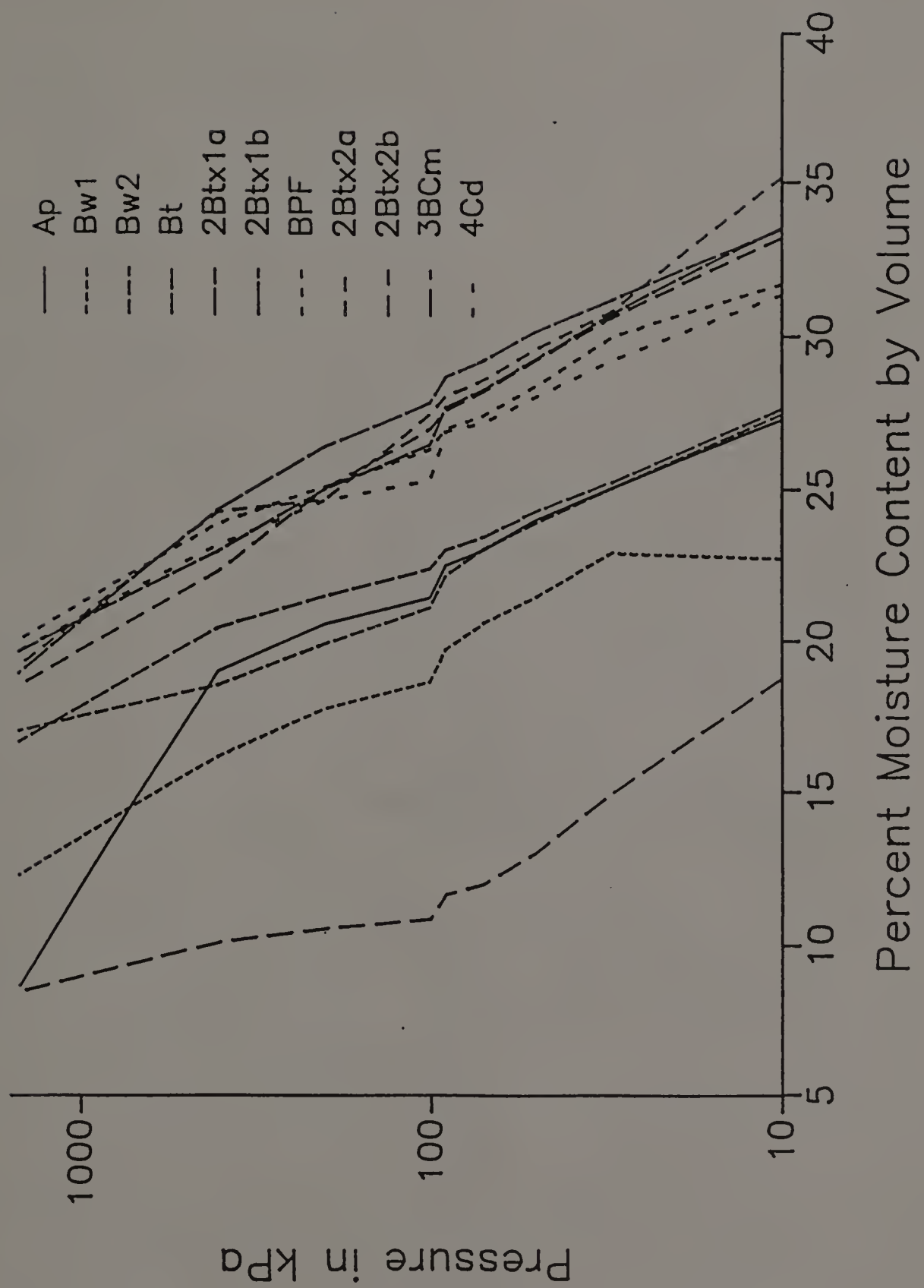
Horizon	Pressure (kPa)								
	10	30	50	70	90	100	200	400	1500
Ap	33.59	25.45	23.37	22.04	20.86	19.71	17.38	15.84	15.42
s.d.	2.14	2.32	2.46	2.67	2.45	2.44	3.33	3.32	1.56
Bw	27.88	23.18	20.65	18.77	17.67	16.56	14.40	13.37	11.29
s.d.	1.40	1.19	1.19	1.26	1.09	1.14	1.37	1.69	2.52
BE	21.53	19.63	19.00	18.58	18.06	17.84	16.72	15.25	13.06
s.d.	1.23	1.24	1.23	1.25	1.24	1.31	1.23	1.30	1.29
2Btx1	23.42	21.28	19.59	19.07	19.03	18.48	17.35	15.76	13.84
s.d.	0.52	0.30	1.53	0.25	0.20	0.25	0.23	0.24	0.25
2Btx2	23.80	22.15	21.27	20.63	20.16	19.37	17.86	15.86	13.88
s.d.	1.43	1.46	1.49	1.52	1.53	1.24	1.16	0.97	0.85
2BCd	25.65	23.51	22.34	21.46	20.61	20.06	18.63	16.68	15.79
s.d.	1.23	1.45	1.34	0.95	0.84	1.98	1.02	1.42	1.09
3Cd1	32.03	25.90	24.41	23.05	22.50	21.61	19.45	16.78	15.15
s.d.	3.37	0.93	1.13	1.43	1.20	1.40	1.54	1.40	1.82
3Cd2	27.85	25.30	24.22	23.44	23.07	22.50	21.42	17.63	16.37
s.d.	2.94	1.48	2.03	1.34	1.42	1.67	1.04	1.33	0.98

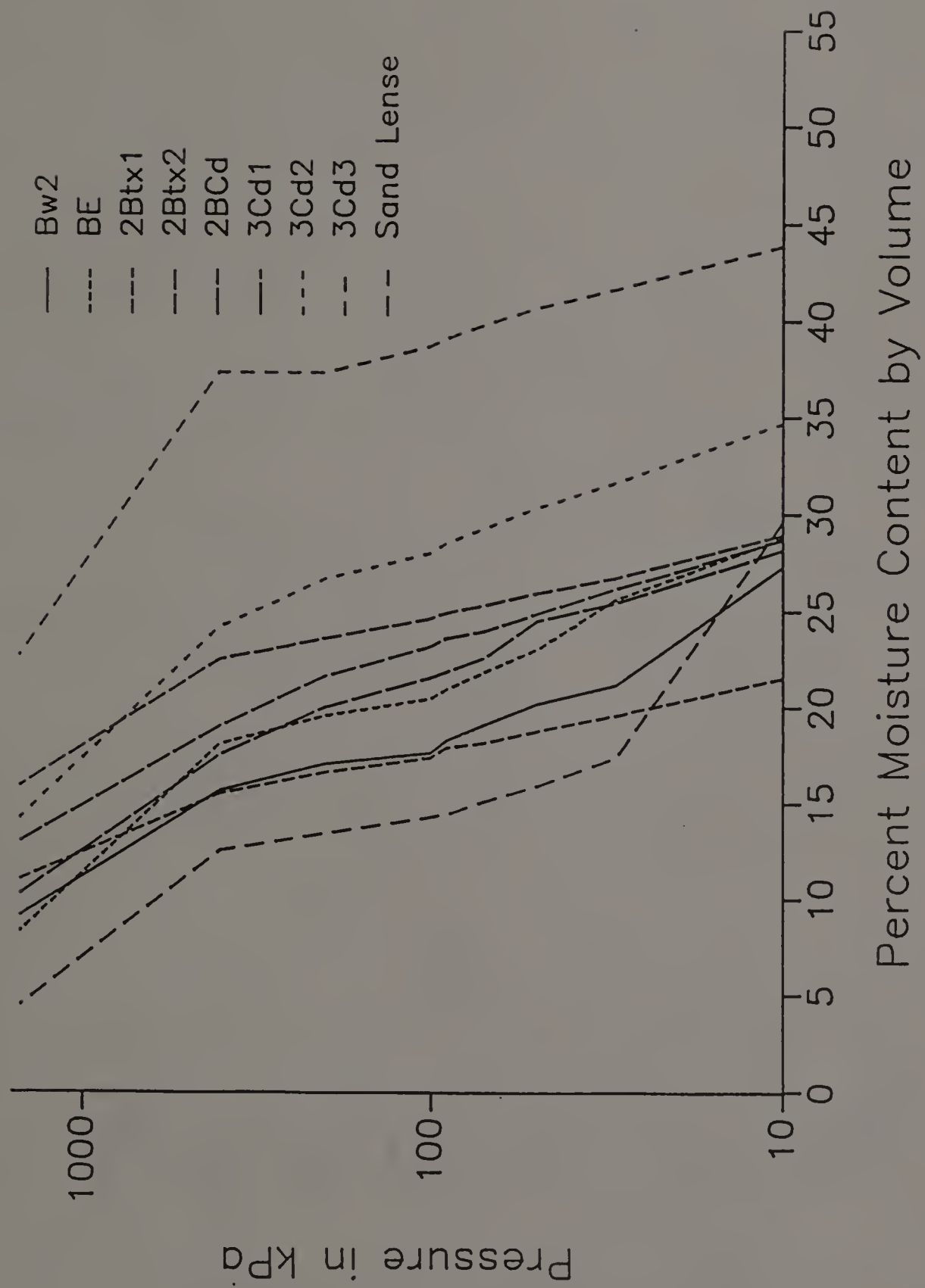
Pedon 4

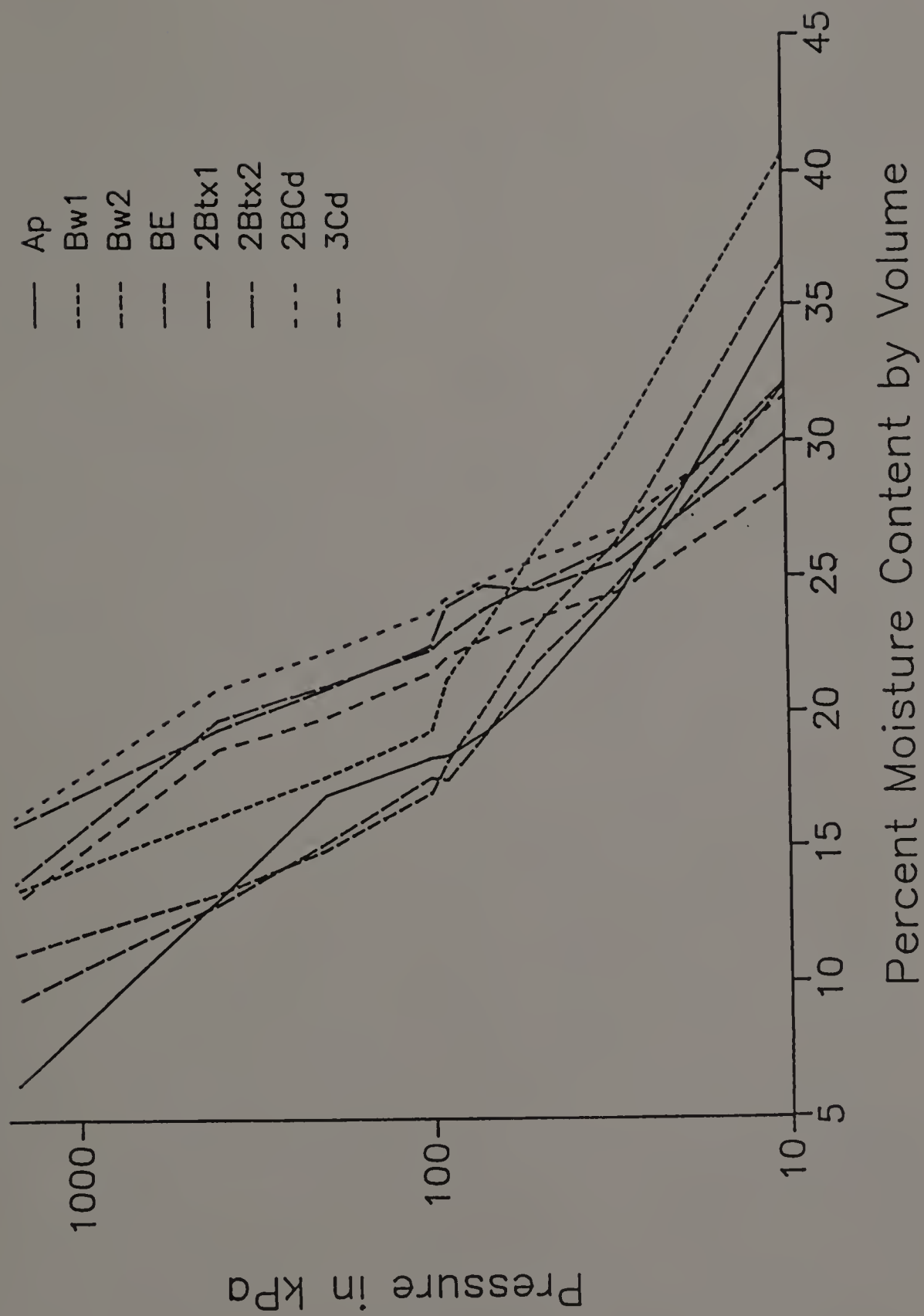
Horizon	Pressure (kPa)								
	10	30	50	70	90	100	200	400	1500
Ap	34.68	24.11	20.89	19.23	18.34	18.26	16.88	13.06	6.82
s.d.	5.98	4.29	4.40	4.59	4.62	4.60	6.40	4.67	5.14
Bw1	40.64	29.73	25.99	23.07	21.14	19.25	17.56	16.09	13.31
s.d.	5.03	4.21	3.75	2.97	2.96	3.00	2.71	2.39	2.18
Bw2	36.67	26.22	23.11	20.17	18.14	16.97	14.82	13.44	11.00
s.d.	2.42	1.49	0.67	0.66	0.65	0.56	0.79	0.70	0.56
BE	31.96	24.59	21.78	19.16	17.46	17.54	15.08	12.84	9.34
s.d.	2.65	2.51	1.99	1.34	0.92	0.87	0.84	1.20	0.18
2Btx1	32.06	26.05	24.69	23.74	22.75	22.20	20.90	19.68	13.61
s.d.	2.31	2.24	2.40	2.46	2.46	2.52	2.43	2.45	2.74
2Btx2	30.19	25.48	24.45	24.62	23.80	22.36	20.78	19.33	15.77
s.d.	1.49	1.01	0.96	0.31	0.34	1.01	1.14	1.21	1.96
2BCd	31.57	26.67	25.57	24.79	24.10	23.57	22.12	20.81	16.07
s.d.	2.66	2.52	2.47	2.45	2.43	2.41	2.32	2.16	1.62
3Cd	28.39	24.34	23.39	22.63	21.95	21.38	19.74	18.61	12.92
s.d.	0.64	0.41	0.44	0.43	0.41	0.44	0.35	0.22	0.77

Pedon 5

Horizon	Pressure (kPa)								
	10	30	50	70	90	100	200	400	1200
Ap	54.55	51.05	45.44	42.57	38.86	37.59	36.03	32.56	26.64
s.d.	5.77	5.82	6.44	6.81	6.38	6.18	6.19	6.02	3.66
Bw	40.51	33.85	30.59	25.20	23.49	22.62	20.85	18.69	11.02
s.d.	2.64	1.82	1.75	2.71	2.36	2.33	2.49	2.65	0.65
BE	30.53	25.94	22.90	21.05	18.92	18.29	17.11	14.44	7.74
s.d.	1.44	1.46	0.67	0.54	0.86	0.83	0.34	0.85	0.62
2EB	24.69	22.98	22.25	21.79	21.31	21.05	20.09	19.25	16.14
s.d.	4.81	4.84	4.83	4.85	4.85	4.86	5.10	4.95	2.86
2Btx1	18.04	15.48	14.71	13.71	13.13	12.74	11.94	10.63	9.76
s.d.	0.65	0.53	0.74	0.50	0.46	0.49	0.46	0.45	0.17
2Btx2	19.67	17.17	16.35	15.64	15.14	14.72	13.88	12.38	11.23
s.d.	0.41	0.43	0.44	0.40	0.36	0.35	0.29	0.23	0.24
2Cd1	18.14	15.83	14.97	14.19	13.68	13.27	12.34	10.81	9.73
s.d.	1.07	0.69	0.50	0.37	0.27	0.27	0.20	0.20	0.58
2Cd2	22.33	19.78	19.06	17.99	17.25	16.63	15.66	13.28	10.59
s.d.	1.41	1.17	1.21	0.98	1.02	0.96	1.07	0.81	0.28
BPFa	22.51	18.90	17.60	16.88	16.15	13.45	11.88	10.56	10.02
s.d.	0.93	0.93	0.94	1.06	0.75	0.51	0.15	0.68	0.84
BPFb	22.84	19.74	18.59	17.73	17.05	16.01	15.11	13.71	11.55
s.d.	0.56	0.34	0.28	0.22	0.23	0.20	0.21	0.25	0.65







Secondary Sites

EHP

Horizon	Pressure (kPa)							
	10	30	50	70	100	200	400	1500
Ap	16.84	15.33	14.38	13.58	12.86	12.29	10.59	8.80
s.d.	0.54	0.33	0.37	0.54	0.65	0.53	0.51	1.02
Bw1	15.09	14.20	13.69	13.33	12.92	12.20	11.08	10.60
s.d.	1.04	1.03	1.00	1.01	1.01	0.99	0.97	1.08
Bw2	13.78	12.87	12.31	11.92	11.53	10.71	9.78	9.71
s.d.	2.12	2.14	2.19	2.16	2.14	2.10	1.97	0.00
45 cm	12.99	12.27	11.88	11.61	11.29	10.76	9.90	7.96
s.d.	2.20	2.05	2.00	1.91	1.85	1.60	1.29	0.00
52.5 cm	12.57	11.68	11.17	10.85	10.50	9.77	8.98	8.53
s.d.	1.67	1.17	1.72	1.74	1.70	1.69	1.59	2.24
60 cm	14.57	13.80	13.31	12.90	12.51	11.75	10.86	9.88
s.d.	0.65	0.79	0.92	0.97	1.02	1.18	1.07	2.15
67.5 cm	14.63	13.87	13.31	13.00	12.66	11.79	10.73	8.76
s.d.	1.00	1.07	1.11	1.13	1.14	1.00	0.98	0.00
75 cm	16.06	15.46	14.96	14.35	13.75	12.90	11.72	10.18
s.d.	0.76	0.89	0.71	0.38	0.00	0.00	0.00	0.00
82.5 cm	13.58	12.92	12.51	12.19	11.89	11.32	10.66	10.48
90 cm	14.72	13.72	13.30	12.99	12.63	11.84	10.94	9.22
s.d.	0.21	0.34	0.34	0.38	0.48	0.55	0.63	0.00

EHW

Horizon	Pressure (kPa)							
	10	30	50	70	100	200	400	1500
Ap	27.03	23.40	22.12	21.12	20.31	19.21	17.72	16.92
s.d.	4.89	4.01	3.39	3.08	2.79	2.91	2.12	4.05
Bw1	15.28	13.57	12.48	11.94	11.47	10.64	9.60	7.47
s.d.	0.94	0.79	0.53	0.50	0.72	0.59	0.70	0.06
Bw2	16.17	14.49	13.62	12.91	12.52	11.65	10.48	9.11
s.d.	1.04	0.80	0.70	0.67	0.65	0.43	0.56	1.52
47.5 cm	17.24	15.60	14.77	13.61	13.20	12.41	11.33	10.43
s.d.	1.53	1.62	1.55	0.71	0.62	0.67	0.20	0.37
55 cm	16.01	14.80	13.80	13.41	13.27	12.63	11.77	9.18
s.d.	1.05	0.87	1.22	1.01	0.67	0.68	0.50	1.91
62.5 cm	15.15	13.73	13.04	12.52	12.04	11.22	10.51	9.32
s.d.	1.39	1.28	1.17	1.13	1.03	0.80	0.73	0.00
70 cm	13.66	12.64	12.09	11.38	10.86	9.79	9.06	9.21
s.d.	2.99	2.87	2.90	2.99	2.76	2.78	2.66	1.41
77.5 cm	14.21	12.72	12.06	11.55	11.10	10.29	9.41	7.82
s.d.	0.61	0.75	0.78	0.79	0.83	0.57	0.75	0.00
85 cm	17.76	16.66	16.13	15.63	15.24	14.54	13.68	8.25
s.d.	1.78	2.03	2.09	2.08	2.09	1.98	1.92	0.74

EHR

Horizon	Pressure (kPa)							
	10	30	50	70	100	200	400	1500
Ap	30.27	24.70	24.00	23.25	22.47	21.80	20.71	12.57
s.d.	2.40	0.62	0.55	0.68	0.96	0.86	1.16	2.17
Bw	31.57	21.83	18.45	17.10	15.63	14.54	13.28	10.70
s.d.	2.83	2.09	2.24	2.60	2.25	2.13	1.78	0.09
40 cm	20.02	17.47	15.97	15.23	14.326	13.30	12.21	8.55
s.d.	0.40	0.48	0.57	0.59	0.76	0.88	0.84	2.12
47.5 cm	21.02	18.44	16.83	16.11	15.40	14.35	13.48	10.36
s.d.	1.04	0.96	0.89	0.84	0.82	0.51	0.54	0.79
55 cm	21.22	18.57	16.71	15.78	14.93	13.92	12.87	6.85
s.d.	0.42	0.90	1.04	1.11	1.24	1.29	1.29	0.76
62.5 cm	19.31	15.37	12.47	11.21	10.07	8.79	7.89	6.19
s.d.	1.25	2.44	2.67	2.67	2.61	2.48	2.33	0.00
70 cm	18.28	14.78	12.53	11.80	10.68	9.81	8.89	5.58
s.d.	1.05	0.96	0.80	0.72	0.98	0.56	0.73	0.80

BHP

Horizon	Pressure (kPa)							
	10	30	50	70	100	200	400	1500
Ap	31.71	29.70	28.48	27.76	25.97	25.04	23.87	3.42
s.d.	2.37	1.42	1.86	1.92	2.03	2.22	2.56	0.37
Bw1	21.21	17.14	14.18	12.97	11.75	10.52	9.38	1.34
s.d.	2.73	2.33	1.73	1.28	1.42	1.30	1.19	0.00
Bw2	19.21	15.20	12.63	11.41	10.10	8.63	7.33	0.87
s.d.	2.47	2.21	1.90	1.68	1.60	1.04	1.23	0.14
BE	16.68	13.00	10.77	9.95	8.63	7.65	6.46	4.42
s.d.	1.59	1.52	1.27	1.61	1.06	1.59	1.40	2.17
60 cm	14.83	13.45	12.26	11.44	10.61	9.15	7.92	0.96
s.d.	2.09	1.75	1.47	1.27	1.22	1.16	1.38	0.09
67.5 cm	11.73	10.73	10.06	9.56	9.12	8.04	6.90	1.76
s.d.	1.46	1.26	1.21	1.22	1.25	1.40	1.61	2.38
72 cm	12.92	11.78	10.99	10.43	9.89	8.85	7.69	3.59
s.d.	1.06	0.94	0.94	1.01	1.02	1.15	1.05	0.49
77.5	13.75	13.04	12.49	11.99	11.58	10.90	9.93	4.07
s.d.	0.63	0.67	0.66	0.77	0.80	0.86	0.42	0.40

250

Horizon	Pressure (kPa)								
	10	30	50	70	100	200	300	400	1500
sp	24.11	20.85	18.96	17.10	16.36	15.79	14.82	14.09	6.83
z.d.	0.99	0.71	0.79	0.18	0.09	0.10	0.22	0.43	0.02
Ev1	21.77	19.62	18.33	17.02	15.26	15.51	14.81	14.23	7.23
z.d.	0.36	0.47	0.72	0.41	0.51	0.46	0.42	0.58	0.00
Ev2	20.34	18.23	17.14	15.78	14.99	14.23	13.34	12.71	7.98
z.d.	1.34	1.33	1.20	1.31	1.03	0.81	0.91	0.90	1.04
45 cm	17.34	15.70	14.91	13.48	13.02	12.13	11.33	10.72	6.80
z.d.	0.66	0.60	0.68	0.60	0.66	0.58	0.61	0.59	0.26
11.5 cm	15.42	14.31	14.01	13.03	12.72	12.24	11.73	11.34	4.52
z.d.	2.23	1.93	1.82	1.28	1.40	1.32	1.31	1.26	0.00
60 cm	16.22	15.44	15.11	14.37	13.96	13.24	12.77	12.19	8.41
z.d.	2.30	2.37	2.43	2.80	2.72	2.95	3.04	3.16	2.71
37.5 cm	14.43	13.79	13.47	12.91	12.62	11.86	11.68	11.19	6.72
z.d.	0.40	0.43	0.44	0.49	0.48	0.28	0.59	0.52	1.97
75 cm	13.24	12.61	12.34	11.81	11.55	11.14	10.78	10.46	6.72
z.d.	0.37	0.34	0.34	0.32	0.36	0.42	0.48	0.51	0.00
22.5 cm	13.34	12.87	12.38	12.18	12.04	11.64	11.21	10.88	7.89
z.d.	1.01	1.09	0.87	1.10	1.14	1.18	1.16	1.21	0.00
90 cm	13.71	13.23	12.98	12.59	12.39	12.11	11.85	11.59	7.68
z.d.	1.48	1.38	1.33	1.29	1.28	1.31	1.31	1.28	0.32

BHR

Horizon	Pressure (kPa)								
	10	30	50	70	100	200	300	400	1500
A	61.79	56.05	28.59	21.58	20.91	19.97	19.28	18.54	16.48
s.d.									
Bw	21.86	15.36	13.65	13.47	11.31	9.97	9.30	7.72	5.76
s.d.	1.59	1.13	1.03	1.53	1.01	0.99	1.06	0.81	0.00
30 cm	14.60	12.74	11.54	10.80	10.20	8.98	8.47	7.52	6.11
s.d.	3.45	2.97	2.61	2.38	2.34	1.72	1.74	1.32	0.97
37.5 cm	13.64	12.02	10.85	10.12	9.43	8.35	7.54	6.89	5.30
s.d.	0.18	0.16	0.28	0.31	0.43	0.65	0.86	0.77	0.59
45 cm	10.97	9.42	8.76	8.33	7.86	7.28	6.88	6.39	4.13
s.d.	0.45	0.32	0.25	0.23	0.31	0.38	0.30	0.35	0.00
52.5 cm	9.42	7.65	6.95	6.57	5.93	5.44	5.08	4.83	4.19
s.d.	0.44	0.30	0.33	0.29	0.63	0.55	0.47	0.43	0.00
60 cm	9.35	7.87	6.98	6.81	6.25	5.73	5.07	5.05	4.12
s.d.	0.38	0.45	0.34	0.48	0.40	0.42	0.68	0.31	0.36

OHW

Horizon	Pressure (kPa)								
	10	30	50	70	100	200	300	400	1500
Ap	30.79	26.36	24.76	20.93	20.30	19.46	18.12	16.28	14.68
s.d.	0.87	1.60	1.95	2.95	2.99	3.04	2.86	2.44	2.74
Bw1	16.31	14.25	13.30	12.37	11.80	11.52	10.62	10.12	8.06
s.d.	2.48	1.85	1.48	1.35	1.01	1.12	1.15	1.09	0.19
Bw2	21.20	16.85	14.91	13.33	12.71	12.09	10.91	9.91	7.20
s.d.	6.26	4.63	3.89	3.37	2.94	2.67	2.13	1.85	1.49
BE	28.15	22.35	19.31	16.39	15.54	14.74	13.12	11.11	10.59
s.d.	5.68	3.93	3.87	2.97	2.86	2.69	2.44	3.54	2.38
85 cm	24.40	18.75	15.98	13.42	12.93	12.70	11.19	9.97	8.14
s.d.	1.66	0.67	0.06	0.27	0.28	0.09	0.54	0.00	0.91
92.5 cm	18.95	15.77	14.00	12.90	12.04	11.81	10.98	9.79	8.25
s.d.	3.93	2.19	1.78	0.91	0.60	0.69	0.27	0.45	0.72
100 cm	14.17	13.14	12.44	12.22	11.46	11.11	10.56	9.92	9.39
s.d.	0.10	0.33	0.49	0.55	0.65	0.37	0.77	0.60	0.58
107.5 cm	16.99	14.44	13.08	12.46	11.50	11.30	10.36	9.62	9.00
s.d.	3.39	2.32	1.96	2.01	1.49	1.56	1.54	1.04	0.36
115 cm	13.70	12.46	11.66	11.13	10.47	10.28	9.78	8.88	6.48
s.d.	0.51	0.52	0.15	0.15	0.07	0.14	0.16	0.54	1.66
122.5 cm	14.11	12.74	12.02	11.37	10.82	10.75	10.03	9.03	7.80
s.d.	0.73	0.53	0.10	0.06	0.66	0.23	0.93	1.66	0.67
130 cm	12.82	11.66	11.08	10.47	10.07	9.45	8.81	8.03	7.58
s.d.	0.09	0.70	0.07	0.49	0.12	0.12	0.41	0.27	0.09
137.5 cm	12.38	11.14	10.72	10.19	9.75	9.49	8.76	8.01	6.37
s.d.	0.95	1.06	0.89	1.04	1.07	0.90	0.76	0.68	0.16
145 cm	13.50	12.44	12.00	11.53	11.06	10.98	10.51	9.91	7.18
s.d.	0.25	0.27	0.22	0.36	0.17	0.30	0.09	0.24	0.53
152.5 cm	12.59	11.59	10.95	10.41	9.55	9.42	9.20	9.12	7.14
s.d.	2.46	2.17	2.28	2.07	1.76	1.81	1.83	2.38	1.42
BPF	14.72	12.89	11.83	10.71	10.21	9.89	9.75	8.97	7.16
s.d.	1.59	1.61	0.96	1.12	1.13	1.12	1.06	0.83	0.72

OHL

Horizon	Pressure (kPa)								
	10	30	50	70	90	100	200	400	1500
Ap	39.86	33.37	29.59	26.12	24.05	22.71	21.22	19.46	14.72
s.d.	3.85	2.67	3.41	3.19	2.08	2.06	1.93	2.26	1.26
Bw	34.43	28.28	26.04	23.51	21.06	19.02	16.83	14.96	10.64
s.d.	0.78	1.44	1.41	1.28	1.46	1.04	1.24	1.27	0.96
Bg1	32.92	30.17	26.72	24.69	23.27	22.54	20.83	18.60	15.16
s.d.	7.15	6.15	6.15	5.85	5.55	5.42	5.59	5.15	4.47
Bg2	24.05	19.97	17.23	15.37	14.70	13.36	11.59	9.98	9.36
s.d.	1.38	1.14	0.97	0.80	0.82	0.78	0.71	0.77	0.85
2Bw	22.79	18.11	16.21	14.23	13.27	12.90	11.37	9.79	8.89
s.d.	2.30	1.52	1.48	1.65	1.60	1.58	1.06	1.03	1.23
2BCm	37.38	33.65	30.82	30.07	29.70	21.07	20.03	12.01	7.31
s.d.	20.51	20.80	22.19	20.46	20.16	11.43	10.72	2.94	0.70
3Cd1	22.98	19.13	17.64	16.52	15.89	15.50	14.63	13.11	12.42
s.d.									
3Cd2	24.29	20.19	18.36	17.26	16.45	15.89	14.74	12.50	10.88
s.d.	0.05	0.14	0.31	0.23	0.24	0.23	0.23	0.22	0.42
3Cd3	22.05	14.26	12.28	10.94	9.47	9.30	8.28	6.04	4.98
s.d.	1.30	0.79	0.88	0.94	0.65	0.61	0.61	0.31	0.40
4Cm	21.37	17.62	15.37	14.46	13.88	13.02	12.51	11.64	10.36
s.d.	2.99	2.32	1.27	1.13	1.01	2.58	2.64	0.81	0.65
5Cd4	15.95	12.76	11.61	10.64	10.04	9.61	8.72	7.68	6.49
s.d.	1.96	1.51	1.39	1.31	1.23	1.30	1.28	1.58	1.57

BTR/S									
Horizon	Pressure (kPa)								
	10	30	50	70	100	200	400	1500	
Ap	27.32	26.29	25.46	24.74	23.84	20.74	19.38	12.36	
s.d.	2.74	2.60	2.56	2.42	2.15	2.27	2.59	0.30	
Bw	20.71	18.60	15.38	14.13	13.15	9.81	8.65	4.80	
s.d.	0.51	1.67	2.05	1.78	2.14	1.09	0.84	0.53	
40 cm	17.37	13.01	10.53	9.58	8.74	6.50	5.98	4.42	
s.d.	1.22	1.78	1.51	1.24	0.94	0.45	0.28	0.64	
50 cm	18.81	13.10	10.98	10.01	9.20	7.22	6.47	5.44	
s.d.	1.62	1.73	1.41	1.39	1.20	0.86	0.44	0.73	
60 cm	12.97	10.25	8.69	8.16	7.22	5.98	4.66	4.21	
s.d.	2.67	2.49	2.38	1.60	0.90	1.10	0.57	0.78	
70 cm	8.08	7.00	6.10	5.59	5.07	3.99	3.47	3.32	
s.d.	0.23	0.10	0.10	0.07	0.01	0.06	0.15	0.19	
80 cm	9.41	8.64	8.12	7.88	7.58	6.90	6.33	5.28	
s.d.	0.84	0.91	0.96	1.04	1.10	1.07	1.19	1.29	
90 cm	10.12	9.78	9.54	9.39	9.21	8.78	8.33	5.86	
s.d.	3.00	2.86	2.86	2.87	2.93	3.00	2.93	0.22	
100 cm	8.51	7.66	7.04	6.75	6.41	5.64	4.94	3.14	
s.d.	0.87	0.70	0.42	0.29	0.14	0.26	0.39	1.30	
110 cm	8.31	7.73	7.33	7.10	6.77	6.24	5.81	4.97	
s.d.	0.15	0.16	0.27	0.32	0.32	0.46	0.49	1.09	

BTR

Horizon	Pressure (kPa)								
	10	30	50	70	100	200	300	400	1500
50 cm	19.99	13.47	12.72	11.76	10.16	8.86	8.11	7.73	5.99
60 cm	17.13	11.22	10.44	9.06	8.70	7.98	7.44	6.99	3.22
70 cm	15.52	8.89	7.38	6.10	5.68	4.46	4.31	3.87	1.68
80 cm	10.71	8.85	7.99	7.57	6.95	5.67	5.56	5.28	2.55
90 cm	10.04	9.34	9.10	9.02	8.75	8.14	8.02	7.84	5.92
BPF	12.55	7.64	6.31	5.71	4.99	3.57	3.37	2.97	1.73
100 cm	8.81	8.40	8.16	8.04	7.82	7.27	7.09	6.94	3.72
110 cm	8.07	7.15	6.82	6.71	6.49	5.78	5.65	5.41	5.29
120 cm	7.26	7.20	5.82	5.67	5.09	4.72	4.58	4.27	2.77
130 cm	8.33	7.34	6.93	6.8	6.41	6.09	5.98	5.44	1.83
140 cm	9.10	7.79	7.14	6.72	6.37	5.64	5.32	4.89	4.31
150 cm	9.72	8.79	8.38	7.92	7.72	6.86	6.75	6.49	2.46
160 cm	9.30	8.18	7.57	7.34	7.11	6.76	6.63	6.30	1.34
170 cm	10.96	8.85	7.92	7.40	7.11	5.91	5.81	5.33	1.13

Till Site

Horizon	Pressure (kPa)								
	10	30	50	70	90	100	200	400	1500
LTD UT	27.95	22.35	18.83	17.06	15.62	14.14	11.91	9.16	7.96
s.d.	1.45	1.96	2.14	2.16	2.02	2.02	1.98	1.72	1.57
LTD UTd	28.90	24.76	22.22	20.18	19.27	18.11	15.99	12.66	11.56
s.d.	0.83	1.20	1.36	1.30	1.34	1.38	1.22	1.18	1.50
LTD OT	24.48	21.68	20.43	19.70	19.05	18.63	17.44	16.59	15.46
s.d.	2.27	1.87	1.88	1.89	1.89	1.93	1.78	2.01	2.02
LTD LT	27.79	25.50	24.32	23.78	23.11	22.65	21.84	20.55	19.50
s.d.	0.60	0.74	0.79	0.78	0.79	0.79	0.82	0.86	0.35
AY UT	23.30	20.76	18.60	16.93	16.09	14.56	11.40	10.15	7.21
s.d.	1.59	1.13	0.99	0.95	0.94	1.42	0.77	0.41	0.48
AY OT	30.30	27.87	26.14	24.68	23.90	22.15	20.79	18.78	18.33
s.d.	2.27	2.02	1.88	1.64	1.48	1.51	1.33	1.28	1.38
AY LT	36.51	32.58	30.36	28.55	27.39	25.62	24.31	22.43	21.29
s.d.	3.71	2.25	1.54	0.94	0.76	0.83	1.01	1.57	1.95
BA UT1	26.65	24.72	23.44	22.37	21.79	20.60	19.24	17.81	17.12
s.d.	0.71	0.46	0.40	0.41	0.48	0.57	0.82	1.13	1.31
BA UT2	26.27	21.51	19.35	17.55	17.08	15.93	12.16	8.31	8.08
s.d.	0.75	0.91	1.29	1.57	1.58	1.78	6.98	2.08	2.45
BA OT	24.81	23.22	22.16	21.39	21.00	20.96	20.55	17.77	14.34
s.d.	0.96	0.95	0.83	0.77	0.73	0.73	1.90	0.75	0.10
BA LT	27.84	25.06	23.76	22.71	22.11	21.45	19.50	18.20	15.45
s.d.	1.01	0.72	0.60	0.49	0.48	0.50	0.53	0.50	0.41
BA Clay	41.92	38.80	37.06	36.80	35.98	35.52	31.89	30.39	25.95
s.d.	1.16	0.97	0.97	0.93	3.04	3.02	0.71	0.76	0.53

Horizon	Pressure (kPa)								
	10	30	50	70	90	100	200	400	1500
CH UT A	26.40	20.47	14.88	13.68	12.72	11.05	9.41	6.68	6.29
s.d.	0.58	1.43	0.77	0.77	0.68	0.70	0.50	0.45	0.47
CH UT B	32.05	24.23	18.69	16.58	15.33	12.66	9.98	7.04	5.49
s.d.	1.24	1.33	1.28	1.33	1.21	0.73	0.80	0.65	0.34
CH UT C	33.08	24.57	20.55	18.51	17.37	14.92	12.19	8.69	5.71
s.d.	1.65	2.07	1.59	1.48	1.65	1.84	1.61	1.15	0.55
CH LT	25.49	23.54	22.62	21.97	21.55	20.91	20.22	19.12	18.85
s.d.	0.97	0.87	0.86	0.80	0.82	0.76	0.82	0.81	1.01

Horizon	Pressure (kPa)								
	10	30	50	70	90	100	200	400	1500
EE TT	11.84	16.83	13.29	10.67	9.52	8.75	6.83	5.19	1.56
s.d.	2.14	2.13	1.46	1.22	1.17	1.12	0.81	0.63	0.03
EE OT	12.36	19.84	18.26	16.89	16.11	15.47	14.43	13.03	9.42
s.d.	1.14	0.70	0.59	0.52	0.49	0.49	0.49	0.44	0.24
EE LT	25.18	22.31	20.56	18.92	17.94	17.03	15.11	13.06	8.78
s.d.	0.60	0.43	0.43	0.35	0.35	0.29	0.39	0.34	0.30
EE T	34.33	34.36	32.83	31.76	31.39	30.22	29.05	27.95	27.74
s.d.	1.57	1.44	1.35	1.33	1.35	1.28	1.24	1.24	1.18
BA Gray	21.25	18.64	17.27	16.48	15.75	15.17	14.13	12.97	10.59
s.d.	2.18	2.23	2.22	2.20	2.19	2.19	2.19	2.17	0.20
BA Red	18.24	16.20	14.94	14.05	13.46	12.59	11.55	10.59	8.57
s.d.	1.40	1.33	1.32	1.25	1.26	1.29	1.33	1.10	0.51
LA	29.97	27.19	25.73	24.56	24.08	23.20	21.82	20.24	16.19
s.d.	1.12	1.11	1.11	1.07	1.08	1.08	0.90	0.71	0.53
LE	30.44	26.45	23.31	21.11	20.62	19.42	17.44	15.92	12.01
s.d.	0.61	0.52	0.41	0.32	0.27	0.33	0.44	0.67	0.44
GA3	29.53	16.95	14.16	9.95	8.79	8.06	6.00	4.44	2.34
s.d.	3.70	2.48	2.26	1.46	1.39	1.33	1.06	0.98	0.17
GU	23.25	15.25	12.02	9.25	8.24	7.56	6.17	5.11	4.09
s.d.	0.47	0.95	0.60	0.68	0.80	0.77	0.69	0.66	0.47

APPENDIX D
COMPUTER PROGRAMS

Bulk Density (in BASIC)

```
10 PRINT "input mass: clod#1, clod#2, clod#3"
20 INPUT X1,X2,X3
30 PRINT "input: gravel#1, gravel#2, gravel#3"
35 INPUT G1,G2,G3
40 PRINT "input: volume#1, volume#2, volume#3"
45 INPUT V1,V2,V3
60 REM COMPUTE B1,B2,B3
66 LET B1=((X1-G1)/(V1-(G1/2.65)))
75 LET B2=((X2-G2)/(V2-(G2/2.65)))
80 LET B3=((X3-G3)/(V3-(G3/2.65)))
85 LET B4=(B1+B2+B3)/3
90 REM
95 REM
100 REM COMPUTE STANDARD DEVIATION
105 LET D=((B1-B4)^2+(B2-B4)^2+(B3-B4)^2)^.5
107 REM
108 REM
110 REM COMPUTE RELATIVE STANDARD DEVIATION
115 LET R=D/B4
117 PRINT "    "
118 PRINT "    "
119 PRINT "    "
120 PRINT "BULK DENSITY OF CLODS #1, #2, and #3"
125 PRINT B1;"g/cm3" B2;"g/cm3" B3;"g/cm3"
127 PRINT "    "
128 PRINT "MEAN=";B4;"g/cm3"
129 PRINT "    "
130 PRINT "STANDARD DEVIATION=";D;"g/cm3"
134 PRINT "    "
135 PRINT "RELATIVE STANDARD DEVIATION=";R;
140 END
```

Moisture Retention (in BASIC)

```
10 KEY OFF
20 CLS
30 PRINT"input number of Wet/Dry/ Coarse number sets:"
40 INPUT NS
50 FOR X=1 TO NS
60 PRINT "Inupt Dry Mass"X
70 INPUT D(X)
80 PRINT "Input Correction Factor"X
90 INPUT C(X)
100 NEXT X
110 PRINT "Input Bulk Density:"
120 INPUT BD
130 CLS
```

```

140 PRINT "Input Number of Wet Masses using same M(D) and C.F.
150 INPUT WML
160 FOR P=1 TO NS
170 FOR Q=1 TO WML
180 PRINT "Input Wet Mass "Q;" of set";P
190 INPUT M(P,Q)
200 NEXT Q
210 NEXT P
220 CLS
230 FOR I=1 TO NS
240 FOR J=1 TO WML
250 LET WUNC(J,I)=(M(J,I)-D(I)/D(I))
260 LET WC(J,I)=WUNC(J,I)/(1-(C(I)/D(I)))
270 LPRINT "Wc number";J;" in set";I;" equals "; USING "#.####";WC(J,I)
280 NEXT J
290 NEXT I
300 PRINT
310 FOR G=1 TO WML
320 FOR F=1 TO NS
330 Z=Z+WC(G,F)
340 IF F=NS THEN LET AV(G)=Z/F ELSE 360
350 Z=0
360 NEXT F
370 NEXT G
380 FOR L=1 TO WML
390 LPRINT "Mean (Wc) ";L;" = "; USING "##.####";AV(L)
400 LET V(L)=BD*AV(L)
410 LPRINT "Volumetric ";L;" = "; USING "##.####";V(L)
420 NEXT L
430 PRINT
440 FOR T=1 TO WML
450 FOR U=1 TO NS
460 LET QD(T)=QD(T)+(WC(T,U)^2)
470 LET WD(T)=WD(T)+(WC(T,U)
480 IF U=NS THEN LET WDX(T)=(WD(T)^2)/NS
490 LET AD(T)=QD(T)-WDX(T)
500 LET SD(T)=(AD(T)/(NS-1))^.5
510 IF U=NS THEN LPRINT "Standard Deviation ";T;" = "; USING
    "##.####";SD(T)
520 NEXT U
530 NEXT T
540 PRINT
550 PRINT
560 PRINT
570 PRINT"Continue? (Y/N)
580 INPUT A$
590 IF A$="y" THEN 20 ELSE 600
600 CLS
610 KEY ON

```

Using the programs

Bulk Density Program

Type: Basic ^

Press: F3

Load"CBD1 ^

Press: F2

Enter masses: #,#,# ^

Enter C.F.: #,#,# ^

Enter volume: #,#,# ^

The program calculates individual BD plus statistics.

Moisture Retention Program

Type: Basic ^

Press: F3

Load"Final ^

Press: F2

Enter number of Reps (sets): # ^

Enter dry mass 1: # ^

Enter C.F. 1: # ^

Repeat until all dry masses and C.F.'s entered.

Enter Bulk Density for the horizon: # ^

Enter the number of pressures (observations): # ^

Enter weight 1 of 1: # ^

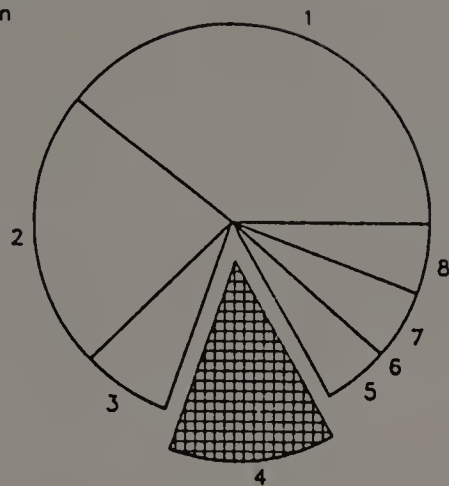
" " 2 of 1: # ^

..... etc

Print out will give you moisture content of each observation by weight first and then by volume. Also statistics will be calculated for each.

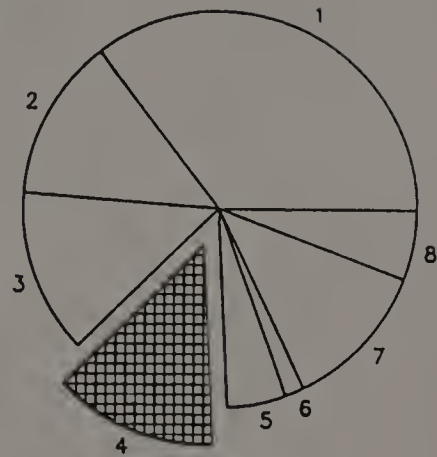
APPENDIX E
MICROMORPHOLOGY

- 1 = S-matrix and fine voids
- 2 = Weathered Grain
- 3 = Unweathered Grain
- 4 = Argillan
- 5 = Grain Cutan
- 6 = Mangan
- 7 = Ferran
- 8 = Void



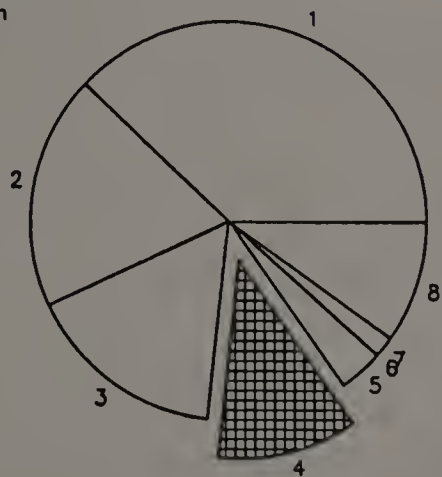
Modal Distribution
Pedon 1
Bt Horizon

- 1 = S-matrix and fine voids
- 2 = Weathered Grain
- 3 = Unweathered Grain
- 4 = Argillan
- 5 = Grain Cutan
- 6 = Mangan
- 7 = Ferran
- 8 = Void



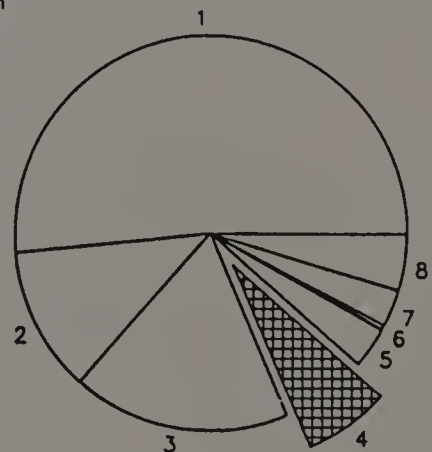
Modal Distribution
Pedon 1
2Btx1 Horizon

- 1 = S-matrix and fine voids
- 2 = Weathered Grain
- 3 = Unweathered Grain
- 4 = Argillan
- 5 = Grain Cutan
- 6 = Mangan
- 7 = Ferran
- 8 = Void



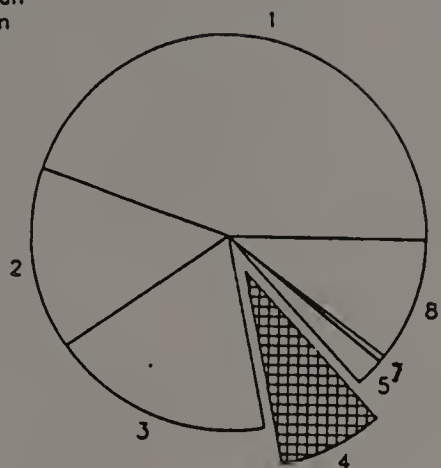
Modal Distribution
Pedon 1
Bleached Prism Face in 2Btx1

- 1 = S-matrix and fine voids
- 2 = Weathered Grain
- 3 = Unweathered Grain
- 4 = Argillan
- 5 = Grain Cutan
- 6 = Mangan
- 7 = Ferran
- 8 = Void



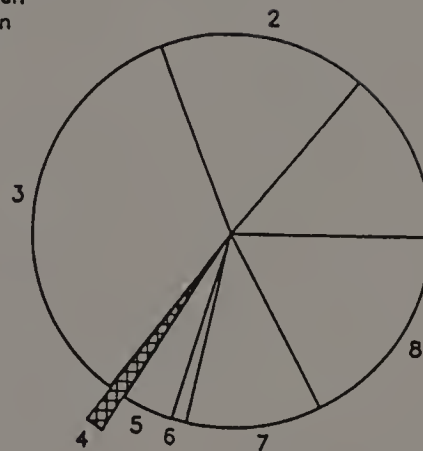
Modal Distribution
Pedon 1
2Btx2 Horizon

- 1 = S-matrix and fine voids
- 2 = Weathered Grain
- 3 = Unweathered Grain
- 4 = Argillan
- 5 = Grain Cutan
- 6 = Mangan
- 7 = Ferran
- 8 = Void



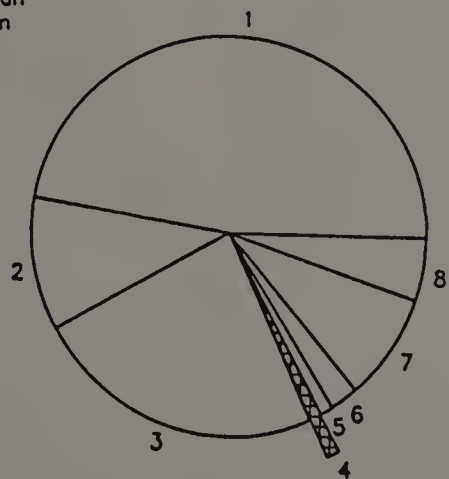
Modal Distribution
Pedon 1
Bleached Prism Face in 2Btx2

- 1 = S-matrix and fine voids
- 2 = Weathered Grain
- 3 = Unweathered Grain
- 4 = Argillan
- 5 = Grain Cutan
- 6 = Mangan
- 7 = Ferran
- 8 = Void



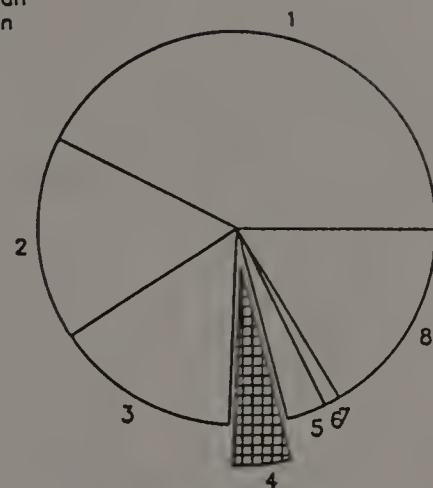
Modal Distribution
Pedon 1
3BCm Horizon

- 1 = S-matrix and fine voids
- 2 = Weathered Grain
- 3 = Unweathered Grain
- 4 = Argillan
- 5 = Grain Cutan
- 6 = Mangan
- 7 = Ferran
- 8 = Void



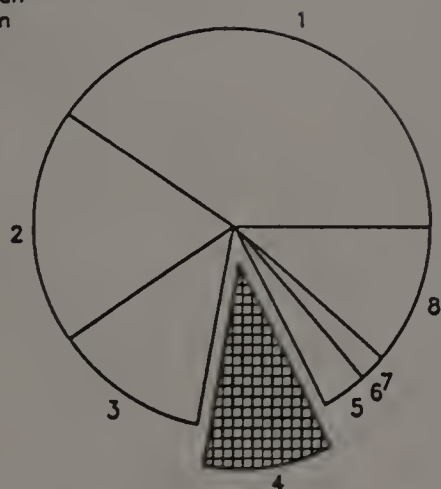
Modal Distribution
Pedon 1
4Cd Horizon

- 1 = S-matrix and fine voids
- 2 = Weathered Grain
- 3 = Unweathered Grain
- 4 = Argillan
- 5 = Grain Cutan
- 6 = Mangan
- 7 = Ferran
- 8 = Void



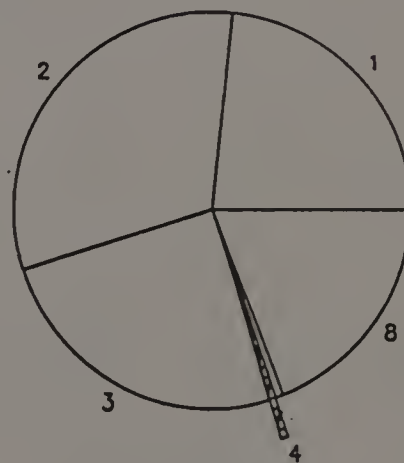
Modal Distribution
Pedon 2
BE Horizon

- 1 = S-matrix and fine voids
- 2 = Weathered Grain
- 3 = Unweathered Grain
- 4 = Argillan
- 5 = Grain Cutan
- 6 = Mangan
- 7 = Ferran
- 8 = Void



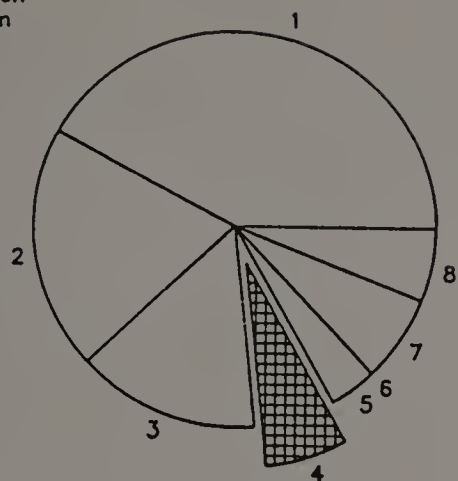
Modal Distribution
Pedon 2
2Btx1 Horizon

- 1 = S-matrix and fine voids
- 2 = Weathered Grain
- 3 = Unweathered Grain
- 4 = Argillan
- 5 = Grain Cutan
- 6 = Mangan
- 7 = Ferran
- 8 = Void



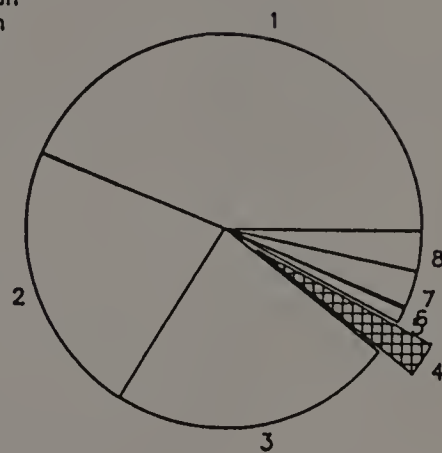
Modal Distribution
Pedon 2
Bleached Prism Face

- 1 = S-matrix and fine voids
- 2 = Weathered Grain
- 3 = Unweathered Grain
- 4 = Argillan
- 5 = Grain Cutan
- 6 = Mangan
- 7 = Ferran
- 8 = Void



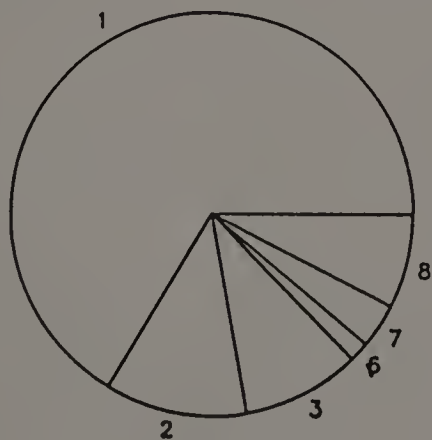
Modal Distribution
Pedon 2
2Btx2 Horizon

- 1 = S-matrix and fine voids
- 2 = Weathered Grain
- 3 = Unweathered Grain
- 4 = Argillan
- 5 = Grain Cutan
- 6 = Mangan
- 7 = Ferran
- 8 = Void



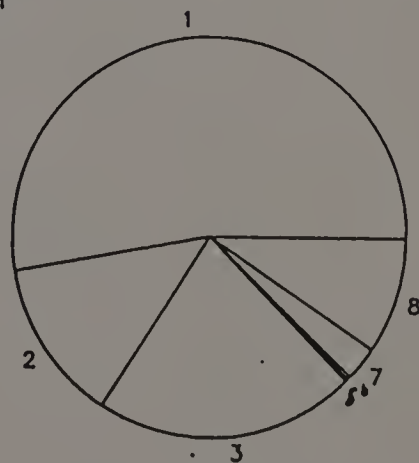
Modal Distribution
Pedon 2
2BCd Horizon

- 1 = S-matrix and fine voids
- 2 = Weathered Grain
- 3 = Unweathered Grain
- 4 = Argillan
- 5 = Grain Cutan
- 6 = Mangan
- 7 = Ferran
- 8 = Void



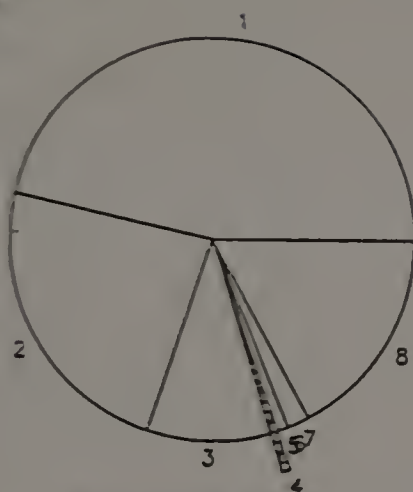
Modal Distribution
Pedon 2
3Cd1 Horizon

- 1 = S-matrix and fine voids
- 2 = Weathered Grain
- 3 = Unweathered Grain
- 4 = Argillan
- 5 = Grain Cutan
- 6 = Mangan
- 7 = Ferran
- 8 = Void



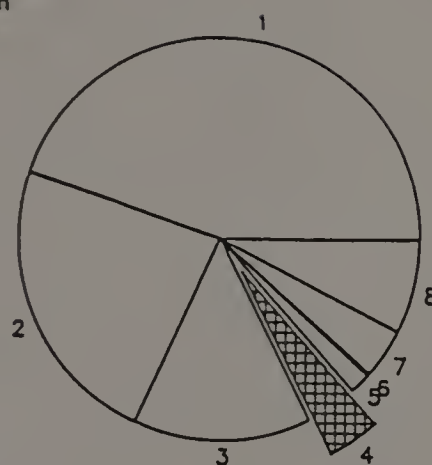
Modal Distribution
Pedon 2
3Cd2 Horizon

- 1 = S-matrix and fine voids
- 2 = Weathered Grain
- 3 = Unweathered Grain
- 4 = Argillan
- 5 = Grain Cutan
- 6 = Mangan
- 7 = Ferran
- 8 = Void



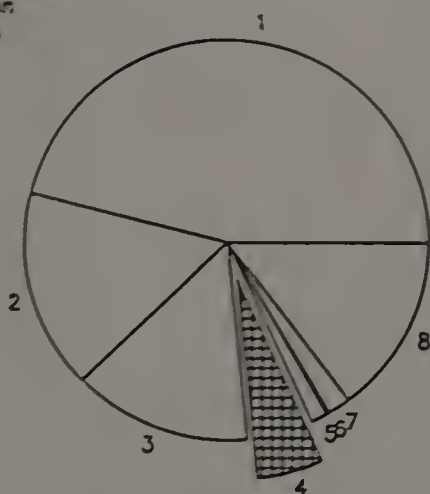
Modal Distribution
Pedon 3
BE Horizon

- 1 = S-matrix and fine voids
- 2 = Weathered Grain
- 3 = Unweathered Grain
- 4 = Argillan
- 5 = Grain Cutan
- 6 = Mangan
- 7 = Ferran
- 8 = Void



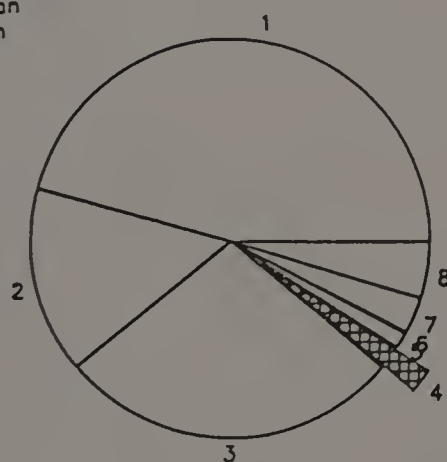
Modal Distribution
Pedon 3
2Btx1 Horizon

- 1 = S-matrix and fine voids
- 2 = Weathered Grain
- 3 = Unweathered Grain
- 4 = Argillan
- 5 = Grain Cutan
- 6 = Mangan
- 7 = Ferran
- 8 = Void



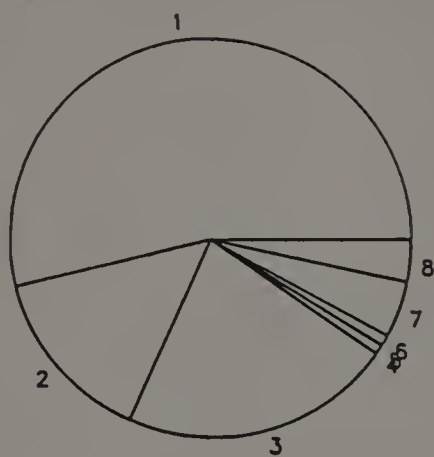
Modal Distribution
Pedon 3
2Btx2 Horizon

- 1 = S-matrix and fine voids
- 2 = Weathered Grain
- 3 = Unweathered Grain
- 4 = Argillan
- 5 = Grain Cutan
- 6 = Mangan
- 7 = Ferran
- 8 = Void



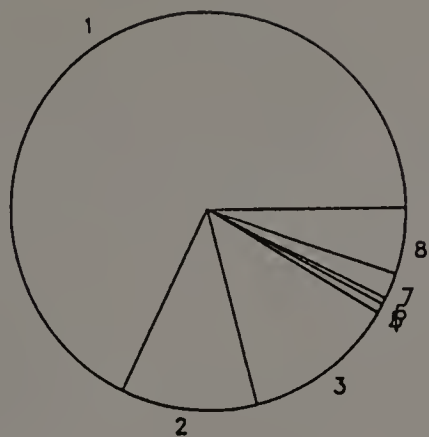
Modal Distribution
Pedon 3
2BCd Horizon

- 1 = S-matrix and fine voids
- 2 = Weathered Grain
- 3 = Unweathered Grain
- 4 = Argillan
- 5 = Grain Cutan
- 6 = Mangan
- 7 = Ferran
- 8 = Void



Modal Distribution
Pedon 3
3Cd Horizon

- 1 = S-matrix and fine voids
- 2 = Weathered Grain
- 3 = Unweathered Grain
- 4 = Argillan
- 5 = Grain Cutan
- 6 = Root
- 7 = Ferran
- 8 = Void



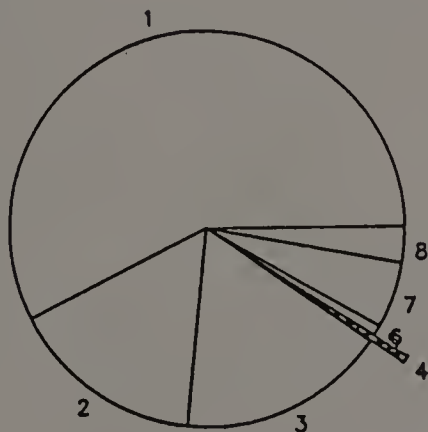
Modal Distribution
Pedon 4
Ap Horizon

- 1 = S-matrix and fine voids
- 2 = Weathered Grain
- 3 = Unweathered Grain
- 4 = Argillan
- 5 = Grain Cutan
- 6 = Root
- 7 = Ferran
- 8 = Void



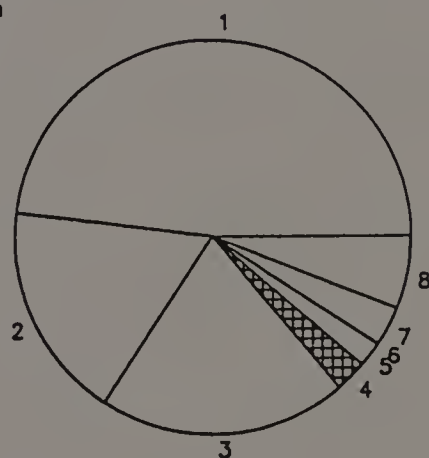
Modal Distribution
Pedon 4
Bw1 Horizon

- 1 = S-matrix and fine voids
- 2 = Weathered Grain
- 3 = Unweathered Grain
- 4 = Argillan
- 5 = Grain Cutan
- 6 = Mangan
- 7 = Ferran
- 8 = Void



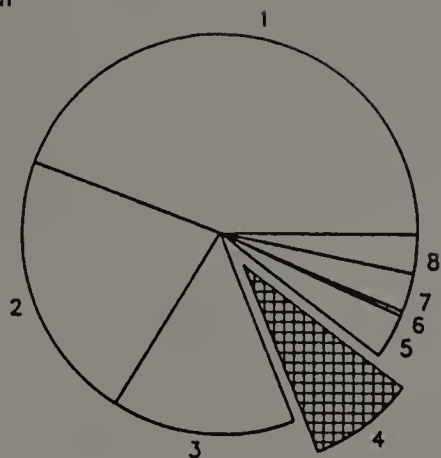
Modal Distribution
Pedon 4
Bw2 Horizon

- 1 = S-matrix and fine voids
- 2 = Weathered Grain
- 3 = Unweathered Grain
- 4 = Argillan
- 5 = Grain Cutan
- 6 = Mangan
- 7 = Ferran
- 8 = Void



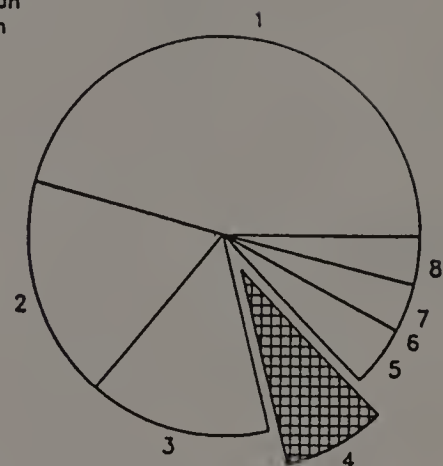
Modal Distribution
Pedon 4
BE Horizon

- 1 = S-matrix and fine voids
- 2 = Weathered Grain
- 3 = Unweathered Grain
- 4 = Argillan
- 5 = Grain Cutan
- 6 = Mangan
- 7 = Ferran
- 8 = Vaid



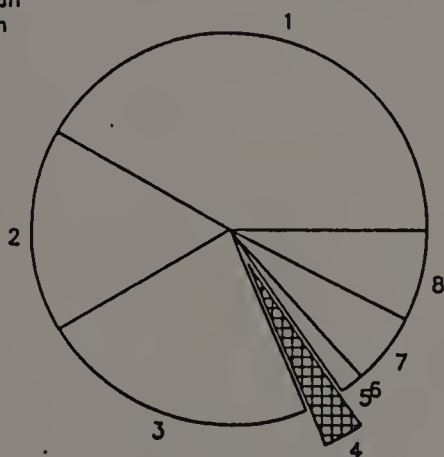
Modal Distribution
Pedon 4
2Btx1 Horizon

- 1 = S-matrix and fine voids
- 2 = Weathered Grain
- 3 = Unweathered Grain
- 4 = Argillan
- 5 = Grain Cutan
- 6 = Mangan
- 7 = Ferran
- 8 = Vaid



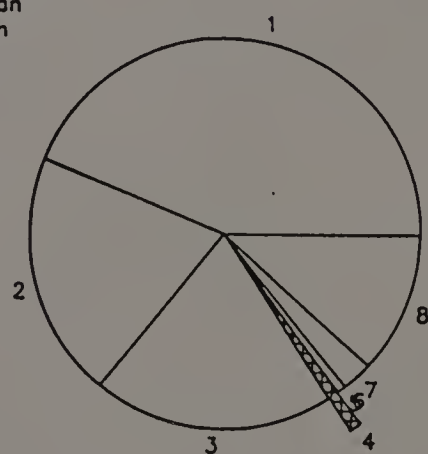
Modal Distribution
Pedon 4
2Btx2 Horizon

- 1 = S-matrix and fine voids
- 2 = Weathered Grain
- 3 = Unweathered Grain
- 4 = Argillan
- 5 = Grain Cutan
- 6 = Mangan
- 7 = Ferran
- 8 = Vaid



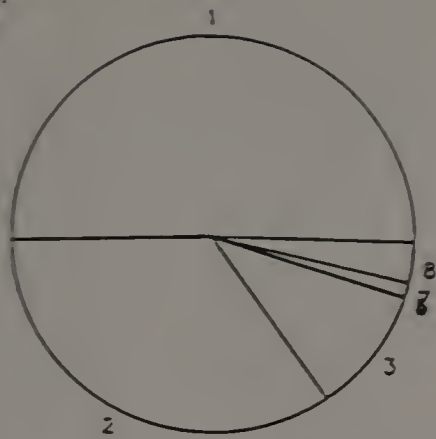
Modal Distribution
Pedon 4
2BCd Horizon

- 1 = S-matrix and fine voids
- 2 = Weathered Grain
- 3 = Unweathered Grain
- 4 = Argillan
- 5 = Grain Cutan
- 6 = Mangan
- 7 = Ferran
- 8 = Vaid



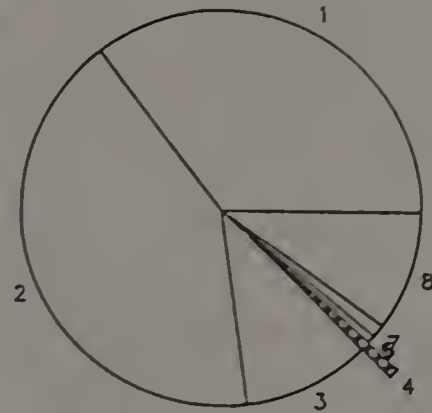
Modal Distribution
Pedon 4
3Cd Horizon

- 1 = S-matrix and fine voids
- 2 = Weathered Grain
- 3 = Unweathered Grain
- 4 = Argillan
- 5 = Grain Cutan
- 6 = Mangan
- 7 = Ferran
- 8 = Void



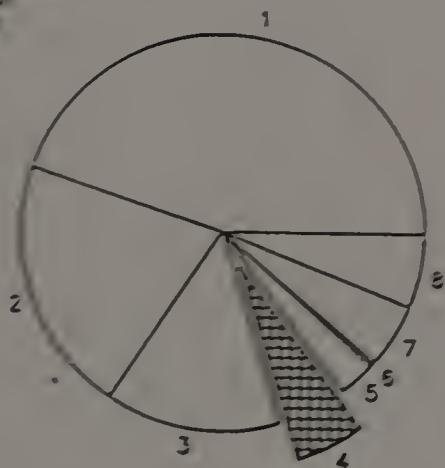
Modal Distribution
Pedon 5
BE Horizon

- 1 = S-matrix and fine voids
- 2 = Weathered Grain
- 3 = Unweathered Grain
- 4 = Argillan
- 5 = Grain Cutan
- 6 = Mangan
- 7 = Ferran
- 8 = Void



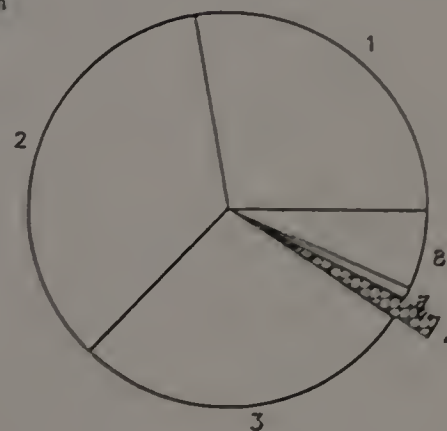
Modal Distribution
Pedon 5
2EB Horizon

- 1 = S-matrix and fine voids
- 2 = Weathered Grain
- 3 = Unweathered Grain
- 4 = Argillan
- 5 = Grain Cutan
- 6 = Mangan
- 7 = Ferran
- 8 = void



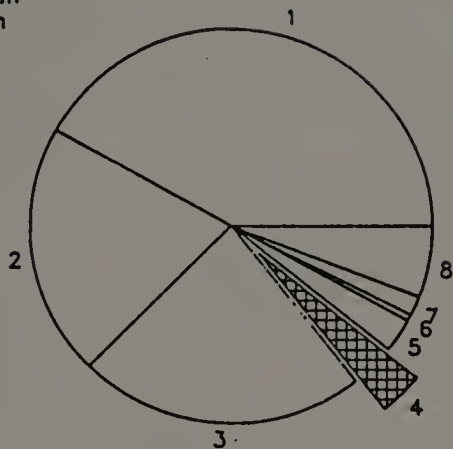
Modal Distribution
Pedon 5
2Bx1 Horizon

- 1 = S-matrix and fine voids
- 2 = Weathered Grain
- 3 = Unweathered Grain
- 4 = Argillan
- 5 = Grain Cutan
- 6 = Mangan
- 7 = Ferran
- 8 = Void



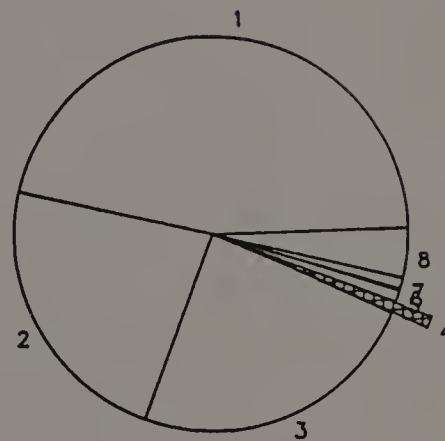
Modal Distribution
Pedon 5
Bleached Prism Face

- 1 = S-matrix and fine voids
- 2 = Weathered Grain
- 3 = Unweathered Grain
- 4 = Argillan
- 5 = Grain Cutan
- 6 = Mangan
- 7 = Ferran
- 8 = Void



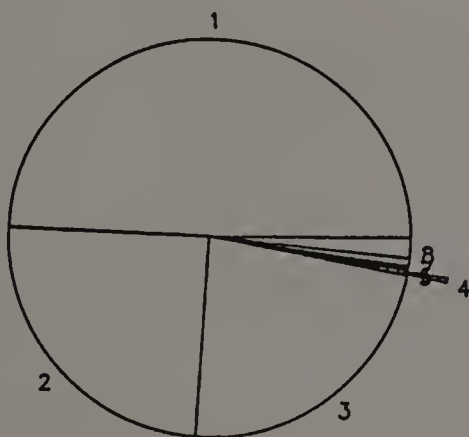
Modal Distribution
Pedon 5
2Btx2 Horizon

- 1 = S-matrix and fine voids
- 2 = Weathered Grain
- 3 = Unweathered Grain
- 4 = Argillan
- 5 = Grain Cutan
- 6 = Mangan
- 7 = Ferran
- 8 = Void



Modal Distribution
Pedon 5
2Cd1 Horizon

- 1 = S-matrix and fine voids
- 2 = Weathered Grain
- 3 = Unweathered Grain
- 4 = Argillan
- 5 = Grain Cutan
- 6 = Mangan
- 7 = Ferran
- 8 = Void



Modal Distribution
Pedon 5
2Cd2 Horizon

APPENDIX F
RIDGEBURY VARIATION

Introduction

The Ridgebury series is common in the uplands of Massachusetts and surrounding states. Approximately 2.5% of the mapped acreage in Massachusetts is in the Ridgebury series (personal communication R. Scanu, 1989) The series has most recently been classified as an Aeric Haplaquept whereas it was previously classified as an Aeric Fragiaquept. The soils are developed on glacial till and have a dense subsurface horizon that is slowly permeable and restricts root penetration. This dense horizon may have some of the common morphologic features of a fragipan, including a polygonal pattern of bleached prism faces (BPF), brittleness, and slaking in water (Soil Survey Staff, 1975; Witty and Knox, 1989). Some of the soils do not show this morphology, yet contain a dense subsurface horizon.

The Ridgebury soils typically are found in the low lying concave areas and toe slope sections of till uplands and on toe slopes of drumlins. Slopes generally are level but can be as great as 15 percent. The till in which the soil has developed is derived from highly metamorphosed rocks and ranges from a loamy to a fine sandy texture. The exact age of the various tills are the source of considerable debate at the present time (Stone, personal communication, 1987; Lindbo, 1990). An aeolian component is typically observed in most of the soils of the region (Fletcher, 1978).

The parent material of the Ridgebury soils varies throughout the region (Newton, 1978) and soil properties differ accordingly. This

study was initiated to characterize some of the morphologic variations observed in the Ridgebury series.

Materials and Methods

Three areas previously mapped or identified as Ridgebury series were selected for investigation (Veneman and Bodine, 1982; Mikelk, personal communication, 1985; Reed, 1989). These areas were chosen to represent a range in parent materials typical for the series. All areas were located in a toe slope position. Pits were excavated to a depth of 2 m for Pedons 1 and 3 and to a depth of 80 cm for BHR. The parent material from which BHR was developed was observed also in a deep pit approximately 100 m upslope. Pit faces were cleaned and prepared for photography prior to description. Photomosaics were taken of Pedons 1 and 3 to assist in the preparation of cross section diagrams (Ryan and McGarity, 1983). Bulk samples and clods were taken after the descriptions were completed.

A minimum of 2 thin section samples were taken from each horizon. A 5 cm x 5 cm x 2.5 cm deep sheet metal box was pressed into the pit face; excess soil was removed from the outside edges, the box removed from the face with minimum disturbance and the orientation noted on the box. The samples were then transported back to the laboratory for analysis.

The samples were air dried for at least 3 months prior to impregnation. The samples were impregnated under vacuum with Spur

resin. After the resin had cured the samples were sectioned and observed. Terminology of Brewer (1976) was used for the descriptions.

Results and Discussion

Macromorphology

The overall morphology of the three pedons differs illustrated in Figures 25-26, 115-117 illustrate. There are however notable similarities among all three pedons. All pedons contain a dense horizon within the upper meter. The soil colors along with height of the water table at the time of sampling indicate that these soils are somewhat poorly to poorly drained (c.f. Appendix B; Profile Descriptions for the three pedons in question). The A horizons, while varying in thickness, have similar colors and contain common medium to large distinct high chroma mottles (Table 31). The mottles occur as neoferrans, ferrans, and iron-rich nodules. The Bw horizons are also similar in regards to color and mottling.

Differences between the pedons also are evident (Table 31). The various subsoil in different pedons does not exhibit the same horizon sequence due to the difference in parent material assemblage of each site. OHL has the strongest influence of aeolian material and also has distinct colluvial layers. BHR essentially lacks the aeolian mantle and is developed directly in the till. Textural differences between the pedon therefore are strongly related to parent material. Whereas a dense horizon occurs within all the pedons it



O
-
A
-
Bw
-
Bx1
-
Bx2

Figure 115. Photograph of the BTR Pedon, Spencer, MA.

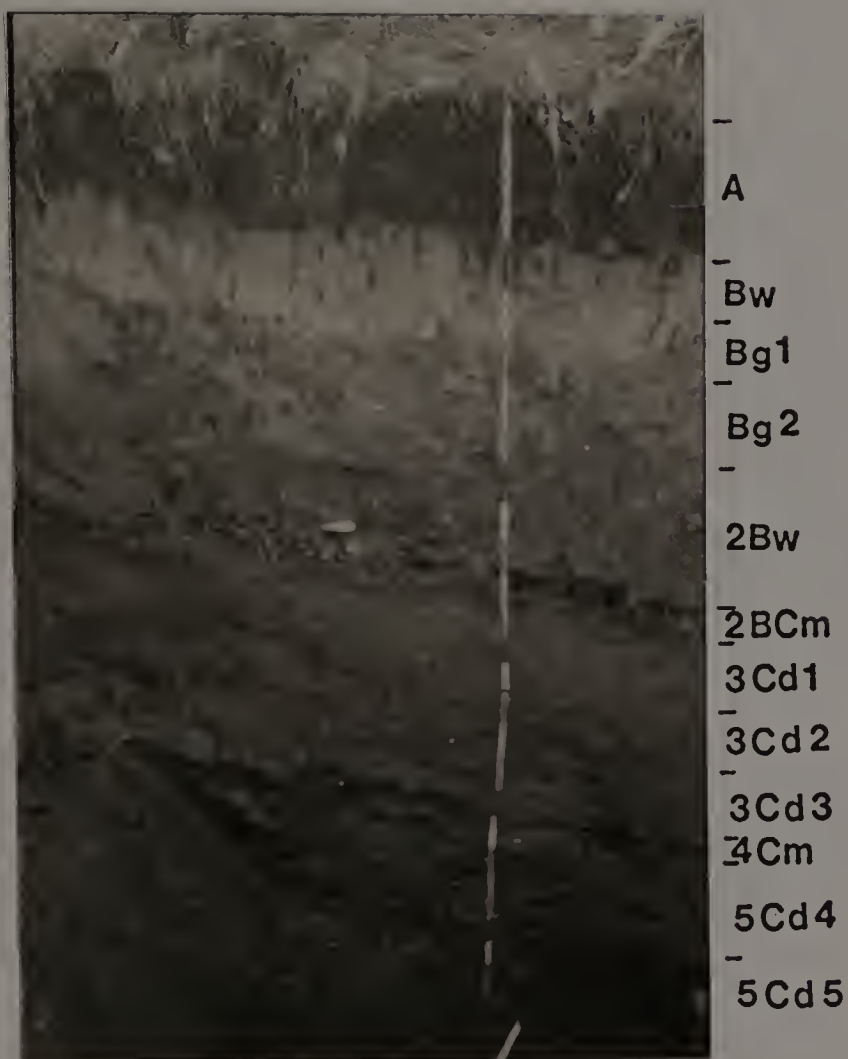


Figure 116. Photograph of the OHL Pedon profile, Amherst, MA.

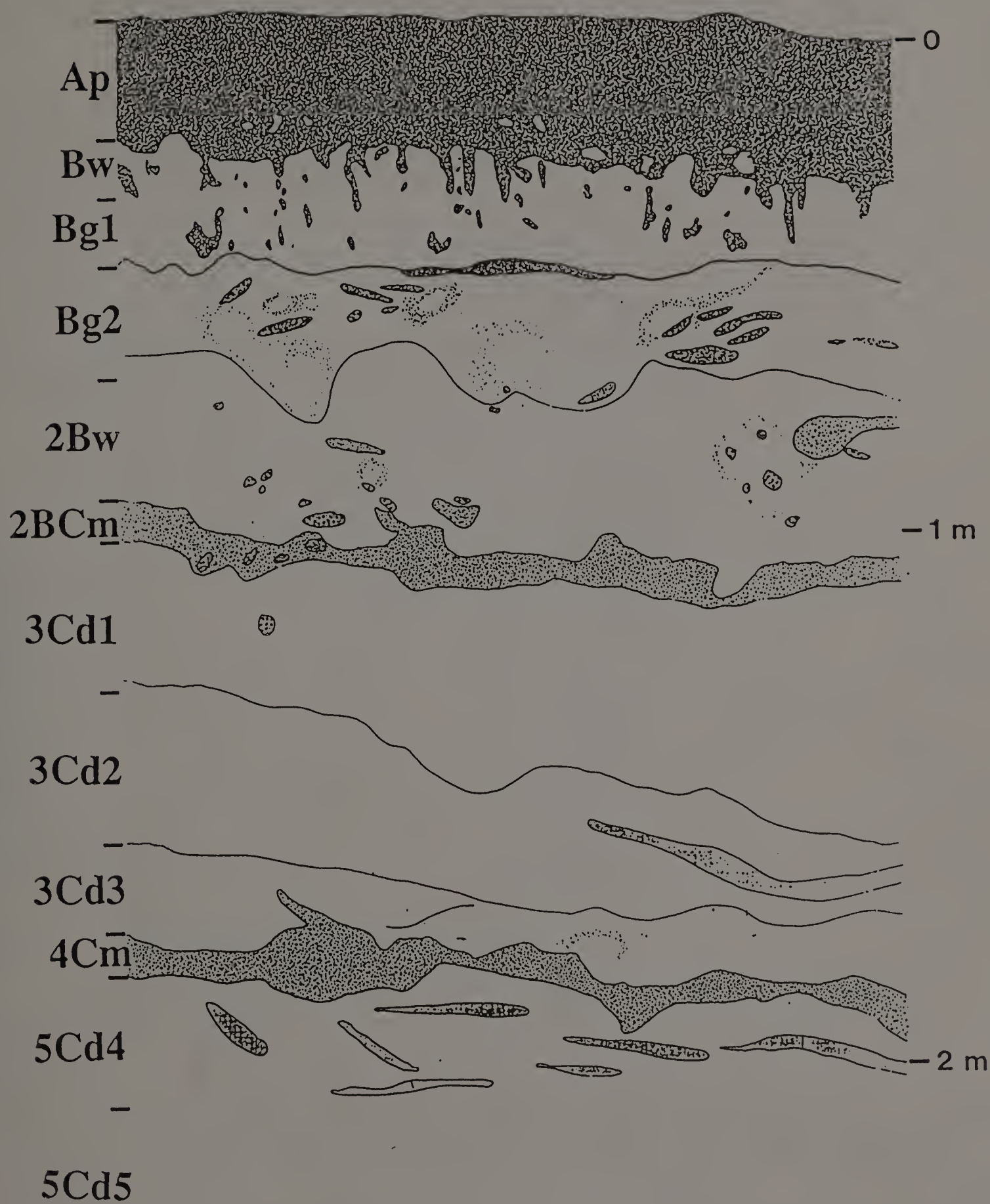


Figure 117. Cross-sectional diagram of the OHL Pedon.

Table 31. Selected morphologic observation of the Ridgebury Pedons.

	Pedon 5	BHR	OHL
<u>A-horizon</u>			
Color, matrix	10YR 3/1	2.5Y 3/2	10YR 3/1
Thickness	25 cm	11 cm	21 cm
Color, mottles	7.5YR 5/6	7.5YR 5/4	2.5Y 6/4 7.5YR 5/6
<u>B-horizon</u>			
Color, matrix	10YR 5/4	2.5Y 5/4	2.5Y 6/4, 5/4
Thickness	19 cm	12 cm	19 cm
Color, mottles	7.5YR 5/6 10YR 7/1	2.5Y 5/2 10YR 4/6	5Y 6/1, 5/1 7.5YR 5/6
<u>Bgd- or Bx-horizon</u>			
Depth to Bgd or Bx	81 cm (2Bx)	23-30 cm (Bx)	40 cm (Bgd)
Color, matrix	10YR 5/3, 6/4	2.5Y 5/2	5GY 6/1 to 5G 6/1
Color, mottles	7.5YR 4/6	5Y 6/2	2.5Y6/6
Bleached Prism Faces in Bx	10YR 7/1 and 5Y 7/1 interior with 10YR 5/4 exterior	5Y 6/2 interior 10YR 4/6 exterior	Not present
<u>Cd-horizon</u>			
Depth to Cd	184 cm	80+ cm	102 cm
Color, matrix	5GY 6/1	n.d.	10YR3/3, 4/4, 2.5Y 4/4, 5YR 4/6, N70, 5Y 6/1
Color, mottles	5Y 6/1	n.d.	5Y 3/3, 2.5Y 4/4, 2.5Y 6/6, 5YR 3/3
Depth to Till	57-81 cm	0-10 cm	187 cm

does not show identical morphologic features. The dense horizons of Pedon 5 and 2 contain bleached prism faces (BPF) and are brittle. The BPF are characterized by light gray to light olive gray interiors with dark to yellowish brown rinds (Figures 28 and 40). These occur as roughly vertical streaks 1 to 10 cm wide and 30 to 50 cm apart. In plan view they demark a polygonal network (Figure 40). This morphology combined with the brittle behavior is typical of a fragipan (Grossman and Carlisle, 1969; Soil Survey Staff, 1975) and these horizons are denoted with a subscript "x".

Also present within the dense layer of Pedons 1 and 2 are vesicles and clay skins. The clay skins are up to 0.7 mm thick. Silt caps are present as well. The dense horizon of OHL lacks the afore mentioned features. OHL does contain two iron stained and cemented horizons. These are much sandier than the overlying horizons and are presumed to be a component of the colluvium which underlies the pedon. The source of the iron and manganese present in the horizon is unclear but perhaps may have been transported laterally from more elevated landscape positions (Veneman and Bodine, 1982; Pickering and Veneman, 1984). The depth to the till also varies considerably, being deepest in OHL and shallowest in BHR (Table 31). Differences in parent material clearly result in a variable macromorphology.

Micromorphology

Similarities also are observed in the A and upper Bw horizon with respect to the micromorphology (Table 32). Root and organic debris are common in the A horizons. The upper horizons are loosely packed and dominated by a silty matrix. Papules and Fe-rich nodules dominate in the upper as well as many of the lower horizons (Figure 45 and 118). Similarities in these horizons are expected since their macromorphology, drainage class, and natural environment are similar.

In the lower subsoil and in the substratum differences are more pronounced. Pedons 1 and 2 show a stonger fabric, denser packing of skeleton grains, and the presence of argillans. Initially, the argillans and ferriargillans are thin and discontinuous, and confined to large continuous voids. The expression of the argillans and ferriargillans increases with depth to the 2Bx2 and Bx2 horizons (Figure 119). Argillans commonly coat voids of all types and act as bridges between skeleton grains (Lindbo and Veneman, 1989). In extreme cases pores are completely filled with illuviated argillans. Geopetal structures are common suggesting that these are illuviation features (Figure 69). Ferrans occur along with the argillans as well as coating grains within the s-matrix. Along the boundaries of the BPF ferrans and ferriargillans coat most surfaces. The interiors of the BPF appear leached, showing very few cutanic features (Figure 55). The abundance of argillans and ferriargillans deceases in the 2Cd1 horizon of Pedon 5. Other features such as papules and nodules also

Table 32. Micromorphological observations of the Ridgebury Pedons.

Horizon	Plasmic Fabric	Pedological Features
Pedon 5		
Bw	Silasepic	Common Fe-nodules and papules
BE	Silasepic	Common papules and diffuse Fe-nodules; very few skeletans
2Bw	Silasepic	Common papules, diffuse Fe-nodules, and thin ferriargillans and argillans; few ferrans
2Bx1	Silasepic to mosepic and skel-vosepik	Common papules, Fe-nodules, argillans, ferriargillans, ferrans, albans, and silt caps, common grain to grain argillans and ferriargillans; very few mangans
2Bx2	Insepik to mosepic and skel-vosepik	Common papules, Fe-nodules, argillans, ferriargillans, ferrans, and silt caps, common grain to grain argillans and ferriargillans; few to common albans; very few mangans; argillans, ferriargillans, and ferrans decrease with depth
2Cd1	Silasepic to mosepic	Few papules, argillans, and diffuse Fe-nodules; very few ferrans

Continued, next page

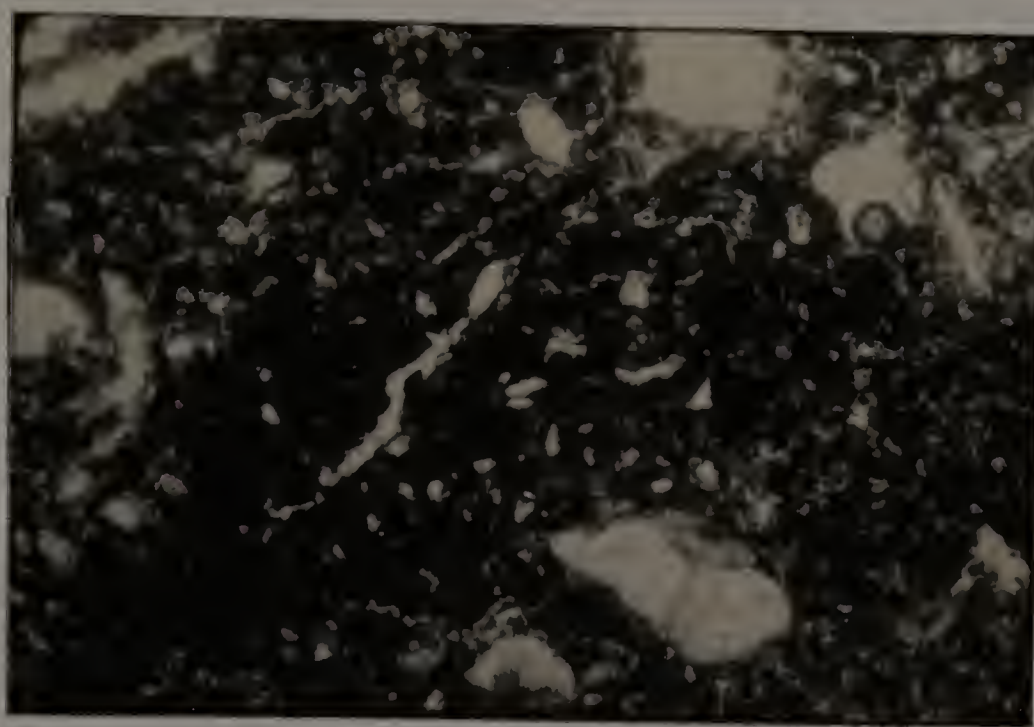
Table 32 cont.

		BHR
A	Silasepic	Common papules, Fe-nodules, fecal pellets, roots, and organic debris
Bw	Insepic with minor vosepic	Common papules, Fe-nodules, roots, and organic debris; few ferrans; very few thin argillans and fecal pellets
Bx1	In- to mosepic minor vo-skelsepic more developed with depth	Common papules, Fe-nodules, and ferrans, few to common argillans and ferriargillans increasing with depth
Bx2	Mosepic with some areas of omniseptic	Common papules, Fe-nodules, and ferrans; few to common argillans and ferriargillans
		OHL
Ap	Silasepic	Common Fe-nodules, fecal pellets, neo ferrans, roots, and organic debris; few ferrans and albans
Bw	Silasepic	Common Fe-nodules, papules, roots, and organic debris; few to common thin channel argillans; few ferrans/and neoferrans
Bg1	Silasepic	Common papules, few to common quassi-, neo-, ferrans; few Fe-nodules, roots, and organic debris; very few thin argillans
Bg2	Silasepic	Common papules, ferrans, Fe-nodules; few thin ferriargillans; very few argillans
2Bw	Silasepic	Common Fe-nodules and ferrans (acting as a cement); few ferriargillans and mangans

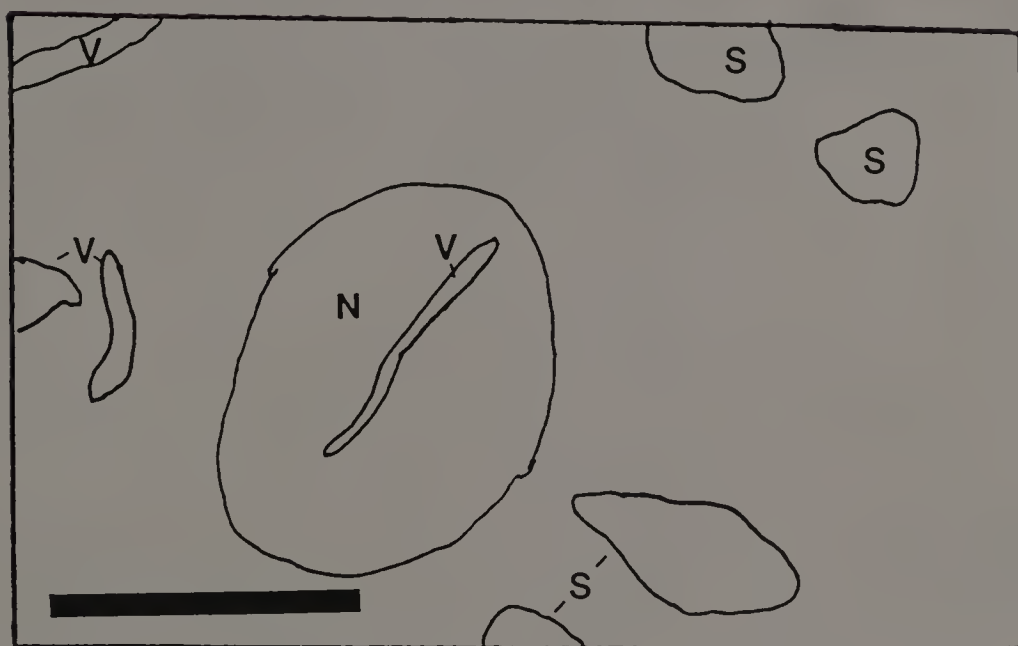
Continued, next page

Table 32 cont.

23Cm	Silasepic	Common ferrans and mangans (acting as a cement); few to common silt caps; few ferriargillans; very few thin argillans; very little plasma overall
3Cd1	Silasepic to skel-insepic	Common Fe-nodules; few ferrans and papules; very few thin ferriargillans (at top of horizon), mangans, and poorly developed silt caps
3Cd2	Silasepic to skel-insepic	Common Fe-nodules; few ferrans and papules; very few mangans and poorly developed silt caps
3Cd3	Silasepic to skel-insepic	Common Fe-nodules; few ferrans, mangans, and papules
4Cm	Silasepic	Common ferrans and mangans (acting as cement); very few Fe-nodules
5Cd4	Silasepic to skelsepic	Common ferrans
5Cd5	Silasepic to skelsepic	Common ferrans

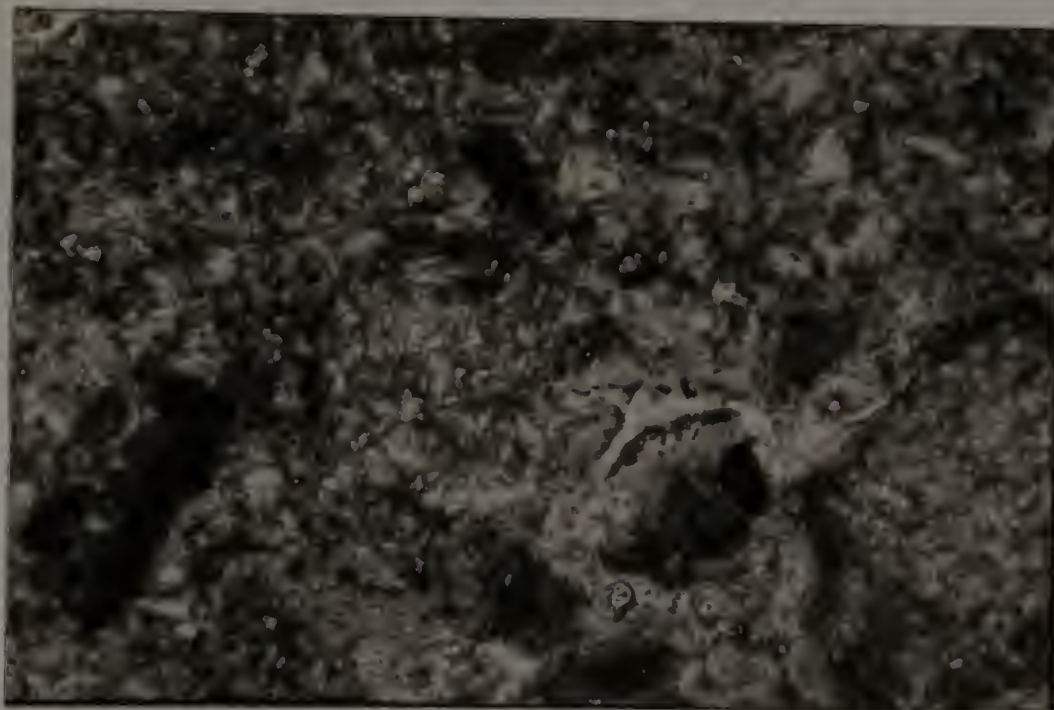


A

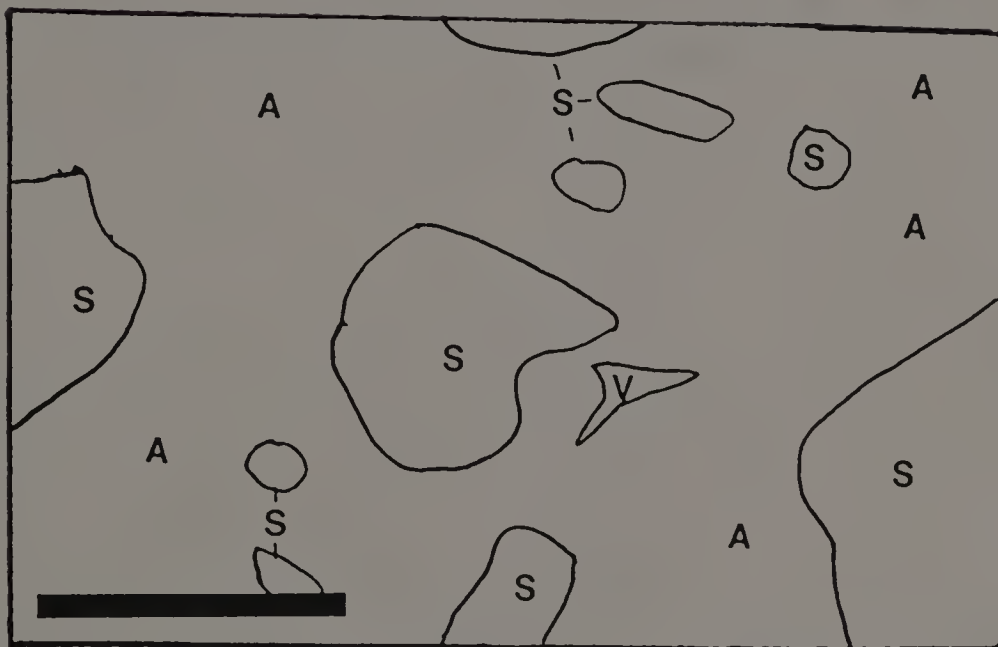


B

Figure 118. Photomicrograph of A horizon, OHL Pedon. N = nodule, S = skeleton grain, V = void. (A) photograph, (B) schematic. The bar is 1 mm long.



A



B

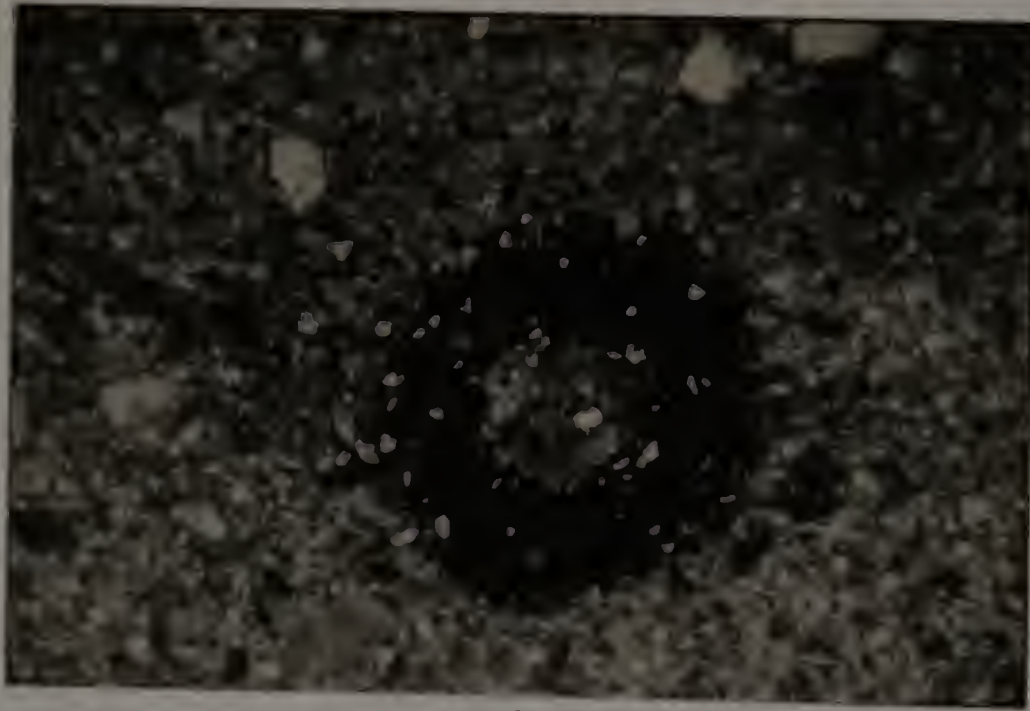
Figure 119. Photomicrograph of Bx2 horizon, BTR Pedon. A = argilan, S = skeleton grain, V = void. (A) photograph, (B) schematic. The bar is 1 mm long.

decrease in abundance in the lower horizon as well. The arrangement of features is typical of those observed in fragipans (Grossman et al., 1959; Horn and Rutledge, 1965; Grossman and Carlisle, 1969; Wang et al., 1974; Smith and Callahan, 1987; Habecker et al., 1990).

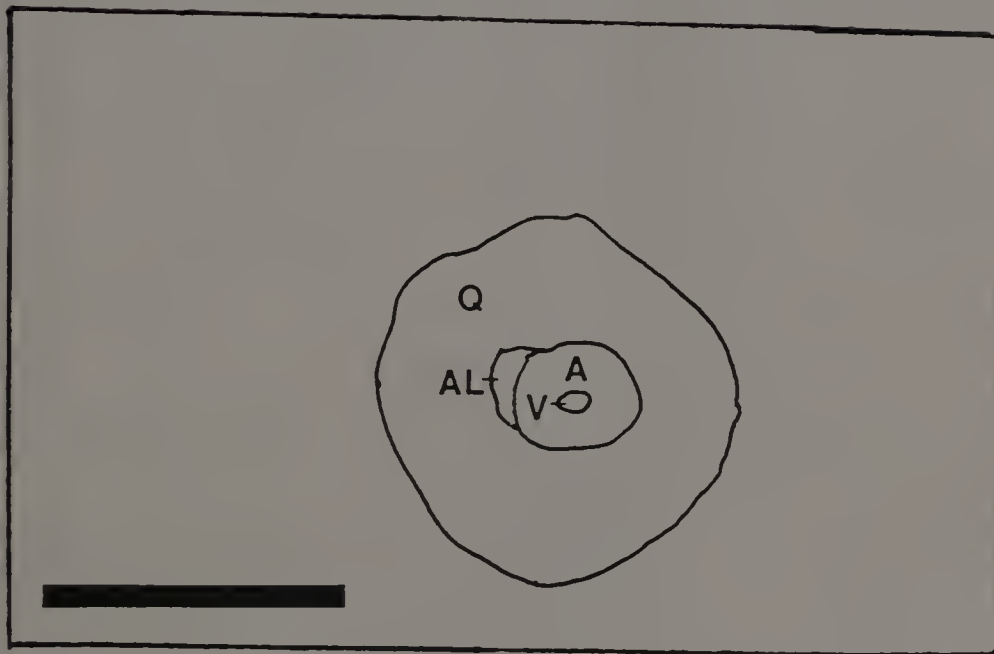
The lower horizons of OHL are quite different from the other pedons. There are few thin argillans present but not as extensive or as well developed as those seen in the 2Bx and Bx horizons of Pedon 5 and 2 (Figure 120). Iron-rich nodules begin to coalesce in the lower portions of the 2Bw. Within the BCm and the deeper Cm horizons ferrans and mangans bridge skeleton grains thus cementing the horizon (Figure 121). The grains are in a simple packing arrangement with the small amount of plasma (not involved in the ferrans or mangans) exhibiting a silasepic fabric. Ferrans are present in all the Cd horizons showing a decrease in 5Cd5 (Figure 122). Overall OHL shows less development than Pedons 1 and 2. The micromorphology confirms both similarities and differences seen in the macromorphology.

Conclusions

The similarities that exist among these profiles are due to climate, drainage, and in part, parent material. All the pedons are poorly to somewhat poorly drained with a dense subsurface horizon. The origin and genesis of the dense horizons as well as its morphology are variable.

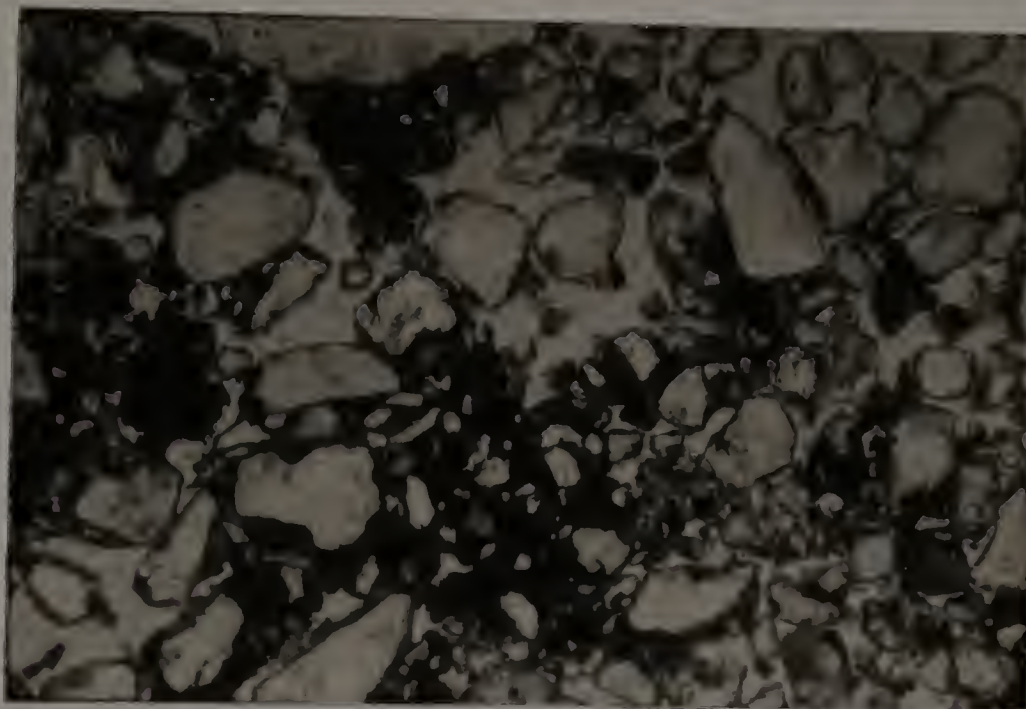


A



B

Figure 120. Photomicrograph of Bgl horizon, OHL Pedon. A = argillan, AL = alban, Q = quassiferran, V = void. (A) photograph, (B) schematic. The bar is 1 mm long.

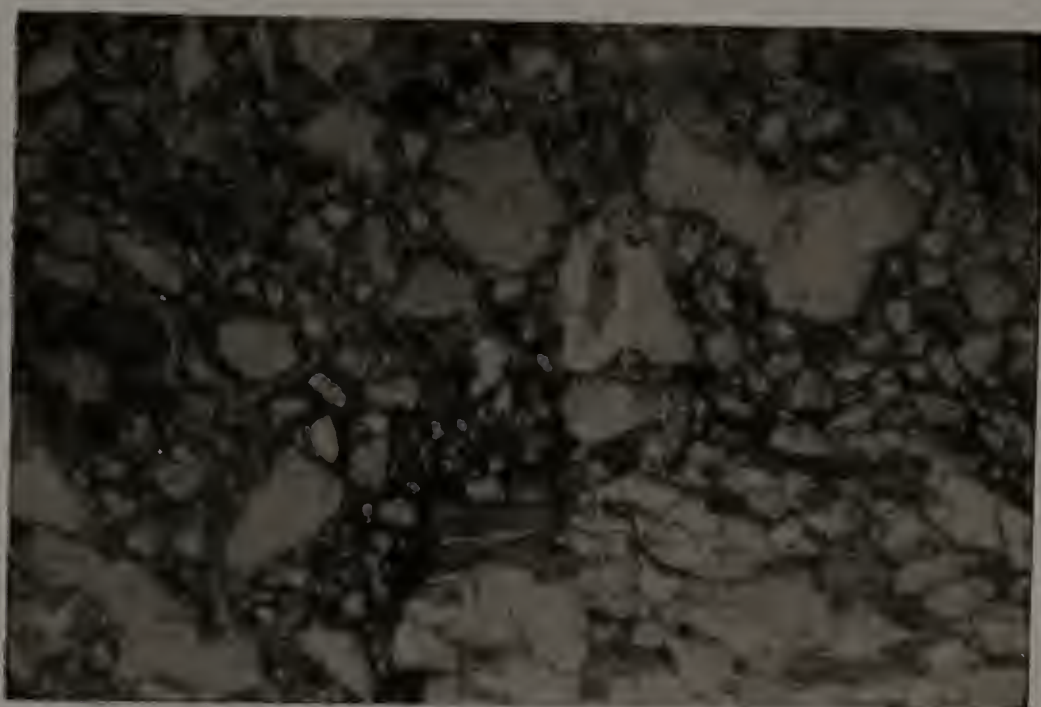


A

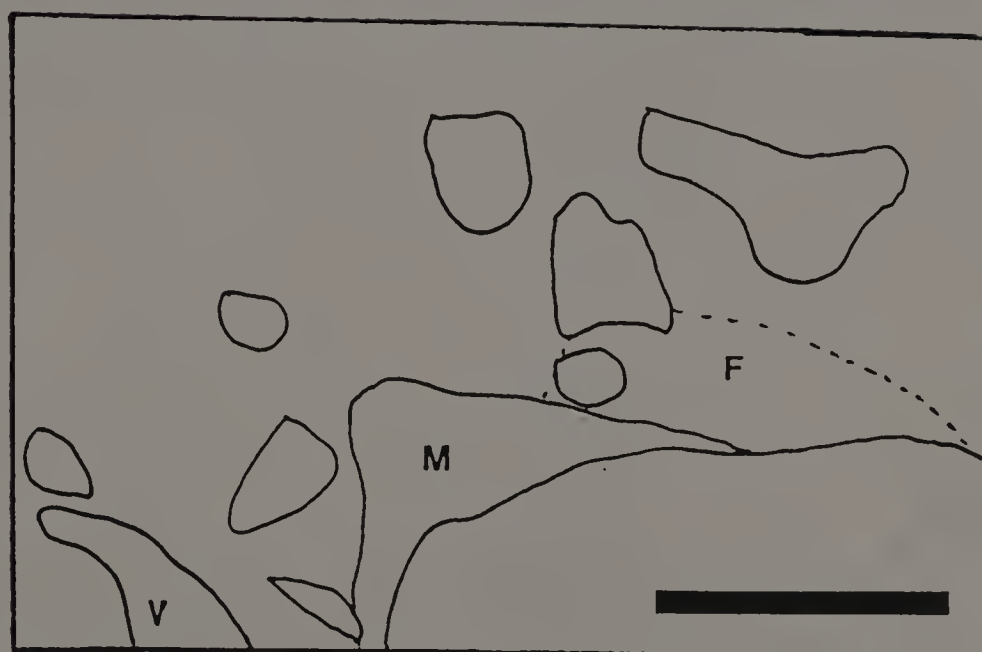


B

Figure 121. Photomicrograph of 2BCm horizon, OHL Pedon. F = ferran, M = mangan, V = void. (A) photograph, (B) schematic. The bar is 1 mm long.



A



B

Figure 122. Photomicrograph of 3Cd3 horizon, OHL Pedon. F = ferran, M = mangan, V = void. (A) photograph, (B) schematic. The bar is 1 mm long.

Pedons 1 and 2 exhibit macro- and micromorphology typical to fragipans (Soil Survey Staff, 1975). This includes the roughly vertical, polygonal bleached prism faces (BPF), dense and brittle behavior, tendency to slake in water, and clay bridges with sepic fabrics. The brittle material consists of 70 to 95% of the horizon.

OHL contains a dense horizon that does not exhibit fragipan morphology and is not brittle. Unlike Pedons 1 and 2, OHL is developed mainly in colluvial material. The cemented horizons are only present in this pedon. The genesis of these horizons remains unclear.

Pedons 1 and 2 fit within the range of characteristics for the Ridgebury series while OHL falls outside of them. OHL may be described as a variant since it does meet the characteristics for part of the profile. An alternative for soils similar to OHL would be to reclassify them, thus creating another series, if extensive areas of this soil are found.

APPENDIX G
GRINDING ANALYSIS

Pedon 1

Percent Extractable Fe; Ground in shatter box

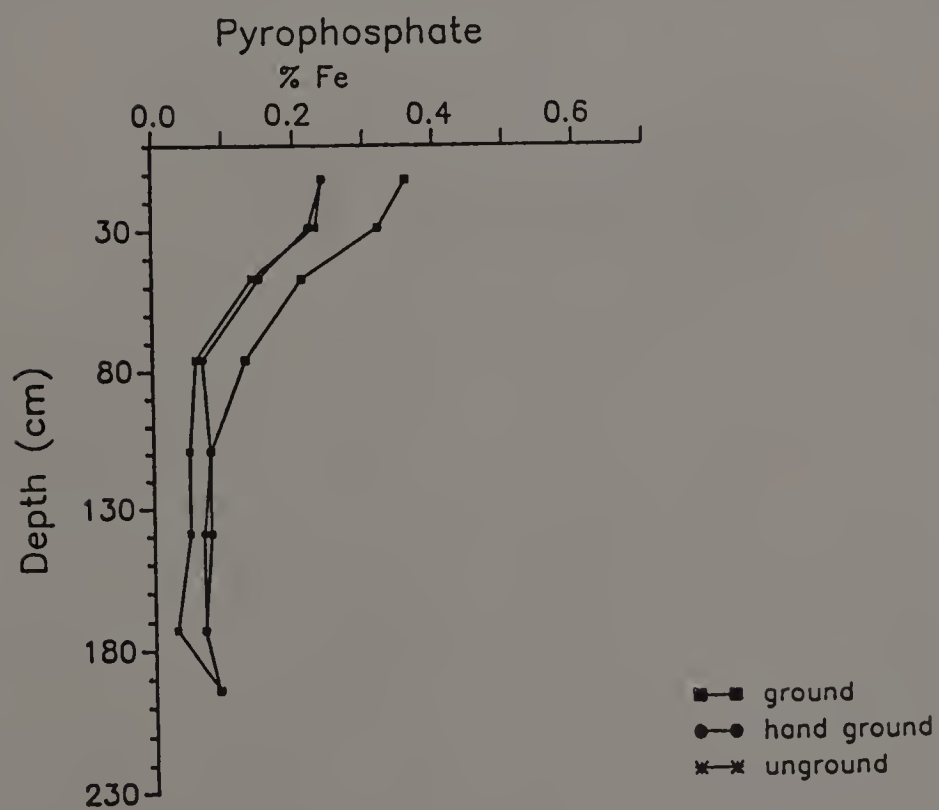
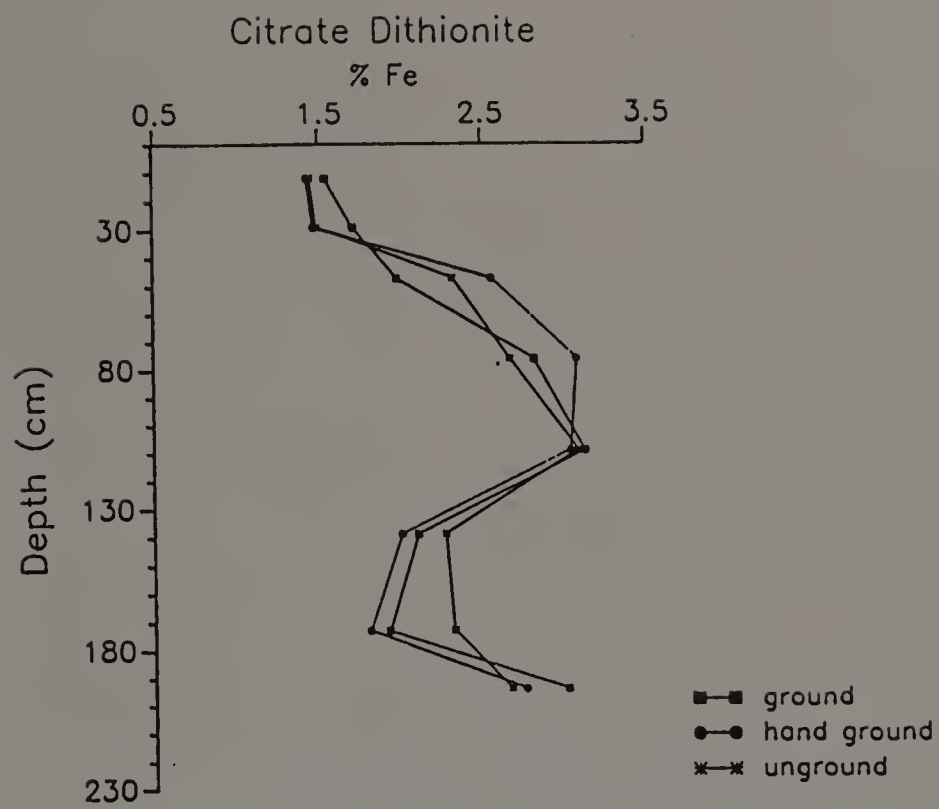
Hori.	C.D.	Pyro	Oxal.	C.B.D.	A.A.	H.H.1	H.H.2	NaOH	NaEDTA
Ap	1.54	0.36	0.930	1.096	0.093	0.247	0.230	1.52	0.130
Bw1	1.71	0.32	0.995	1.113	0.068	0.236	0.326	0.133	0.095
Bw2	1.98	0.21	0.900	0.918	0.055	0.145	0.262	0.158	0.058
Bt	2.82	0.13	1.765	1.789	0.075	0.203	0.354	0.134	0.079
2Btx1	3.13	0.08	2.335	1.915	0.093	0.220	0.398	0.165	0.082
2Btx2	2.10	0.08	1.525	1.457	0.093	0.277	0.463	0.170	0.089
3BCm	1.92	0.07	1.680	1.416	0.092	0.241	0.256	0.124	0.106
4Cd	3.02	0.09	2.490	1.680	0.108	0.289	0.525	0.144	0.117
BPF	1.71	0.08	1.520	1.227	0.098	0.364	0.428	0.136	0.093

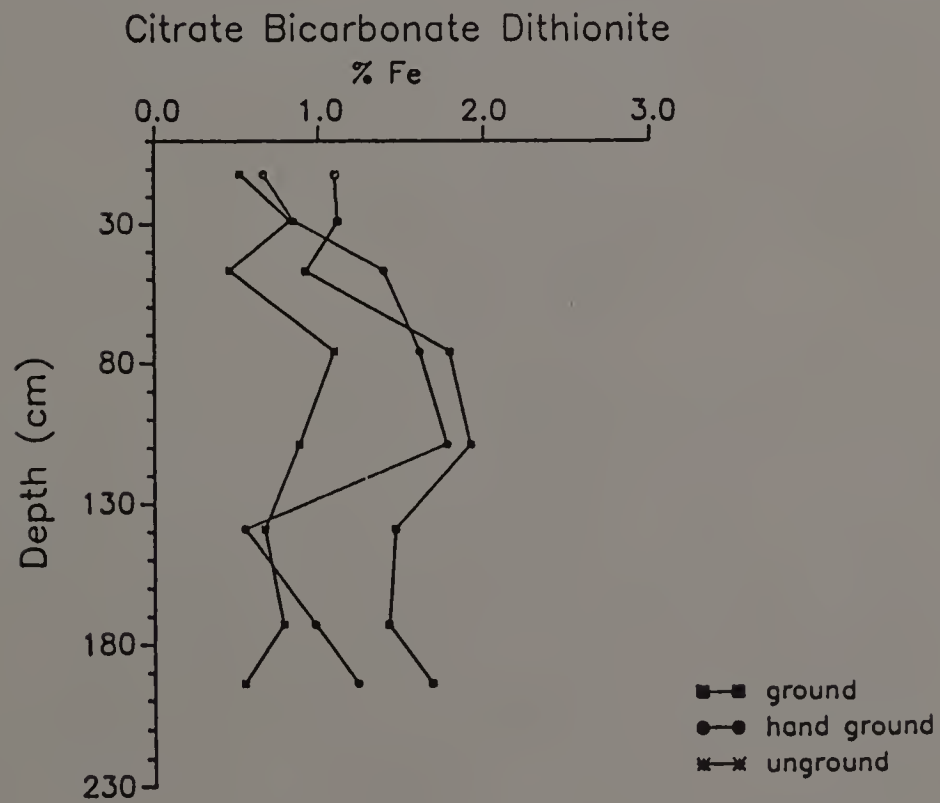
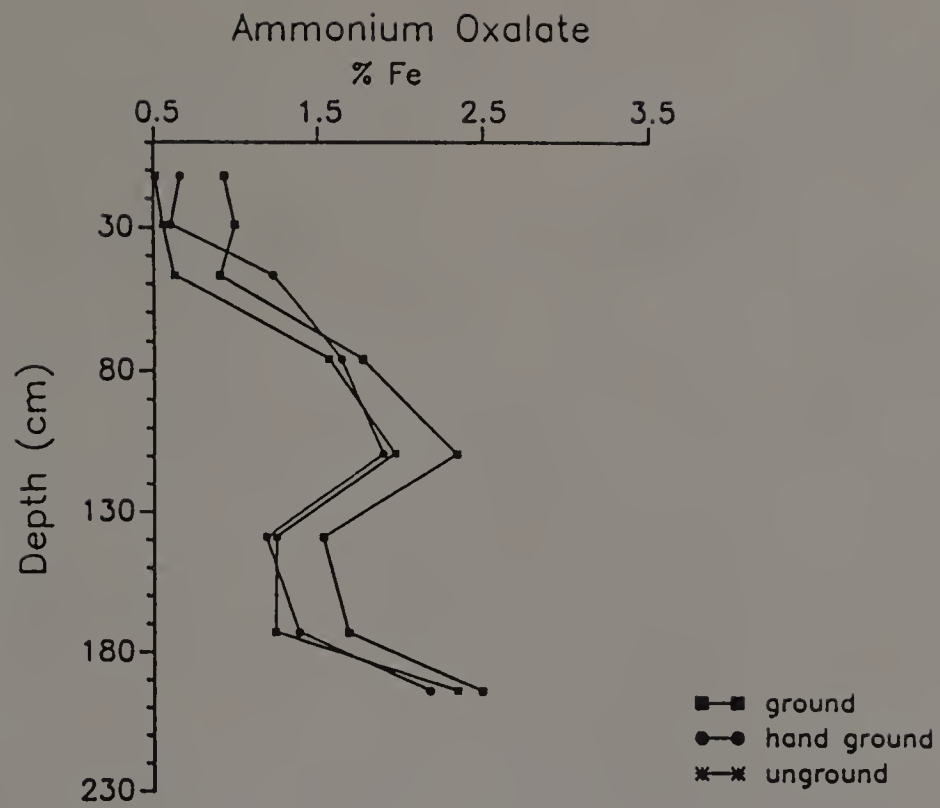
Percent Extractable Fe; Ground by hand to pass a 0.5 mm sieve

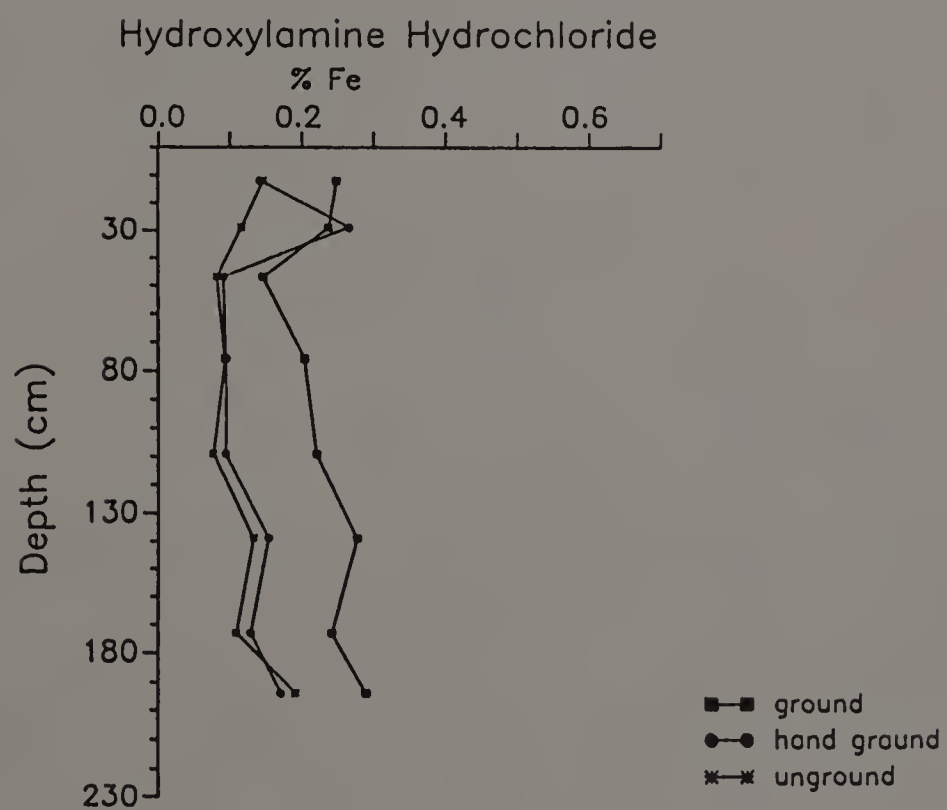
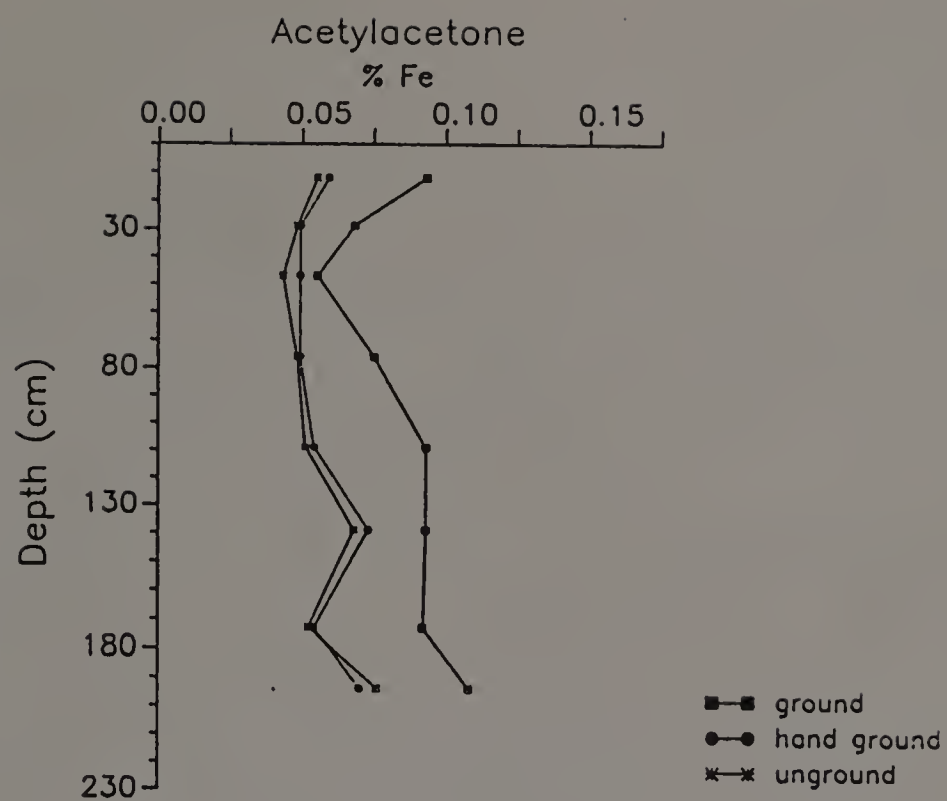
Hori.	C.D.	Pyro	Oxal.	C.B.D.	A.A.	H.H.1	H.H.2	NaOH	NaEDTA
Ap	1.43	0.24	0.660	0.665	0.059	0.141	----	0.115	0.077
Bw1	1.47	0.22	0.600	0.847	0.049	0.265	----	0.103	0.050
Bw2	2.56	0.15	1.225	1.393	0.049	0.090	----	0.075	0.030
Bt	3.08	0.07	1.635	1.608	0.049	0.094	----	0.096	0.032
2Btx1	3.04	0.08	1.890	1.773	0.054	0.093	----	0.605	0.034
2Btx2	2.00	0.07	1.180	0.550	0.073	0.153	----	0.150	0.059
3BCm	1.80	0.06	1.380	0.972	0.054	0.128	----	0.076	0.072
4Cd	2.76	0.09	2.175	1.231	0.07	0.17	----	0.095	0.065

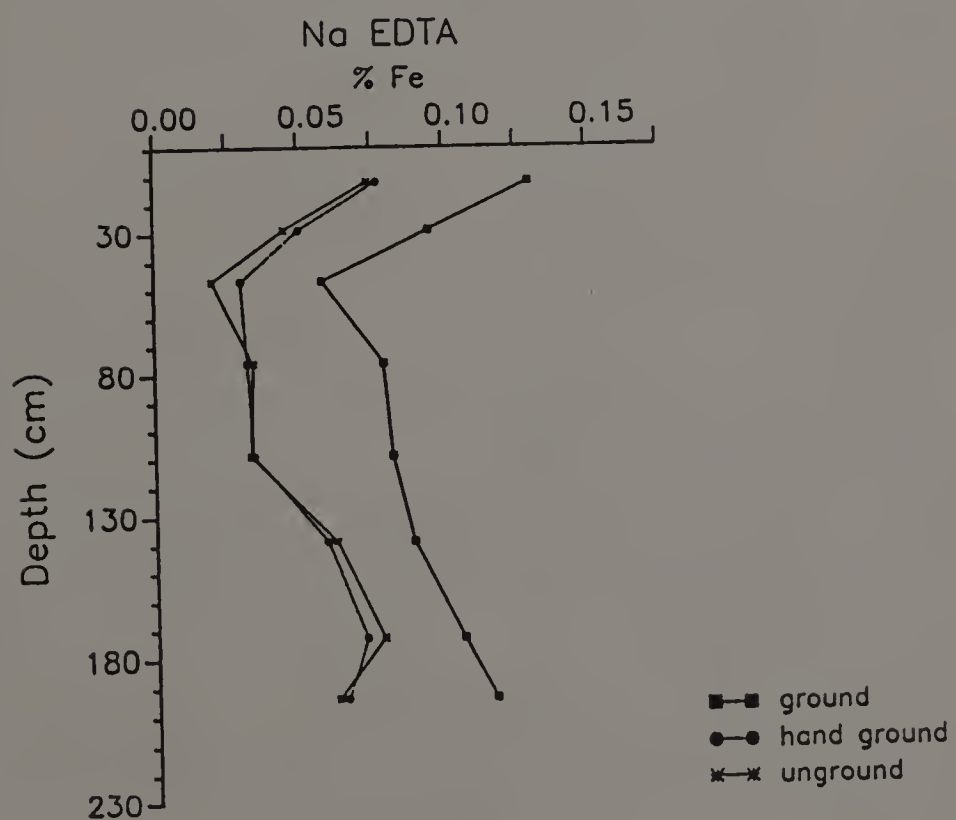
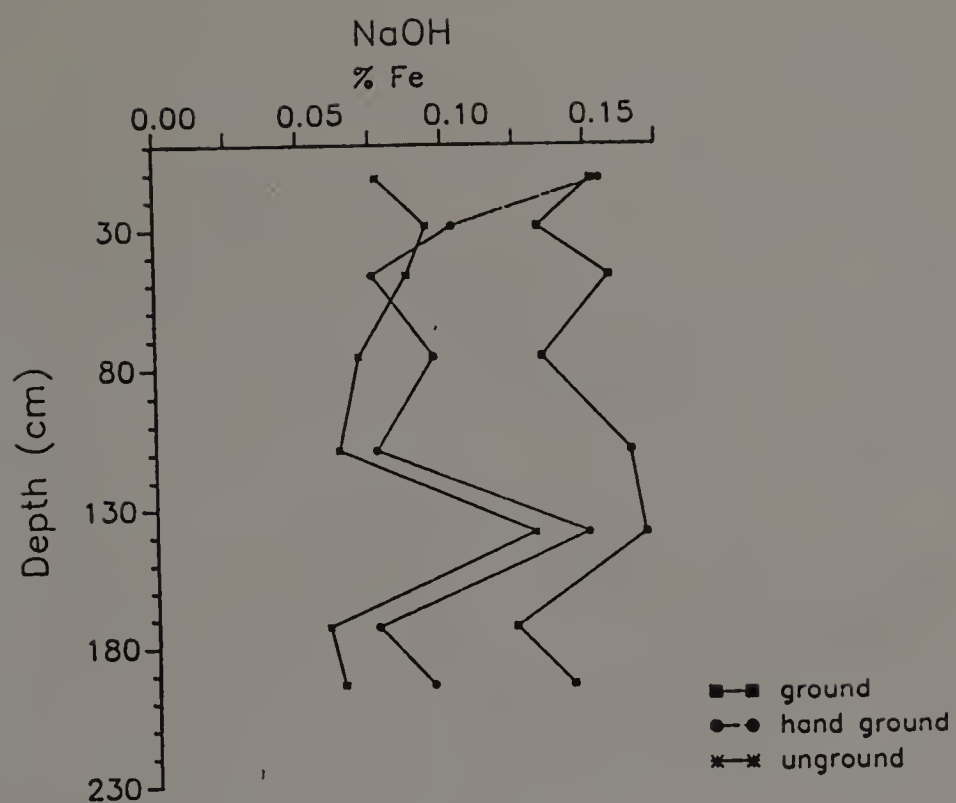
Percent Extractable Fe; Unground

Hori.	C.D.	Pyro	Oxal.	C.B.D.	A.A.	H.H.1	H.H.2	NaOH	NaEDTA
Ap	1.45	0.24	0.510	0.524	0.055	0.145	----	0.077	0.074
Bw1	1.49	0.23	0.55	0.827	0.048	0.115	----	0.094	0.045
Bw2	2.32	0.14	0.625	0.457	0.043	0.081	----	0.087	0.020
Bt	2.67	0.06	1.560	1.088	0.048	0.092	----	0.070	0.034
2Btx1	3.01	0.05	1.960	0.876	0.051	0.076	----	0.063	0.033
2Btx2	2.27	0.05	1.240	0.667	0.068	0.132	----	0.131	0.062
3Bcm	2.32	0.03	1.235	0.781	0.052	0.108	----	0.059	0.078
4Cd	2.67	0.09	2.340	0.545	0.076	0.190	----	0.064	0.062









Pedon 1

Percent Extractable Al; Ground in shatter box

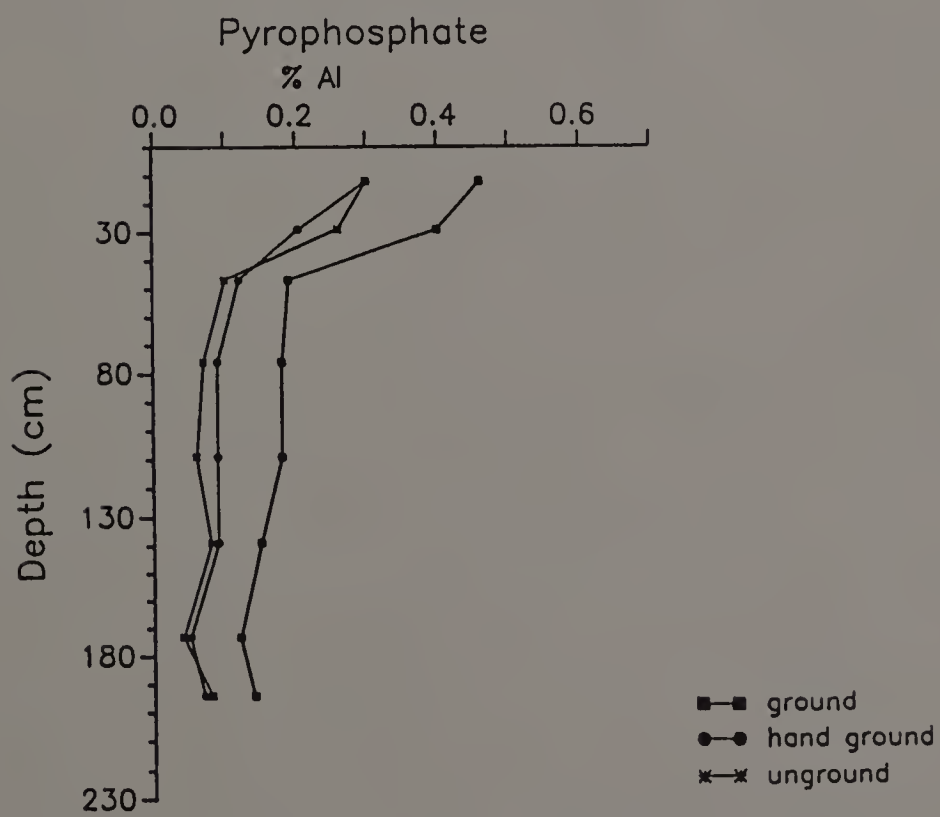
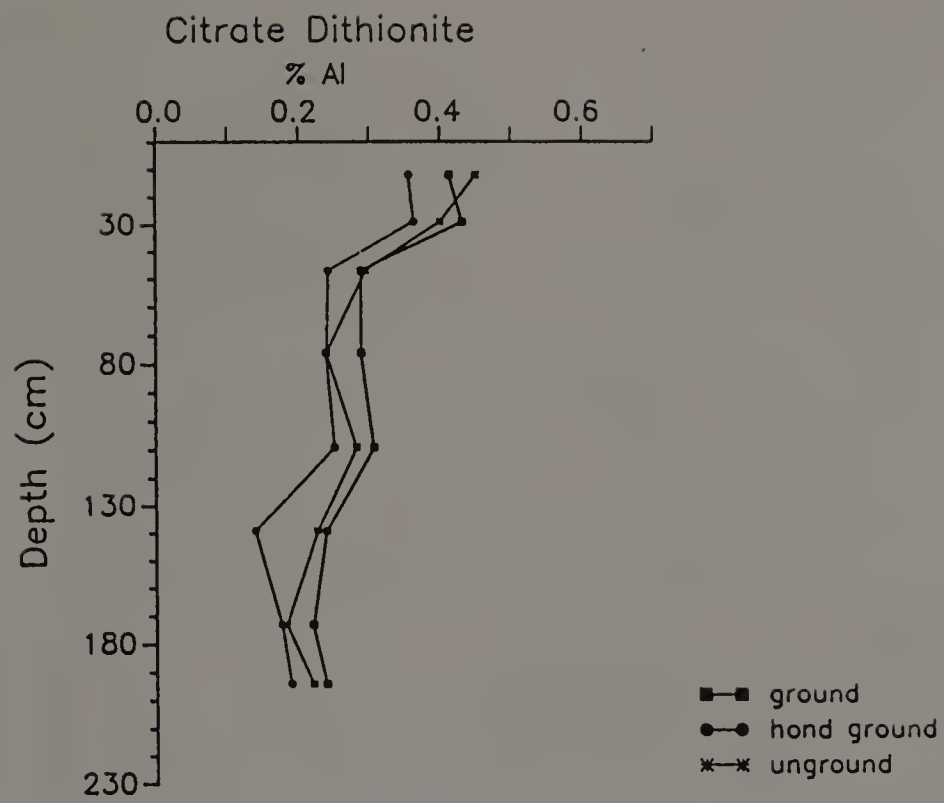
Hori.	C.D.	Pyro	Oxal.	C.B.D.	A.A.	H.H.1	H.H.2	NaOH	NaEDTA
Ap	0.413	0.460	0.83	0.416	0.249	0.575	0.387	1.218	----
Bw1	0.431	0.400	0.85	0.376	0.190	0.515	0.390	1.333	----
Bw2	0.288	0.190	0.05	0.114	0.117	0.265	0.304	1.293	----
Bt	0.288	0.180	0.61	0.250	0.134	0.310	0.322	1.515	----
2Btx1	0.306	0.180	0.53	0.245	0.144	0.315	0.359	1.103	----
2Btx2	0.238	0.150	0.45	0.145	0.131	0.335	0.338	1.175	----
3BCm	0.219	0.120	0.61	0.148	0.124	0.220	0.200	0.823	----
BPF	0.213	0.190	0.38	0.149	0.158	0.415	0.428	1.348	----

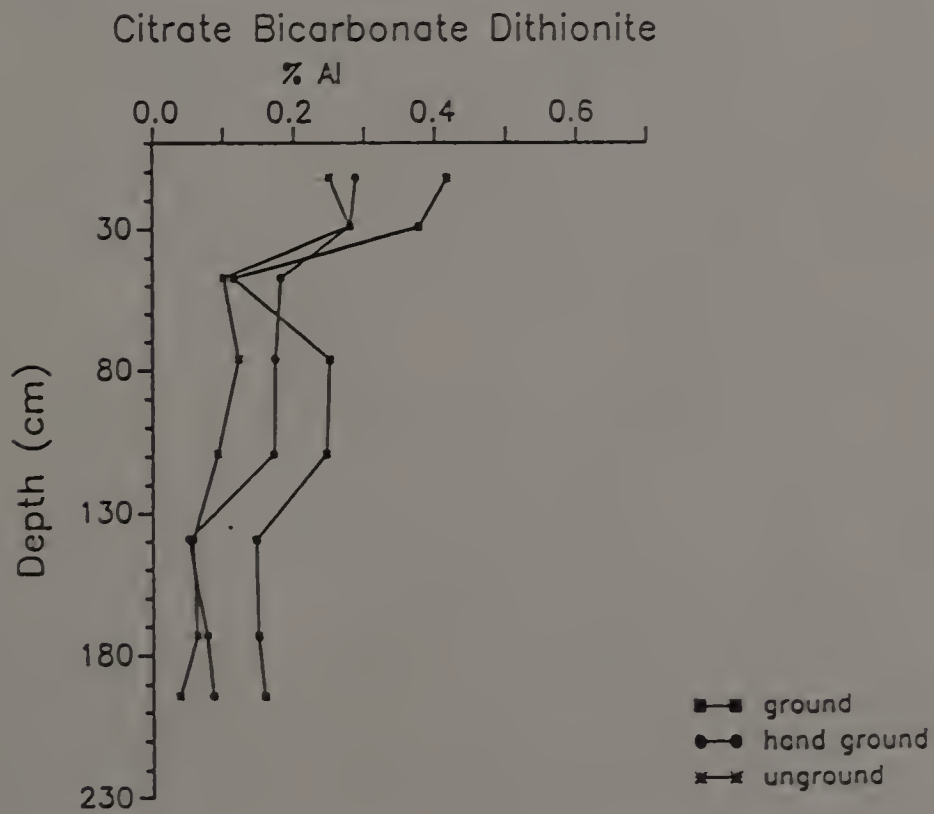
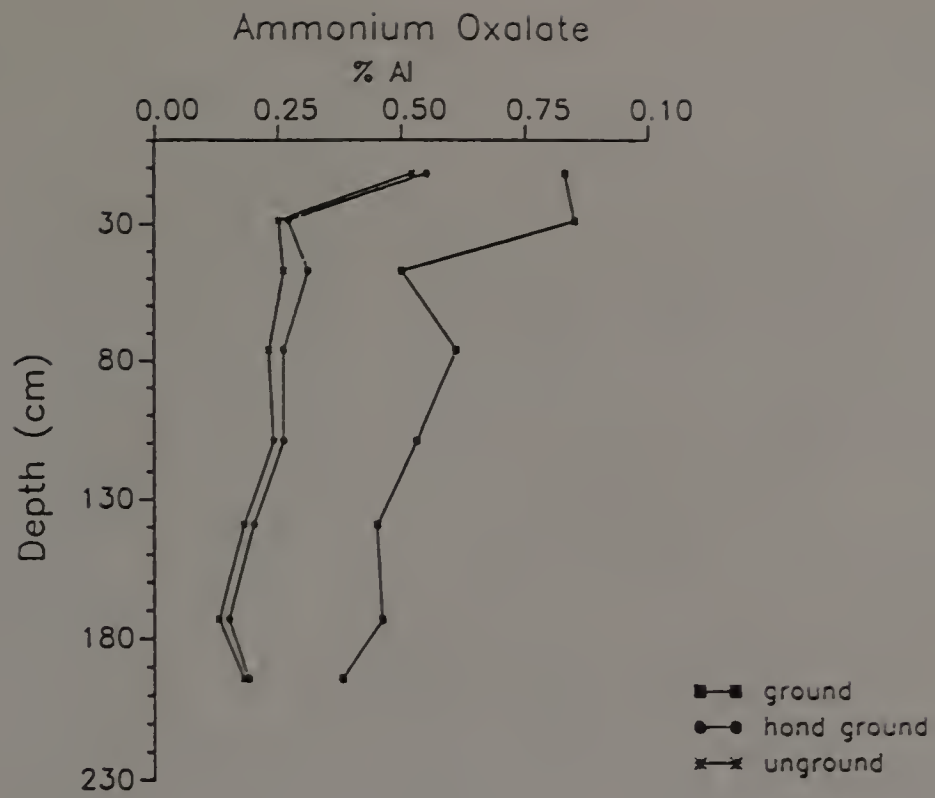
Percent Extractable Al; Ground by hand to pass a 0.5 mm sieve

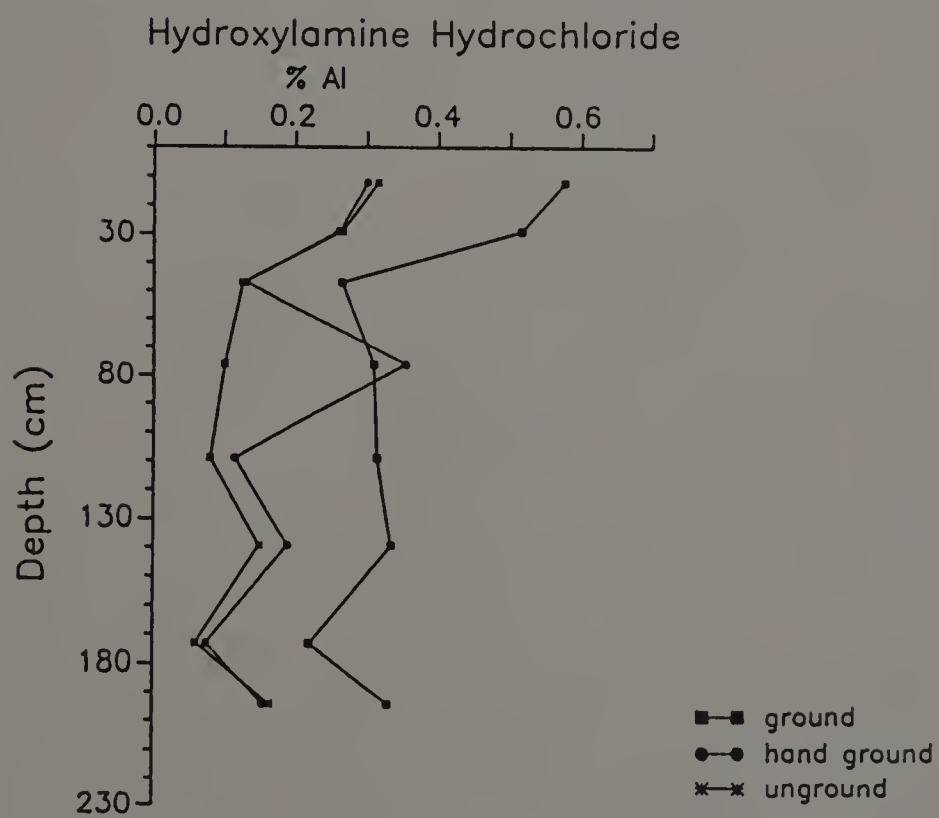
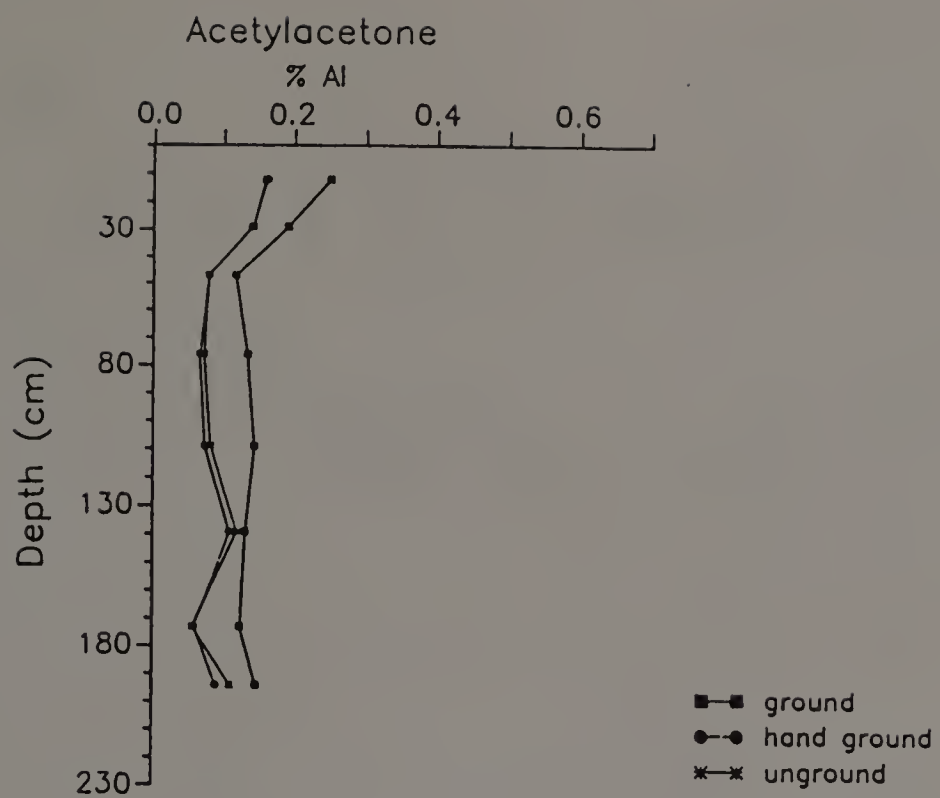
Hori.	C.D.	Pyro	Oxal.	C.B.D.	A.A.	H.H.1	H.H.2	NaOH	NaEDTA
Ap	0.356	0.300	0.55	0.287	0.161	0.300	----	0.953	----
Bw1	0.363	0.300	0.27	0.279	0.139	0.260	----	1.060	----
Bw2	0.244	0.120	0.31	0.180	0.079	0.130	----	1.007	----
Bt	0.238	0.090	0.26	0.172	0.066	0.355	----	1.215	----
2Btx1	0.256	0.090	0.26	0.170	0.074	0.115	----	1.220	----
2Btx2	0.138	0.090	0.20	0.050	0.109	0.190	----	1.058	
3BCm	0.175	0.050	0.15	0.076	0.059	0.075	----	0.493	----
4Cd	0.188	0.070	0.19	0.085	0.090	0.155	----	0.775	----

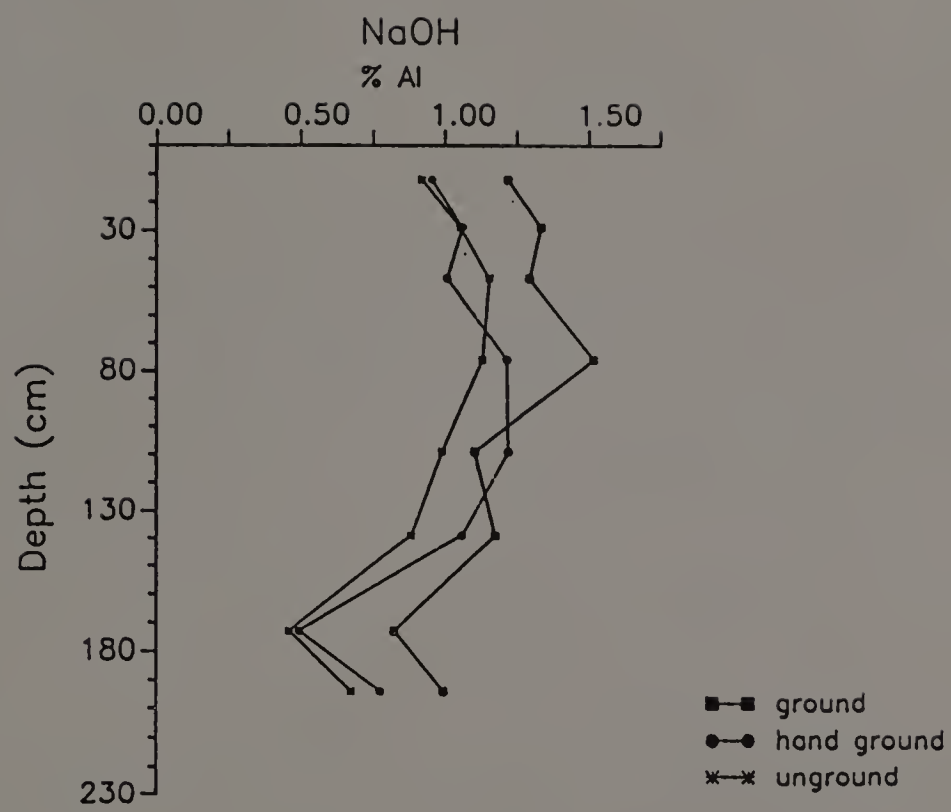
Percent Extractable Al; Unground

Hori.	C.D.	Pyro	Oxal.	C.B.D.	A.A.	H.H.1	H.H.2	NaOH	NaEDTA
Ap	0.450	0.300	0.52	0.250	0.158	0.315	----	0.918	----
Bw1	0.400	0.260	0.25	0.279	0.141	0.265	----	1.053	----
Bw2	0.294	0.100	0.26	0.100	0.078	0.125	----	1.153	----
Bt	0.238	0.070	0.23	0.121	0.072	0.100	----	1.128	----
2Btx1	0.281	0.060	0.24	0.091	0.082	0.080	----	0.988	----
2Btx2	0.225	0.080	0.18	0.056	0.119	0.150	----	0.880	----
3BCm	0.181	0.040	0.13	0.062	0.056	0.060	----	0.458	----
4Cd	0.219	0.080	0.18	0.037	0.110	0.165	----	0.673	----









Pedon 1

Percent Extractable Mn; Ground in shatter box

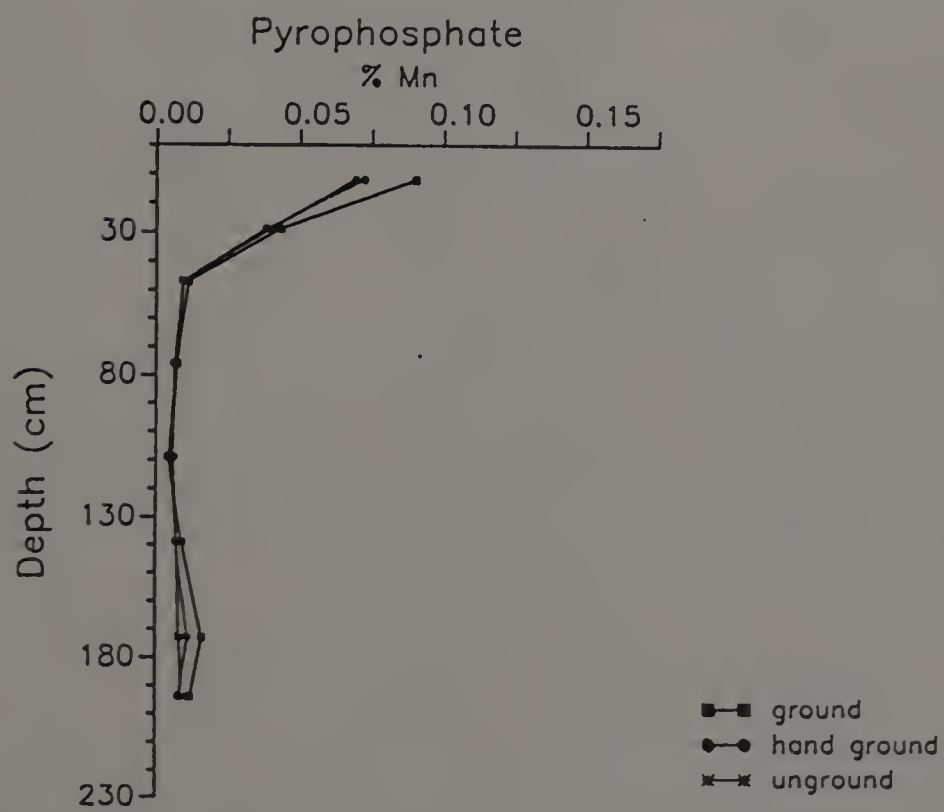
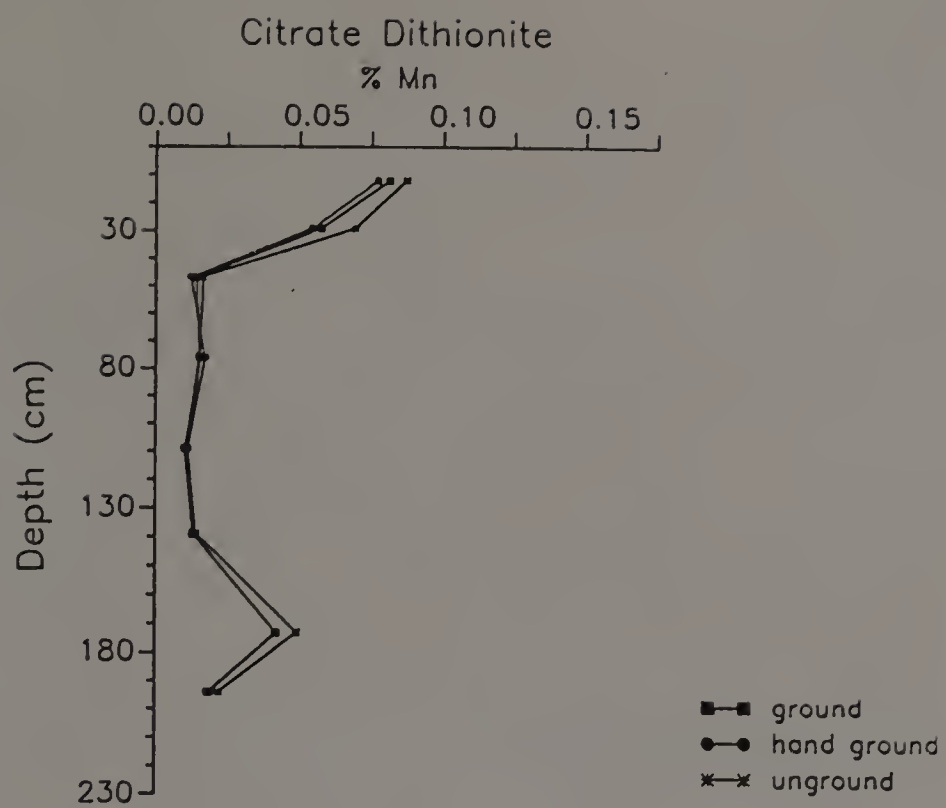
Hori.	C.D.	Pyro	Oxal.	C.B.D.	A.A.	H.H.1	H.H.2	NaOH	NaEDTA
Ap	0.081	0.090	0.028	0.067	0.025	0.066	0.045	----	0.095
Bw1	0.057	0.043	0.003	0.047	0.009	0.047	0.029	----	0.046
Bw2	0.014	0.011	0.004	0.008	0.004	0.011	0.007	----	0.009
Bt	0.015	0.007	0.005	0.011	0.005	0.011	0.007	----	0.006
2Btx1	0.010	0.004	0.003	0.006	0.004	0.006	0.004	----	0.004
2Btx2	0.013	0.009	0.004	0.010	0.008	0.011	0.008	----	0.009
3BCm	0.042	0.016	0.020	0.035	0.014	0.037	0.019	----	0.035
4Cd	0.018	0.012	0.008	0.013	0.010	0.015	0.009	----	0.013
BPF	0.004	0.003	0.002	0.002	0.002	0.003	0.002	----	0.001

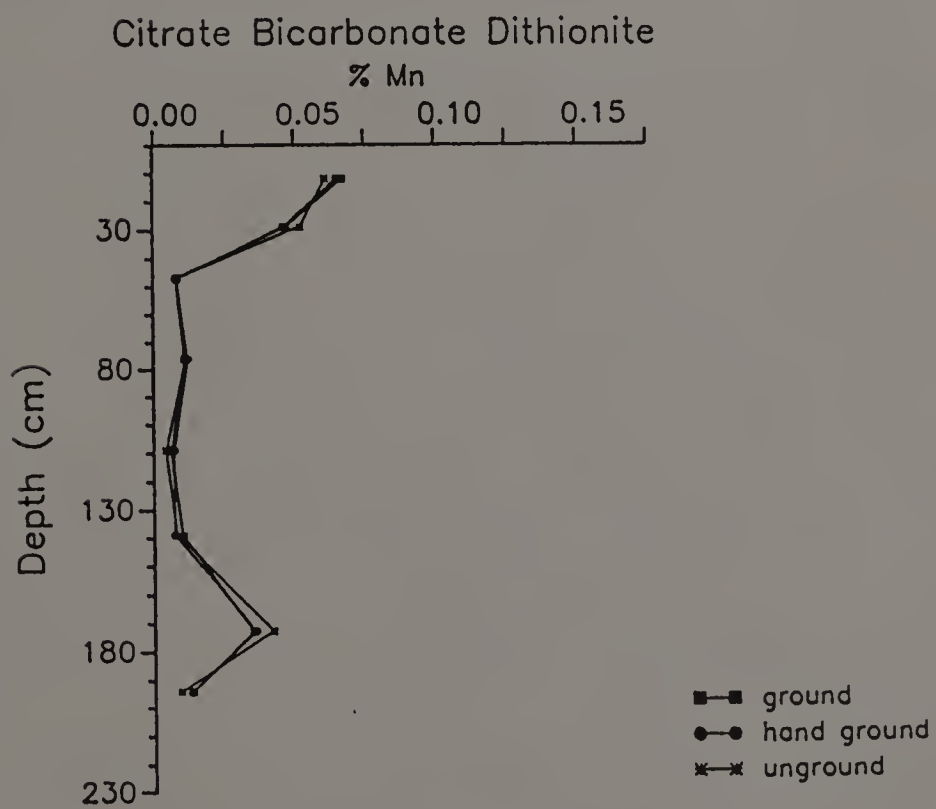
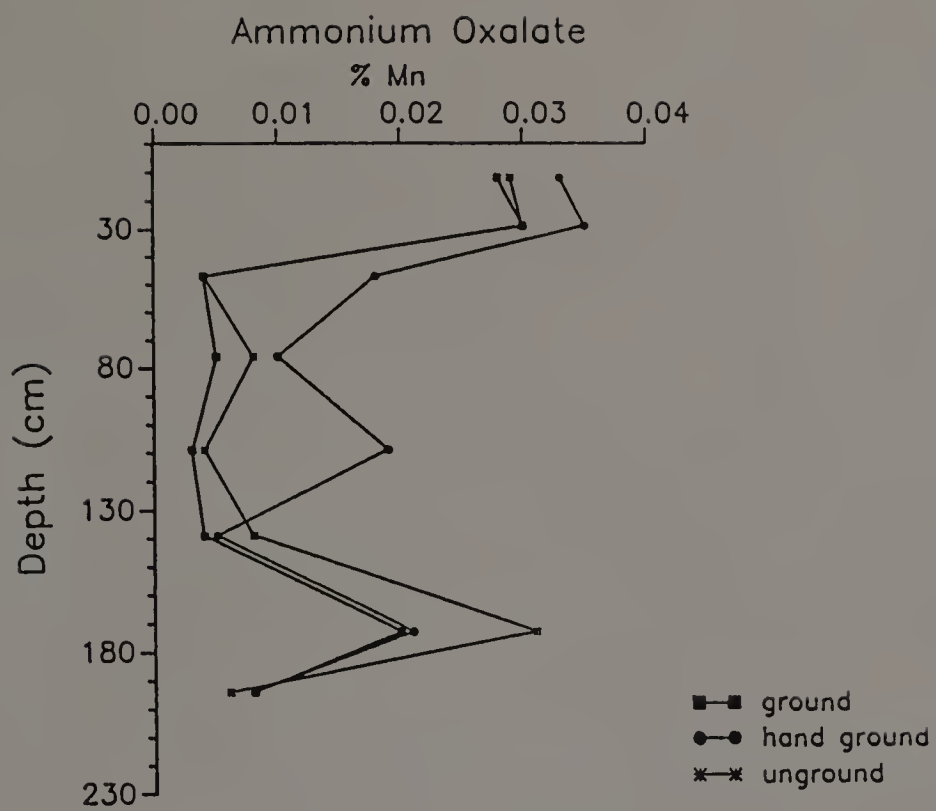
Percent Extractable Mn; Ground by hand to pass a 0.5 mm sieve

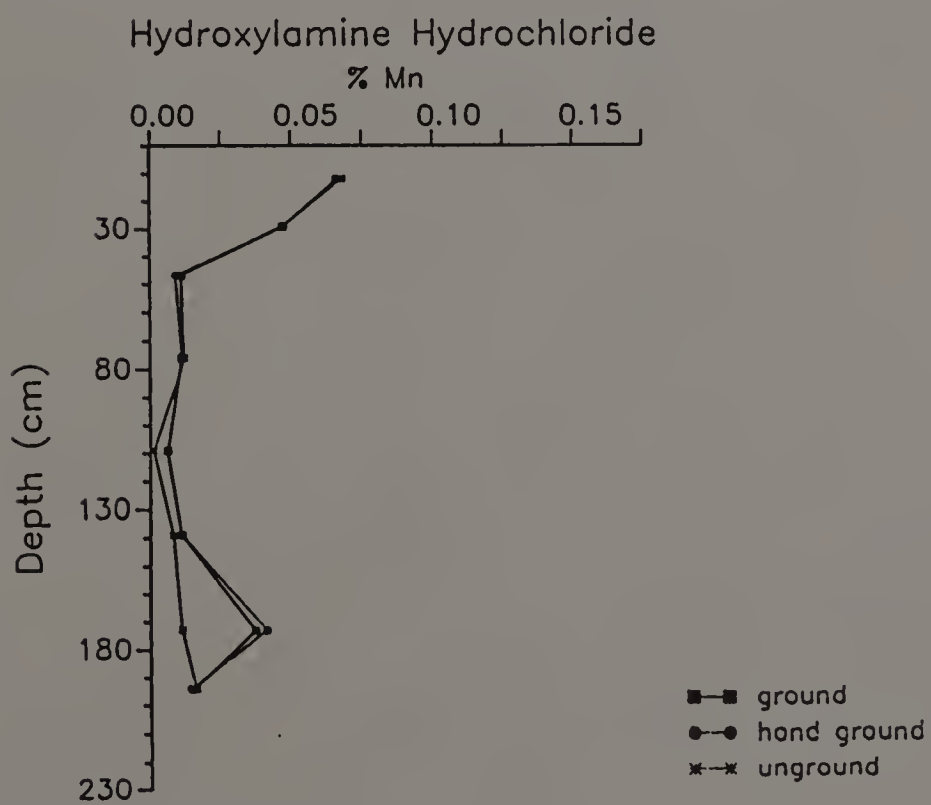
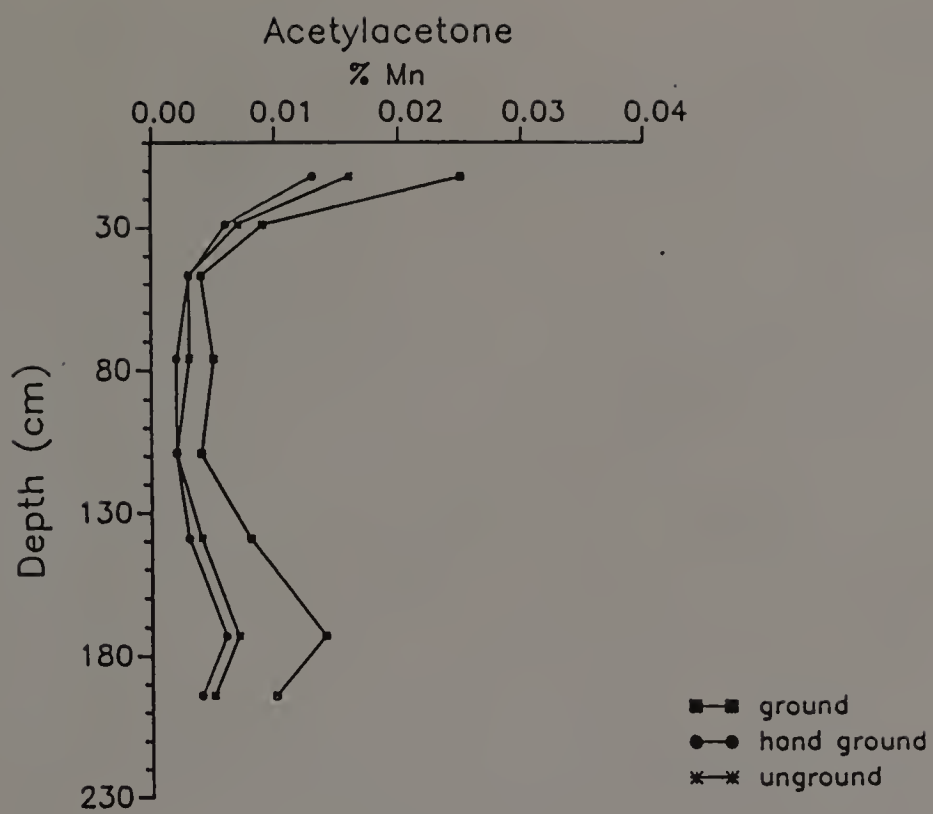
Hori.	C.D.	Pyro	Oxal.	C.B.D.	A.A.	H.H.1	H.H.2	NaOH	NaEDTA
Ap	0.077	0.072	0.033	0.065	0.013	0.066	----	----	0.088
Bw1	0.054	0.038	0.035	0.046	0.006	0.046	----	----	0.044
Bw2	0.012	0.009	0.018	0.008	0.003	0.009	----	----	0.006
Bt	0.017	0.006	0.010	0.012	0.002	0.011	----	----	0.009
2Btx1	0.011	0.006	0.019	0.007	0.002	0.066	----	----	0.003
2Btx2	0.013	0.007	0.005	0.007	0.003	0.011	----	----	0.010
3BCm	0.042	0.011	0.021	0.036	0.006	0.041	----	----	0.036
4Cd	0.019	0.008	0.008	0.013	0.004	0.014	----	----	0.016

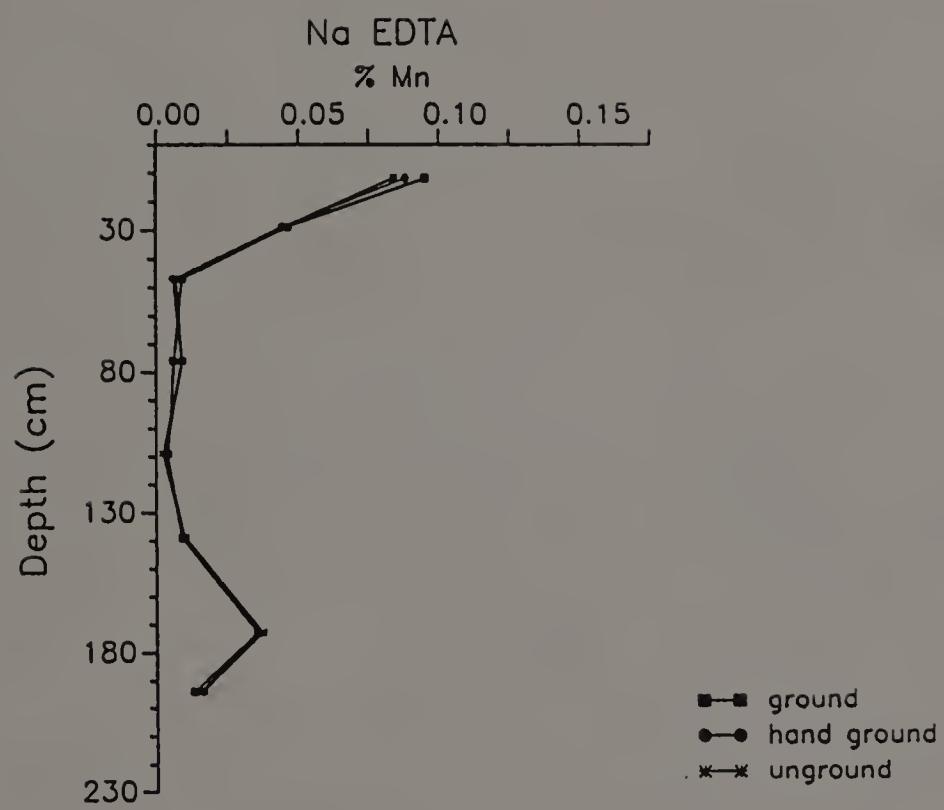
Percent Extractable Mn; Unground

Hori.	C.D.	Pyro	Oxal.	C.B.D.	A.A.	H.H.1	H.H.2	NaOH	NaEDTA
Ap	0.087	0.069	0.029	0.061	0.016	0.068	----	----	0.084
Bw1	0.069	0.040	0.030	0.052	0.007	0.047	----	----	0.045
Bw2	0.016	0.009	0.004	0.008	0.003	0.011	----	----	0.007
Bt	0.015	0.007	0.008	0.011	0.003	0.012	----	----	0.009
2Btx1	0.011	0.005	0.004	0.004	0.002	0.001	----	----	0.002
2Btx2	0.014	0.007	0.008	0.008	0.004	0.008	----	----	0.010
3BCm	0.049	0.008	0.031	0.042	0.007	0.011	----	----	0.037
4Cd	0.022	0.009	0.006	0.009	0.005	0.016	----	----	0.015









Pedon 1

Percent Extractable Si; Ground in shatter box

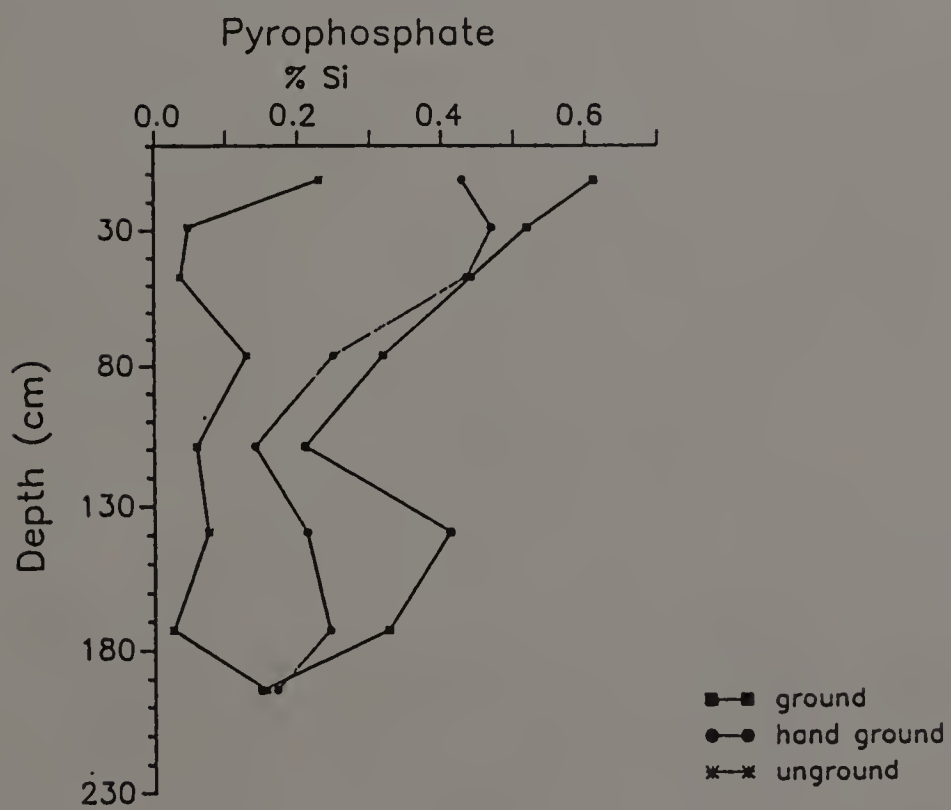
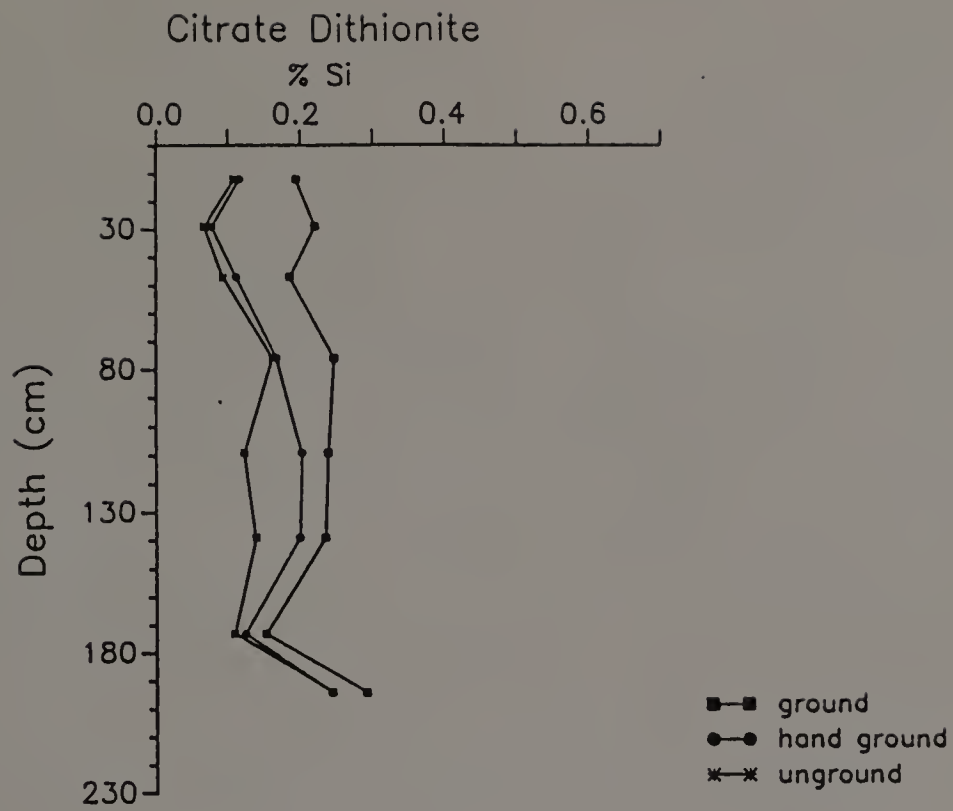
Hori.	C.D.	Pyro	Oxal.	C.B.D.	A.A.	H.H.1	H.H.2	NaOH	NaEDTA
Ap	0.194	0.611	0.197	0.043	1.722	----	0.537	5.06	0.064
Bw1	0.220	0.518	0.261	0.049	1.513	----	0.850	6.24	0.026
Bw2	0.185	0.440	0.122	0.047	1.251	----	0.530	8.64	0.032
Bt	0.246	0.317	0.242	0.055	1.520	----	0.596	9.72	0.073
2Btx1	0.238	0.209	0.162	0.072	1.645	----	0.581	8.34	0.104
2Btx2	0.234	0.411	0.144	0.059	1.332	----	0.559	6.94	0.071
3BCm	0.152	0.324	0.147	0.051	1.534	----	0.341	1.40	0.071
4Cd	0.291	0.148	0.210	0.057	1.770	----	0.390	6.64	0.114
BPF	0.339	0.396	0.137	0.047	1.550	----	0.828	7.53	0.077

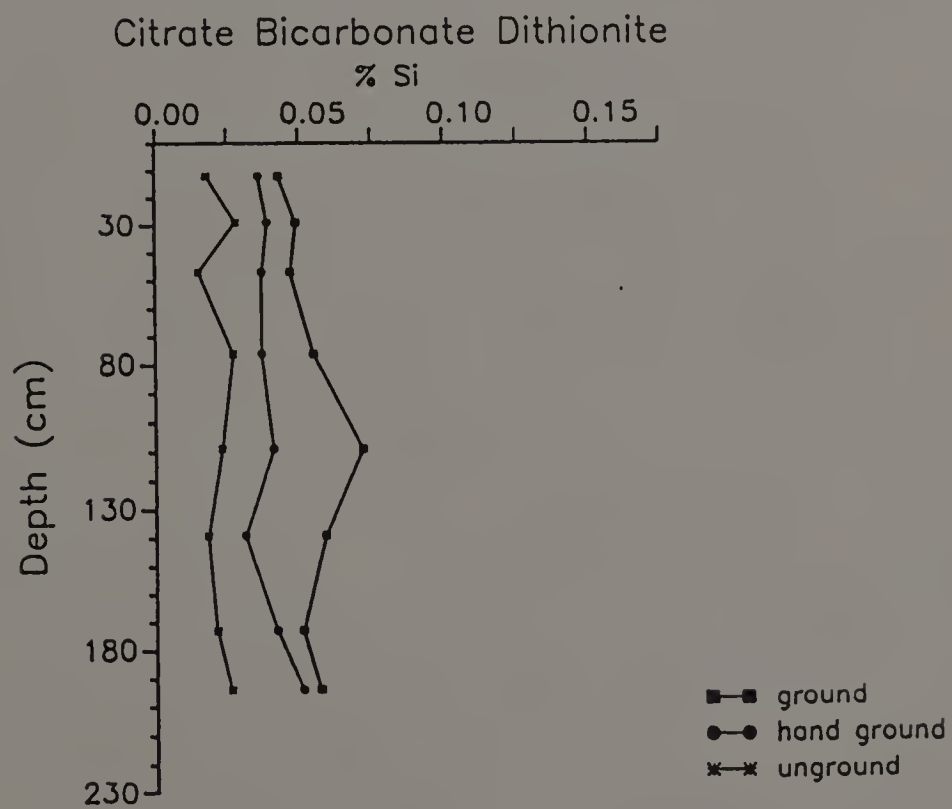
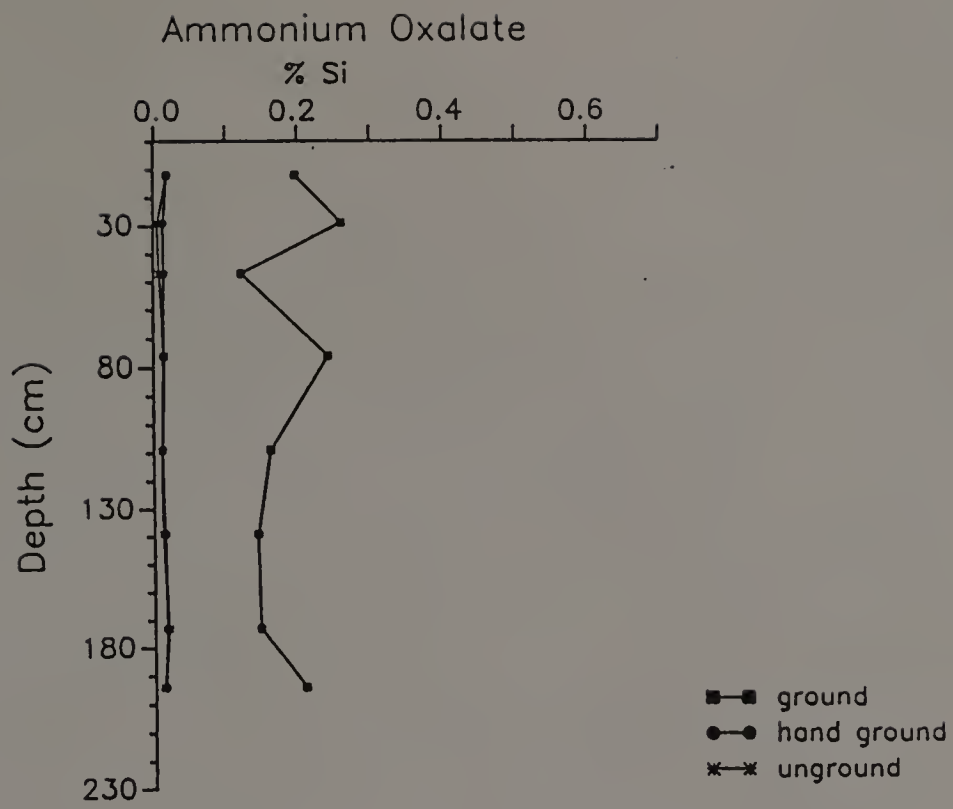
Percent Extractable Si; Ground by hand to pass a 0.5 mm sieve

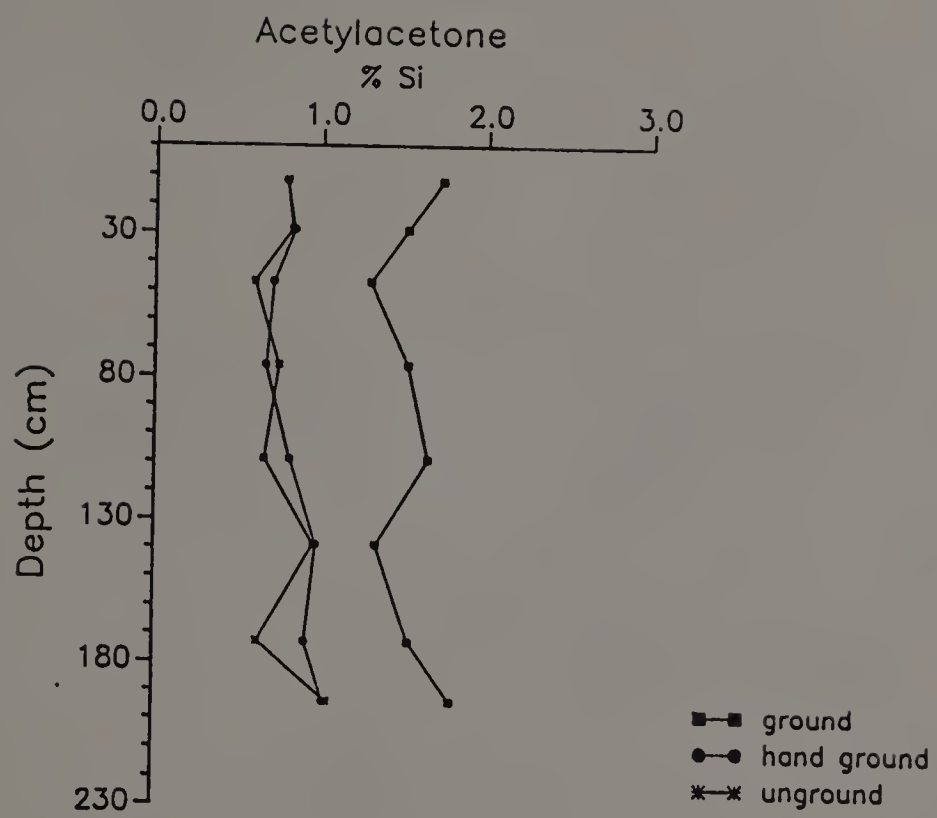
Hori.	C.D.	Pyro	Oxal.	C.B.D.	A.A.	H.H.1	H.H.2	NaOH	NaEDTA
Ap	0.115	0.428	0.018	0.036	0.782	----	----	4.15	0.035
Bw1	0.077	0.469	0.013	0.039	0.831	----	----	4.77	0.016
Bw2	0.111	0.434	0.014	0.037	0.706	----	----	5.84	0.028
Bt	0.167	0.248	0.013	0.037	0.664	----	----	6.34	0.038
2Btx1	0.202	0.140	0.011	0.041	0.810	----	----	7.82	0.033
2Btx2	0.166	0.212	0.015	0.031	0.970	----	----	6.24	0.036
3BCm	0.123	0.243	0.016	0.042	0.908	----	----	0.83	0.045
4Cd	0.243	0.169	0.014	0.051	1.023	----	----	4.57	0.031

Percent Extractable Si; Unground

Hori.	C.D.	Pyro	Oxal.	C.B.D.	A.A.	H.H.1	H.H.2	NaOH	NaEDTA
Ap	0.108	0.229	0.018	0.018	0.789	----	----	3.57	0.030
Bw1	0.067	0.047	0.005	0.028	0.817	----	----	3.38	0.015
Bw2	0.093	0.036	0.008	0.015	0.594	----	----	5.65	0.017
Bt	0.161	0.128	0.014	0.027	0.741	----	----	3.77	0.030
2Btx1	0.122	0.059	0.011	0.023	0.657	----	----	4.46	0.021
2Btx2	0.138	0.075	0.012	0.018	0.956	----	----	4.56	0.023
3BCm	0.108	0.025	0.019	0.021	0.622	----	----	0.40	0.043
4Cd	0.243	0.155	0.011	0.026	1.040	----	----	3.12	0.025







Pedon 5

Percent Extractable Fe; Ground in shatter box

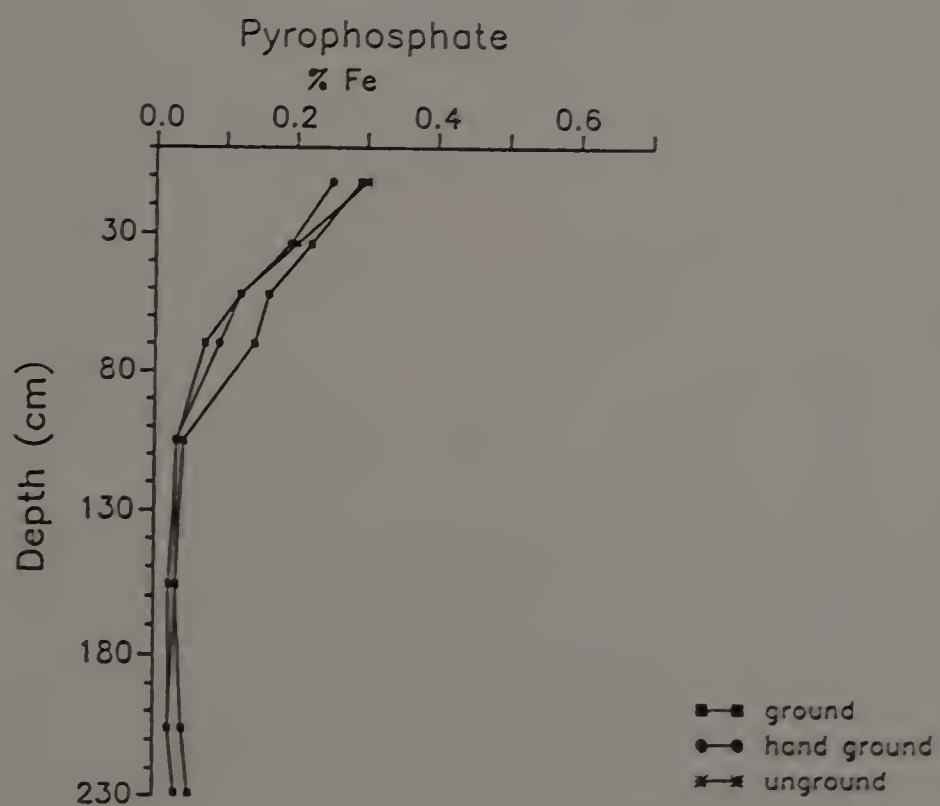
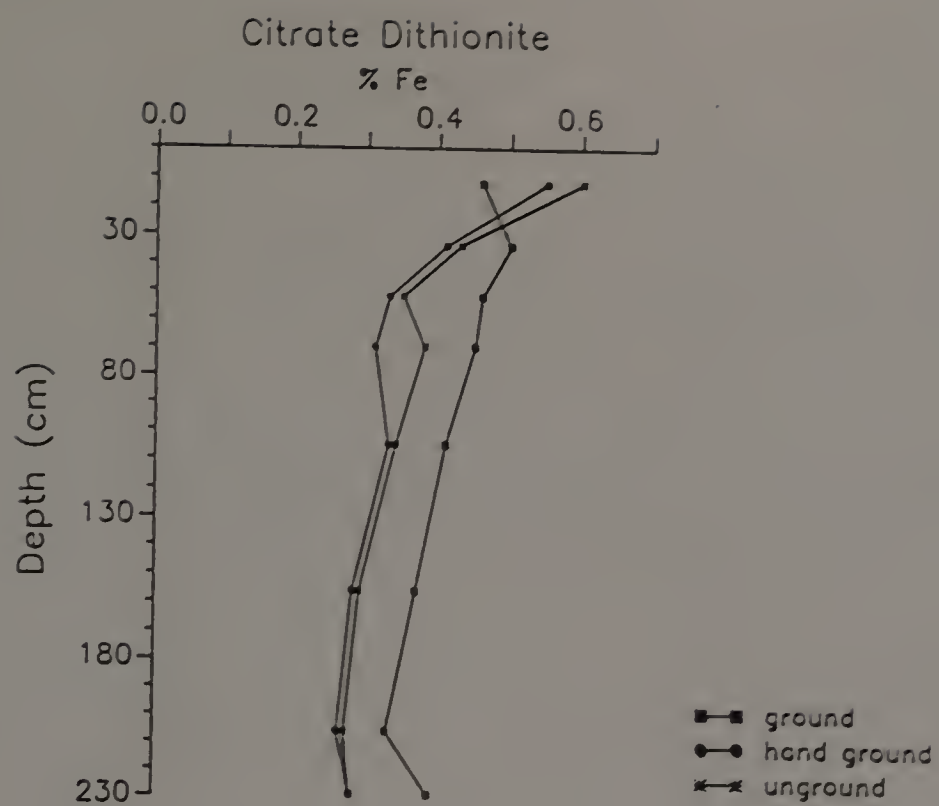
Hori.	C.D.	Pyro	Oxal.	C.B.D.	A.A.	H.H.1	H.H.2	NaOH	NaEDTA
Ap	0.46	0.29	0.695	0.262	0.089	0.240	0.228	0.102	0.196
Bw	0.50	0.22	0.440	0.224	0.081	0.158	0.136	0.095	0.101
BE	0.46	0.16	0.345	0.160	0.089	0.114	0.143	0.114	0.075
2EB	0.45	0.14	0.385	0.242	0.066	0.107	0.112	0.115	0.049
2Btx1	0.41	0.04	0.270	0.212	0.080	0.143	0.128	0.091	0.048
2Btx2	0.37	0.03	0.150	0.131	0.049	0.092	0.071	0.061	0.028
2Cd1	0.33	0.04	0.155	0.090	0.042	0.078	0.064	0.078	0.032
2Cd2	0.39	0.05	0.245	0.077	0.072	0.122	0.091	0.091	0.056
BPF	0.39	0.08	0.265	0.097	0.081	0.146	0.110	0.114	0.072

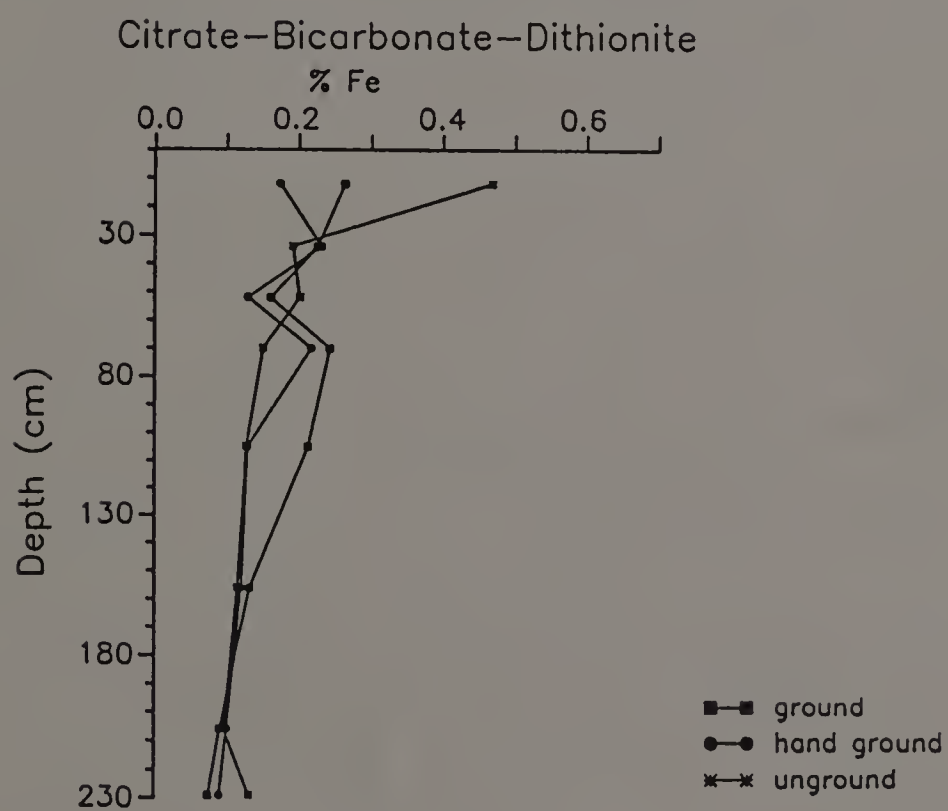
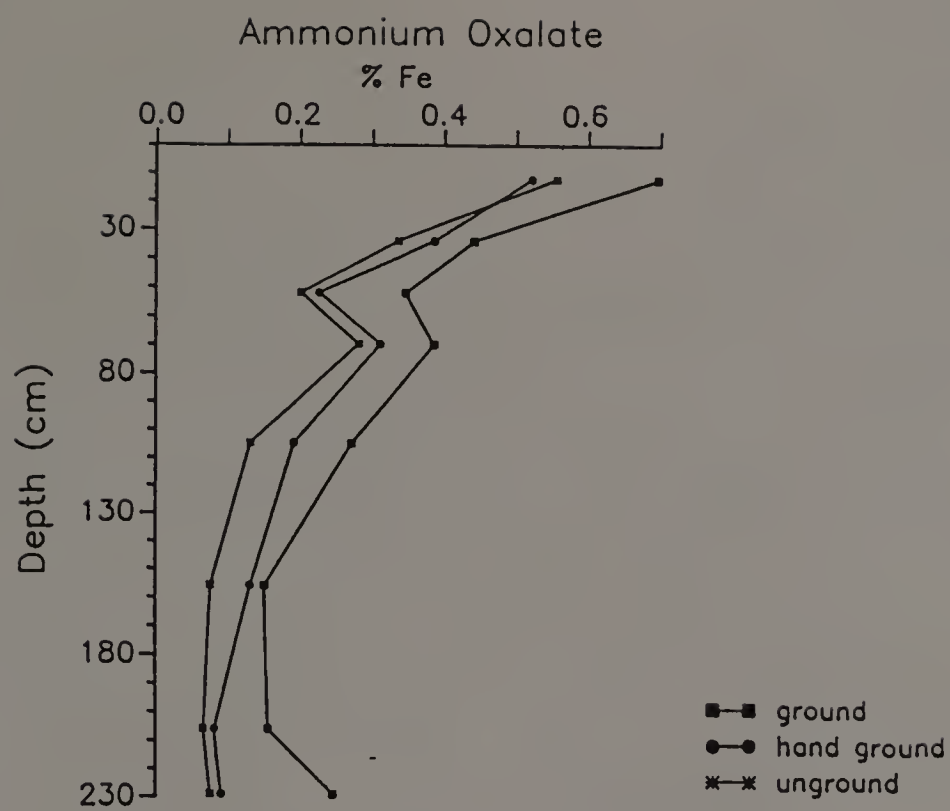
Percent Extractable Fe; Ground by hand to pass a 0.5 mm sieve

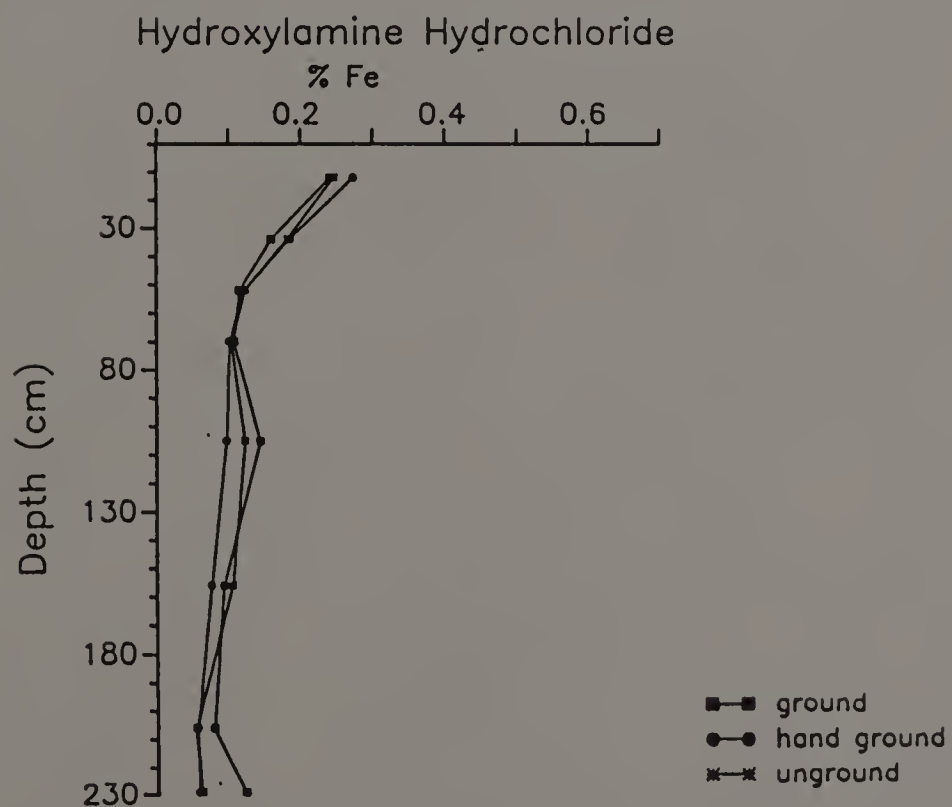
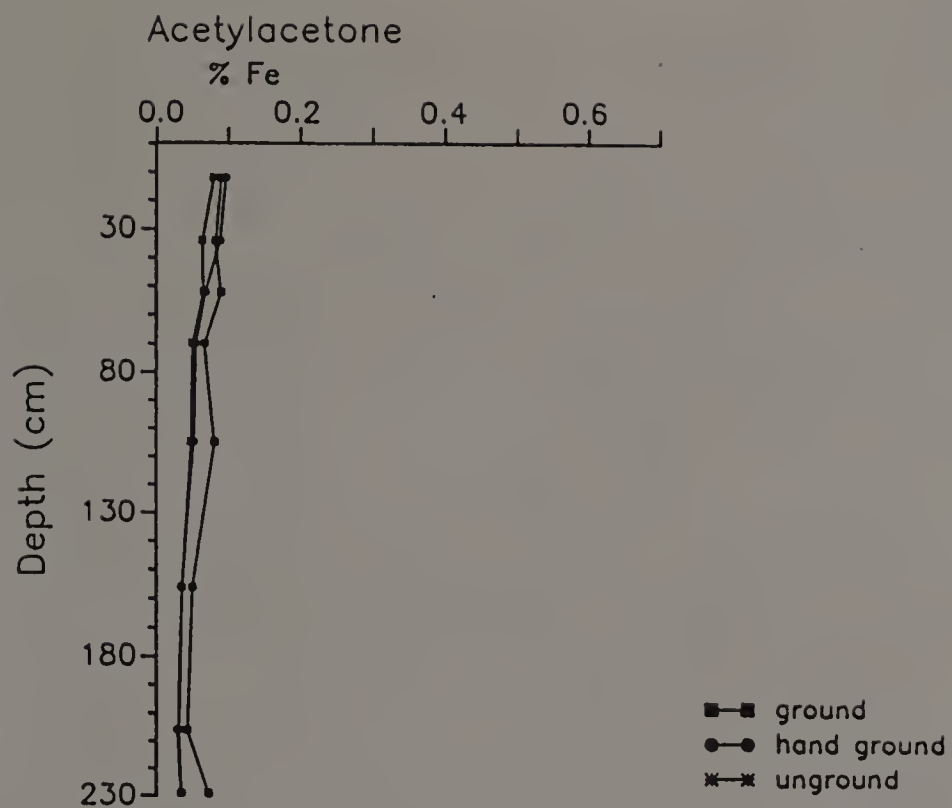
Hori.	C.D.	Pyro	Oxal.	C.B.D.	A.A.	H.H.1	H.H.2	NaOH	NaEDTA
Ap	0.55	0.25	0.580	0.172	0.095	0.272	----	0.141	0.181
Bw	0.41	0.19	0.385	0.230	0.087	0.184	----	0.106	0.079
BE	0.33	0.12	0.225	0.128	0.067	0.121	----	0.094	0.060
2EB	0.31	0.09	0.310	0.216	0.054	0.100	----	0.096	0.034
2Btx1	0.33	0.03	0.190	0.128	0.051	0.096	----	0.107	0.021
2Btx2	0.28	0.03	0.130	0.119	0.034	0.075	----	0.088	0.023
2Cd1	0.26	0.02	0.080	0.099	0.028	0.055	----	0.065	0.021
2Cd2	0.28	0.03	0.090	0.089	0.034	0.057	----	0.071	0.022
BPF	0.24	0.05	0.095	0.113	0.038	0.065	----	0.078	0.036

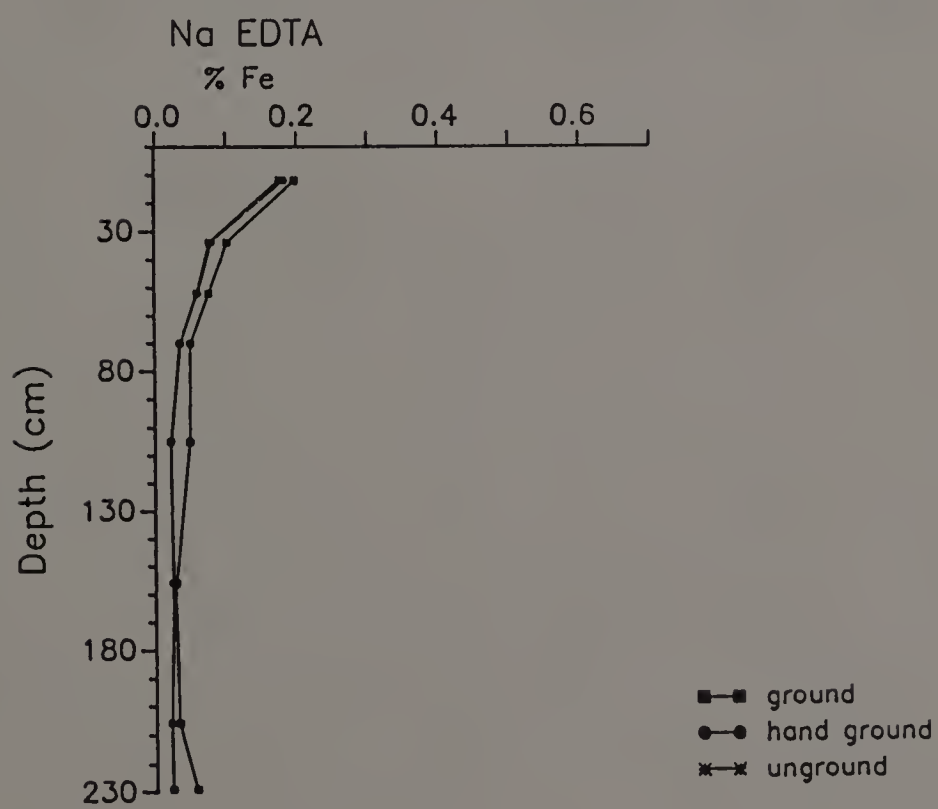
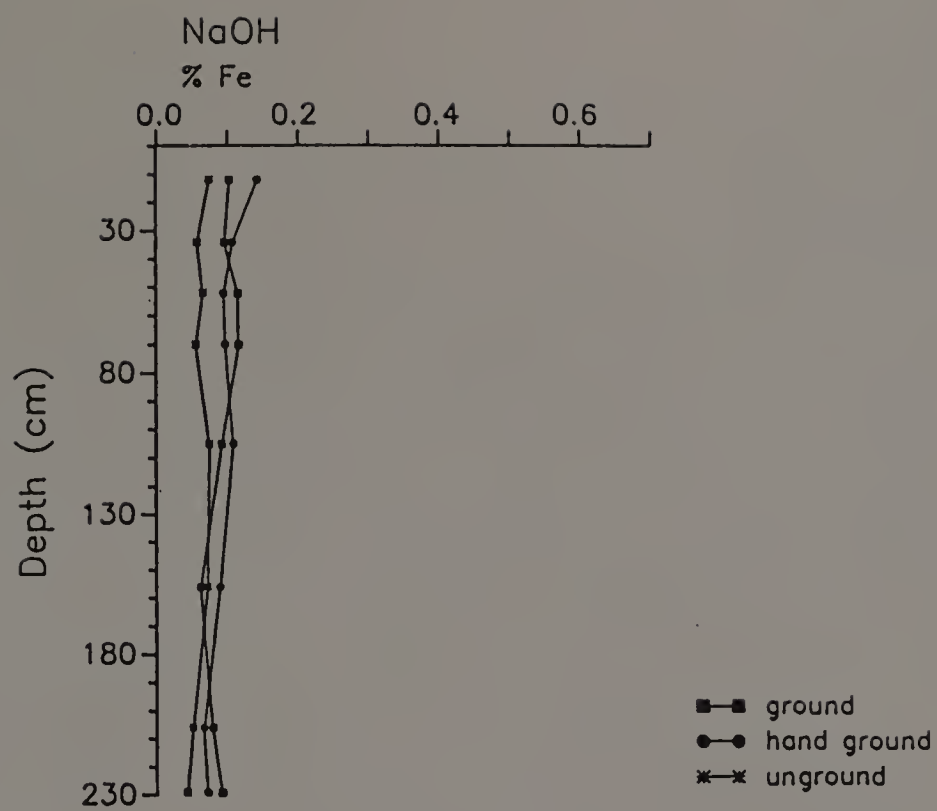
Percent Extractable Fe; Unground

Hori.	C.D.	Pyro	Oxal.	C.B.D.	A.A.	H.H.1	H.H.2	NaOH	NaEDTA
Ap	0.60	0.30	0.555	0.467	0.079	0.246	----	0.074	0.175
Bw	0.43	0.20	0.335	0.190	0.063	0.181	----	0.057	0.076
BE	0.35	0.12	0.200	0.200	0.065	0.122	----	0.065	0.058
2EB	0.38	0.07	0.280	0.149	0.049	0.103	----	0.055	0.035
2Btx1	0.34	0.03	0.130	0.126	0.047	0.122	----	0.074	0.021
2Btx2	0.29	0.02	0.075	0.114	0.035	0.104	----	0.071	0.025
2Cd1	0.27	0.02	0.065	0.095	0.031	0.053	----	0.050	0.020
2Cd2	0.28	0.03	0.075	0.131	0.034	0.061	----	0.042	0.022
BPF	0.32	0.03	0.100	0.106	0.042	0.125	----	0.060	0.033









Pedon 5

Percent Extractable Al; Ground in shatter box

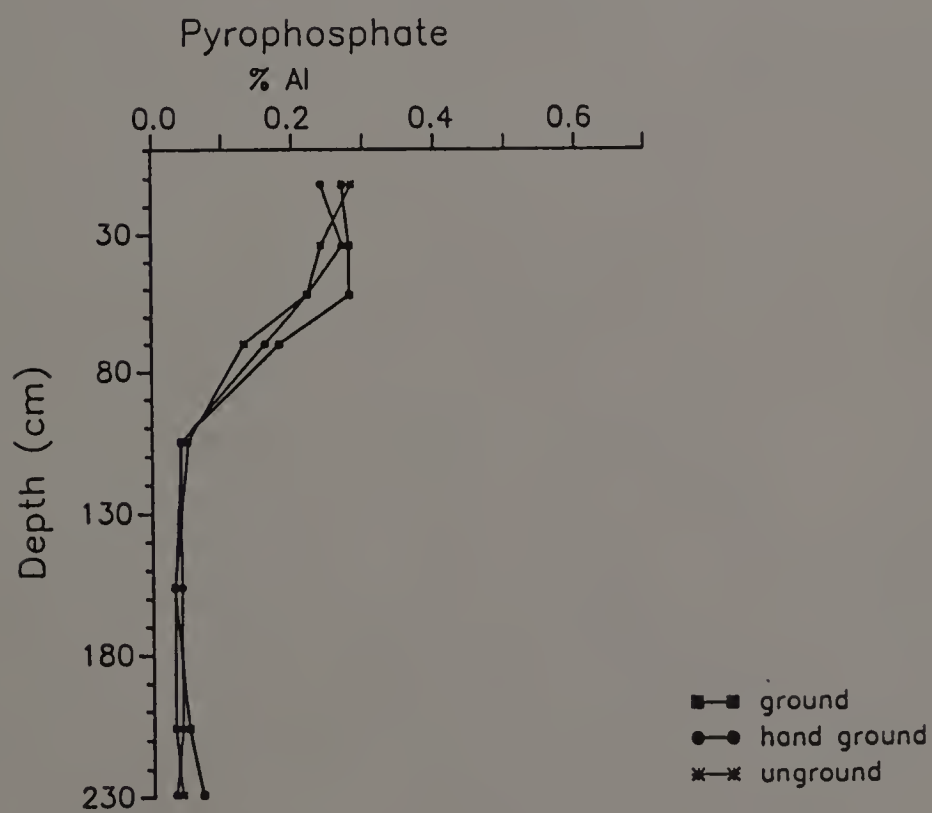
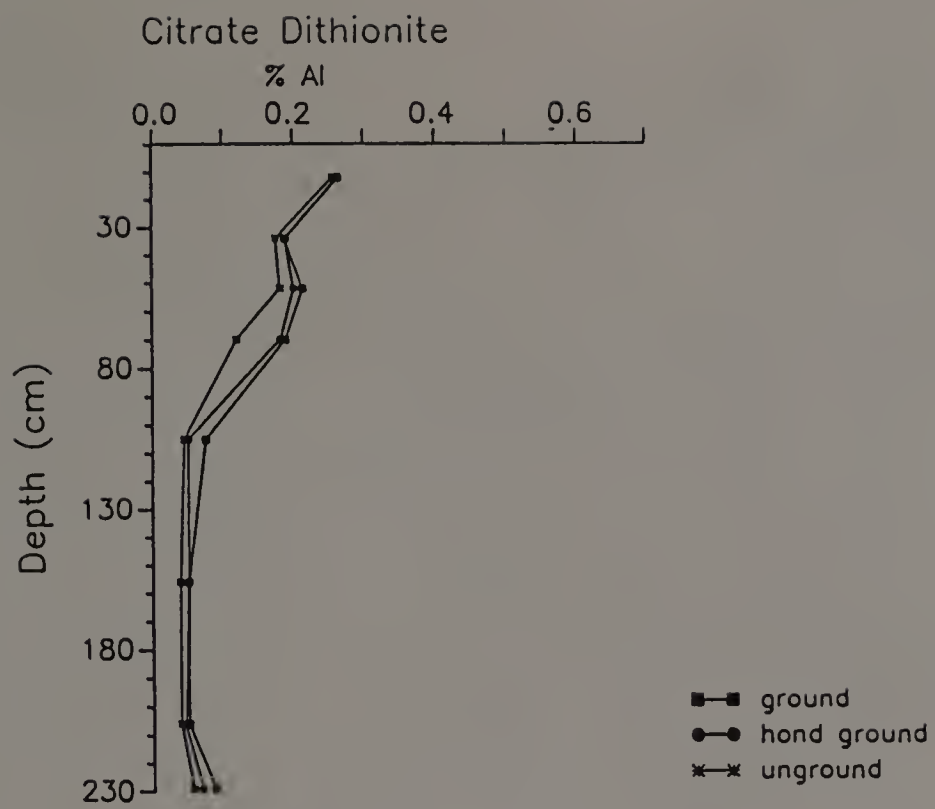
Hori.	C.D.	Pyro	Oxal.	C.B.D.	A.A.	H.H.1	H.H.2	NaOH	NaEDTA
Ap	0.263	0.270	0.63	0.183	0.209	0.350	0.246	0.625	----
Bw	0.188	0.280	0.38	0.116	0.185	0.230	0.179	0.833	----
BE	0.213	0.280	0.38	0.101	0.249	0.230	0.244	0.073	----
2EB	0.188	0.180	0.38	0.085	0.187	0.220	0.153	0.655	----
2Btx1	0.075	0.040	0.43	0.013	0.107	0.145	0.114	0.360	----
2Btx2	0.050	0.030	0.16	0.005	0.072	0.085	0.070	0.388	----
2Cd1	0.050	0.050	0.13	0.006	0.083	0.085	0.073	0.350	----
2Cd2	0.088	0.070	0.17	0.007	0.123	0.130	0.084	0.350	----
BPF	0.138	0.150	0.30	0.029	0.190	0.210	0.124	0.583	----

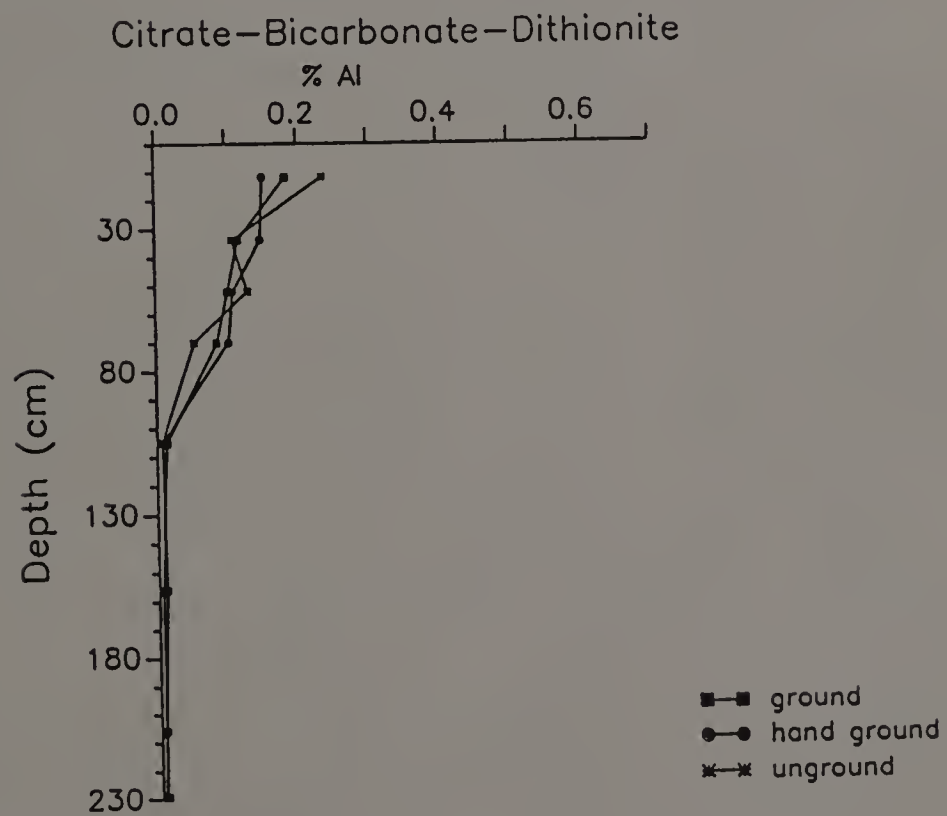
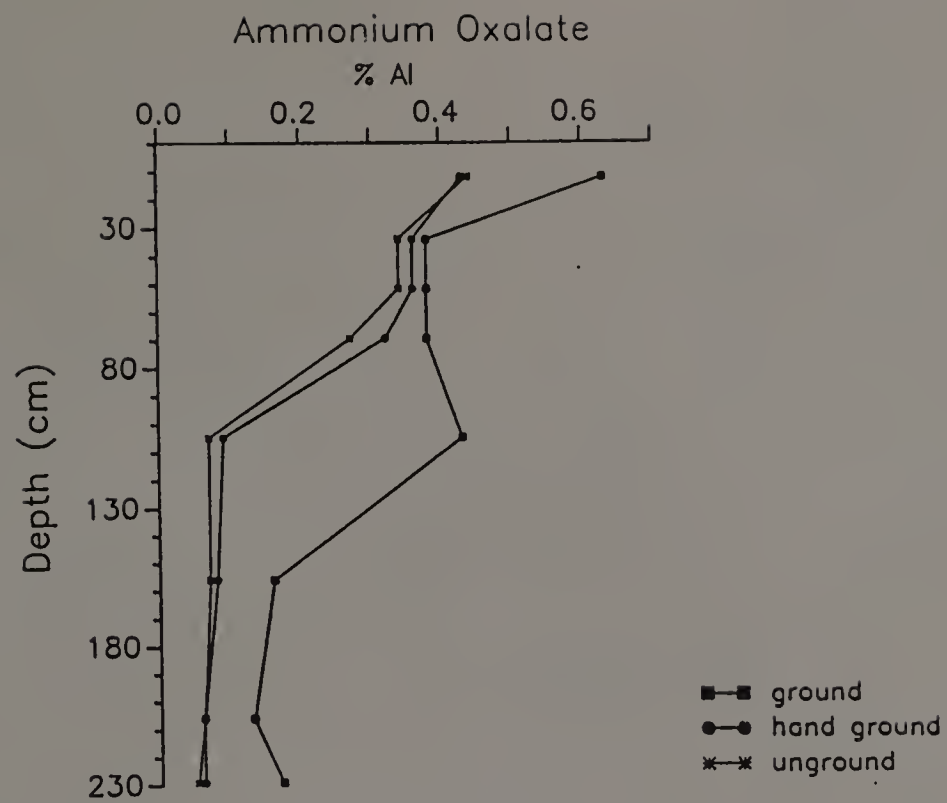
Percent Extractable Al; Ground by hand to pass a 0.5 mm sieve

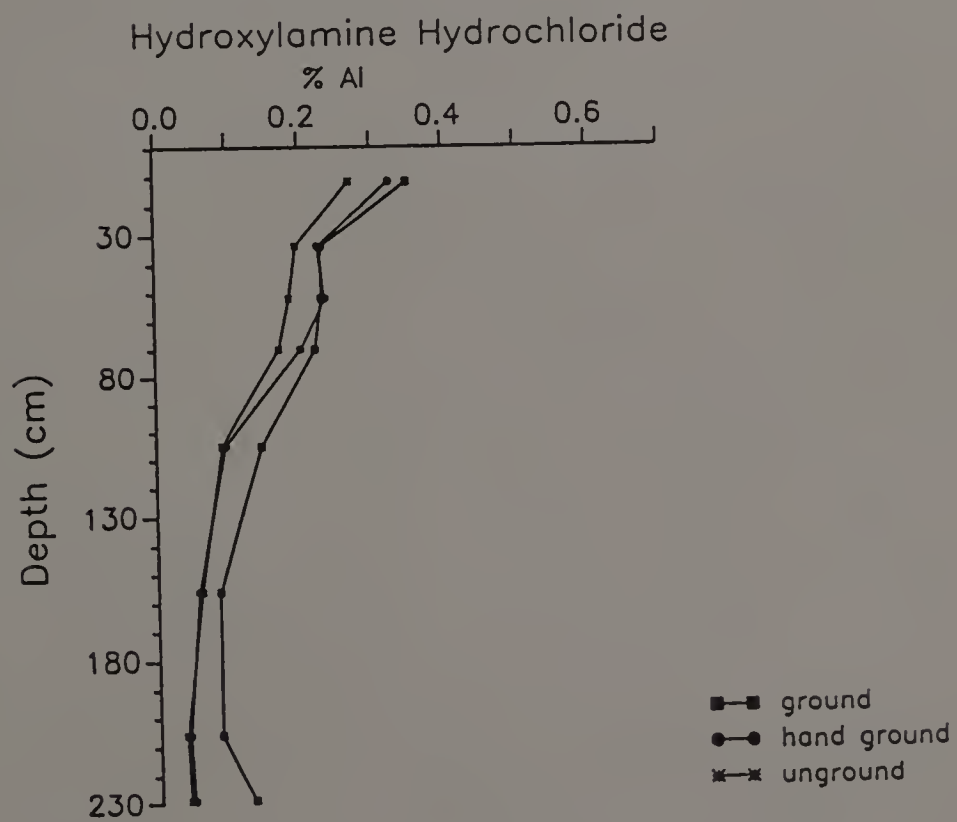
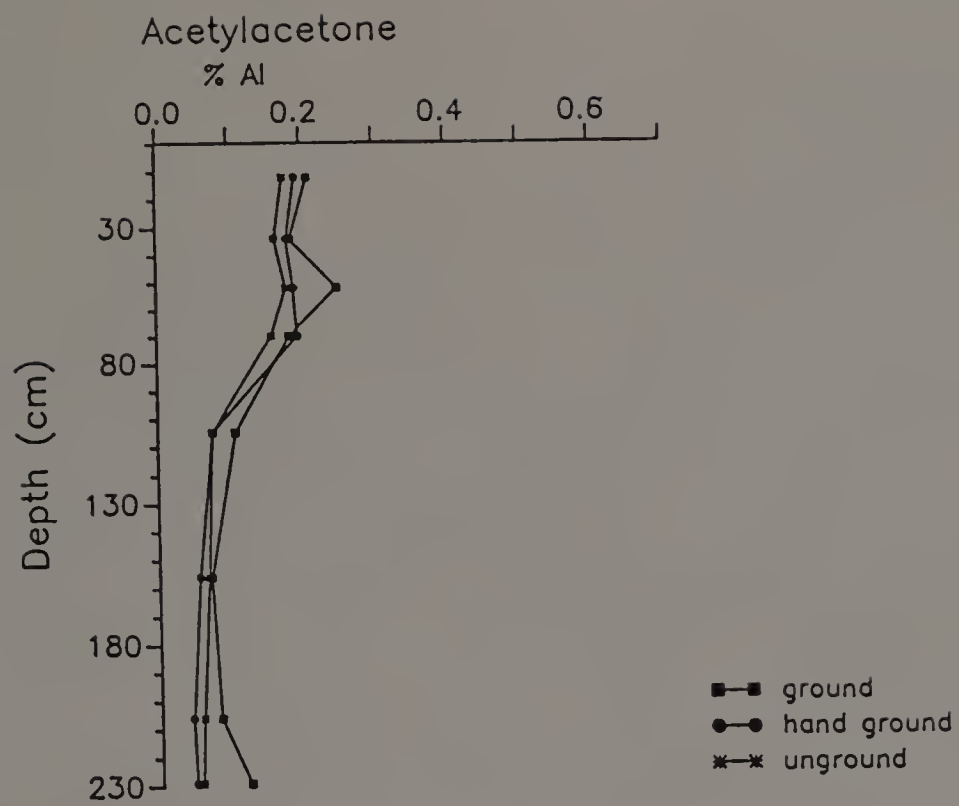
Hori.	C.D.	Pyro	Oxal.	C.B.D.	A.A.	H.H.1	H.H.2	NaOH	NaEDTA
Ap	0.263	0.240	0.43	0.151	0.192	0.325	----	0.723	----
Bw	0.188	0.270	0.36	0.147	0.180	0.225	----	0.833	----
BE	0.200	0.220	0.36	0.108	0.189	0.235	----	0.820	----
2EB	0.181	0.160	0.32	0.101	0.194	0.200	----	0.715	----
2Btx1	0.050	0.040	0.09	0.007	0.075	0.095	----	0.378	----
2Btx2	0.050	0.040	0.08	0.010	0.055	0.055	----	0.375	----
2Cd1	0.044	0.040	0.06	0.006	0.043	0.040	----	0.333	----
2Cd2	0.069	0.030	0.06	0.004	0.047	0.045	----	0.290	----
BPF	0.044	0.050	0.10	0.022	0.051	0.050	----	0.508	----

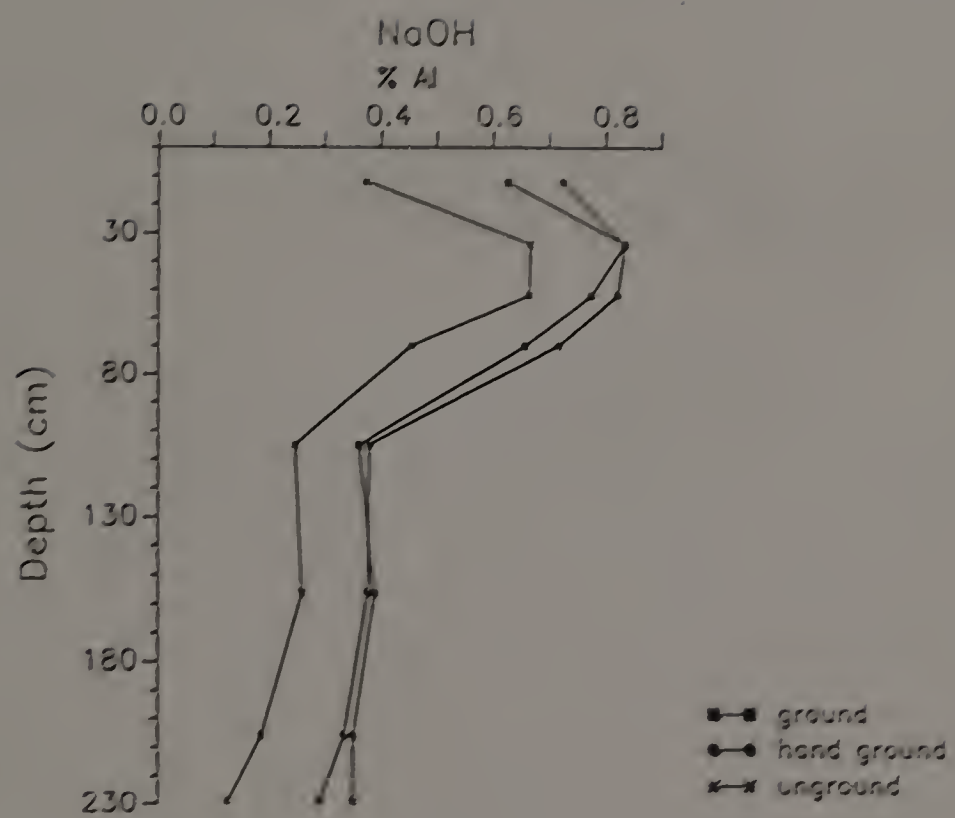
Percent Extractable Al; Unground

Hori.	C.D.	Pyro	Oxal.	C.B.D.	A.A.	H.H.1	H.H.2	NaOH	NaEDTA
Ap	0.256	0.280	0.44	0.236	0.176	0.270	----	0.373	----
Bw	0.175	0.240	0.34	0.108	0.164	0.195	----	0.665	----
BE	0.181	0.220	0.34	0.129	0.179	0.185	----	0.663	----
2EB	0.119	0.130	0.27	0.053	0.158	0.170	----	0.453	----
2Btx1	0.044	0.050	0.07	0.006	0.075	0.090	----	0.245	----
2Btx2	0.038	0.030	0.07	0.011	0.068	0.060	----	0.258	----
2Cd1	0.038	0.030	0.06	0.006	0.058	0.035	----	0.185	----
2Cd2	0.056	0.040	0.05	0.006	0.055	0.040	----	0.125	----
BPF	0.056	0.060	0.09	0.014	0.068	0.075	----	0.330	----









Pedon 5

Percent Extractable Mn; Ground in shatter box

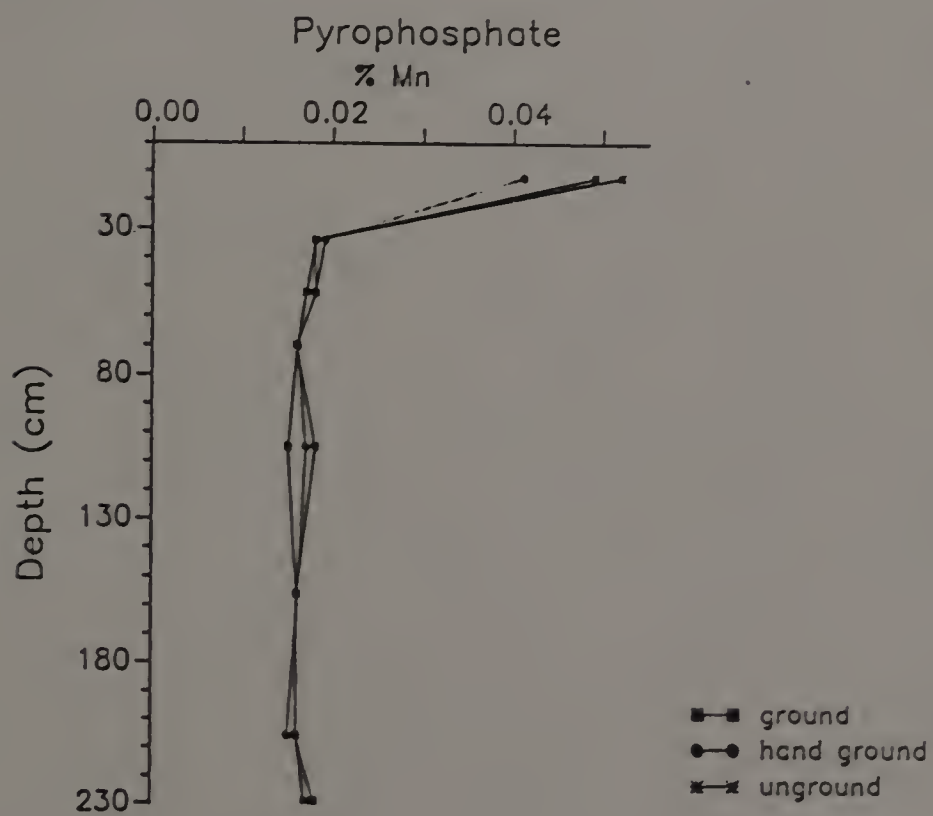
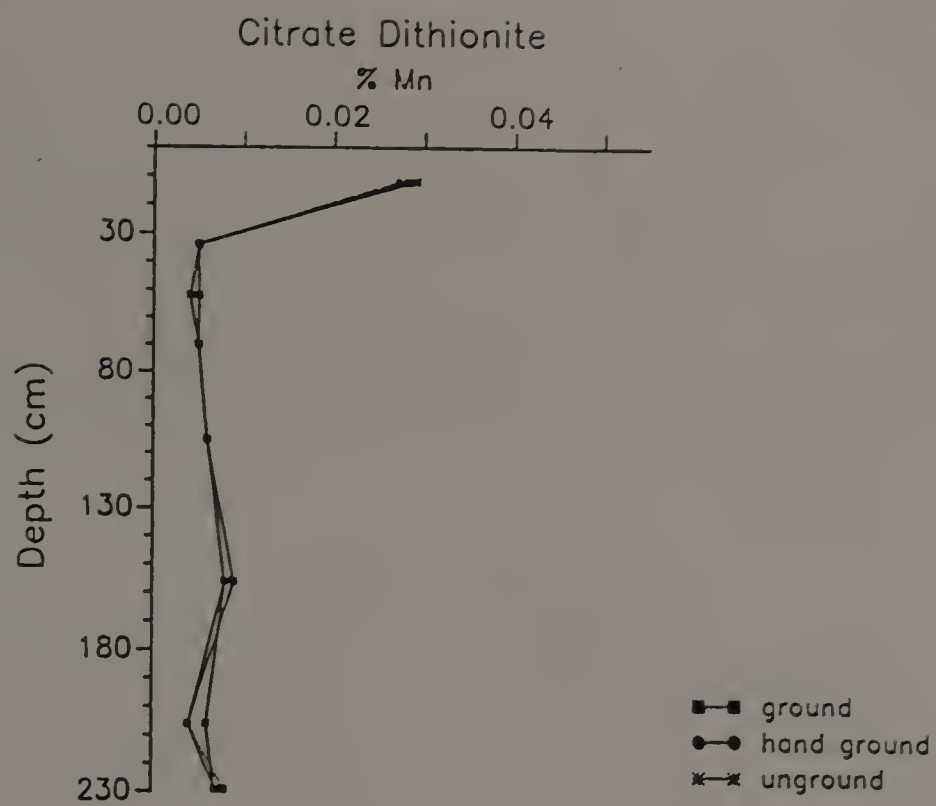
Hori.	C.D.	Pyro	Oxal.	C.B.D.	A.A.	H.H.1	H.H.2	NaOH	NaEDTA
Ap	0.028	0.049	0.027	0.019	0.019	0.027	0.017	----	0.029
Bw	0.005	0.018	0.002	0.002	0.002	0.003	0.001	----	0.003
BE	0.005	0.018	0.002	0.002	0.003	0.002	0.002	----	0.002
2EB	0.005	0.016	0.003	0.003	0.002	0.002	0.001	----	0.001
2Btx1	0.006	0.015	0.004	0.004	0.004	0.005	0.003	----	0.003
2Btx2	0.009	0.016	0.005	0.006	0.005	0.007	0.004	----	0.005
2Cd1	0.004	0.016	0.002	0.002	0.003	0.003	0.002	----	0.003
2Cd2	0.008	0.018	0.004	0.004	0.006	0.006	0.004	----	0.005
BPF	0.004	0.015	0.002	0.001	0.002	0.002	0.001	----	0.001

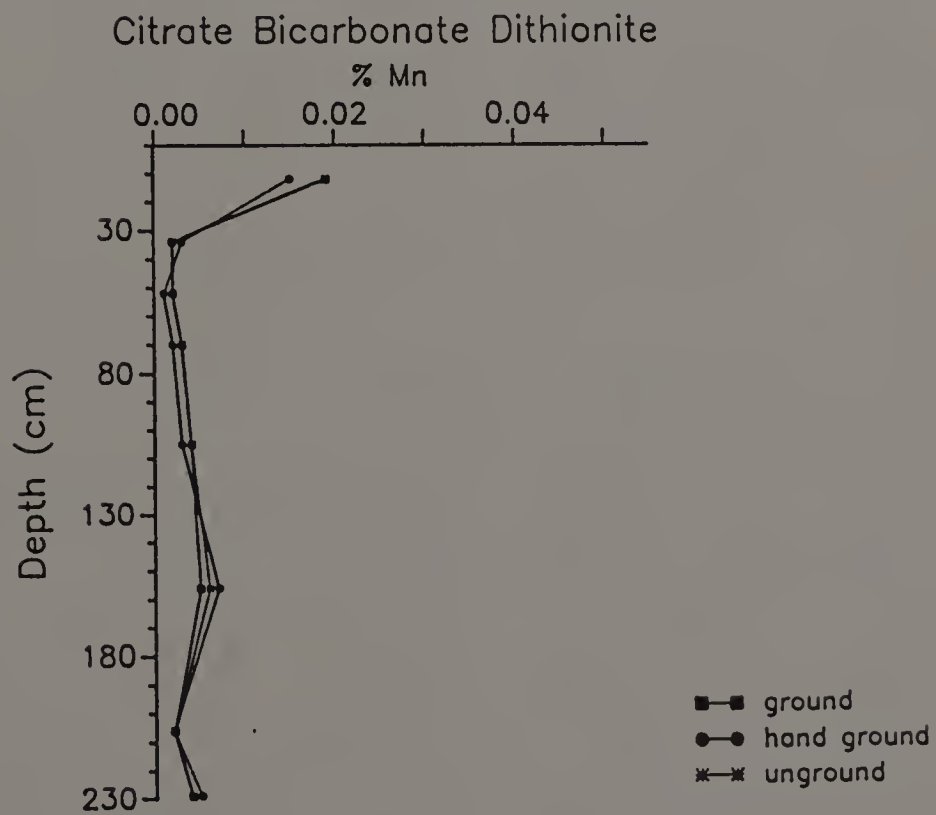
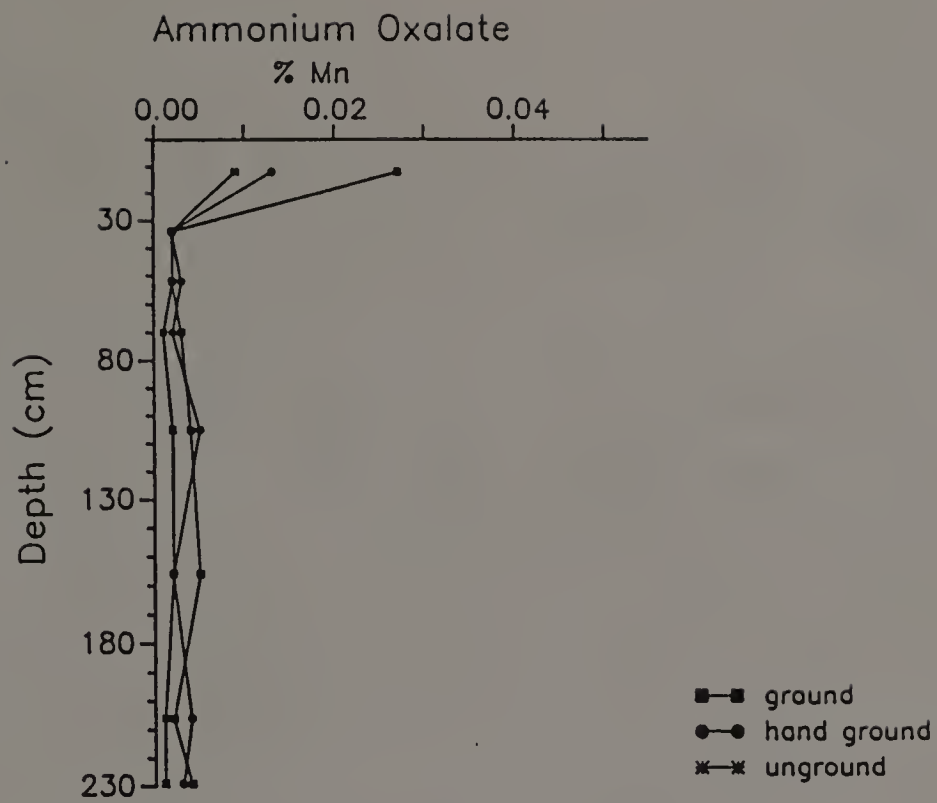
Percent Extractable Mn; Ground by hand to pass a 0.5 mm sieve

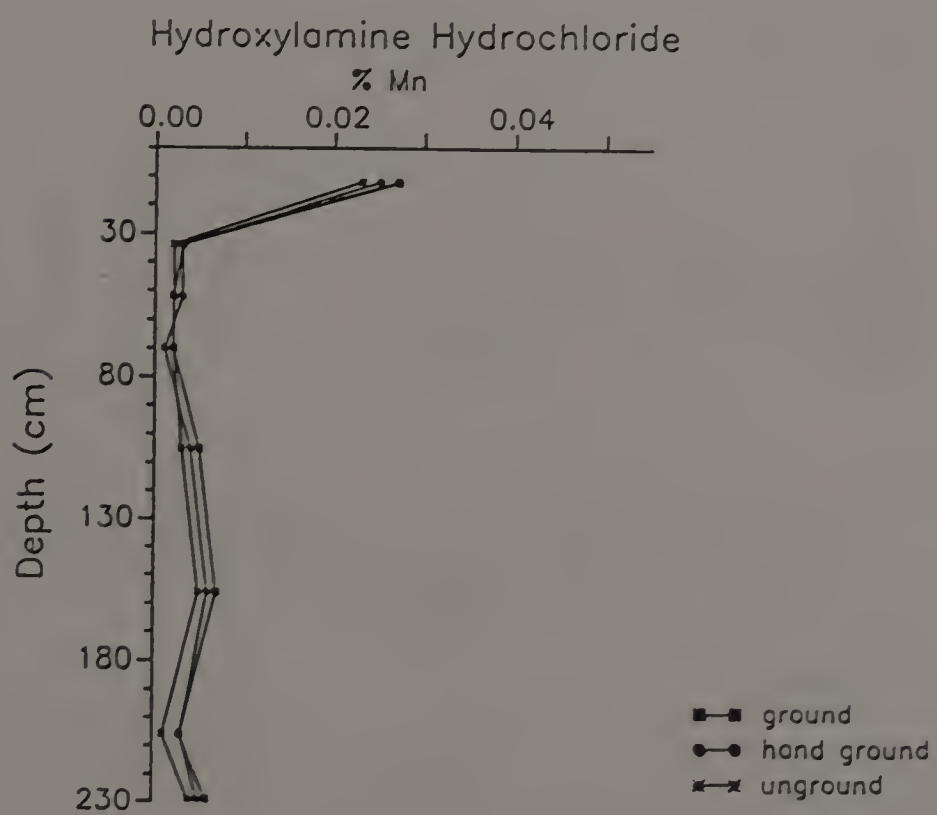
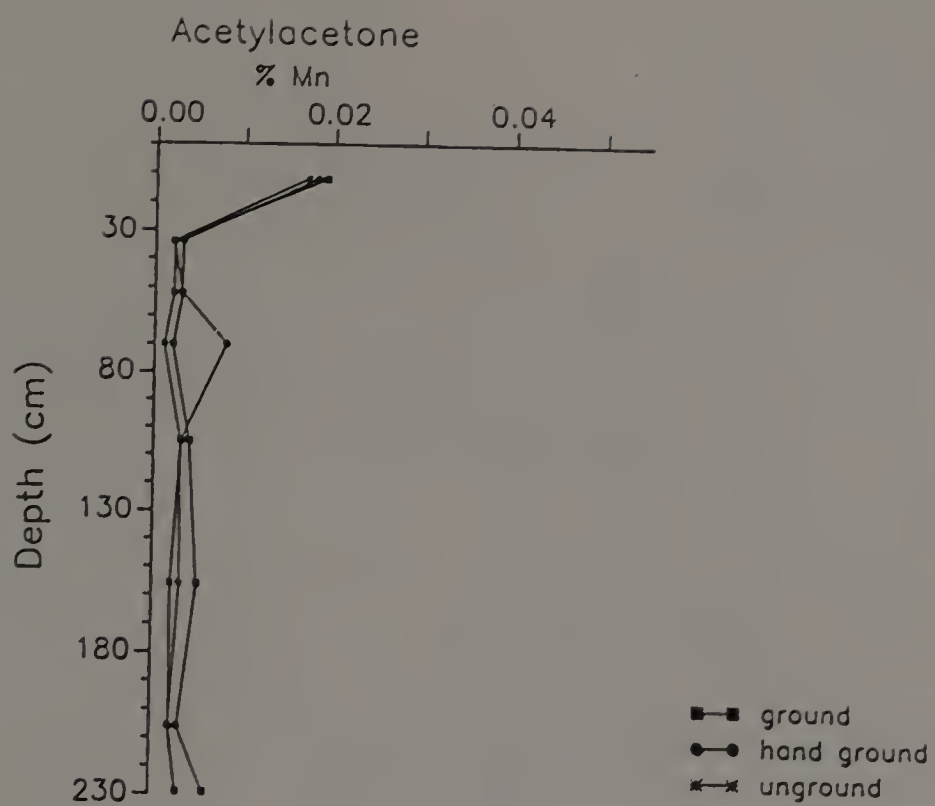
Hori.	C.D.	Pyro	Oxal.	C.B.D.	A.A.	H.H.1	H.H.2	NaOH	NaEDTA
Ap	0.027	0.041	0.013	0.015	0.018	0.025	----	----	0.026
Bw	0.005	0.019	0.002	0.003	0.003	0.003	----	----	0.003
BE	0.005	0.018	0.003	0.001	0.003	0.003	----	----	0.002
2EB	0.005	0.016	0.002	0.002	0.008	0.001	----	----	0.008
2Btx1	0.006	0.017	0.005	0.003	0.003	0.004	----	----	0.002
2Btx2	0.008	0.016	0.002	0.007	0.003	0.006	----	----	0.003
2Cd1	0.004	0.015	0.004	0.002	0.002	0.003	----	----	0.001
2Cd2	0.007	0.017	0.003	0.005	0.003	0.005	----	----	0.003
BPF	0.003	0.016	0.001	0.001	0.002	0.001	----	----	----

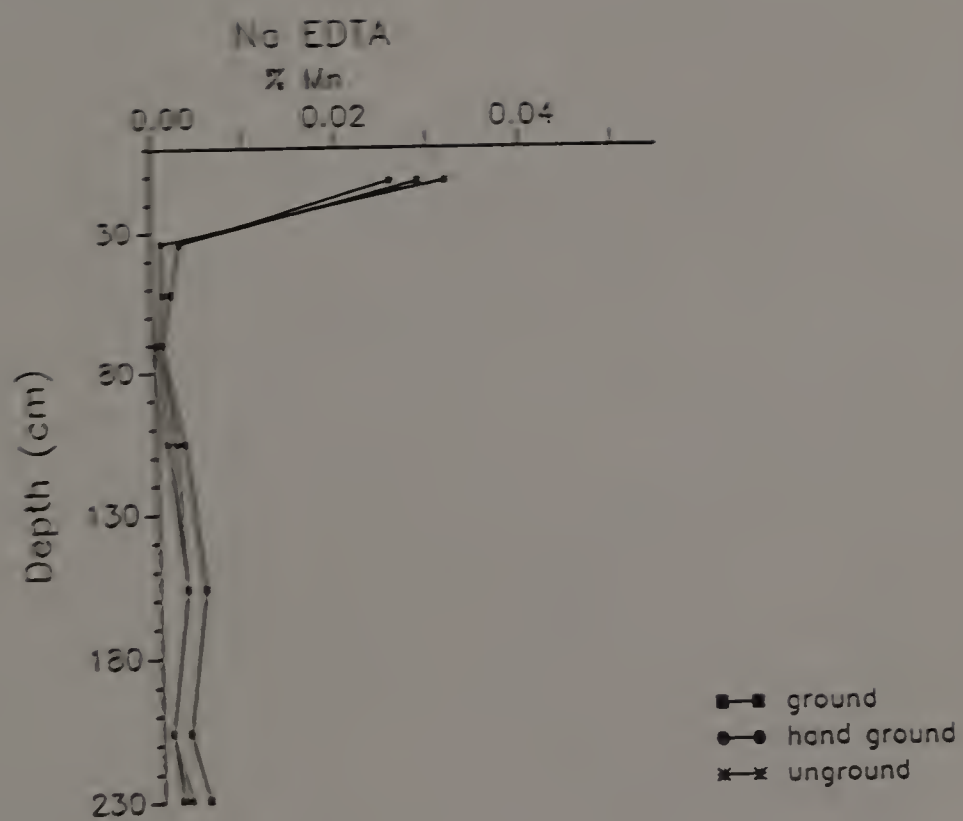
Percent Extractable Mn; Unground

Hori.	C.D.	Pyro	Oxal.	C.B.D.	A.A.	H.H.1	H.H.2	NaOH	NaEDTA
Ap	0.029	0.052	0.009	0.019	0.017	0.023	----	----	0.032
Bw	0.005	0.018	0.002	0.002	0.002	0.002	----	----	0.001
BE	0.004	0.017	0.002	0.002	0.002	0.002	----	----	0.001
2EB	0.005	0.016	0.001	0.003	0.001	0.002	----	----	0.001
2Btx1	0.006	0.018	0.002	0.004	0.003	0.003	----	----	0.001
2Btx2	0.008	0.016	0.002	0.006	0.002	0.005	----	----	0.003
2Cd1	0.006	0.016	0.001	0.002	0.002	0.001	----	----	0.001
2Cd2	0.007	0.017	0.001	0.004	0.003	0.004	----	----	0.002
BPF	0.003	0.016	0.001	0.001	0.008	0.001	----	----	----









Pedon 5

Percent Extractable Si; Ground in shatter box

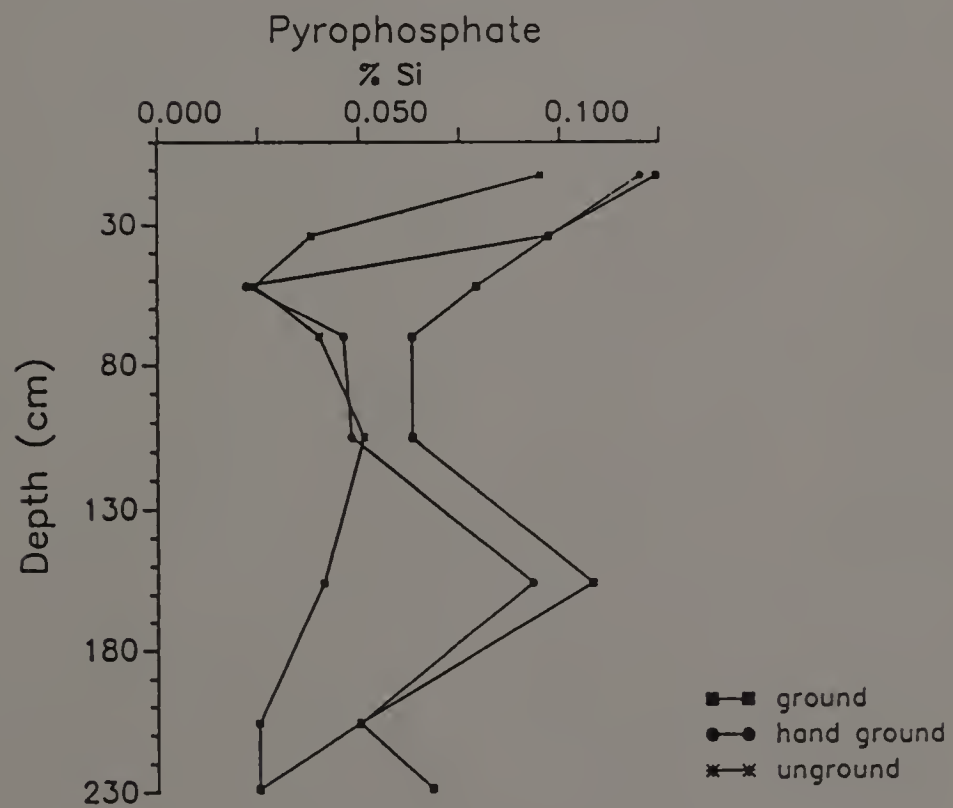
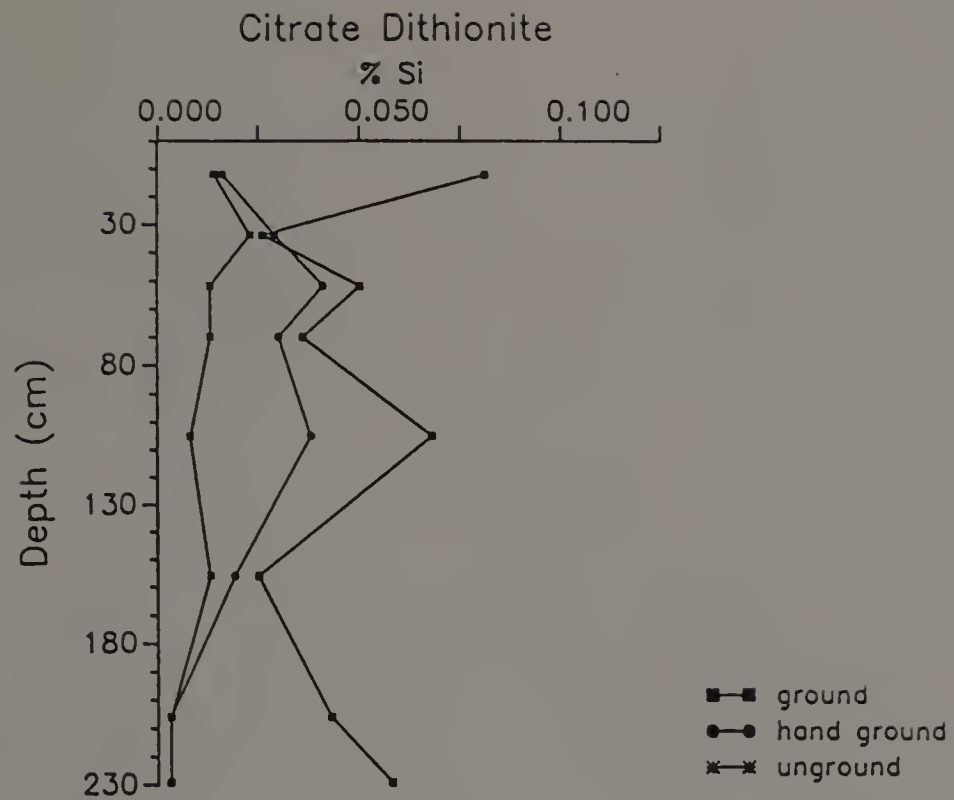
Hori.	C.D.	Pyro	Oxal.	C.B.D.	A.A.	H.H.1	H.H.2	NaOH	NaEDTA
Ap	0.081	0.124	0.190	0.050	1.25	----	0.122	7.31	0.087
Bw	0.026	0.097	0.197	0.036	1.38	----	0.122	9.69	0.064
BE	0.050	0.079	0.144	0.046	2.22	----	0.275	5.80	0.113
2EB	0.036	0.063	0.132	0.037	2.14	----	0.281	0.42	0.103
2Btx1	0.068	0.063	0.193	0.042	2.47	----	0.428	6.67	0.119
2Btx2	0.025	0.108	0.199	0.029	2.01	----	0.210	4.60	0.076
2Cd1	0.043	0.050	0.169	0.033	1.58	----	0.348	4.34	0.052
2Cd2	0.058	0.068	0.223	0.038	2.45	----	0.261	5.17	0.106
BPF	0.096	0.073	0.168	0.028	2.26	----	0.422	5.33	0.152

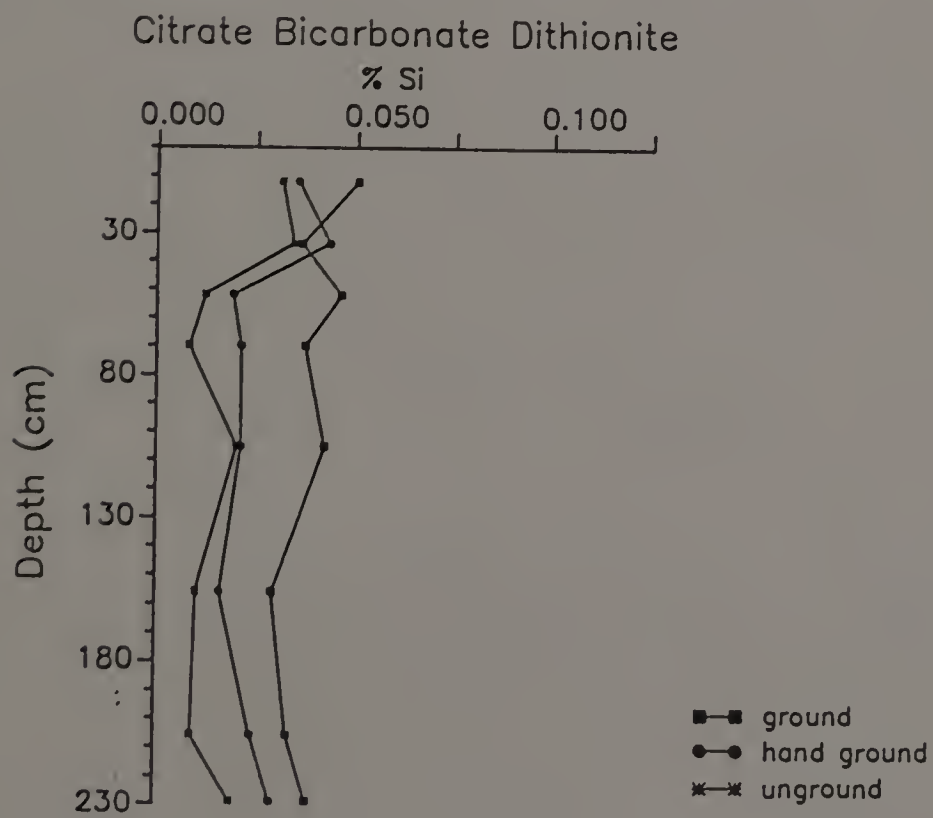
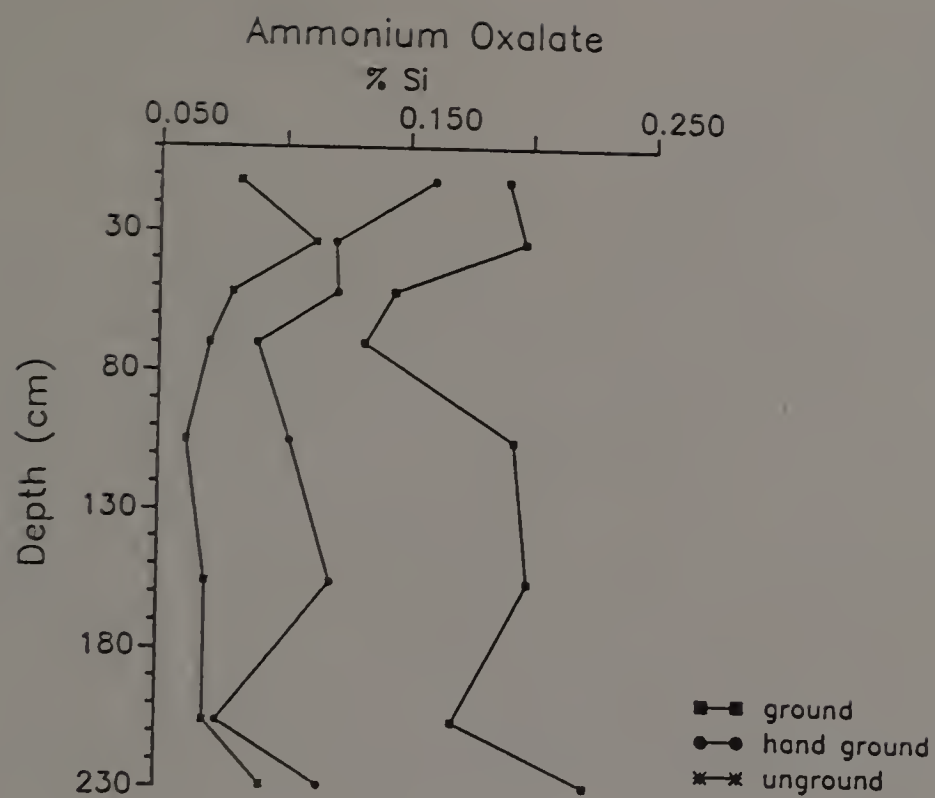
Percent Extractable Si; Ground by hand to pass a 0.5 mm sieve

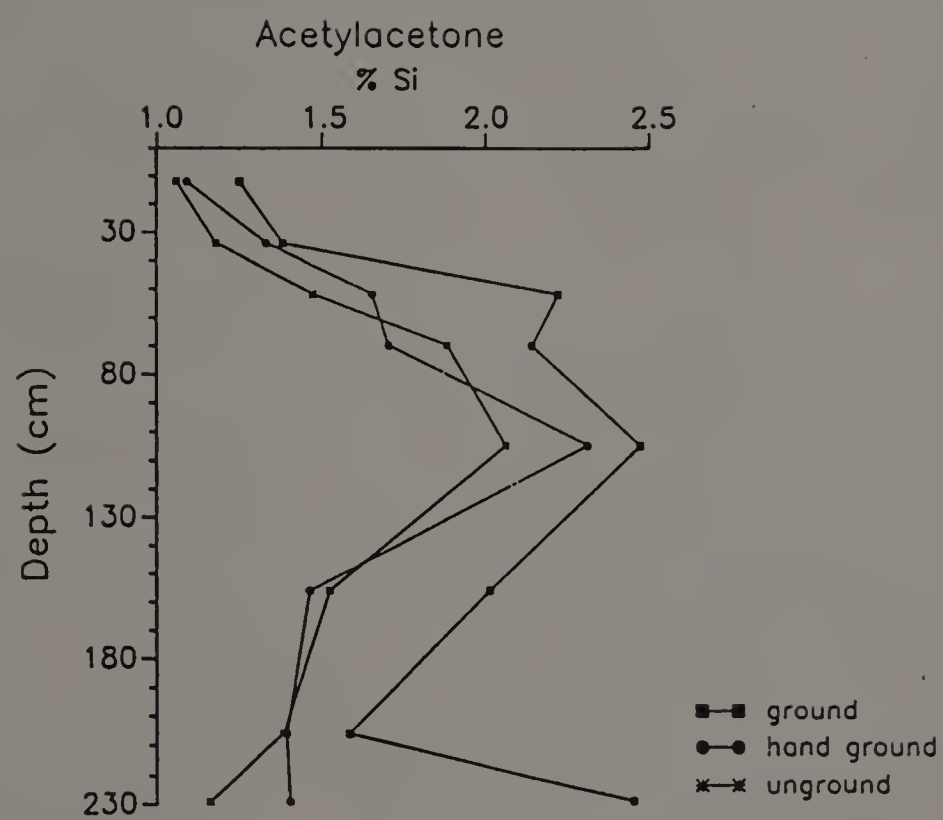
Hori.	C.D.	Pyro	Oxal.	C.B.D.	A.A.	H.H.1	H.H.2	NaOH	NaEDTA
Ap	0.016	0.120	0.160	0.035	1.09	----	----	4.99	0.083
Bw	0.024	0.097	0.120	0.043	1.33	----	----	3.56	0.042
BE	0.041	0.022	0.121	0.019	1.65	----	----	3.99	0.079
2EB	0.030	0.046	0.089	0.021	1.70	----	----	0.40	0.036
2Btx1	0.038	0.048	0.102	0.021	2.31	----	----	3.50	0.042
2Btx2	0.019	0.093	0.119	0.016	1.46	----	----	3.36	0.042
2Cd1	0.003	0.050	0.074	0.024	1.39	----	----	3.53	0.048
2Cd2	0.003	0.025	0.115	0.029	1.40	----	----	5.51	0.074
BPF	0.014	0.147	0.106	0.019	0.97	----	----	4.55	0.063

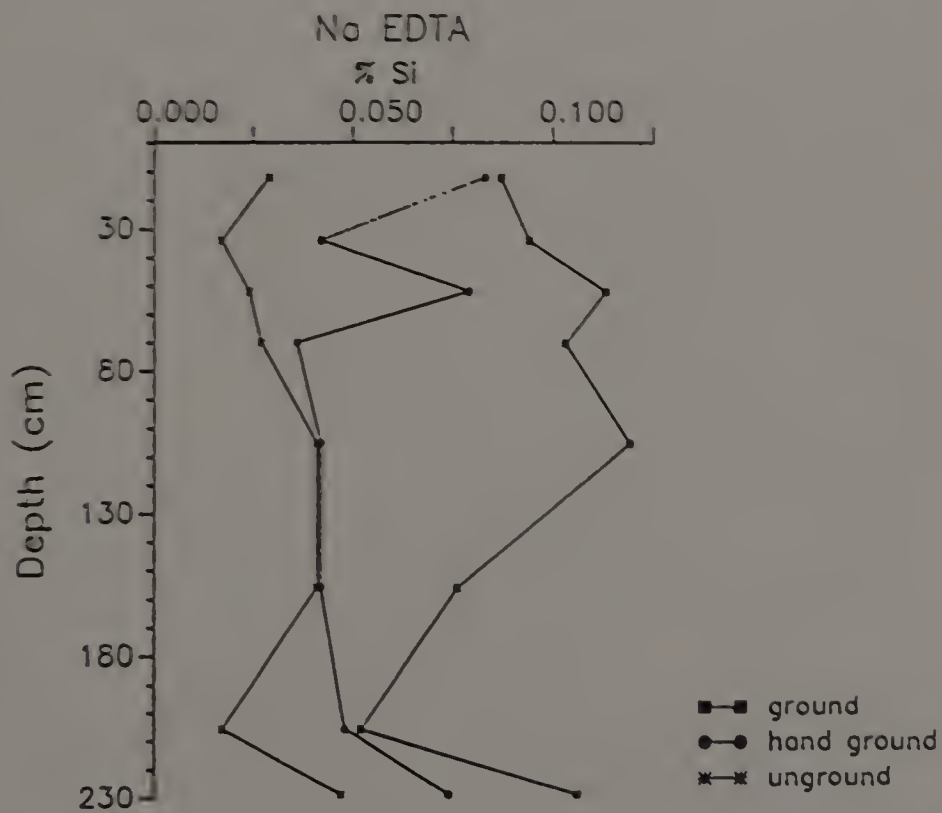
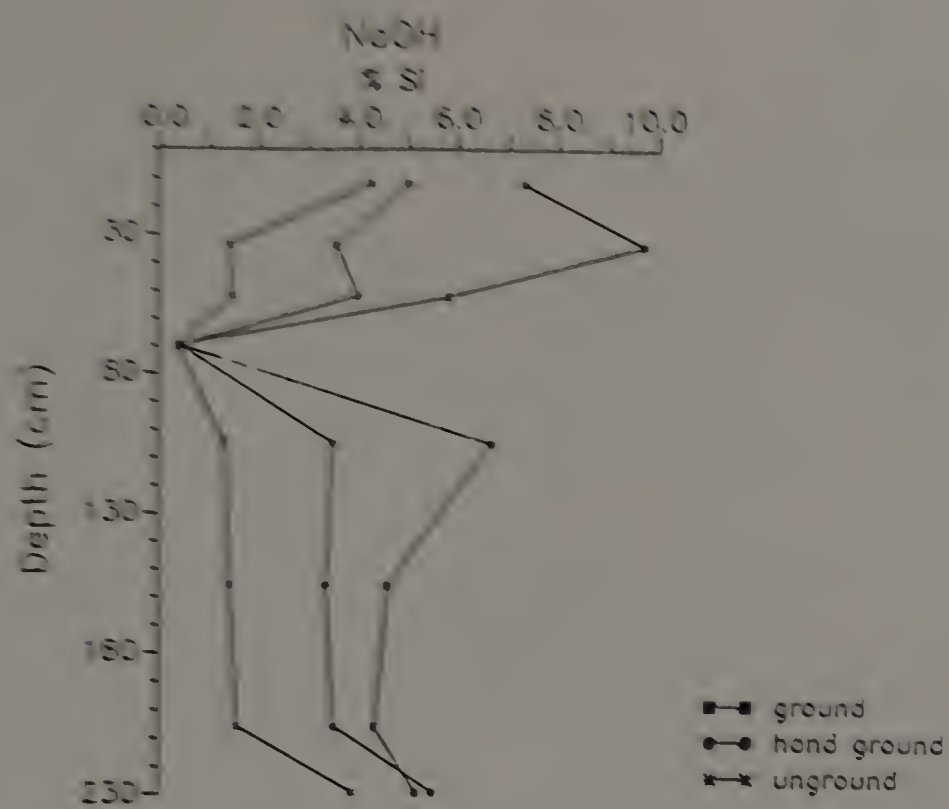
Percent Extractable Si; Unground

Hori.	C.D.	Pyro	Oxal.	C.B.D.	A.A.	H.H.1	H.H.2	NaOH	NaEDTA
Ap	0.014	0.095	0.082	0.031	1.06	----	----	4.25	0.029
Bw	0.023	0.038	0.112	0.034	1.18	----	----	1.41	0.017
BE	0.013	0.024	0.079	0.012	1.47	----	----	1.47	0.024
2EB	0.013	0.040	0.070	0.008	1.88	----	----	0.38	0.027
2Btx1	0.008	0.051	0.061	0.020	2.06	----	----	1.33	0.041
2Btx2	0.013	0.041	0.069	0.010	1.52	----	----	1.43	0.041
2Cd1	0.003	0.025	0.069	0.009	1.38	----	----	1.58	0.017
2Cd2	0.003	0.025	0.097	0.019	1.16	----	----	3.88	0.047
BPF	0.013	0.089	0.042	0.022	1.07	----	----	3.65	0.030









APPENDIX H
CHEMICAL DATA

Primary Pedons

Pedon 1

Hor.	Depth	H ₂ O	pH KCl	CaCl ₂	O.C.	Ex Acid	Ca	CEC		K	Sum Bases
Ap	0-23	5.09	4.00	4.40	1.52	12.96	0.025	0.481	0.069	0.413	0.988
Bw1	23-34	4.95	4.01	4.25	0.86	12.54	0.015	0.222	0.065	0.314	0.616
Bw2	34-59	5.19	3.90	4.34	0.43	6.87	0.017	0.308	0.062	0.300	0.687
Bx	59-91	5.21	3.70	4.43	0.21	6.54	0.042	0.489	0.067	0.253	0.851
2Btx1	91-125	5.01	3.61	4.30	0.15	7.06	0.044	0.946	0.078	0.147	1.215
2Btx2	125-152	4.90	4.32	3.00	0.12	6.49	0.043	1.604	0.108	0.218	1.973
3BCd	152-194	5.27	3.99	4.50	0.07	3.44	0.028	0.806	0.080	0.166	1.080
4Cd	194+	5.19	3.51	4.46	0.13	6.02	0.057	2.420	0.113	0.289	2.879
PCF	124	4.85	3.03	4.01	0.19	--	--	--	--	--	--

Pedon 2

Hor.	Depth	H ₂ O	pH KCl	CaCl ₂	O.C.	Ex Acid	Ca	CEC		K	Sum Bases
Ap	0-14	4.38	5.27	4.09	3.98	16.94	3.029	0.465	0.052	0.328	3.874
Bw1	14-25	4.69	4.30	4.17	1.05	9.03	0.205	0.008	0.047	0.074	0.334
Bw2	25-39	4.77	4.49	4.32	0.59	6.33	0.095	0.025	0.039	0.055	0.214
BE	39-55	4.85	4.52	4.23	0.27	5.10	0.150	0.016	0.040	0.068	0.274
2Btx1	55-86	4.15	4.69	4.16	0.16	4.30	1.230	0.218	0.061	0.133	1.642
2Btx2	86-136	4.30	4.69	4.08	0.12	4.79	1.325	0.230	0.059	0.127	1.741
2BCd	136-160	4.49	4.98	4.01	0.13	5.05	2.959	0.485	0.119	0.116	3.676
3Cd1	160-183	4.50	4.99	4.09	0.09	4.11	3.847	0.535	0.120	0.169	4.671
3Cd2	183-210	5.89	4.19	4.22	0.11	2.86	6.045	0.794	0.123	0.183	7.145
3Cd3	210+	5.78	5.50	4.27	0.12	2.69	7.784	1.069	0.127	0.245	9.225
Sand	196	5.13	4.81	4.29	0.03	0.94	0.644	0.074	0.038	0.040	0.796
PCF	148	--	--	--	0.15	3.43	1.218	0.239	0.065	0.082	1.604

Pedon 3

Hor.	Depth	H ₂ O	pH KCl	CaCl ₂	O.C.	Ex Acid	Ca	CEC		K	Sum Bases
Ap	0-20	5.11	4.82	4.20	1.86	10.72	2.742	0.296	0.017	0.186	3.240
Bw	20-37	5.60	5.11	4.25	0.52	4.40	0.447	0.119	0.024	0.160	0.750
BE	37-61	5.92	5.23	4.56	0.21	2.50	1.689	0.128	0.028	0.183	2.028
2Btx1	61-100	5.85	5.01	4.53	0.13	2.75	0.991	0.366	0.027	0.229	1.613
2Btx2	100-137	5.79	4.98	4.50	0.08	2.48	1.222	0.358	0.034	0.221	1.833
2BCd	137-183	5.62	4.82	4.18	0.14	3.59	2.016	0.465	0.037	0.224	2.742
3Cd1	183-216	6.14	4.89	4.93	0.14	2.38	4.815	1.563	0.041	0.138	6.557
3Cd2	216+	6.30	5.84	4.99	0.13	2.84	4.756	1.892	0.066	0.147	6.861

Pedon 4

Hor.	Depth	H ₂ O	pH		O.C.	Ex Acid	Ca	CEC		K	Sum Bases
			KCl	CaCl ₂				Mg	Na		
Ap	0-25	5.80	5.31	4.80	2.27	11.03	4.646	1.041	0.032	0.123	5.840
Bw1	25-43	5.89	5.29	4.81	0.74	7.32	1.819	0.621	0.042	0.079	2.561
Bw2	43-57	6.09	5.26	4.91	0.23	4.94	1.964	0.831	0.060	0.103	2.958
BE	57-71	6.11	5.19	5.00	0.29	3.28	1.669	0.720	0.044	0.118	2.947
2Btx1	71-102	6.06	5.00	4.88	0.18	3.64	2.218	1.114	0.036	0.150	3.518
2Btx2	102-132	5.99	4.92	4.71	0.16	3.78	2.605	1.360	0.038	0.155	4.158
2BCd	132-169	5.89	4.79	4.65	0.18	2.35	3.428	1.473	0.039	0.171	5.111
3Cd	169+	6.12	4.96	5.12	0.13	2.50	5.122	2.641	0.070	0.176	8.009

Pedon 5

Hor.	Depth	H ₂ O	pH		O.C.	Ex Acid	Ca	CEC		K	Sum Bases
			KCl	CaCl ₂				Mg	Na		
Ap	0-25	6.39	5.84	6.36	2.21	5.31	8.949	1.547	0.079	0.136	10.710
Bw	25-45	6.21	5.22	6.27	0.46	3.88	2.143	0.851	0.068	0.129	3.191
BE	45-60	6.07	5.04	6.12	0.39	3.34	1.599	0.633	0.055	0.089	2.376
2EB	60-81	6.16	5.14	6.15	0.17	1.85	0.679	0.144	0.054	0.112	0.989
2Btx1	81-130	6.31	4.28	6.39	0.04	0.00	2.572	0.712	0.072	0.047	3.403
2Btx2	130-184	6.15	4.48	6.19	0.03	0.43	1.839	0.444	0.067	0.035	2.385
2Cd1	184-229	6.49	4.95	6.49	0.03	0.00	1.245	0.317	0.059	0.026	1.647
2Cd2	229+	6.82	5.38	7.07	0.02	0.00	1.292	0.341	0.057	0.026	1.716
BPF		6.13	4.77	6.19	0.12	1.63	1.505	0.411	0.062	0.049	2.027

Secondary Sites

EHP

Hor.	Depth	H ₂ O	pH	CaCl ₂	O.C.	Ex Acid	Ca	CEC		K	Sum Bases
			KCl					Mg	Na		
Ap	0-18	4.91	3.99	4.94	1.30	11.52	1.800	0.707	0.036	0.415	2.958
Bw1	18-30	4.95	3.87	4.32	0.45	8.60	1.098	0.383	0.036	0.347	1.864
Bw2	30-51	4.86	3.79	4.39	0.34	7.68	0.474	0.119	0.003	0.256	0.852
Bt	51-76	4.90	3.73	4.42	0.18	7.47	1.821	0.522	0.035	0.125	2.503
2Btx1	76+	4.80	3.64	4.28	0.16	6.83	2.121	0.728	0.033	0.111	2.993

EHW

Hor.	Depth	H ₂ O	pH	CaCl ₂	O.C.	Ex Acid	Ca	CEC		K	Sum Bases
			KCl					Mg	Na		
Ap	0-23	5.03	4.21	4.71	3.06	18.08	3.718	1.946	0.084	0.222	5.970
Bw1	23-41	4.51	3.70	4.05	0.40	9.27	0.599	0.206	0.018	0.086	0.909
Bw2	41-56	4.50	3.61	4.03	0.25	10.28	0.873	0.498	0.045	0.134	1.550
2Btx1	56-76	4.29	3.65	4.00	0.16	9.03	0.898	0.559	0.041	0.159	1.657
2Btx2	76+	4.49	3.59	4.12	0.19	8.29	0.599	0.197	0.011	0.136	0.943

EHR

Hor.	Depth	H ₂ O	pH	CaCl ₂	O.C.	Ex Acid	Ca	CEC		K	Sum Bases
			KCl					Mg	Na		
Ap	0-25	4.98	4.25	4.70	2.87	19.77	2.520	0.880	0.064	0.212	3.676
Bw1	25-41	4.57	4.27	4.42	0.89	12.42	0.274	0.111	0.048	0.141	0.574
BE	41-56	4.45	3.89	4.14	0.38	10.24	0.399	0.239	0.045	0.218	0.901
2Bx1	56-66	4.51	3.87	4.18	0.35	8.63	0.424	0.222	0.050	0.196	0.892
2Bx2	66+	4.50	3.81	4.19	0.21	6.68	0.324	0.206	0.040	0.170	0.740

EHDP2

Hor.	Depth	H ₂ O	pH	CaCl ₂	O.C.	Ex Acid	Ca	CEC		K	Sum Bases
			KCl					Mg	Na		
Ap	0-25	4.60	3.79	4.00	2.61	17.37	0.006	0.130	0.068	0.309	0.513
Bw1	25-38	4.67	3.88	3.92	0.48	8.74	0.004	0.058	0.050	0.226	0.338
Bw2	38-50	4.89	3.80	3.39	0.24	7.68	0.006	0.119	0.066	0.297	0.488
BE	50-78	5.21	4.01	4.31	0.17	5.81	0.549	0.366	0.059	0.463	1.439
2BCx	78-108	5.23	3.94	4.30	0.13	5.17	0.019	0.531	0.071	0.443	1.064
3BCm	108+	5.20	3.90	4.35	0.13	5.17	0.024	0.777	0.055	0.372	1.228

EHDP3

Hor.	Depth	H ₂ O	pH		O.C.	Ex Acid	Ca	CEC		K	Sum Bases
			KCl	CaCl ₂				Mg	Na		
Ap	0-24	4.18	3.91	3.99	3.10	20.90	0.006	0.123	0.107	0.382	0.618
Bw1	24-37	4.67	4.03	4.10	0.51	9.26	0.003	0.062	0.074	0.303	0.442
Bw2	37-63	4.86	3.99	4.16	0.32	8.72	0.002	0.095	0.072	0.436	0.605
2BCd	63-96	5.03	4.29	4.49	0.17	6.30	0.001	0.082	0.053	0.240	0.376
3BCm	96-138	5.05	4.00	4.30	0.11	4.58	0.701	0.658	0.057	0.336	1.752
4Cr	138+	5.20	4.42	4.67	0.16	2.85	0.010	0.239	0.054	0.274	0.577

BHP

Hor.	Depth	H ₂ O	pH		O.C.	Ex Acid	Ca	CEC		K	Sum Bases
			KCl	CaCl ₂				Mg	Na		
Ap	0-20	4.29	3.91	4.02	3.33	16.54	0.540	0.177	0.018	0.053	0.698
Bw1	20-36	4.61	4.20	4.49	1.15	9.31	0.374	0.090	0.047	0.047	0.558
Bw2	36-48	4.48	4.38	4.54	0.76	6.95	0.399	0.049	0.061	0.045	0.554
BE	48-58	4.79	4.35	4.61	0.46	5.37	0.324	0.045	0.045	0.045	0.459
2Btx1	58-74	4.84	4.38	4.90	0.25	4.67	0.250	0.049	0.040	0.054	0.393
2Btx2	74+	5.11	4.07	4.65	0.15	5.07	1.347	0.045	0.068	0.081	1.541

BHW

Hor.	Depth	H ₂ O	pH		O.C.	Ex Acid	Ca	CEC		K	Sum Bases
			KCl	CaCl ₂				Mg	Na		
Ap	0-20	4.67	4.02	4.29	1.93	10.66	0.524	0.107	0.077	0.083	0.791
Bw1	20-30	5.00	4.23	4.31	0.92	7.80	1.198	0.095	0.065	0.071	1.429
Bw2	30-48	5.21	4.24	4.72	0.61	6.62	1.073	0.099	0.053	0.061	1.286
2Bx1	48-61	5.09	4.21	4.99	0.24	2.38	0.549	0.053	0.046	0.078	0.726
2Bx2	61+	5.25	4.17	4.68	0.18	2.42	1.023	0.123	0.057	0.123	1.326
BPF		5.40	4.19	4.95	0.17	3.80	2.171	0.358	0.074	0.167	2.770

BHR

Hor.	Depth	H ₂ O	pH		O.C.	Ex Acid	Ca	CEC		K	Sum Bases
			KCl	CaCl ₂				Mg	Na		
A	3-11	4.12	3.88	3.89	4.66	19.60	0.424	0.239	0.084	0.160	0.907
Bw	11-28	4.42	4.14	4.61	0.92	8.51	0.424	0.086	0.062	0.037	0.609
Bx1	28-46	4.69	3.81	4.32	0.15	3.70	1.572	0.317	0.046	0.048	1.983
Bx2	46+	5.04	3.94	4.73	0.09	2.44	2.246	0.411	0.051	0.075	2.783
BPF		5.20	3.90	4.81	0.11	2.99	3.792	0.823	0.059	0.897	5.571

OHW

Hor.	Depth	H ₂ O	pH		O.C.	Ex Acid	Ca	CEC		K	Sum Bases
			KCl	CaCl ₂				Mg	Na		
Ap	0-31	5.29	4.77	5.15	2.32	11.43	1.145	0.596	0.035	0.126	1.902
Bw1	31-53	5.35	4.37	4.98	0.59	4.50	1.240	0.884	0.030	0.120	2.274
Bw2	53-74	5.40	4.40	5.13	0.32	4.73	1.250	0.819	0.035	0.129	2.233
BE	74-94	5.49	4.54	5.11	0.48	5.92	1.205	0.753	0.045	0.248	2.251
2Btx1a	94-107	5.38	4.22	4.99	0.21	4.28	1.654	0.901	0.027	0.123	2.705
2Btx1b	107-122	5.20	4.19	4.89	0.20	3.33	1.609	0.946	0.023	0.117	2.695
2Btx2a	122-137	5.12	4.11	4.80	0.16	3.72	1.722	0.905	0.009	0.110	2.746
2Btx2b	137+	5.20	4.10	4.89	0.15	3.58	1.786	1.041	0.013	0.118	2.958

OHL

Hor.	Depth	H ₂ O	pH		O.C.	Ex Acid	Ca	CEC		K	Sum Bases
			KCl	CaCl ₂				Mg	Na		
Ap	0-21	3.87	3.72	3.76	5.66	20.81	0.372	0.062	0.064	0.142	0.640
Bw	21-40	4.67	3.92	4.10	1.37	7.51	0.721	0.119	0.066	0.069	0.975
Bg1	40-52	5.01	3.69	4.29	0.39	4.66	0.871	0.564	0.065	0.121	2.621
Bg2	52-76	5.08	3.94	4.40	0.20	2.38	0.392	0.366	0.059	0.098	1.915
2Bw	76-90	5.41	4.43	4.80	0.13	1.85	0.918	0.206	0.056	0.077	1.257
2BCm	90-102	5.63	--	5.18	0.09	2.16	1.043	0.288	0.052	0.062	1.445
3Cd1	102-144	5.60	4.21	4.87	0.11	1.69	2.131	0.502	0.056	0.083	2.772
3Cd2	144-160	5.76	4.43	5.12	0.04	2.73	2.191	0.473	0.053	0.059	2.776
3Cd3	160-175	5.87	4.44	5.12	0.16	1.63	1.859	0.391	0.053	0.047	2.350
4Cm	175-187	5.79	4.40	5.07	0.05	2.02	2.211	0.477	0.053	0.059	2.800
5Cd4	187-220	5.90	4.59	5.16	0.07	1.63	1.889	0.420	0.048	0.029	2.386
5Cd5	220+	5.83	4.60	5.20	0.33	0.41	1.001	0.259	0.056	0.035	1.351

BTR/S

Hor.	Depth	H ₂ O	pH		O.C.	Ex Acid	Ca	CEC		K	Sum Bases
			KCl	CaCl ₂				Mg	Na		
Ap	0-18	6.61	6.19	6.26	2.77	5.33	2.141	1.024	0.024	0.121	3.314
Bw1	18-46	6.64	5.92	6.23	0.94	2.50	--	--	--	--	--
Bw2	46-71	6.39	5.60	5.90	0.28	2.22	0.439	0.280	0.010	0.044	0.773
2BE a	71-81	6.17	5.40	5.69	0.21	1.56	0.242	0.185	0.003	0.034	0.464
2BE b	81-91	6.00	5.19	5.58	0.19	1.66	0.202	0.140	0.007	0.047	0.396
2Bxt1a	91-102	5.93	4.80	5.49	0.12	1.78	0.367	0.160	0.016	0.079	0.622
2Bxt1b	102+	5.99	4.71	5.60	0.07	1.21	0.644	0.296	0.011	0.067	1.018
BPF	85	5.87	4.76	5.50	0.09	0.65	0.744	0.259	0.002	0.060	1.065

BTR

Hor.	Depth	H ₂ O	pH	CaCl ₂	O.C.	Ex Acid	Ca	CEC		K	Sum Bases
			KCl					Mg	Na		
2Btx1a	91	6.03	4.38	5.46	0.07	0.58	2.021	0.843	0.048	0.096	3.008
2Btx1b	107	6.09	4.34	5.50	0.06	1.11	1.996	0.769	0.047	0.077	2.889
2Btx2a	122	6.00	4.30	5.80	0.05	1.28	2.420	0.979	0.074	0.097	3.570
2Btx2b	137	6.02	4.49	5.51	0.05	0.71	1.347	0.522	0.039	0.060	1.968
BPF	115	5.19	4.41	5.35	0.06	1.95	1.297	0.485	0.071	0.092	1.945

Till Sites

Upper Till

Sample	HOH	pH KCl	CaCl2	O.C.	Ex. Acid	Ca	Mg	CEC Na	K	Total CEC
<u>LTD</u>										
UT1	5.58	4.30	4.82	0.08	1.67	0.090	0.012	0.054	0.152	1.978
UT2	5.53	4.22	4.80	0.05	2.10	0.047	0.012	0.063	0.139	2.361
UT3	5.49	4.18	4.79	0.11	2.83	0.798	0.062	0.041	0.152	3.883
UT4	5.42	4.17	4.72	0.22	5.74	0.047	0.016	0.036	0.111	5.950
UT5	5.34	4.28	4.66	0.27	8.00	0.025	0.016	0.046	0.148	8.235
<u>AY</u>										
UT1	5.45	4.20	5.20	0.09	0.51	4.012	0.975	0.062	0.331	5.890
UT2	5.72	4.42	5.80	0.16	1.53	0.225	0.037	0.051	0.121	1.964
UT3	5.86	4.31	4.88	0.10	2.08	0.398	0.169	0.123	0.119	2.889
UT4	6.04	4.24	5.50	0.08	0.98	1.240	0.284	0.089	0.072	2.665
UT5	6.16	4.40	5.24	0.08	1.51	0.534	0.378	0.087	0.072	2.581
<u>BA</u>										
UT1	5.13	4.13	4.80	0.29	1.02	1.435	1.143	0.069	0.345	4.012
UT2	3.84	3.58	3.71	0.38	1.87	0.873	0.345	0.025	0.123	3.236
<u>CH</u>										
CH UTA	5.13	4.45	5.10	0.12	1.10	0.063	0.021	0.009	0.006	1.199
CH UTB	6.06	4.62	6.23	0.10	0.45	0.354	0.230	0.014	0.005	1.353
CH UTC	6.37	4.59	6.38	0.11	0.14	0.726	0.413	0.012	0.005	1.300

Oxidized Lower Till

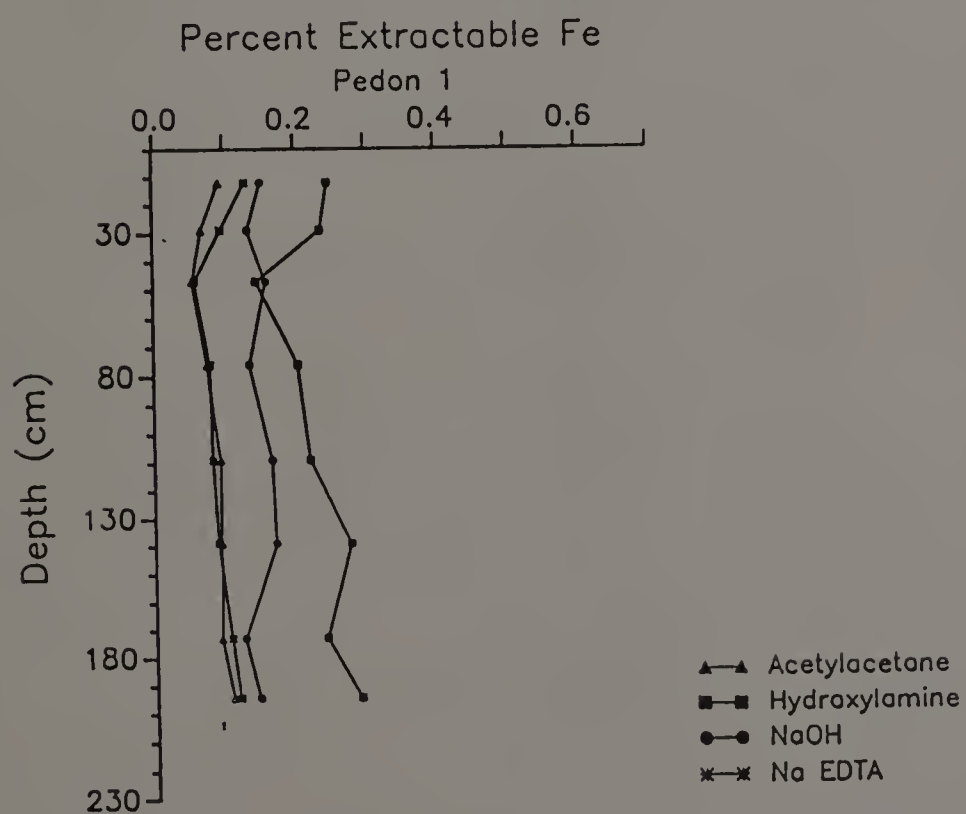
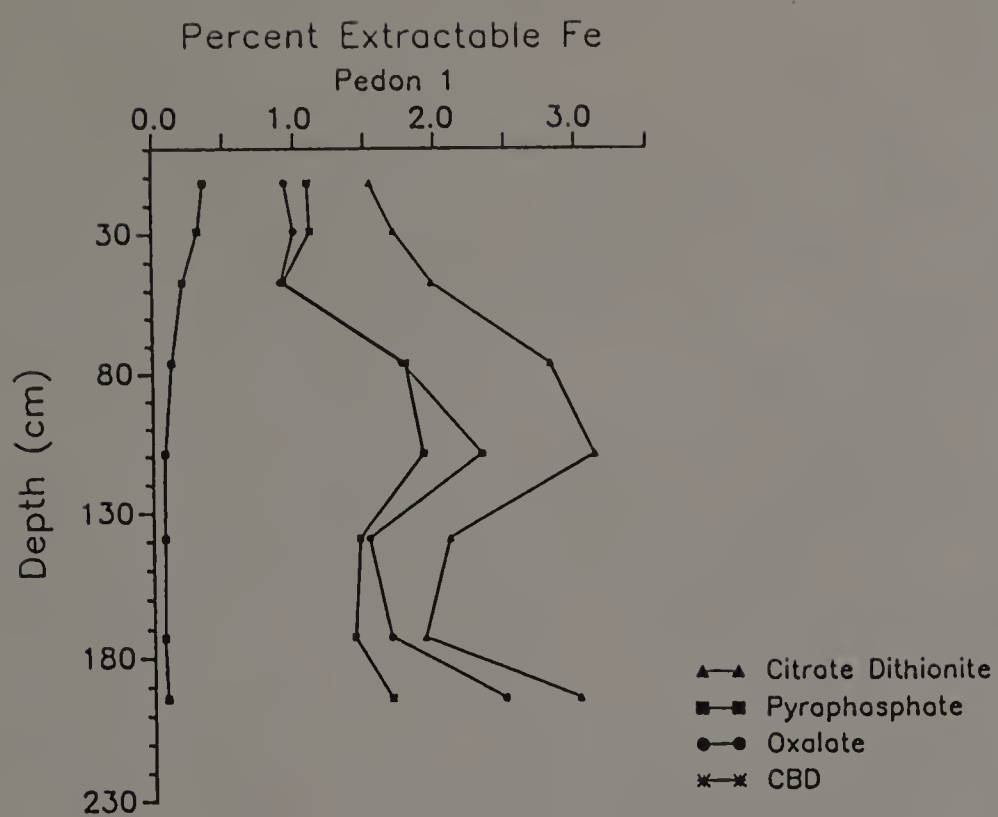
Sample	HOH	pH KCl	CaCl2	O.C.	Ex. Acid	Ca	Mg	CEC Na	K	Total CEC
<u>LTD</u>										
OT1	6.63	4.53	5.40	0.16	1.45	3.962	0.798	0.069	0.258	6.537
OT2	6.94	4.39	5.60	0.07	1.47	3.121	0.767	0.078	0.228	5.664
OT3	6.87	4.47	5.75	0.06	1.63	3.548	0.843	0.090	0.223	6.334
OT4	6.98	4.01	5.72	0.14	2.83	4.835	0.629	0.124	0.243	8.661
OT5	6.62	4.06	5.63	0.09	2.95	5.082	0.498	0.116	0.250	8.896
<u>AY</u>										
OT1	6.72	4.51	5.96	0.09	2.28	2.565	0.847	0.043	0.236	5.971
OT2	6.43	4.42	5.65	0.09	1.47	2.557	0.823	0.034	0.309	5.193
OT3	6.90	4.62	6.16	0.08	1.20	2.507	0.913	0.037	0.132	4.789
OT4	7.18	5.00	6.45	0.09	0.45	2.727	1.538	0.062	0.286	5.063
OT5	6.82	4.49	6.01	0.08	0.00	2.490	1.016	0.068	0.187	3.761
<u>BA</u>										
OT1	5.70	4.18	5.24	--	3.71	2.692	1.279	0.059	0.219	7.959
OT2	--	--	--	0.24	3.62	0.973	0.979	0.047	0.339	5.958

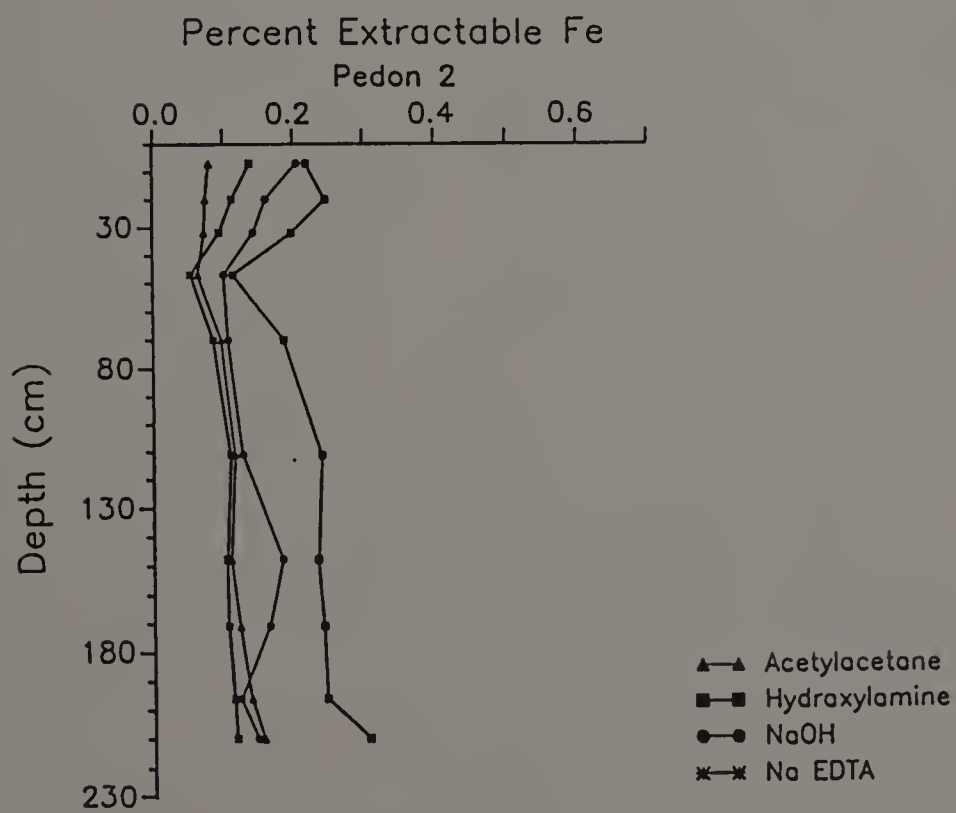
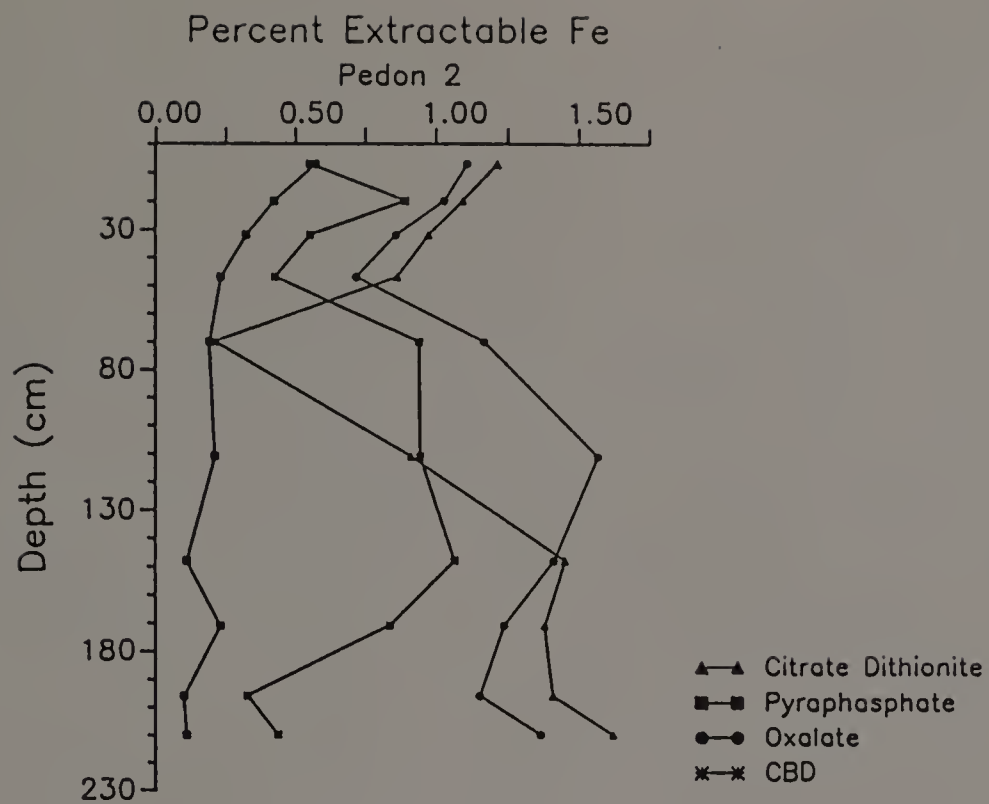
Unoxidized Lower Till

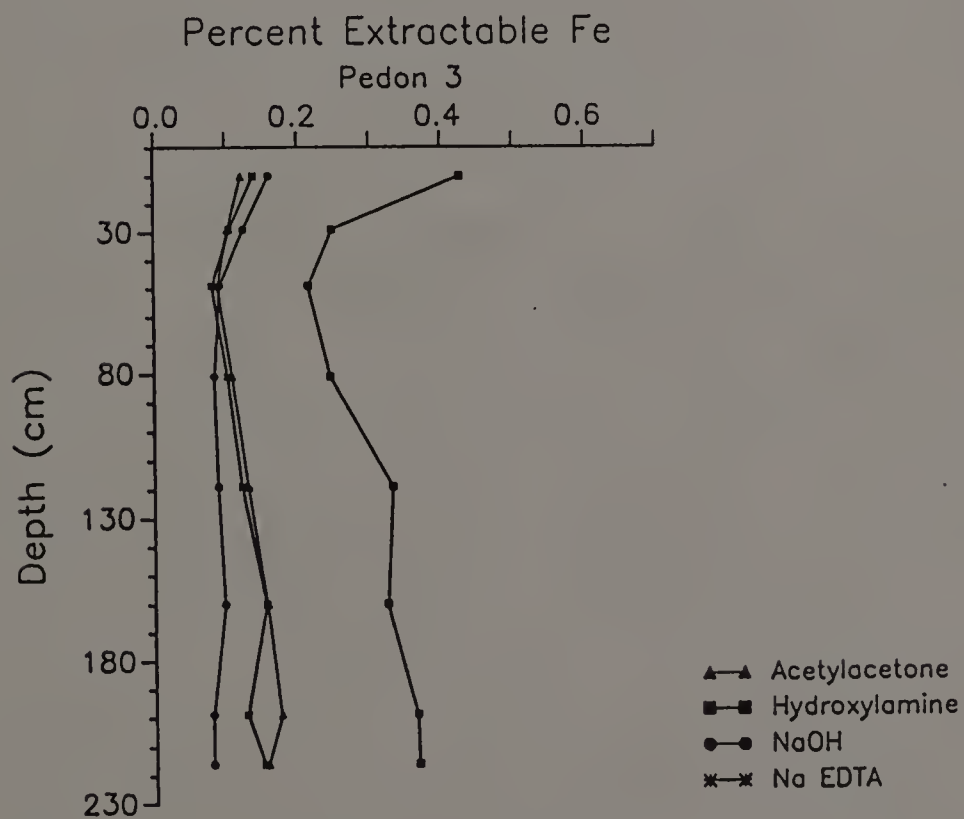
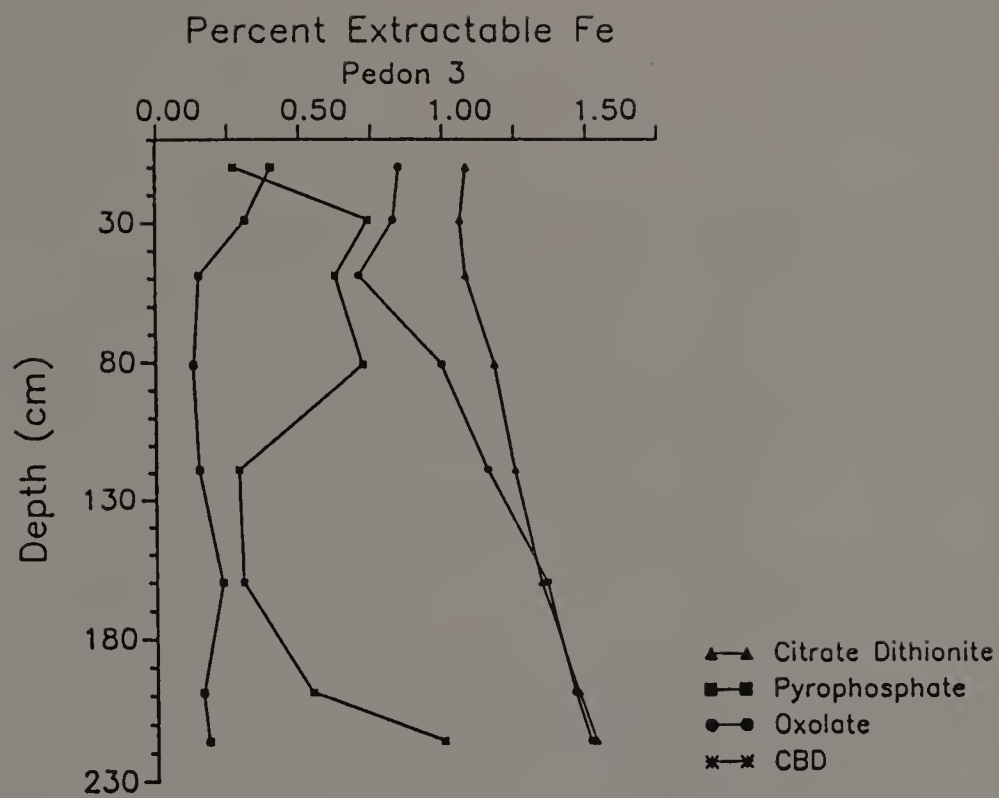
Sample	HOH	pH KCl	CaCl2	O.C.	Ex. Acid	Ca	Mg	CEC Na	K	Total CEC
<u>LTD</u>										
LT1	6.51	6.39	6.91	0.22	0.00	3.847	0.967	0.123	0.432	5.378
LT2	7.08	6.51	6.63	0.22	0.57	3.154	1.246	0.110	0.527	5.607
LT3	7.14	6.53	6.73	0.20	0.67	3.318	1.259	0.050	0.545	5.842
LT4	7.17	6.24	6.73	0.21	1.12	2.395	1.493	0.048	0.587	5.643
LT5	5.50	4.25	5.99	0.17	1.91	1.946	1.571	0.051	0.448	5.926
<u>AY</u>										
LT1	8.17	6.58	7.57	0.14	0.00	3.865	1.341	0.063	0.434	5.703
LT2	8.68	7.55	8.12	0.14	0.00	3.660	1.000	0.048	0.523	5.231
LT3	8.50	6.91	7.80	0.11	0.00	3.268	1.111	0.041	0.302	4.722
LT4A	8.63	7.55	8.15	0.14	0.00	1.589	1.177	0.046	0.120	2.932
LT4B	8.63	7.04	7.91	0.13	0.00	4.004	1.213	0.042	0.510	5.769
LT5	8.68	7.77	8.28	0.12	0.00	3.867	0.724	0.042	0.352	4.985
<u>BA</u>										
LT1	6.36	5.15	6.02	0.30	1.51	2.043	1.584	0.141	0.458	5.736
LT2	6.52	5.10	5.45	0.26	4.46	1.504	1.366	0.055	0.470	7.855
BU LT	8.01	6.83	8.02	0.30	0.0	5.539	0.506	0.054	0.329	6.428
CH LT	8.13	7.11	8.09	0.15	0.06	2.752	1.514	0.020	0.251	4.597

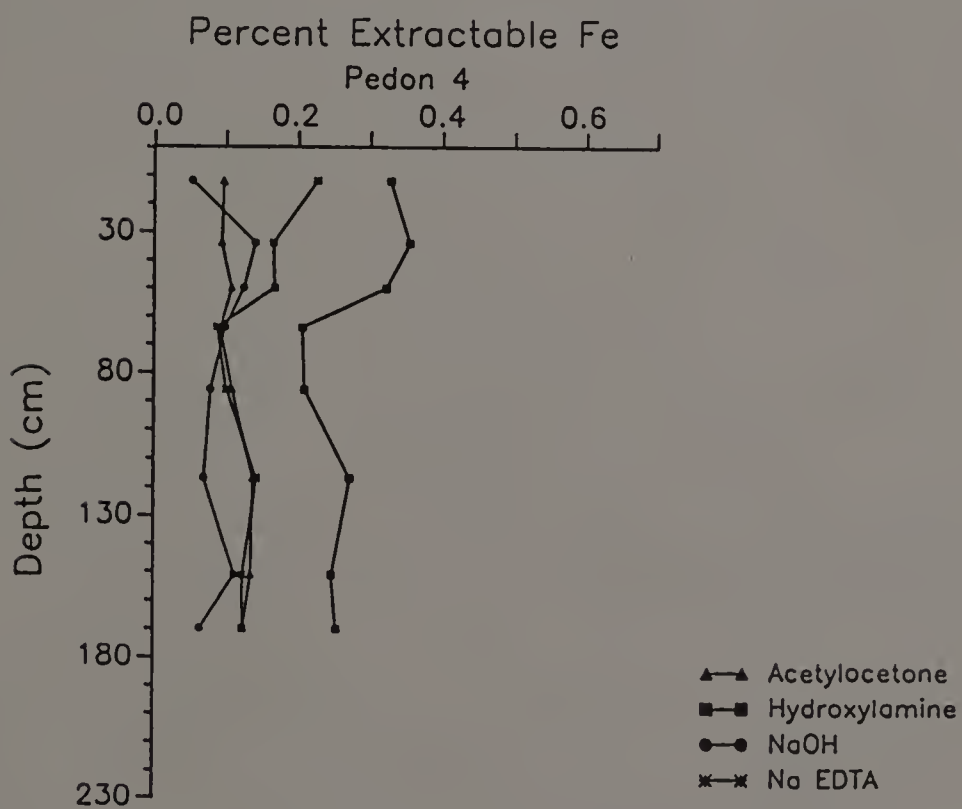
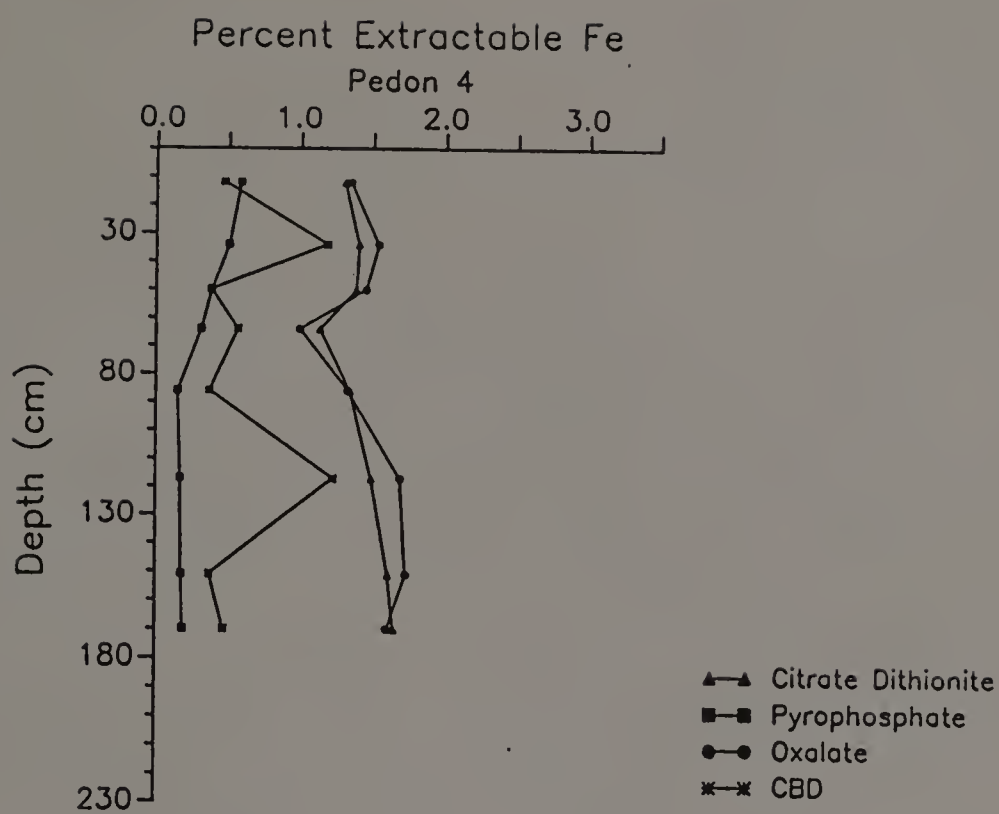
APPENDIX I
EXTRACTION GRAPHS

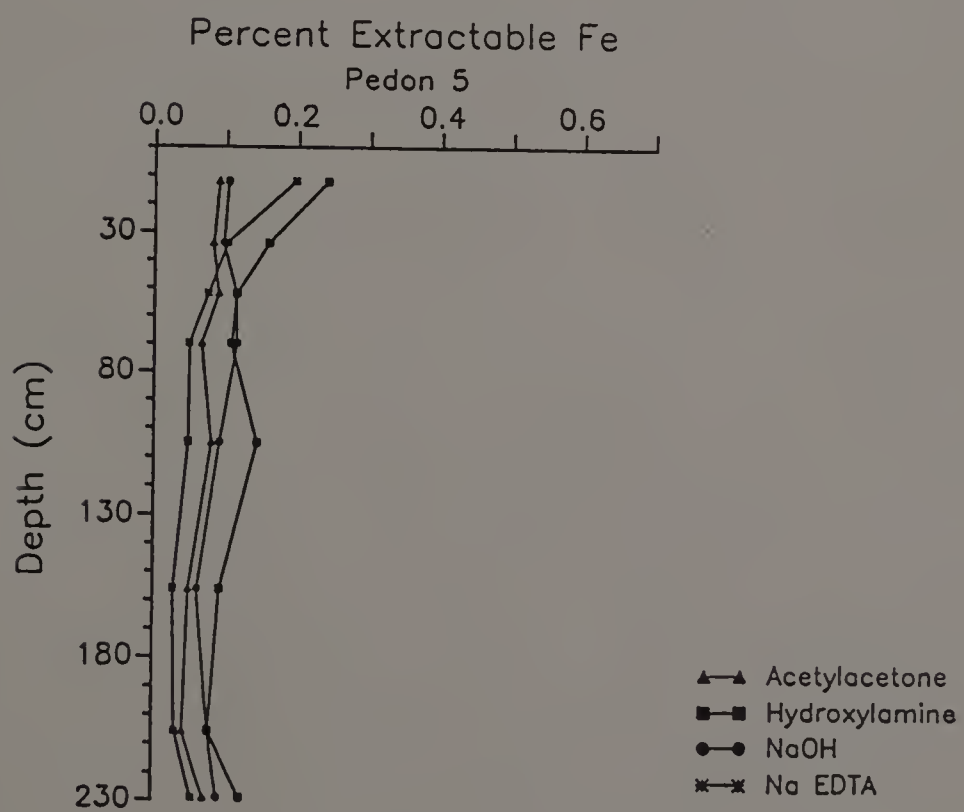
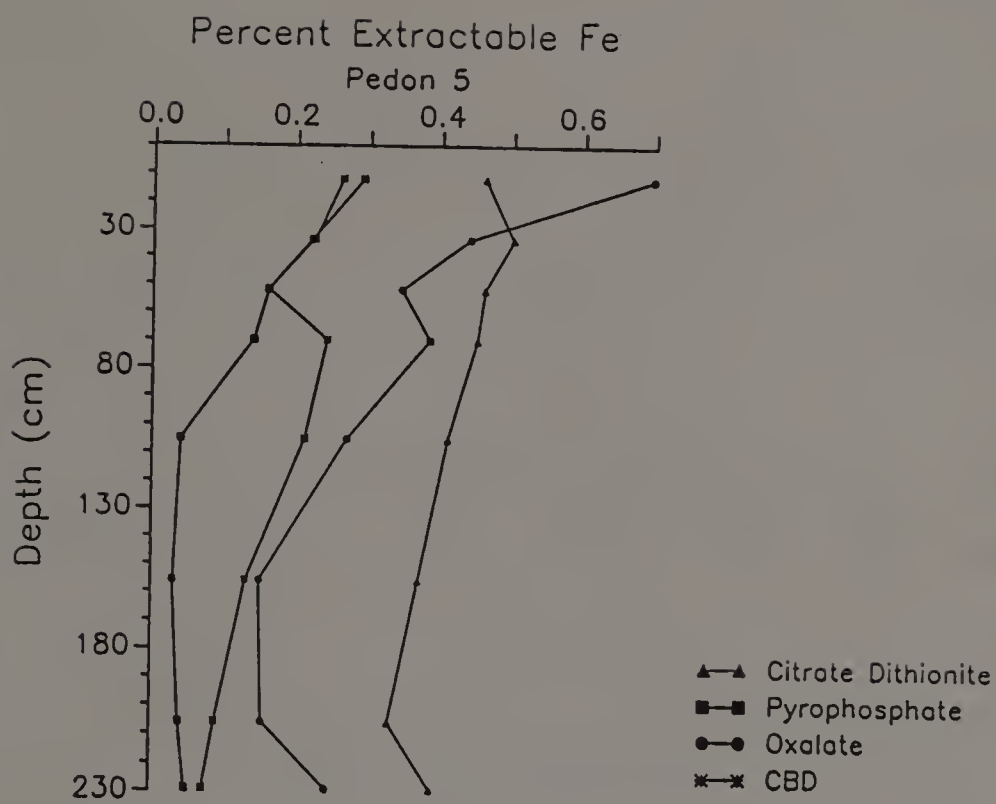
Extractable Fe Graphs



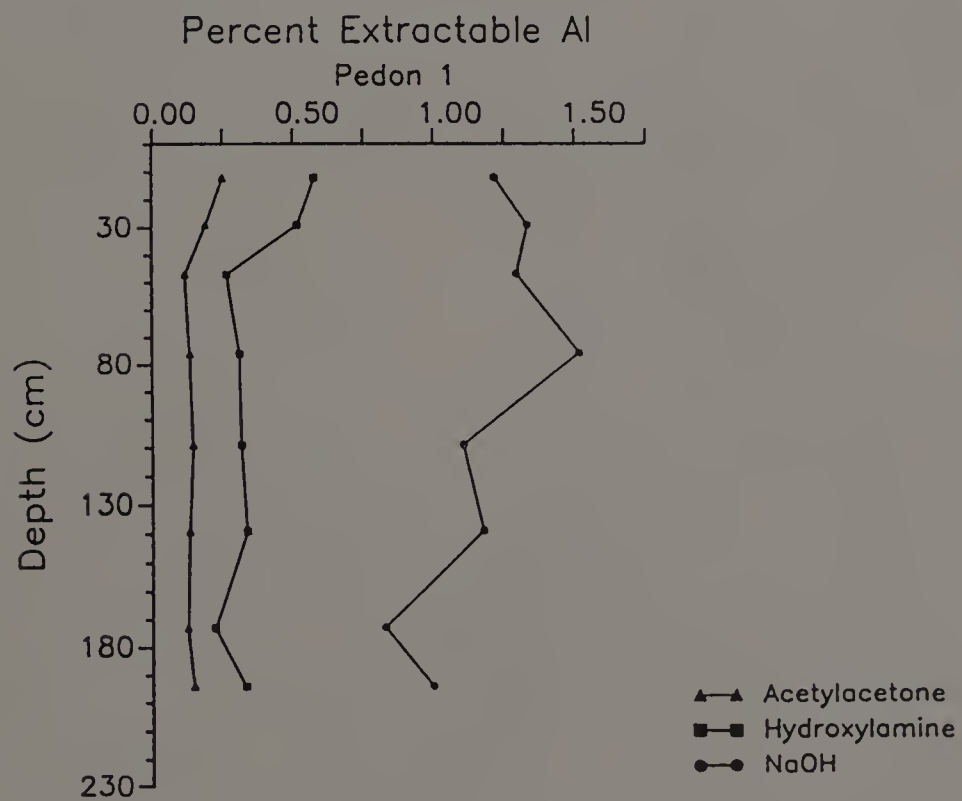
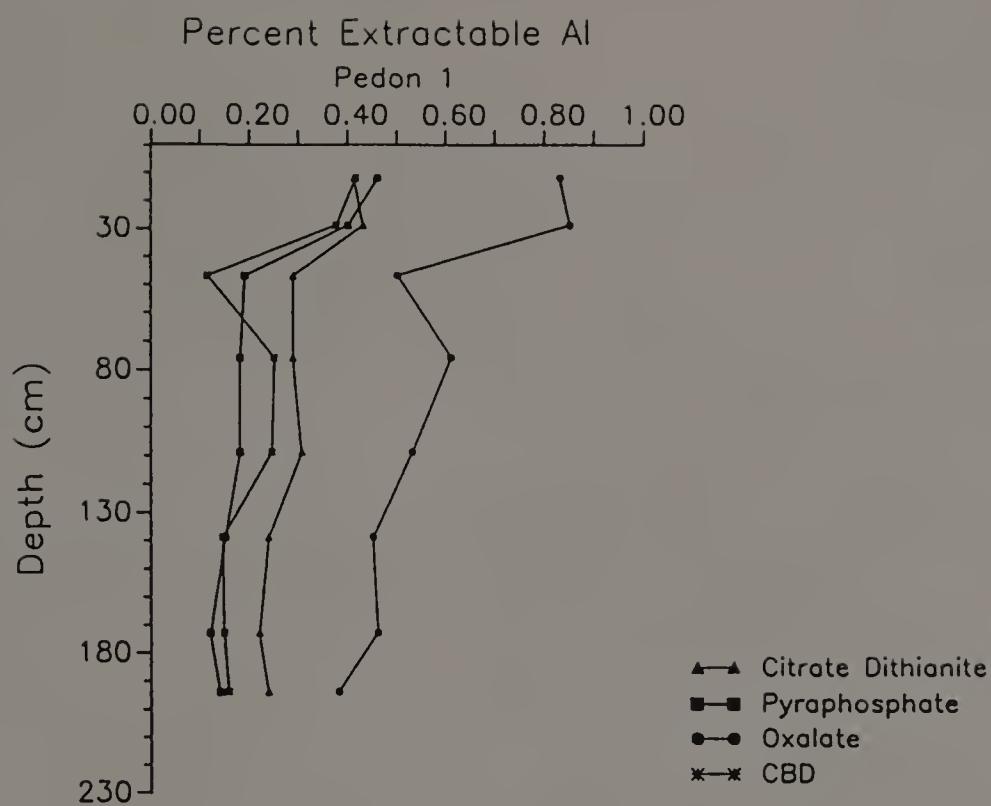


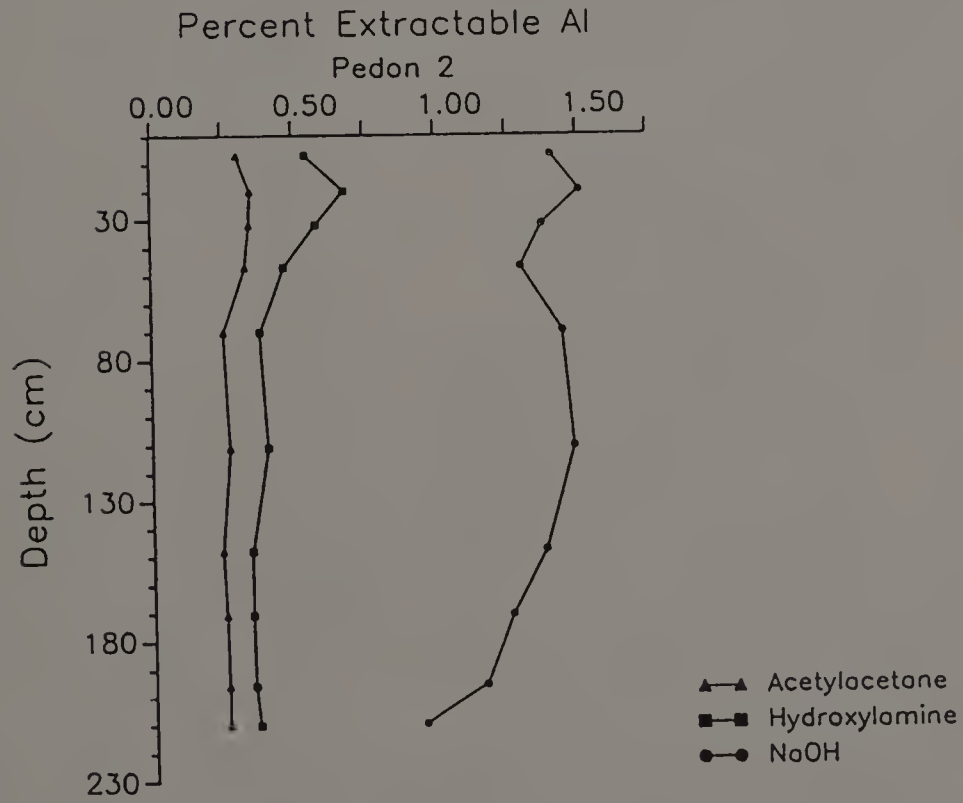
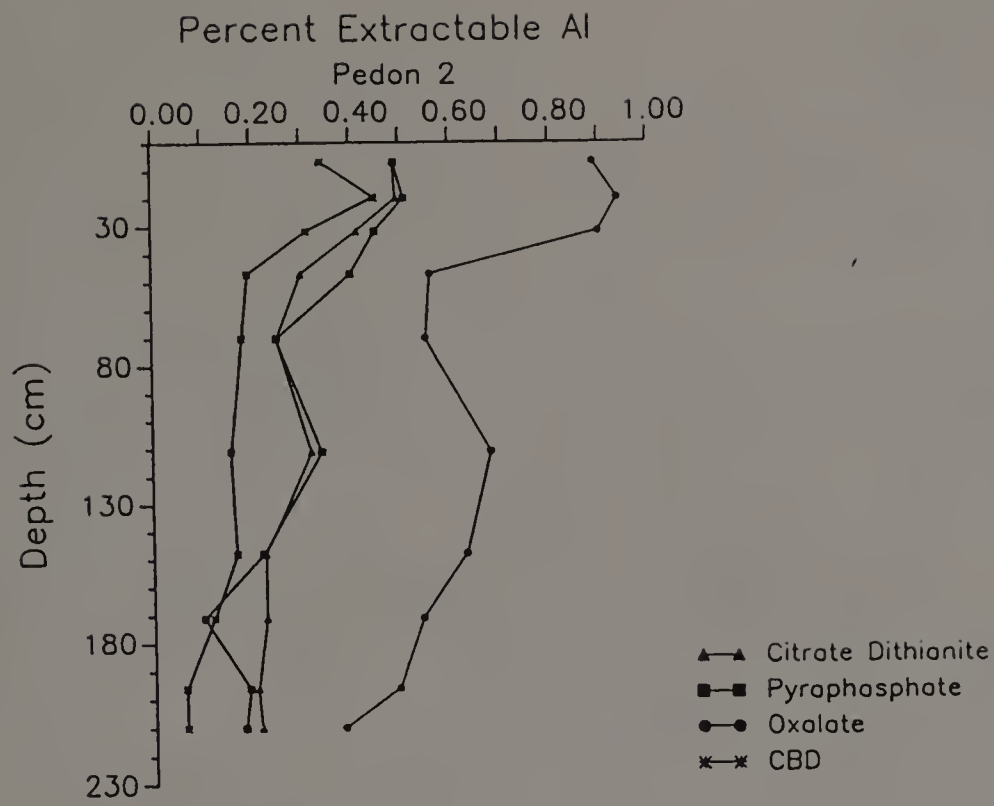


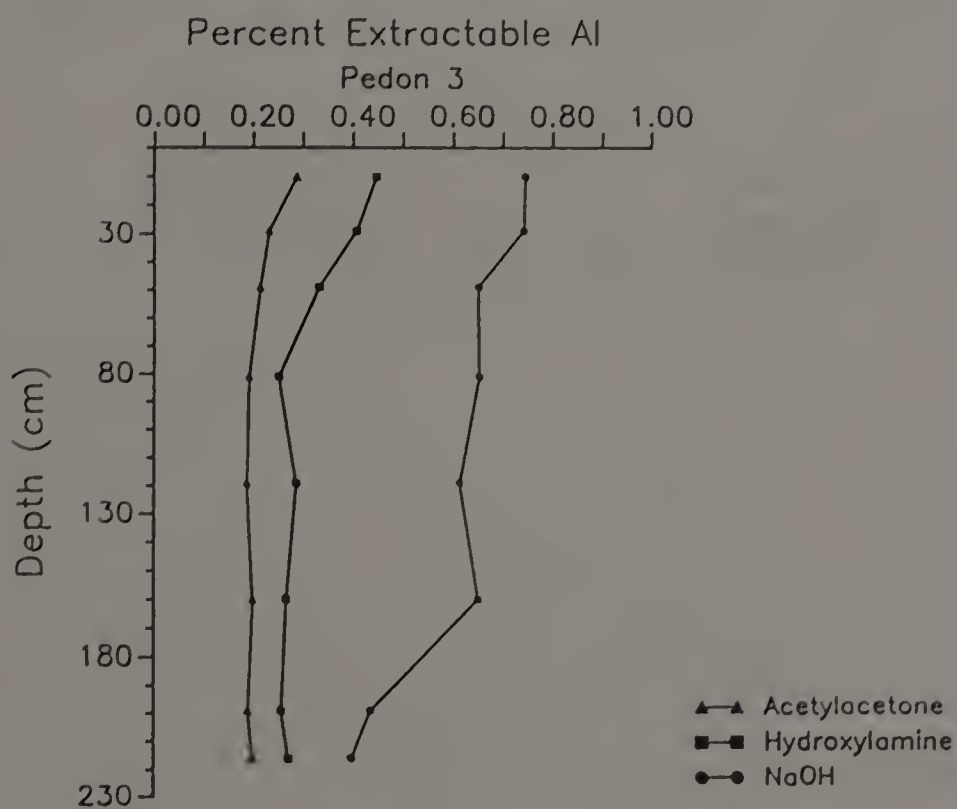
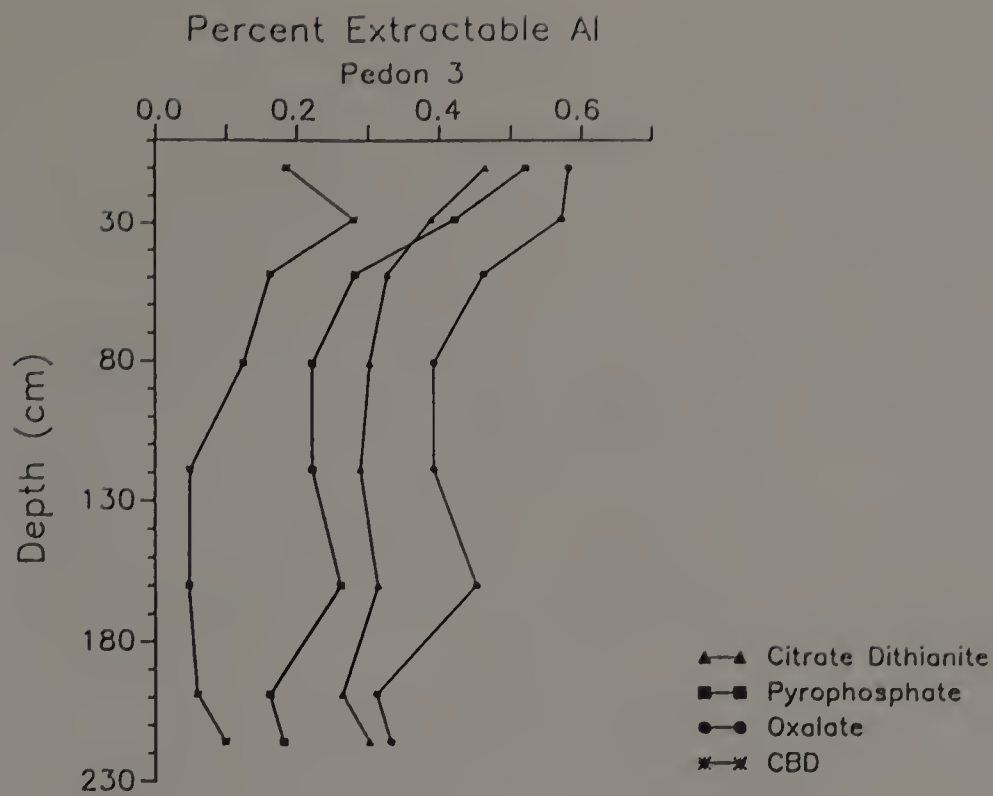


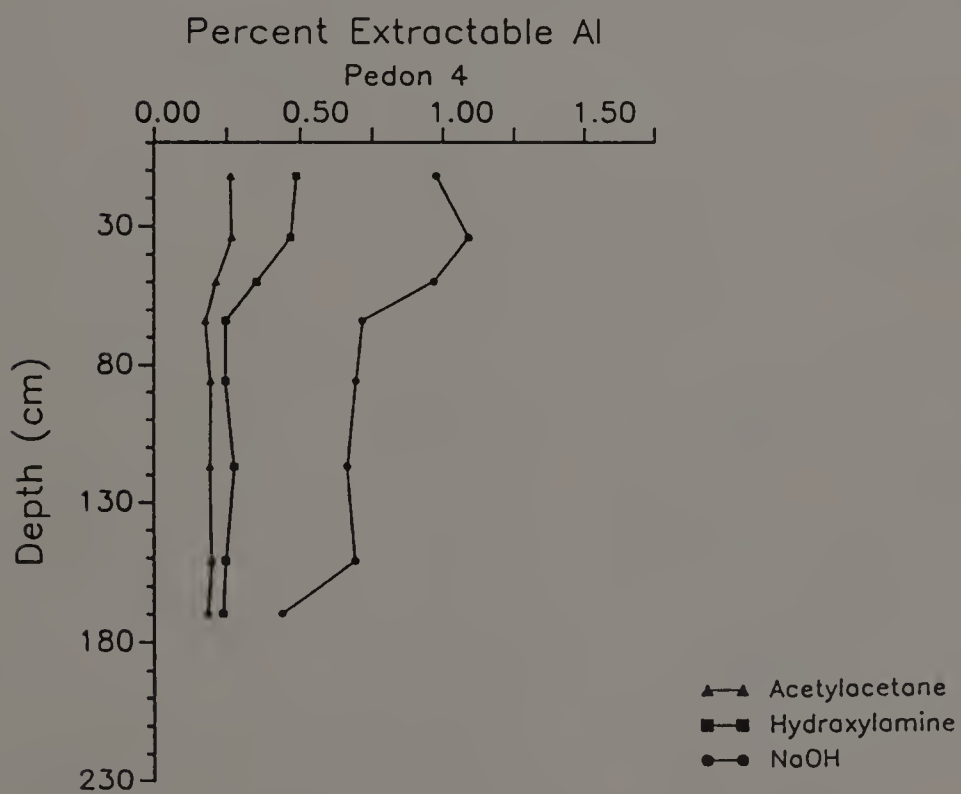
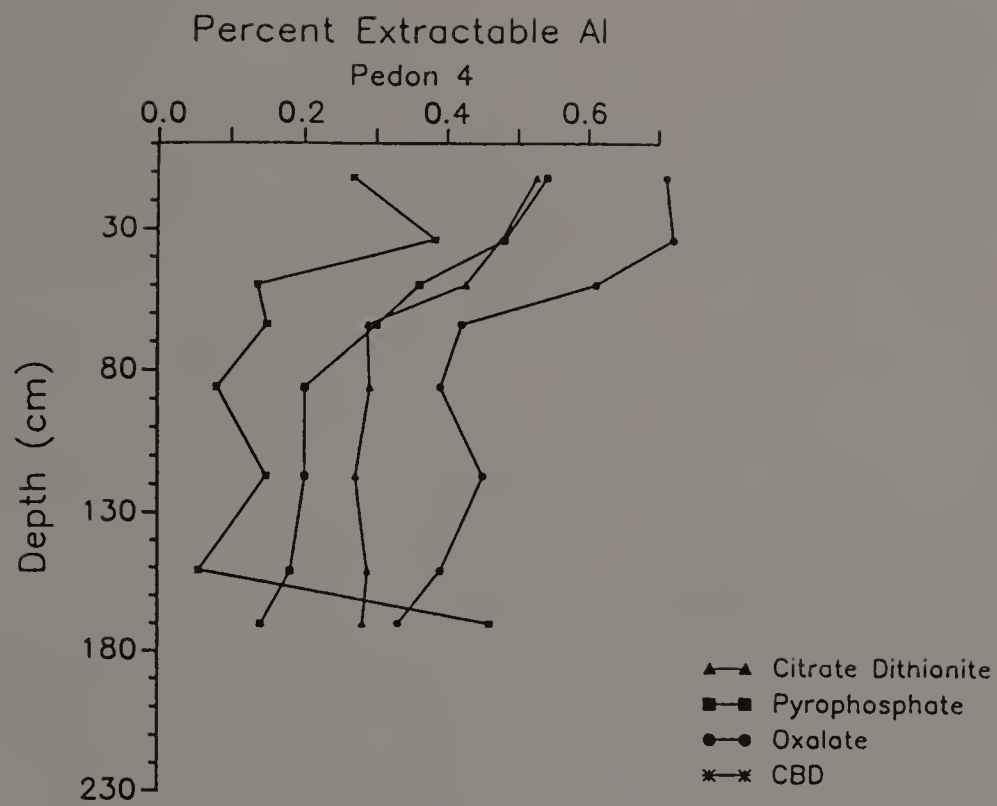


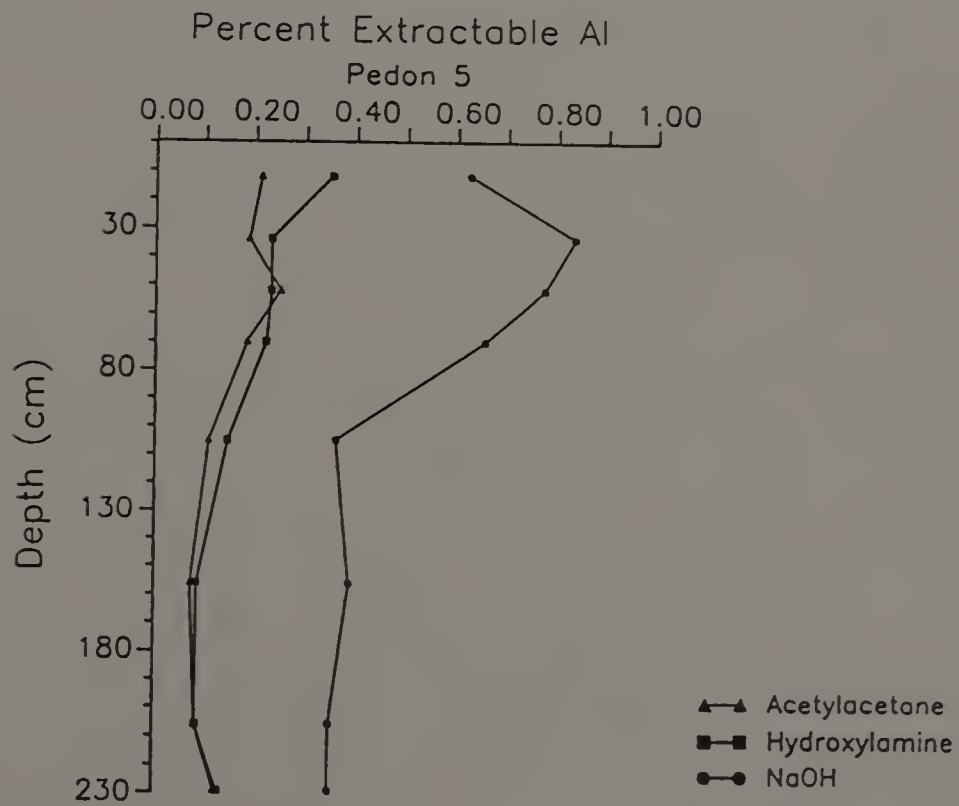
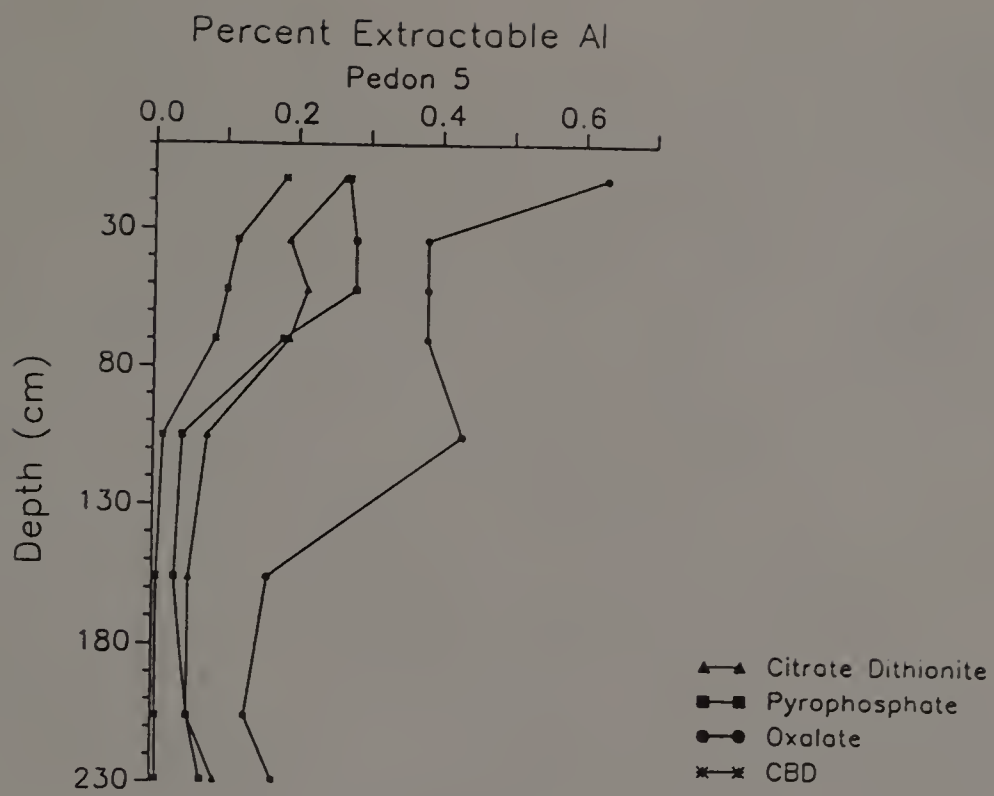
Extractable AI Graphs



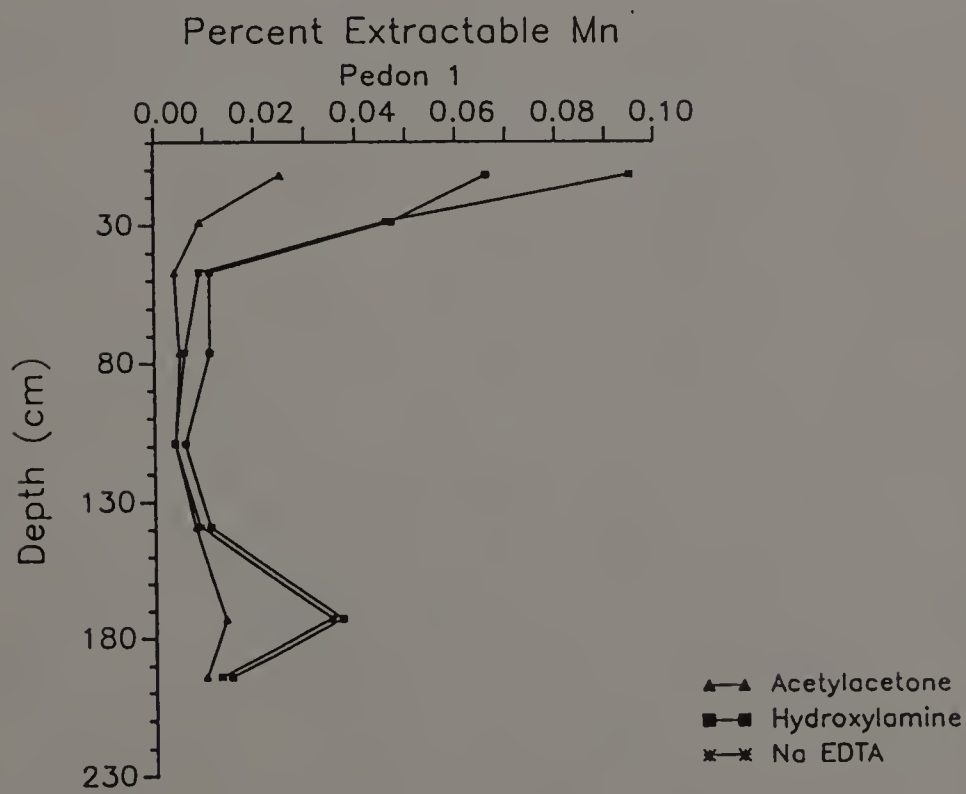
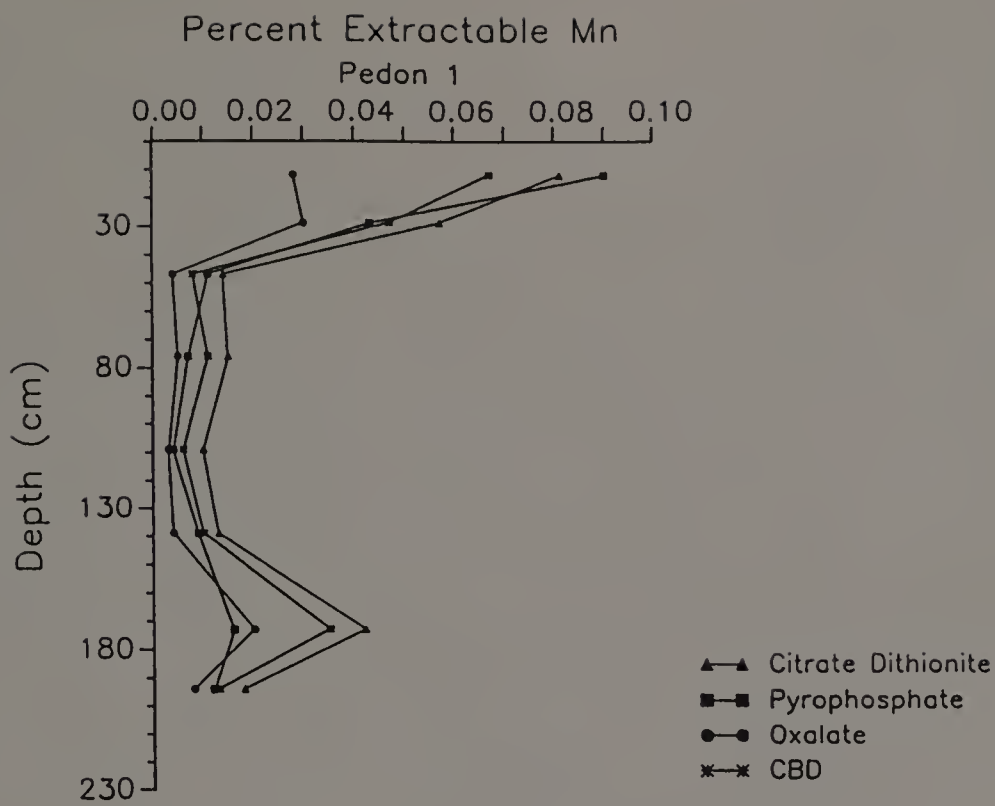


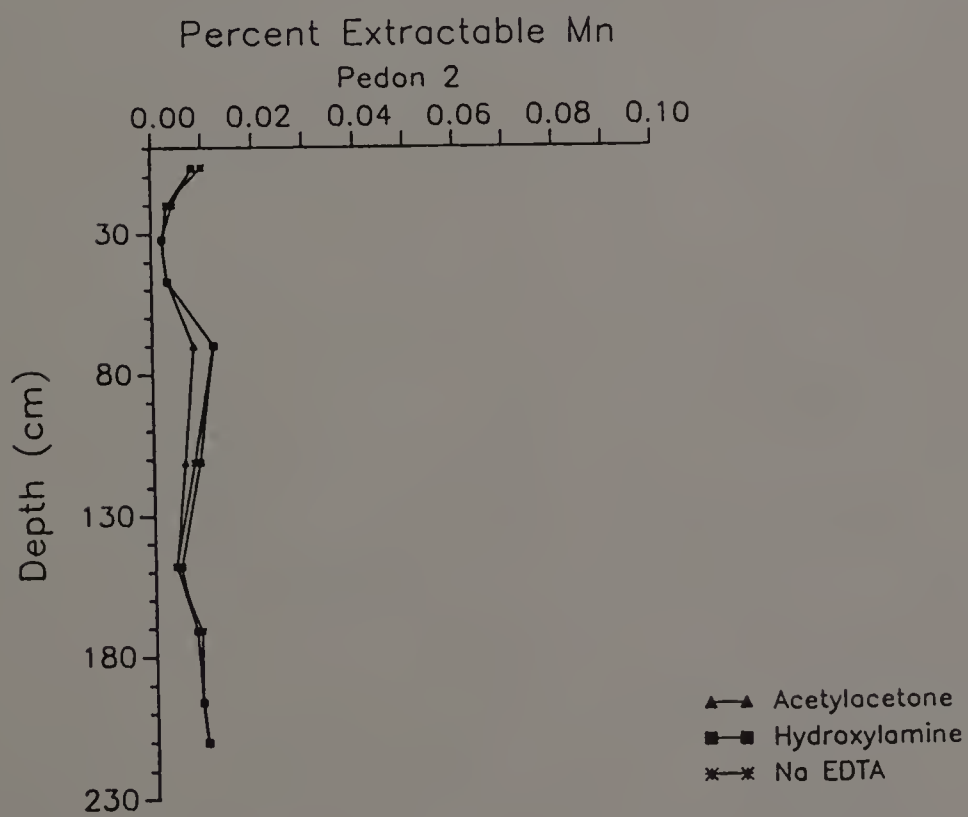
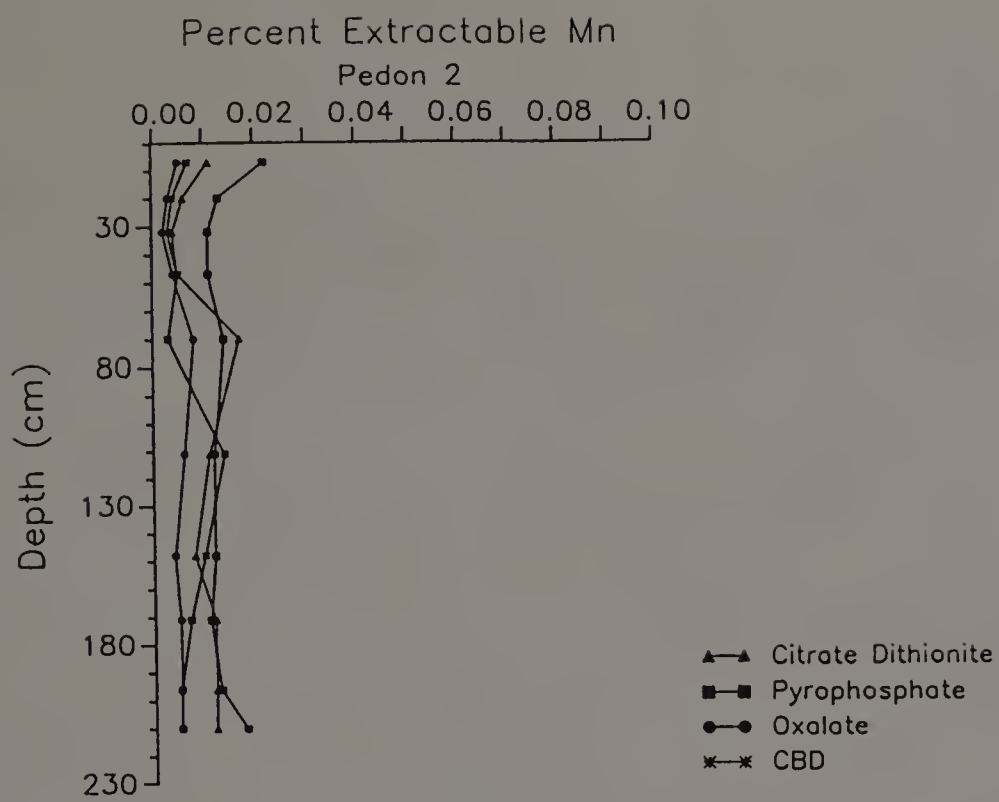


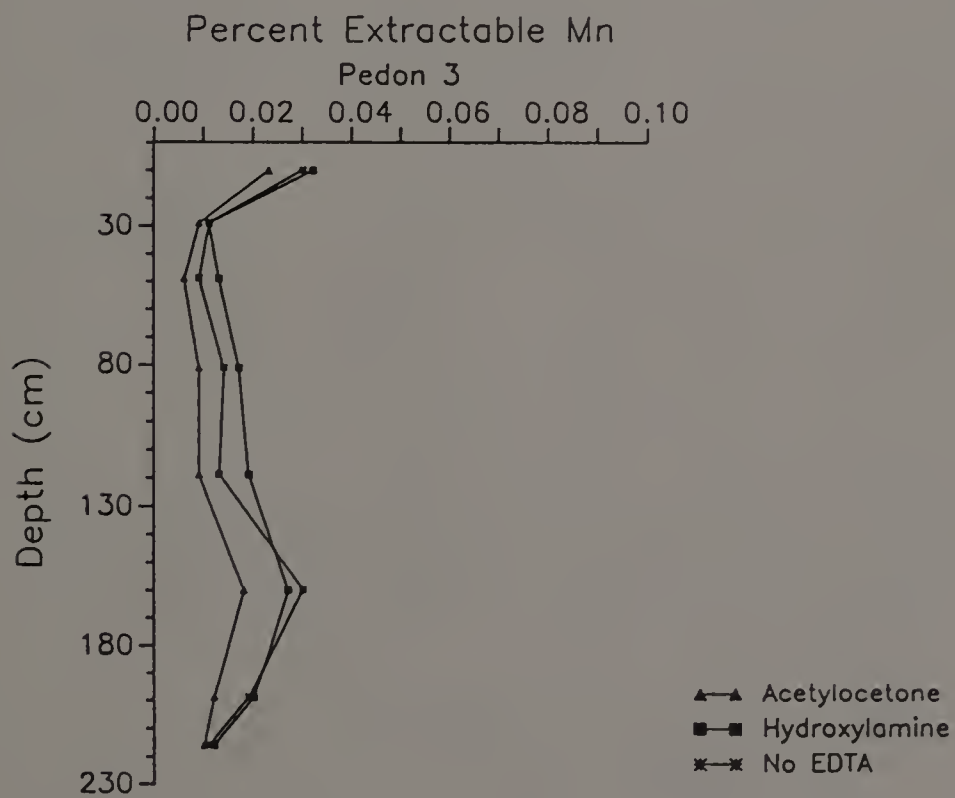
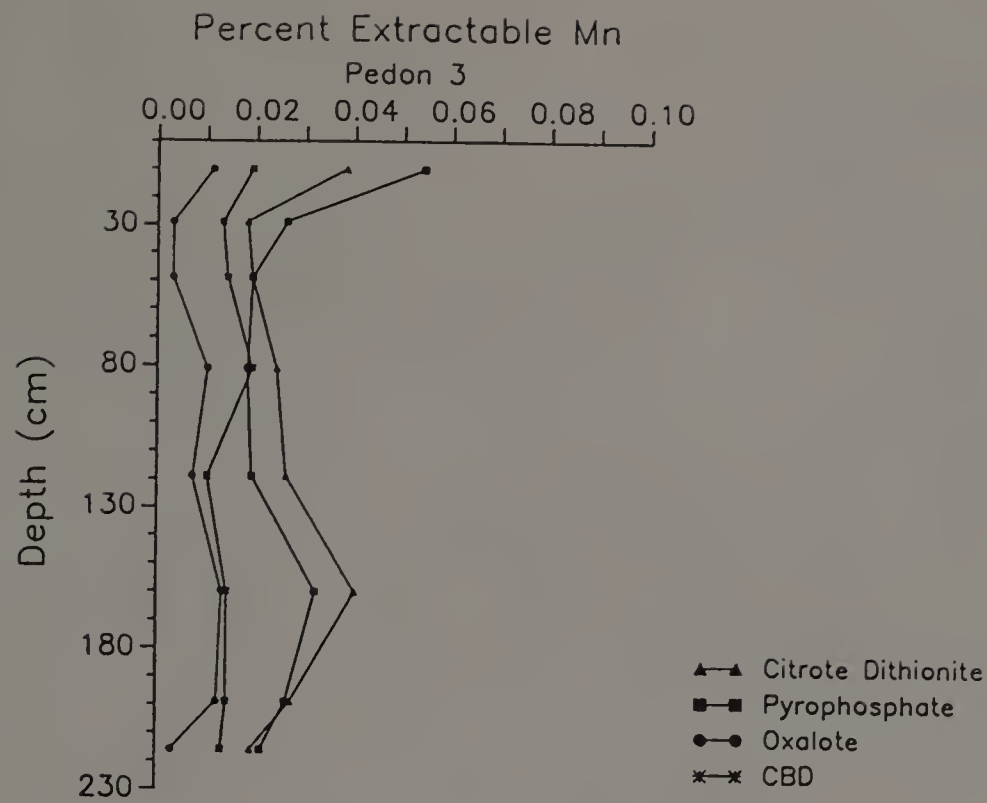


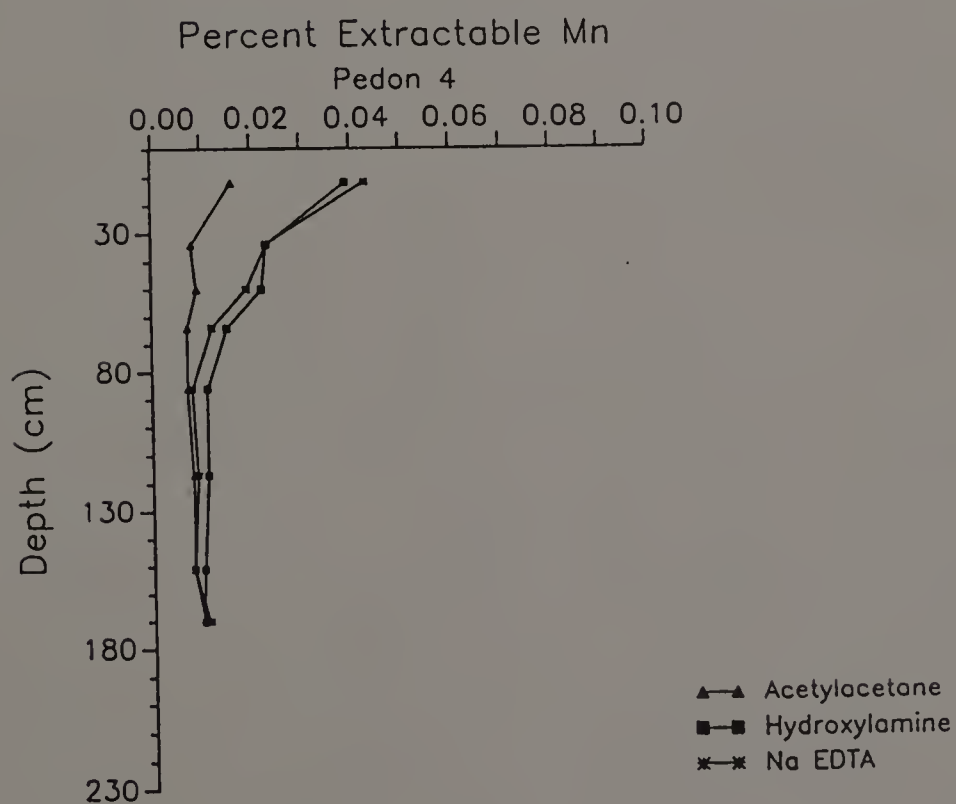
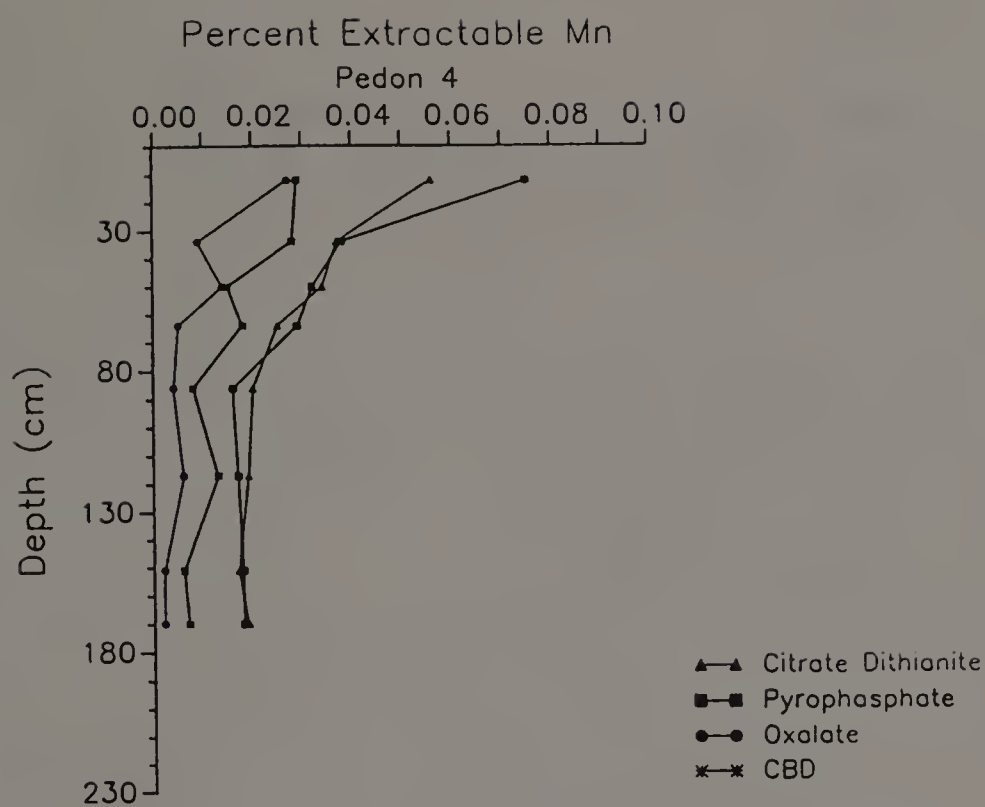


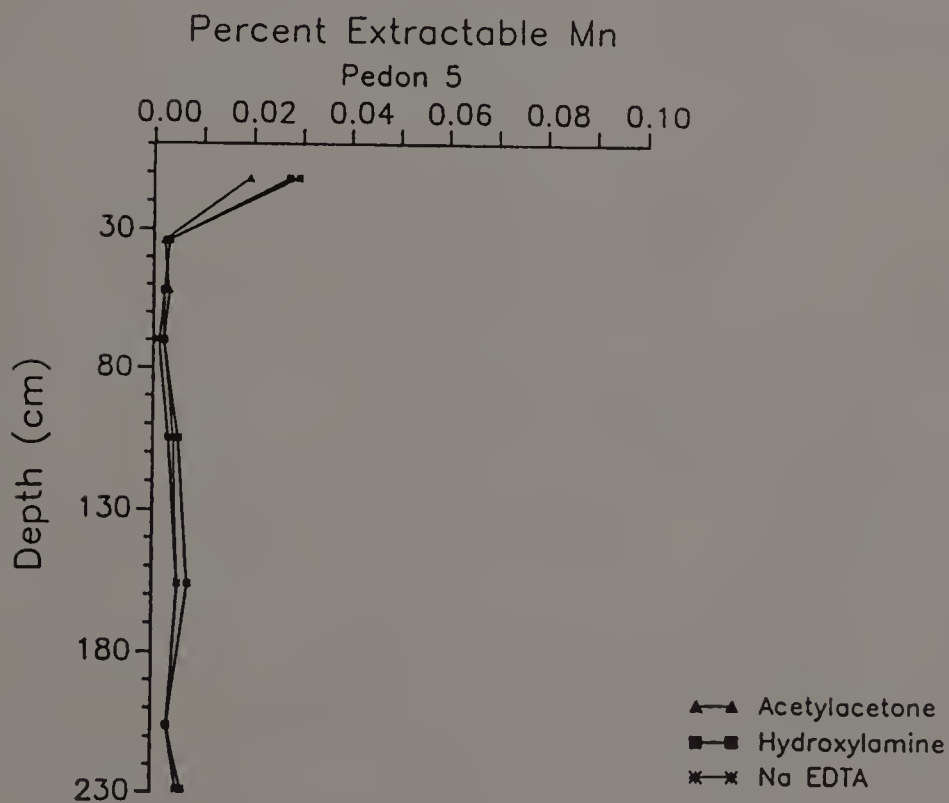
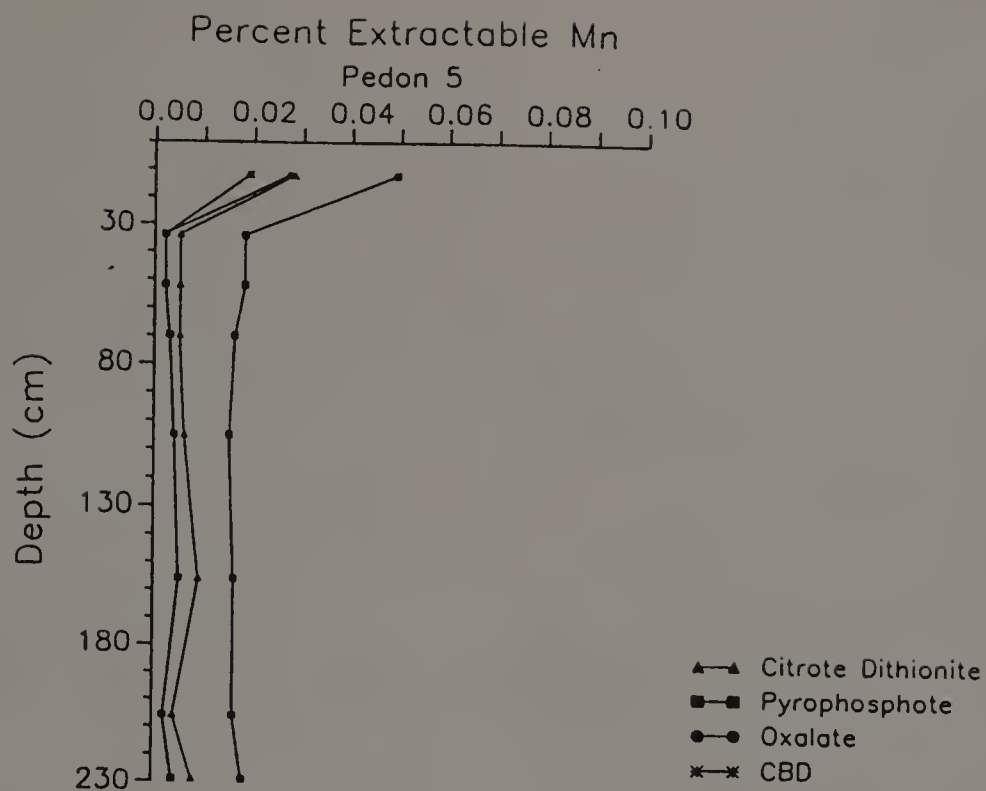
Extractable Mn Graphs



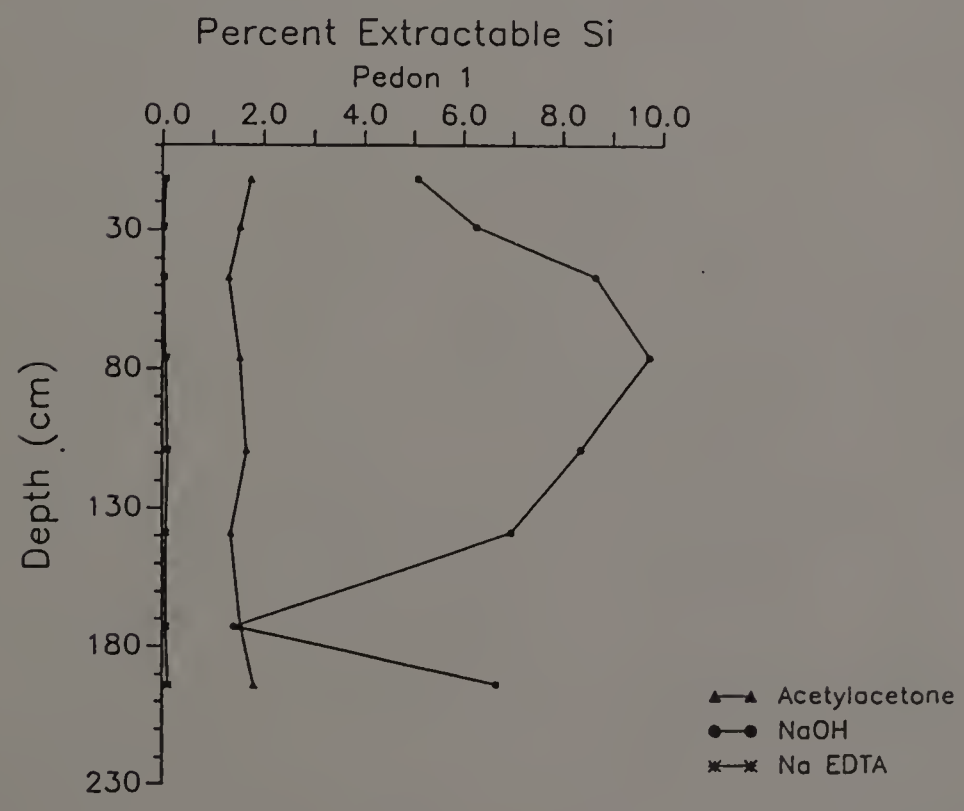
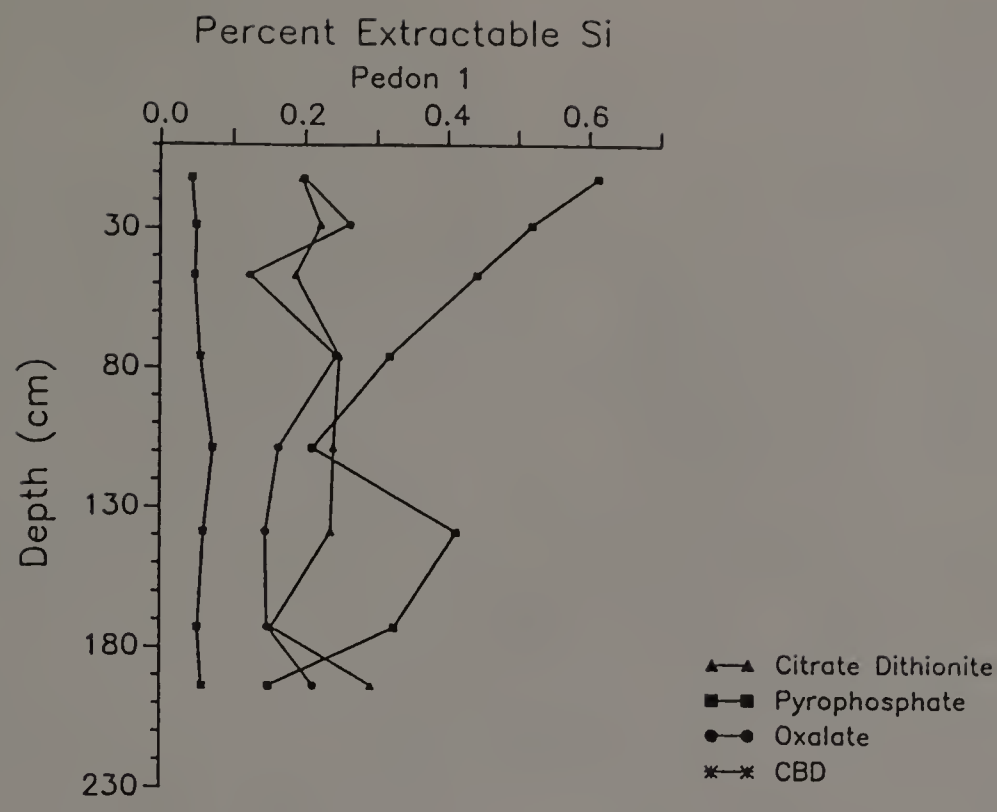


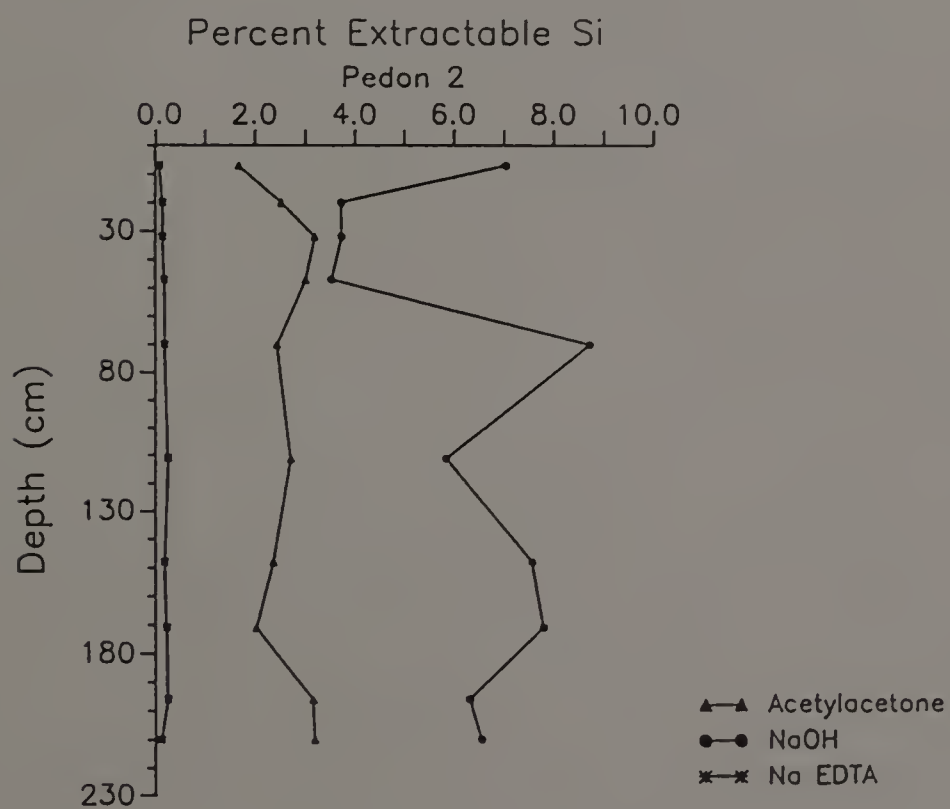
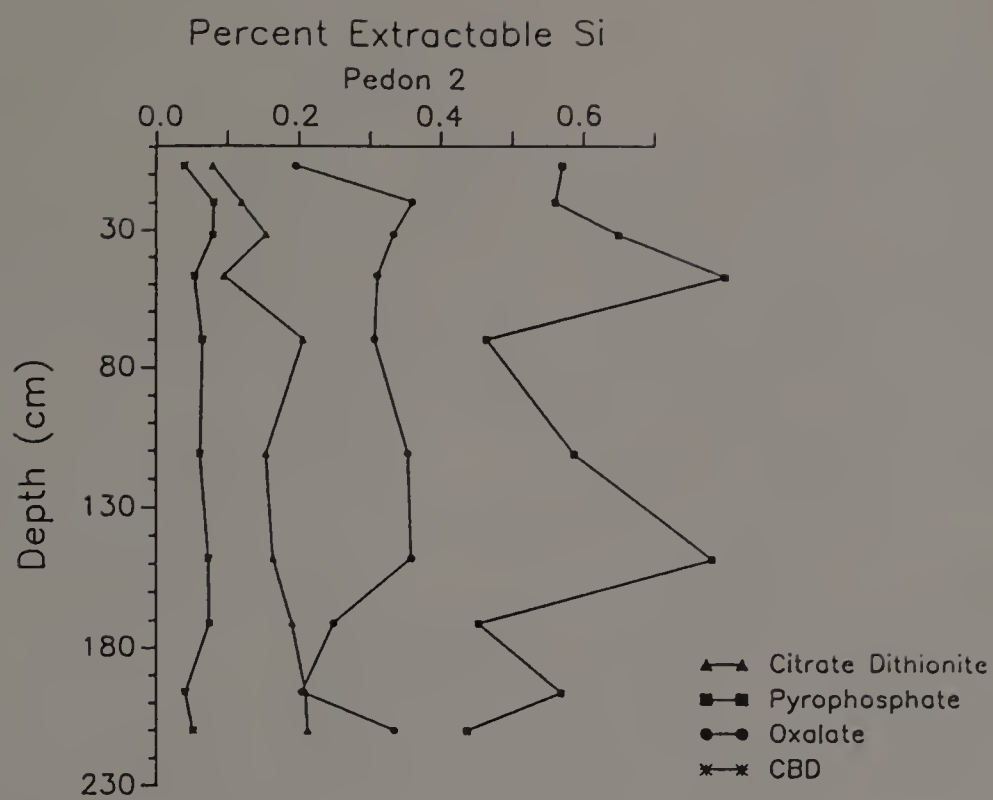


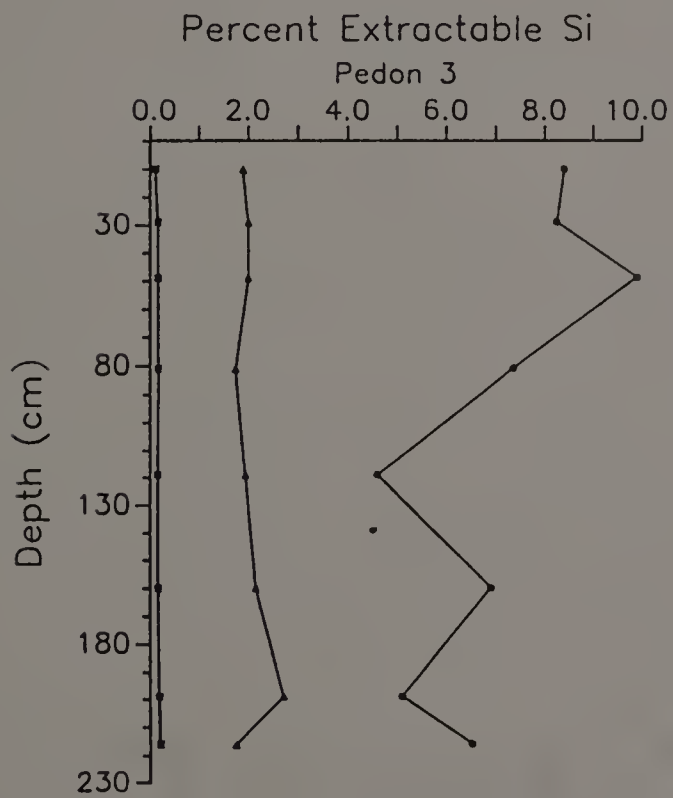
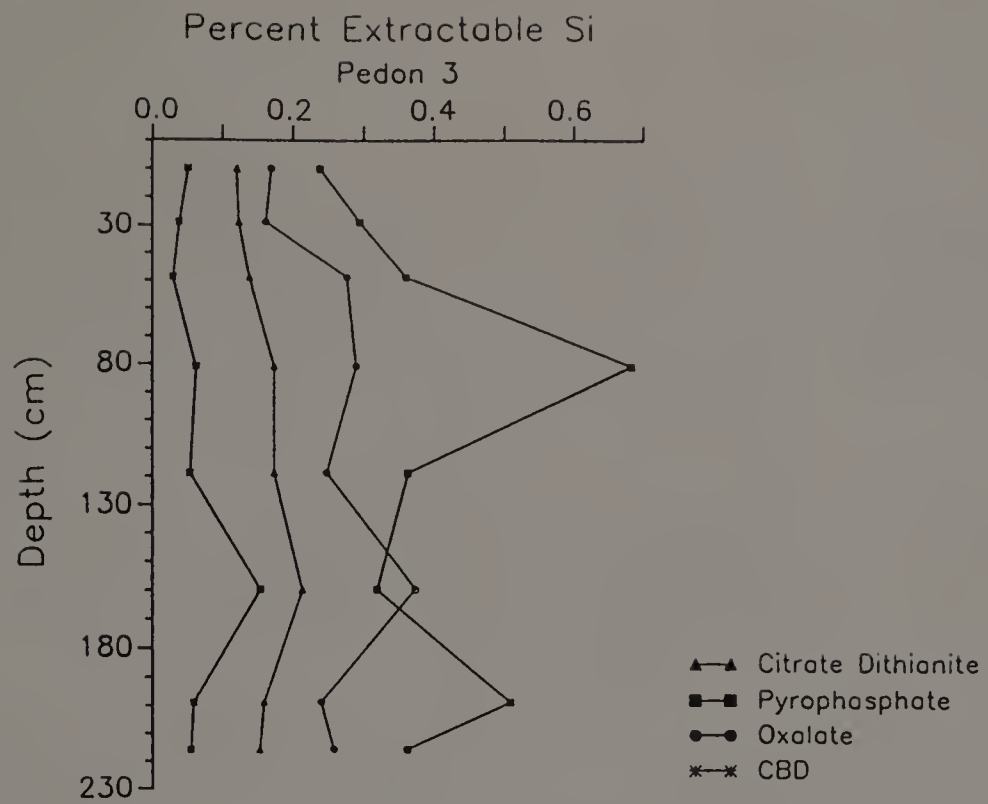


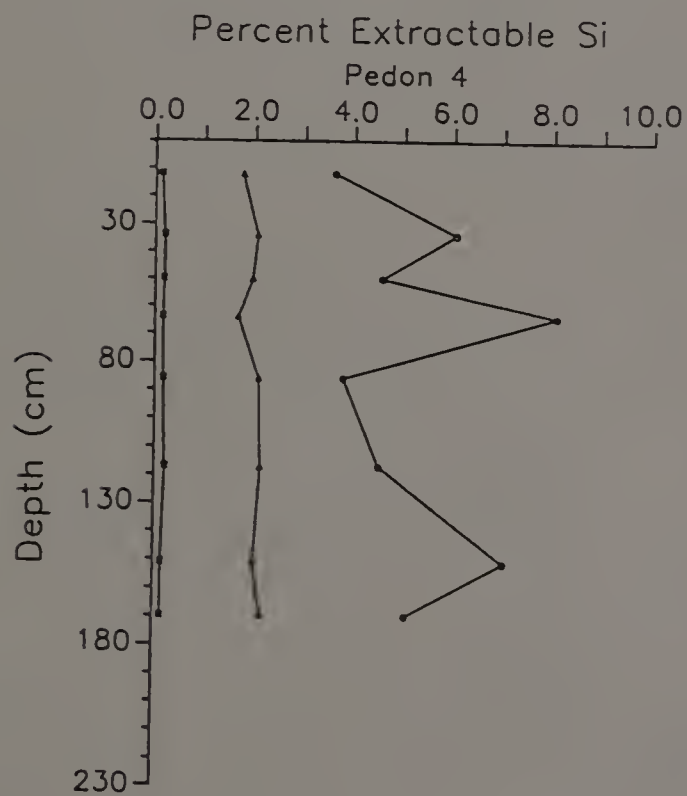
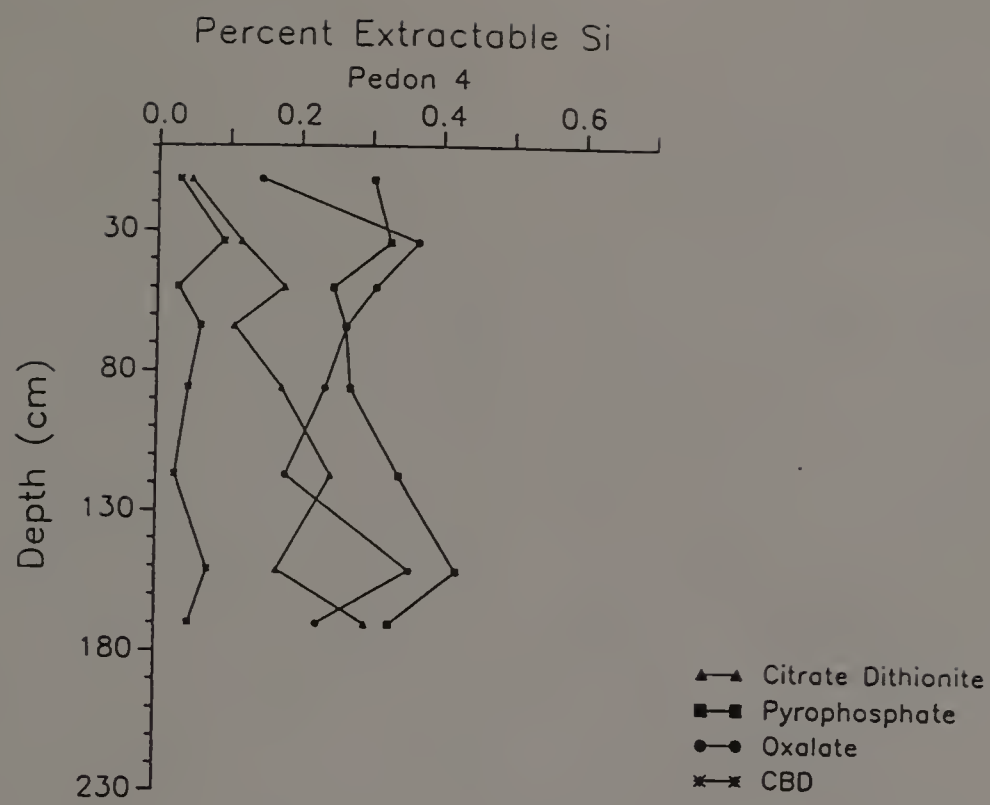


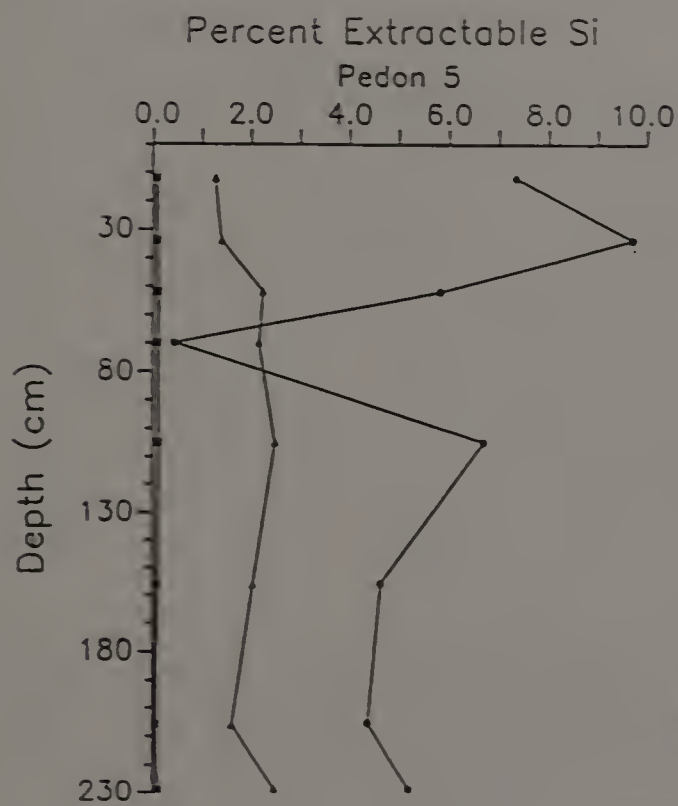
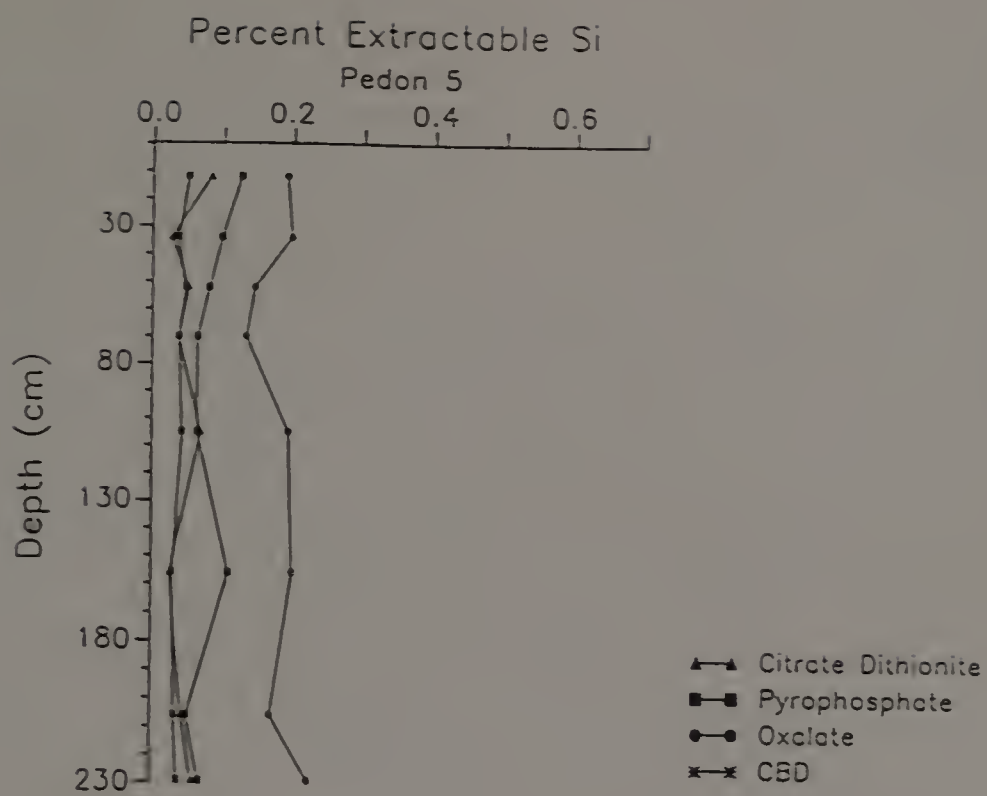
Extractable Si Graphs











Secondary Sites

Percent Extractable Fe

EHP

Hori.	C.D.	Pyro	Oxal.
Ap	1.58	0.33	0.820
Bw1	2.40	0.22	0.965
Bw2	2.58	0.15	1.300
Bt	2.44	0.15	1.510
2Btx2	2.36	0.14	1.555

EHW

Hori.	C.D.	Pyro	Oxal.
Ap	1.92	0.57	1.415
Bw1	1.86	0.24	1.455
Bw2	2.08	0.20	1.540
2Btx1	2.38	0.16	1.820
2Btx2	2.41	0.12	1.775

EHR

Hori.	C.D.	Pyro	Oxal.
Ap	2.00	0.68	1.460
Bw1	1.77	---	1.570
BE	0.92	0.33	1.350
2Bx1	1.07	0.28	1.030
2Bx2	0.72	0.18	0.840

EHDP2

Hori.	C.D.	Pyro	Oxal.
Ap	1.67	0.61	1.170
Bw1	1.75	0.38	1.390
Bw2	2.00	0.26	1.400
BE	2.14	0.14	1.210
2BCx	1.98	0.18	1.335
3BCm	2.60	0.14	1.985

EHDP3

Hori.	C.D.	Pyro	Oxal.
Ap	1.91	0.59	1.420
Bw1	2.02	0.65	1.465
Bw2	2.37	0.55	1.840
2BCd	1.77	0.38	1.315
3BCm	2.33	0.15	1.445
4Cr	3.10	0.16	1.960

BHP

Hori.	C.D.	Pyro	Oxal.
Ap	1.37	0.58	1.250
Bw1	1.53	0.42	1.240
Bw2	0.94	0.29	1.855
BE	0.71	0.17	0.890
2Btx1	1.29	0.10	0.705
2Btx2	1.23	0.09	0.975

BHW

Hori.	C.D.	Pyro	Oxal.
Ap	1.34	0.47	1.465
Bw1	1.38	0.41	1.130
Bw2	1.24	0.29	1.620
2Bx1	0.93	0.12	1.025
2Bx2	1.18	0.10	1.140
BPF	1.16	0.09	1.680

BHR

Hori.	C.D.	Pyro	Oxal.
A	0.91	0.61	1.040
Bw	0.71	0.31	0.810
Bx1	0.72	0.14	0.930
Bx2	0.90	0.08	1.060
BPF	0.57	0.09	0.795

OHW

Hori.	C.D.	Pyro	Oxal.
Ap	1.21	0.46	1.325
Bw1	1.31	0.20	1.525
Bw2	1.58	0.18	1.525
BE	1.92	0.31	2.200
2Btx1a	1.53	0.15	----
2Btx1b	1.54	0.11	1.490
2Btx2a	1.62	0.11	1.490
2Btx2b	1.67	0.08	1.650

OHL

Hori.	C.D.	Pyro	Oxal.
Ap	0.132	0.265	0.321
Bw	0.092	0.121	0.243
Bg1	0.063	0.023	0.227
Bg2	0.063	0.012	0.158
2Bw	0.048	0.040	0.255
2BCm	0.105	0.104	0.267
3Cd1	0.031	0.006	0.250
3Cd2	0.024	0.011	0.305
3Cd3	0.010	0.013	0.330
4Cm	0.101	0.016	0.278
5Cd4	0.099	0.024	0.541
5Cd5	0.030	0.041	0.191

BTR/S

Hori.	C.D.	Pyro	Oxal.
Ap	0.77	0.38	0.560
Bw1	0.62	0.25	0.445
Bw2	0.42	0.20	0.280
2BE a	0.42	0.16	0.465
2BE b	0.36	0.13	0.395
2Btx1a	0.35	0.07	0.325
2Btx1b	0.38	0.04	0.295
BPF	0.30	0.08	0.305

BTR

Hori.	C.D.	Pyro	Oxal.
2Btx1a	0.40	0.007	0.235
2Btx1b	0.37	0.09	0.160
2Btx2a	0.40	0.09	0.160
2Btx2b	0.29	0.07	0.100
BPF	0.44	0.13	0.315

Percent Extractable Al

EHP

Hori.	C.D.	Pyro
Ap	0.325	0.300
Bw1	0.294	0.230
Bw2	0.275	0.190
Bt	0.250	0.220
2Btx1	0.250	0.200

EHW

Hori.	C.D.	Pyro
Ap	0.463	0.450
Bw1	0.313	0.270
Bw2	0.269	0.280
2Btx1	0.319	0.280
2Btx2	0.256	0.210

EHR

Hori.	C.D.	Pyro
Ap	0.600	0.530
Bw1	0.588	----
BE	0.231	0.440
2Bx1	0.275	0.330
2Bx2	0.213	0.260

EHDP2

Hori.	C.D.	Pyro
Ap	0.489	0.450
Bw1	0.394	0.320
Bw2	0.325	0.230
BE	0.306	0.220
2BCx	0.256	0.170
3BCm	0.331	0.510

EHDP3

Hori.	C.D.	Pyro
Ap	0.581	0.520
Bw1	0.394	0.390
Bw2	0.413	0.340
2BCd	0.350	0.330
3BCm	0.325	0.180
4Cr	0.363	0.160

BHP

Hori.	C.D.	Pyro
Ap	0.581	0.520
Bw1	0.631	0.510
Bw2	0.488	0.520
BE	0.400	0.470
2Btx1	0.375	0.380
2Btx2	0.281	0.200

BHW

Hori.	C.D.	Pyro
Ap	0.425	0.480
Bw1	0.475	0.440
Bw2	0.450	0.400
2Bx1	0.288	0.290
2Bx2	0.250	0.230
BPF	0.188	0.180

BHR

Hori.	C.D.	Pyro
A	0.413	0.470
Bw	0.150	0.400
Bx1	0.131	0.180
Bx2	0.131	0.140
BPF	0.106	0.150

OHW

Hori.	C.D.	Pyro
Ap	0.419	0.440
Bw1	0.225	0.170
Bw2	0.238	0.150
BE	0.350	0.280
2Btx1a	0.213	0.120
2Btx1b	0.069	0.120
2Btx2a	0.065	0.100
2Btx2b	0.062	0.120

OHL

Hori.	C.D.	Pyro	Oxal.
Ap	0.030	0.072	0.042
Bw	0.015	0.028	0.033
Bg1	0.010	0.002	0.029
Bg2	0.005	----	0.022
2Bw	0.008	----	0.021
2BCm	0.008	----	0.019
3Cd1	0.007	----	0.023
3Cd2	0.007	----	0.015
3Cd3	0.006	----	0.020
4Cm	0.010	----	0.017
5Cd4	0.005	----	0.013
5Cd5	0.005	----	0.013

BTR/S

Hori.	C.D.	Pyro
Ap	0.375	0.41
Bw1	0.375	0.39
Bw2	0.312	0.31
2BE a	0.250	0.24
2BE b	0.237	0.24
2Btx1a	0.194	0.22
2Btx1b	0.137	0.12
BPF	0.125	0.14

BTR

Hori.	C.D.	Pyro
2Btx1a	0.137	0.12
2Btx1b	0.131	0.12
2Btx2a	0.119	0.13
2Btx2b	0.106	0.12
BPF	0.125	0.17

Percent Extractable Mn

EHP

Hori.	C.D.	Pyro	Oxal.
Ap	0.039	0.054	0.015
Bw1	0.013	0.019	0.004
Bw2	0.009	0.015	0.003
Bt	0.010	0.016	0.003
2Btx1	0.011	0.017	0.004

EHW

Hori.	C.D.	Pyro	Oxal.
Ap	0.071	0.086	0.029
Bw1	0.032	0.030	0.018
Bw2	0.028	0.026	0.012
2Btx1	0.030	0.024	0.013
2Btx2	0.037	0.023	0.016

EHR

Hori.	C.D.	Pyro	Oxal.
Ap	0.064	0.047	0.020
Bw1	0.011	----	0.005
BE	0.018	0.021	0.008
2Bx1	0.037	0.029	0.014
2Bx2	0.025	0.023	0.015

EHDP2

Hori.	C.D.	Pyro	Oxal.
Ap	0.058	0.079	0.039
Bw1	0.027	0.028	0.016
Bw2	0.020	0.019	0.017
BE	0.026	0.019	0.010
2BCx	0.029	0.020	0.013
3BCm	0.059	0.020	0.036

EHDP3

Hori.	C.D.	Pyro	Oxal.
Ap	0.084	0.098	0.058
Bw1	0.049	0.050	0.020
Bw2	0.049	0.038	0.019
2BCd	0.017	0.022	0.006
3BCm	0.076	0.031	0.030
4Cr	0.084	0.029	0.035

BHP

Hori.	C.D.	Pyro	Oxal.
Ap	0.012	0.023	0.002
Bw1	0.005	0.012	0.002
Bw2	0.004	0.011	0.004
BE	0.003	0.010	0.001
2Btx1	0.005	0.009	0.003
2Btx2	0.009	0.011	0.006

BHW

Hori.	C.D.	Pyro	Oxal.
Ap	0.010	0.016	0.005
Bw1	0.007	0.010	0.000
Bw2	0.005	0.009	0.002
2Bx1	0.006	0.007	0.002
2Bx2	0.006	0.007	0.002
BPF	0.004	0.007	0.001

BHR

Hori.	C.D.	Pyro	Oxal.
A	0.002	0.004	0.001
Bw	0.002	0.004	0.000
Bx1	0.006	0.006	0.002
Bx2	0.009	0.008	0.005
BPF	0.006	0.008	0.003

OHW

Hori.	C.D.	Pyro	Oxal.
Ap	0.047	0.061	0.025
Bw1	0.019	0.015	0.003
Bw2	0.028	0.013	0.014
BE	0.021	0.013	0.008
2Btx1a	0.007	0.012	0.003
2Btx1b	0.016	0.009	0.006
2Btx2a	0.024	0.011	0.010
2Btx2b	0.016	0.009	0.004

OHL

Hori.	C.D.	Pyro	Oxal.
Ap	0.001	0.001	0.001
Bw	0.001	0.001	0.001
Bg1	0.001	----	0.001
Bg2	0.001	----	0.001
2Bw	0.001	----	0.001
2BCm	0.005	----	0.007
3Cd1	0.002	----	0.003
3Cd2	0.002	----	0.002
3Cd3	0.001	----	0.002
4Cm	0.027	----	0.047
5Cd4	0.001	----	0.002
5Cd5	0.001	----	0.003

BTR/S

Hori.	C.D.	Pyro	Oxal.
Ap	0.015	0.021	0.002
Bw1	0.003	0.003	0.001
Bw2	0.002	0.002	0.000
2BE a	0.004	0.004	0.001
2BE b	0.004	0.003	0.001
2Btx1a	0.007	0.004	0.001
2Btx1b	0.007	0.004	0.001
BPF	0.002	0.003	0.001

BTR

Hori.	C.D.	Pyro	Oxal.
2Btx1a	0.010	0.004	0.002
2Btx1b	0.009	0.006	0.002
2Btx2a	0.008	0.006	0.003
2Btx2b	0.008	0.006	0.002
BPF	0.004	0.003	0.001

Till sites

Percent Extractable Fe

Sample	C.D.	Pyro	Oxal.
<u>Upper Till</u>			
LTD UT1	0.313	0.016	0.084
UT2	0.269	0.013	0.075
UT3	0.336	0.021	0.076
UT4	0.447	0.027	0.097
UT5	0.452	0.031	0.090
AY UT1	0.226	0.015	0.039
UT2	0.258	0.025	0.068
UT3	0.261	0.019	0.068
UT4	0.323	0.021	0.086
UT5	0.344	0.029	0.069
BA UT1	0.521	0.041	0.178
UT2	0.193	0.097	0.061

Lower Till - Oxidized

LTD OT1	0.696	0.037	0.206
OT2	0.212	0.017	0.062
OT3	0.293	0.093	0.048
OT4	0.687	0.035	0.192
OT5	0.617	0.032	0.198
AY OT1	0.454	0.028	0.102
OT2	0.316	0.028	0.101
OT3	0.400	0.034	0.113
OT4	0.383	0.039	0.079
OT5	0.373	0.038	0.112
BA OT	0.841	0.035	0.173
OT/LT	0.559	0.039	0.170

Lower Till - Unoxidized

LTD LT1	0.305	0.044	0.177
LT2	0.322	0.030	0.158
LT3	0.319	0.028	0.177
LT4	0.383	0.022	0.186
LT5	0.413	0.028	0.166
AY LT1	0.477	0.024	0.170
LT2	0.241	0.033	0.142
LT3	0.333	0.039	0.140
LT4A	0.334	0.027	0.154
LT4B	0.368	0.048	0.131
LT5	0.169	0.054	0.140
BA LT1	0.633	0.036	0.212
LT2	0.631	0.049	0.202

Percent Extractable Al

Sample	C.D.	Pyro	Oxal.
<u>Upper Till</u>			
LTD UT1	0.435	0.053	0.172
UT2	0.443	0.066	0.200
UT3	0.355	0.093	0.202
UT4	0.670	0.123	0.366
UT5	0.774	0.130	0.520
AY UT1	0.379	0.049	0.162
UT2	0.499	0.091	0.197
UT3	0.376	0.071	0.198
UT4	0.556	0.067	0.155
UT5	0.484	0.061	0.198
BA UT1	0.354	0.022	0.194
UT2	0.503	0.023	0.121

Lower Till - Oxidized

LTD OT1	0.480	0.006	0.251
OT2	0.504	0.057	0.235
OT3	0.604	0.015	0.177
OT4	0.459	0.013	0.156
OT5	0.433	0.025	0.196
AY OT1	0.461	0.056	0.166
OT2	0.498	0.055	0.183
OT3	0.424	0.050	0.149
OT4	0.331	0.060	0.152
OT5	0.519	0.055	0.194
BA OT	0.476	0.033	0.154
OT/LT	0.516	0.019	0.149

Lower Till - Unoxidized

LTD LT1	0.359	0.022	0.220
LT2	0.419	0.014	0.198
LT3	0.493	0.018	0.191
LT4	0.474	0.011	0.268
LT5	0.344	0.010	0.171
AY LT1	0.505	0.022	0.196
LT2	0.503	0.029	0.179
LT3	0.501	0.028	0.199
LT4A	0.601	0.032	0.149
LT4B	0.381	0.027	0.159
LT5	0.246	0.036	0.150
BA LT1	0.483	0.018	0.180
LT2	0.339	0.026	0.153
BU	0.100	0.040	--

Percent Extractable Si

Sample C.D. Pyro Oxal.

Upper Till

LTD	UT1	0.114	0.232	0.109
	UT2	0.063	0.194	0.110
	UT3	0.099	0.194	0.328
	UT4	0.255	0.139	0.471
	UT5	0.471	0.176	0.622
AY	UT1	0.058	0.202	0.126
	UT2	0.176	0.172	0.169
	UT3	0.114	0.127	0.278
	UT4	0.094	0.136	0.219
	UT5	0.094	0.155	0.286
BA	UT1	0.140	0.139	0.236
	UT2	0.145	0.122	0.135

Lower Till - Oxidized

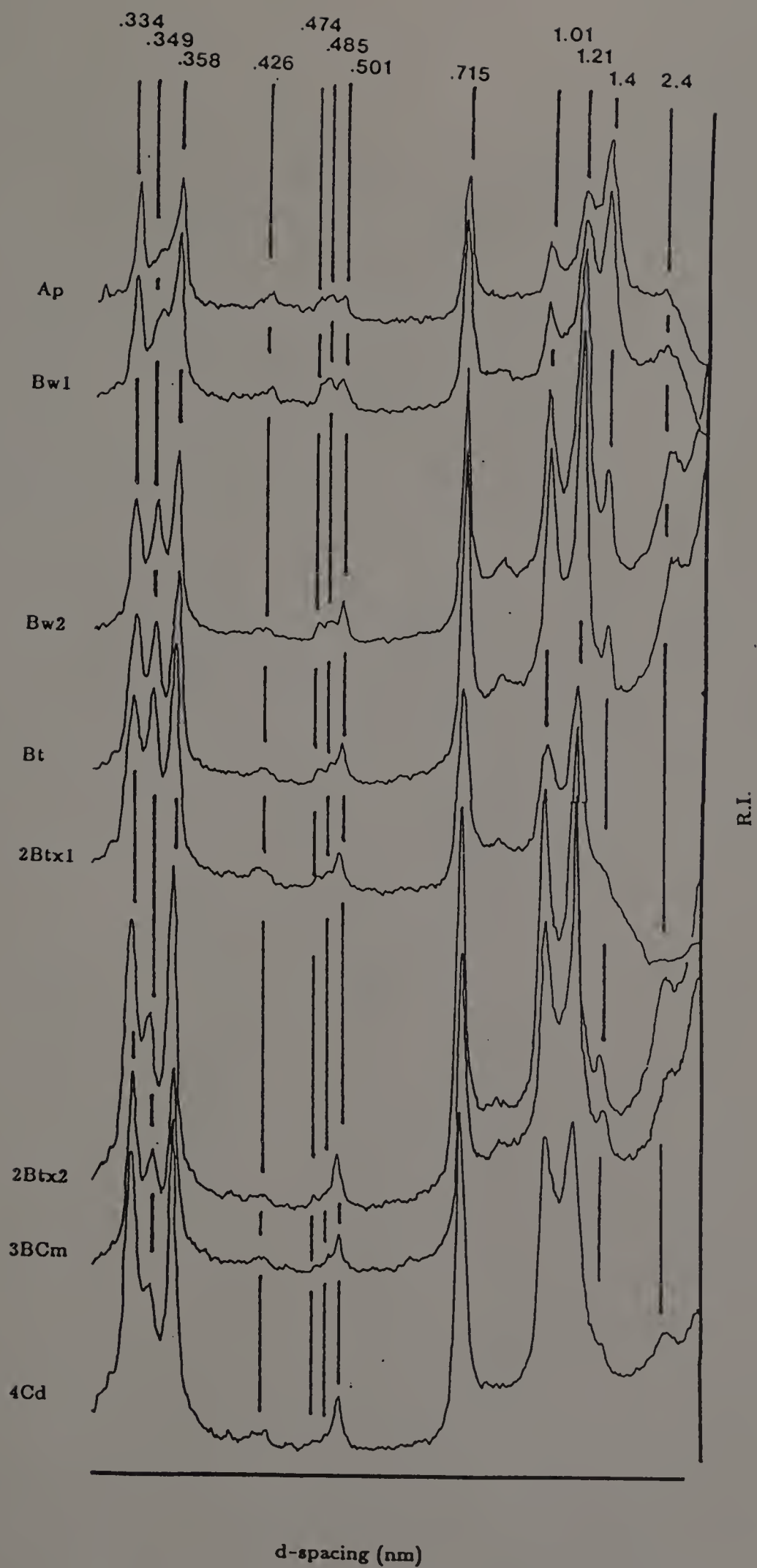
LTD	OT1	0.068	0.204	0.345
	OT2	0.099	0.101	0.219
	OT3	0.288	0.162	0.244
	OT4	0.441	0.143	0.188
	OT5	0.252	0.073	0.185
AY	OT1	0.084	0.142	0.379
	OT2	0.094	0.110	0.345
	OT3	0.170	0.197	0.463
	OT4	0.140	0.134	0.228
	OT5	0.247	0.334	0.362
BA	OT	0.084	0.106	0.202
	OT/LT	0.160	0.185	0.253

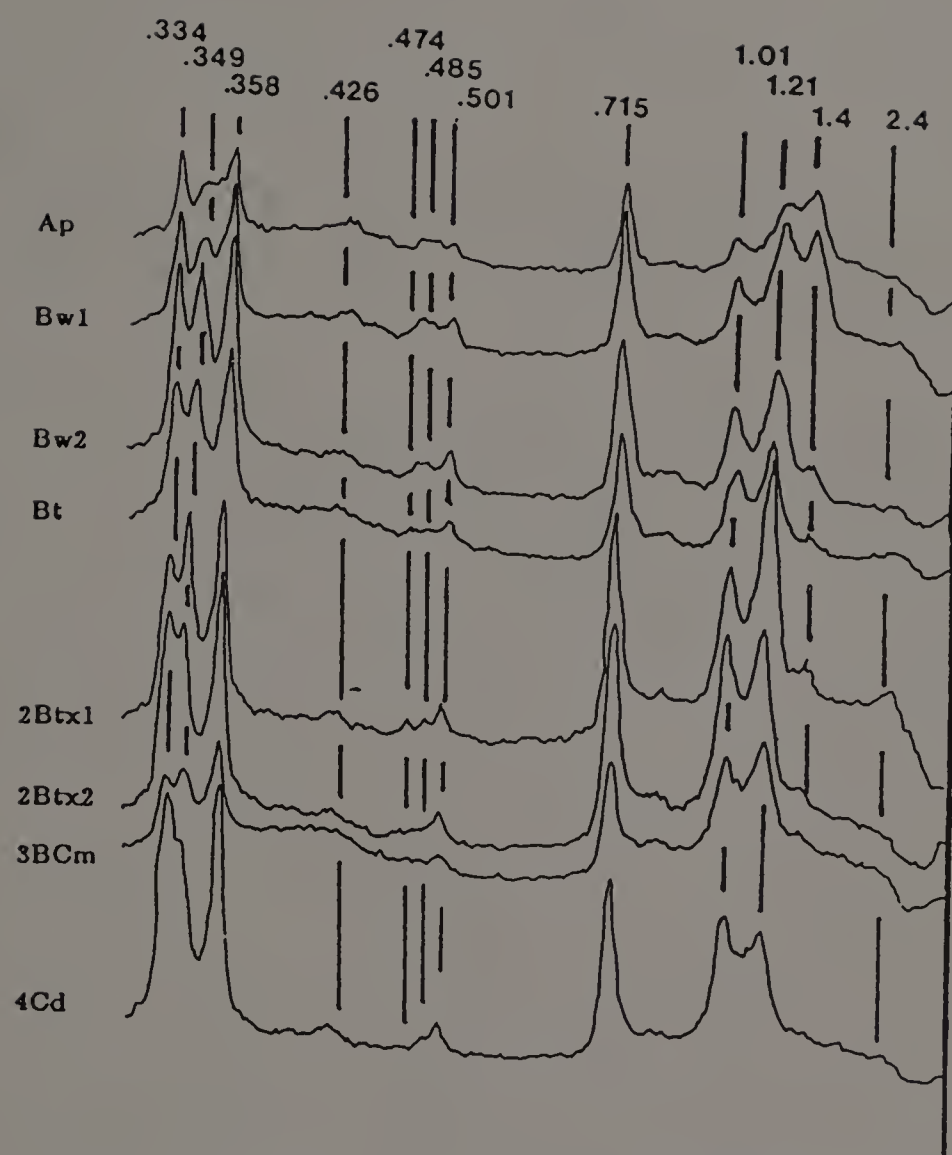
Lower Till - Unoxidized

LTD	LT1	0.227	0.092	0.421
	LT2	0.119	0.157	0.269
	LT3	0.063	0.078	0.253
	LT4	0.104	0.180	0.371
	LT5	0.063	0.078	0.353
AY	LT1	0.104	0.131	0.488
	LT2	0.102	0.106	0.328
	LT3	0.308	0.162	0.261
	LT4A	0.252	0.122	0.454
	LT4B	0.267	0.250	0.328
	LT5	0.160	0.190	0.337
BA	LT1	0.114	0.218	0.144
	LT2	0.115	0.141	0.152

APPENDIX J
CLAY MINERAL ANALYSIS

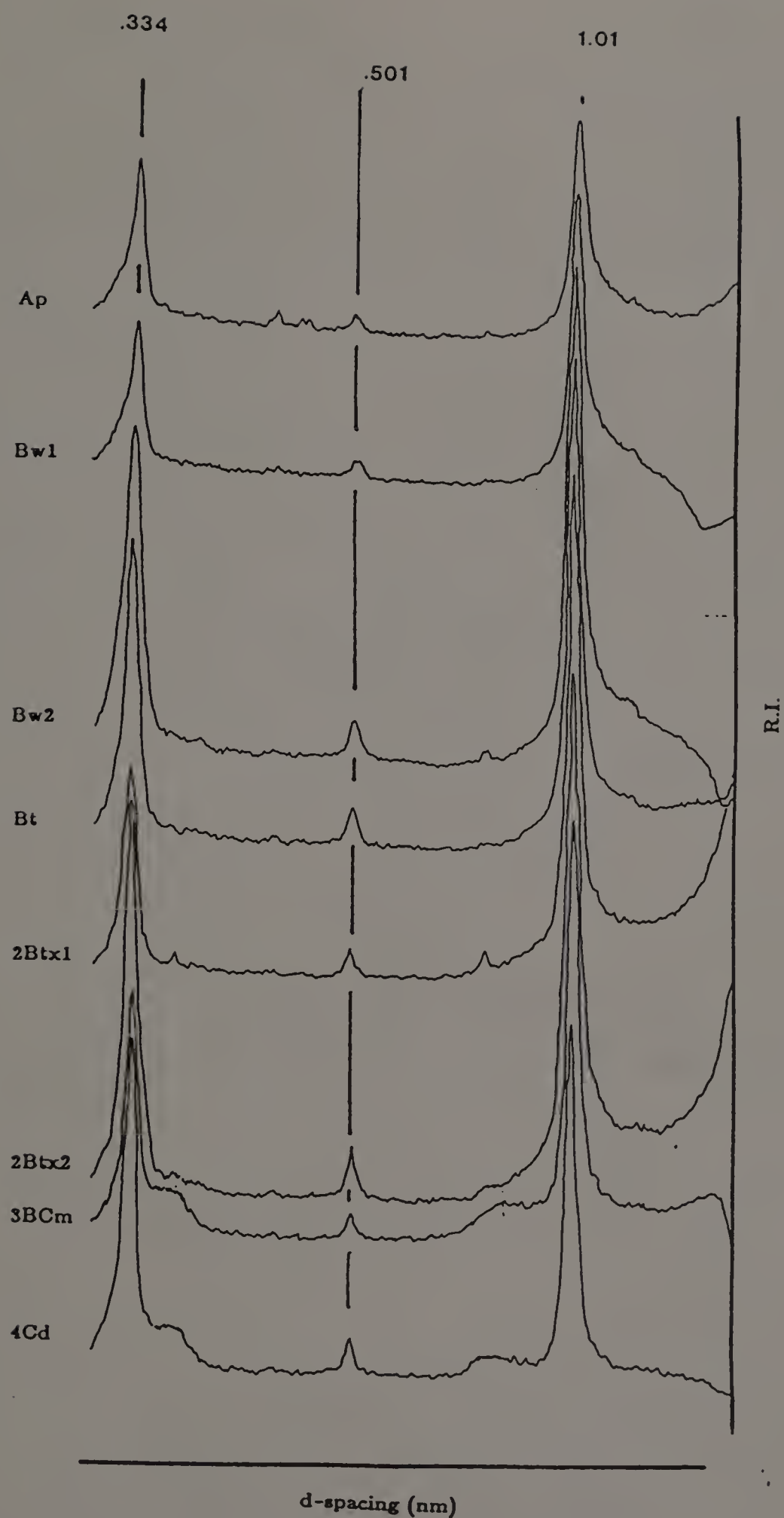
Pedon 1



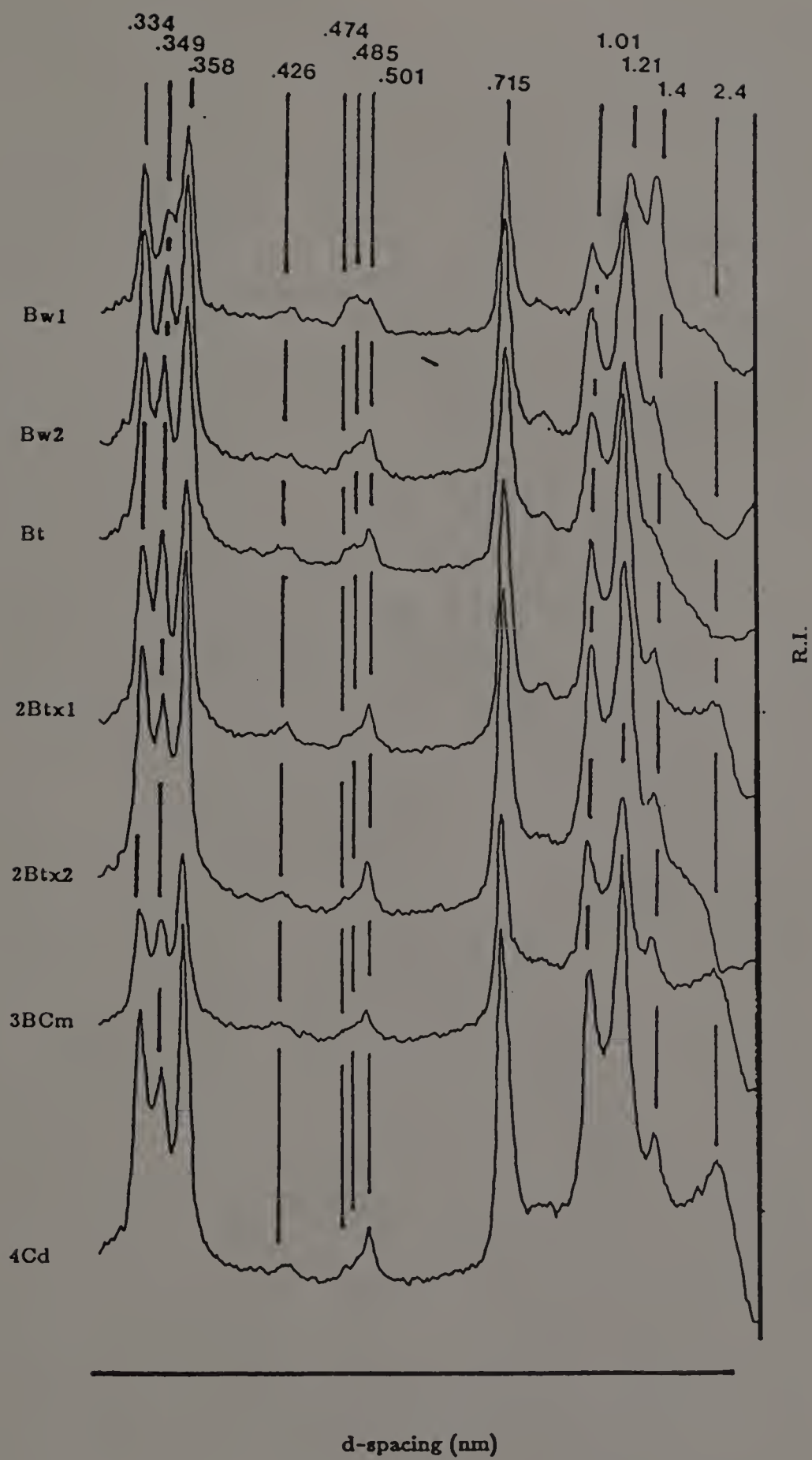


d-spacing (nm)

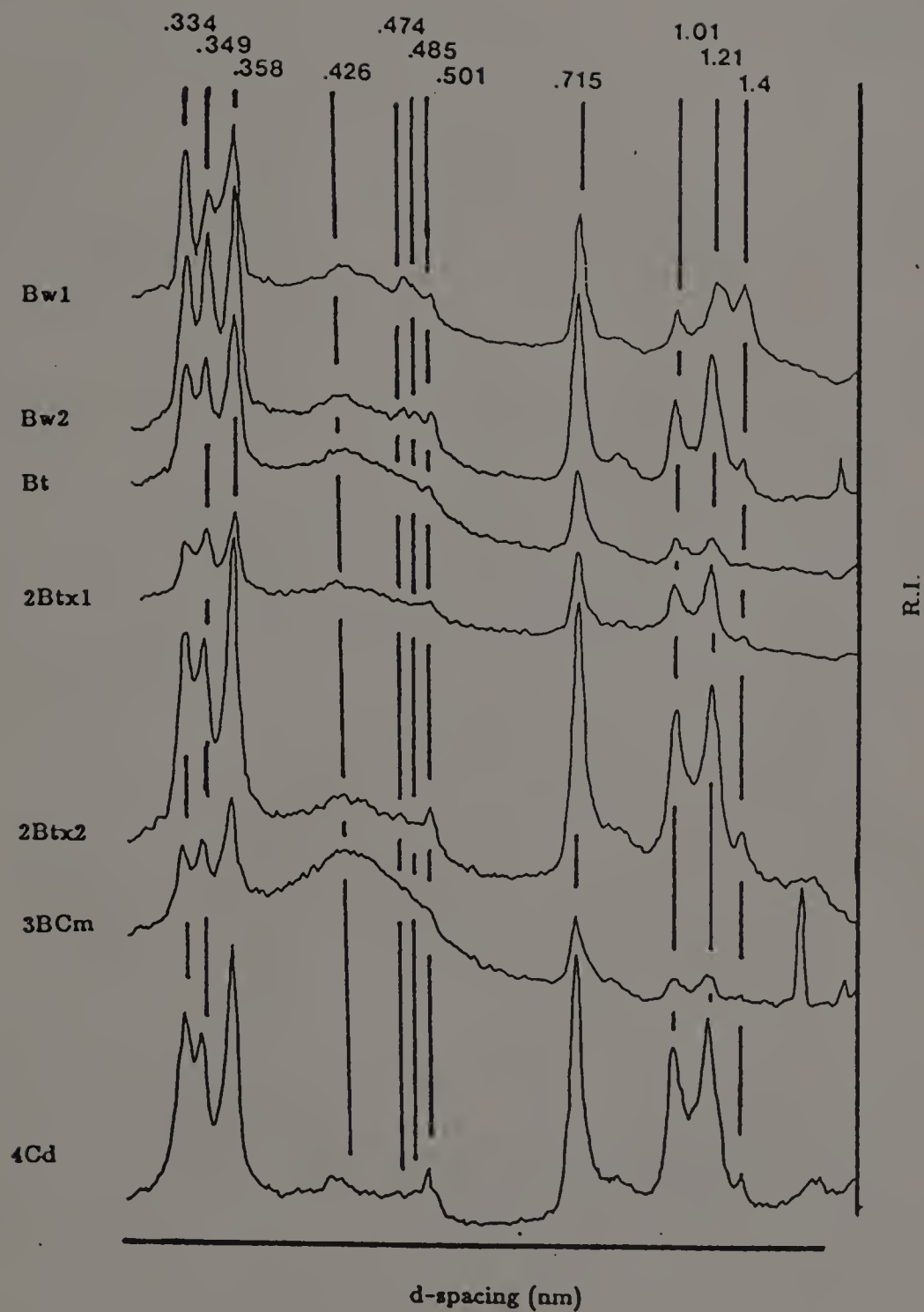
Glycol.



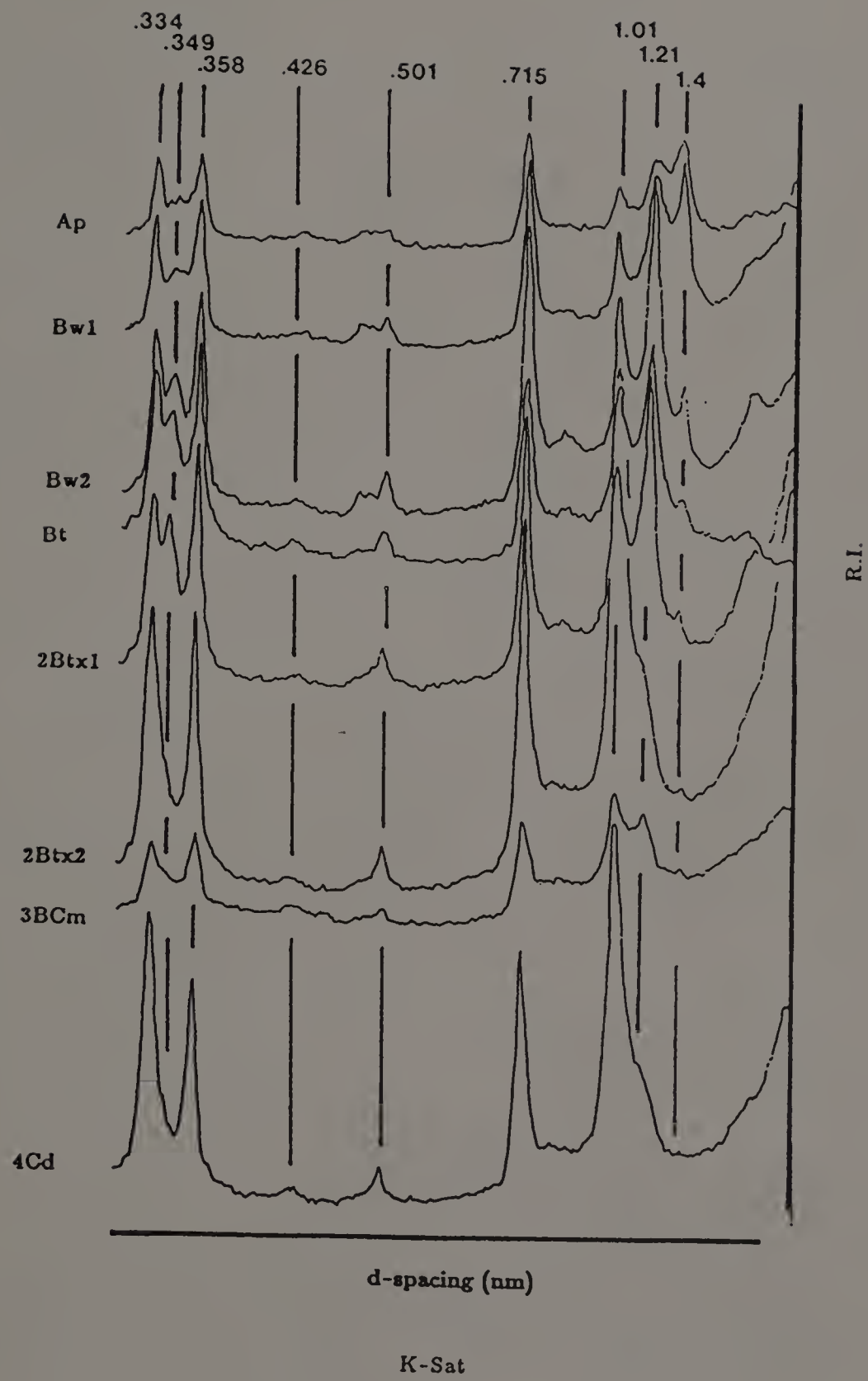
550°

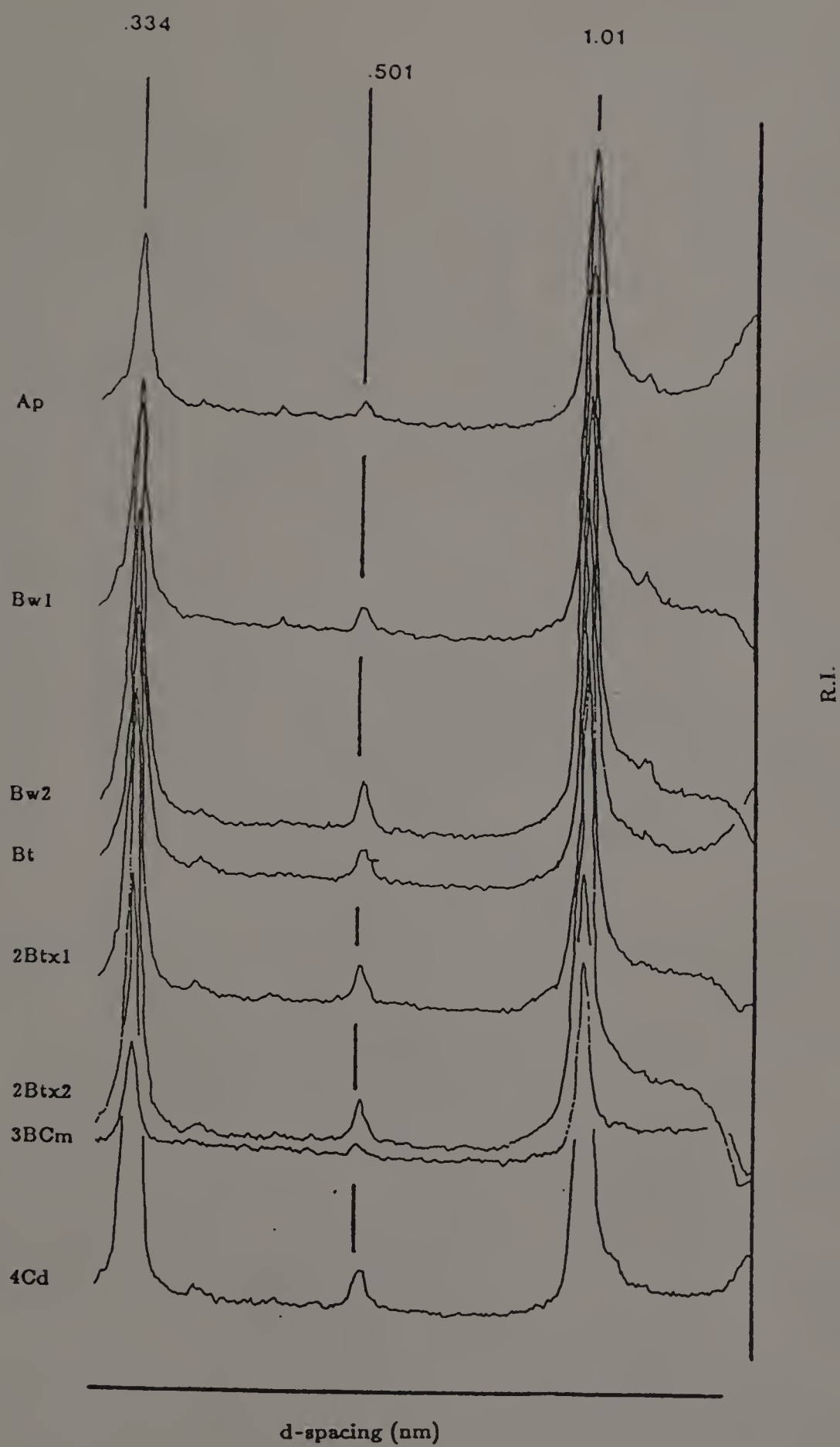


Mg-Sat.



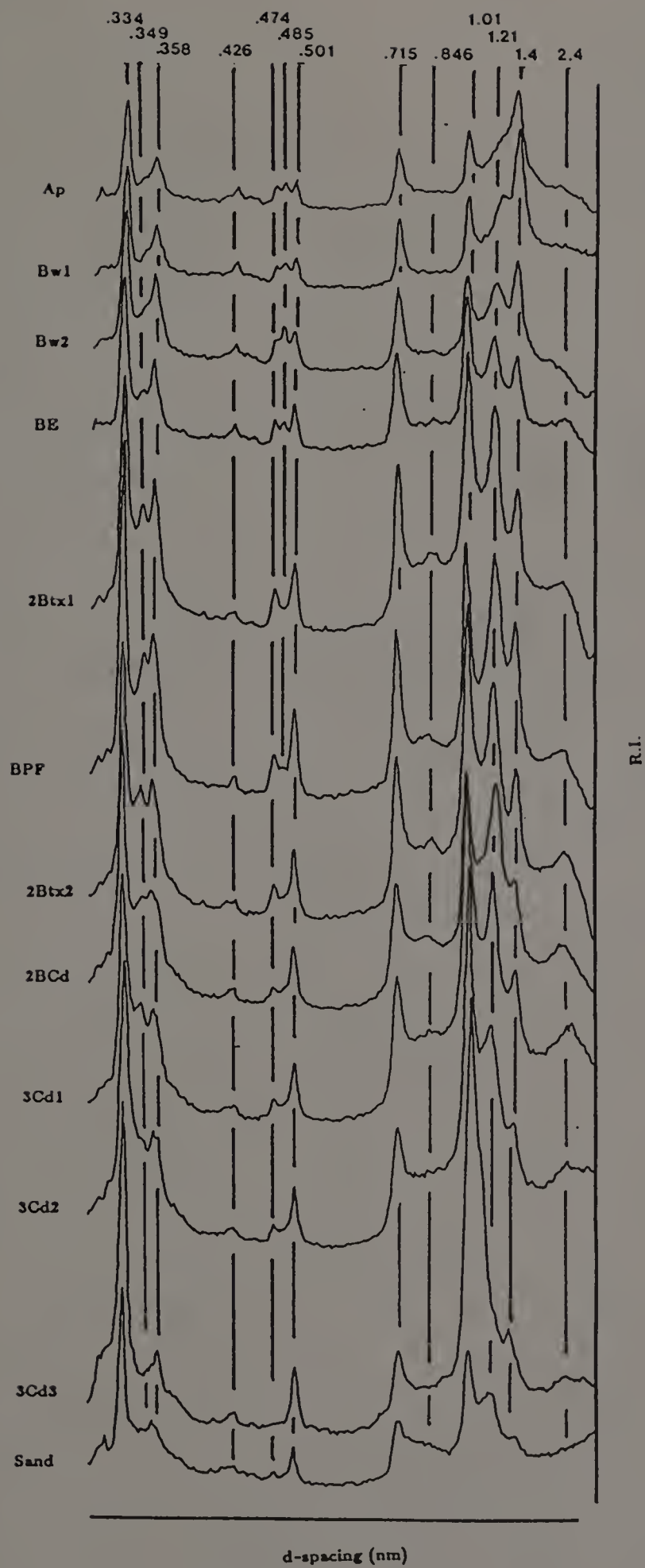
Mg-Glycer.



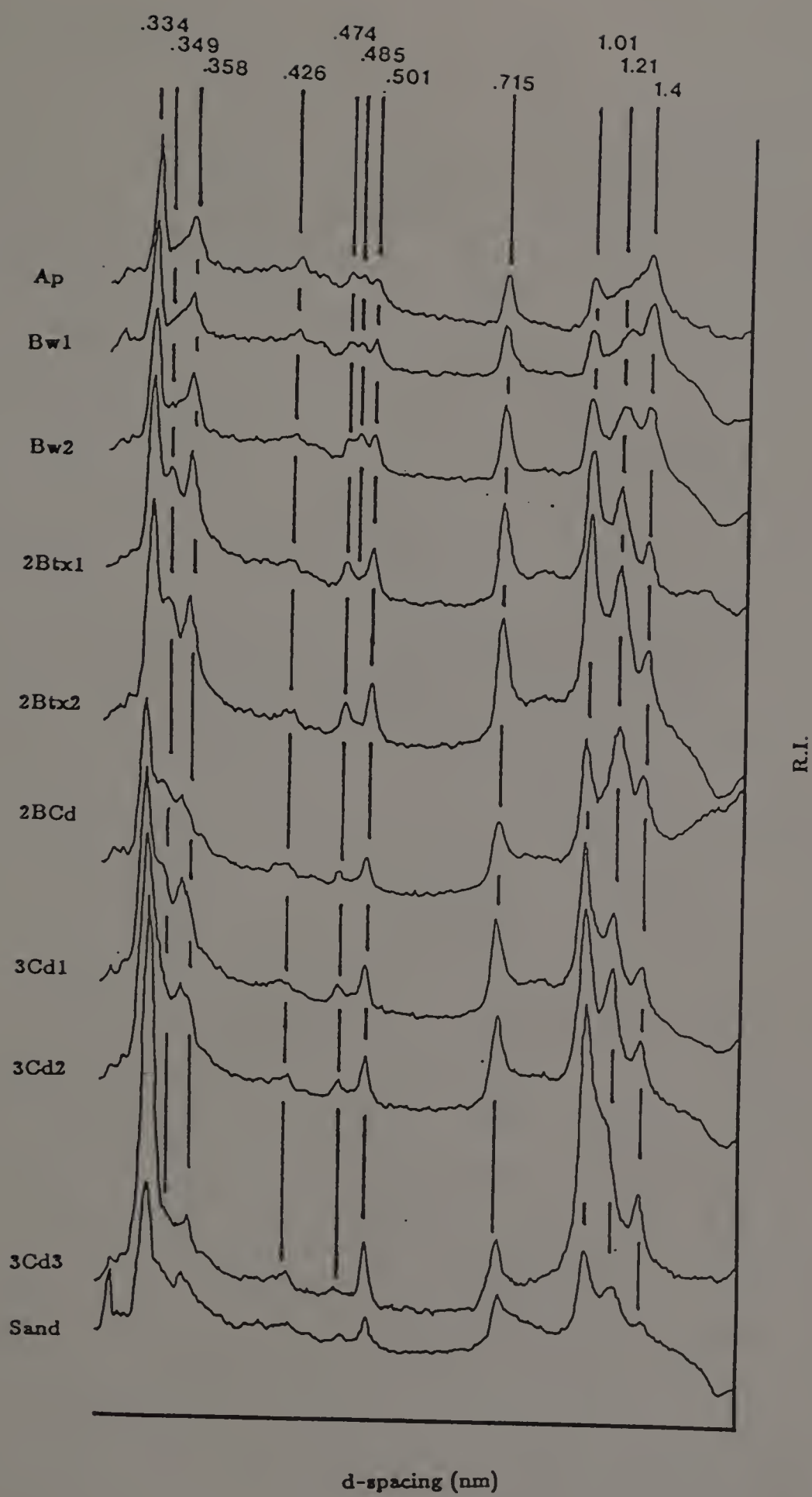


K-Sat. 550°

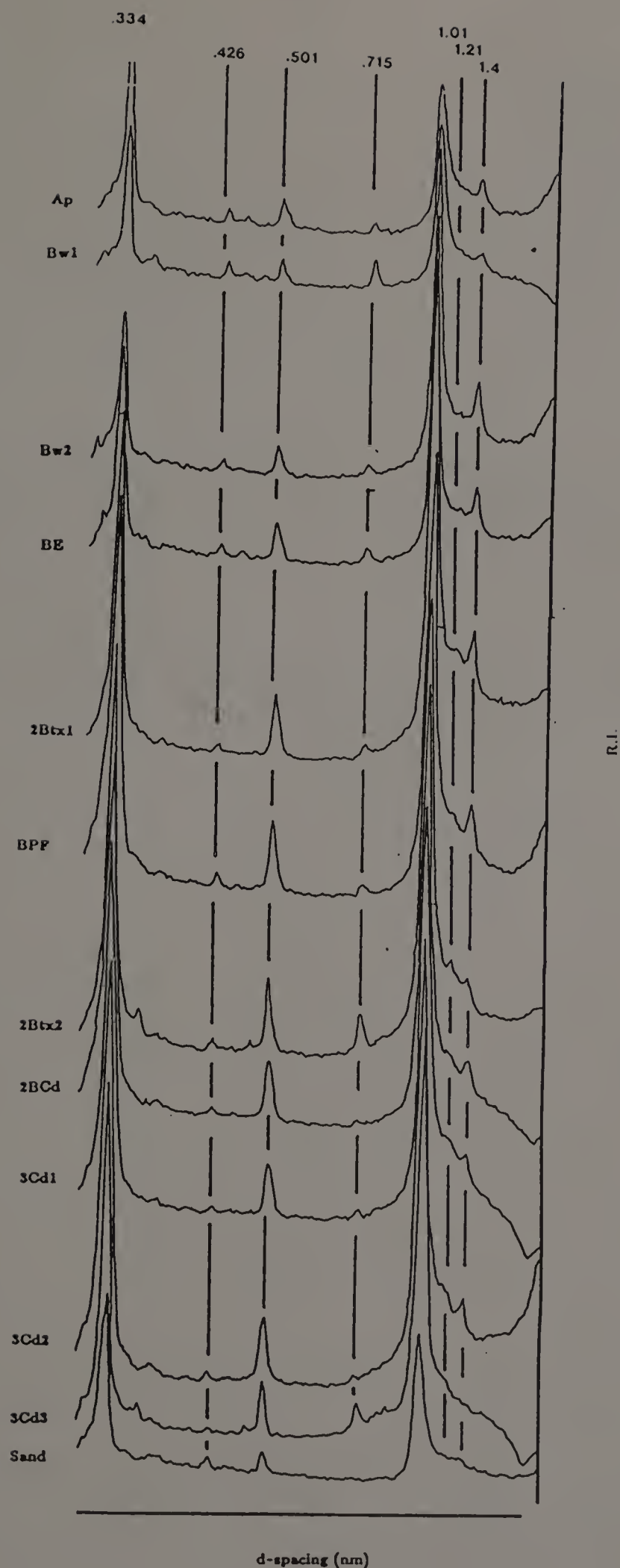
Pedon 2

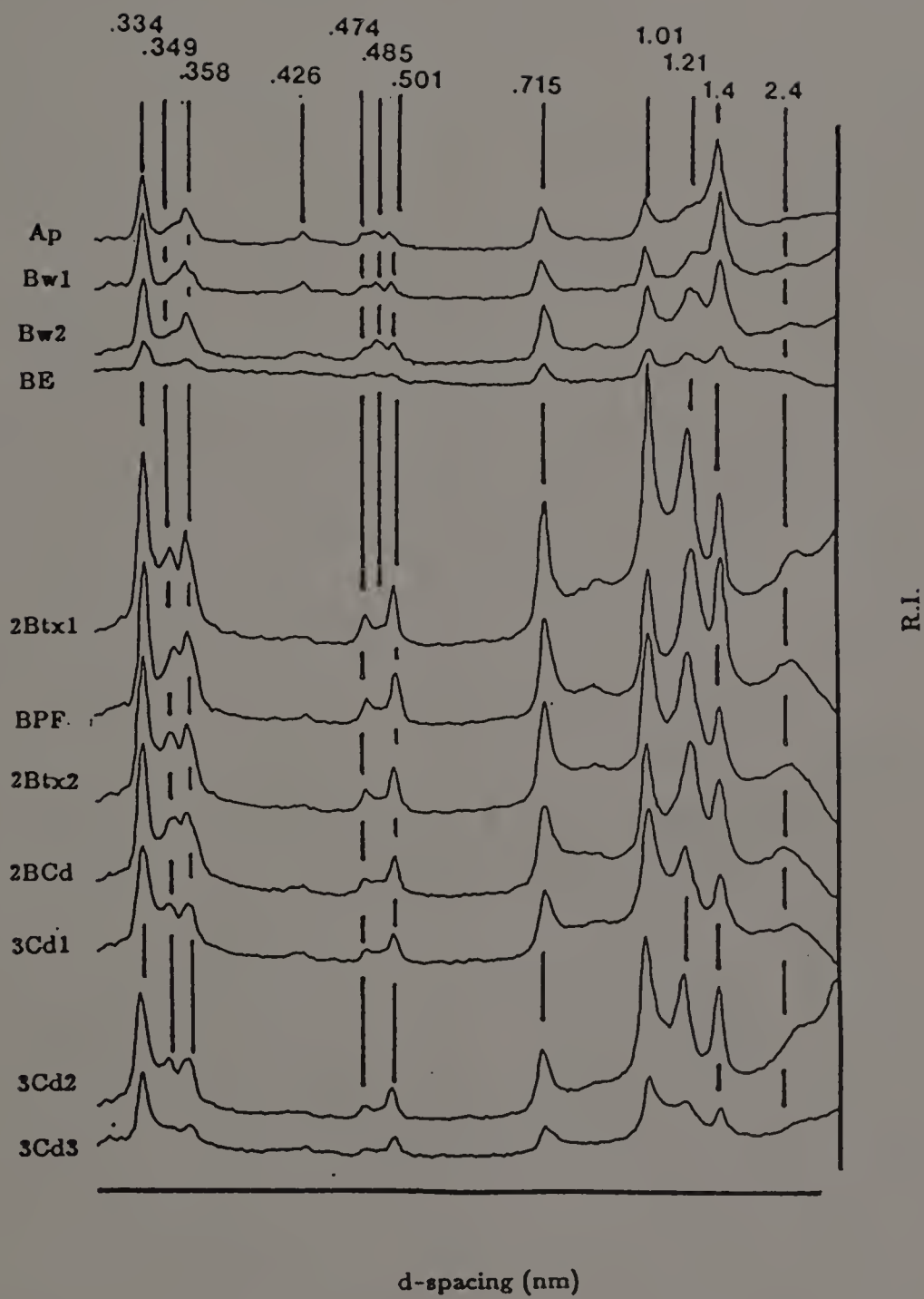


Na-Sat.

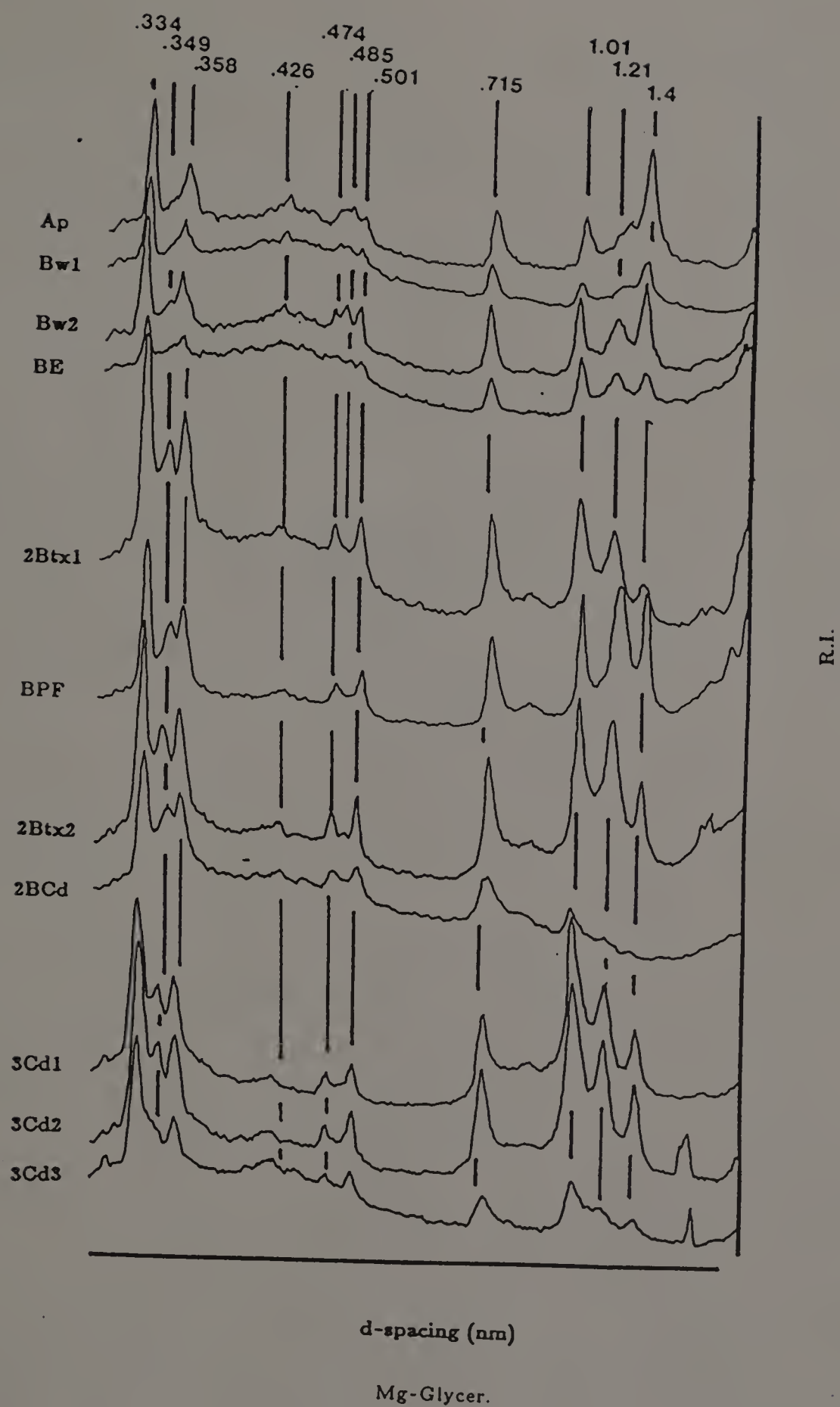


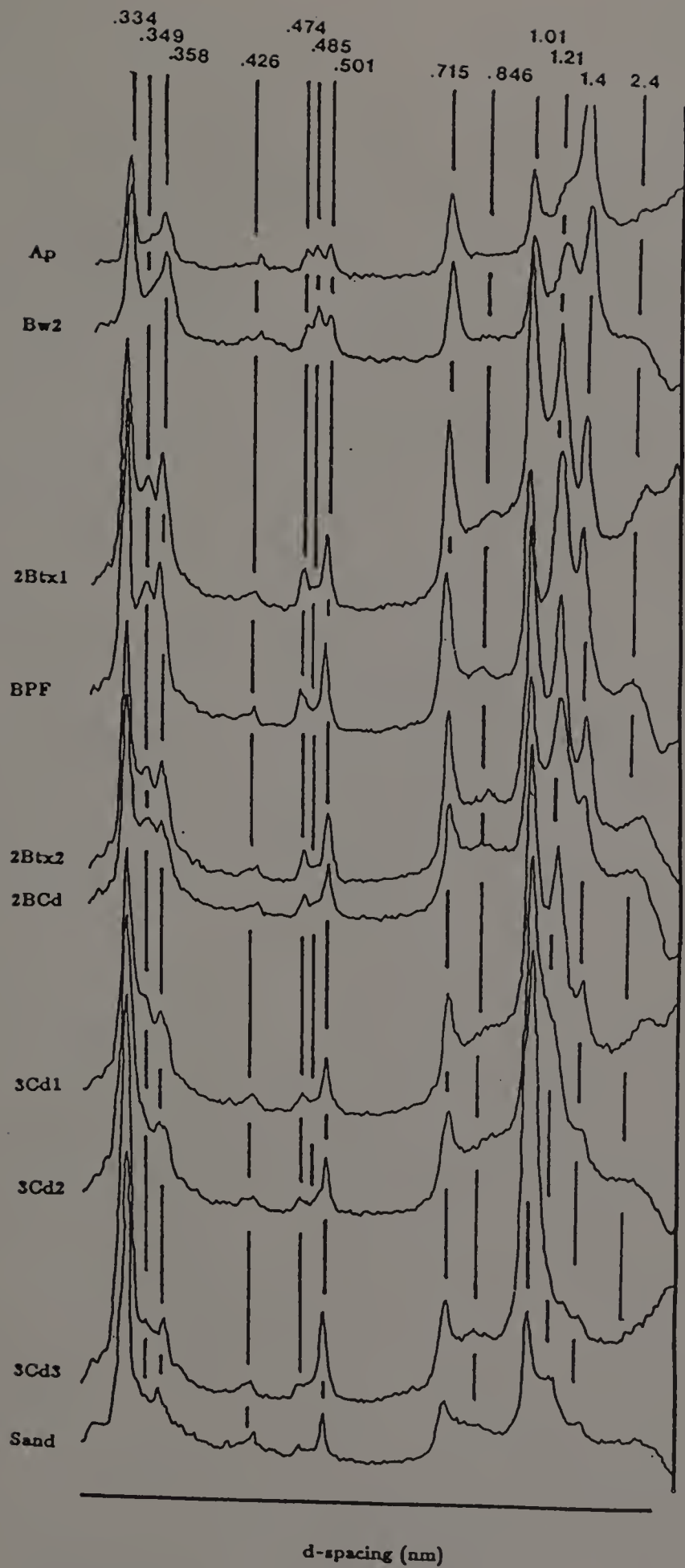
Glycol.





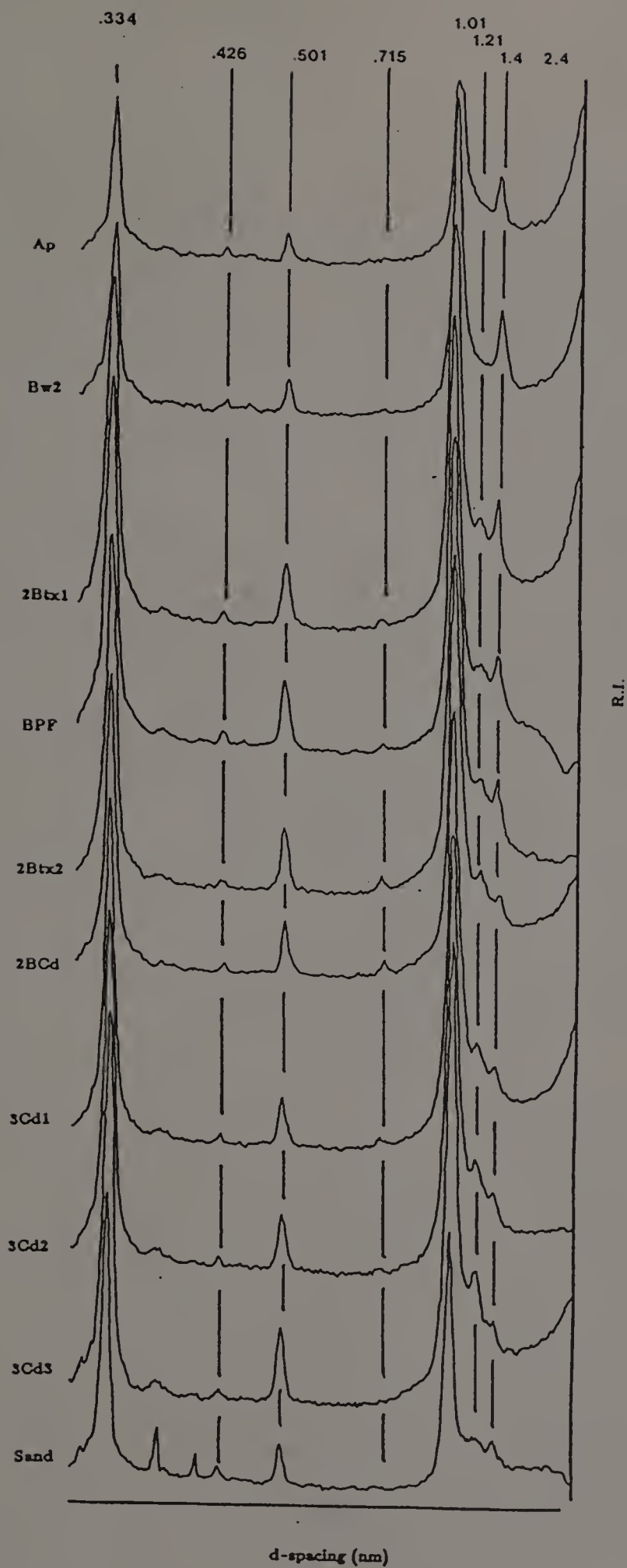
Mg-Sat.





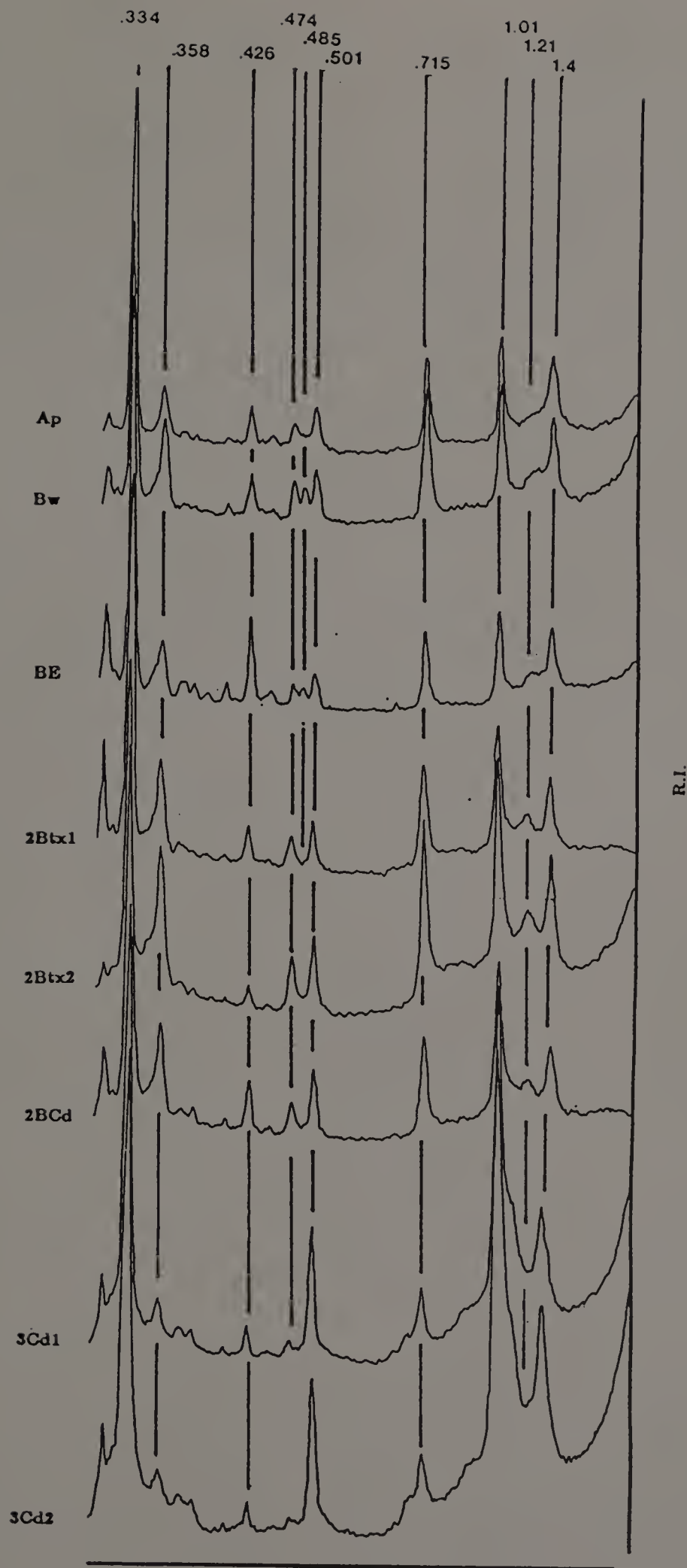
R.I.

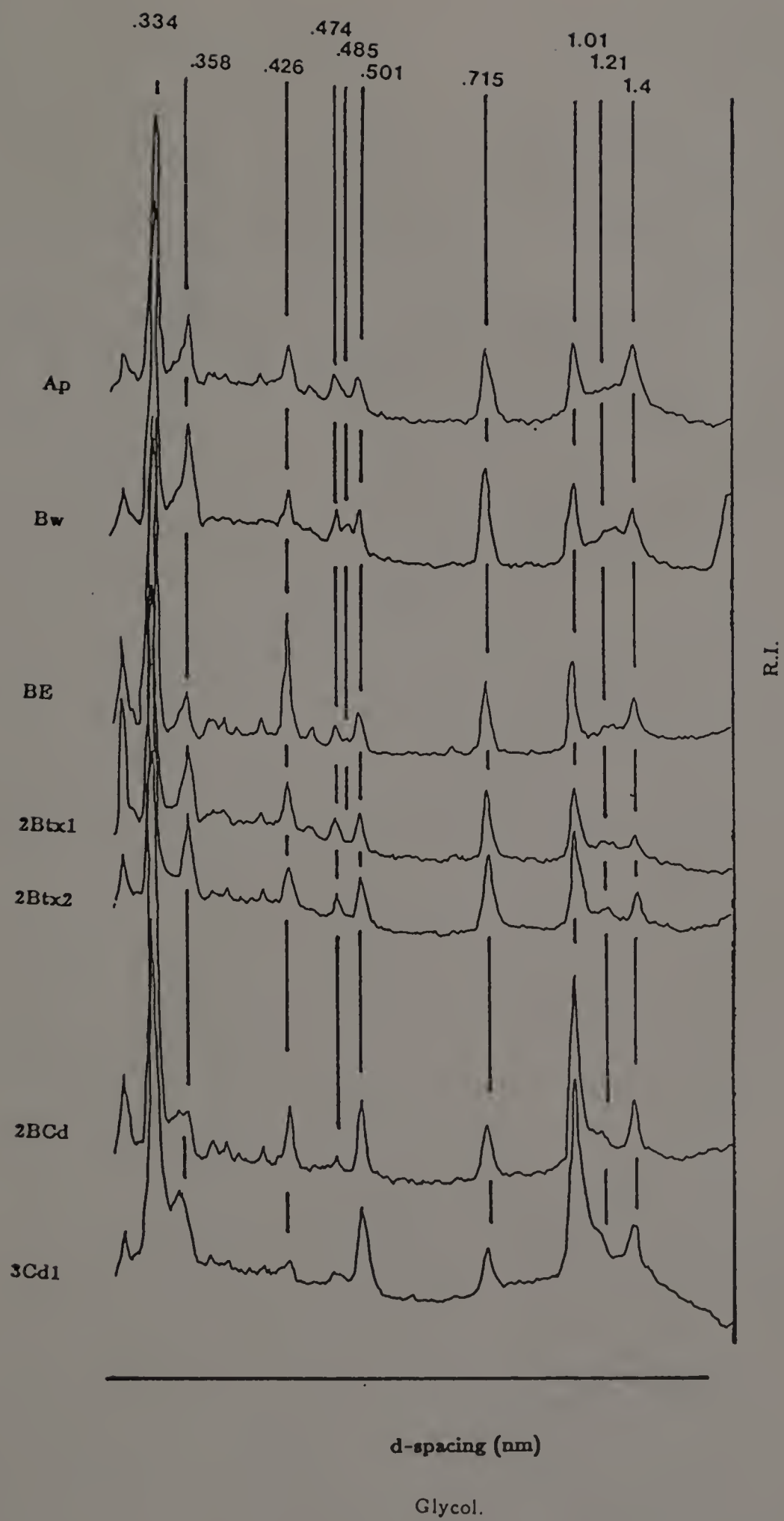
K-Sat

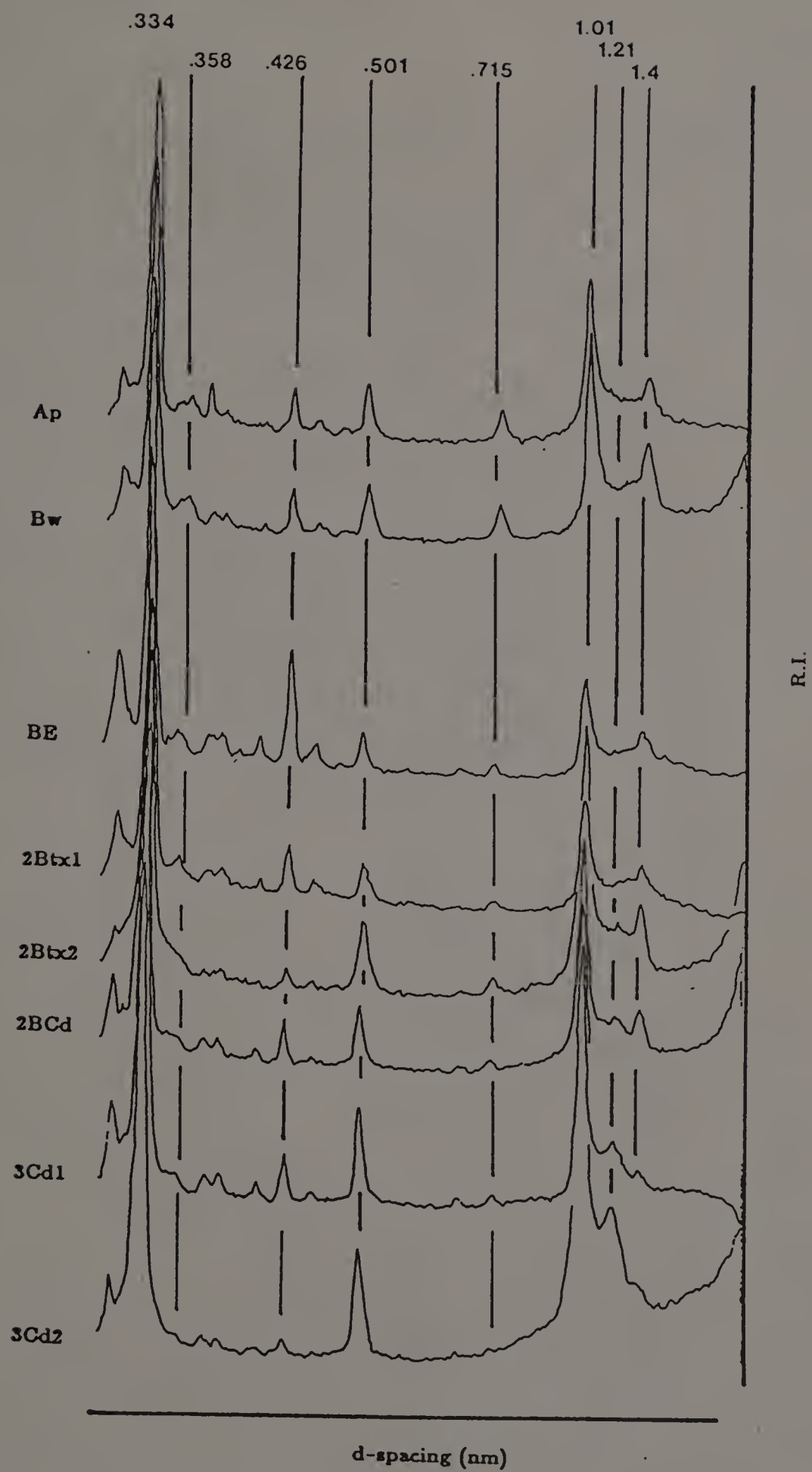


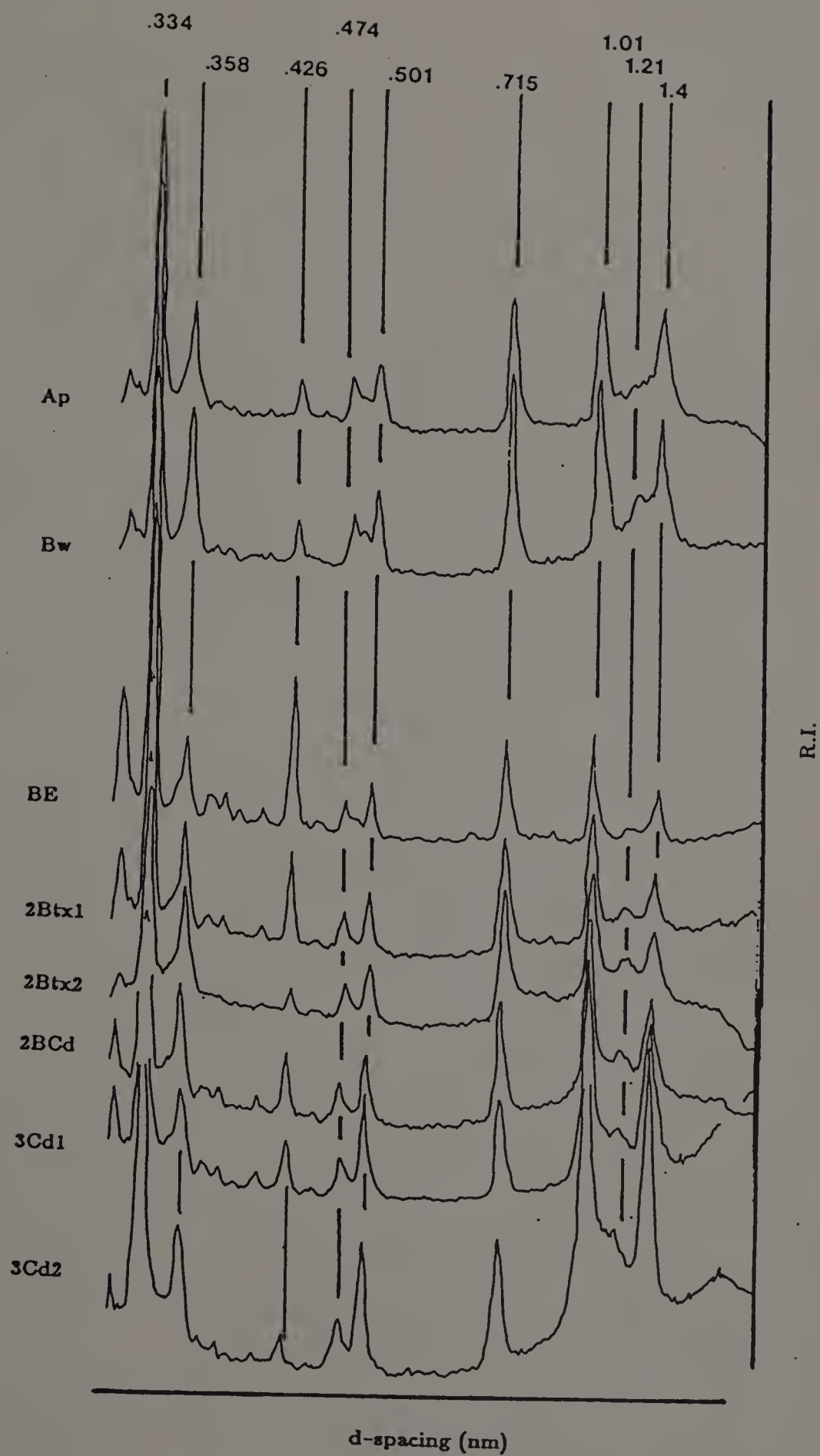
K-Sat. 550°

Pedon 3

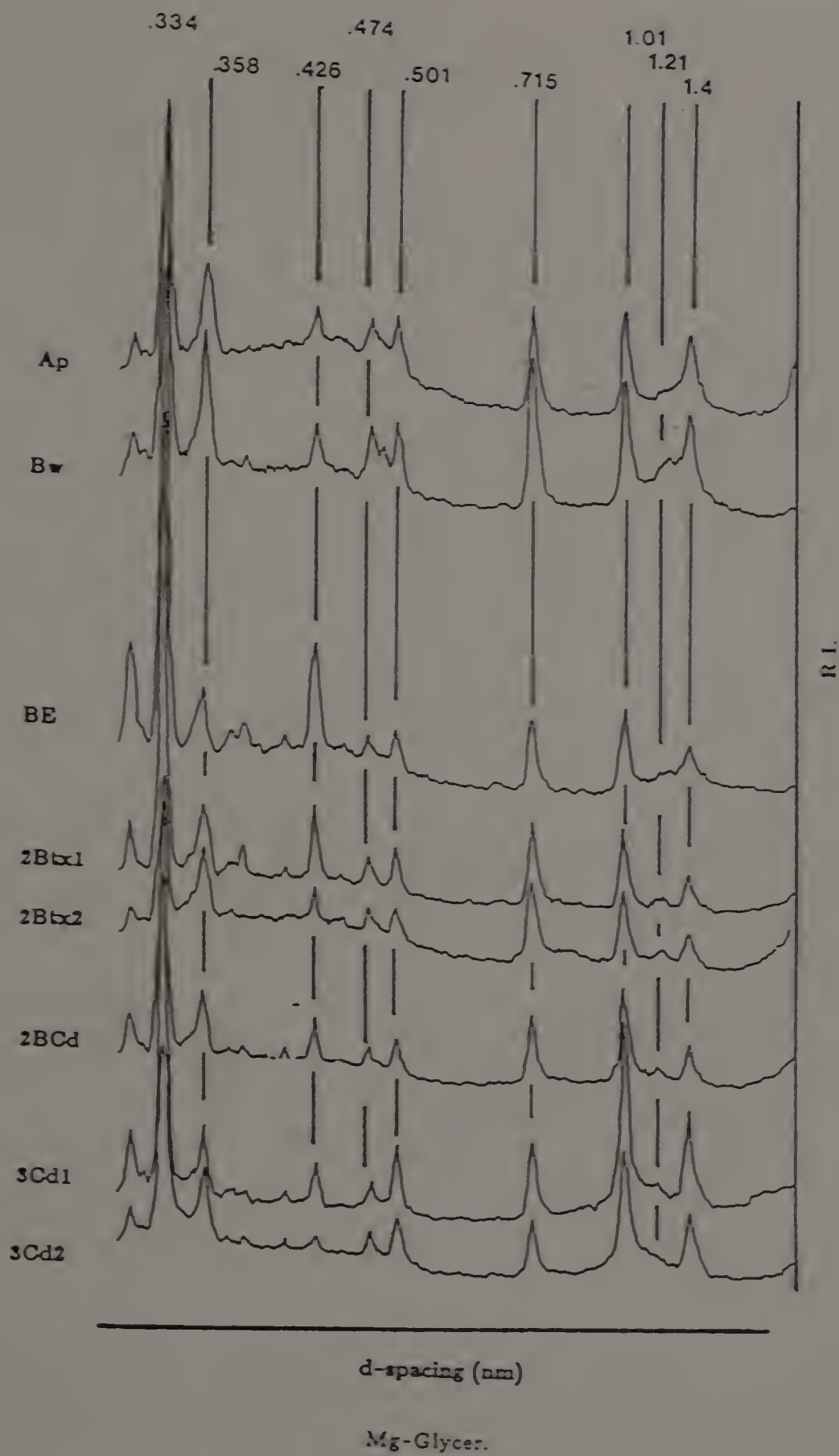


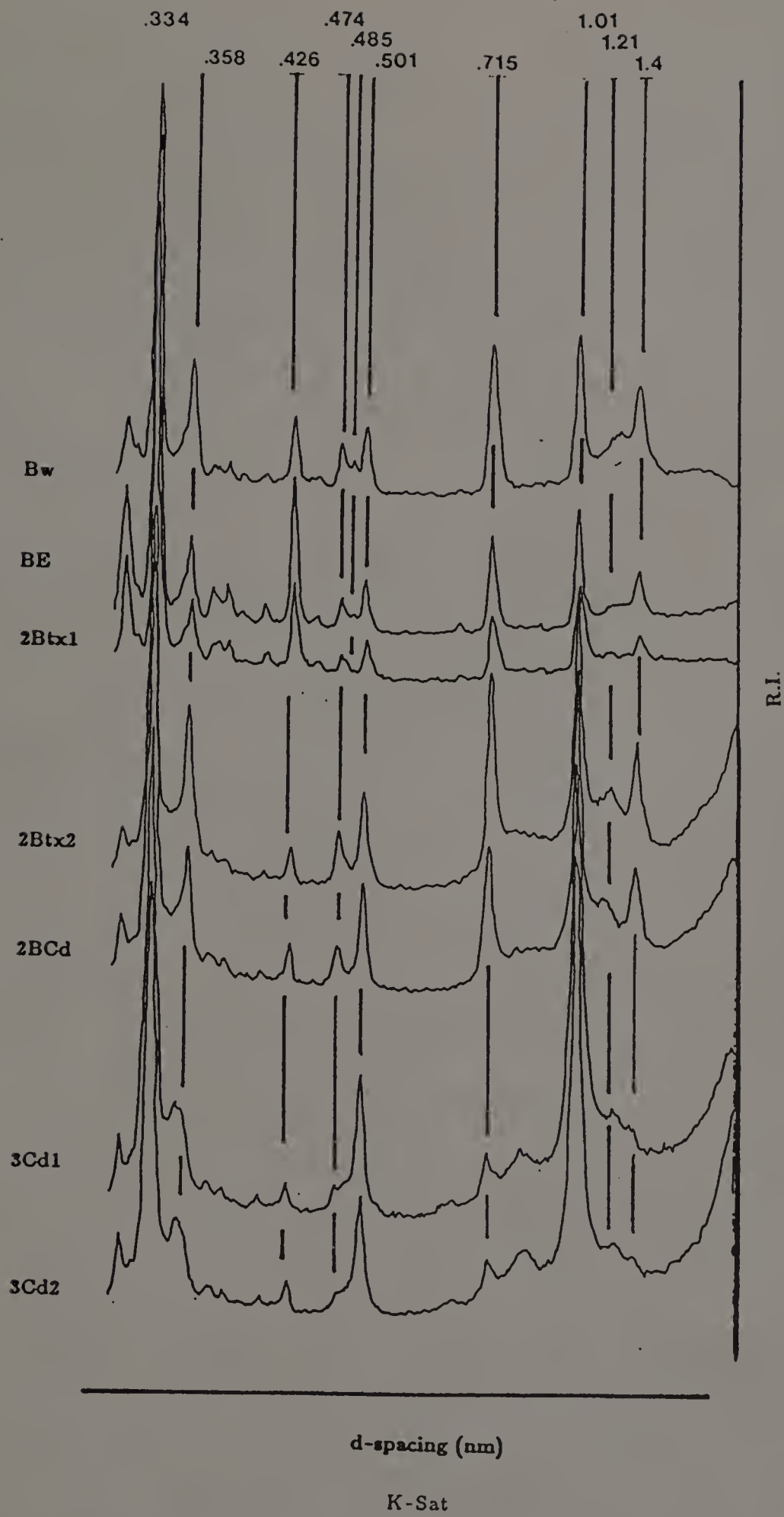


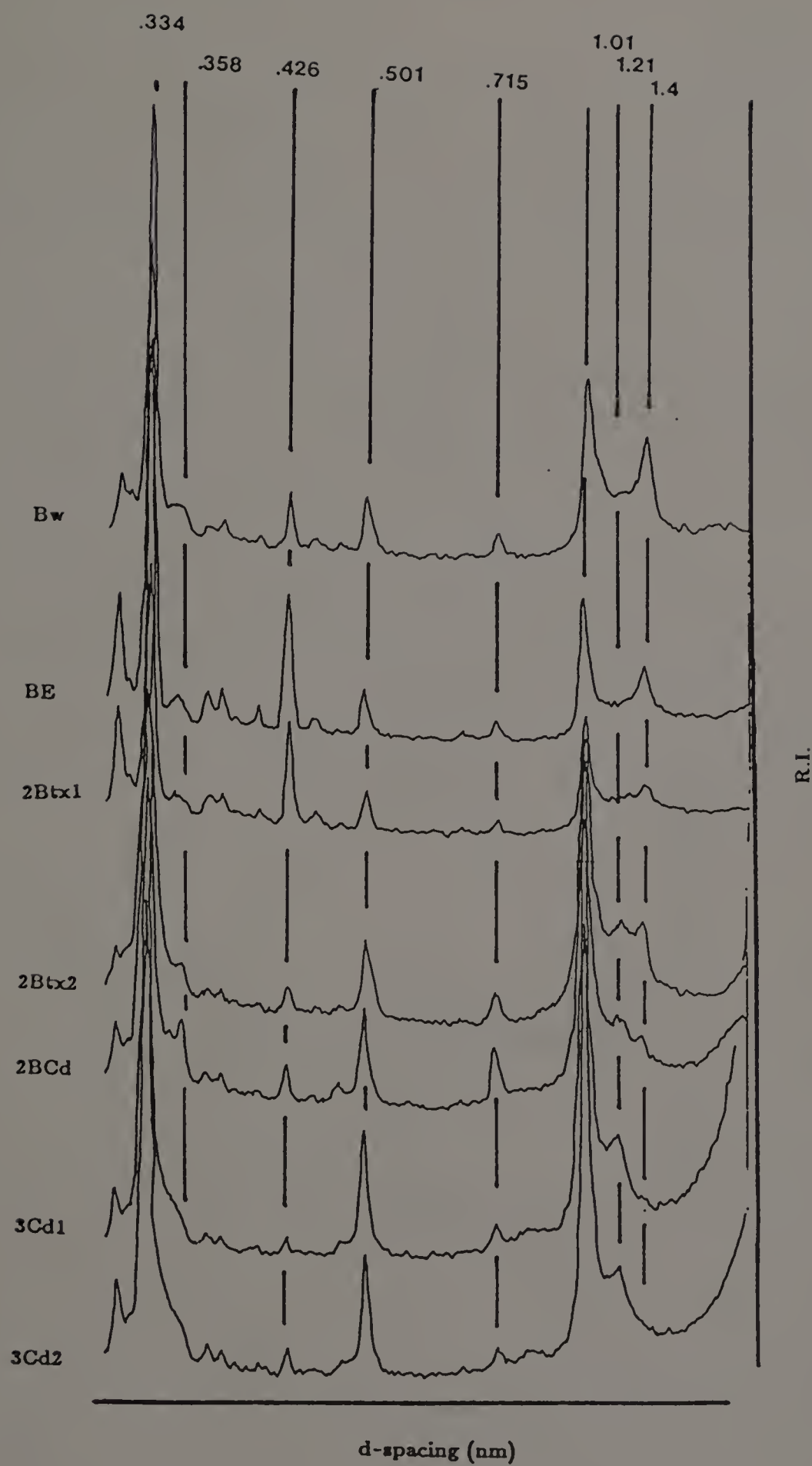




Mg-Sat.







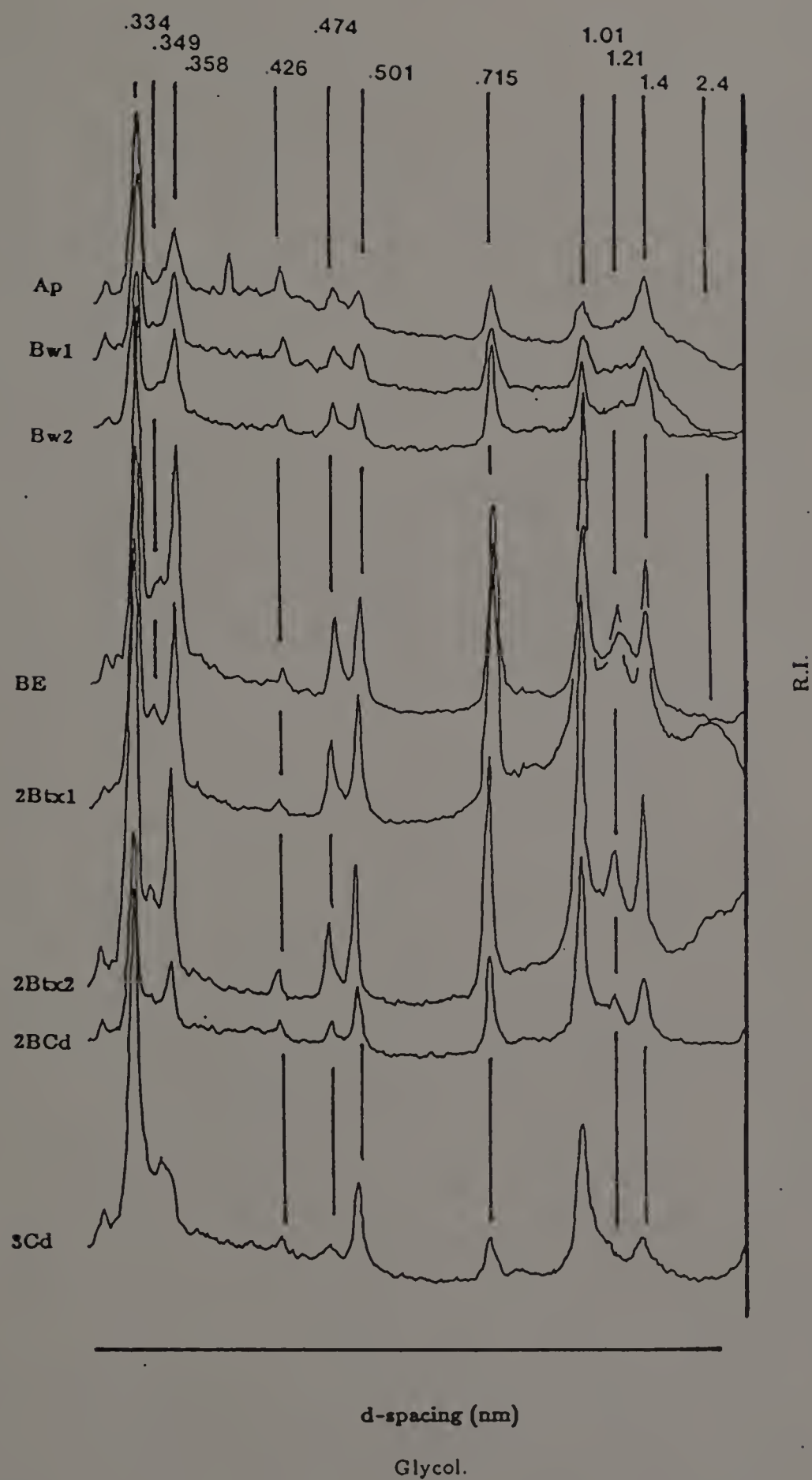
K-Sat. 550°

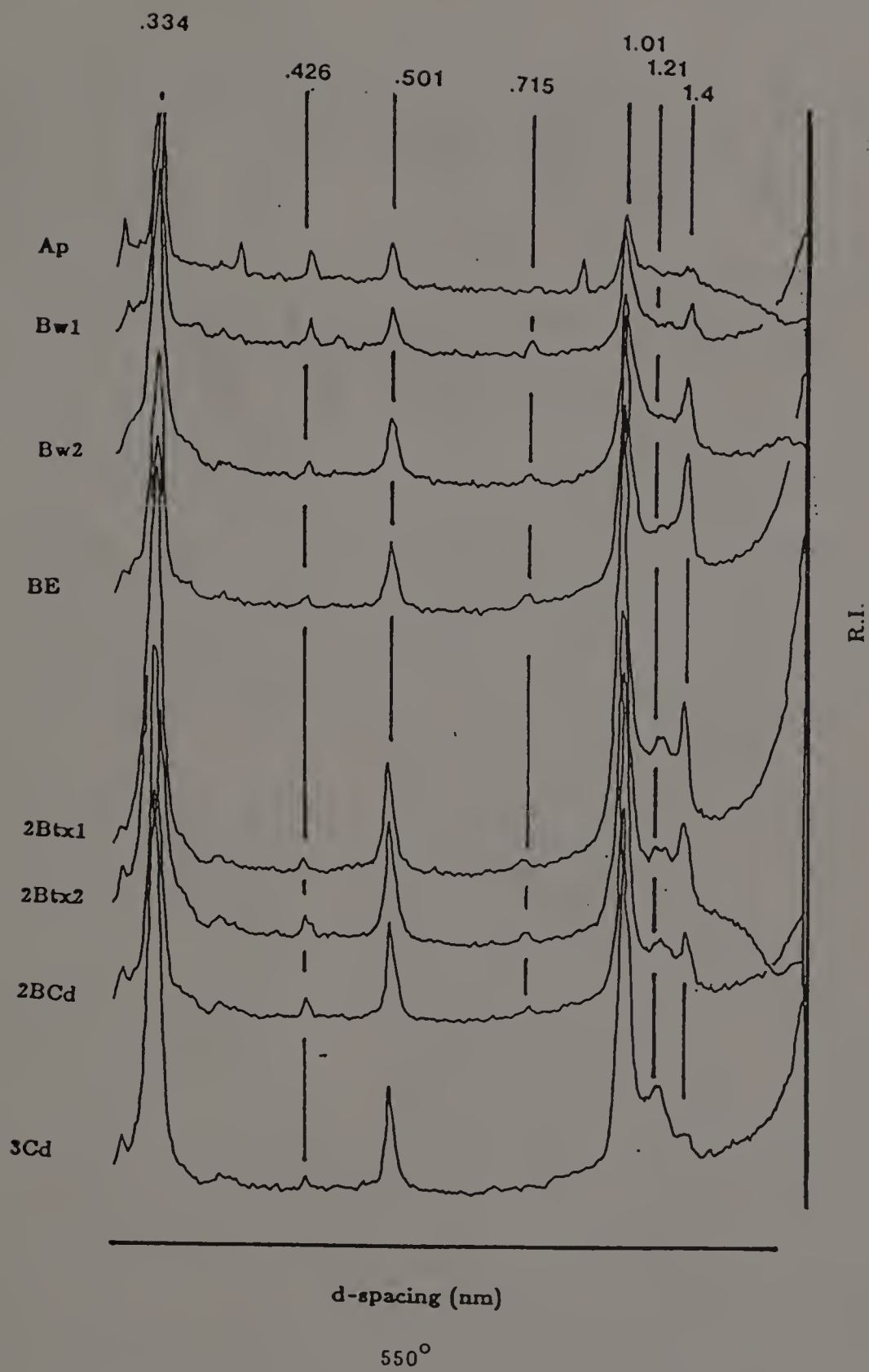
Pedon 4

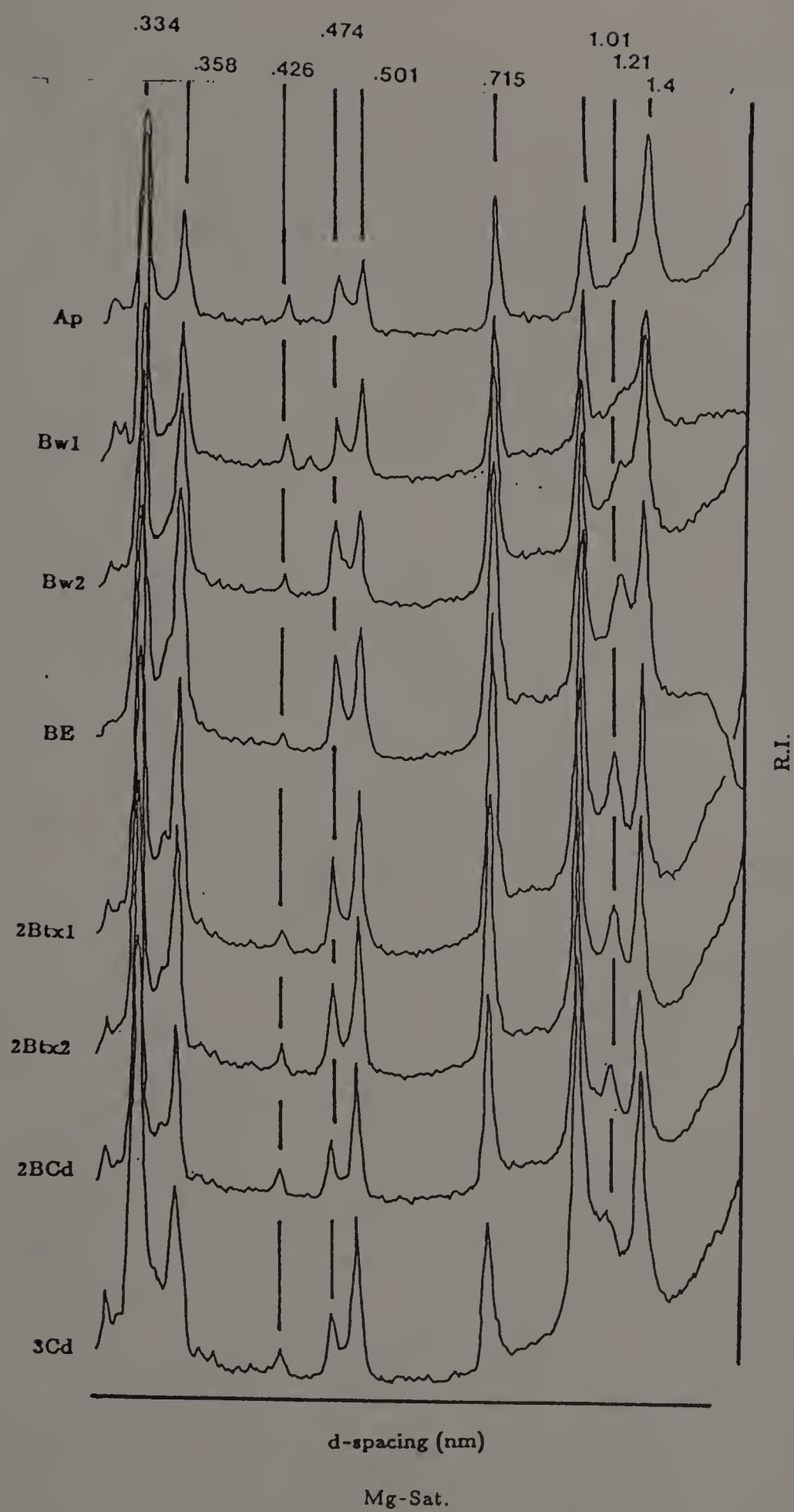


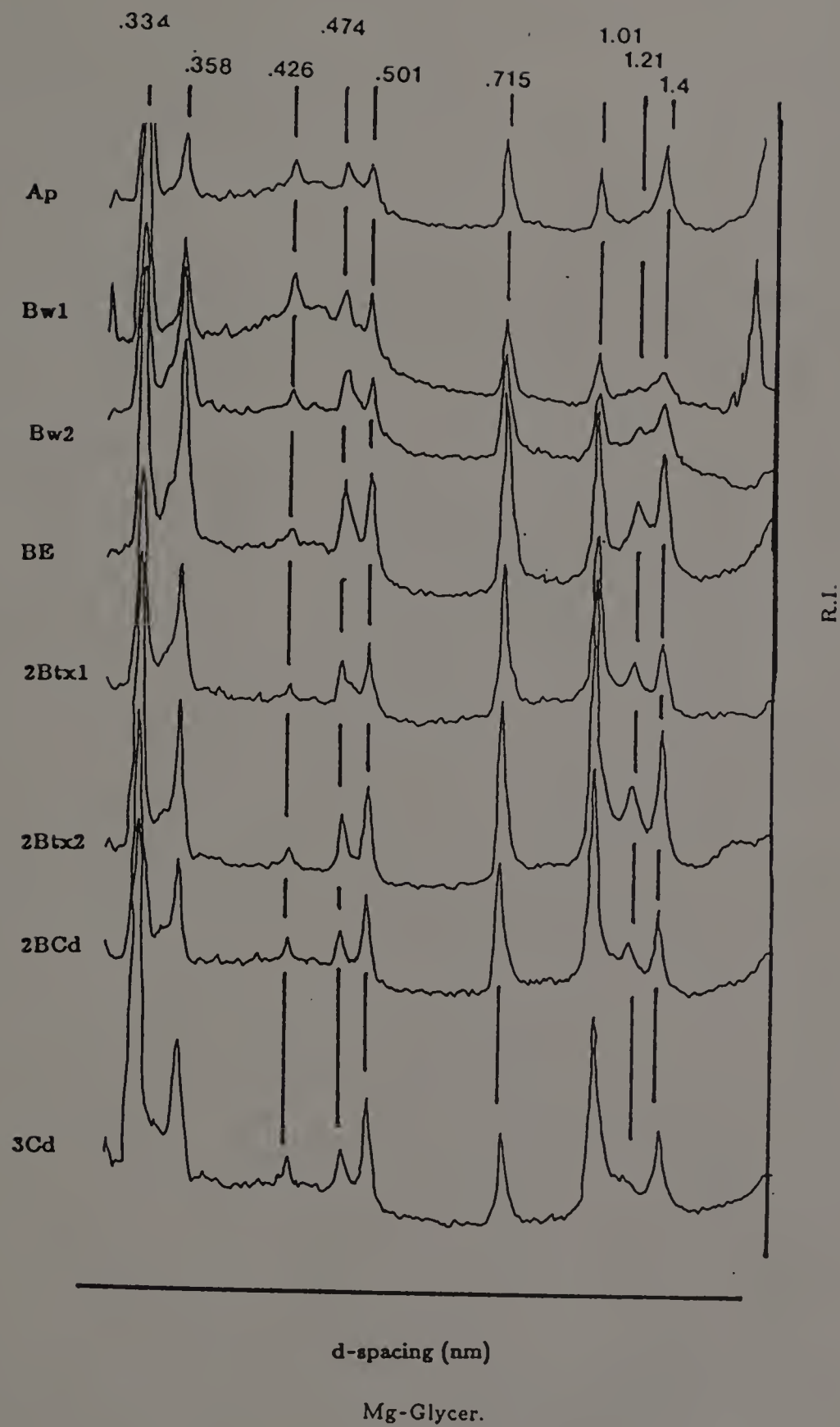
d-spacing (nm)

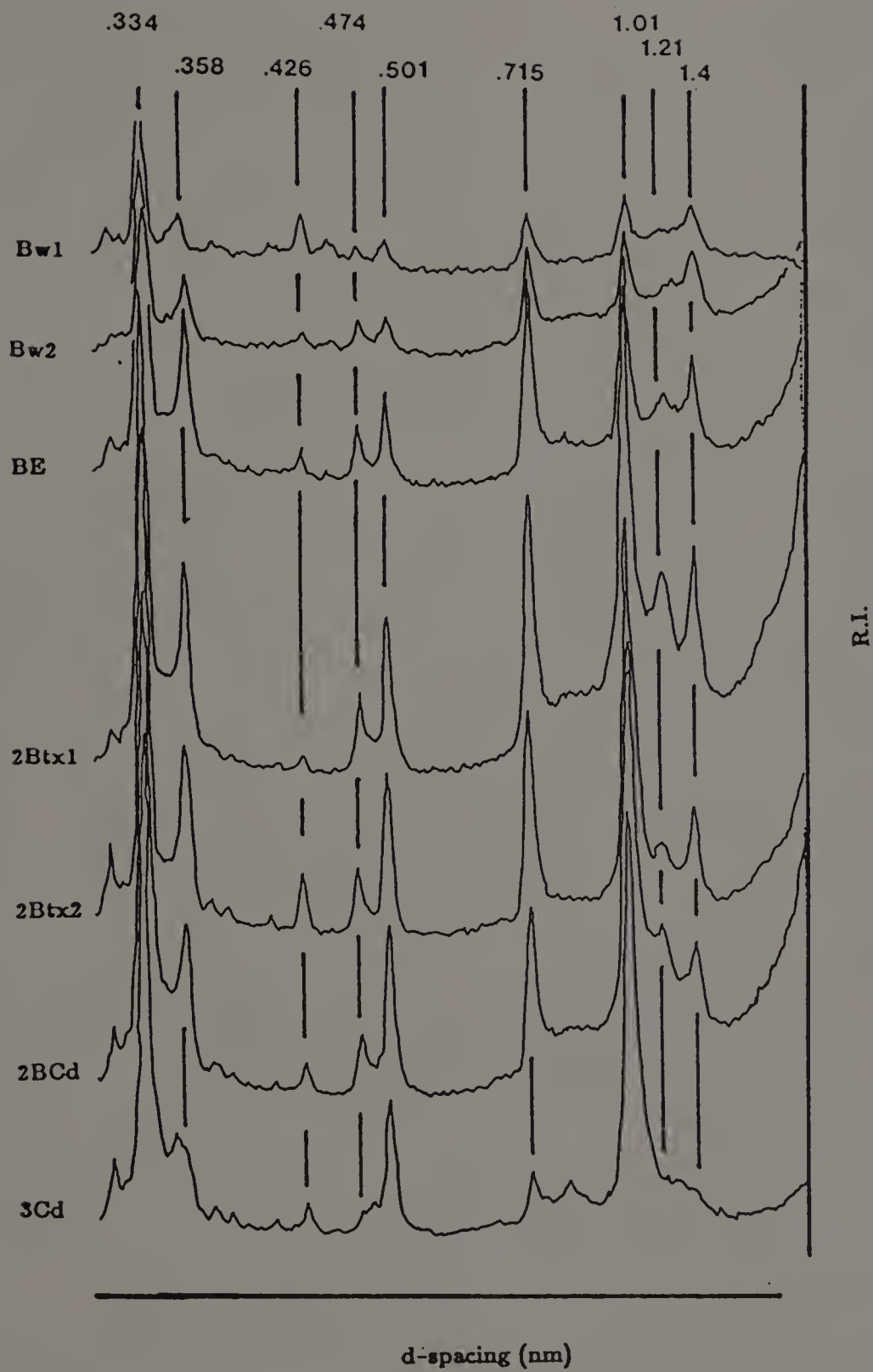
Na-Sat.



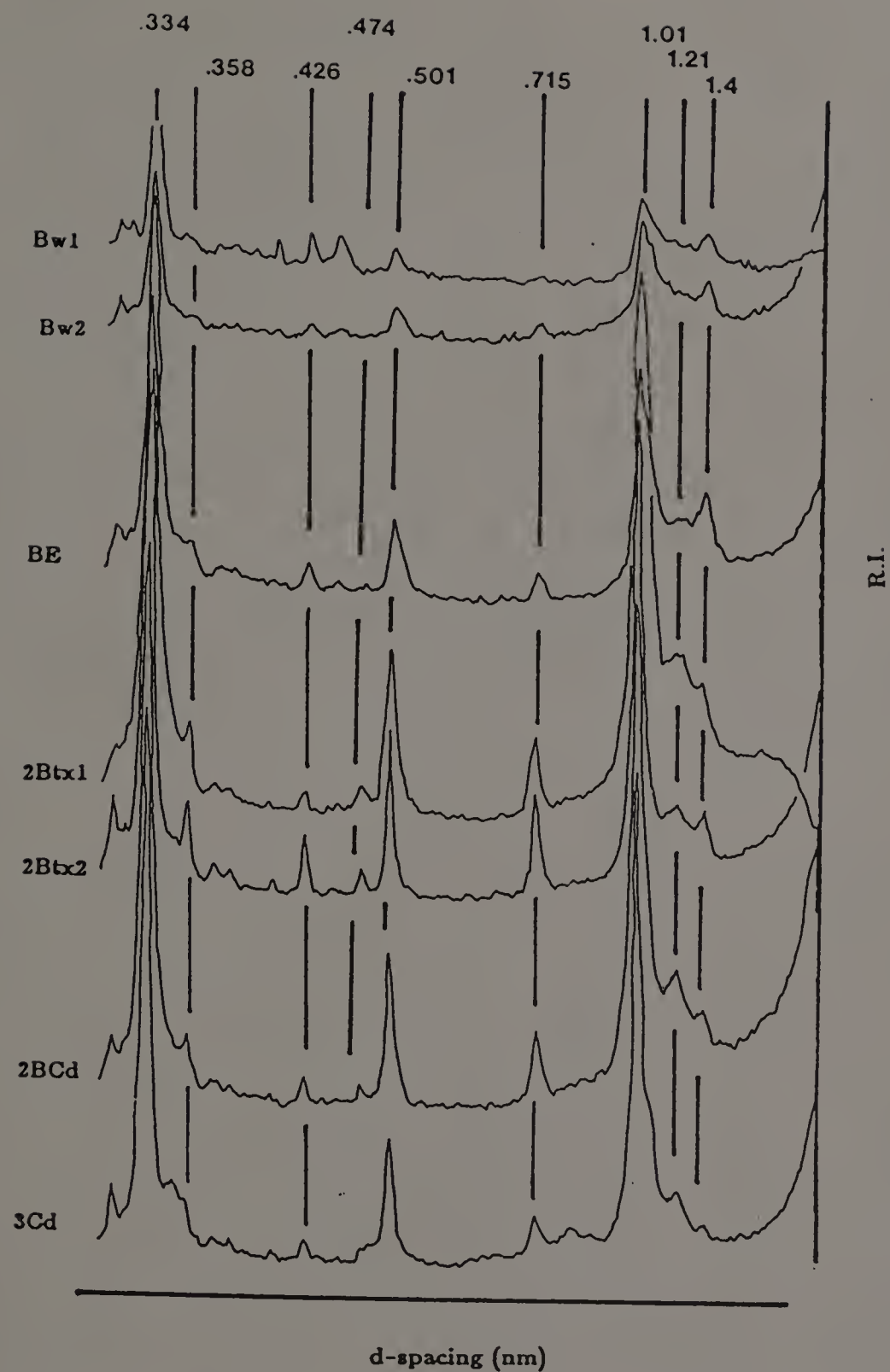






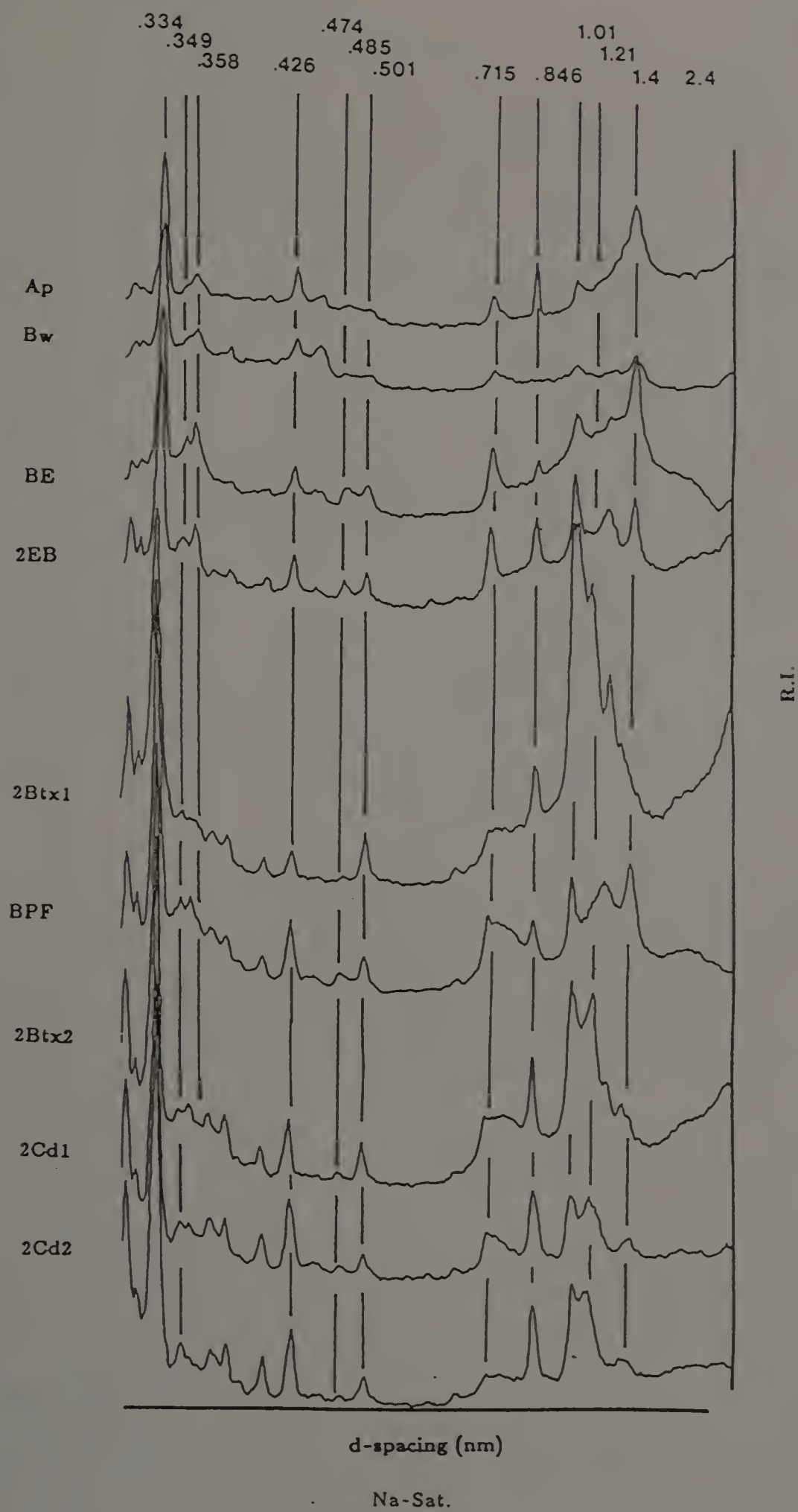


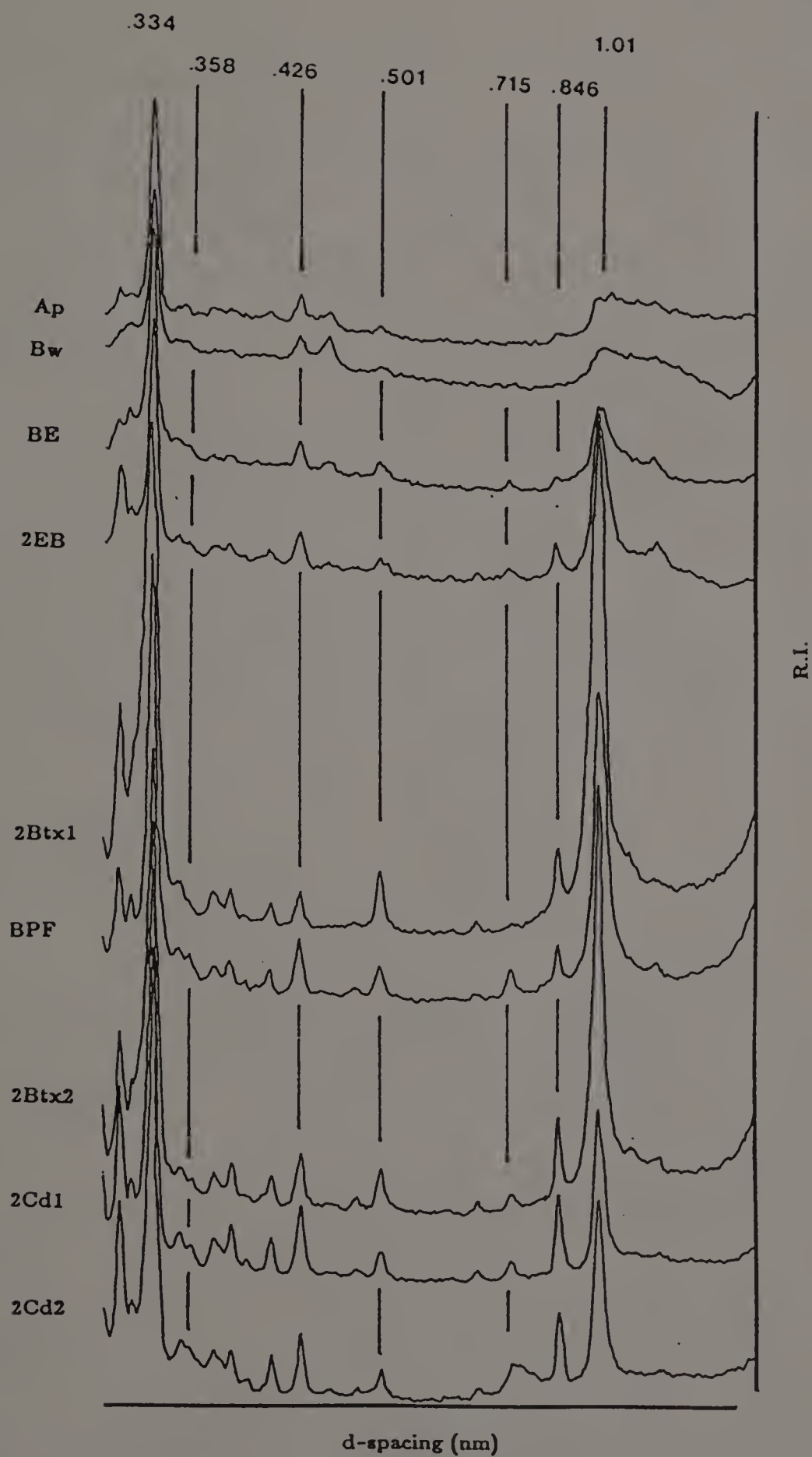
K-Sat



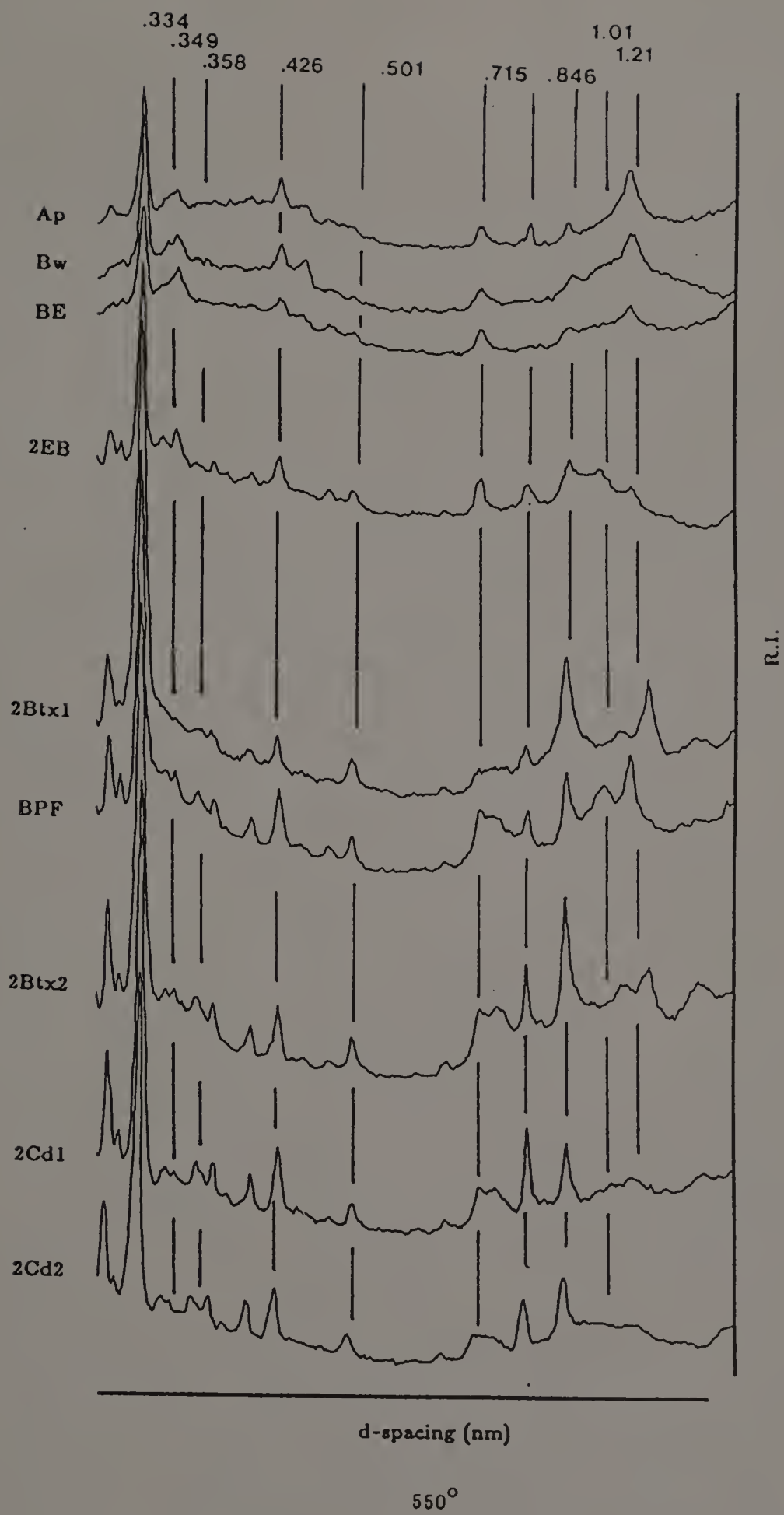
K-Sat. 550°

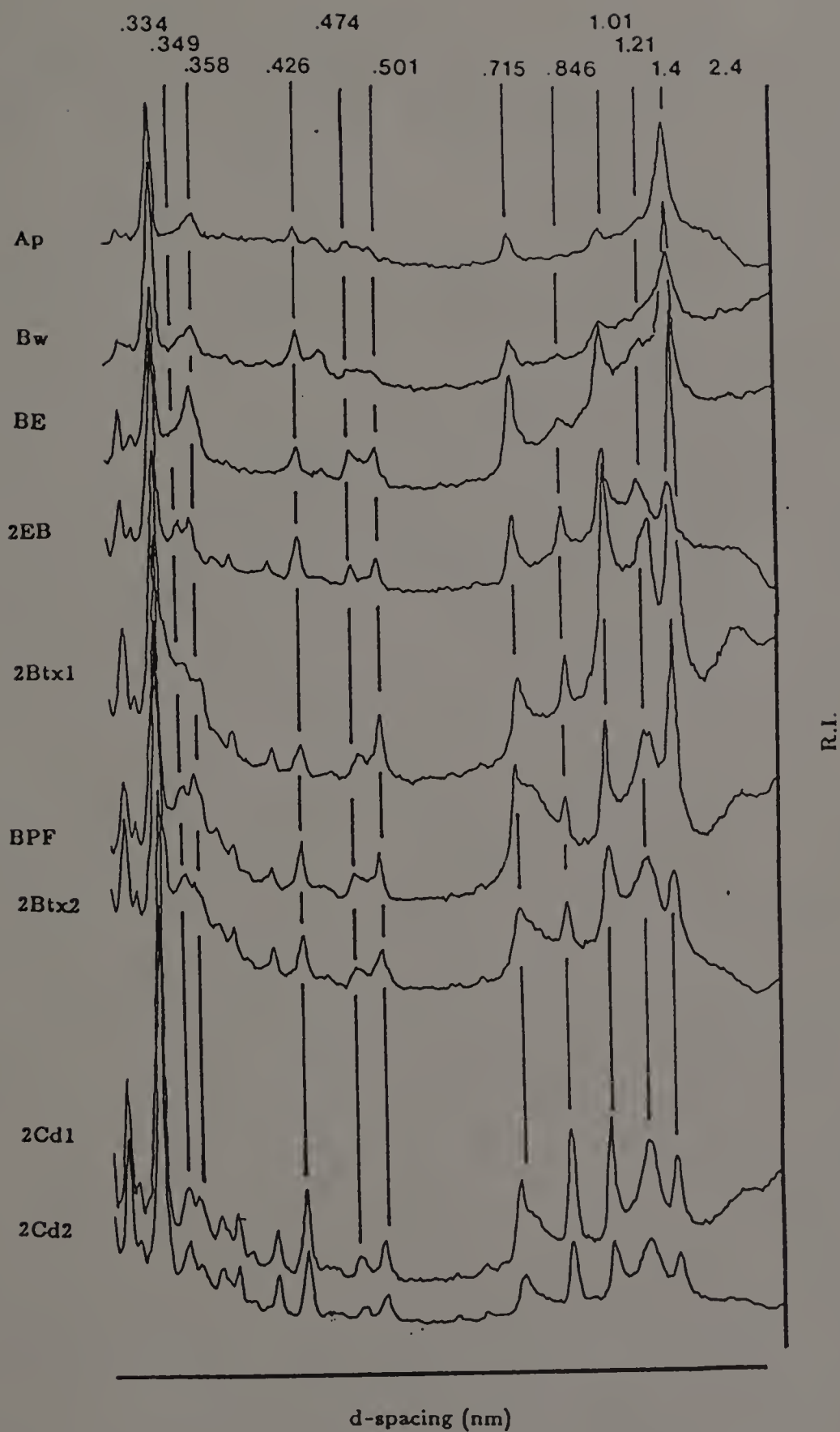
Pedon 5



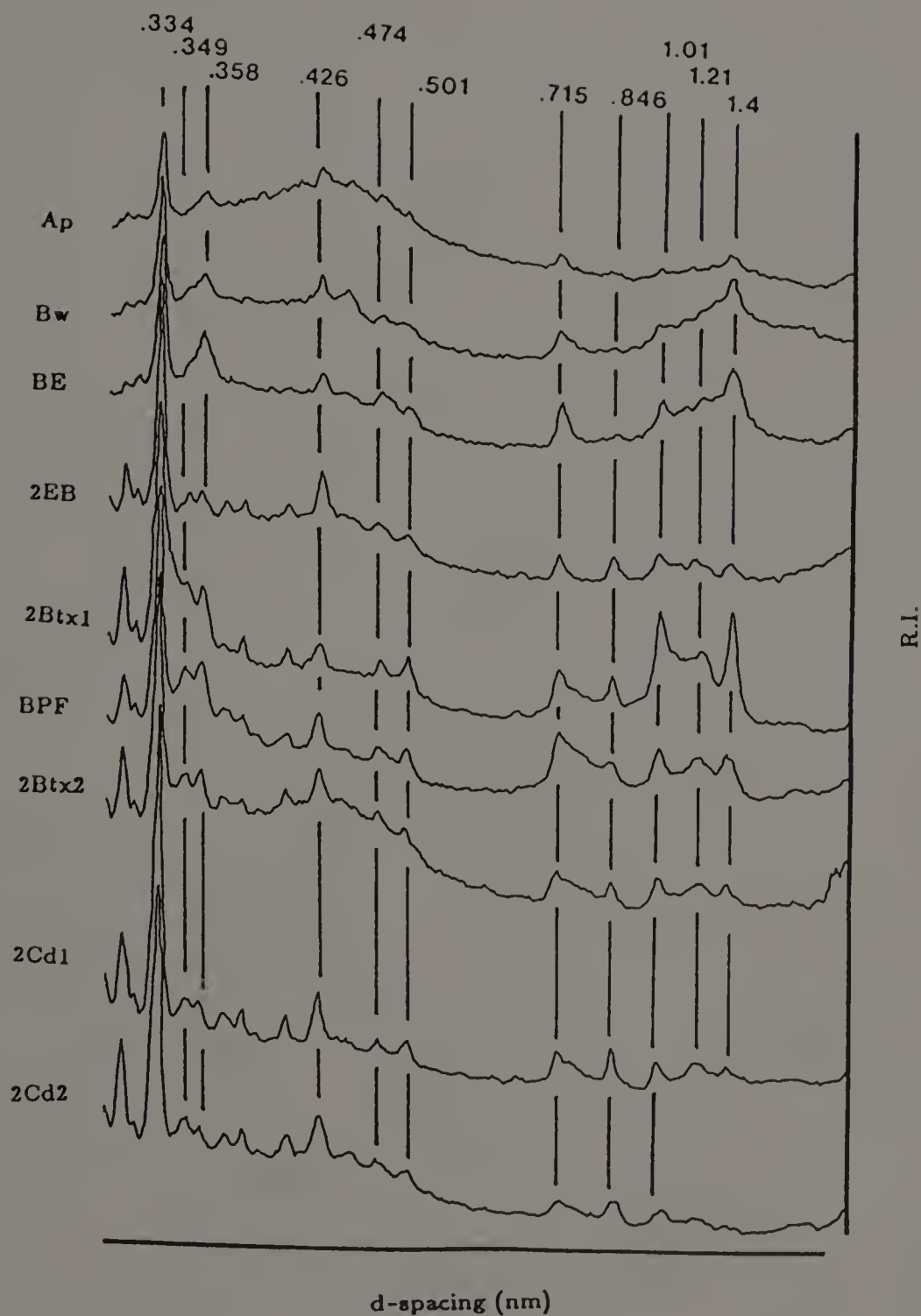


Glycol.

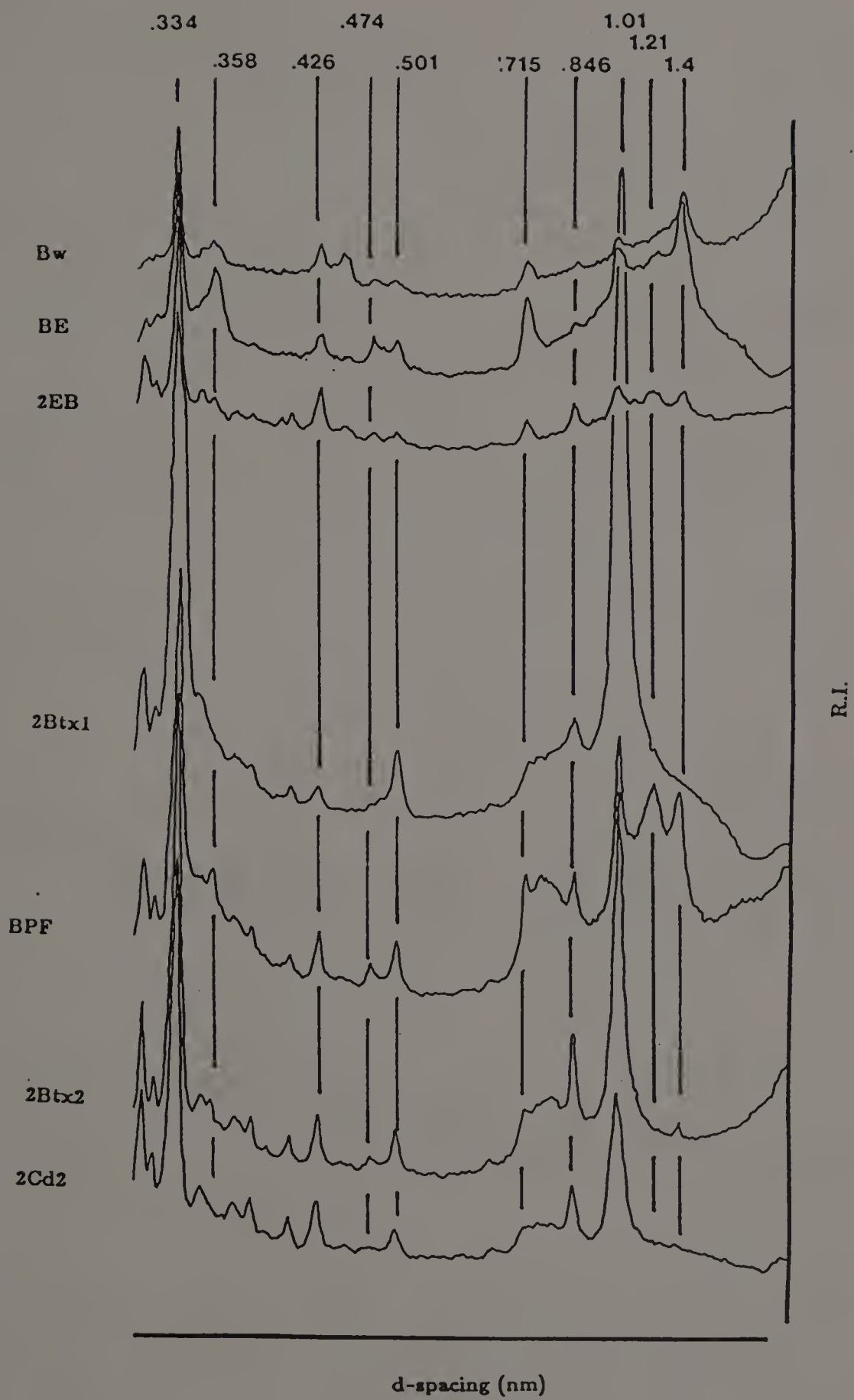




Mg-Sat.

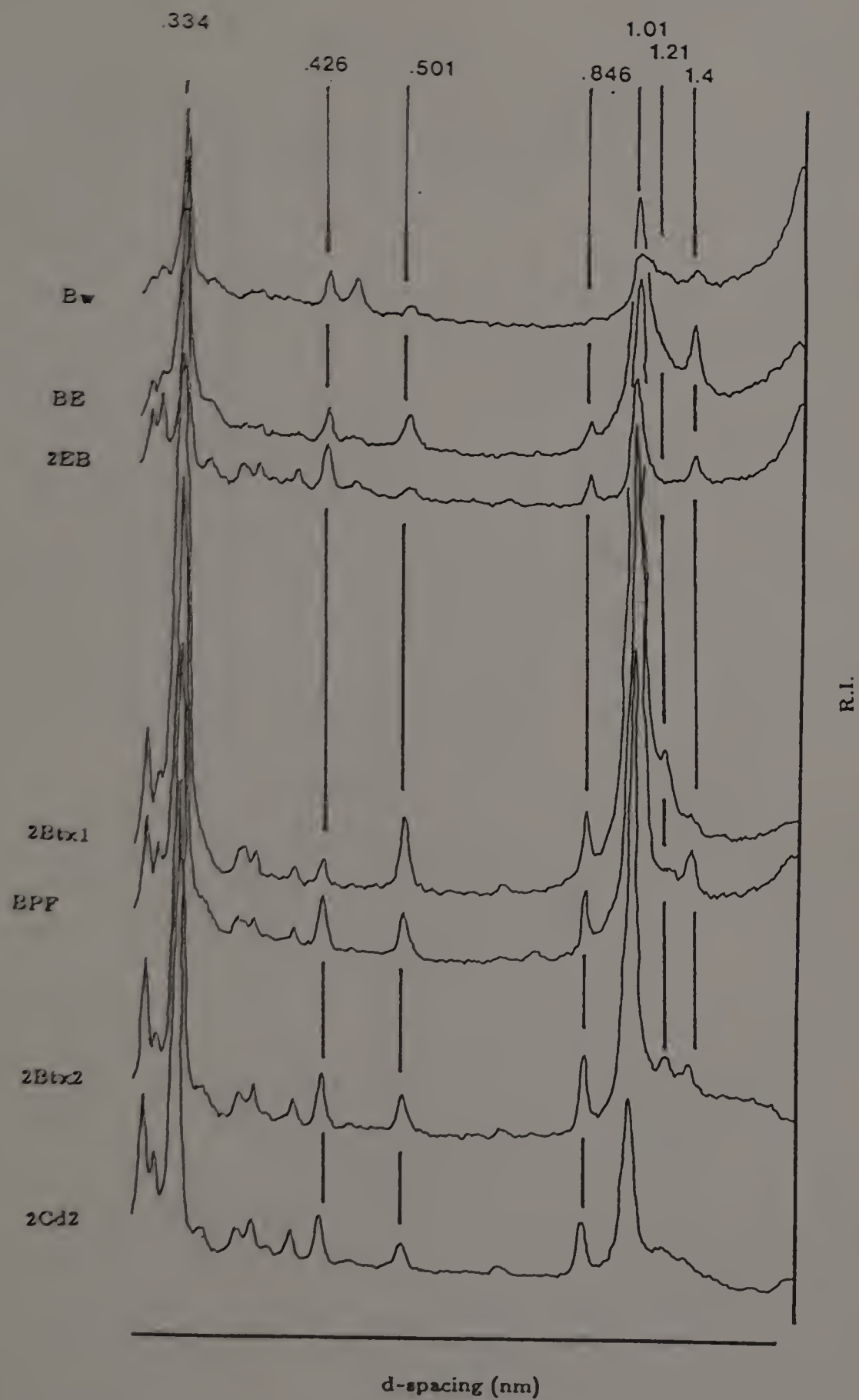


Mg-Glycer.



d-spacing (nm)

K-Sat



K-Sat. 550°

APPENDIX K

HEAVY MINERAL ANALYSIS

Pedon 1

	Ap	Bw1	Bw2	Bt	2Btx1	2Btx2	BPF	3BCm	4Cd	5Cr
Andalusite	1.5	1.3	0.6	0.2	0.7	0.4	0.3	7.5	1.2	0.3
Apatite										
Pyroxene	0.3	1.0	0.3	0.5	0.3	0.4	1.6	3.0	1.8	0.8
Epidote	5.1	4.6	3.5	3.6	4.6	5.2	4.5	2.3	4.0	1.3
Garnet Total	8.7	9.9	7.5	10.1	8.2	6.9	6.1	8.3	3.7	22.4
Red	0.6	0.5	0.6	0.2	1.1	0.4	0.3	0.8		6.9
Clear	8.1	9.4	6.9	9.9	7.1	6.5	5.8	7.5	3.7	15.5
Hornblende Total	8.7	6.8	6.9	4.8	6.4	8.1	8.0	25.9	6.7	7.5
Green	4.2	3.2	3.8	2.6	4.3	3.6	3.5	21.8	4.3	5.1
Brown	0.9	0.8	0.3			1.6	1.0	4.1	0.6	1.3
Blue	3.6	2.8	2.8	2.2	2.1	2.8	3.5		1.8	1.1
Monazite										
Rutile	2.7	3.8	5.3	4.1	5.7	3.6	3.5	0.3	1.5	4.3
Sillimanite	0.6	0.8	0.6	1.2	0.3	0.8	0.3	0.7	0.9	0.8
Staurolite					0.3					
Tourmaline	0.3	0.3	0.6	1.0	1.4	1.2	0.6	10.9	0.9	0.5
Tremolite	69.0	66.5	67.9	69.5	64.6	67.7	65.9	13.1	68.3	57.6
Zircon	1.2	2.3	2.5	1.7	4.3	2.0	4.2	13.9	3.4	2.9
Clino/Zoisite	1.8	2.8	4.1	3.4	2.9	3.0	4.8	13.9	7.6	2.9

Pedon 2

	Ap	Bw1	Bw2	BE	2Btx1	2Btx2	2BCd	3Cd1	3Cd2	3Cd3
Andalusite	3.9	1.8	0.9	1.6	1.7	1.3	1.9	1.1	3.0	2.3
Apatite										
Pyroxene	1.0	0.3		0.3	0.3	0.2				1.1
Epidote	3.4	2.5	1.2	2.5	1.7	2.1	1.9	1.5	2.6	2.3
Garnet Total	21.6	15.4	13.0	10.1	14.0	7.5	12.5	8.4	9.3	11.0
Red	8.2	4.3	3.4	2.4	5.0	2.4	1.9	2.3	1.1	1.5
Clear	13.4	11.1	9.6	7.7	9.0	5.1	10.6	6.1	8.2	9.5
Hornblende Total	23.5	16.0	20.9	19.7	16.3	24.3	21.7	23.4	22.3	17.1
Green	16.3	12.3	18.6	16.2	13.2	20.7	17.5	21.1	18.6	14.1
Brown	2.6	2.1	0.9	0.5	0.9	1.5	1.4	0.8	1.5	0.8
Blue	4.6	2.1	1.4	3.0	2.2	2.1	2.8	1.5	2.2	2.3
Monazite	0.3			0.5	0.3	0.2				
Rutile	3.9	4.6	3.5	4.4	5.1	3.6	3.7	4.2	3.7	4.6
Sillimanite	1.3	0.9	1.4	2.2	2.5	1.1	2.3	0.8	1.5	1.5
Staurolite						0.2				
Tourmaline	2.3	1.2	1.4	1.9	2.2	1.5	1.4	3.4	1.1	2.7
Tremolite	48.4	41.5	46.7	47.7	46.0	48.8	46.3	46.4	43.5	43.3
Zircon	8.2	7.7	5.5	4.7	4.5	4.5	4.6	8.0	7.4	7.6
Clino/Zoisite	5.9	8.0	5.5	4.4	5.3	4.7	3.7	2.7	5.6	6.5

Pedon 3								
	Ap	Bw	BE	2Btx1	2Btx2	2BCd	3Cd1	3Cd2
Andalusite								
Apatite								
Pyroxene	2.7	1.0	2.4	3.3	2.5	5.7	4.6	5.4
Epidote	25.3	26.6	23.4	23.2	21.7	15.3	21.3	23.4
Garnet Total	11.3	14.3	19.5	21.1	23.5	20.0	16.7	14.6
Red	1.1	1.7	1.8	1.8	3.7	2.7	2.5	1.3
Clear	10.7	12.6	17.7	19.3	20.4	17.2	14.2	13.4
Hornblende Total	40.0	40.5	30.8	33.1	27.6	27.1	22.5	27.6
Green	8.4	7.5	7.1	4.3	7.5	8.3	7.1	7.9
Brown		1.0	1.2	0.6	0.9		0.8	0.4
Blue	31.6	32.0	32.5	28.2	18.2	18.8	14.6	19.2
Monazite	0.4	0.3	1.2	0.9		1.2	1.7	0.4
Rutile	0.8	2.0	3.3	4.2	5.9	3.9	9.2	10.0
Sillimanite	0.8		0.9	0.9	1.5	1.2	0.8	1.3
Staurolite	0.8	2.3	4.1	0.9	1.9	3.9	2.9	0.4
Tourmaline	0.8	2.3	2.4	3.3	2.5	4.7	2.9	2.1
Tremolite								
Zircon	0.4	0.7	1.2	1.2	1.5	3.9	4.6	2.9
Clino/Zoisite	16.2	10.0	11.2	8.0	11.5	9.0	13.8	11.7

Pedon 4								
	Ap	Bw1	Bw2	BE	2Btx1	2Btx2	2BCd	3Cd
Andalusite	1.7	2.5	0.8	0.4	1.8	1.1	1.8	3.0
Apatite								
Pyroxene	2.6	1.7	1.9	1.7	3.3	3.4	5.7	7.2
Epidote	23.2	25.2	24.3	28.5	18.0	14.3	13.2	11.9
Garnet Total	12.0	8.0	9.3	9.7	19.5	18.3	17.6	18.2
Red	1.7	0.4	1.9	0.4	1.8	2.3	3.9	3.4
Clear	10.2	7.6	7.4	9.2	17.6	16.0	13.7	14.8
Hornblende Total	38.6	43.7	39.0	35.5	23.2	21.7	26.9	27.5
Green	7.7	8.4	6.2	3.9	5.5	5.1	5.3	7.6
Brown	0.9	0.8	1.5	0.4	0.4	2.3	0.8	0.4
Blue	30.0	34.5	31.3	31.1	17.3	14.3	20.9	19.5
Monazite	0.9	1.7	1.5	1.3	1.5	2.3	1.8	0.8
Rutile	0.4	1.7	1.9	6.1	11.0	14.9	10.1	9.3
Sillimanite	1.7	0.4	0.8	0.9	0.7	2.3	0.4	0.4
Staurolite	0.4	0.4	0.8	0.4	2.9	3.4	4.0	1.7
Tourmaline	2.6	2.9	1.5	1.3	4.0	3.4	3.5	3.0
Tremolite								
Zircon	8.6	2.9	6.6	6.6	9.2	8.0	10.6	10.6
Clino/Zoisite	7.3	8.8	11.6	7.5	4.8	6.9	4.4	6.8

Pedon 5

	Ap	Bw	BE	2BE	2Btx1	2Btx2	2Cd1	2Cd2	BPF
Andalusite	0.4	2.3	3.5	1.8	2.9	4.1	4.0	3.7	1.4
Apatite									
Pyroxene	1.3	1.5	0.9	1.1	0.3	1.2	0.9	1.4	0.5
Epidote	13.6	11.7	11.6	10.8	9.8	11.7	12.4	10.4	9.8
Garnet Total	4.3	8.3	9.1	11.5	5.5	5.1	5.3	3.1	3.6
Red	0.9	1.9	1.9	2.2	0.6	1.9	2.2	1.1	1.9
Clear	3.4	6.4	7.2	9.3	4.1	3.2	3.1	2.0	1.7
Hornblende Total	60.9	61.1	59.7	62.2	66.7	65.9	70.0	66.2	72.5
Green	11.1	12.8	10.4	12.6	11.7	12.7	9.3	6.0	6.9
Brown	1.7	1.1	1.2		0.6	0.7	0.3	0.3	1.4
Blue	48.1	47.2	48.1	49.6	54.3	52.5	60.4	59.9	64.3
Monazite									
Rutile		0.4	0.3	0.3	0.6	0.5		0.3	0.3
Sillimanite	3.0	1.1	0.6	0.7	0.3				
Staurolite		0.4		0.3					0.3
Tourmaline	0.9	0.4	1.9	1.1	1.3	0.5		1.4	0.5
Tremolite	2.1	2.3	2.5	1.4	2.9	2.7	2.2	2.6	2.7
Zircon	4.7	2.6	2.5	1.4	1.6	4.9	1.5	3.4	2.5
Clino/Zoisite	0.4	1.5			0.3				

APPENDIX L

COLUMN DATA

Particle Size Analysis

BTR Column

Hori.	VC	C	Sand M	F	VF	Total Sand	Silt		Clay
							C	F	
CaCl ₂	5.60	9.01	15.25	18.56	20.92	69.34	9.01	13.54	8.02
AmOx	3.97	7.54	14.70	17.45	21.08	64.74	12.69	14.50	8.07
Pyro	5.31	8.14	15.83	17.53	21.46	67.27	10.73	14.99	7.01
NaOH	4.89	8.43	16.57	17.85	20.60	68.34	10.10	14.52	7.04

BTR/S Column

Hori.	VC	C	Sand M	F	VF	Total Sand	Silt		Clay
							C	F	
CaCl ₂	3.99	7.52	14.73	26.31	10.90	63.45	12.60	12.93	11.03
AmOx	2.70	7.55	16.13	27.14	12.03	65.55	13.49	10.49	10.48
Pyro	3.50	8.07	16.42	28.06	7.99	64.04	7.62	17.18	11.17
NaOH	3.96	9.22	16.12	25.75	11.52	66.57	9.46	12.75	11.23

EHP Column

Hori.	VC	C	Sand M	F	VF	Total Sand	Silt		Clay
							C	F	
CaCl ₂	3.62	6.32	8.71	15.44	17.87	51.97	15.09	7.00	25.94
AmOx	4.54	6.74	9.41	15.20	18.84	54.73	8.14	8.08	29.03
Pyro	4.95	6.64	8.38	14.35	19.41	53.55	7.81	12.74	25.90
NaOH	6.00	7.76	9.67	14.91	11.84	51.67	10.17	11.05	27.11

OHW Column

Hori.	VC	C	Sand M	F	VF	Total Sand	Silt		Clay
							C	F	
CaCl ₂	6.56	10.75	14.28	21.27	6.09	59.75	9.82	15.79	14.65
AmOx	6.88	9.26	12.33	17.81	7.41	53.77	14.35	14.42	17.46
Pyro	8.90	9.87	12.91	19.05	7.06	58.69	10.17	17.98	10.17
NaOH	6.47	10.85	13.92	24.46	7.14	62.84	7.89	13.31	15.97

OH Till (3Cd) Column

Hori.	VC	C	Sand M	F	VF	Total Sand	Silt C	F	Clay
CaCl ₂	6.86	9.81	12.25	15.28	10.82	55.02	11.61	10.16	23.21
AmOx	6.08	9.28	12.13	15.52	11.71	54.72	10.15	10.04	25.09
Pyro	6.90	9.43	12.29	15.35	11.66	55.65	10.69	11.29	22.37
NaOH	6.87	10.21	12.46	17.04	10.23	56.81	9.38	10.50	23.31

BHW Column

Hori.	VC	C	Sand M	F	VF	Total Sand	Silt C	F	Clay
CaCl ₂	3.79	6.07	9.58	13.53	19.19	52.16	12.34	15.41	20.09
AmOx	3.49	6.24	10.46	14.30	18.79	53.28	10.96	14.55	21.21
Pyro	3.28	7.01	12.82	13.80	17.55	36.91	31.50	12.02	19.57
NaOH	4.66	7.42	11.05	13.87	18.08	37.00	30.56	17.03	15.41

BHR Column

Hori.	VC	C	Sand M	F	VF	Total Sand	Silt C	F	Clay
CaCl ₂	8.92	9.78	12.74	13.93	18.49	63.86	18.03	12.07	6.04
AmOx	12.88	14.00	14.35	14.09	18.14	73.46	12.50	8.62	5.42
Pyro	8.86	11.48	14.66	15.75	19.98	70.73	18.19	7.05	4.03
NaOH	8.71	11.31	13.46	15.13	19.03	67.64	12.24	10.06	10.06

BH Till (3Cd) Column

Hori.	VC	C	Sand M	F	VF	Total Sand	Silt C	F	Clay
CaCl ₂	3.29	5.10	9.36	23.35	14.59	55.71	14.36	8.13	21.80
AmOx	4.89	5.28	8.34	14.81	15.58	48.89	15.94	10.02	25.15
Pyro	4.38	8.38	10.03	22.77	12.97	58.54	11.76	6.76	22.94
NaOH	3.23	5.77	9.45	16.94	17.80	53.20	13.46	9.61	23.73

Selected Chemical Analysis

BTR Column

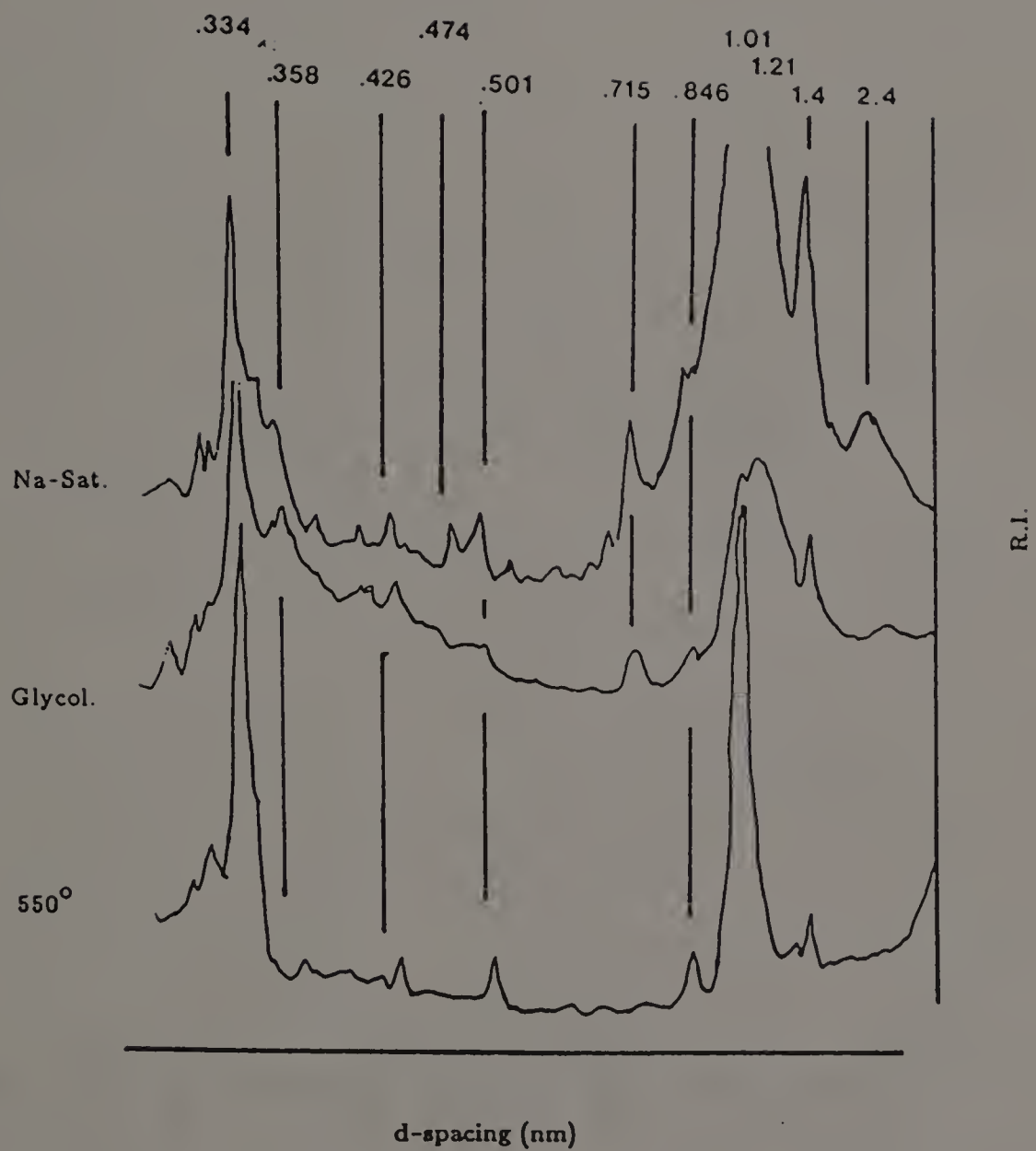
Hor.	H ₂ O	pH		O.C.	Ex Acid	Ca	CEC			Sum Bases	Total CEC
		KCl	CaCl ₂				Mg	Na	K		
CaCl ₂	5.59	4.69	5.50	0.08	0.54	4.741	0.276	0.045	0.051	5.113	5.653
AmOx	7.01	4.83	6.77	0.08	0.00	2.894	0.058	0.015	0.015	2.982	2.982
Pyro	7.10	7.02	7.00	0.07	0.14	3.094	0.045	--	0.031	--	--
NaOH	8.61	8.14	7.73	0.09	0.00	2.819	0.086	--	0.027	--	--

BHW Column

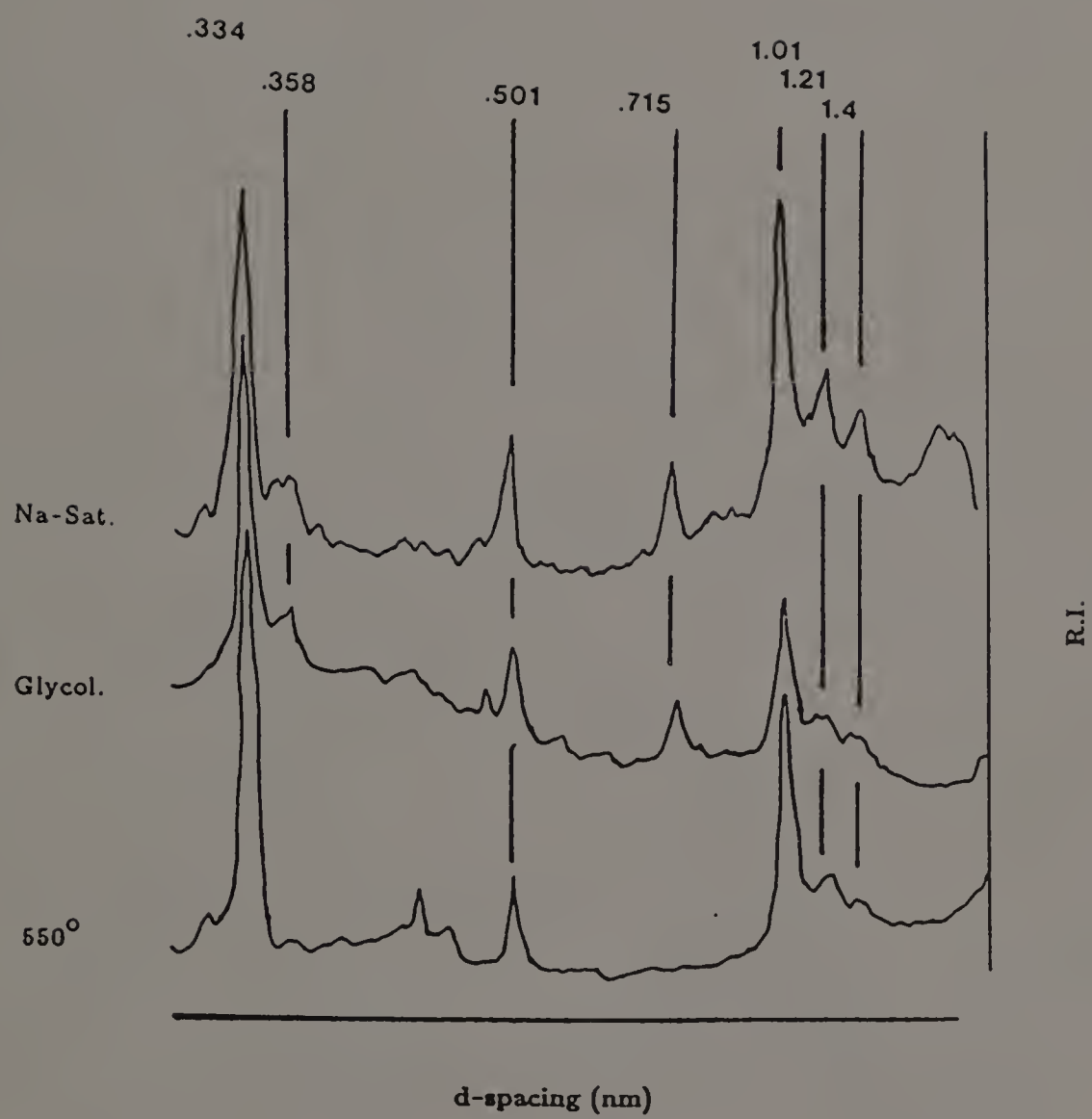
Hor.	H ₂ O	pH		O.C.	Ex Acid	Ca	CEC			Sum Bases	Total CEC
		KCl	CaCl ₂				Mg	Na	K		
CaCl ₂	4.59	4.14	4.81	--	2.71	4.167	0.062	0.039	0.181	4.449	7.159
AmOx	4.58	3.80	4.32	--	4.30	0.549	0.333	0.022	0.042	0.946	5.246
Pyro	9.23	8.84	9.30	--	0.97	0.574	0.095	--	0.135	--	--
NaOH	10.31	9.93	10.32	--	0.00	1.422	0.062	--	0.080	--	--

BHR Column

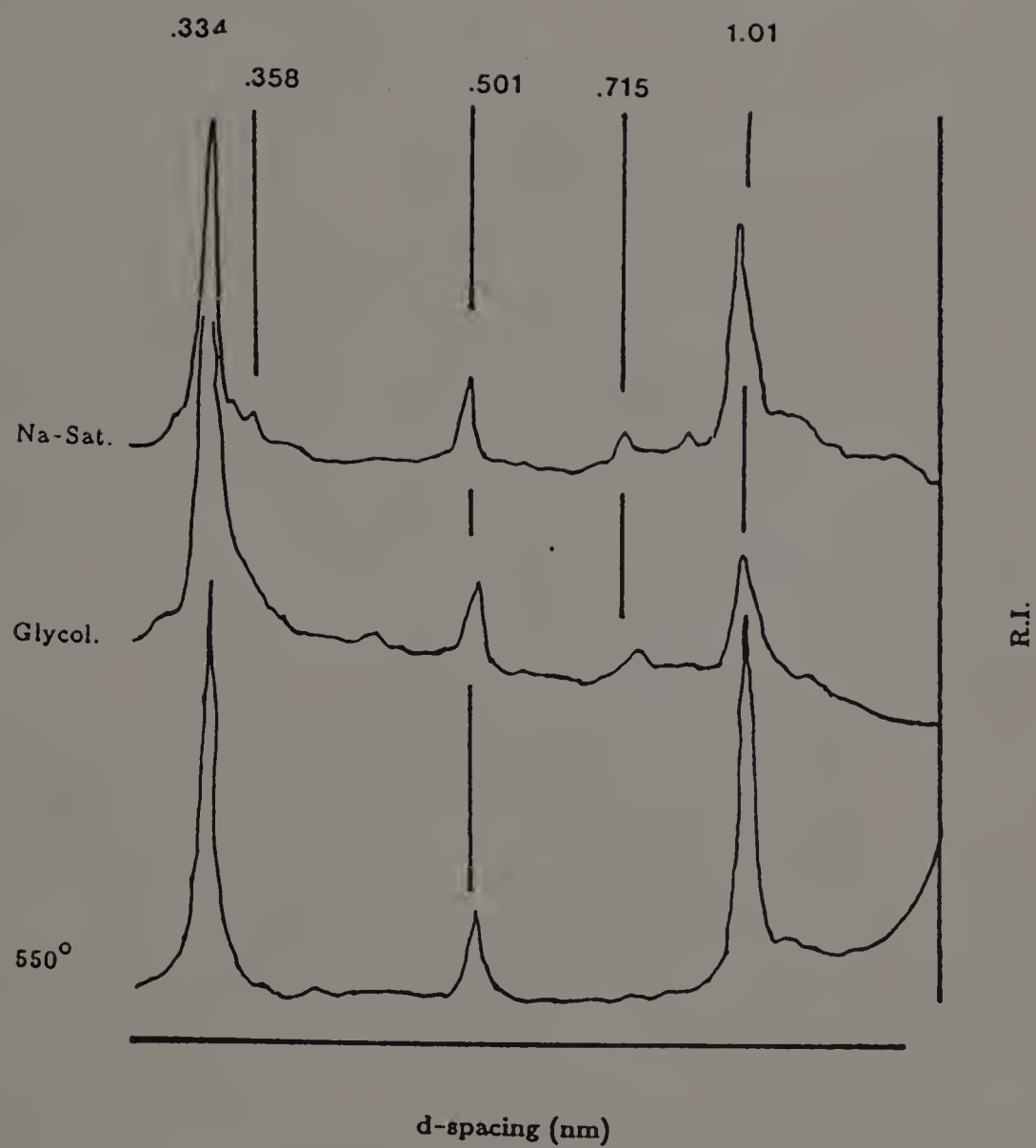
Hor.	H ₂ O	pH		O.C.	Ex Acid	Ca	CEC			Sum Bases	Total CEC
		KCl	CaCl ₂				Mg	Na	K		
CaCl ₂	5.22	4.52	5.29	0.20	1.90	4.391	0.082	0.007	0.068	4.548	6.448
AmOx	3.89	3.64	3.91	0.21	2.06	2.146	0.156	0.013	0.027	2.342	4.402
Pyro	9.19	8.49	8.42	0.29	0.00	1.322	0.078	--	0.069	--	--
NaOH	10.10	9.64	9.20	0.20	0.26	1.272	0.185	--	0.036	--	--



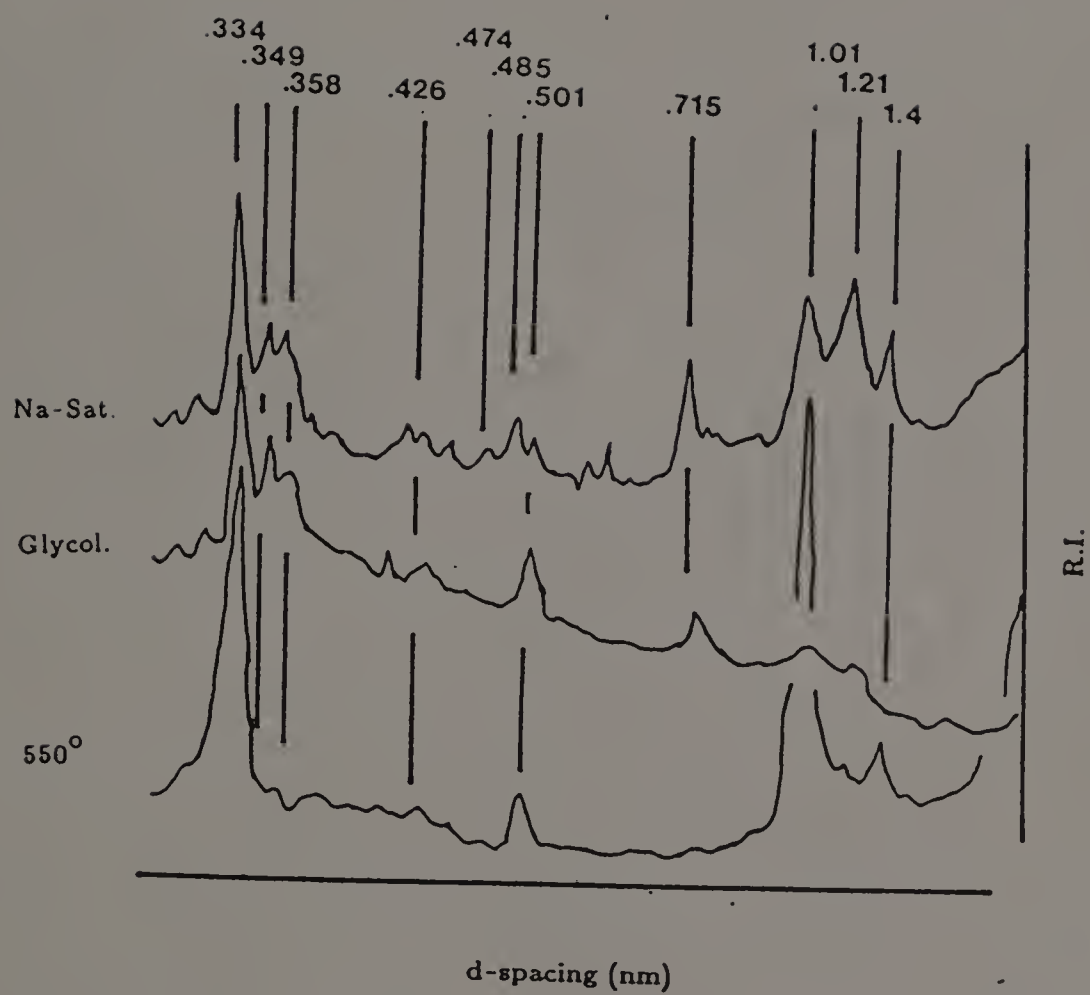
Belchertown Ridgebury/Scituate (BTR/S)



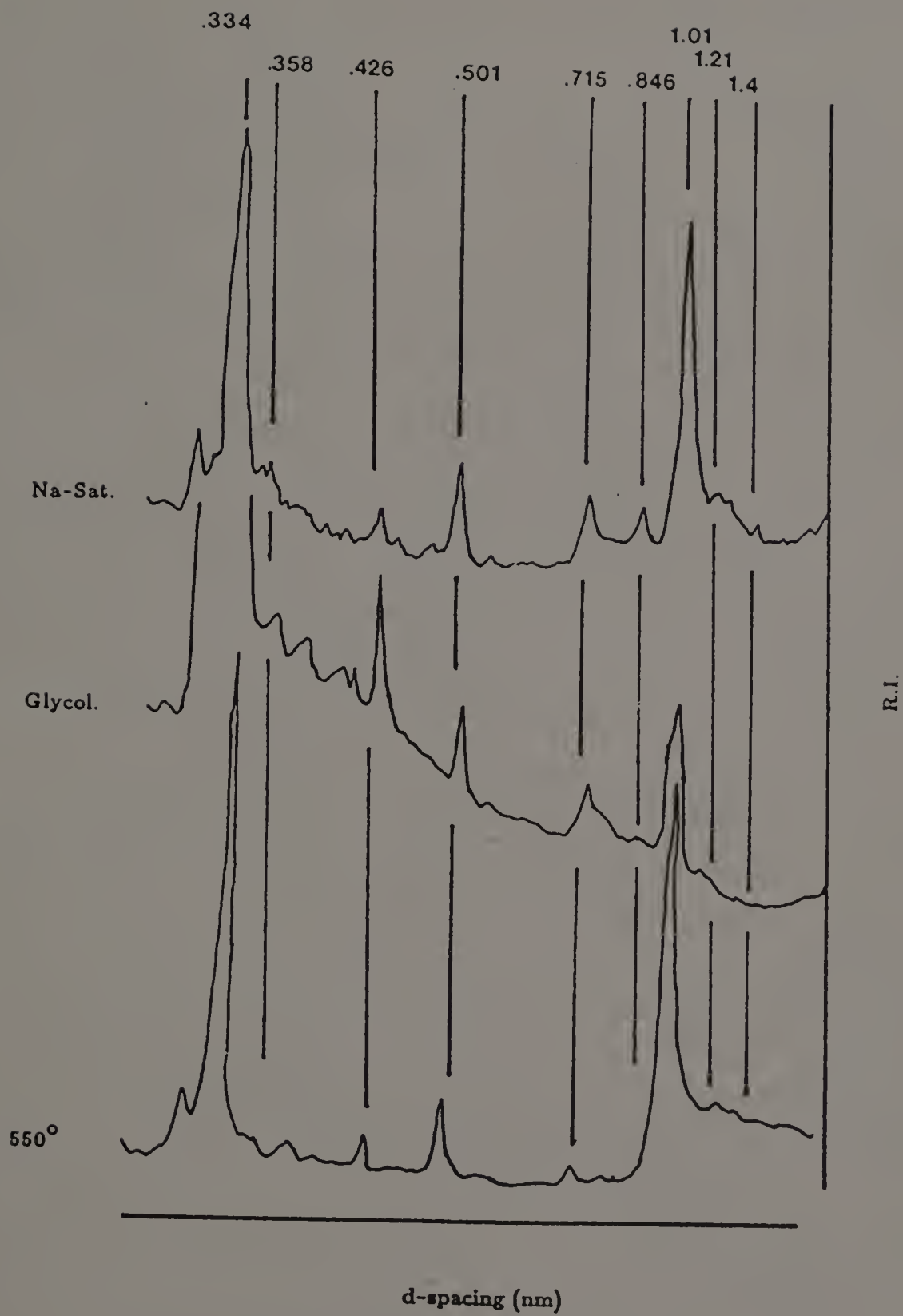
Orchard Hill Woodbridge (OHW)



Orchard Hill Woodbridge 3Cd (OHD)



Buck Hill Woodbridge (BHW)



Buck Hill Paxton 3Cd3 (BHD)

APPENDIX M

GROUND PENETRATING RADAR

Introduction

Ground-Penetrating-Radar (GPR) can be used to delineate numerous features within the soil. In this study GPR was used on two areas of a drumlin located in central Massachusetts. The first was situated on the north slope of the drumlin extending from the summit to the footslope, the second was located on the west side of the drumlin extending from the upper sideslope to the footslope. Two transects 10 meters apart and over 100 meters long were established on the north slope and a area 24 by 67 meters was established on the west slope. The GPR results showed that the Btx horizon on the north-facing site was roughly parallel to the ground surface. The west-facing site lacked the parallel features possibly due to solifluction or the presence of a terrace along the lower portions of the slope. Overall, the GPR data was useful in delineating the subsurface topography of fragipans in this area.

Objectives

1. Investigate the suitability of using GPR to delineate a Bx horizon.
2. Investigate the relationship between the ground surface and the surface of a fragipan across the slope of a drumlin.

Materials and Methods

The ground-penetrating radar was the SIR System-8 manufactured by Geophysical Surveys Systems, Inc. System components used consisted of the model 4800 control unit, ADTEK SR 8004H graphic recorder, power distribution unit, and the 120 MHz antenna with the model 705DA transceiver. A scanning time of 80 nanoseconds (ns) was used in this study.

The study site was located on a drumlin in Brookfield, Worcester County, MA. The north facing site is currently an orchard with five year old dwarf apple trees. Before planting the older apple trees including stumps were removed causing some subsurface disturbance. The west facing site is located at the far edge of the orchard and has only been used as pasture and hayland.

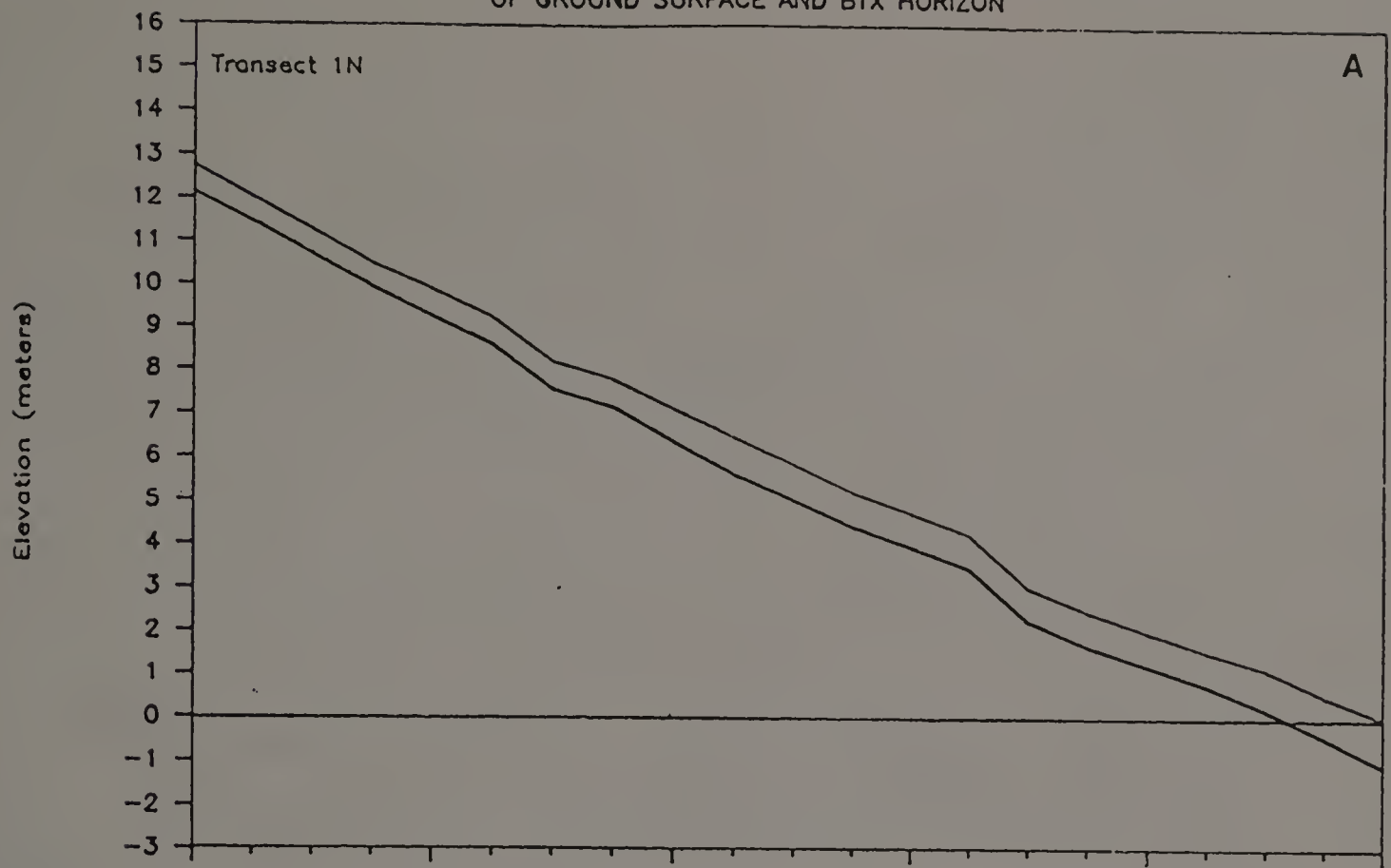
Elevations were taken at specific points to establish a detailed topographic map of the surface at each area. The subsurface topography was mapped using the depths to contacts established by the GPR and confirmed by test pits and augered holes.

The transects on the north slope were 122 meters (transect 1N) and 110 meters (transect 2N) in length with observations points spaced at 6.1 meter intervals. Transect 1N consists of 21 observation points on a 10% north-facing slope with relief of 12.75 meters. Transect 2N consists of 19 observation points on a 12% north-facing slope with a relief of 13.49 meters (Figure 123 and 124).

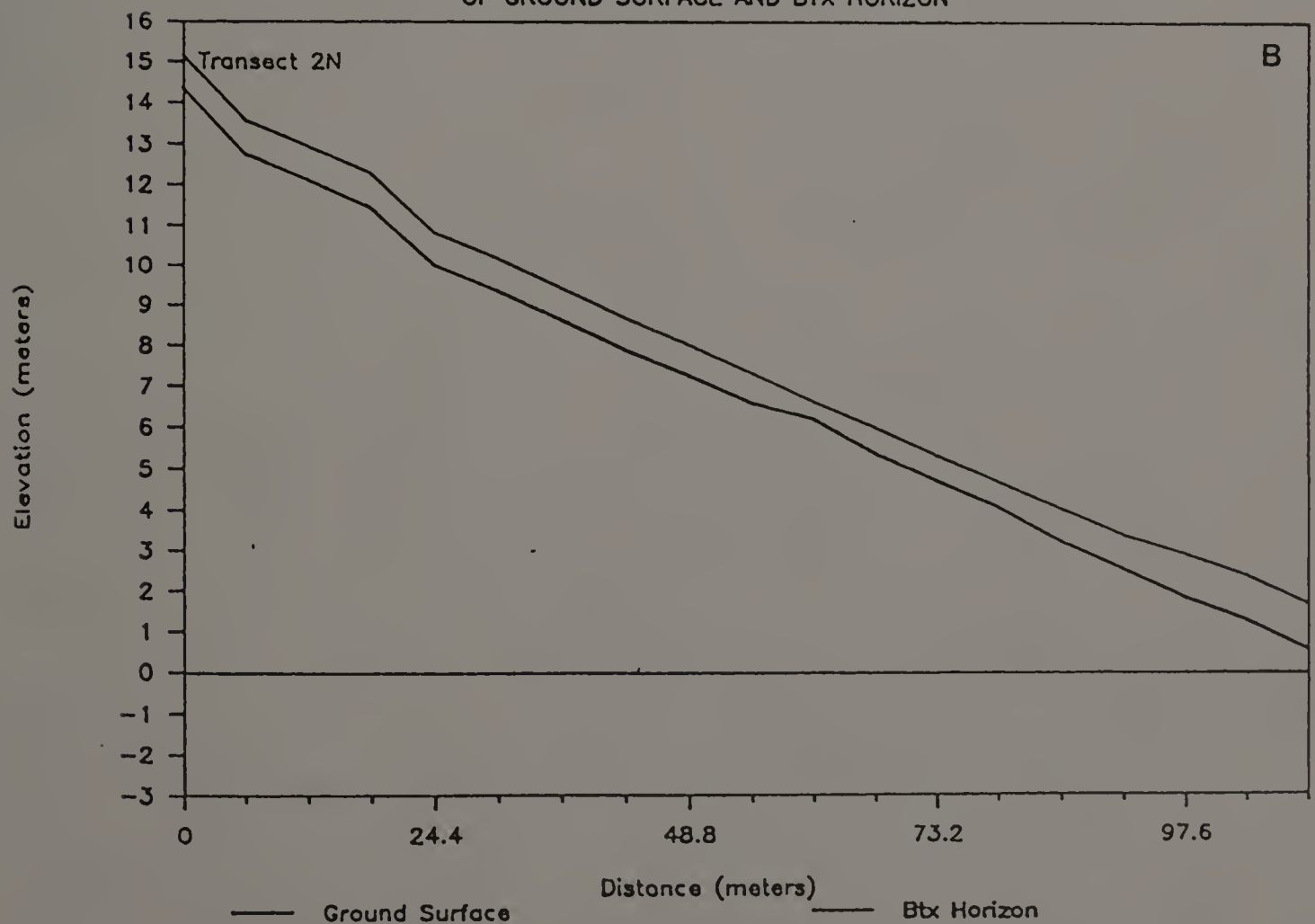
On the west-facing slope data from eight transects (three shown here) were compiled. Transects were 67.1 meters in length with

Figure 123. Cross section of transects (A) 1N and (B) 2N
illustrating relationship of pan to the surface.

RELATIVE ELEVATIONS ALONG NORTH SLOPE OF GROUND SURFACE AND BTX HORIZON



RELATIVE ELEVATIONS ALONG NORTH SLOPE OF GROUND SURFACE AND BTX HORIZON



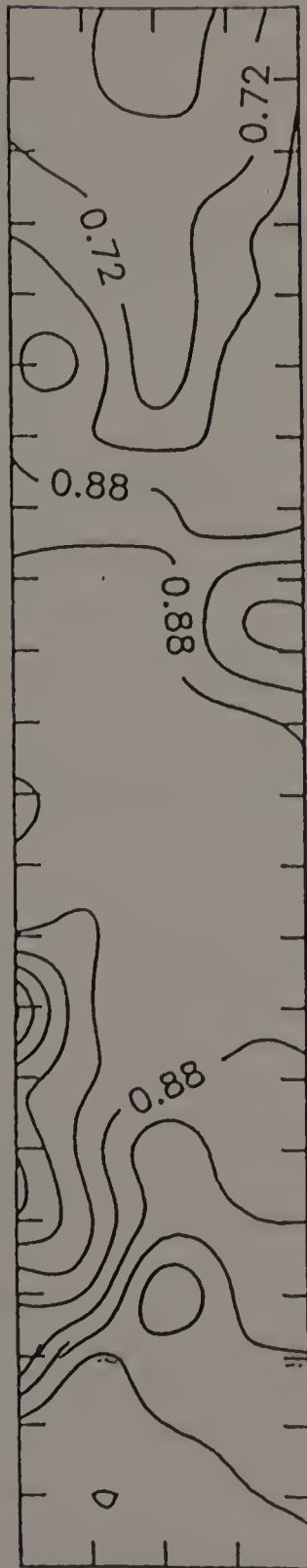


Figure 124. Subsurface topography of the north slope area.

observations points spaced at 3.05 meter intervals. Transect 1W consist of 23 observation points on a 14% west-faccing slope with relief of 9.37 meters. Transect 2W consists of 23 observation points on a 15% west-facing slope with relief of 9.92 meters. Transect 3W consists of 21 observation points on 13% west-facing slope with relief of 8.09 meters (Figure 125).

Results

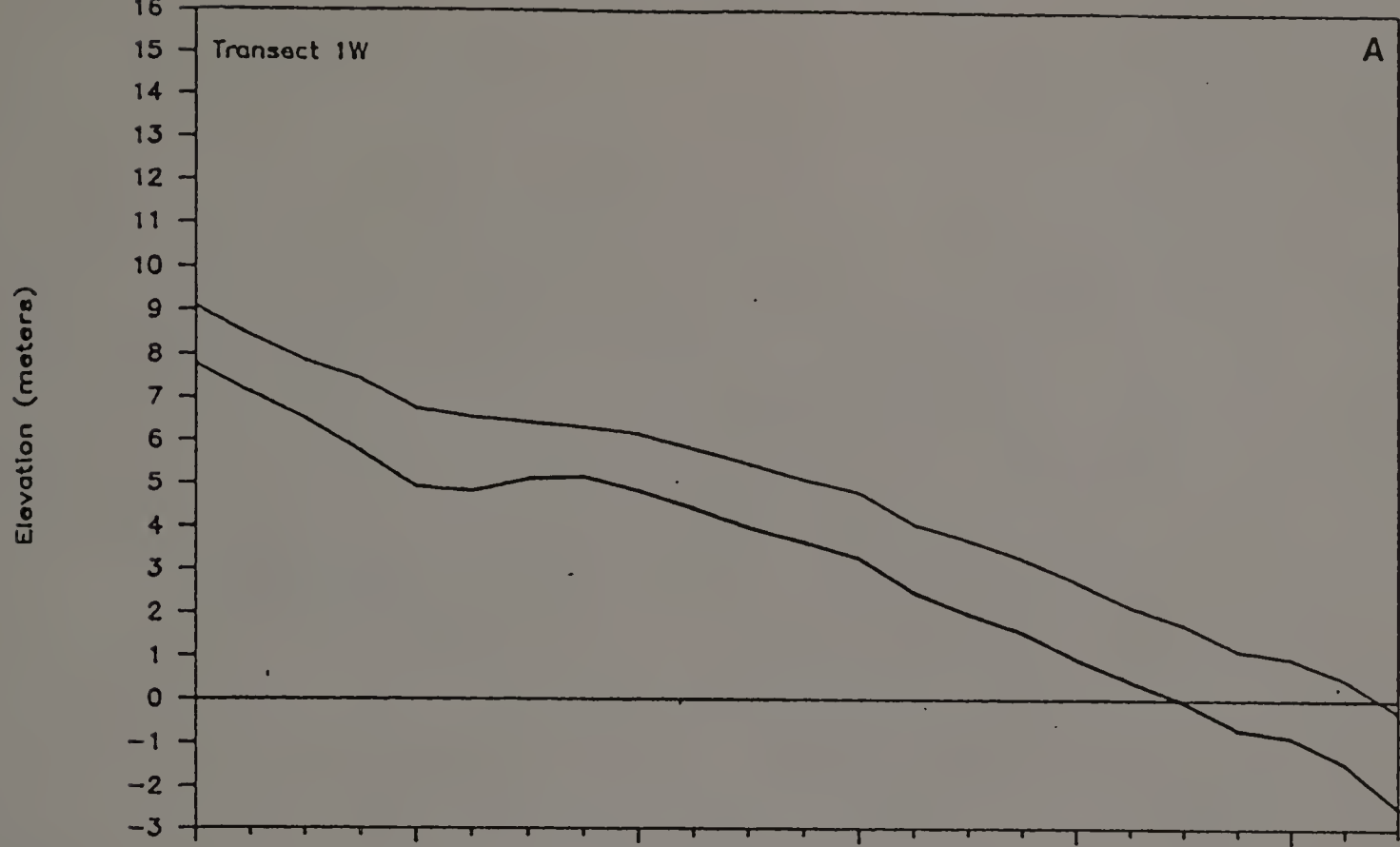
North Slope

The radar imagery was exceedingly difficult to interpret on the north facing slope as a result of multiple, segmented interfaces believed to be a product of the up-rooting of apple trees.

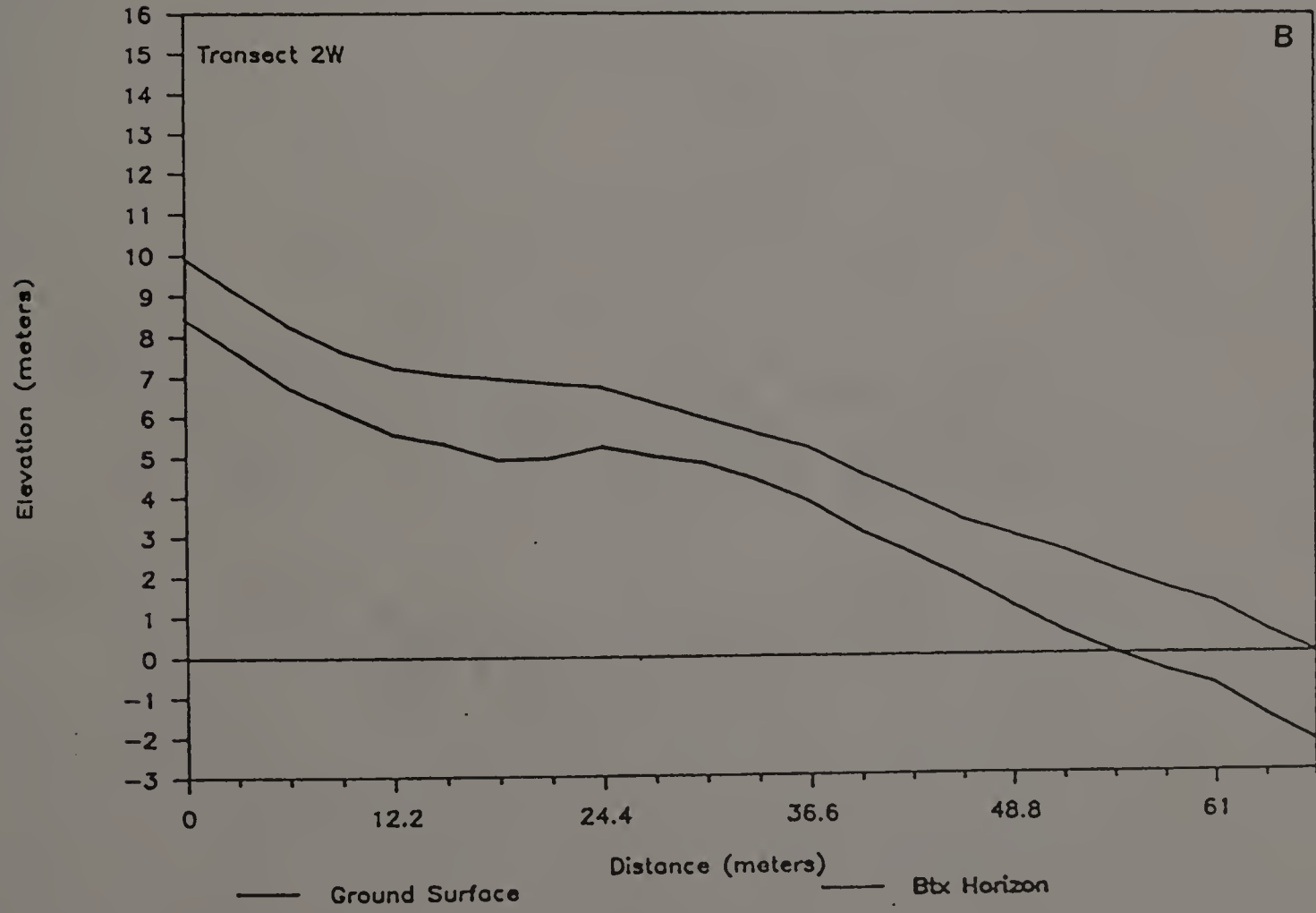
Transects from the north-facing slopes (Figures 123 and 124) revealed relatively shallow and uniform depths to the Btx horizon. The sample correlation coefficient, r , between elevation and depth to Btx horizon for these transects is 0.495. While no significant trend is obvious from the data, a slight deepening in the depth to the Btx horizon may be noted along the lower portion of each transects. This may be due to mass wasting processes. The average depth to the Btx horizon on transects 1N and 2N is 0.80 m with a standard deviation of 0.16. The median depth to the Btx horizon is 0.82 m, and is nearly identical with the mean. This data attest to the low variability and relative uniformity in the depth to the Btx horizon along the north-facing slope.

Figure 125. Cross section of transects (A) 1W, (B) 2W, and (C) 3W illustrating the relationship of the pan to the surface.

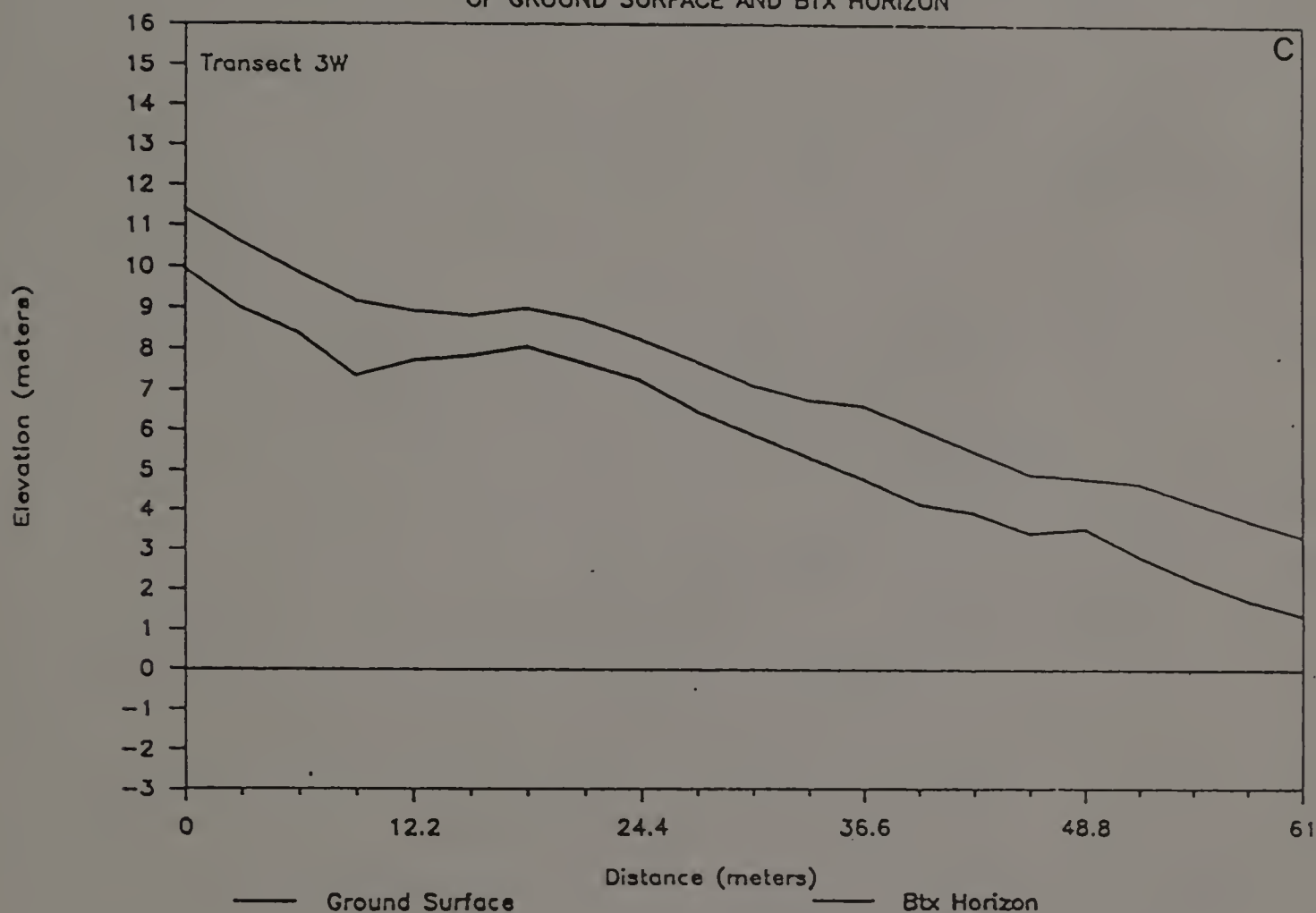
RELATIVE ELEVATIONS ALONG WEST SLOPE
OF GROUND SURFACE AND BTX HORIZON



RELATIVE ELEVATIONS ALONG WEST SLOPE
OF GROUND SURFACE AND BTX HORIZON



RELATIVE ELEVATIONS ALONG WEST SLOPE OF GROUND SURFACE AND BTX HORIZON



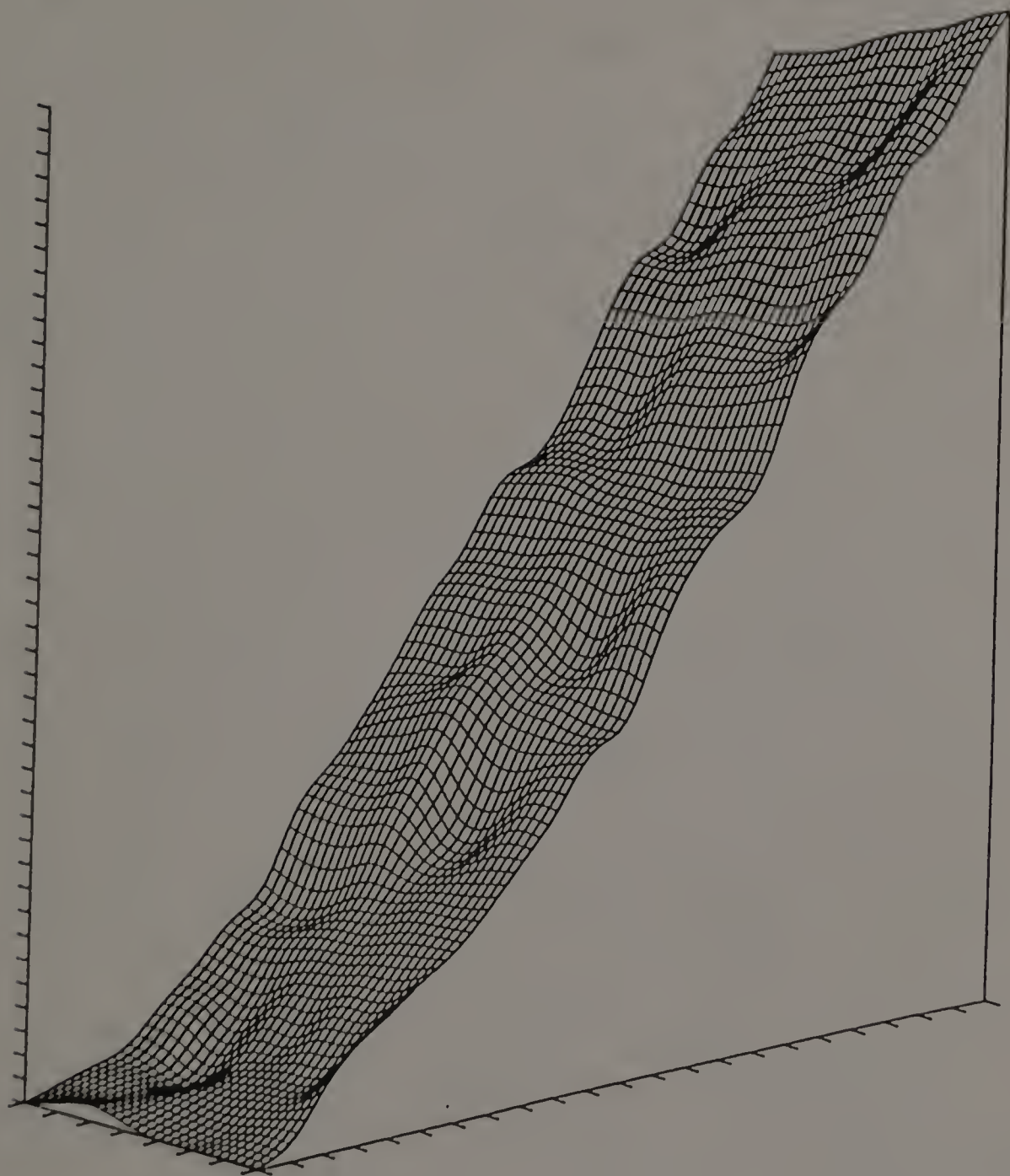
West Slope

Transects from the west-facing slopes (Figure 125) as well as topographic map developed from the data (Figure 126 and 127) reveal relatively deeper and more variable depths to the Btx horizon. The radar imagery was more interpretable here than on the north-facing slope, as this site did not experience the severe up-rooting of apple trees. The area can be divided into three sections: a concave upper sideslope with generally deeper depths to the Btx horizon; a convex middle sideslope with generally shallow depths to the Btx horizon; and a concave footslope with the depth to the Btx horizon deepening with lower slope positions. The sample correlation coefficient, r , between elevation and depth to Btx horizon for these transects is -0.647. These relationships may be attributed to a terrace along the lower portions of the slope and/or to solifluction.

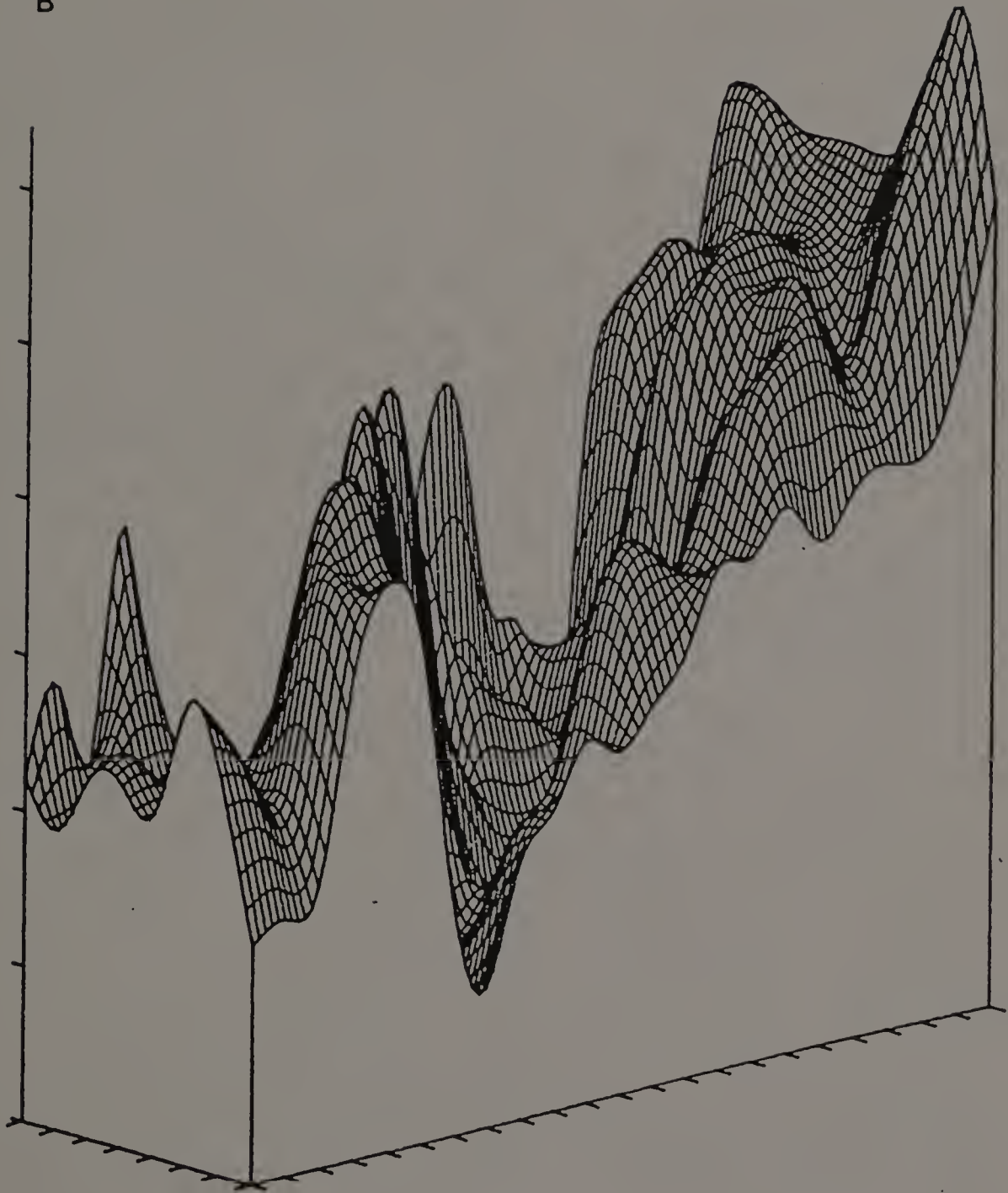
The average depth to the Btx horizon along these transects is 1.62 m with a standard deviation of 0.32. The median depth to the Btx horizon is 1.55 m, and is nearly identical with the mean. This data attest to the higher variability in the depth to the Btx horizon along the west-facing slope.

Figure 126. Three dimensional plot of (A) surface and (B)
subsurface of the west slope area.

A



B



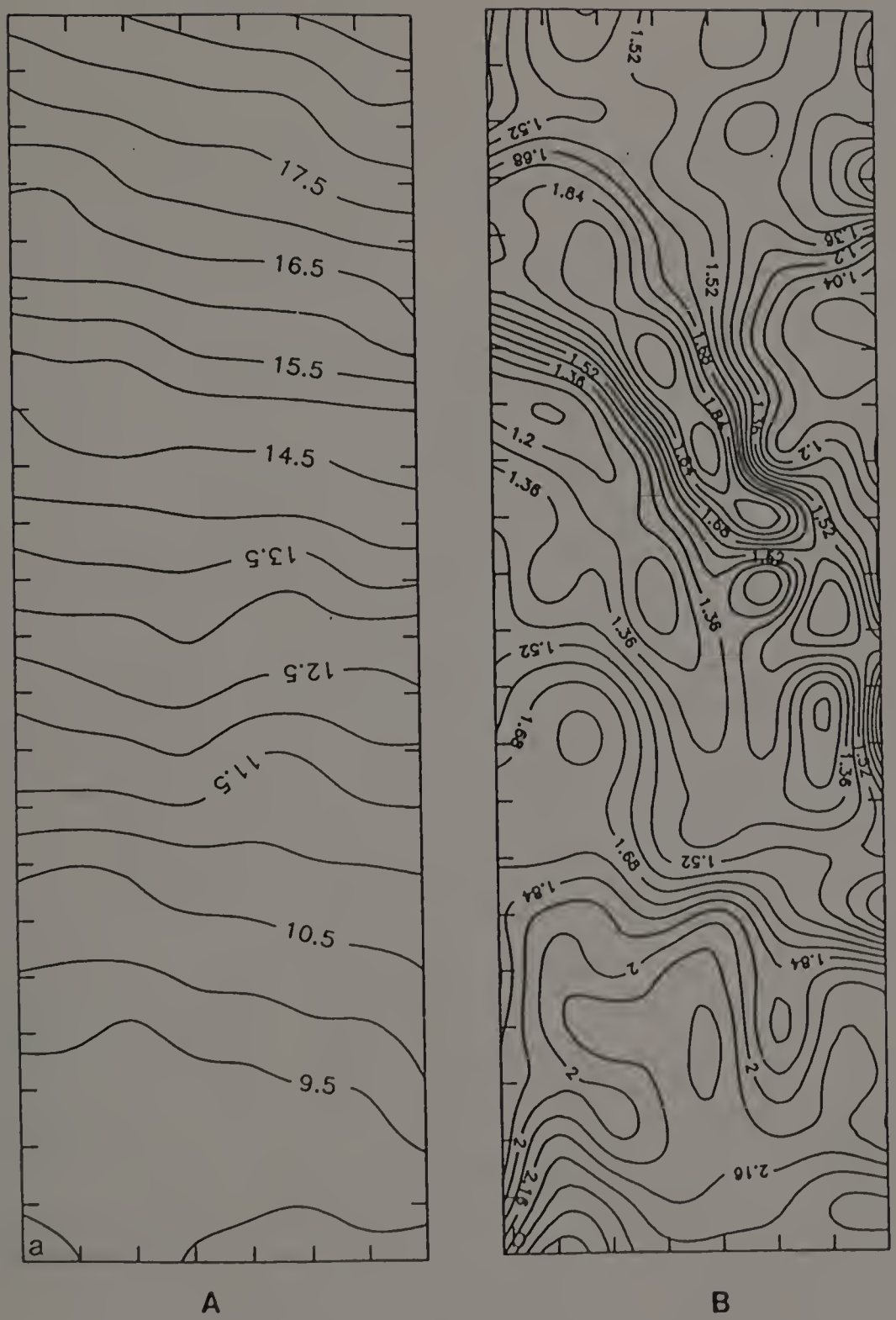


Figure 127. Surface (A) and subsurface (B) topography of the west slope area.

Conclusions

1. GPR results illustrate the relation of the Btx horizon to the surface even if there has been disturbance on the site.
2. Although the results were hindered by past management practices (tree removal) the radar unit was able to identify the Btx horizon as well as some of the effects of past management practices.
3. The results aid in interpreting and possibly qualifying or quantifying geomorphic processes such as soil creep. More work needs to be done with this aspect of the device.

This work was presented at the 1988 ASA Annual Meetings in Anaheim, CA and was co-authored by James Doolittle, SCS, Chester, PA. The topographic plots were prepared by Dr. Mary Collins, University of Florida, Gainesville, FL.

BIBLIOGRAPHY

- Anderson, J.U., J.L. White. 1958. A study of fragipans in some southern Indiana soils. Soil Sci. Soc. Proc. 22:450-454.
- Andrews, J.T. 1971a. Methods in the analysis of till fabric. In R. P. Goldthwait (ed.) Till: A Symposium, Ohio State University Press. p.321-327.
- Andrews, J.T. 1971b. Techniques of till fabric analysis. Tech. Bull. Brit. Geomorph. Res. Group. 1-43.
- Antoine, P.P. 1970. Mineralogical, chemical, and physical studies on the genesis and morphology of a Rockwood sandy loam (Typic Fragiboralf). Ph.D. Dissertation. Univ. of Minnesota, St. Paul.
- Arshad, M.A., R.J. St. Arnaud, P.M. Huang. 1972. Dissolution of trioctahedral layer silicates by ammonium oxalate, sodium dithionite-citrate-bicarbonate, and potassium pyrophosphate. Can. J. Soil Sci. 52:19-26.
- Bascomb, C.L. 1968. Distribution of pyrophosphate-extractable iron and organic carbon in soils of various groups. J. Soil Sci. 19:251-268.
- Bascomb, C.L., K. Thanigasalam. 1978. Comparison of aqueous acetylacetone and potassium pyrophosphate solutions for selective extraction of organic bound Fe from soils. J. Soil Sci. 29:382-287.
- Bilzi, A.F., E.J. Ciolkosz. 1977. Time as a factor in the genesis of four developed soils in recent alluvium in Pennsylvania. Soil Sci. Soc. Am. J. 41:122-127.
- Birkeland, P.W. 1974. Pedology, Weathering, and Geomorphological Research. Oxford University Press. Inc., London. 285 p.
- Bisdorf, E.A.B., R. Nouta, B. Volbert. 1983. STEM-EDXRA and SEM-EDXRA investigations of iron coated organic matter in thin sections with transmitted, secondary and backscattered electrons. Geoderma. 30:77-92.
- Black, R.F. 1982. Modes of deglaciation in Connecticut. In G. J. Larson and B. D. Stone (eds.) Late Wisconsinan Glaciation of New England. p. 70-100.
- Bodine, S.M. 1986. Lithological controls on the clay mineralogy of selected Massachusetts soils. M.S. Thesis. Univ. of Massachusetts. 322p.

- Bonnichesen, R., G.L. Jacobson, Jr., R.B. Davis, H.W. Borns, Jr. 1985. The environmental setting for human colonization of northern New England and adjacent Canada in Late Pleistocene time. In H. W. Borns, Jr., P. LaSalle, and W. B. Thompson. Late Pleistocene History of Northeastern New England and adjacent Quebec. GSA Special Paper 197. P. 151-9.
- Borggaard, O.K. 1976. Selective extraction of amorphous iron oxide by EDTA from a mixture of amorphous iron oxide, goethite and hematite. J. Soil Sci. 27:978-486.
- Borns H.W., Jr., P.E. Calkin. 1977. Quaternary glaciations, west-central Maine. GSA Bull. 88:1773-84.
- Boulton, G.S. 1987. A theory of drumlin formation by subglacial sediment deformation. In J. Menzies, J. Rose (eds.) Drumlin Symposium. A. A. Balkema, Rotterdam, Netherlands. p. 25-80.
- Boulton, G.S. 1972. Modern arctic glaciers as depositional models for former ice sheets. J. Geol. Soc. London. 128:361-393.
- Boulton, G.S. 1971. Till genesis and fabric in Svalbard, Spitsbergen, In R. P. Goldthwait (ed.) Till: A Symposium. Ohio State University Press. p.41-72.
- Boulton, G.S. 1968. Flow tills and related deposits on some Vestspitsbergen glaciers. J. Glaciol. 7:391-412.
- Boulton, G.S., D.L. Dent. 1974. The nature and rates of post-depositional changes in recently deposited till from Southeast Iceland. Geografiska Annaler. 56:121-134.
- Boulton, G.S., M.A. Paul. 1976. The influence on genetic processes on some geotechnical properties of glacial tills. Q. J. Eng. Geol. 9:159-94.
- Brewer, R. 1976. Fabric and Mineral Analysis of Soils. Robert F. Krieger Publishing Company. Melbourne, Florida. 482p.
- Bryan, K. 1949. The geological implications of cryopedology. J. Geol. 57:101-4
- Bryant, R.B. 1989. Strength characteristics and related physical properties of fragipans. In N. E. Smeck and E. J. Ciolkosz (eds.) Fragipans: Their Occurrence, Classification, and Genesis. Soil Sci. Soc. Am. Special publication Number 24. p. 141-150.
- Budel, J. 1959. Periodische und episodische solifluktion im Rahmen der Klimatischen Solifluktionstypen. Erkunde. 13:297-314.

- Buurman, P., A.G. Jongmans. 1975. The Neerepen soil, an early Oligocene podzol with a fragipan and gypsum concretions from Begian and Dutch Limburg. *Pedologie* 25:105-117.
- Caggiano, J.A., Jr. 1978. Surficial and applied surficial geology of the Belchertown Quadrangle, Massachusetts. Ph.D. Dissertation. Univ. of Massachusetts. 179p.
- Calhoun, T.E. 1980. Recommended reclassification or disposition of Northeast region series now classified as having fragipans. In E. J. Ciolkosz (ed.) *Proc. Northeast Cooperative Soil Survey Conference*, University Park, PA. June 23-27, 1980. Agron. Series no. 5.
- Carlisle, F.J., E.G. Knox, R.B. Grossman. 1957. Fragipan horizon in New York soils: I. General characteristics and distribution. *Soil Sci. Soc. Proc.* 21:320-321.
- Chao, T.T., P.K. Theobald, Jr. 1976. The significance of secondary iron and manganese oxides in geochemical exploration. *Econ. Geol.* 71:1560-9.
- Chao, T.T., L. Zhou. 1983. Extraction techniques for selectives dissolution oxides from soils and sediments. *Soil Sci. Soc. Am. J.* 47:225-32.
- Chartes, C.J. 1985. A preliminary investigation of hardpan horizons in Northwest New South Wales. *Aust. J. Soil Res.* 23:325-337.
- Clark, P.U. 1986. Subglacial sediment dispersal and till composition. *J. Geology.* 95:527-41
- Commission of the European Communities. 1985. Soil map of the European Communities-1:1,000,000. Directorate-General Information Market and Innovation. Luxembourg, Luxembourg.
- Cowan, W.R. 1968. Ribbed moraine: till fabric analysis and origin. *Can. J. Earth Sci.* 5:1145-60.
- Crampton, C.B. 1965. An indurated horizon in soils of South Wales. *J. Soil Sci.* 16:230-241.
- Creameens, D.L., L.D. Norton, R.G. Darmody, I.J. Jansen. 1988. Etch-pit measurements on scanning electron micrographs of weathered grain surfaces. *Soil Sci. Soc. Am. J.* 52:883-5.
- Creameens, D.L., R.G. Darmody, I.J. Jansen. 1987. SEM analysis of weathered grains: Pretreatment effects. *Geology.* 15:401-4.

- Cummingham, R.L., E.J. Ciolkosz. 1984. Soils of the northeastern United States. The Pennsylvania State Univ. College of Agriculture, Agric. Exp. Stn. Bull. 848. University Park, PA.
- Currier, L.W. 1941. Tills of eastern Massachusetts. GSA Bull. 52:1895-6.
- Dabney, S.M., H.M. Selim. 1987. Anisotropy of a fragipan soil: Vertical vs. horizontal hydraulic conductivity. Soil Sci. Soc. Am. J. 51:3-6.
- Daniels, R.B., W.D. Nettleton, R.J. McCracken, E.E. Gamble. 1966. Morphology of soils with fragipans in parts of Wilson County North Carolina. Soil Sci. Soc. Am. Proc. 30:376-380.
- Day, P.R. 1965. Particle fractionation and particle size analysis. In C.A. Black (ed.) Methods of Soil Analysis Part I. ASA, Madison, Wisconsin. p. 545-567.
- DeJong, J., M.C.H. Harris. 1971. Settlements of two multistory building in Edmonton Alberta. Can. Geotech. J. 10:261-281.
- DeKimpe, C. 1970. Chemical, physical, and mineralogical properties of a podzol soil with fragipan derived from glacial till in the Province of Quebec. Can. J. Soil Sci. 50:317-330.
- DeKimpe, C.R., G.A. Bourbeau, R.W. Baril. 1976. Pedological aspects of till deposits in the province of Quebec. In R.F. Legget (ed.) Glacial Till Special Publication No.12 of the Royal Society of Canada. 156-69.
- DeKimpe, C.R., R.W. Baril, R. Rivard. 1972. Characterization of a toposequence with fragipan: The Leeds-Ste Marie-Brompton series of soils, Province of Quebec. Can. J. Soil Sci. 52:135-150.
- DeKimpe, C.R., M.R. Laverdiere. 1982. Dissolution of organometallic complexes and silica from the clay fraction of podzolic soils. Commun. in Soil Sci. Plant Anal. 13:387-400.
- DeKimpe, C.R., J.A. McKeague. 1974. Micromorphological, physical, and chemical properties of a podzolic soil with a fragipan. Can. J. Soil Sci. 54:29-38.
- Denny, C.S. 1982. Geomorphology of New England. U. S. Geol. Survey Prof. Paper 1208. 18 p.
- Denny, C.S. 1941. Glacial drift near Canaan, New Hampshire. GSA Bull. 52:1898.
- Derbyshire, E., A. McGown, and A. Radwan. 1976. Total fabric of some till landforms. Earth Surface Processes. 1:17-26.

- Derry, D.R. 1933. Heavy minerals of the Pleistocene beds of the Don Valley, Toronto, Ontario. *J. Sed. Pet.* 3:113-118.
- Deshpande, T.L., D.J. Greenland, J.P. Quirk. 1968. Changes in soil properties associated with the removal of Fe and Al oxides. *J. Soil Sci.* 19:108-122.
- Drake, L.D. 1974. Till fabric control by clast shape. *GSA Bull.* 85:247-50.
- Drake, L.D. 1971. Evidence for ablation and basal till in East-Central New Hampshire. In R.P. Goldthwait (ed.) *Till: A Symposium*, Ohio State University Press. p. 73-91.
- Dremer, M.S. 1981. The mineralogy and sedimentology of some Long Island tills, and their correlation with lobes of the late Wisconsinan ice sheet, Long Island, New York. M. S. Thesis. Univ. of Massachusetts, Amherst. 192 p. (unpublished)
- Ehlers, J., H.J. Stephan. 1983. Till fabric and ice movement. In J. Ehlers (ed.). *Glacial Deposits in North-West Europe*. A. A. Balkema, Rotterdam. p. 267-74.
- Fanning, D.S., M.C.B. Fanning. 1989. Soil: Morphology, genesis, and classification. John Wiley and Sons, New York. 395 p.
- Fitzpatrick, E.A. 1987. Preiglacial features in the soils of northeast Scotland. In J. Boardman (ed.), *Periglacial Processes and Landforms in Britain*. Cambridge University Press. p. 153-62.
- Fitzpatrick, E.A. 1980. The Micromorphology of Soils. Univ. of Aberdeen, Scotland. 433 p.
- Fitzpatrick, E.A. 1956. An indurated soil horizon formed by permafrost. *J. of Soil Sci.* 7:248-255.
- Fletcher, P.C. 1979. The presence of a wind blown component in Massachusetts soils. M.S. Thesis. University of Mass. 166 p. (unpublished)
- Flint, R.F. 1961. Two tills in southern Connecticut. *GSA Bull.* 72:1687-92.
- Franzmeier, D.P., B.F. Hajek, C.H. Simonson. 1965. Use of amorphous material to identify spodic horizons. *Soil Sci. Soc. Am. Proc.* 29:737-43.

- Franzmeier, D.P., L.D. Norton, G.C. Steinhardt. 1989. Fragipan formation in loess of the Midwestern United States. In N. E. Smeck and E. J. Ciolkosz (eds.) Fragipans: Their Occurrence, Classification, and Genesis. Soil Sci. Soc. Am. Special publication Number 24. p. 69-98.
- Franzmeier, D.P., G.C. Steinhardt, L.D. Norton. 1978. A model for the formation of fragipans in loess. ISSS Meetings Poster session.
- Fritton, D.D., F.N. Swader, K. Hoddinott. 1983. Profile modification persistence in a fragipan soil. Soil Sci. 136:124-30.
- Fritton, D.D., G.W. Olson. 1972. Bulk density of a fragipan soil in natural and disturbed profiles. Soil Sci. Soc. Am. Proc. 36:686-689.
- Fuchtbauer, W. 1972. Diagenesis of heavy minerals. In Arenaceous deposits: Sedimentation and diagenesis. Alberta Univ. Dep.Ext. and Alberta Soc. Pet. Geol., Edmonton. p. 267-72.
- Fuller, M.L. 1901. Probable representatives of PreWisconsin till in southeastern Massachusetts. J. Geology. 9:311-329.
- Fuller, M.L. 1914. The geology of Long Island. U. S. Geologic Survey Prof. Paper 82, 231p.
- Gephart, C. 1979. Use of polyolefin shrinkable tubing to encase soil cores for hydraulic conductivity determinations. Soil Survey Horizons. 20:11-14.
- Gerath, R.F., B.K. Fowler, G.M. Haselton. 1985. The deglaciation of the northern White Mountains of New Hampshire. In H.W. Borns, Jr., P. LaSalle, and W.B. Thompson. Late Pleistocene History of Northeastern New England and Adjacent Quebec. GSA Special Paper 197. p. 21-28.
- Giovannini, G., P. Sequi. 1976. Iron and aluminum as cementing substances of soil aggregates. J. Soil Sci. 27:140-147.
- Glass, H.D., M.M. Killey. 1986. Principles and application of clay mineral composition in Quaternary stratigraphy: Examples from Illinois, USA. In J. J. van der Meer (ed.). Tills and Glaciotectonics. A. A. Balkema, Rotterdam. p. 117-125.
- Glen, J.W., J.J. Donner, R.G. West. 1957. On the mechanism by which stones in till become oriented. Am. J. Science. 255:194-205.
- Goldthwait, L. 1948. Glacial Till in New Hampshire. New Hampshire Planning and Development Comm., Concord, 11p.

- Grossman, R.B. 1954. Studies of physical properties of fragipans in New York State. M. S. Thesis. Cornell Univ., Ithaca, NY. (unpublished)
- Grossman, R.B., F.J. Carlisle. 1969. Fragipan soils of the Eastern United States. *Advan. Agron.* 21:237-279.
- Grossman, R.B., M.G. Cline. 1957. Fragipan horizons in New York soils: II. Relationships between rigidity and particle size distribution. *Soil Sci. Soc. Proc.* 21:322-325.
- Grossman, R.B., J.B. Fehrenbacher, A.H. Beavers. 1959a. Fragipan soils of Illinois: I. General characteristics and field relationships of the Hosmer Silt Loam. *Soil Sci. Soc. Am. Proc.* 23:65-70.
- Grossman, R.B., F. Stephen, J.B. Fehrenbacher, A.H. Beavers. 1959b. Fragipan soils of Illinois: III. Micromorphological studies of Hosmer Silt Loam. *Soil Sci. Soc. Am. Proc.* 23:73-75.
- Grossman, R.B., F. Stephen, J.B. Fehrenbacher, A.H. Beavers, J.M. Parker. 1959c. Fragipan soils of Illinois: II. Mineralogy in reference to parent material uniformity of Hosmer Silt Loam. *Soil Sci. Soc. Am. Proc.* 23:70-73.
- Gustavson, T.C., J.C. Boothroyd. 1987. A depositional model for outwash, sediment sources, and hydrologic characteristics, Malaspina Glarier, Alaska: A modern analog of the southeastern margin of the Laurentide Ice Sheet. *GSA Bull.* 99:187-200.
- Gywn, Q.H. J., A. Dreimanis. 1979. Heavy mineral assemblages in till and their use in distinguishing glacial lobes in the Great Lakes. *Can. J. Earth Sci.* 16:2219-35.
- Habecker, M.A., K. McSweeney, F.W. Madison. 1990. Identification and genesis of fragipans in Ochrepts of North Central Wisconsin. *Soil Sci. Soc. Am. J.* 54:139-46.
- Hallmark, C.T., N.E. Smeck. 1979a. The effect of extractable aluminum iron and silicon on strength and bonding of fragipans of northeastern Ohio. *Soil Sci. Soc. Am. J.* 43:145-150.
- Hallmark, C.T., N.E. Smeck. 1979b. A rupture technique to determine fragipan strength. *Soil Sci. Soc. Am. J.* 43:198-200.
- Hallmark, C.T., L.P. Wilding, N.E. Smeck. 1982. Silicon. In A.L. Page (ed.) *Methods of Soil Analysis Part II*. ASA Madison Wisconsin. p. 263-274.
- Handy, R.L. 1973. Collapsible loess in Iowa. *Soil Sci. Soc. Am. Proc.* 37:281-284.

- Hanna, W.E., L.A. Daugherty, R.W. Arnold. 1975. Soil geomorphic relationships in a first-order valley in Central New York. *Soil Sci. Soc. Am. Proc.* 39:716-722.
- Harlan, P.W., D.P. Franzmeier. 1977. Soil formations on loess in Southwestern Indiana: I. Loess stratigraphy and soil Morphology. *Soil Sci. Soc. Am. J.* 41:93-98.
- Harlan, P.W., D.P. Franzmeier, C.B. Roth. 1977. Soil formation of loess in south western Indiana: II. Distribution of clay and free oxides and fragipan formation. *Soil Sci. Soc. Am. J.* 41:99-103.
- Hill, A.R. 1968. An experimental test of the field technique of till marcfabric analysis. *Trans. Inst. Brit. Geogr.* 45:93-106.
- Holmes, C.D. 1941. Till Fabric. *GSA Bull.* 52:1299-1354.
- Holmgren, G. 1967. A rapid citrate-dithionite extratable iron procedure. *Soil Sci. Soc. Am. Proc.* 31:205-212.
- Hoppe, G. 1952. Hummocky moraine regions with special reference to the interior of Norbotten. *Geogr. Ann.* 34:1-72.
- Horn, M.E., E.M. Rutledge. 1965. The Dickson and Zanesville soil of Washington County, Arkansas: II. Micromorphology of their fragipans. *Soil Sci. Soc. Am. Proc.* 29:443-448.
- Hubert, J.F. 1973. Analysis of heavy mineral assemblages. In R. E. Carver (ed.), *Procedures in Sedimentary Petrology*. Wiley Interscience, New York. p.453-478.
- Hutcheson, T.B., Jr., H.H. Bailey. 1964. Fragipan soils: Certain genetic implications. *Soil Sci. Soc. Am. Proc.* 28:684-685.
- Hutcheson, T.B., Jr., R.J. Lewis, W.A. Seay. 1959. Chemical and clay mineralogical properties of certain Memphis catena soils of western Kentucky. *Soil Sci. Soc. Am. Proc.* 23:474-478.
- Innes, R.P., D.J. Pluth. 1970. Thin section preparation using an epoxy impregnation for petrographic and electron microprobe analysis. *Soil Sci. Soc. Am. Proc.* 34:483-485.
- Jha, P.P., M.G. Cline. 1963. Morphology and genesis of a sol Brun Acide with fragipan in uniform silty material. *Soil Sci. Soc. Proc.* 27:339-344.
- Johnson, W.H., H.D. Glass, D.L. Gross, S.R. Moran. 1971. Glacial drift of the Shelbyville Moraine at Shelbyville, Illinois. *Illinois Geological Survey Circular* 459. 24 p.

- Judson, S. 1949. The Pleistocene stratigraphy of Boston, Massachusetts and its relation to the Boylston Street fishweir, in The Boylston Street fishweir II a study of the geology, paleobotany, and biology of a site on Stuart Street in the Back Bay district of Boston, Massachusetts. Papers of the Robert S. Peabody Foundation for Archaeology. 4:7-78.
- Karathanasis, A.D. 1989. Solution chemistry of fragipans- Thermodynamic approach to understanding fragipan formation. In N. E. Smeck and E. J. Ciolkosz (eds.) Fragipans: Their Occurrence, Classification, and Genesis. Soil Sci. Soc. Am. Special publication Number 24. p. 113-140.
- Karathanasis, A.D. 1987. Mineral solubility relationships in Fragiudalfs of western Kentucky. Soil Sci. Soc. Am. J. 51:474-81.
- Karathanasis, A.D. 1987. Thermodynamic evaluation of amorphous aluminosilicate binding agents in fragipans of western Kentucky. Soil Sci. Soc. Am. J. 51:819-824.
- Kaye, C.A. 1967. Kaolinization of bedrock of the Boston, Massachusetts area. U. S. Geol. Survey Prof. Paper 575C. P. C165-72.
- Kaye, C.A. 1964. Illinoian and early Wisconsinan moraines of Martha's Vineyard, Massachusetts. U. S. Geol. Survey Prof. Paper 501C. p.C134-139.
- Kaye, C.A. 1961. Pleistocene stratigraphy of Boston, Massachusetts. U. S. Geol. Prof. Paper. 424. p.B73-78.
- Kempton, J.P., P.B. DuMontello, H.D. Glass. 1971. Subsurface stratigraphy of the Woodfordian tills in the McLean County region, Illinois. In R. P. Goldthwait (ed.). Til: A Symposium. Ohio State University Press. p. 217-33.
- Knox, E.G. 1957. Fragipan horizons in New York Soils: III. The basis of rigidity. Soil Sci. Soc. Proc. 21:326-330.
- Koteff, C., F. Pessl, Jr. 1985. Till stratigraphy in New Hampshire: Correlation with adjacent New England and Quebec. In H.W. Borns, Jr., P. LaSalle, and W.B. Thompson. Late Pleistocene History of Northeastern New England and Adjacent Quebec. GSA Special Paper 197. p. 1-12.
- Krohelski, J.T. 1976. Genesis and morphology of two soils with fragipans in Massachusetts: The Paxton and Millis series. M.S. Thesis. Univ. of Massachusetts. 85 p. (unpublished)

- Langohr, R. 1987. Characteristics and genesis of fragipans and associated root inhibiting consolidated soil horizons in Western Europe. Agron. Abstr. p. 227.
- Larsen, F.D., J.H. Hartshorn. 1982. Deglaciation of the southern portion of the Connecticut Valley of Massachusetts. In G. J. Larson, B. D. Stone (eds.) Late Wixconsinan Glaciation of New England. p. 115-28.
- Lawson, D.E. 1980. Acomparison of the pebble orientations in ice and deposits of the Matanuska Glacier, Alaska. J. Geology. 87:629-45.
- Lenhardt, D.R. 1983. Characterization and strength analysis of representative fragipans of New York state. Ph.D. Dissertation. Cornell Univ. 388 p. (unpublished)
- Lindbo, D.L. 1990. Characterization of selected tills in Massachusetts. M.S. Thesis. Univ. of Massachusetts, Amherst, MA. 239 p. (unpublished)
- Lindbo, D.L., P.L.M. Veneman. 1989. Fragipans in the Northeastern United States. In N. E. Smeck and E. J. Ciolkosz (eds.) Fragipans: Their Occurrence, Classification, and Genesis. Soil Sci. Soc. Am. Special publication Number 24. p. 11-32.
- Lord, H.J. 1979. The clay mineralogy of some Massachusetts soils developed in till. M. S. Thesis, University of Massachusetts, Amherst. 160 p. (unpublished)
- Lozet, J.M., A.J. Herbillon. 1971. Fragipan soils of Condroz (Belgium): Mineralogical, chemical, and physical aspects in relation with their genesis. Geoderma 5:325-343.
- Lyford, W.H., J.C. Goodlett, W.H. Coates. 1963. Land forms, soils with fragipans, and forest on a slope in the Harvard Forest. Harvard Forest Bulletin. No. 30.
- Lynn, W.C., R.B. Grossman. 1970. Observations of certain soil fabrics with the scanning electron microscope. Soil Sci. Soc. Am. Proc. 34:645-648.
- Marsan, F.A., J.Torrent. 1989. Fragipan bonding by silica and iron oxide in a soil from northwestern Italy. Soil Sci. Soc. Am. J. 53:1140-5.
- Mark, D.M. 1974. On the interpretation of till fabrics. Geology. 2:101-4.
- Matthews, B. 1976. Fragipan in Cumbrian soils: Its origin and significance. Proc. Cumberland Geol. Soc. 3/4:267-268.

- McCabe, F., J.F. Collins, M. Walsh. 1978. 'Channel' (Fragipan like) horizons in the soils of a drumlin in north central Ireland. Proc. Royal Irish Acad. 78:133-144.
- McCarrick, T., R. Protz. 1978. The effects of soil composition upon three acrylic soil impregnating resins. Commun. in Soil Sci. and Plant Anal. 9:955-962.
- McCracken, R.J., S.B. Weed. 1963. Pan horizons in Southeastern soils: Micromorphology and associated chemical, mineralogical, and physical properties. Soil Sci. Soc. Am. Proc. 27:330-334.
- McIlvride, W.A. 1982. Surficial geology of the northeastern part of the Mt. Holyoke Quadrangle, Massachusetts. M.S. Thesis. Univ. of Massachusetts, Amherst. 105 p. (unpublished)
- McKeague, J.A. 1967. An evaluation of 0.1M pyrophosphate and pyrophosphate dithionite in comparison with oxalate as extractants of the accumulation products in podzols and some other soils. Can. J. Soil Sci. 47:95-99.
- McKeague, J.A., J.E. Brydon, N.M. Miles. 1971. Differentiation of forms of extractable iron and aluminum in soils. Soil Sci. Soc. Am. Proc. 35:33-8.
- McKeague, J.A., J.H. Day 1966. Dithionite and oxalate extractable Fe and Al as aids in differentiating various classes of soils. Can. J. Soil Sci. 46:13-22.
- McKeague, J.A., J.H. Day. 1969. Oxalate extractable Al as a criterion for identifying podzol B horizons. Can. J. Soil Sci. 49:161-163.
- McKeague, J.A., P.N. Sprout. 1975. Cemented subsoils (Puric Horizons) in some soils of British Columbia. Can. J. Soil Sci. 55:189-203.
- McLean, E.O., 1982. Soil pH and lime requirement. In A.L. Page (ed.) Methods of Soil Analysis Part II. p. 199-224.
- Menzies, J. 1986. Inverse-graded units within till in Drumlins near Caledonia, southern Ontario. Can. J. Earth Sci. 23:774-86.
- Miller, F.P., N. Holowaychuk, L.P. Wilding. 1971a. Canfield Silt Loam a fragiudalf: I. Macromorphological, physical, and chemical properties. Soil Sci. Soc. Am. Proc. 35:319-324.
- Miller, F.P., L.P. Wilding, N. Holowaychuk. 1971b. Canfield Silt Loam a fragiudalf: II. Micromorphology, physical, and chemical properties. Soil Sci. Soc. Am. Proc. 35:324-331.

- Millfred, C.J., F.D. Hole. 1970. Soils of Jefferson County, Wisconsin. The University of Wisconsin, Univ. Extension, Bull. 86, Soil Series No. 61, Madison, WI.
- Moss, J.H. 1943. Two tills in the Concord quadrangle, Massachusetts. GSA Bull. 54:1826.
- Mullholland, J.W. 1976. Texture of tills, central Massachusetts. J. Sed. Pet. 46:778-87.
- Nelson, D.W., L.E. Sommers. 1982. Total carbon, organic carbon, and organic matter. In A. L. Page, R. H. Miller, D. R. Keeney (eds.) Methods of Soil Analysis, Part 2. 2nd ed. Agronomy 9:539-579.
- Nettleton, W.D., R.B. Daniels, R.J. McCracken. 1968a. Two North Carolina coastal plain catenas: I. Morphology and fragipan development. Soil Sci. Soc. Am. Proc. 32:577-582.
- Nettleton, W.D., R.J. McCracken, R.B. Daniels. 1968b. Two North Carolina coastal plain catenas: II. Micromorphology, composition and fragipan genesis. Soil Sci. Soc. Am. Proc. 32:582-587.
- Newton, R.M. 1978. Stratigraphy and structure of some New England tills. Ph.D. Dissertaion. University of Massachusetts. 241 p.
- Nikiforoff, C.C. 1955. Hardpan soils of the coastal plain of southern Maryland. Geological Survey Professional Paper 267-B. US Government Printing Office, Washington, DC. 63 p.
- Nikiforoff, C.C., R.P. Humbert, J.G. Cady. 1948. The hardpan in certain soils of the Coastal Plain. Soil Sci. 65:135-153.
- Norton, L.D., J.M. Bigham, G.F. Hall, N.E. Smeck. 1983. Etched thin sections for coupled optical and electron microscopy and microanalysis. Geoderma 30:55-64.
- Norton, L.D., D.P. Franzmeier. 1978. Toposequence of loess derived soils in southwestern Indiana. Soil Sci. Soc. Am. J. 42:622-627.
- Norton, L.D., G.F. Hall, N.E. Smeck, J.M. Bigham. 1984. Fragipan bonding in a late Wisconsinan loess-derived soil in East Central Ohio. Soil Sci. Soc. Am. J. 48:1360-1366.
- Oldale, R.N., D.M. Eskenasy. 1983. Regional significance of pre-Wisconsinan till from Nantucket Island, Massachusetts. Quaterary Res. 19:302-11.

- Oldale, R.N., P.C. Valentine, T.M. Cronin, E.C. Spiker, B.W. Blackwelder, D.F. Belknap, J.F. Wehmiller, B.J. Szabo. 1982. Stratigraphy, structure, absolute age, and paleontology of the upper Pleistocene deposits at Sankaty Head, Nantucket Island, Massachusetts. *Geology*. 10:246-52.
- Olson, G.W., F.D. Hole. 1968. The fragipan soils of northeastern Wisconsin. *Transactions of the Wisconsin Academy of Sciences, Arts, and Letters* (1967-68). 56:173-184.
- Osmond, D.A. 1958. Micropedology. *Soils and Fert.* 21:1-6.
- Payton, R.W. 1980. Pedogenic compaction: the character and formation of compact soil horizons. *Proceedings of the North of England Soils Discussion Group* (1979). 16:103-126.
- Pease, M.H. 1970. Pleistocene stratigraphy observed in a pipeline in East Central Connecticut and its bearing on the two till problem. *USGS Prof. Paper* 700D. D36-48.
- Peech, M., R.L. Cowan, J.H. Baker. 1962. A critical study of the BaCl_2 -Triethanolamine and ammonium acetate methods for determining the exchangeable hydrogen content of soils. *Soil Sci. Soc. Am. Proc.* 26:37-40.
- Pessl, F., Jr. 1966. A two till locality in northwestern Connecticut. *USGS Prof. Paper* 550D. D89-93.
- Pessl, F., Jr. 1971. Till fabrics and till stratigraphy in western Connecticut. *In* R.P. Goldthwait (ed.) *Till: A Symposium*, Ohio State University Press. p. 92-105.
- Pessl, F., Jr., J. P. Schafer. 1968. Two-till problem in Naugatuck-Torrington area, western Connecticut. *In* P. Orville (ed.). *NEIGC Guidebook for Field Trips in Connecticut*. State Geological and Natural History Survey. Guidebook No. 2. p. 1-25.
- Petersen, G.W., R.W. Ranney, R.L. Cunningham, R.P. Matelski. 1970. Fragipans in Pennsylvania soils: A statistical study of laboratory data. *Soil Sci. Soc. Am. Proc.* 34:719-722.
- Pickering, E.W. 1983. Hardpan strength characteristics, moisture regimes, and morphology of soils in a Paxton catena in central Massachusetts. M.S. Thesis. Univ. of Massachusetts. 119 p. (unpublished)
- Pickering, E.W., P.L.M. Veneman. 1984. Strength characteristics of three indurated horizons in Massachusetts. *Soil Sci. Soc. Am. J.* 48:133-137.

- Price, F.R., D.A. Jenkins. 1980. Removal of resin from standard soil thin sections by low temperature ashing as a means of following transmitted optical by scanning electron microscopy. *Clay Minerals*. 15:309-315.
- Pritchett, W.L. 1979. Properties and Management of Forest Soils. John Wiley and Sons, New York.
- Quigley, R.M., T.A. Ogunbadejo. 1976. Till geology, mineralogy and geotechnical behavior Sarnia, Ontario. In R.F. Legget (ed.) *Glacial Till Special Publication No. 12 of The Royal Society of Canada*. p. 336-345.
- Ramsden, J., J. A. Westgate. 1971. Evidence of reorientation of a till fabric in Edmonton area, Alberta. In R. P. Goldthwait (ed.) *Till: A Symposium*. Ohio State University Press. p. 335-44.
- Ranney, R.W., E.J. Ciolkosz, R.L. Cunningham, G.W. Petersen, R.P. Matelski. 1975. Fragipans in Pennsylvania soils: properties of bleached prism face materials. *Soil Sci. Soc. Am. Proc.* 39:695-698.
- Reed, M.G. 1989. Moistures regimes, water flow patterns, and related soil characteristics of upland soils in central Massachusetts. M. S. Thesis. University of Massachusetts. 160 p. (unpublished)
- Reed, M.G., P.L.M. Veneman. 1986. Hydraulic characterization of a Canton, Scituate, and Ridgebury hydrosequence. *Agron. Abstr.* p. 236.
- Retelle, M.J. 1979. Surficial geology of the Bernardston quadrangle, Massachusetts-Vermont. M.S. Thesis. Univ. of Massachusetts. 98 p.
- Ritcher, K. 1936. Gefugestudien in Engraebræ, Fondalsbræ, und ihren Volrlandsedimenten. *Zeits. Gletcherkunde*. 24:22-30.
- Ritter, D.F. 1986. Process Geomorphology. William C. Brown Publishers. 579 p.
- Rhoades, J.D. 1982. Cation exchange capacity. In A.L. Page (ed.) *Methods of Soil Analysis Part II*. p. 149-158.
- Ross, G.J., C. Wang, P.A. Schuppli. 1985. Hydroxylamine and ammonium oxalate solutions as extractions for Fe and Al from Soils. *Soil Sci. Soc. Am. J.* 49:783-785.
- Ruark, G.A. 1985. A refined soil coring system. *Soil Sci. Soc. Am. J.* 49:278-281.

- Ruhe, R.V. 1969. Soils, paleosols, and environment. In W. Dort, Jr., J. K. Jones, Jr. (eds.) Pleistocene and recent environments of the central Great Plains. Univ. Press of Kansas, Lawrence. p. 37-52.
- Ruhe, R.V. 1956. Geomorphic surfaces and the nature of soils. Soil Sci. 82:441-5.
- Ryan, P.J., J.W. McGarity. 1983. Procedure for recording spatial variability of soil properties along trench faces. Soil Sci. Soc. Am. J. 47:332-4.
- St. Arnaud, R.J. 1976. Pedological aspects of glacial till. In R.F. Legget (ed.) Glacial Till. Special Publication No.12 of the Royal Society of Canada. p133-153.
- Schafer, J.P., J.H. Hartshorn. 1965. The quaternary of New England. In H.E. Wright and D.G. Frey (eds.) The Quaternary of the United States. Princeton University Press.
- Scotter, D.R., B.E. Clothier, R.B. Corker. 1979. Soil water in a fragiaqualf. Aust. J. Soil Res. 17:443-453.
- Shaler, N. S. 1889. The geology of Nantucket. U. S. Geol. Survey Bull. v.53, 55 p.
- Smalley, I.J., J.E. Davin. 1982. Fragipan horizons in soils: A bibliographic study and review of some of the hard layers in loess and other material. New Zealand Soil Bureau Bibliographic Report 30. 122 p.
- Smeck, N.E., M.L. Thompson, L.D. Norton, M.J. Shipitalo. 1989. Weathering discontinuities: A key to fragipan formation. In N. E. Smeck and E. J. Ciolkosz (eds.) Fragipans: Their Occurrence, Classification, and Genesis. Soil Sci. Soc. Am. Special publication Number 24. p. 99-112.
- Smeck, N.E., E.J. Ciolkosz. 1989. Fragipans: Their Occurrence, Classification, and Genesis. Soil Sci. Soc. Am. Special publication Number 24. 153 p.
- Smith, B.R., L.L. Callahan. 1987. Soils with Bx horizons in the Upper Costal Plains of South Carolina. Soil Sci. Soc. Am. J. 51:158-164.
- Smith, B.R., R.B. Daniels. 1989. Occurrence and characteristics of fragipans on the Coastal Plains of the Southeastern United States. In N. E. Smeck and E. J. Ciolkosz (eds.) Fragipans: Their Occurrence, Classification, and Genesis. Soil Sci. Soc. Am. Special publication Number 24. p. 33-42.

- Snyder, K.E., R.B. Bryant. 1985. Slope processes and fragipan expression in soils of the Saamanca re-entrant, New York. Agron. Abstr. p. 198.
- Soil Survey Staff. 1988. Keys to Soil Taxonomy (fourth printing). SMSS technical monograph no. 6. Cornell University.
- Soil Survey Staff. 1985. Keys to Soil Taxonomy (third printing). SMSS technical monograph no. 6. Cornell University.
- Soil Survey Staff. 1984. Procedures for collecting soil samples and methods of analysis for Soil Survey. USDA-SCS Soil Survey Investigations Report. U.S. Government Printing Office.
- Soil Survey Staff. 1979. Soil survey laboratory data and descriptions for some soils of Louisiana. USDA-SCS Soil Survey Investigations Rep. No. 35.
- Soil Survey Staff. 1975. Soil Taxonomy. Agric. Handb. No. 436. USDA. U.S. Government Printing Office, Washington, D.C.
- Soil Survey Staff. 1974. Soil Survey Investigations Report. Soil Survey Laboratory Methods and Procedures for Collecting Soil Samples. SCS, USDA. U.S. Government Printing Office. 67 p.
- Soil Survey Staff. 1974. Soil survey laboratory data and descriptions for some soils of New York. USDA-SCS Soil Survey Investigations Rep. No. 25.
- Soil Survey Staff. 1968. Soil survey laboratory data and descriptions for some soils of the New England States. USDA-SCS. Soil Survey Investigations Rep. No. 20
- Soloyanis, S.C. 1978. Paleomagnetic properties of some New England tills. Ph.D. dissertation, Univ. of Massachusetts, Amherst, MA. 78 p. (unpublished)
- Soloyanis, S.C., L.L. Brown 1979. Late Pleistocene magnetic stratigraphy recorded in some New England tills. Geophys. Res. Letters. 6:256-68.
- Steele, F., R.B. Daniels, E.E. Gamble, L.A. Nelson. 1969. Fragipan horizons and BE Masses in the Middle Coastal Plain of North Central North Carolina. Soil Sci. Soc. Am. Proc. 33:752-755.
- Steinhardt, G.C., D.P. Franzmeier, L.D. Norton. 1982. Silica associated with fragipan and non-fragipan horizons. Soil Sci. Soc. Am. J. 46:656-657.

- Steinhardt, G.C., D.P. Franzmeier. 1979. Chemical and mineralogical properties of the fragipans of the Cincinnati Catena. Soil Sci. Soc. Am. J. 43:1008-1013.
- Steward, M.T., D.M. Mickelson. 1976. Clay mineralogy and relative age of tills in north-central Wisconsin. J. Sed. Pet. 46:200-6.
- Stewart, D.P., and P. MacClintock. 1971. Ablation till in Northeastern Vermont. In R. P. Goldthwait (ed.), Till: A Symposium, Ohio State University Press. p.106-114.
- Stone, B.D., J.D. Peper. 1982. Topographic control of the deglaciation of eastern Massachusetts: Ice lobation and the marine incursion. In B. D. Stone, G. J. Larson (eds.) Late Wisconsinan Glaciation of New England. p. 145-82.
- Stout, B.B. 1952. Species distribution and soils in the Harvard Forest. Harvard Forest Paper no. 24. Harvard Univ. Harvard Forest, Petersham, MA 29 p.
- Thomas, G.M. 1984. A comparison of the paleomagnetic character of some varves and tills from the Connecticut Valley. M. S. Thesis. Univ. of Massachusetts, Amherst, MA. 136 p. (unpublished)
- Upham, W. 1878. Modified drift in New Hampshire. In C. H. Hitchcock (ed.) The Geology of New Hampshire, part III. Concord, New Hampshire. p. 3-176.
- Upham, W. 1879. The till of New England. Geol. Mag. 6:283-284.
- van Vliet, B., R. Langohr. 1981. Correlation between fragipans and permafrost with special reference to silty Weichelian deposits in Belgium and northern France. Catena 8:137-154.
- van Vliet-Lanoe, B. 1985. Frost effects in soils. In J. Broadman (ed.) Soils and Quaternary landscape evolution. John Wiley and Sons, New York. p. 117-58.
- Veneman, P.L.M., S.M. Bodine. 1982. Chemical and morphological soil characteristics in a New England drainage toposequence. Soil Sci. Soc. Am. J. 46:359-363.
- Waldron, P. F. 1984. The influence of conservation tillage on edaphic properties of a typic dystrocrept in Massachusetts. M.S. Thesis. Univ. of Massachusetts. 148 p.
- Wang, C. 1971. Genetic studies of Lansing and Langford soils. Ph.D. Dissertation. Cornell Univ. 166p. (unpublished).

- Wang, C., J.L. Nowland, H. Kodama. 1974. Properties of two fragipan soils in Nova Scotia including scanning electron micrographs. *Can. J. Soil Sci.* 54:159-170.
- Weedle, T.K., D.W. Caldwell. 1986. Surficial deposits in the lower Sandy River valley and adjacent areas. In NEIGC Guidebook for Field Trips in Southwestern Maine. p. 216-239.
- Weedle, T.K. 1988. On the lack of early and middle Wisconsinan deposits at New Sharon, Maine-implications for middle Wisconsinan ice centers. *AMQUA Programs and Abstracts*. p. 160.
- Westgate, J.A., A. Dreimanis. 1967. The Pleistocene sequence at Zorra, southwestern Ontario. *Can. J. Earth Sci.* 14:1127-43.
- White, S.E. 1947. Two tills and the development of glacial drainage in the vicinity of Stafford Springs, Connecticut. *Am. J. Sci.* 245:754-78.
- Willman, H.B., H.D. Glass, J.C. Frye. 1966. Mineralogy of glacial tills and their weathering profiles in Illinois. Part II. Weathering profiles. *Illinois State Geological Survey Circular* 400.
- Winters, E. 1942. Silica hardpan development in the red and yellow podzolic region. *Soil Sci. Soc. Am. Proc.* 7:437-440.
- Winters, E., R.W. Simonson. 1951. The Subsoil. *Adv. Agron.* 3:2-86.
- Witty, J.E., E.G. Knox. 1989. Identification, role in soil taxonomy, and world wide distribution of fragipans. In N. E. Smeck and E. J. Ciolkosz (eds.) *Fragipans: Their Occurrence, Classification, and Genesis*. *Soil Sci. Soc. Am. Special publication* Number 24. p. 1-10.
- Woodworth, J.B., E. Wigglesworth. 1934. Geography and geology of the region including Cape Cod, the Elizabeth Islands, Nantucket, Martha's Vineyard, No Mans Land, and Block Island. *Harvard Coll. Mus. Comp. Zool. Mem.* vol. 52. 338 p.
- Wright, H.E. 1957. Stone orientation in the Wadena drumlin field, Minnesota. *Geogr. Ann.* 39:19-31.
- Whittig, L.D., V.J. Kilmer, R.C. Roberts, J.G. Cody. 1957. Characteristics and genesis of Cascade and Powell soils of northwestern Oregon. *Soil Sci. Soc. Am. Proc.* 21:226-32.
- Williams, R.F., R.N. Fanvolden. 1967. The influence of joints on the movement of ground water through glacial till. *J. Hydrology* 5:163-170.

- Yassoglou, N.J., E.P. Whiteside. 1960. Morphology and genesis of some soils containing fragipans in northern Michigan. Soil Sci. Soc. Proc. 24:396-407.
- Zen, E. 1983. Bedrock Geologic Map of Massachusetts. U. S. Geol. Survey, Alexandria, Virginia. 3 maps.

